CONSEIL INTERNATIONAL DES UNIONS SCIENTIFIQUES

UNION GEODESIQUE ET GEOPHYSIQUE INTERNATIONALE

ASSOCIATION DE SÉISMOLOGIE
ET DE
PHYSIQUE DE L'INTÉRIEUR DE LA TERRE

PUBLICATIONS DU BUREAU CENTRAL SÉISMOLOGIQUE INTERNATIONAL

Sous la direction de J. P. ROTHÉ

SECRÉTAIRE DE L'ASSOCIATION DE SÉISMOLOGIE ET DE PHYSIQUE DE L'INTÉRIEUR DE LA TERRE

SÉRIE A

TRAVAUX SCIENTIFIQUES

Fascicule 20

Publié avec le concours financier de l'U. N. E. S. C. O.

TOULOUSE
ÉDOUARD PRIVAT & Cie Libraire-Éditeur
14, RUE DES ARTS, 14

1959

AVERTISSEMENT

Le présent fascicule contient, dans l'ordre où elles ont été présentées, le texte de quelques-unes des communications scientifiques discutées au cours des séances de la conférence de Toronto.

Les autres communications destinées à être publiées dans différents périodiques scientifiques n'ont pas été réimprimées. On en trouvera les références bibliographiques dans les Comptes Rendus N° 12, Association de Séismologie et de Physique de l'Intérieur de la Terre, comptes rendus des séances de la XI[e] conférence réunie à Toronto du 3 au 14 septembre 1957, Strasbourg, 1958, pp. 69-197.

J.-P. Rothé,
Secrétaire de l'Association Internationale
de Séismologie et de Physique
de l'Intérieur de la Terre.

Strasbourg
15 avril 1958.

TABLE DES AUTEURS

INDEX ALPHABÉTIQUE DES MATIÈRES

Géographie Séismologique.

Géothermie.

Magnitude.

Microséismes.

Voir Agitation microséismique.

Ondes séismiques.

Radioactivité.

Séismographes.

Tectonophysique.

ON A NEW METHOD
OF DETERMINING EARTHQUAKE MAGNITUDES

By E. BISZTRICSÁNY*.

The magnitude determination of earthquakes was based by RICHTER [1] upon the amplitudes of the long-period waves of shallow shocks. Of course, the registrated amplitude is dependent on epicentral distance and influenced also by the instrumental parameters. Thus the unit magnitude and the intensity of the zero-magnitude shock had to be defined arbitrarily. The equation of the zero-magnitude shock, as defined by GUTENBERG [2] is as follows :

$$- \log B = 5{,}04 + \tfrac{1}{2} [48{,}25 \chi (\Delta^\circ - 90^\circ) +$$
$$\log \sin \Delta^\circ + \frac{1}{3} (\log \Delta^\circ - 1{,}954)]$$

This equation may be within a broad interval substituted by a straight line which yields acceptable results even in epicentral distances as small as $\Delta^\circ = 10^\circ$. However, the magnitudes of nearer shocks will be overestimated by this method. An excellent example is the Grecian series of shocks, whose epicentral distance related to *Prague* was about 12°, its magnitudes were determined by *Prague* and *Athens* as well. On comparing the magnitudes of the 22 shocks occurred 1953 to 1955 [3] it is seen that the magnitude determined by *Athens* is invariably some 0,4 units above the values given by *Prague* (S. *fig.* 1). By investigating several Hungarian earthquakes of small epicentral intensity a similar result was obtained. The magnitude equation for *Budapest* has yielded on the average values one-half unit above the expected ones. As the period of recurrence of Hungarian shocks felt at distances above 5-6° is rather long (as much as 20 to 30 years), we were at a loss how to determine the magnitudes of smaller shocks. Thus the need arose to seek a different way of magnitude determination.

A possibility to carry out this intention was given by the *Prague Seismological Report for 1953-1955* [3], containing the data of 25 blastings of given explosive mass and wave duration. We have chosen from these the ones of identical locality, so that the only variable parameter was the mass of explosive. By studying these data it became evident that the duration of earth motion is proportional to the quantity of explosives used (*fig.* 2).

* Geophysical Institute, Eötvös University Budapest (Hungary).

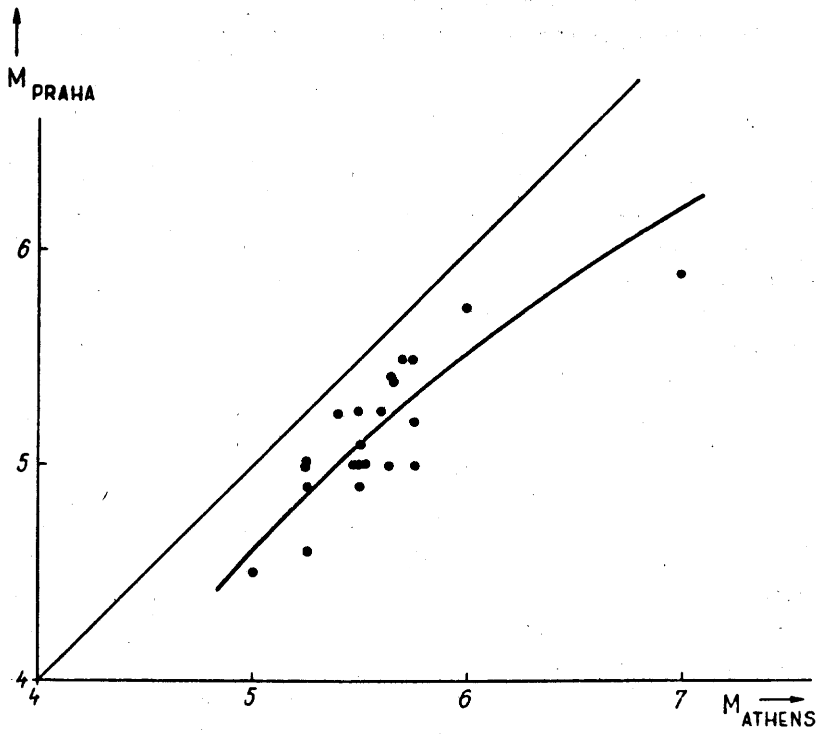

FIG. 1. — Magnitudes determined by *Prague* plotted against magnitudes determined by *Athens.* (If the Athens equation of magnitude would be correct, the points should lie upon line bisecting the angle of coordinate axes.)

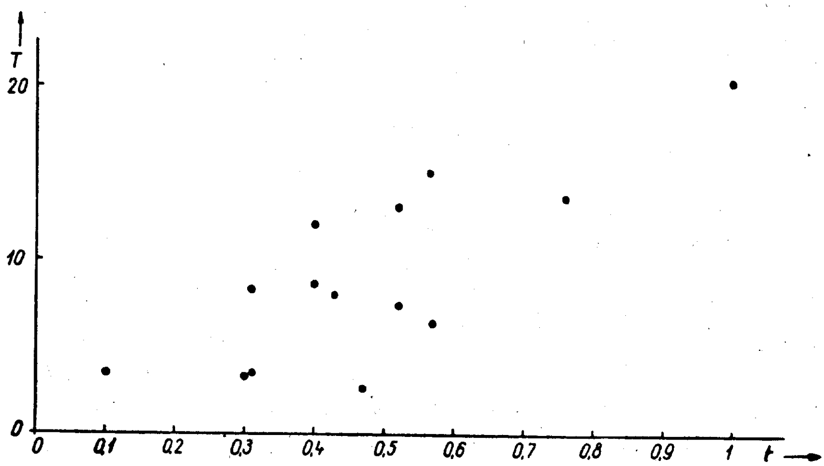

FIG. 2. — Explosion registered at a distance of 27 km. Mass of explosive /T/ plotted against duration of surface wave /t/.

If a certain degree of similarity may be assumed between natural and artificial shocks, it will be logical to assume that in the former case there will be a similar relation of magnitude and duration of ground motion. This assumption is wholly justifiable, as shown by the following considerations (having originated from L. EGYED) :

If the duration of surface waves (t) is dependent on the mass of the explosive (D) and if the relation may be assumed to take the form

$$D = ct^{\beta}$$

and further if the amount of elastic energy generated by the blast may be assumed to be proportional to the mass of explosive, *i. e.*

$$E = \gamma D$$

then the relation

$$\log E = \log \gamma + \log D = \log \gamma + \log C + \beta \log t$$

will hold, wherein substituting

$$\log \gamma + \log C = \alpha$$

the relation

$$\log E = \beta \log t + \alpha$$

will be obtained. On comparing with the Equation of GUTENBERG

$$\log E = aM + b$$

M being the magnitude, we obtain

$$M = c \log t + d$$

According to this line of thought there is a linear relation between magnitude and the logarithm of wave duration.

In the case of earthquake waves this simple relation is obscured by the distance-dependent superposition of different phases and by the consequent change in wave durations. This was eliminated by studying surface waves only. Of course the dependence of duration changes on frequency dispersion had to be reckoned with even in this case.

The most reliable Hungarian seismograph is the WIECHERT pendulum in *Budapest* ($V \sim 190$, $T_0 \sim 10$, $\varepsilon \sim 5$). This is why our studies were restricted to the records of this instrument.

The magnitudes of 166 shocks of the interval 1931-1955 were determined by Equation

$$M = \log A_{20} + 1{,}37 \log \Delta^{\circ} + 2{,}63 \qquad (1)$$

and plotted against log t. In the following « t » will be defined as the time difference between L and F in minutes, as usually given by literature, L being the inset and F the end of the surface wave.

Performing a least-squares approximation, a straight line

$$M = 2{,}12 \log t + 0{,}0005\, \Delta^\circ + 2{,}98 \qquad (2)$$

was obtained for the set of points of *fig.* 3, *M* being the magnitude, Δ° the epicentral distance in degrees. Because of the smallness of its coefficient, this member was neglected in the following. As a next step, the magnitudes of Hungarian shocks were determined by the method of GUTENBERG and RICHTER, and plotted against log *t* (unfilled circles in *fig.* 3). The values thus plotted came to

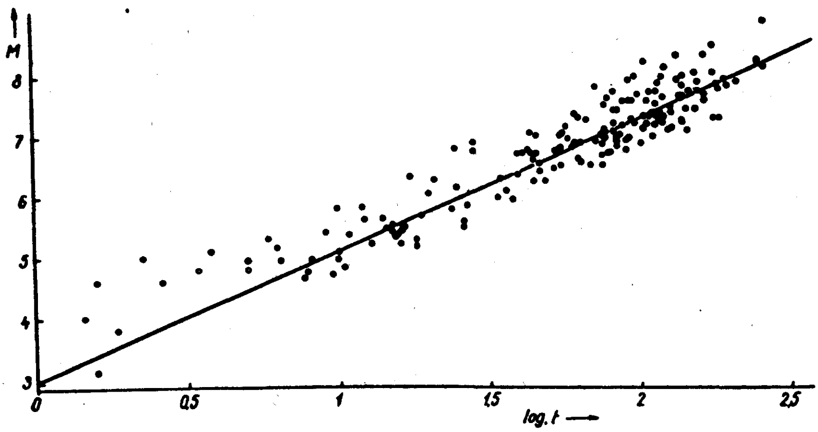

FIG. 3. — Magnitudes determined by the *Budapest* magnitude equation plotted against log *t*. Full circles designate shocks of $\Delta^\circ > 10^\circ$, empty circles near shocks with $\Delta^\circ < 3^\circ$.

lie above the straight line of Equation (1), thus corroborating the efficiency of the outlined method.

For the sake of checking our results the same work was carried out for the WIECHERT-pendulum of *Prague*. According to the Prague reports (V and T_0 are nearly identical with the similar data for Budapest) the equation obtained is

$$M = 1{,}85 \log t + 0{,}007\, \Delta^\circ + 2{,}66 \qquad (3)$$

For near shocks the member containing Δ° may likewise be neglected, which is, however, not the case for shocks of greater epicentral distances. The expression 0,007 was subtracted from the values *M* and the differences obtained were plotted, as above, against log *t* (*fig.* 4).

The standard deviation of M, was found to equal here $\sqrt{\frac{[xx]}{n}} = 0{,}30$

It was further attempted to determine the magnitudes of medium and deep shocks by the outlined method, by attaching a depth dependent coefficient to the above equation. We had access to the data of 86 shocks whose magnitude has been determined by *Pasadena*.

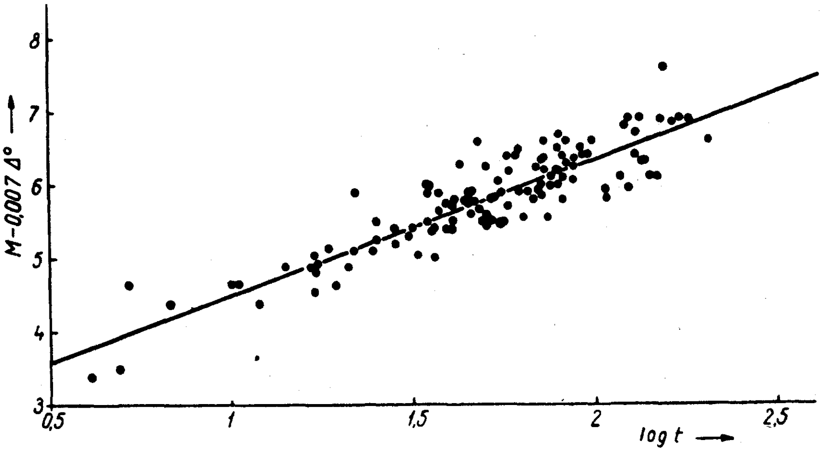

FIG. 4. — M — 0,007 $\Delta°$ values, as determined by the *Prague* magnitude equation, plotted against log t.

These values were added to the data of 208 shallow shocks whose depth of focus was substituted by an assumed average of 25 km. The magnitudes of these were likewise given by *Pasadena* [4]. The equation obtained after a least-squares approximation was

$$M = 1{,}58 \log t + 0{,}002\, \Delta° + 0{,}0007\, h + 4{,}02 \qquad (3/a)$$

On substituting $\Delta°$ and h into the equation and subtracting the members dependent upon these variables from M the set of points of *fig.* 5 is obtained. The standard deviation from the straight line

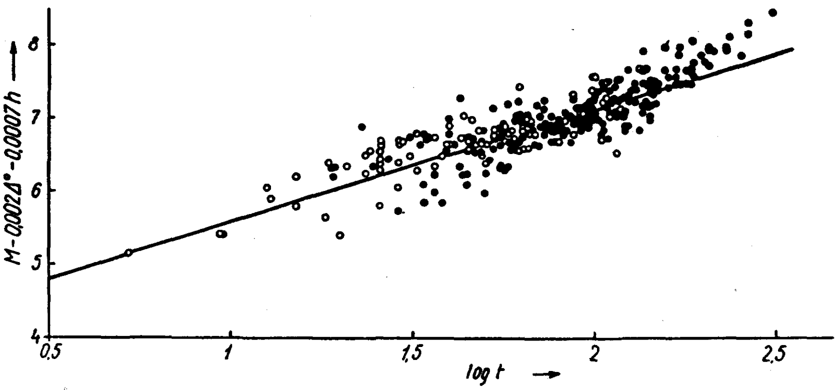

FIG. 5. — M — 0,002 $\Delta°$ — 0,0007 h values, as computed from the observations oft the WIECHERT seismograph of *Budapest,* plotted against log t. The magnitudes of the shocks have been given by *Pasadena.*

is for this set of points $\sqrt{\frac{[xx]}{n}} = 0{,}27$. Considering that the standard deviation of values determined by the method of GUTENBERG and RICHTER amounts to 0,33, and the same for the values determined by the *Prague*-equation [5] amounts to 0,34, the standard deviation of Equations (2) and (3) is highly acceptable.

It was shown above, partly on the basis of theoretical considerations, partly by analyzing the data of several earthquake observatories that there is a linear relation between the magnitude of the earthquakes and the time of decay of their surface waves. This relation also holds for deep-focus earthquakes. Consequently, the procedure above described represents a new, readily applicable method of magnitude determination. The standard deviation of the new method is much better than that of the standard ones.

The applicability of the method seems to be deteriorated by returning waves and aftershocks.

In the case of shocks with a magnitude of 8 or above the returning waves may disturb the determination of the end of the decay interval. However, the fact that in case of Figs 3-4 the points cluster around one and the same line indicates that the surface disturbance should continue even if there would be no returning wave. The scatter of the points above Magnitude 8 does not exceed that of the points below.

The determination of the end of the wave duration may also meet with difficulties because of aftershocks. For the case of an estimate of errors we have scanned the 1946 to 48 reports of *Pasadena* and the 1953 to 55 reports of *Prague*. No more than 2 per cents of the shocks was disturbed by aftershocks. Thus it seems that the method is applicable in an overwhelming majority of cases.

The advantages of the method are :

1. Rapidity.
2. The exact knowledge of instrumental constants is unnecessary.
3. Magnitude determination is reliable even around M = 0.
4. The method may be applied to small-distance shocks.
5. It may be likewise applied to deep-focus shocks.

The *eL* and *F* values of Equation (3/a) were adopted from the *Microseismic Report of the Hungarian Earthquake Observatory* by M^me^ SZILBER.

SUMMARY.

It is shown that there is a linear relation between magnitude and duration of the surface wave. An interesting feature of the relation is

that it is as good as independent on epicentral distance, especially for small distances. The equation obtained is also applicable to deep-focus earthquakes. The standard-deviation of the magnitudes thus determined was found to be 0,27, i.e. smaller than the standard deviation of magnitudes determined by the method of GUTENBERG and RICHTER.

REFERENCES.

1. RICHTER (C. F.). : An Instrumental Earthquake Magnitude Scale. *Bull. Seism. Soc. Am. 25.* 1-32. 1935.
2. GUTENBERG (B.). Amplitudes of Surface Waves and Magnitude of Earthquakes. *Bull. Seism. Soc. Am. 35,* 3-12, 1945.
3. KÁRNÍK (V.), VANĚK (J.), NYKLES (J.) : Bull. Československých Stanic Praha 1953-55.
4. GUTENBERG (B.) and RICHTER (C. F.) : Seismicity of the Earth and Associated Phenomena. *Princeton University Press,* 1954.
5. ZÁTOPEK (A.) and VANĚK (J.) : On the Regional Repartition of Magnitude Differences between Pasadena and Praha. Kartograficky Přehled. 4. 41-55. 1950.

LA « MAGNITUDO UNIFICATA » PER I TERREMOTI A PROFONDITA' NORMALE, E LA MAGNITUDO DEI TERREMOTI PROFONDI PER LA STAZIONE SISMICA DI ROMA

Domenico DI FILIPPO-Liliana MARCELLI

I PARTE
(*terremoti a profondità normale*).

Generalità e richiami.

In questi ultimi anni il concetto di magnitudo dei terremoti, (sorto inizialmente in America per opera di Richter cui si affiancò immediatamente Gutenberg) ha avuto una vasta diffusione in tutto il mondo, e molti sono oggi gli Osservatori che insieme ai rilievi sismici quotidiani indicano questa grandezza che caratterizza in maniera oggettiva (anche se ancora non rigorosamente esatta) l'entità di un sisma all'ipocentro.

Com'é noto, la magnitudo M dei sismi veniva data tramite formule che tenevano conto delle ampiezze delle onde superficiali orizzontali A (limitatamente ad un periodo oscillante in un piccolo intorno di 20 sec.) e delle distanze epicentrali $\Delta°$. Tali formule sono del seguente tipo :

$$M = \log A + \alpha \log \Delta° + \beta \tag{1}$$

α, β sono dei termini numerici, caratteristici delle singole stazioni in cui viene effettuato il rilievo.

Successivamente Gutenberg stabilì alcune relazioni che tengono conto anche degli altri tipi di onde (P, PP, ed S) le quali entrano nelle formule con i loro periodi e le loro ampiezze.

Recentemente poi, un ulteriore perfezionamento al concetto di tale grandezza é stato apportato da Gutenberg e Richter con l'introduzione della « *magnitudo unificata* », grandezza quest'ultima che, ponendo un legame tra le magnitudo di uno stesso terremoto calcolate con tutti i tipi di onde (PZ, PH, PPZ, PPH, SH, MH) dà un valore risultante unificato, valore a cui ogni onda ha portato il proprio contributo.

Una equazione lineare consente il passaggio dalla magnitudo calcolata con le onde superficiali Ms a quella calcolata con le onde spaziali : questa equazione è per Pasadena, la seguente :

$$(2) \qquad m_B = 0{,}63\ Ms + 2{,}5 = Ms - 0{,}37\ (Ms - 6{,}76)$$

Dai rilievi diretti delle onde spaziali, la m_B é calcolata con le formule

$$(3) \qquad \begin{cases} m = \log \dfrac{u}{T} + Q + s \text{ (orizzontale) oppure} \\ m = \log \dfrac{w}{T} + Q + s \text{ (verticale)} \end{cases}$$

essendo u la risultante delle ampiezze orizzontali (espressa in micron) w l'ampiezza verticale, T i corrispondenti periodi, Q i valori dati da Gutenberg e Richter mediante una serie di grafici, ed s una costante che dipende dalla stazione.

Metodo e materiale usato per la determinazione della « magnitudo unificata » nella stazione di Roma.

Allo scopo di adeguarci a tali recenti sviluppi abbiamo effettuato anche noi un aggiornamento sui rilievi fatti per il passato.

Attualmente la magnitudo a Roma viene calcolata con la formula

$$(4) \qquad M = \log A + 1{,}526 \log \Delta^\circ + 2{,}439$$

del tipo della (1) e i risultati che ne conseguono sono in genere abbastanza concordi con i valori dati da altre stazioni.

In questo lavoro abbiamo seguito le orme di Gutenberg e Richter.

Per poter giungere anche noi ad una relazione tra la magnitudo calcolata con le onde superficiali di 20 sec. e quella calcolata con le spaziali, abbiamo effettuato lo spoglio di due anni di registrazioni, ottenute presso la stazione sismica di Roma, con apparecchi Galitzin-I.N.G. e Galitzin-Wilip. Le annate in istudio (1949-1950) fanno seguito a quelle di cui ci siamo serviti nel precedente lavoro.

Rilevate, dove era possibile (e limitatamente ai terremoti di profondità normale) le ampiezze ed i periodi delle P (orizzontali e verticali) delle PP (orizzontali e verticali) delle S (orizzontali) e delle M (orizzontali con periodi di 20 sec. circa) abbiamo calcolato, per ogni terremoto, le sei magnitudo, servendoci per le onde spaziali delle formule (3) di Gutenberg e Richter e adoperando per le Q i loro stessi grafici, omettendo la costante di stazione che fa parte di un calcolo successivo. Nel servirci delle onde superficiali abbiamo usato la formula (4).

Tutti i rilievi sono riportati nella Tabella 1. Con il metodo dei minimi quadrati siamo passati a calcolare poi separatamente le formule che legano le M (PH), M (PZ), M (PPH), M (PPZ), M (SH), con la M rilevata dalla (4).

Le equazioni ottenute sono le seguenti

(5)	m (PH)	$= 0{,}375\ \mathrm{M} + 4{,}352 = \mathrm{M} - 0{,}625\ (\mathrm{M} - 6{,}963)$	(con 44 equaz.)
(6)	m (PZ)	$= 0{,}401\ \mathrm{M} + 3{,}964 = \mathrm{M} - 0{,}599\ (\mathrm{M} - 6{,}618)$	(— 48 —)
(7)	m (PPH)	$= 0{,}360\ \mathrm{M} + 4{,}493 = \mathrm{M} - 0{,}640\ (\mathrm{M} - 7{,}017)$	(— 52 —)
(8)	m (PPZ)	$= 0{,}503\ \mathrm{M} + 3{,}298 = \mathrm{M} - 0{,}497\ (\mathrm{M} - 6{,}640)$	(— 52 —)
(9)	m (SH)	$= 0{,}648\ \mathrm{M} + 2{,}425 = \mathrm{M} - 0{,}352\ (\mathrm{M} - 6{,}882)$	(— 39 —)

Questi risultati sono abbastanza confrontabili con quelli analoghi che Båth ha trovato in un suo recente lavoro per Uppsala e Kiruna :

(5′)	m (PH)	$= \mathrm{M} - 0{,}46\ (\mathrm{M} - 6{,}4)$	(Uppsala)
	m (PH)	$= \mathrm{M} - 0{,}50\ (\mathrm{M} - 6{,}5)$	(Kiruna)
(6′)	m (PZ)	$= \mathrm{M} - 0{,}45\ (\mathrm{M} - 6{,}3)$	(Uppsala)
	m (PZ)	$= \mathrm{M} - 0{,}59\ (\mathrm{M} - 6{,}2)$	(Kiruna)
(9′)	m (SH)	$= \mathrm{M} - 0{,}23\ (\mathrm{M} - 5{,}6)$	(Uppsala)
	m (SH)	$= \mathrm{M} - 0{,}30\ (\mathrm{M} - 6{,}1)$	(Kiruna)

Conglobando inoltre i risultati parziali (5) (6) (7) (8) e (9) in un unico risultato generale, abbiamo ottenuto la formula seguente, confrontabile con la (2) di Gutenberg e Richter

(10) $$m = 0{,}474\ \mathrm{M} + 3{,}590 = \mathrm{M} - 0{,}526\ (\mathrm{M} - 6{,}822)$$

Messe in grafico le due equazioni (2) e (10) (v. *fig.* 1) si vede che

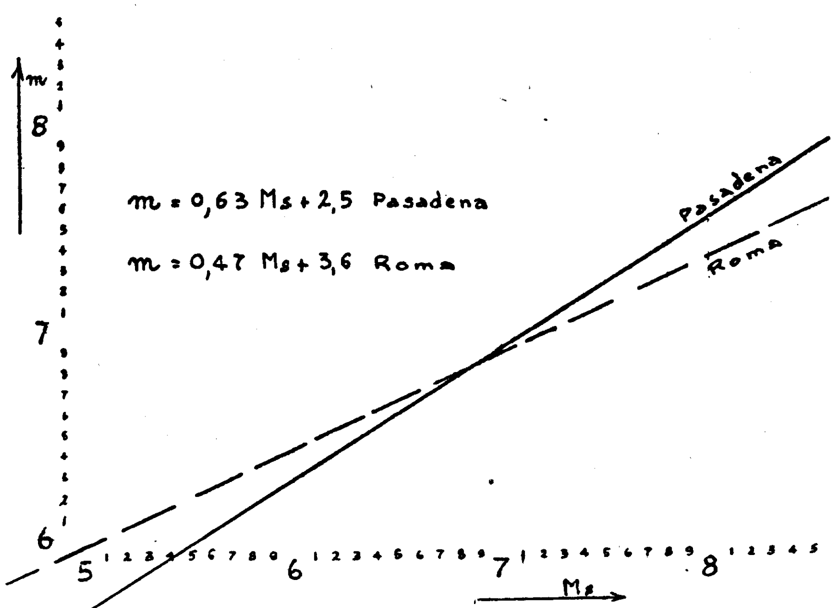

FIG. 1.

esse coincidono praticamente in un intorno di M = 7 differenziandosi, a destra e a sinistra di tale intorno, per valori simmetricamente opposti.

Della (10) ci siamo valsi per determinare, di ciascun terremoto, la « *magnitudo unificata* » (a meno della correzione di stazione), mediando i valori calcolati direttamente dalle onde spaziali (facendo uso delle (3), con quello calcolato applicando la (10).

Il fattore di correzione ε per la stazione di Roma.

I risultati sin qui conseguiti sono ancora, come s'é detto, incompleti : é necessario renderli confrontabili con i rilievi delle altre stazioni sismiche per ottenere una uniformità di valutazione.

Come termine di confronto per la ricerca del fattore correttivo ε (che nella (3) di Gutenberg e Richter é indicato con s) abbiamo ritenuto opportuno, per ovvie ragioni, scegliere le magnitudo date da Pasadena.

La ricerca é stata molto laboriosa : numerosi tentativi sono andati falliti prima di giungere a quello che riteniamo il più soddisfacente anche perché ci sembra piuttosto ragionevole.

E' ragionevole infatti supporre che le ampiezze delle onde ed i periodi relativi possano essere influenzati dai particolari tragitti sismici, per cui riteniamo di poter accettare la possibilità di una distribuzione azimutale degli scarti $\varepsilon = M_{\text{Pasadena}} - m_{\text{unificata Roma}}$.

Questa supposizione, suffragata dai risultati sperimentali, porterebbe ad assegnare ad ε i valori come nella *fig.* 2.

Con centro Roma, proiettata la superficie terrestre in proiezione stereografica e tracciata la raggiera degli azimut in ottanti (con α che va da 1 à 16) si é trovato che per i terremoti con epicentro compreso nel settore E-NNE (comprendente perciò le zone delle isole Curili, il Giappone, le Marianne, le Filippine, le Nuove Ebridi, le Salomone e una larga fascia continentale asiatica) vale la relazione

$$M = m_{\text{unif. Roma}} + 0{,}10.$$

Per i terremoti provenienti dal settore NN-E — NNW (comprendente la zona fortemente sismica delle Aleutine) la correzione è nulla

$$M = m_{\text{unif. Roma}} + 0{,}00$$

e per quelli con epicentro compreso nel settore NNW-W (America centrale e buona parte del'America settentrionale) si ha invece

$$M = m_{\text{unif. Roma}} + 0{,}30.$$

Per i terremoti provenienti dalla zona al di sotto della linea E-W non si può dire per il momento nulla di preciso poiché disponiamo di pochi elementi : scarsi sono infatti i sismi a fuoco normale con

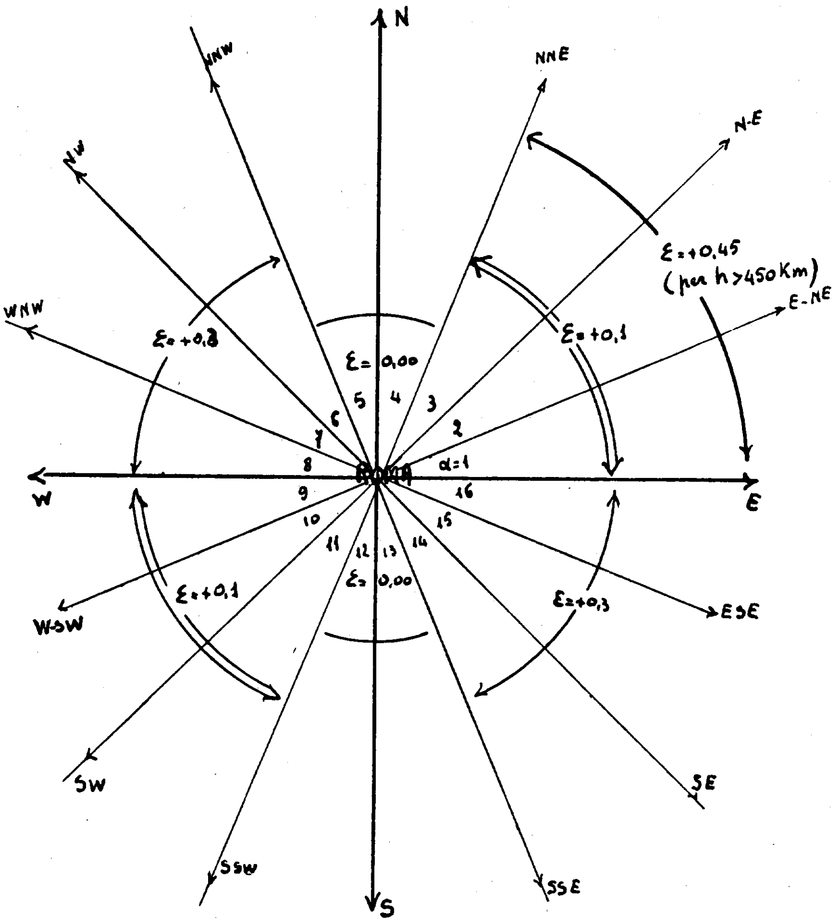

Fig. 2.

quella provenienza; è notorio che prevalgono ivi i telesismi con profondità notevoli, per cui torneremo sull'argomento nella II parte del nostro lavoro.

Naturalmente i risultati esposti non vogliono imporsi come definitivi : essi rappresentano solo un tentativo suscettibile di critica. Successive ricerche potranno confermarli, o modificarli, o addirittura annullarli.

Applicazione dei risultati.

Allo scopo di poter dimostrare l'attendibilità dei risultati conseguiti, abbiamo effettuato i calcoli su una nuova serie di terremoti, ed abbiamo scelto a questo scopo il primo quadrimestre 1957.

Nella Tabella 2 sono esposti i valori delle magnitudo unificate di Roma (complete del termine correttivo) e messi a confronto con le relative magnitudo calcolate a Pasadena. (Se per qualche terremoto manca la determinazione di Pasadena, vi si é sostituita quella di qualche altra stazione indicata.)

I nostri calcoli vanno fino alla IV cifra decimale, ma ne riportiamo solo le prime due.

Naturalmente il fattore correttivo é stato apportato con il criterio precedentemente esposto, conoscendosi per ogni terremoto la posizione epicentrale.

Notiamo a questo punto, per confutare qualche possibile obiezione che, poiché la magnitudo di un terremoto non é di carattere così assolutamente urgente da giustificarne l'immediata valutazione (a meno che non si tratti di scosse molto vicine o particolarmente intense, per le quali possono subentrare altre considerazioni), é sempre possibile conoscere l'epicentro al momento dei calcoli, si da poter attribuire a ciascuna scossa l'ε che le compete (ammesso che le cose vadano come abbiamo detto).

II Parte.

La magnitudo dei terremoti profondi nella stazione di Roma.

La trattazione precedente, come abbiamo detto, si riferisce ai soli terremoti superficiali, attribuendo loro una profondità media normale di 25 km. dove non era esplicitato altro valore, ed includendo fino ad un massimo di 50 km. di profondità.

Qui ci proponiamo invece l'esame dei terremoti profondi, e per averne una gamma estesa che ne abbracci tutte le possibili profondità, ne abbiamo scelti 64 tra le registrazioni degli anni 1938-39-40-41-1946-48-49-1950-51 con h variabili tra i 60 e i 660 km.

Fatto la spoglio e i rilievi (dove era possibile) delle ampiezze e dei periodi delle P, PP, S ed M, abbiamo calcolato anche qui le magnitudo relative, servendoci per le onde spaziali delle formule (3) (limitatamente ai primi due termini) e servendoci altresì, per le Q, delle relative curve di Gutenberg e Richter, e, per le onde superficiali ancora della nostra formula (4).

Chiariamo a questo punto che le onde superficiali, in quanto verremo ora esponendo, non sono tenute in considerazione. Trattandosi di terremoti profondi esse perdono l'importanza fondamentale che invece hanno nei terremoti a profondità normale. Tuttavia le riprenderemo in esame più tardi.

Nella Tabella 3 è riportato l'elenco dei 64 terremoti disposti in ordine di profondità, e con i dati dei rilievi.

I valori delle singole magnitudo calcolate per le sole onde spaziali, sono stati mediati per ciascun terremoto. Il confronto di questi valori con quelli dati da Pasadena ci ha permesso il calcolo della *correzione di stazione* ε. E' interessante notare che tale correzione è ancora quella relativa ai terremoti superficiali, per lo meno fino ad una profondità di 450 km. Pare che a questo punto, come noteremo tra breve, tale correzione debba subire una modifica.

Diciamo intanto che, poiché molti dei terremoti profondi si trovano nella America meridionale e nell'Oceano Pacifico, questa volta gli epicentri si distribuiscono intorno a Roma in tutte le direzioni.

Sulla correzione di stazione si nota ancora una sorprendente simmetria riguardo alla distribuzione azimutale : sembra infatti che i valori di tale correzione possano ritenersi distribuiti come in figura, uguali per settori opposti ugualmente orientati lungo una stessa direzione.

Questo vale, come s'è detto, per *tutti i terremoti fino ad una profondità ipocentrale di 450 km.* (Applicate inaftti queste correzioni ai pochi terremoti superficiali che si trovano a Sud della linea EW di Roma, se ne riscontra l'attendibilità.)

Invece, per profondità superiori ai 450 km. il valore di ε relativo ai soli terremoti provenienti dal settore NNE-E va mutato in

$$\varepsilon = + 0{,}45$$

fermi restando invece gli ε relativi alle altre provenienze.

Discussione dei risultati ottenuti.

Dall'esame della Tabella 3 risulta il buon accordo dei risultati trovati a Roma con quelli dati da Pasadena.

Non di tutti i terremoti è stato possibile il prelievo completo dei dati, ed è da prevedere l'eventualità di poter disporre soltanto di una parte delle onde, o anche addirittura di un unico tipo.

Meglio, potendolo fare, mediare su tutti i rilievi : buoni anche i risultati ottenuti con l'uso delle sole P (nel 60 % dei casi questi valori coincidono o al più differiscono di 0,1). Meno buoni, ma ancora attendibili, i risultati ottenuti con l'uso delle sole S (nel 41 % dei casi si hanno buoni risultati). Ci sembra invece sconsigliabile l'uso della sole PP, poiché i risultati che se ne traggono sono discontinui : mentre talvolta coincidono addirittura con le magnitudo di Pasadena, talaltra se ne differenziano anche di molto, passando senza regolarità da valori molto più alti a valori molto più bassi. Questa discontinuità potrebbe forse esser dovuta al fatto che per certe distanze le dromocrone delle PP coincidono con quelle delle SKP e quindi si rischia di prendere l'una per l'altra e i due tipi di onde hanno evidentemente caratteristiche diverse.

Concludendo questa discussione suggeriamo la preferenza netta alle onde P, anche per il fatto che, essendo le prime a comparire sul sismogramma non si rischia di vederne periodo e ampiezze alterate da altre onde.

Tentativi per ottenere une curva di correzione facendo unso delle onde superficiali.

Poiché le onde superficiali diminuiscono di ampiezza via via che l'ipocentro di un terremoto scende a profondità sempre maggiori, é evidente che non ci si può servire di esse per calcolare la magnitudo dei terremoti profondi, poiché i risultati sarebbero ovviamente inferiori alla realtà.

Tuttavia abbiamo voluto fare un tentativo per vedere se, con opportune correzioni, si possa egualmente giungere a risultati soddisfacenti. La cosa sarebbe auspicabile, giacché il rilievo di onde superficiali di 20 sec. di periodo essendo più facile e più sicuro renderebbe più sollecita la determinazione della magnitudo.

Diciamo subito che il risultato cui siamo pervenuti è soltanto un tentativo.

Calcolate con la (4) le magnitudo di tutti i terremoti profondi che abbiamo prese in esame e confrontate con le magnitudo dedotte con le onde spaziali, abbiamo riportato in grafico i risultati ottenuti. Ponendo in ascisse le profondità ipocentrali e in ordinate gli scarti m — M (m = media delle magnitudo calcolate con le onde spaziali ed M = magn. calcolata con le superficiali), abbiamo tentato di raccordare i punti tracciando il grafico della fig. 3. Da questo risulterebbe che mentre le correzioni aumentano abbastanza rapidamente da 0,1 à 0,7 fino a circa 200 km. di profondità, invece poi nell'intervallo $250 < h < 450$ km. si mantengono costantemente vicine al valore 0,8 per riaumentare poi quando h supera i 450 km.

Se questo tentativo troverà conferma sperimentale, si potrà in seguito calcolare l'equazione della curva.

Riassunto

Per adeguarci agli sviluppi più recenti del concetto di Magnitudo dei terremoti, abbiamo effettuato un aggiornamento sui rilievi fatti per il passato.

Com'è noto, la magnitudo dei sismi veniva data tramite formule che tenevano conto delle ampiezze delle onde superficiali orizzon-

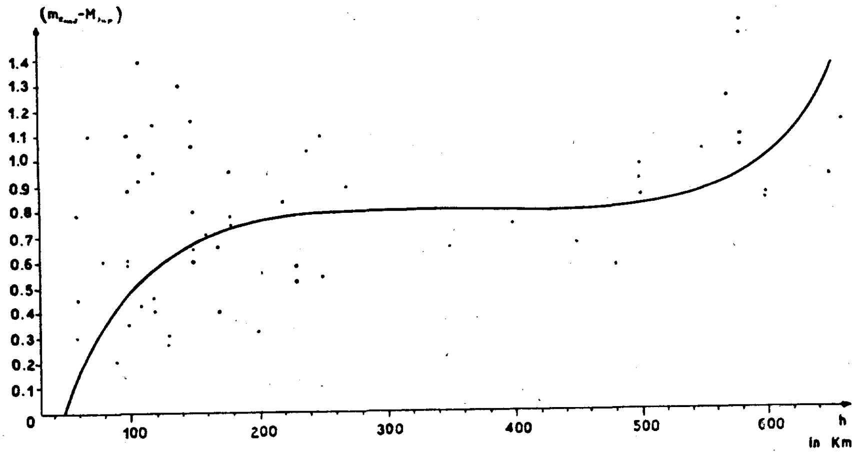

Fig. 3.

tali (limitatamente ad un periodo oscillante in un piccolo intorno di 20 sec.). C'è inoltre, com'è ovvio, una stretta dipendenza con la distanza epicentrale. Alcuni termini numerici, caratteristici delle singole stazioni, differenziano le formule tra loro.

Successivamente Gutenberg ha stabilito delle relazioni che tengono conto anche delle onde P,PP ed S le quali entrano nelle formule con i loro periodi e le loro ampiezze.

Una equazione lineare consente il passaggio dalla magnitudo calcolata con le onde superficiali a quella calcolata con le onde spaziali : questa equazione è per Pasadena

$$m_B + 0.63\ M_S + 2.5 = M_S - 0.37\ (M_S - 6.76).$$

Dai rilievi diretti delle onde spaziali, la m_B è calcolata con la formula

$$m = \log u/T + Q + s \quad \text{(orizzontale) oppure}$$
$$m = \log w/T + Q + s \quad \text{(verticale).}$$

Per poter giungere anche noi ad una relazione tra la magnitudo calcolata con le onde superficiali e quella calcolata con le spaziali, abbiamo effettuato lo spoglio di due anni di registrazioni. Rilevate, dove era possibile (e limitamente ai terremoti a profondità normale) le ampiezze e i periodi delle P (oriz. e vertic.) delle PP (orizz. e vertic.) delle S (orizzontali) e delle M (con T = 20 sec. circa), abbiamo calcolato per ogni terremoto le 6 magnitudo (M(PH), M(PZ), M(PPH), M(PPZ), M (SH)ed $M_{sup.}$) servendoci per le onde spaziali delle formule di Gutenberg e Richter e adoperando per le Q le loro stesse tabelle, omettendo la costante di stazione che fa parte di un calcolo a parte. Calcolate separamente (con il metodo dei minimi quadrati) le formule che legano le varie M (spaziali) con la M superficiale, si trovano dei coefficienti confrontabili con quelli che Båth ha trovato in un suo recente lavoro. Conglobando inoltre i risultati parziali in un risultato generale abbiamo ottenuto la formula seguente (controntabile con l'analoga di Gutenberg e Richter) :

$$m = 0.474\ M_s + 3.590 = M_s - 0.526\ (M_s - 6.822).$$

Messe in grafico le due equazioni (di Roma e Pasadena) si vede che esse coincidono praticamente in un intorno di $M_s = 7$ differenziandosi a destra e a sinistra per valori simmetricamente opposti..

Di questa equazione ci siamo valsi per determinare, di ciascun terremoto, la *magnitudo unificata,* mediando i valori calcolati direttamente dalle onde spaziali, con quello calcolato facendo uso delle onde superficiali di 20 sec. di periodo.

Un confronto tra le « magnitudo unificate » così ottenute e le corrispondenti magnitudo calcolate da Pasadena, permette la determinazione di un coefficiente per la stazione sismica di Roma, che consentirà, ci auguriamo, una uniformità di risultati almeno con l'America, poichè Pasadena è stata da noi assunta come punto di riferimento.

Vengono discussi i risultati conseguiti.

Allo scopo di dimostrare la bontà o meno delle formule e delle correzioni trovate, è stata poi calcolata la magnitudo di una serie di terremoti e messe a confronto con le analoghe valutazioni di Pasadena.

La II parte del lavoro è riserbata ad uno studio sui terremoti profondi. Per questi, esclusi dalla precedente trattazione, viene calcolata la magnitudo con le onde spaziali, facendo uso della formula di Gutenberg (priva del termine correttivo)

$$M = q + Q \qquad (q = \log u/T \text{ oppure } q = \log w/T).$$

Si è trovato che la correzione di stazione si mantiene ancora quella dei terremoti superficiali, salvo una variazione che si verifica per i telesismi a profondità superiori ai 450 km. e provenienti dal settore E-NNE.

Per i terremoti profondi inoltre, si è fatto un tentativo per la ricerca di una funzione che leghi la magnitudo calcolata con le onde spaziali con quella calcolata con le onde superficiali (di $T = 20$ sec. ca.)

Riportati in ascisse i valori delle profondità ipocentrali e in ordinate le differenze $m_{spaziali} - M_{superf.}$ si trova una curva che sembra presentare per un ampio intervallo della profondità ipoc. (250 < h < 450) la stessa correzione (+ 0.8 ca.) mentre al di sotto e al di sopra di tale intervallo gli scarti aumentano piuttosto rapidamente.

BIBLIOGRAFIA.

GUTENBERG (B.). (1945 *a*) « Amplitudes of Surfaces Waves and Magnitude of Shallow Earthquakes ». (Bull. Seismol. Soc. Amer., vol. 35, pp. 3-12).

(1945 *b*) Amplitudes of P,PP and S and Magnitude of Shallow Earthquakes. » (Bull. Seismol. Soc Amer., vol. 35, pp. 57-69).

(1945 *c*) « Magnitude Determination for Deep-focus Earthquakes ». (Bull. Seismol. Soc. Amer., vol. 35, pp. 117-130.)

GUTENBERG (B.) and C. F. RICHTER : 1942 « Earthquake Magnitude, Intensity, Energy and Acceleration ». (Bull. Seismol. Soc. Amer., vol. 32., p. 163-191)

1942 « Earthquake Magnitude, Intensity, Energy and Acceleration », 2e Paper. (Bull. Seismol. Soc. Amer.)

1956 « Magnitude and Energy of Earthquakes ». (Annali di Geofisica, vol. IX, n. 1.)

D. DI FILIPPO-L. MARCELLI : « La magnitudo dei terremoti e la sua determinazione nella stazione sismica di Roma ». (Annali di Geofisica, vol. II, n. 4 (1949).

BÅTH (Markus) : « The Problem of Earthquakes, Magnitude Determination ». (Travaux Scientifiques, fascicule 19, série A.)

TABELLA 1

N°	Data	Zona epicentrale	α	H (Tem. ori.)	Δ° da Roma	M_{PH}	M_{PZ}	M_{PPH}	M_{PPZ}	M_{SH}	Msup.	m unificata	M_{Pas}
1	23 febb. 1949	Turkestan	2	16h 08m	53.° 7	7.35	6.83	6.94	6.40	6.44	6.66	6.78	7.3
2	27 marzo —	Mar di Celebès	1	06 34	105. 8	—	6.82	7.13	7.15	—	7.14	7.02	7.0
3	13 apr. —	Tra Olimpia e Tacoma	6	19 56	82. 8	6.78	6.62	6.50	6.38	6.91	6.54	6.65	7.0
4	24 apr. —	Golfo Persico	16	04 22	38. 4	6.25	6.27	6.45	6.23	—	6.81	6.41	6 1/2 (Praga) 6 (Strasburgo)
5	9 magg. —	Sumatra	16	13 36	81	6.97	6.63	6.52	6.11	6.06	6.44	6.49	6 3/4
6	21 magg. —	Honshu (Giappone)	3	21 40	88. 9	6.55	6.67	6.80	6.62	6.32	6.61	6.61	6 1/2
7	25 magg. —	Turkestan	2	08 24	51. 1	6.48	6.25	6.33	6.08	6.45	6.06	6.35	—
8	24 giug. —	A.S.W. di Giava	16	22 39	90, 9	6.94	6.89	6.87	6.62	6.79	6.21	6.77	7
9	2 lugl. —	Marianne	2	19 57	108. 9	7.55	7.11	7.02	7.14	6.70	6.84	7.13	7.1
10	4 lugl. —	Golfo Persico	16	03 40	38	6.06	5.92	6.00	5.61	5.98	5.95	6.00	—
11	7 lugl. —	Nord Atlantico	8	04 32	37. 4	—	6.21	—	—	5.69	4.95	5 95	—
12	8 lugl. —	Oceano Artico	4-5	18 18	30. 3	—	5.83	—	—	5.36	5.15	5.74	—
13	11 lugl. —	Giappone	2	16 10	86. 4	6.55	6.38	6.63	6.31	6.45	6.01	6.46	—
14	23 agos. —	Isole Reg. Carlotta	5	20 24	80. 1	6.51	6.54	6.61	6.55	6.74	6 47	6.60	6 1/4
15	14 sett. —	Isole Celebes	1	19 50	106. 2	—	7.12	6.93	6.81	6.80	7.09	6.92	7.2
16	21 sett. —	Messico merid.	7-8	12 55	90. 6	7.32	6.74	—	—	6.91	6 29	6.89	—
17	27 sett. —	Alaska	5	15 30	77	6.71	6.47	6.52	6.46	6.78	6.19	6.58	7
18	4 ott. —	Alaska merid.	11	10 20	52. 2	7.25	7.05	6.64	6.54	6.99	6.45	6 85	6 1/4
19	7 ott. —	A S.-E. Madagascar	14	12 02	84. 8	7.19	7.16	7.24	7.05	6.55	6.48	6.97	6 3/4
20	31 ott. —	Alaska	5	01 39	79. 2	6.39	6.25	6.37	6.03	6.45	6.13	6.33	6 1/4
21	25 dicem. —	Giappone	2	23 17	87. 5	6.62	6.41	7.11	—	—	6.38	6.69	6
22	25 dicem. —	Giappone	2	23 25	87. 5	6.84	6.41	6.93	6.58	—	6.66	6.70	6 1/4 ±
23	27 dicem. —	Is. Sandwiches	12	23 57	105. 5	7.12	7.03	7.13	6.94	—	6.64	6 99	7.1
24	29 dicem. —	Filippine	2	03 04	91. 4	6.93	6.80	7.21	7.18	7.09	7.30	7 04	7.2
25	3 genn. 1950	Filippine	2	02 51	91. 4	6.87	6.46	—	6.73	6.64	6.62	6.68	6 1/2
26	17 genn. —	Cresta Mediana Atl.	10	10 58	52. 8	7.10	6.31	6.81	6.29	6.97	5.62	6.46	—
27	3 febb. —	Yunnan (Cina)	1	02 51	73. 8	6.54	6.21	6.97	6.44	6.66	6.66	6.59	6 1/2 ~
28	2 marzo —	Is. Sandwiches	11	18 39	106. 3	—	—	7.16	6.71	—	6.26	6.81	6.9
29	7 marzo —	Filippine	1	02 07	100. 4	6.93	6.58	7.02	6.96	—	6.86	6.87	6 3/4 ~
30	27 marzo —	Aleutine	4	13 04	83. 3	6.94	6.61	6.98	6.76	6.82	6.53	6 80	6 3/4
31	29 marzo —	Nuova Guinea	2	17 41	117	—	—	6.96	6.86	—	6.00	6.75	—
32	4 apr. —	Conf. Mongol.-U.R.S.S.	3	18 44	57. 2	6.87	6.29	6.83	—	—	6.47	6.66	6 3/4
33	26 aprile —	Honshu (Giappone)	3	07 04	86. 9	—	5.98	7.09	7.57	—	6.30	6.80	6 3/4

SEGUE TABELLA 1

N°	Data		Zona epicentrale	α	H (Tem. ori.)	Δ° da Roma	M_{PH}	M_{PZ}	M_{PPH}	M_{PPZ}	M_{SH}	Msup.	m unificata	M_{Pas}
34	9 magg.	1950	Turchia	1	11h 17m	34.° 2	6.30	6.41	6.46	6.32	6.10	5.84	6.32	—
35	19 magg.	—	Nuove Ebridi	2	02 38	151. 0	—	—	6.96	6.47	—	6.55	6.71	6 1/2-3/4
36	26 magg.	—	Nuove Ebridi	2	01 17	151. 0	—	—	7.12	6.58	—	7.21	6 90	7.2
37	31 magg.	—	Giappone.	2	13 13	87. 6	6.39	5.90	6.50	6.09	5.76	6.23	6.20	—
38	24 giug.	—	Nuove Ebridi	2	22 25	151. 5	—	—	7.20	6.77	—	7.03	6.97	7.2
39	25 giug.	—	Mindanao	1	11 05	105. 7	7.08	6.84	7.05	6.56	—	6.23	6.81	6.5 ±
40	27 giug.	—	Giappone	3	15 41	80. 6	6.47	6.21	6.43	5.95	6.20	6.56	6.33	6 1/2-3/4
41	3 lug.	—	Is. Caroline	2	10 03	111. 2	—	—	7.03	6.84	6.54	6.69	6.79	—
42	12 lug.	—	Is. Aleutine.	5	11 09	85. 5	6.78	6 53	5.98	5.42	6.15	5.75	6.19	6 1/4
43	7 agos.	—	Is. Filippine	1	02 44	103.05	6.96	6.97	6.93	6.89	—	6.43	6.88	6 3/4 ~
44	18 agos.	—	Cina-Burma-India	1	01 07	68. 0	6.61	6.34	6.71	6.05	6.61	6.34	6.49	7 ±
45	22 agos.	—	Kamtchatka	4	07 40	81. 5	6.57	6.25	—	—	5.88	5.56	6.23	—
46	23 agos.	—	Tibet merid.	1	03 09	65. 7	6.43	6.11	6.64	6.25	6.02	5.72	6.29	—
47	23 agos.	—	Cina-Burma-India	1	18 47	68. 0	6.62	6.40	—	—	6.13	5.79	6.37	—
48	31 agos.	—	Mindanao	1	07 05	102. 8	—	—	6.83	6.68	6.49	6.43	6.66	7
49	10 sett.	—	Giappone	3	03 21	89. 7	6.44	6.27	6.94	6.51	6.20	6.41	6.50	6 3/4
50	24 sett.	—	Zona de l'Iran	16	22 58	36. 0	6.68	6.32	6.45	5.83	5.77	5.25	6.19	—
51	30 sett.	—	Assam settentr.	1	07 28	65. 9	6.51	6.14	6.89	6.66	6.18	5.97	6.47	—
52	5 ottob.	—	America centr.	8	16 09	88. 4	7.24	7.24	7.29	7.24	7.19	7.75	7.24	7.7
53	8 ottob.	—	Celebes	1	03 23	111. 6	7.72?	7.56?	7.36	7.39	7.78	7.37	7.48	7.6
54	23 ottob.	—	Messico	8	16 13	90. 8	6.86	6.96	6.99	6.76	6.77	7.41	6.91	7.1
55	2 nov.	—	Arco della Sonda	1	15 27	114. 7	7.78?	7.48?	7.27	6.89	7.80?	7.22	7.37	7.5
56	5 nov.	—	Isole Riukyu	3	17 37	88. 2	6.54	6.18	6.74	6.74	6.84	7.04	6.66	6.9
57	8 nov.	—	Salomone	2	02 18	136. 3	—	—	7.04	6.61	—	7.12	6.87	7 1/4
58	14 dic.	—	Messico	7	14 15	92. 2	7.07	7.08	7.16	7.20	7.05	7.12	7.09	7.3

TABELLA 2

N°	Data		Zona epic.	h km.	α	H	Δ° da Roma	MPH	MPZ	MPPH	MP Z	MSH	Msup.	munif. + ε	MPas.
1	2 genn.	1957	Aleutine	—	4	00 39	85.23	6.79	6.56	—	—	6.71	6.23	6.65	6 1/2-3/4
2	2 genn.	1957	Aleutine	—	4	02 17	85.77	7.35	7.03	—	—	6.87	6.38	6.97	6 3/4
3	2 genn.	—	Aleutine	—	4	10 49	85.77	7.08	6.46	—	—	6.45	5.85	6.59	6 1/2
4	3 genn.	—	Manciuria	600	3	12 48	77.67	6.65	—	7.28	—	7.00	—	7.08	7
5	23 febb.	—	Formosa	—	2	20 26	87.57	7.23	6.72	7.19	6.86	6.57	6.72	6.99	7-7 1/4
6	2 marzo	—	Giamaica	(50)	8	00 27	78.21	6.66	5.99	6.44	6.14	6.54	6.15	6.68	6 3/4
7	5 marzo	—	Oc. Nord. Atlant.	—	8	12 24	38.03	6.20	5.84	—	—	6.29	5.34	6.40	6 1/2-3/4
8	9 marzo	—	Aleutine	—	4	20 39	85.86	7.04	7.05	6.97	6.92	7.04	7.13	7.00	6 3/4-7
9	10 marzo	—	Is. Andreanof	—	4	03 06	86.04	6.54	6.54	7.01	6.69	6.37	6.75	6.66	6 1/2-6 3/4
10	10 marzo	—	Is. Andreanof	—	4	15 26	86.22	6.48	6.39	—	—	6.36	6.55	6.48	6 1/2 (Strasb.)
11	12 marzo	—	Is. Andreanof	—	4	11 45	86.85	7.20	6.37	7.25	6.83	6.77	7.12	6.90	7-7 1/4
12	13 marzo	—	Is. Andreanof	—	4	15 42	86.40	6.66	6.53	6.99	6.71	6.45	6.73	6.69	6 3/4
13	14 marzo	—	Is. Andreanof	—	4	14 48	86.40	6.96	6.78	7.43	7.02	—	6.90	7.01	7 1/2
14	15 marzo	—	Is. Fox	—	5	02 52	85.28	7.14	6.87	—	—	6.45	6.35	6.76	6 3/4
15	16 marzo	—	Is. Andreanof	—	4	02 34	85.77	6.92	6.81	6.91	7.12	6.95	7.34	6.96	6 3/4
16	17 marzo	—	Is. Andreanof	—	5	22 45	84.42	6.83	6.73	6.93	6.37	—	6.39	6.70	6.5
17	29 marzo	—	Is. Fox	—	5	05 10	85.14	6.89	6.94	6.74	6.49	6.71	6.96	6.78	6 3/4-7
18	29 marzo	—	Is. Aleutine	—	4	22 50	85.41	6.68	6.49	6.50	6.21	6.26	5.78	6.42	6-6 1/4
19	2 apr.	—	Is. Andreanof	—	4	00 39	87.12	6.77	6.59	—	—	5.98	5.59	6.39	6.3 (Uppsala)
20	2 apr.	—	Is. Andreanof	—	4	21 28	87.12	6.61	6.33	—	6.32	6.29	5.69	6.37	6.3 (Uppsala)
21	8 apr.	—	Panama-Costa Rica	—	8	20 18	88.47	6.87	6.51	7.00	6.32	6.18	5.76	6.83	6 1/2
22	9 apr.	—	Honshu (Giapp.)	450	3	00 24	92.25	6.60	6.08	6.75	6.37	6.06	5.77	6.82	6 3/4
23	14 apr.	—	Tibet merid.	(50)	1	07 11	57.33	6.93	6.36	6.42	6.20	6.25	6.76	6.59	6 1/4
24	14 apr.	—	Samoa	—	4	19 18	153.36	—	—	7.19	6.72	—	7.55	7.03	7.5
25	15 apr.	—	Is. Fox	(75)	5	21 33	85.50	6.79	6.48	—	6.70	6.53	5.75	6.63	6.4 (Uppsala)
26	16 apr.	—	Mar di Giava	600	1-16	04 04	96.03	7.20	7.05	7.29	6.88	—	6.07	7.30	7 1/2 ±
27	19 apr.	—	Is. Fox	—	4	15 45	86.76	6.58	6.35	—	—	6.30	5.63	6.37	6.7 (Uppsala)
28	19 apr.	—	Is. Fox	—	5	22 19	86.40	7.60	7.43	—	—	7.29	6.39	7.23	7-7 1/4
29	21 apr.	—	Venezue la-Columbia	—	8	21 12	81.00	6.73	6.38	—	—	6.67	6.65	6.93	6 1/2-6 3/4
30	29 apr.	—	Mindanao	—	1-2	01 23	105.12	—	—	6.88	6.81	6.56	6.17	6.60	5 3/4-6

N°	Data	Zona epic.	h (km.)	α	H (origine)	Δ° (da Roma)	M_{PH}	M_{PZ}	M_{PPH}	M_{PPZ}	M_{SH}
1	29 sett. 1950	Largo coste Messico	60	7	06h 32m~	97.83	6.65	6.59	6.80	6.91	6.51
2	1 dic. —	Oc. Atlantico	60	9	14 50	56.34	7.36	6.84	6.56	6.43	7.04
3	8 giug. —	Oc. Atlantico	60	12	16 07	92.10	7.53	7.13	6.99	6.55	7.11
4	29 luglio —	Molucca	70	1	16 45	107.1	—	7.14	7.04	6.66	6.73
5	29 luglio —	Salomone	70	2	23 49	131.2	—	—	6.37	6.02	—
6	10 dic. —	Sud America	80	9	02 50	98.10	6.99	6.80	6.99	6.77	—
7	25 magg. —	Is. Caroline	90	2	18 35	108.5	—	7.02	6.95	6.60	6.90
8	10 sett. —	Nuove Ebridi	100	2	15 16	145.53	—	—	7.10	6.80	—
9	3 magg. 1949	Is. Curili	100	3	15 57	83.3	7.07	6.67	—	—	6.07
10	22 dic. —	Messico	100	8	09 30	90.5	—	6.25	7.17	6.77	6.14
11	30 magg. —	Cile sett.	100	9	01 33	97.2	—	6.68	6.95	6.53	6.71
12	9 dic. 1950	Argentina sett.	100	10	21 39	99.0	7.21	7.14	—	—	7.25
13	23 genn. 1949	Sumatra	100	16	06 31	90.0	—	6.60	7.15	6.96	6.41
14	1 dic. 1950	Solomone	110	2	16 28	129.33	—	—	6.69	6.73	—
15	25 apr. 1949	Cile sett.	110	9	13 55	97.2	—	6.69	7.03	6.98	7.29
16	7 agos. 1940	Coste del Cile	110	9	02 56	99.0	—	—	6.59	6.41	—
17	7 giug. 1950	Sud America	110	9	16 52	92.3	7.18	6.82	—	—	6.68
18	7 ott. 1938	Arco Sonda	120	1	16 24	77.4	—	—	6.76	—	5.62
19	8 magg. 1949	Cile sett.	120	10	21 25	98.1	—	—	7.02	6.45	6.44
20	30 april. —	Mindanao	130	1	01 23	103.2	7.01	7.04	7.12	7.31	6.99
21	1 agos. 1939	Giappone	140	3-4	15 56	79.2	6.50	6.67	7.53	6.65	6.09
22	24 genn. 1950	Nuove Ebridi	150	2	16 47	144.45	—	—	7.07	6.61	—
23	21 magg. 1951	Is. Solomone	150	2	08 27	131.4	—	—	6.36	6.07	—
24	26 sett. 1940	Nuove Ebridi	150	3	03 56	133.2	—	—	6.66	5.95	—
25	24 agos. 1951	Curili	150	3	14 21	83.7	6.51	6.31	6.66	6.35	6.49
26	23 lugl. 1949	Nuove Ebridi	150	2-3	10 27	149.4	—	—	7.51	6.93	—
27	4 marzo 1951	Perù merid.	150	9	11 17	98.1	6.92	6.59	6.55	6.27	6.51
28	3 nov. 1949	Curili	160	3	01 12	83.7	6.78	6.64	6.77	6.46	6.75
29	5 marzo 1951	Is. Riukyu	170	2	20 12	88.0	7.05	6.60	6.71	6.25	6.11
30	27 genn. 1941	Birmania	180	1	02 30	63.9	6.53	—	6.76	—	6.05
31	21 nov. 1948	Is. Reg. Carlotta	180	2-3	19 10	143.2	—	—	7.15	6.60	—
32	12 agos. 1939	Nuove Ebridi	180	2-3	02 07	145.8	—	—	7.24	6.88	—
33	20 febb. 1940	Nuove Ebridi	200±	2-3	02 18	144	—	—	7.35	6.98	—
34	12 febb. 1940	Is. Tonga	200	3	08 21	158.4	—	—	6.77	6.52	—
35	21 nov. 1939	Hindu Kush	220	1	11 02	59.9	7.08	6.78	7.36	7.05	7.03
36	4 mar. 1949	Afghanistan	230	1	10 19	44.4	7.39	7.22	—	—	7.19
37	22 dic. 1940	Sud America	230	9	18 59	90	6.78	6.20	6.72	6.48	6.61
38	27 magg. —	Hindu Kush	240	1	04 10	46.0	5.96	5.67	6.32	5.81	—
39	21 sett. —	Hindu Kush	250	1	13 40	44.5	6.06	5.70	6.53	6.26	6.51
40	10 dic. 1950	Isole Tonga	250	3	13 23	163.2	—	—	7.19	7.17	—
41	14 april. 1951	Argentina Sett.	250	10	00 45	97.2	—	—	6.79	6.37	—
42	3 april. 1941	Sud America	260	10	15 21	99.0	7.12	6.83	6.79	6.56	—
43	3 april. —	Sud America	260	10	14 55	98.1	6.83	6.19	6.39	6.07	—
44	31 genn. —	Isole Timor	270	1	02 38	111.4	—	—	7.00	6.57	—
45	23 mar. 1951	Isole Kermadec	270	2-3	21 39	166.5	—	—	6.65	6.30	—
46	28 febb. 1950	Giappone	340	3	10 21	81.9	7.55	7.38	7.41	7.13	6.64
47	21 magg. 1940	Isole Tonga	350	3	18 40	156.6	—	—	6.63	6.12	—
48	20 april. —	Giappone	400	2	20 18	83.7	6.23	5.88	6.38	6.15	—
49	22 sett. 1950	Isole Figi	450	3	23 53	155.7	—	—	7.06	6.66	—
50	11 lugl. 1951	Isole Bonin	480	2	18 22	94.2	6.74	6.35	6.40	6.20	—
51	13 lugl. 1950	Isole Bonin	500	2-3	04 04	95.0	6.51	6.12	6.62	6.34	5.80
52	1 agos. 1940	Isole Tonga	500	3	12 39	157.5	—	—	6.47	5.81	—
53	7 nov. 1940	Isole Marianne	500	2-3	13 58	90.0	—	6.04	—	6.57	5.94
54	12 genn. 1950	Isole Fiji	550	3	12 00	154.4	—	—	6.78	6.41	—
55	18 giug. 1940	Isole Filippine	570	1	13 52	100.3	—	—	6.64	6.41	—
56	10 lugl. —	Manciuria	580	3	05 50	77.9	6.61	6.14	7.84	7.13	6.75
57	11 genn. 1946	Manciuria	580	3	01 33	64.8	6.93	6.68	7.39	7.13	6.85
58	5 april. 1949	Wladiwostok	580	3	09 27	78.3	5.98	5.74	6.65	6.82	6.37
59	17 magg. 1950	Corea	580	3	11 47	81.9	6.44	6.21	—	—	6.55
60	26 sett. 1946	Isole Tonga	600	3	10 53	153.0	—	—	6.65	6.06	—
61	30 magg. 1950	Isole Tonga	600	3	15 04	156.6	—	—	6.50	5.97	—
62	2 dic. —	Brasile W	650	9	15 20	90.9	6.54	6.03	6.62	6.19	6.60
63	9 lugl. —	Brasile	650	9	04 40	90.5	6.95	6.61	7.13	6.55	7.02
64	14 agos. —	Argentina	660	10	22 51	98.1	7.38	7.10	7.34	6.86	—

m(médiato) + ε	M Pasad.	M superf.	m Roma	$\delta =$ Mpas — m (Roma)	$\delta_P =$ $M_{Pas} - \overline{M}_P$	$\delta_{PP} =$ $M_{Pas} - \overline{M}_{PP}$	$\delta_S =$ $M_{Pas} - M_S$	m Roma — M sup.
6.69 + ε	7	6.53	7.0	+0.008	+0.082	—0.155	+0.185	+0.461
6.83 + ε	7 1/4	6.64	6.9	+0.323	+0.052	+0.651	+0.211	+0.288
7.06 + ε	7.1	6.29	7.1	+0.038	—0.230	+0.322	—0.014	+0.773
6.90 + ε	7	5.88	7.0	+0.005	—0.245	+0.047	+0.172	+1.111
6.20 + ε	7.1	6.55	6.3	+0.802	—	+0.802	—	?
6.89 + ε	7.0	6.38	7.0	+0.014	+0.003	+0.021	—	+0.611
6.87 + ε	7.0	6.79	7.0	+0.034	—0.118	+0.126	0.000	+0.206
6.95 + ε	7.0	6.69	7.5	+0.053	—	+0.053	—	+0.353
6.60 + ε	7 ~	5.82	6.7	+0.296	+0.030	—	+0.826	+0.886
6.58 + ε	6 1/2	6.26	6.9	—0.382	—0.053	—0.769	—0.064	+0.620
6.72 + ε	7	5.65	6.8	+0.182	+0.216	+0.162	+0.185	+1.164
7.20 + ε	8	7.63	7.3	+0.702	+0.727	—	+0.654	?
6.78 + ε	7-7 1/4	6.47	7.1	+0.047	+0.101	—0.229	+0.419	+0.610
6.71 + ε	7.2	6.86	6.8	+0.391	—	+0.391	—	?
7.00 + ε	7.3	6.66	7.1	+0.203	+0.506	+0.199	—0,694	+0.435
6.50 + ε	6 1/4	5.56	6.6	—0.351	—	—0.351	—	+1.040
6.90 + ε	6.8	5.60	7.0	—0.197	—0.303	—	+0.015	+1.400
6.19 + ε	6 1/4	5.84	6.3	—0.041	—	—0.609	+0.527	+0.451
6.63 + ε	6 3/4 ~	5.58	6.7	+0.014	—	—0.084	+0.209	+1.161
7.09 + ε	7.4	6.92	7.2	+0.206	+0.271	+0.086	+0.315	+0.270
6.49 + ε	6 1/2	5.31	6.6	—0.088	—0.182	—0.192	+0.306	+1.278
6.84 + ε	6.4	6.29	6.9	—0.539	—	—0.539	—	+0.649
6.22 + ε	7.0	6.37	6.3	+0.683	—	+0.683	—	?
6.31 + ε	6 3/4	6.42	6.4	+0.345	—	+0.345	—	?
6.46 + ε	6 1/2	5.49	6.6	—0.064	—0.012	—0.103	—0.091	+1.074
7.22 + ε	7.2	6.15	7.3	—0.121	—	—0.121	—	+1.171
6.57 + ε	6 3/4-7	5.87	6.7	+0.204	+0.018	+0.362	+0.260	+0.802
6.68 + ε	6.8	6.04	6.8	+0.020	—0.011	+0.089	—0.054	+0.741
6.55 + ε	6.9	6.24	6.6	+0.255	—0.023	+0.317	+0.687	+0.663
6.45 + ε	6 1/2	5.76	6.5	—0.046	—0.129	—0.357	+0.348	+0.786
6.87 + ε	6.8	6.22	7.0	—0.172	—	—0.172	—	+0.752
7.06 + ε	7.2	6.20	7.2	+0.039	—	+0.039	—	+0.961
7.16 + ε	7.0	6.94	7.3	—0.261	—	—0.261	—	+0.320
6.65 + ε	6 3/4	6.51	6.7	+0.005	—	+0.005	—	+0.555
7.06 + ε	6.9	6.32	7.2	—0.261	—0.130	—0.405	—0.234	+0.841
7.27 + ε	7.5	6.85	7.4	+0.131	+0.092	—	+0.211	+0.517
6.56 + ε	7.1	6.07	6.7	+0.343	+0.511	+0.401	+0.393	+0.587
5.94 + ε	6 1/4	5.00	6.0	+0.212	+0.332	+0.085	—	+1.042
6.21 + ε	6 1/4	5.21	6.3	—0.062	+0.270	—0.243	—0.361	+1.102
7.18 + ε	7 1/4	7.37	7.3	—0.030	—	—0.030	—	—0.090?
6.58 + ε	7	6.13	6.7	+0.323	—	+0.323	—	+0.547
6.82 + ε	7.2	6.89	6.9	+0.277	+0.124	+0.429	—	+0.033
6.37 + ε	6 1/2	6.75	6.5	+0.031	—0.110	+0.173	—	—0.281?
6.79 + ε	6 3/4	6.00	6.9	—0.136	—	—0.136	—	+0.886
6.48 + ε	7.0	6.61	6.6?	+0.425	—	+0.425	—	—0.035?
7.22 + ε	7.8	7.32	7.3	+0.477	+0.730	+0.430	+1.065	+0.005
6.37 + ε	6 1/2	5.83	6.5	+0.025	—	+0.025	—	+0.645
6.16 + ε	6	5.52	6.3	—0.260	—0.153	—0.366	—	+0.740
6.86 + ε	7	6.28	7.0	+0.045	—	+0.045	—	+0.675
6.42 + ε	7	6.29	6.9	+0.129	+0.007	+0.251	—	+0,576
6.28 + ε	6 3/4-7	5.75	6.7	+0.145	+0.109	—0.059	+0.624	+0.985
6.14 + ε	6 3/4	5.67	6.6	+0.160	—	+0.160	—	+0.920
6.18 + ε	6 3/4	5.77	6.7	+0.116	+0.260	—0.269	+0.358	+0.864
6.59 + ε	6.8	6.0	7.0	—0.245	—	—0.245	—	+1.045
6.53 + ε	6 1/2	5.72	7.0	—0.479	—	—0.479	—	+1.259
6.89 + ε	7.3	5.84	7.3	—0.043	+0.479	—0.637	+0.105	+1.503
7.00 + ε	7.2	6.38	7.4	—0.247	—0.054	—0.512	—0.095	+1.067
6.31 + ε	6.7	5.65	6.8	—0.064	+0.388	—0.486	—0.121	+1.115
6.40 + ε	6.7	5.29	6.8	—0.148	—0.074	—	—0.295	+1.555
6.36 + ε	7±	5.95	6.8	+0.191	—	+0.191	—	+0.859
6.23 + ε	6 1/4	5.83	6.7	—0.434	—	—0.434	—	+0.850
6.39 + ε	6 3/4	—	6.5	+0.255	+0.365	+0.246	+0.050	—
6.85 + ε	7	6.02	7.0	+0.048	+0.121	+0.061	—0.124	+0.935
7.17 + ε	7 1/4	6.13	7.3	—0.019	—0.086	+0.049	—	+1.139

CORRELATION BETWEEN MAGNITUDE AND INTENSITY OF EARTHQUAKES; ASTHENOSPHERE

by N. V. SHEBALIN.

The problem of low velocity layers in upper parts of the Earth is much discussed at present (1-3). A method of observations may be proposed, the existence of sudden decreasing of seismic velocity at some discontinuity being directly shown. Indeed, the influence of such a change of velocity for the seismic rays emissing vertically upwards is not significant. That is why the foci lying nearly under and over the above-mentioned boundary and having equal energy must be feeling at the surface with equal intensity. At the same time this boundary must exert an essential influence to the rays emissing in various lateral directions. Surface waves, f. i. Love-waves, may be considered as the result of interference of such « lateral » rays, and therefore the surface waves' amplitudes will hardly depend on the location of foci as regards to this discontinuity.

Thus the existence of low velocity layer may be proved by comparing intensity of earthquakes with its magnitude for various focal depths.

For testing these speculations a study of correlation between the epicentral intensity of earthquakes and its magnitude in dependence on the focal depth was undertaken.

Magnitude M of all the earthquakes was determined by the surface waves method (4,5). The initial data were taken from records of some Russian seismic stations and different bulletins. In determining M of deep-focus earthquakes, the observed amplitudes of irregular surface waves characteristic of deep-focus earthquakes were used. No corrections for focal depth were applied. The usual error in determination M was ± 0.3-0.4.

The focal depth h was taken from summary bulletins (6-8) or determined by the phases pP and sS. The focal depths less than 80-100 km (within the Earth's crust) were determined by the phase sP (Kondorskaya's method 9). The error of focal depth changed from ± 20-30 km for the deepest foci to ± 3-5 km for the shallowest ones.

The data on intensity I were taken from numerous publications, bulletins, catalogues etc. The error might be ± 1/2 grade (for well-studied earthquakes) or ± 1 grade (for other ones).

Data on magnitude M, intensity I and focal depth h were obtained for 225 earthquakes with the focal depths from 3-5 to 640 km, magnitude from 3.3 to 8.3 and intensity from 3 to 11-12 grades.

A study for the depths down to 60-80 km (10) ascertained no peculiarities in respect of velocity's lowering, perhaps because of insufficient accuracy of method being applied.

The equation linking intensity and magnitude for depths down to 60-80 km has been got :

$$I = \beta M - k\, lgh + c,$$

$$\beta = 1.52 \pm 0.10;\ k = 3.5 \pm 0.3;\ c = 3.0 \pm 0.3$$

It is easy to show that k in this equation is a coefficient in the wellknown Blake's formula (11)

$$I_2 - I_1 = k\, lg\, \frac{D_1}{D_2}\ ,$$

which gives the difference of the intensity observed at two hypocentral distances D_1 and D_2. The value of $k = 3.5$ gives good results by using the Blake's formula for the shallow earthquakes.

Further the conduct of function $\delta(h) = 1.5\,M - I$ characterizing a relative level of surface vawes' amplitudes was studied for all the depths down to 640 km (*Fig.* 1). At the depths $0 < h < 60\text{-}80$ km the value $\delta(h)$ according to the equation

$$\delta(h) = -3.0 + 3.5\, lg\, h$$

changes from -1 to $+4$ which means that intensity decreases with the focal depth much more rapidly than the amplitudes of surface waves.

Beginning from depths of 80-100 km the value $\delta(h)$ feels a sudden decreasing appoximately by 2.5 units after which it goes up again. For the interval of depths from 80-100 to 640 km the analogous equation is

$$\delta(h) = -5.4 + 3.4\, lg\, h.$$

Such a rapid decrease of $\delta(h)$ can be explained only by an essential reduction of the surface waves' amplitudes of the foci underlying at some discontinuity. Just as the upper boundary of the low velocity layer (asthenosphere) must screen the body waves from underlying foci forming then the surface waves, so there is a reason to identify the boundary of a rapid decrease of $\delta(h)$ and the upper boundary of the asthenosphere.

The screening of « lateral » rays may be also noted to have a consequence in more rapid decrease of intensity at far epicentral distances than it ensued from the Blake's formula with $k = 3.5$.

It is remarkable that the analogous equation of $\delta(h)$ may be received from two equations given by B. Gutenberg and C. F. Richter (12) :

$$lg\,\mathrm{E} = 8.8 + 2\,lg\,h + 1.8\,\mathrm{M},$$
$$lg\,\mathrm{E} = 9.5 + 3.2\,lg\,h + 1.1\,\mathrm{I}.$$

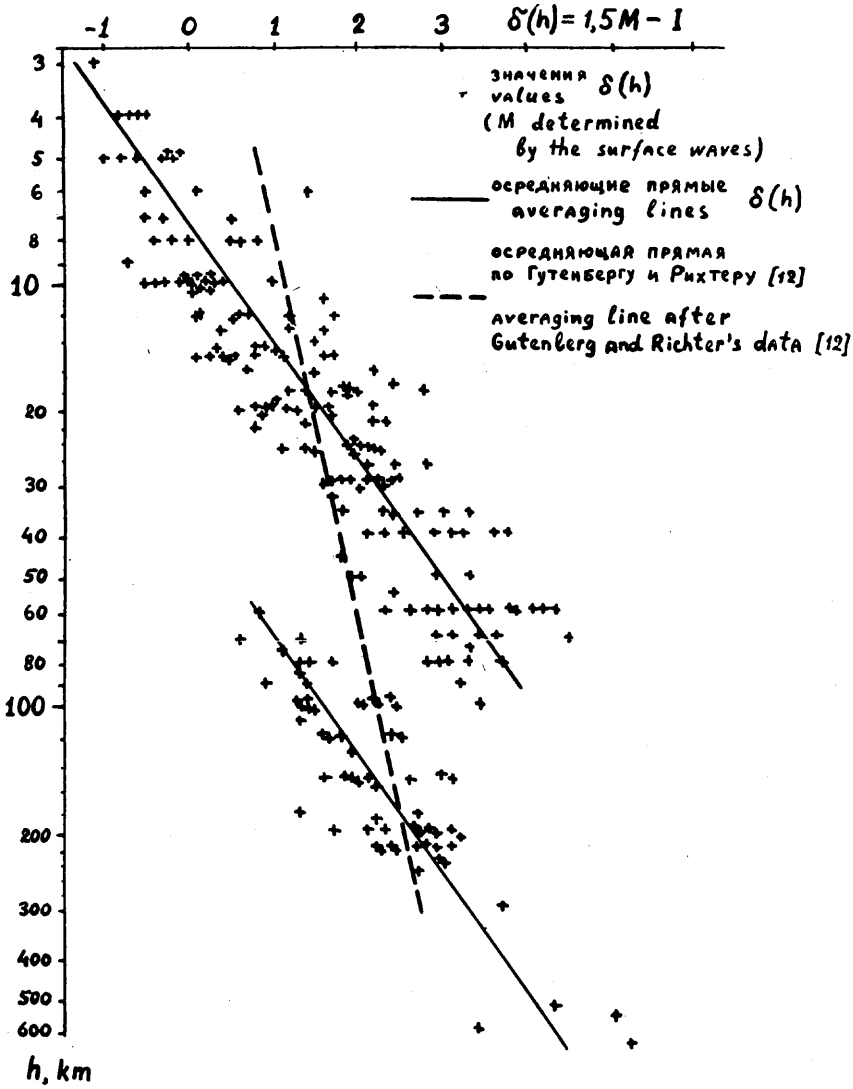

FIG. 1.

Striking off $lg\,\mathrm{E}$ we get

$$\mathrm{I} = -\,0.6 + 1.6\,\mathrm{M} - 1.1\,lg\,h.$$

Gutenberg and Richter had not divided ones from anothers shallow-and deep-focus earthquakes. That is why the function $\delta(h)$ taking from the last equation

$$\delta(h) = 1.5\,\mathrm{M} - \mathrm{I} = 1.1\,lg\,h + 0.6 - 0.1\,\mathrm{M}$$

or (considering the mean quantity of M to be 6)

$$\delta(h) = 1.5\,\mathrm{M} - \mathrm{I} = 1.1\,lg\,h$$

goes with averaging the two our branches of $\delta(h)$ without any jump at the depth of 80-100 km (see *fig.* 1).

The passage from the upper to the lower branch of $\delta(h)$ may be seen to take place on the large interval of depths from 60 to 100 km. But this is not a result of mistakes in determining the focal depth. If divided to different regions the values of $\delta(h)$ show the jump for all the earthquakes of some definite region taking place at a definite depth (*Fig.* 2). A jump of $\delta(h)$ in each region is made

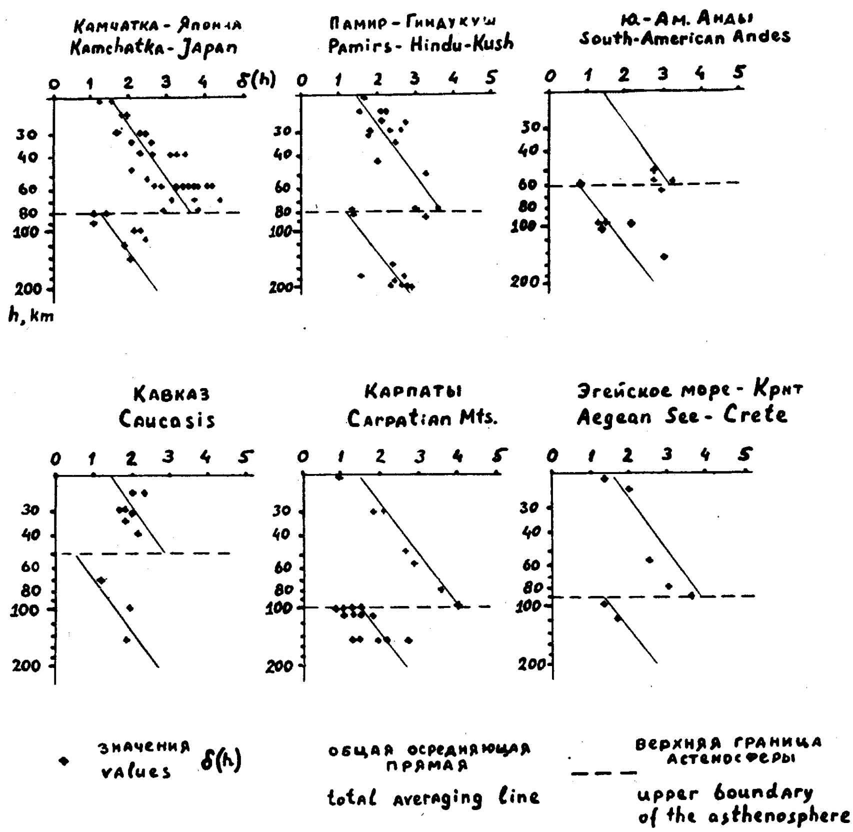

FIG. 2.

with a change of the focal depth by 10 or 15 km only. This testifies to a sudden decrease of the velocity on the upper boundary of the asthenosphere. The following data have been obtained of the depth of this boundary.

Kamchatka - Japan	ca 80 km
Pamirs - Hindu-Kush	ca 80 km
South-American Andes	ca 65 km
The Caucasis	ca 55 km
Carpathian Mts	ca 100 km
The Aegean Sea - Crete	ca 90 km

These data are to be taken as preliminaries.

As a conclusion the problem of M-determination of deep-focus earthquakes may be considered from point of view of above-mentioned results.

At first, the observed surface waves' amplitudes of deep-focus earthquakes are noted to be a sufficiently steady sign to use them for M-determination. But it is not clear what corrections must be used for deep-focus earthquakes.

The paths of body waves coming to the far stations are not exposed to the influence of the asthenosphere, so if M determined by body waves (13, 14) contains no error that may appear with increasing of focal depth, the value $\delta'(h) = 1.5\,M_{p,s} - I$ ($M_{p,s}$ means M determined by P- and S-waves amplitudes) is due to have no peculiarities at the depths of 80-100 km.

Our results show (*Fig.* 3) that down to the depth of 80 km $\delta'(h)$ and $\delta(h)$ coincide, and then $\delta'(h)$ also displaces to the left but not so strong as $\delta(h)$. This displacement shows that the curves $f(\Delta, h)$ by Gutenberg [14] serving to determine M of deep-focus earthquakes by body waves contain a systematic error ca 0.7 down from the depths of ca 80 km.

By reason of this the corrections to be added to M of deep-focus earthquakes depend on whether we aspire to equalize $M_{p,s}$ and M_L (M_L means M determined by surface waves — « undae longae ») for all the focal depths, or we want to have equal M for earthquakes with equal energy, or etc.

We reckon that the most correct way in M-determinations is not to use any corrections and to be based only on the actually observed amplitudes of surface or any other waves. The inevitable influence of focal depth and other factors must be taken into consi-

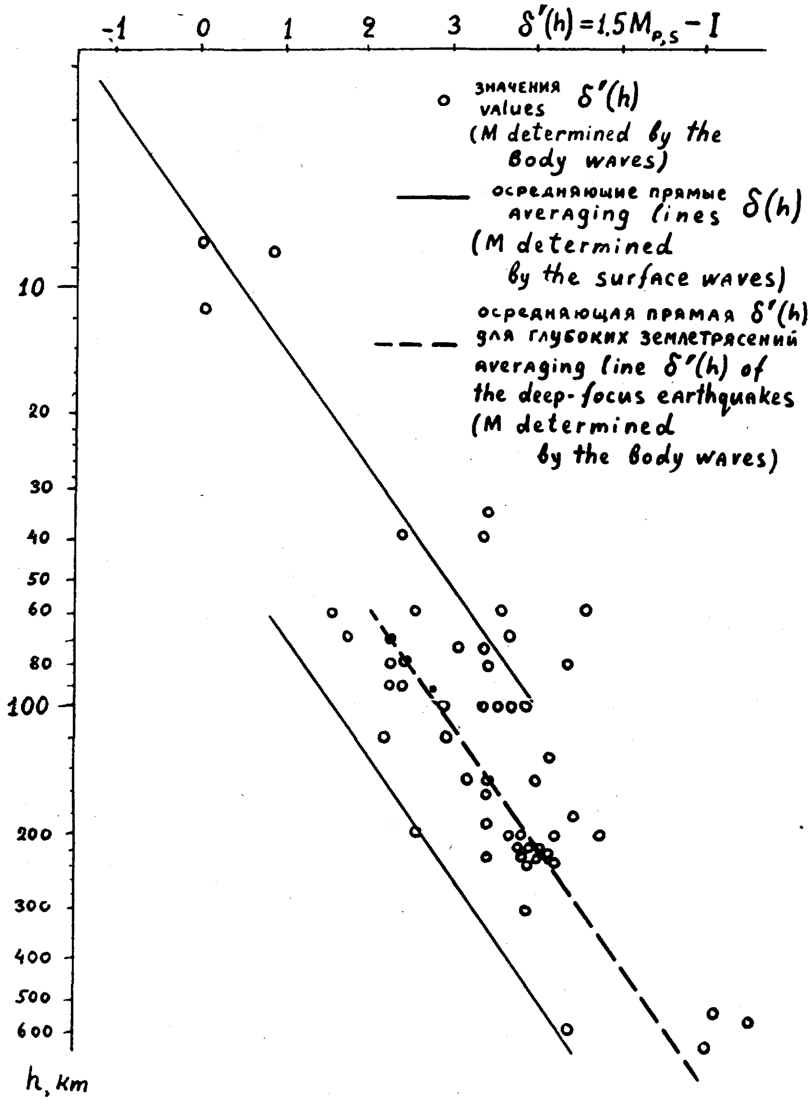

FIG. 3.

deration by studying the correlation between magnitude and energy of earthquakes. The latter must be different for different kinds of M ($M_{p,s}$, M_L etc.).

Institute of the Earth's physics
Moscow

References.

1. B. Gutenberg. The layer of relative low wave velocity at a depth of 80 kilometers. Bull. Seism. Soc. Am., 38, 1948.

2. B. Gutenberg. Low-velocity layers in the Earth mantle. Bull. Geol. Soc. Am., 65, 1954.

3. B. Gutenberg. Low-velocity lithosphere channel. Bull. Geol. Soc. Am., 66, 1955.

4. B. Gutenberg. Amplitudes of surface waves and magnitudes of shallow earthquakes. Bull. Seism. Soc. Am., 35, 1945.

5. С.Л. СОЛОВЬЕВ, Н.В. ШЕБАЛИН. Определение интенсивности землетрясений по смещениям в поверхностных волнах Извстия АН СССР, серия геофизическая, №7, 1957. (S.L. Solovyov, N.V. Shebalin, magnitude determination by amplitudes of surface waves).

6. International Seismological Summary. Kew, 1932-1944.

7. Bulletin mensuel, Bureau Central International Seismologique. Strasbourg, 1945-1956.

8. Бюллетень сети сейсмичечких станций СССР.

9. Н.В. КОНДОРСКАЯ. Выделение волны sP при неглубоких землетрясениях и её использование для определеиия глубины очага (N.V. Kondorskaya. Ascertaining the wave sP by shallow earthquakes and its using for determination of focal depth). Труды Геофизическаго институти АН СССР, № 36 (163), 1956.

10. Н.В. ШЕБАЛИН. Соотношение между балльностью и интенсивностью землетрясений в зависимости от глубины очага (N.V. Shebalin. Correlation between intensity and magnitude of earthquakes in dependence on focal depth). Бюллетень Совета по сейсмологии АН СССР, № 6. 1957 (в печати).

11. A. Blake. On the estimation of focal depth from macroseismic data. Bull. Seism. Soc. Am., 31, 1941.

12. B. Gutenberg, C. F. Richter. Earthquake magnitude, intensity, energy and acceleration. Bull. Seism. Soc. Am., 32, 1942.

13. B. Gutenberg. Amplitudes of P, PP and S and magnitude of shallow earthquakes. Bull. Seism. Soc. Am., 35, 1945.

14. B. Gutenberg. Magnitude determination for deep-focus earthquakes. Bull. Seism. Soc. Am., 35, 1945.

MAGNITUDE AND ENERGY OF EARTHQUAKES

S. L. SOLOVYOV.

The investigations of different objective methods of earthquakes classification and especially of those based on energy or magnitude of earthquakes are developed in the USSR mainly during the last few years. There are at least two reasons, stimulating these investigations, namely, the work at the Atlas of Seismicity of the USSR* and the increase of the annual number of earthquakes registered on the territory of the country, this increase being the consequence of the recent development of the seismic stations network and of the improvement of seismic equipment.

The earthquake magnitude scale, introduced in seismological practice by C. Richter and B. Gutenberg (1956 a) was first used in the USSR approximately in 1953 when the analysis of different methods of magnitude determination was made (Solovyov, 1953). This work has shown that the most simple and stable (and the only possible for the earthquakes of previous years) is the magnitude determination based on the surface waves. But the well-known formula by B. Gutenberg (1945 a) :

$$M = lg\, A_{20} - lg\, A^{*}_{20} + C + D \tag{1}$$

$$lg\, A^{*}_{20} = 1.818 - 1.656\, lg\, \Delta^{\circ} \quad 15^{\circ} < \Delta < 130^{\circ}, \tag{2}$$

where A_{20} is the horizontal component of the maximum ground movement in microns in surface waves having periods of about 20 sec, C is the station correction and D — correction for focal depth and other parameters of earthquakes, could not be applied at stations of the USSR, such long-period waves being not registered at stations for many distant earthquakes.

So it was necessary to look for some other forms of magnitude determination. Taking into consideration that the velocity of oscillation $\left(\frac{A}{T}\right)$ is more strictly connected than its amplitude with the energy of the wave, it was suggested (Solovyov S. L., 1955) to determine the magnitude according to the next expression :

$$M = lg\, \frac{A}{T} - lg\, \left(\frac{A}{T}\right)^{*} \tag{3}$$

Here A is the maximum amplitude of the surface wave and T is the period of this wave. It is useful to point out that the usual

* See the communication by S. F. Savarensky at present meeting.

values of T are enclosed approximately between 3 sec. and 30 sec. Average periods of maximum phase of surface waves corresponding to different epicentral distances are represented in Table 1, the records being obtained with Kirnos or Galitzin instruments.

TABLE 1.

Approximate mean values of the period of maximum phase of surface waves corresponding to different epicentral distances

Δ km.	T sec.	Δ km.	T sec.
250- 400	6	3500- 5500	14
400- 600	7	5500- 7500	16
600- 900	8	7500-10000	18
900-1300	9	10000-13000	20
1300-2000	10	13000-16000	22
2000-3500	12	16000-20000	24

It is possible to say formally that this function $lg\left(\frac{A}{T}\right)^*$ gives a change of $lg\ \frac{A}{T}$ with epicentral distance for the earthquake with zero magnitude. The values of this function have been found, the necessary data corresponding to earthquakes of main continental seismic regions of the USSR (Caucasus, Turkmenistan, Central Asia) being used (Solovyov S. L. 1955, Solovyov S. L., Shebalin N. V. 1957). The following approximate equation of the function was established :

$$lg\left(\frac{A}{T}\right)^* = -3.20 - 1.60\ lg\ \Delta^\circ \quad 4^\circ \leqslant \Delta \leqslant 90^\circ \qquad (4)$$

At the same time some other methods of magnitude determination were examined including that represented by the formula :

$$M = lg\,A - lg\,A^* \qquad (5)$$

Here A means the same as in formula (3), i. e. the maximum ground displacement in surface waves. The possibility to measure magnitude from (5) has both principal and practical importance, especially for nearby earthquakes when the estimation of wave period is very uncertain; besides that no information about periods of waves is available for many old earthquakes.

Statistic methods applied to values of A corresponding to earthquakes of the above-mentioned seismic regions have given mean values of $lg\,A^*$ (Solovyov S. L., Shebalin N. V. 1957). The approximate, equation of the function $lg\,A^* = f(\Delta)$ is

$$lg\,A^* \approx -2.60 - 1.25\ lg\ \Delta^\circ \qquad 4^\circ \leqslant \Delta \leqslant 90^\circ \qquad (6)$$

The agreement between the values of M, determined from formulae (3) and (5), was examined. It was found that the mean (using many earthquakes) difference between these two ranges of magnitude values depended on the earthquake magnitude :

$$M_A - M_{A/T} \approx 0.05\,(M - 6) \tag{7}$$

Here $M_{A/T}$ is the value of M from (3) and M_A — from (5). The correlation (7) means by the way that the period of a surface wave depends a little on the magnitude of an earthquake. Taking into consideration that the usual accuracy of magnitude determination is equal to $\pm$ 1/4 and that the values of M determined from surface waves change from 3 to 8 1/2 one can see on basis of (7) that formulae (3) and (5) give on the average the same values of M.

The comparision of formulae (2), (4) and (6) shows that the maximum amplitude of surface wawe changes with distance as $\Delta^{-1.25}$ and the maximum amplitude of wave with fixed period (20 sec) changes as $\Delta^{-1.6}$, the last attenuation being consequently more strong than the previous one and approximately the same as the attenuation of the maximum velocity of ground oscillations. It confirms in particular the validity of the expression :

$$lg\left(\frac{A}{T}\right)^{*} = lg\, A^{*}_{20} - lg\, 20 \tag{8}$$

used by many authors.

It is interesting to compare the values of M determined in the USSR and in other countries. The functions $lg\left(\frac{A}{T}\right)^{*}$ and $lg\, A^{*}$ were established in such a way that the values of M determined by using (3) or (5) were equal to those calculated from (1) when C = D = O. No corrections to M (station, for focal depth or for geographical situation of epicentre) are used in the USSR because of the uncertain nature of these corrections. At the same time some corrections C and D are in use at other stations of the world. For instance at Prague C = 0.33 and corrections D depending on the focal depth are used sometimes (Zatopek A. et Vanek I., 1952). At Swedish stations Uppsala and Kiruna C $\approx$ 0.3 (Båth M., 1956). This circumstance as well as the use of body waves for magnitude determination leads to a systematic discrepancy between the values of M published in Soviet bulletins and in bulletins of other countries. Detailed comparison (Solovyov S. L., 1958, b has shown that values of M from Soviet Bulletins coincide on the average with the values of M which can be found by using (1), C and D being zero, (2) and amplitudes from Prague bulletin. At the same time these values are less by 0.3, that is by the Prague station correction, than the magnitudes published in the bulletin of Prague.

The introduction of corrections C equal approximately to 0.3 at European stations is caused by intention to put into agreement the values of M, calculated at these stations, and those published in bulletins of Pasadena or in the well-known summary by B. Gutenberg and C. Richter (1954). In connection with this comparison (for the first quarter of 1955) of magnitudes published in bulletins of Pasadena and of the seismic stations of the USSR is represented in Table 2.

TABLE 2.

Comparison of magnitudes given by seismic stations network of the USSR and by station Pasadena. The first quarter of 1955.

Date	Région	M_{USSR}	$M_{Pasadena}$	$M^{cal.}_{Pasadena}$	$M_{Pasadena}$ - $M^{cal.}_{Pasadena}$	M_{USSR} — $M^{cal}_{Pasadena}$
5 Jan 00^h	New Zealand	6 3/4	6 1/2-6 3/4	6,3	1/4	+0,45
5 Jan 17^h	New Hebrides	6 1/4	6 3/4	6,4	1/4	—0,15
5 Jan 23^h	New Hebrides	6 1/2	6 3/4-7	6,5	1/4-1/2	—0
13 Jan 02^h	Aleutian Islands	6 3/4	6,9	6,6	0,3	+0,15
31 Jan 02^h	Kurile Islands	6 1/2	6 1/4-6 1/2	5,85	1/2	+0,65
27 Febr 20^h	Kermadec Islands	7 1/2	8 ±	8	0	—0,5
1 March 04^h	Canada	6	6 1/2-6 3/4	6,7	0	—0,7
18 March 00^h	Kamchatka	6	7 1/4-7 1/2	7	1/4-1/2	—1
31 March 18^h	Philippines	7 1/4	7,5 ±	6,9	0,6	+0,35
				mean :	1/4	—0,07

This Table gives also the values of $M^{cal}_{Pasadena}$, which can be calculated by using (1), C and D being zero, (2) and amplitudes registered at Pasadena. One can see that there are many discrepancies between M_{USSR} and $M^{cal}_{Pasadena}$ and it is unlike to the previous comparison. On the other hand there is no systematic discrepancy between $M_{Pasadena}$ and $M^{cal}_{Pasadena}$. The last fact indicates that the magnitudes from two bulletins have different physical sense and consequently it is necessary to be very cautious when comparing these values.

The application of equations (3) and (5) at seismic stations of the USSR has revealed the existence of a systematic disagreement between the values of M calculated at Far-East stations (Klyuchi, Kurilsk, Magadan, Petropavlovsk, Uglegorsk, Vladivostok, Juzhno-Sakhalinsk) and at other continental stations of the country. This phenomenon is the most remarkable for Kurile-Kamchatka earthquakes. In Fig. 1 the mean differences between individual station

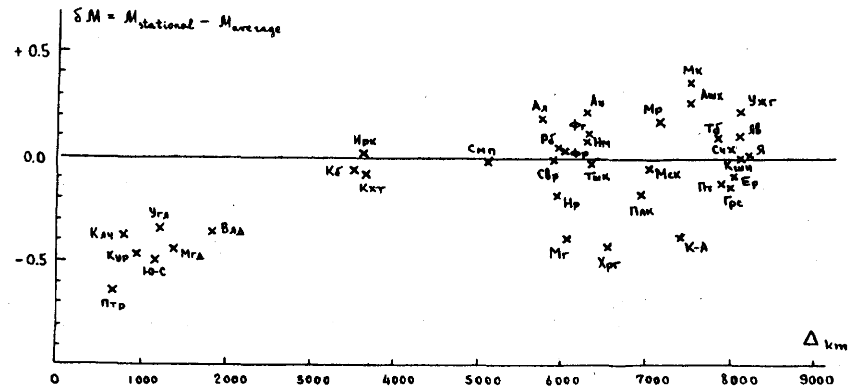

FIG. 1. — Mean differences between individual station and average values of M. KURILE-KAMCHATKA earthquakes of 1953-54. The data of only continental stations were used for calculations of average values. Abbreviations according to the Bulletin of the net of seismic stations of the USSR.

values of M and the mean values for these earthquakes are represented, the mean values of M being found only from data of continental stations (Solovyov S. L., 1958 a, b). One can see that all far-east stations have in this case negative values of δM, the mean values of δM for these stations being equal to —0.45. It means that in the region of far-east stations as well as in the region of continental stations the amplitude of the surface wave of a Kurile-Kamchatka earthquake and its velocity of oscillation diminish with distance in agreement with the angular coefficients from (4) and (6) but both those values increase or at least do not diminish when the waves passes from the first region to the seconds one. The investigation of seismograms, and bulletins shows that in reality for Kurile-Kamchatka earthquakes the ground displacement at far-east stations is often less than the displacement at more distant continental stations.

The special investigation shows that negative values of δM at the far-east stations are typical not only for Kurile-Kamchatka earthquakes but for the majority of Pacific earthquakes originating in the regions of oceanic troughs. On the contrary, the continental earthquakes give in general the positive sign of δM. These facts are illustrated by Fig. 2, where the differences between the values of M calculated at Vladivostok and determined as the average at Moscow, Pulkovo, Sverdlovsk, Irkutsk and other continental stations are represented for some earthquakes of 1930-1955 with different location of epicentres.

The obtained geographical distribution of δM agrees approximately with the distribution found by B. Gutenberg (1945 a) for differences between magnitudes determined from surface waves at Pasadena and, as the average, at other stations of the world. The distribution from Fig. 2 agrees also, except the region of Central Asia, with the results by A. Zatopek and I. Vanek (1952) who have compared the values of M determined at Praha and at Pasadena. It seems to be possible to think that when we have two stations, one of them being situated on the Pacific coast, negative values of $\delta M = M_{Pacific} - M_{Continental}$ are typical for Pacific earthquakes and positive values predominate for continental earthquakes whatever is the location of the station on the coast. Of course it is necessary to study many new data in order to check the validity of this hypothesis.

So far the body waves are not used in the USSR for magnitude determination. It seems that it would be better to study first the agreement between the corresponding tables and figures by B. Gutenberg and C. Richter (1956 b) and the empirical data of seismic stations of the USSR. Besides, it is necessary to work out the most reliable and most convenient mode of correlation of different M-scales. It seems to us in particular that it is necessary to distinguish the values of M determined by using transverse waves from the values determined by using longitudinal waves (Solovyov S. L., 1956).

The magnitude of earthquakes, the methods of whose determination being described above, was used in the Atlas of Seismicity of the USSR. The classification of earthquakes the magnitude of which could not be estimated was based on the principle of the registration limit. In connection with this Table 3 includes the distances beyond which the registration is not possible, corresponding to different values of M.

TABLE 3.

Magnitude and maximum distance of registration.

Δ km.	75-150	150-300	300-700	700-1500	1500-3000	3000-6000	6000-10000
M	(2 1/2)	(3)	3 1/2	4	4 1/2	5	5 1/2

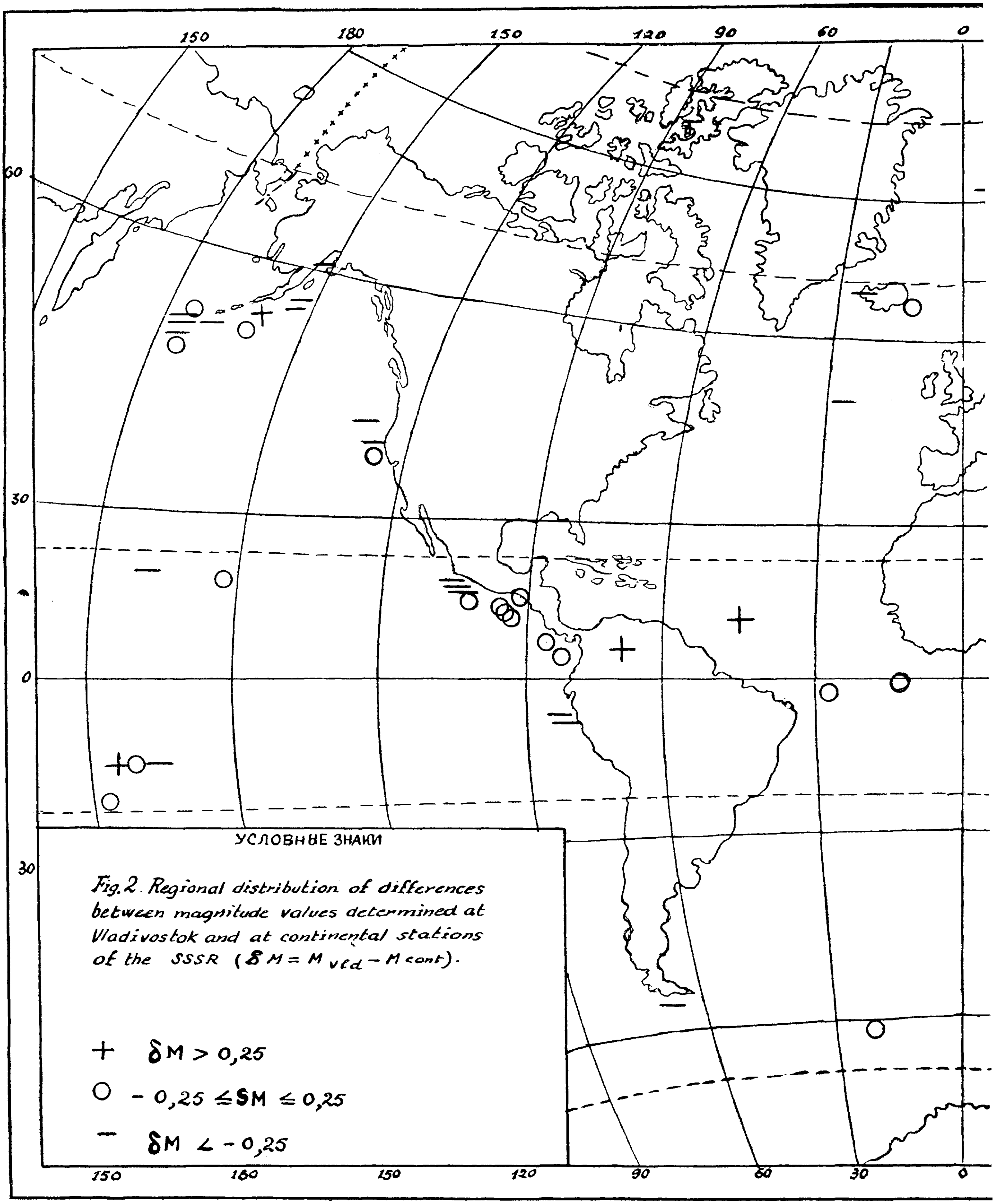

Fig. 2. Regional distribution of differences between magnitude values determined at Vladivostok and at continental stations of the SSSR ($\delta M = M_{Vld} - M_{cont}$).

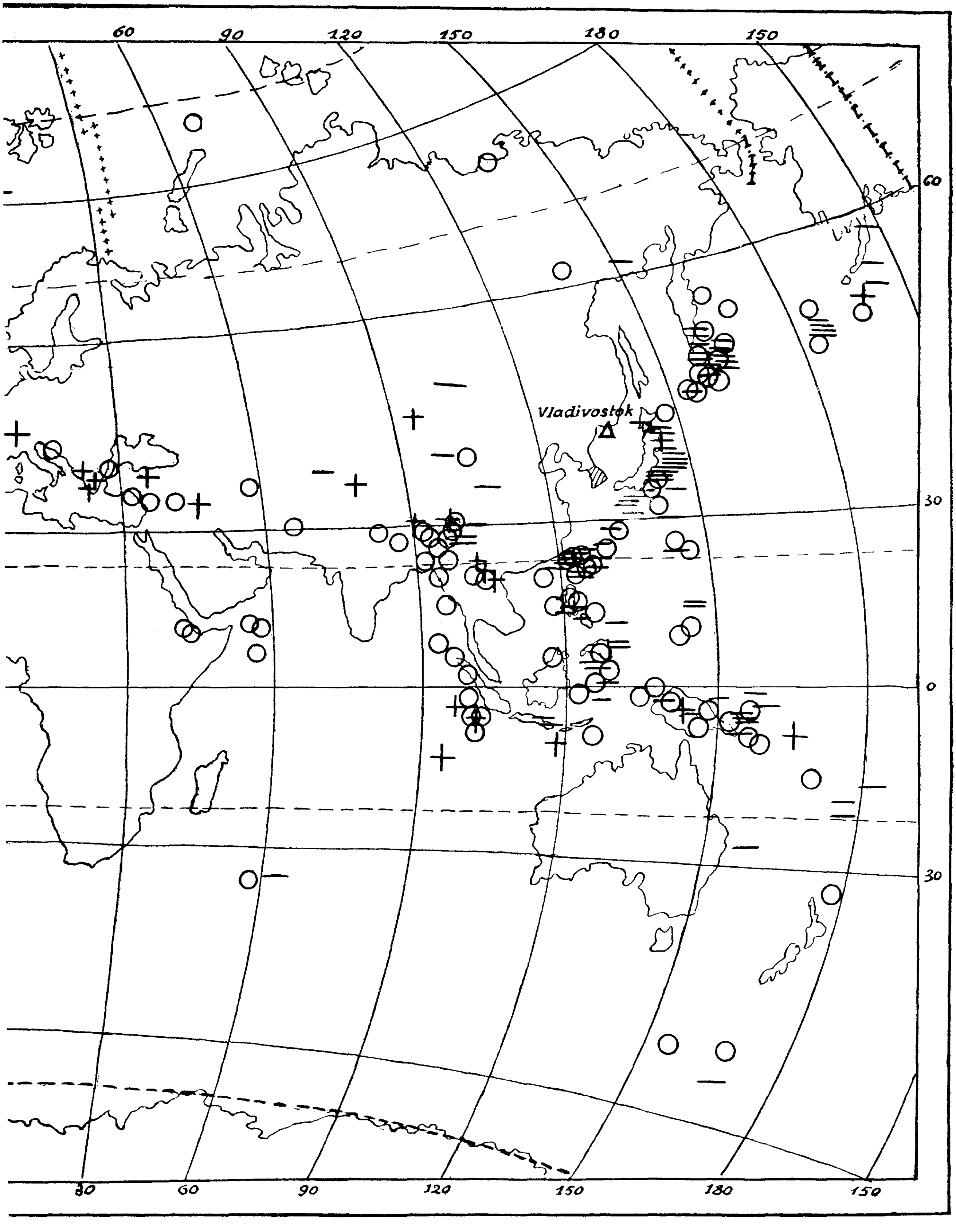

60
90
120
150
180
150
Vladivostok
60
30
0
30
30
60
90
120
150
180
150

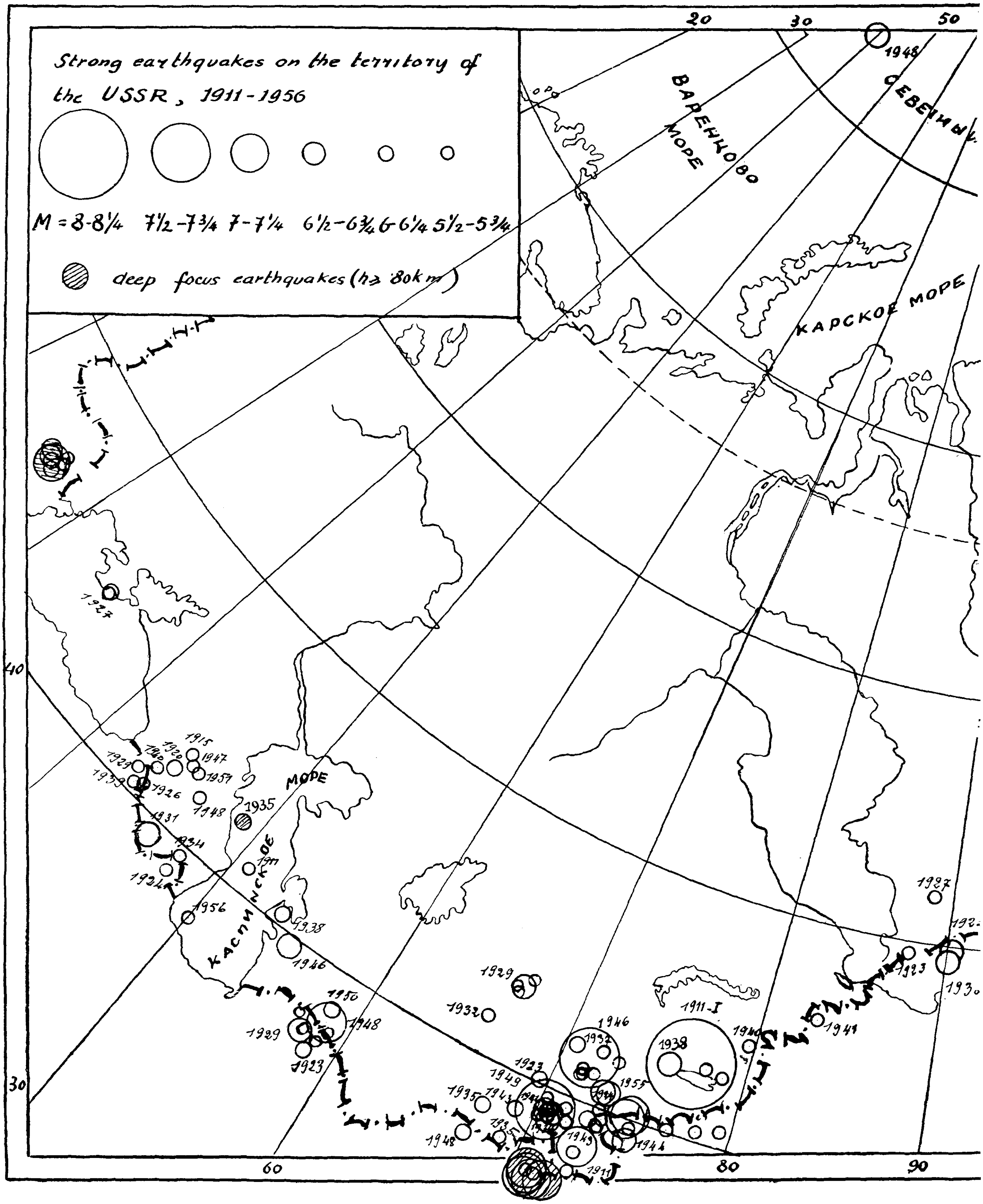

Strong earthquakes on the territory of the USSR, 1911-1956
M = 8-8¼ 7½-7¾ 7-7¼ 6½-6¾ 6-6¼ 5½-5¾
deep focus earthquakes (h ≥ 80 km)
БАРЕНЦОВО МОРЕ
КАРСКОЕ МОРЕ
КАСПИЙСКОЕ МОРЕ
20
30
50
40
30
60
80
90

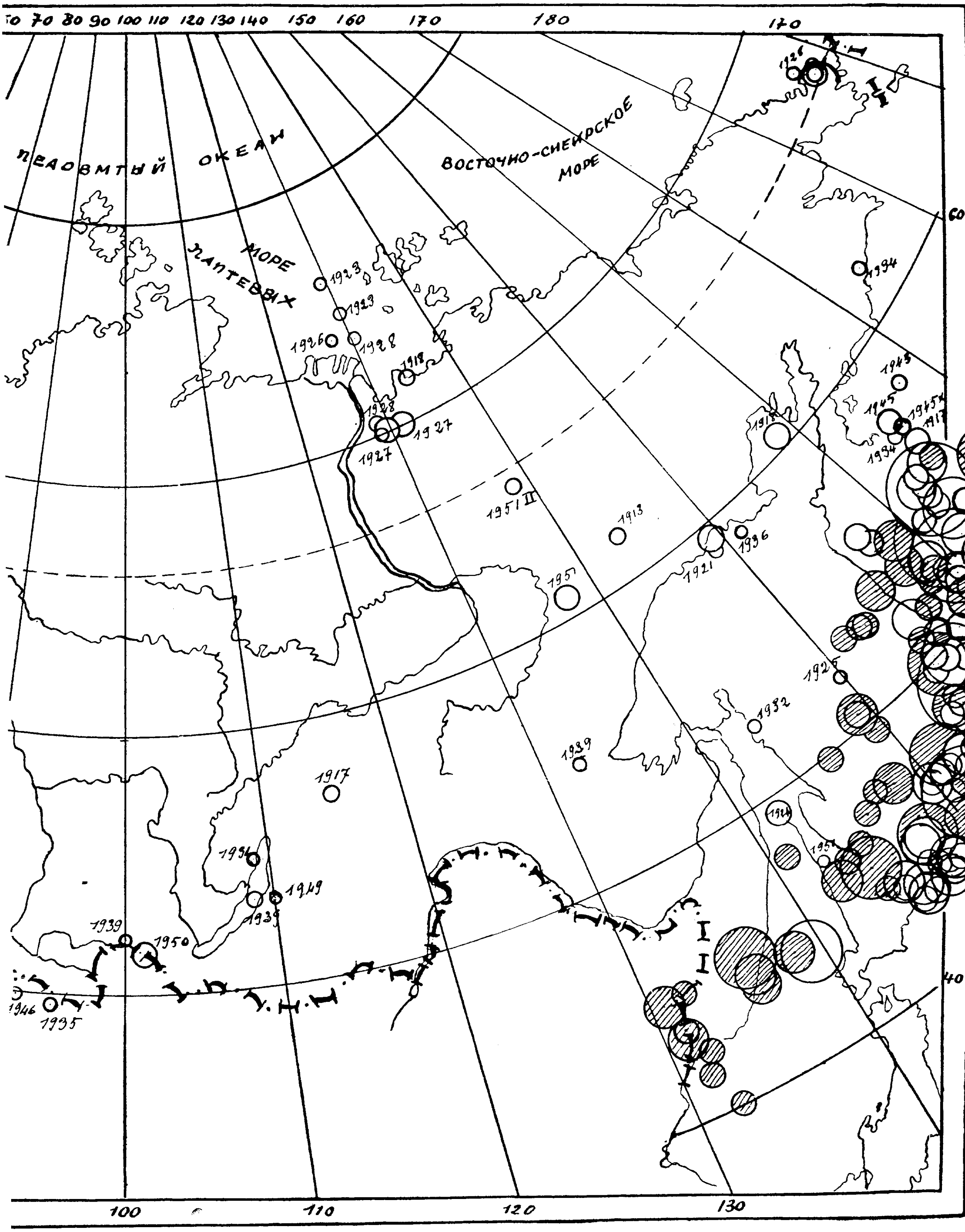

70 80 90 100 110 120 130 140 150 160 170 180 170
ЛЕДОВИТЫЙ ОКЕАН
МОРЕ ЛАПТЕВЫХ
ВОСТОЧНО-СИБИРСКОЕ МОРЕ
60
40
100
110
120
130

The distances are those of the stations terminating the corresponding lists in the Bulletin, the stations being equipped by Kirnos or Galitzin instruments.

In Fig. 3 the map of strong earthquakes on the territory of the USSR during 1912-1955 is given. The earthquakes of Kurile-Kamchatka region and deep earthquakes of Hindukush with $M \geqslant 6\ 1/4$ and earthquakes of other regions with $M \geqslant 5\ 1/2$ are shown here. For magnitude determination in case of deep earthquakes the same methods as for shallow earthquakes were employed, the correction equal to $\approx +1$ being added when $h \geqslant 80\text{-}100$ km*. In some cases magnitudes of deep earthquakes were taken from the summary prepared by B. Gutenberg and C. Richter (1954).

After the compilation of this map as well as the maps of the Atlas former opinions about the seismicity of some remote districts of the country have changed.

2. Energy of earthquake and its relation to magnitude.

The magnitude scale is almost a perfect instrument for the relative energy classification of earthquakes. But it is necessary to measure the energy of earthquakes in absolute units so that to quantify seismological phenomena and to compare them with other geological and geophysical events.

The problem of energy determination is sufficiently difficult. It would be correct to define the energy of the earthquake as the potential energy of an elastic medium deformation which is delivered during the earthquake and is transformed to other forms of energy. It seems that only a negligible part of this energy is radiated from the focus as the energy of the waves. One cannot measure this potential energy directly; it can be estimated approximately and indirectly and only in most favourable cases. On the contrary the energy of seismic waves can be determined, at least in the main, for every registered earthquake. Thus energy classification of earthquakes reduces to-day to that based on seismic waves energy. This last quantity is also often called as energy of earthquake. Further on the term « energy of an earthquake » will be used just in this particular sense.

The following sum will be regarded as the energy of an earthquake :

$$E = E_P + E_S \qquad (9)$$

* See the communication by N. V. Shebalin at present meeting.

where E_P is the energy of the longitudinal wave and E_S is the energy of the transverse wave.

Observations show that as rule $E_S \gg E_P$; so when approximate calculations are fulfilled it is possible to suppose that

$$E \approx E_S \tag{10}$$

There are some other definitions of the energy of an earthquake. H. Jeffreys (1952) supposes that

$$E \approx 2\, E_{surf} \tag{11}$$

when E_{surf} is the energy of surface waves. It seems to the author that this point of view is not absolutely correct because I) E_{surf} is the quantity of the second origin, the source of E_{surf} being the energy of body waves, II) equation (11) is not correct for deep erthquakes, III) the energy of surface waves is as a rule, less than the energy of body waves and the relation of these two energies depends on the magnitude of the earthquake. At last the formulae recommended for the determination of the energy of surface waves/those by H. Jeffreys (1923), S. Kosenko (1953) / are based on the representation of energy propagating through a spherical or a flat layer, the energy flux being proportional to $\left(\frac{A}{T}\right)^2 \Delta t \approx n\, A^2$ (Δt — time of oscillations, n — number of oscillations). As the consequence of this representation the following relation must exist : $A^2 \backsim \Delta^{-1}$. On the other hand observations give [(see 6)] $A^2 \backsim \Delta^{-(2-3)}$. It is difficult to explain such a strong disagreement between theoretical and empirical data simply as the influence of the absorption of energy. It makes oneself to doubt the validity of above-mentioned formulae.

When sufficiently big distances (say, $\Delta > 20°$) are used the estimation of the energy of S wave can be carried out with the help of the well-known formula by Zoppritz — Geiger — Gutenberg — Wiechert (1912) which can be written for the wave SH (the wave with oscillations in the horizontal plane) in the following form :

$$E = 2\pi^3 \rho c\, R^2\, e^{k\Delta}\, \frac{\sin\Delta \sin e_0}{\cos e_h\, de_h / d\Delta} \left(\frac{A}{T}\right)^2 \Delta t \tag{12}$$

$$= \Phi(\Delta)\left(\frac{A}{T}\right)^2 \Delta t$$

Here ρ — the density of the ground at the point of observation : c — velocity of the transverse wave at the point of observation; Δ — epicentral distance; k — absorption factor; e_0 — angle of wave emergence at the point of observation; e_h — angle of wave immersion at the focus, A, T, Δt — amplitude, period and duration of harmonic oscillation which approximates the real movement of the ground.

To use the expression (12) it is necessary to know the values of the function $\Phi(\Delta)$. One could think that these values could be found by double differentiation of the travel-times following the well-known rule by Benndorf. Such differentiation is unfortunately very uncertain because of many errors accumulating during the procedure. Most reliable is the calculation of this function on the basis of some velocity distribution in the Earth's mantle and crust. Smoothed values of function $lg\ \Phi(\Delta)$ found on basis of Jeffreys-Bullen (1939) distribution are represented in Table 4. They correspond to the focus situated in the « basaltic » layer of the Earth's crust. The absorption factor was to be taken equal to 0,00024 km^{-1} according to the results by B. Gutenberg (1945 b).

TABLE 4.

Approximate values of $lg\ \phi(\Delta) =$

$$= lg\ 2\pi^3 \rho c\ R^2 e^{k\Delta} \frac{\sin\Delta \sin e}{\cos e_h\ d e_h/d\Delta}$$

Δ	0°	1°	2°	3°	4°	5°	6°	7°	8°	9°
20°	4.10	4.20	4.30	4.45	4.60	4.70	4.80	4.90	4.95	5.05
30°	5.20	5.30	5.40	5.50	5.50	5.55	5.60	5.65	5.70	5.70
40°	5.70	5.75	5.75	5.80	5.80	5.85	5.85	5.90	5.90	5.90
50°	5.90	5.95	5.95	6.00	6.00	6.00	6.00	6.05	6.05	6.10
60°	6.10	6.10	6.15	6.15	6.15	6.20	6.20	6.20	6.25	6.25
70°	6.30	6.30	6.30	6.30	6.30	6.35	6.35	6.40	6.40	6.40
80°	6.45	6.45	6.45	6.50	6.50	6.50	6.50	6.55	6.55	6.60

Yet the works by A. Vvedenskaya and L. Balakina[2] show that the function $\Phi(\Delta)$ must have some peculiarities at the distances from 20° to 100°. So the values of Table 4 must be looked upon only as the first approximation to the real values of the function $\Phi(\Delta)$.

At small distances the calculation of energy is not easy either. Usually a formula suitable to the symmetrical source in the homogeneous indefinite media is applied in these cases, the formula being first used in seismology perhaps by B. B. Galitzin (1915) :

$$E = 2\pi^3 \rho c\ \Delta^2 \left(\frac{A}{T}\right)^2 \Delta t \qquad (13)$$

2. See the report of these authors at the present meeting.

Yet some theoretical works (the first well-known work by H. Lamb (1904) and some laboratory experiments as well as direct seismological observations (see, for instance, (Solovyov S. L. and Dzhibladze E. A. 1955) indicate that the flux of energy from the source situated near the surface of a hemispace changes with distance approximately as Δ^{-4}. So it seems that it would be more correct to put into (13) at least the factor $\left(\frac{\Delta}{h}\right)^4 h^2$ (h — focal depth) instead of Δ^2. These considerations made the author compare the values of E which could be found by using (13) at small distances (100 km — 200 km) and by using (12) at distances exceeding 20°. Such comparing can be fulfilled only for earthquakes which are already registered at distant stations and are still sufficiently clear recorded at near-by stations. It was assumed that the values of $\frac{\Delta T}{T^2}$ were approximately the same at near and remote stations and these values were omitted during the calculations. The comparison (see Table 5) shows that the values of the energy determined at distant and near stations coincide in the limits of the usual accuracy of *lg* E determination (± 1/2).

TABLE 5.

Comparison of energy estimations carried out at different epicentral distances.

Date	Region	Station	Δ	A μ	$lg\ \frac{ET^2}{\Delta t}$ C. G. S.
15 February 1953, 8^h	Hindu Kush	Andijan	175 km	80	18
		Moscow	27°	0,5	17 1/2
5 September 1953, 22^h	Pamir	Fergana	115 km	40	17
		Moscow	28°	0,3	17
31 January 1954, 11^h	Kamchatka	Petropavlovsk	210 km	200	19
		Moscow	62°	1.5	19 1/2
14 March 1954, 17^h	Kamchatka	Petropavlovsk	280 km	200	19 1/4
		Moscow	64°	0,8	19
26 April 1954, 20^h	Kamchatka	Petropavlovsk	140 km	1600	20 1/2
		Moscow	62°	2	19 3/4

It has given the author the possibility to use the formula (13) without any modification though the values of E resulting from this formula are somewhat doubtful.

The relation between energy and magnitude was supposed to be a linear function, the change of M being limited :

$$lg\,E = \alpha + \beta\,M \tag{14}$$

The energy was calculated following (12) and (13). To make these calculations more simple it was assumed that T and Δt do not depend on the magnitude in the restricted ranges of M values. Average values of T and Δt were taken for these ranges (see Table 6). The amplitudes of waves were taken from seismograms and bulletins, the last ones being used only in the case of near stations. The records obtained from Kirnos seismographs were used. So only the energy of the low-frequency ($T \geqslant 1$ sec) component of the wave was estimated.

The magnitude of earthquakes was determined according to § 1.

The solution of two most numerous groups of observation gave $\beta = 1{,}7$. This value of the angular coefficient was taken as « standard » though the lines with other factors (for example 1.4 or 2) also sufficiently well approximate the empirical data.

The final results of the work are represented in Fig. 4 and in Table 6.

TABLE 6.

Correlation between energy and magnitude (parameters α and β from equation [14]).

N	Region	Ranges of magnitude	Method of energy determination	Number of earthquakes	$T_{av.}$ sec.	$\Delta t_{av.}$ sec.	α	β
1	Central Asia	$3 \leqslant M \leqslant 5{,}5$	Equation (13)	98	1	—	11	1,7
2	Central Asia	$4{,}5 \leqslant M \leqslant 8$	Equation (12)	12	4	30	10	1,7
3	Far East	$3{,}5 \leqslant M \leqslant 6{,}5$	Equation (13)	73	2	10-20	10	1,7
4	Far East	$5{,}5 \leqslant M \leqslant 8$	Equation (12)	23	8	35-40	9	1,7

The break between two lines corresponding to the same seismic region can be explained by the peculiarities of the employed methods, different values of T and Δt being attributed to the same earthquake when different formulae of energy determination have been used. It should be more correct consequently to draw a single line for the given region. For example such a line for Central Asia could have the equation :

$$lg\, E \approx 11.5 + 1.5\, M \qquad (15)$$

Yet the reliable drawing of a mean line requires some supplementary investigations in particular the study of the exact value of absorption factor.

The displacement of lines for the Far East in relation to the lines for Central Asia can also be explained by the peculiarities of

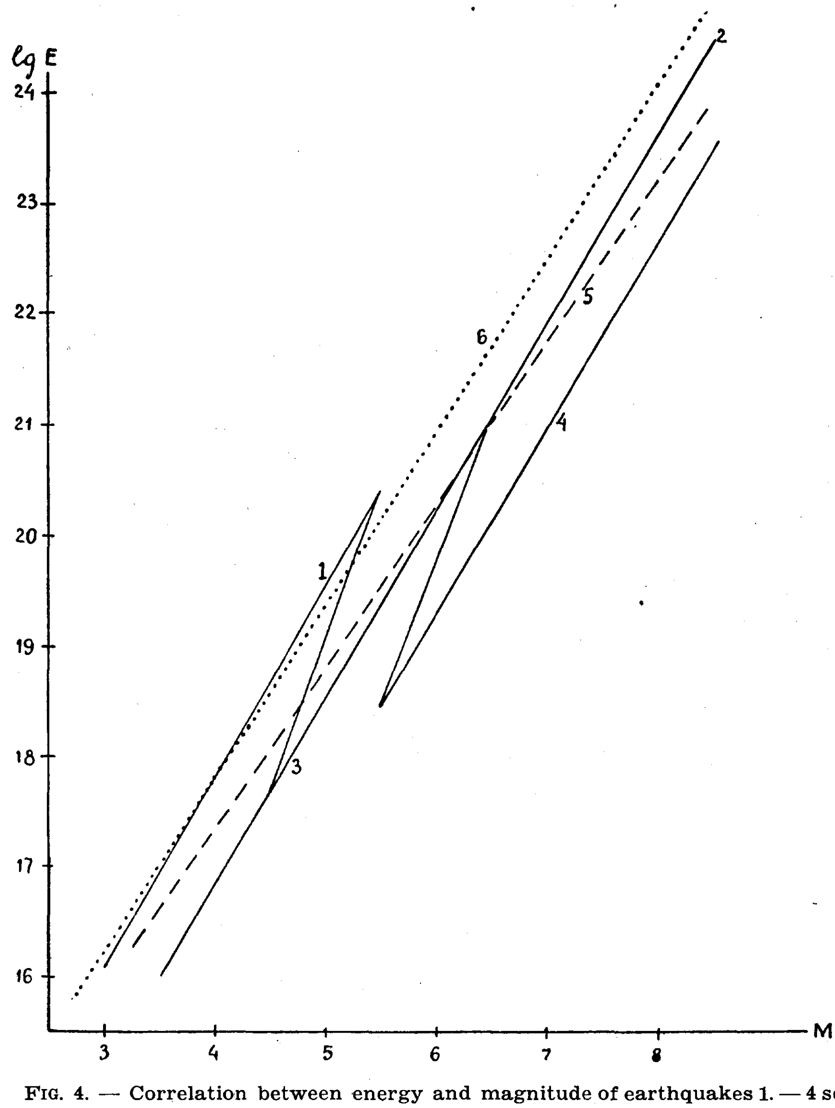

FIG. 4. — Correlation between energy and magnitude of earthquakes 1. — 4 see table 6; 5 — according to Solovvyov S. L. 1956; 6 — according to Gutenberg B. and Richter C 1956.

methods. In the case of weak earthquakes it is the use of a positive correction to M equal to 1/4-1/2 at the Far East stations, which can cause such a discrepancy. On the other hand distant stations of the USSR lie in the direction of the minimum energy radiation from foci of Kurile Kamchatka earthquakes and it can be the cause of the discrepancy in the case of strong earthquakes.

The results by B. Gutenberg and C. Richter (1956 a) about the relation between the energy of body waves and the magnitude calculated from surface waves are also represented in fig 4. The energy of the high-frequency component ($T \leqslant 1$ sec) was estimated in the epicentre by using the Galitzin formula. The sum of $E_P + E_S$ being taken equal to $1.5\ E_S$, factor 2 in (13) was replaced by factor 3. One can see that these results are in good agreement with the results obtained by the author for Central Asia earthquakes.

In one of the author's works (1956) the relation between M and E having the angular coefficient equal to 1 — 1.5 was suggested. This relation was established without the separation of the data relating to different regions and obtained by different methods. It is clear from Fig. 4 that this method has given too little value of β.

Some considerations about the relation between M and E can be exposed. Let us regard first the problem when both quantities are determined on the basis of the same wave.

Let the magnitude be defined as the velocity of ground oscillations, i.e.

$$M_{a/t} = lg\,\frac{A}{T} - lg\,\left(\frac{A}{T}\right)^*$$

Let E be the energy of a given shock and E^* — the energy of a shock with $M = 0$. Then

$$lg\left(\frac{E}{E}\right)^* = 2\,M_{a/t} + lg\,\frac{t}{t}^*$$

Time of oscillations increases when the magnitude increases; consequently

$$lg\,E = \alpha + \beta\,M_{a/t} \quad \beta > 2 \tag{16}$$

In particular if, as it is usual supposed, $T \backsim \sqrt[3]{E}$ and $t \backsim T$

$$\beta \approx 2.17 \tag{16'}$$

If M is defined as the amplitude of wave, i.e.

$$M_a = lg\,A - lg\,A^*$$

the relation has the form :

$$lg\,E = \alpha' + \beta'\,M_A \qquad \beta' < 2 \tag{17}$$

and in the above-mentioned particular case

$$\beta' \approx 1.82 \tag{17'}$$

In our work the relation between the magnitude determined a from the surface wave and the energy of transverse wave was examined. Bearing in mind the used methods (constancy of T and Δt) one can say that the factor must be equal to 2 if the amplitudes of both waves increase with the same speed, the magnitude of earthquake increasing. In fact it was found that $\beta = 1.7$. It means that the amplitudes of surface waves increase more rapidly than the amplitudes of body waves, the fact revealed by many investigators.

The author expresses his acknowledgement to prof. E. F. Savarensky, under whose direction and at whose suggestion the research was undertaken.

References.

Бюллетень сети сейсмических станций СССР, 1955, № 1, Изд. АН СССР, 1956 (Bulletin of the net of the seismic stations of the USSR)

ГОЛИЦЫН Б. Б. (GALITZIN B. B.)

1915. "О землетрясении 18 февраля 1911 г." (On the earthquake of 18 February 1911) Известия Академии Наук, Петроград (Izvestiya Akademii Nauk, Petrograd), 991-998

КОСЕНКО С. К. (KOSENKO S. K).

1953. " К вопросу о вычислении энергии земетрясений " (On the question of earthquake energy calculation). Труды Геофизического института (Trudy Geofizicheskogo Instituta), № 21/148/, 3-15

СОЛОВЬЕВ С. Л. (SOLOVYOV S. L.)

1953. " Применение шкалы интенсивности к Ашхабадскому землетрясению 1948 г." (Application of magnitude scale to the Ashkabad earthquake of 1948). Рукопись. Библиотека Института физики Земли АН СССР. (Unpublished. Library of the Institute of the Physics of the Earth. Moscow)

1955. " О классификации землетряесний по величине их энергии" (On the classification of earthquakes according to their energy). Труды Геофизического института (Trudy Geofizicheskogo Instituta), № 30/157/, 3-21

1956. " О связи энергии и интенсивности землетрясения" (On the relation between energy and magnitude of an earthquake). Известия АН СССР, серия геофизическая, (Isvestiya Akademii Nauk SSSR, seriya geofizicheskaya), № 3, 357-359

1957 (a) "К вопросу о соотношении между энергией об'емных волн и интенсивностью землетрясения" (On the question of correlation between energy of body waves and magnitude of an earthquake). Бюллетень Совета по сейсмологии (Bulletin Sovjeta po seismologii), № 6, 109-121.

1958 (a) "Об изменении с расстоянием амплитуды колебания почвы в поверхностных волнах курило-камчатских землетряеений (Amplitude of ground oscilation in surface waves of Kurile-Kamchatka earthquakes and its variation with distance). Известия АН СССР, серия геофизическая (Isvestiya Akademii Nauk SSSR, seriya geofizicheskaya), № II, 1323-1324.

в печати (b) (in press) 1958 "Некоторые результаты применения шкалы интенсивности землетрясений на сейсмических станциях СССР" (Earthquake magnitude scale and some results of its application at seismological stations of the USSR). Studia Geophysica et Geodaetica.

СОЛОВЬЕВ С.Л., ДЖИБЛАДЗЕ Э.А. (SOLOVJEV S.L., DZHIBLADZE E.A.)

1955. "Об изменении потока сейсмической энергин с эпицентральным расстоянием" (On the changing of the flux of seismic energy with epicentral distance) Известия АН СССР, серия геофизическая, (Isvestiya Academii Nauk SSSR, seriya geofisicheskaya), № 5, 462-463.

СОЛОВЬЕВ С.Л., ШЕБАЛИН Н.В. (SOLOVYOV S.L., SHEBALIN N.V.)
1957. "Определение интенсивности землетрясения по смещению почвы в поверхностных волнах (Earthquake magnitude determination from ground displacement in surface waves). Известия АН СССР, серия геофизическая.

(Isvestiya Akademii Nauk SSSR, seriya geophisicheskaya) N° 7, 926-930.

BÅTH M.
1956. "The problem of earthquake magnitude determination." Un. Geoph. et Geod. Int., Ass. de Seism., Travaux Scient., 19, 5-94.

GUTENBERG B.
1945 a "Amplitudes of surface waves and magnitudes of shallow earthquakes. " Bull. Seism. Soc. Amer., 35, N° 1, 3-12.
1945 b "Amplitudes of P, PP and S and magnitude of shallow earthquakes." Bull. Seism. Soc. Amer., 35, 57-69.

GUTENBERG B. and RICHTER C. F.
1954. " Seismicity of the Eearth and associated phenomena. " Princeton, Princeton University Press.
1956 a "Earthquake magnitude, intensity, energy and acceleration (second paper) ", Bull. Seism. Soc. Amer., 46, N° 2, 105-146.
1956 b "Magnitude and energy of earthquakes." Annali di geofisica, 9, N° 1, 1-15.

JEFFREYS H.
1923. « The Pamir earthquake of 1911 February 18, in relation to to the depths of earthquake foci. « Month. Not. Royal Astr. Soc., Geoph. Suppl., 1, N° 2.
1952. « The Earth ». 3rd ed., Cambrige University Press.

JEFFREYS H. and BULLEN K. E.
1939. « The times of P,S and SKS and velocities of P and S. » Month. Not. Royal Astr. Soc., Geoph. Suppl., 4 N° 7.

LAMB H.
1904. « On the propagation of tremors over the surface of an elastic solid. » Phil. Trans. Royal Soc., London, 203.

ZÁTOPEK A. et VANĚK J.
1952. « Les magnitudes de Praha et leur relation avec les revised values de Pasadena. » Un. Geoph. et Geod. Int., Ass. de Seism., Travaux Scient., 18, 137-152.

ZÖPPRITZ K., GEIGER Z. und GUTENBERG B.
1912. « Über Erdbebenwellen, V ». Nachr. K. Ges. Wiss. Göttingen, Math. phys. Klasse, 123-143.

ENERGY REPRESENTED BY SEISMIC WAVES FROM SMALL EXPLOSIONS

B. F. HOWELL, Jr.

ABSTRACT.

The energy contained in seismic waves may divide unequally into kinetic and potential energy at any point, preventing dependable calculation of energy flux from a seismogram. The case of horizontally polarized shear waves reflected at the surface is developed as a simple example. The energy represented by a seismic pulse of a given amplitude depends also on transmission velocity and, in the case of surface waves, on wavelength, as well as on other less critical factors. Equations showing the penetration of Rayleigh waves are developed in some detail to illustrate this.

. . . .

DIVISION INTO KINETIC AND POTENTIAL ENERGY.

In studying seismograms one of the pieces of information which is frequently sought is the amount of energy released by the original disturbance which caused the observed ground motion. This paper will be concerned with an evaluation of some of the difficulties which must be overcome to estimate energy from the seismogram.

The seismologist measures the motion of the ground at one or more individual points as a function of time. From this he must calculate the flow of energy past his observation station. To obtain the total energy originally released, this calculated energy flux must then be multiplied by a proper geometric factor, determined from a knowledge of the earth's structure.

In doing this, the first difficulty that is encountered is that the seismometer measures only a part of the total energy. At any instant the energy is partly kinetic in the form of velocity of motion of the ground and partly potential in the form of stress of the rock. If only a single wave is present, these two forms of the energy can be shown to be equal at all times, and the total energy present is twice that observed with either a velocity or a strain seismograph (Timoshenko and Goodier, 1951, Chapter 15). However, if more than one pulse is present, interference results, and the ratio of kinetic to potential energy can have any value.

At the surface of the ground, to the approximation that it is a free surface with no stress existing across the surface, the vertical stress components must vanish, and reflected waves will so interfere with incident waves that all energy on the vertical component of motion will be kinetic. This is not the case for waves having a component parallel to the boundary, since the stresses across surfaces perpendicular to the boundary need not vanish.

Interference is easily illustrated by considering the reflection of horizontally polarized shear waves (*Figure* 1). The particle dis-

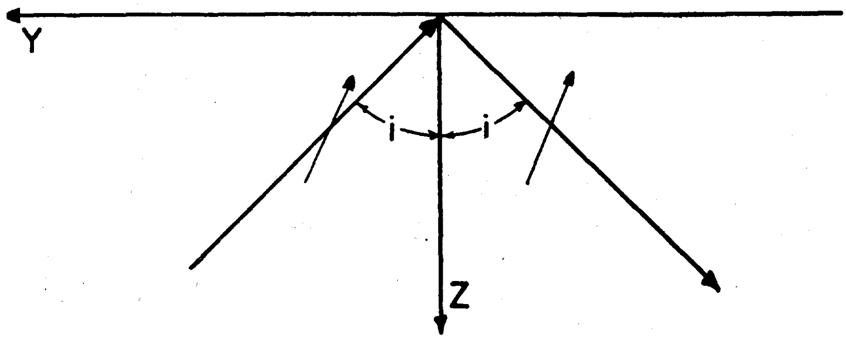

1. Horizontally polarized shear wave reflected at free surface.

placement of such a wave incident on a free surface at an angle i in the yz plane (z downward) with maximum amplitude u_o will be :

$$u_i = u_o \sin p_1 (y \sin i + z \cos i - V_s t) \qquad (1)$$

where $p_1 = 2\pi/$wavelength and V_s is its transmission velocity. The amplitude of the reflected wave will be :

$$u_r = u_o \sin p_1 (y \sin i - z \cos i - V_s t) \qquad (2)$$

The instantaneous kinetic energy of a particle will be

$$E_K = \frac{\rho}{2}\left(\frac{\delta u}{\delta t}\right)^2 = \frac{\rho}{2}\left(\frac{\delta (u_i + u_r)}{\delta t}\right)^2 = \frac{\rho}{2} u_o^2 p_1^2 V_s^2 (A + B)^2 \qquad (3)$$

where u is the total displacement resulting from the incident plus the reflected waves, ρ is the density of the ground and

$$A = \cos p_1 (y \sin i + z \cos i - V_s t) \qquad (4A)$$
$$B = \cos p_1 (y \sin i - z \cos i - V_s t) \qquad (4B)$$

The potential (strain) energy of the particle is (Timoshenko and Goodier, 1951, p. 147) :

$$E_s = \frac{1}{2}\left(X_y \frac{\delta u}{\delta y} + X_z \frac{\delta u}{\delta z}\right) = \frac{\mu}{2}\left[\left(\frac{\delta u}{\delta y}\right)^2 + \left(\frac{\delta u}{\delta z}\right)^2\right]$$
$$= \frac{\mu}{2} u_o^2 p_1^2 [(A + B)^2 \sin^2 i + (A - B)^2 \cos^2 i] \qquad (5)$$

where X_y and X_z are the tractions across the *yz* plane. (For motion in the *x*-direction travelling in the *yz* plane all the other terms of the general equation are zero.) The ratio of the energies is :

$$\frac{E_s}{E_K} = \frac{\mu (A + B)^2 \sin^2 i + (A - B)^2 \cos^2 i}{\rho V_s^2 (A + B)^2} \qquad (6A)$$

Remembering that $V_s{}^2 = \mu/\rho$, and noting that $A = B$ at the surface $z = 0$:

$$\frac{E_{SO}}{E_{KO}} = \sin^2 i \qquad (6B)$$

Therefore, the ratio of shear to kinetic energy can have any value from zero for waves coming directly from below to the expected value of one for waves travelling parallel to the surface.

The proof is less simple for other types of waves, but it is obvious that similar interference must occur. This means that the total energy can not be determined by measurement of velocity alone, or of strain alone, without additional information which generally will not be available. Lacking complete knowledge of the division of energy, one should ideally record with both a strain and a velocity-sensitive seismometer and add the energies calculated from the two records. In practice this is rarely if ever done.

An interesting case of what is believed to be at least in part interference of this sort was recorded by E. Stengel (1954). Figure 2 is a plot of the percentage of the total kinetic energy appearing on each of three perpendicular components of motion as a function of shot depth. The method of computing energies has been described by Howell and Budenstein (1955). The angle of arrival of the waves at the surface was kept fixed within narrow limits. There is a definite oscillation of energy between the different components. Other similar examples could be cited.

These data were all obtained at short distances where the several compressional, shear and surface pulses arrive together. They are presented here as evidence suggesting that interference may alter the apparent strength of an observed pulse in a seismogram. Under natural conditions such as those in which these records were obtained, many other factors, such as shot efficiency and ground inhomogeneities, complicate the results.

EFFECT OF TRANSMISSION VELOCITY

A second factor is the effect of varying velocity of transmission. The various pulses on a seismogram travel at different velocities;

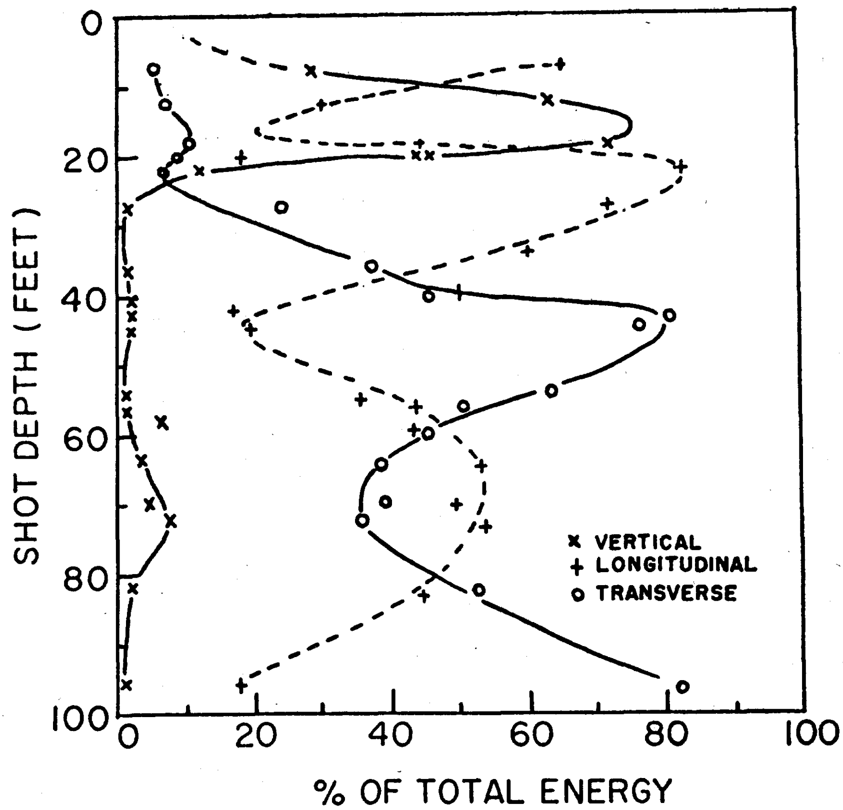

2. Per cent of total energy appearing on individual components.

and in the case of the surface waves, the various parts of one pulse have different transmission velocities because of dispersion. The kinetic energy of a pulse is :

$$E_K = \int_V \frac{\rho v^2}{2}\, dV = \int_A \int_t \frac{\rho v^2}{2}\, C\, dt\, dA \qquad (7)$$

where $C = dx/dt$ is the transmission velocity; v is instantaneous particle velocity; ρ is density; V, the volume of the ground disturbed at any instant; and A, any area thru which the energy flows normally.

Thus, if a seismogram is made with an ideal seismometer whose response characteristic is flat with particle velocity, and if the various pulses, dilatational, shear, and surface waves, all have comparable amplitudes, the dilatational pulse will have the greatest energy density, because of its greatest velocity of transmission. Note for instance the two almost equal pulses at approximatively

$$+\frac{R^2-P^2}{P^4}\left[e^{-2q_1 z}+\frac{4R^4}{(2R^2-S^2)^2}e^{-2q_2 z}-\frac{4R^2}{2R^2-S^2}e^{-(q_1-q_2)z}\right]\sin^2(fx+pt)\Big\}\quad(13)$$

The energy density passing through a vertical slit of unit width would be

$$E_\rho=\int_0^\infty\frac{\rho v^2}{2}dz=\int_0^\infty E_K\,dz$$

$$=\frac{\rho}{2}\Big\{-\frac{R^2}{P^4}\left[-\frac{1}{2q_1}-\frac{(2R^2-S^2)^2}{8q_2R^4}+\frac{2R^2-S^2}{(q_1+q_2)R^2}\right]\cos^2(fx+pt)$$

$$-\frac{R^2-P^2}{P^4}\left[-\frac{1}{2q_1}-\frac{4R^4}{2q_2(2R^2-S^2)^2}+\frac{4R^2}{(q_1+q_2)(2R^2-S^2)}\right]\sin^2(fx+pt)\Big\}\quad(14)$$

Clearing this of q_1 and q_2 and factoring out $V_P^3T/2\pi$, where T is the period of the waves :

$$E_\rho=\frac{\rho V_P^3T}{4\pi}\Big\{\frac{R}{P}\left[\frac{1}{2\left(1-\frac{P^2}{R^2}\right)^{1/2}}+\frac{\left(2-\frac{S^2}{R^2}\right)^2}{8\left(1-\frac{S^2}{R^2}\right)^{1/2}}-\frac{2-\frac{S^2}{R^2}}{\left(1-\frac{P^2}{R^2}\right)^{1/2}+\left(1-\frac{S^2}{R^2}\right)^{1/2}}\right]\cos^2(fx+pt)$$

$$+\left(\frac{R}{P}-\frac{P}{R}\right)\left[\frac{1}{2\left(1-\frac{P^2}{R^2}\right)^{1/2}}+\frac{2}{\left(1-\frac{S^2}{R^2}\right)^{1/2}\left(2-\frac{S^2}{R^2}\right)^2}-\frac{4}{\left(2-\frac{S^2}{R^2}\right)\left[\left(1-\frac{P^2}{R^2}\right)^{1/2}+\left(1-\frac{S^2}{R^2}\right)^{1/2}\right]}\right]\sin^2(fx+pt)\Big\}\quad(15)$$

Thus, the energy passing thru a slit at any instant is a function of the density of the medium, the period and wavelength of the waves, the transmission velocities, and the distance x. If the density of energy flow at the surface is known, the total energy flow per unit of surface width (width measured horizontally along the circumference of the wave front) can be found by multiplying by the factor :

$$F=\frac{E_\rho}{E_0}=\frac{\int_0^\infty\frac{\rho v^2}{2}dz}{\frac{\rho v_0^2}{2}}\quad(16)$$

where E_0 is found from (13) on substitution of $z = 0$:

$$E_0 = \frac{\rho V_p^2}{2} \left\{ \frac{R^2}{P^2} \left[1 + \frac{\left(2 - \frac{S^2}{R^2}\right)^2}{4} - \left(2 - \frac{S^2}{R^2}\right) \right] \cos^2 (fx + pt) \right.$$

$$\left. + \left(\frac{R^2}{P^2} - 1\right) \left[1 + \frac{4}{\left(2 - \frac{S^2}{R^2}\right)^2} - \frac{4}{2 - \frac{S^2}{R^2}} \right] \sin^2 (fx + pt) \right\} \tag{17}$$

Equation (16) can be reduced to the form :

$$\begin{aligned} F &= \frac{V_P\, T}{2\pi} \left[\frac{A + B \sin^2 (fx + pt)}{C + D \sin^2 (fx + pt)} \right] \\ &= \frac{\lambda_P}{2\pi} \left[\frac{A + B \sin^2 (fx + pt)}{C + D \sin^2 (fx + pt)} \right] \end{aligned} \tag{18}$$

where A, B, C, and D are constants depending only on Poisson's ratio, and λ_P is the wavelength of dilatational waves of period T in the medium. Values of F/λ_P are given in Table I.

TABLE 1.

Values of F/λ_P *where* $F = E\rho/E_0$
for various values of Poisson's ratio, σ, *and phase* $(fx + pt)$.
Poisson's ratio.

$sin^2(fx + pt)$	*0.25*	*0.33*	*0.40*	*0.45*	*0.49*
0	0.037	0.039	0.038	0.031	0.016
0.5	0.184	0.188	0.189	0.156	0.080
1	0.252	0.250	0.243	0.197	0.100

These equations bring out a number of important factors. First of all, the "penetration" of Rayleigh Waves is small. The factor by which surface energy density needs to be multiplied to get total energy is on the average of the order of magnitude of 0.15 of a wavelength of dilatational waves, and it fluctuates with time and distance. A large surface amplitude does not mean nearly as much energy for a Rayleigh wave as for a body wave. Howell and Budenstein (1955) have published figures on the energy flux in observed pseudo-Rayleigh waves from small explosions. The figures for the energy found in their study were based on the assumption that the penetration factor, F, equalled one wavelength of Rayleigh waves. Because of this, they were probably too large by a factor of the order of 3.5 ($= \lambda_R/1.5\,\lambda_P$), assuming that the energy of pseudo-Rayleigh waves decreases with depth at the same rate as

0.1 and 0.2 sec on the longitudinal (middle) component of Figure 3. These are the two largest amplitudes on the record. The quantity

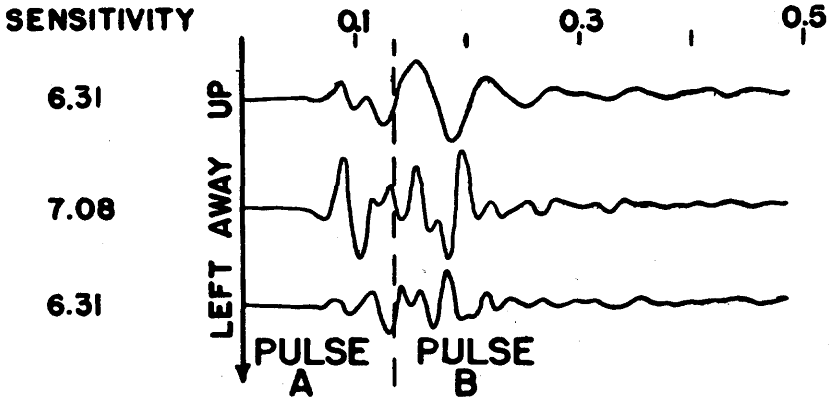

3. Seismogram recorded 90 feet from shot.

$v^2C = v^2x/t$ for the first of these pulses is 5.74 (in/sec)^3 compared to 2.84 (in/sec)^3 for the second, assuming both started from the shot point simultaneously and travelled the same path. Thus, the largest amplitude on a seismogram should be used with caution as a measure of the maximum energy, inasmuch as it may not represent the most energetic pulse.

Effect of Wavelength.

In the case cited above the first pulse was a dilatational pulse spreading radially, whereas the second was part of a coupled wave as defined by Leet (1946). Coupled waves are believed to be either bound waves, confined to a low velocity surface layer by internal reflections, or a form of pseudo-Rayleigh wave representing a higher mode than the first (Howell, 1949; Keller, 1955). In either case, they are spreading thru a different area than that over which the energy of the dilatational pulse is distributed. For a body wave from a shallow source in a homogeneous medium, the total energy can be found from the energy flux by multiplying by the area of a hemisphere whose radius is the distance to the recording location. This is equivalent to assuming that the energy is radiated equally in all directions from a surface source.

In the case of surface waves, the energy flux decreases with depth. Furthermore, it is not a constant, but varies with time and horizontal distance. Note, for instance, what happens in the case of plane Rayleigh waves. For waves travelling in the x-direction, the horizontal and vertical particle displacements are, in complex notation (Byerly, 1942) :

$$u = \frac{if}{h^2}\left\{ -e^{-q_1 z} + \frac{2q_1 q_2}{f^2 + q_2^2} e^{-q_2 z} \right\} e^{i(fx+pt)} \tag{8A}$$

$$w = \frac{q_1}{h^2}\left\{ e^{-q_1 z} - \frac{2f^2}{f^2 + q_2^2} e^{-q_2 z} \right\} e^{i(fx+pt)} \tag{8B}$$

where :

$$f = \frac{p}{V_R} = \frac{2\pi}{\lambda_R \ V_R} = pR \tag{9A}$$

$$h = \frac{p}{V_P} = pP \tag{9B}$$

$$k = \frac{p}{V_S} = pS \tag{9C}$$

$$q_1^2 = f^2 - h^2 = p^2 (R^2 - P^2) \tag{9D}$$

$$q_2^2 = f^2 - k^2 = p^2 (R^2 - S^2) \tag{9E}$$

and V_R, V_P and V_S are the transmission velocities of Rayleigh, dilatational and shear waves respectively in the medium, and λ_R is the wavelength of the waves.

In this notation the existence equation for Rayleigh waves is :

$$(2 R^2 \quad S^2)^2 = 4R^2 (R^2 - S^2)^{\frac{1}{2}} (R^2 - P^2)^{\frac{1}{2}} \tag{10}$$

The instantaneous particle velocities are, using (9) to simplify the notation, and reducing to sine-cosine notation :

$$\frac{\delta u}{\delta t} = \frac{R}{P^2}\left\{ e^{-q_1 z} - \frac{2 (R^2 \quad P^2)^{\frac{1}{2}} (R^2 - S^2)^{\frac{1}{2}}}{2R^2 - S^2} e^{-q_2 z} \right\}$$
$$(\cos (fx+pt) + i \sin (fx + pt)) \tag{11A}$$

$$\frac{\delta w}{\delta t} = \frac{(R^2 - P^2)^{\frac{1}{2}}}{P^2}\left\{ e^{-q_1 z} - \frac{2R^2}{2R^2 - S^2} e^{-q_2 z} \right\}$$
$$(- \sin (fx + pt) + i \cos (fx + pt)) \tag{11B}$$

The kinetic energy of a unit volume is

$$E_K = \frac{\rho v^2}{2} = \frac{p}{2}\left[\left(\frac{\delta u}{\delta t}\right)^2 + \left(\frac{\delta w}{\delta t}\right)^2\right] \tag{12}$$

Substituting the real part of (11) in (12) and using (10) to simplify the result :

$$E_K = \frac{\rho}{2}\left\{ \frac{R^2}{P^4} \left[e^{-2q_1 z} + \frac{(2R^2 - S^2)^2}{4R^4} e^{-2q_2 z} - \frac{2R^2 \quad S^2}{R^2} e^{-(q_1+q_3) z} \right] \right.$$
$$\cos^2 (fx+pt)$$

derived above for true Rayleigh waves. A corrected table for the energies spreading from small explosions is shown in Table II.

TABLE II.

Energy in seismogram pulses.
(From explosions of 0.5 kg. dynamite, releasing approx. 2 × 10^{13} ergs.)

Energy in ergs				
Surface distance in feet	Pulse A (dilatational)	Pulse B (coupled)	Pulse C (pseudo-Rayleigh)	Ratios A:B:C
10	850 $\times 10^9$	170 $\times 10^9$	—	5.0 :1: —
40	1150 $\times 10^9$	180 $\times 10^9$	—	6.2 :1: —
70	530 $\times 10^9$	270 $\times 10^9$	—	2.0 :1: —
150	47 $\times 10^9$	33 $\times 10^9$	—	1.4 :1: —
180	46 $\times 10^9$	10 $\times 10^9$	6.9 $\times 10^9$	4.6 :1:0.69
400	0.17 $\times 10^9$	0.58 $\times 10^9$	1.4 $\times 10^9$	0.30:1:2.4
450	0.38 $\times 10^9$	2.3 $\times 10^9$	2.7 $\times 10^9$	0.16:1:1.2
500	—	0.56 $\times 10^9$	1.2 $\times 10^9$	— :1:2.1
700	—	0.13 $\times 10^9$	0.83 $\times 10^9$	— :1:6.4
1000	—	0.12 $\times 10^9$	0.16 $\times 10^9$	— :1:1.3
1172	—	.0048 $\times 10^9$	0.03 $\times 10^9$	— :1:6.0

On the basis of data supplied by the manufacturer, the chemical energy released by the dynamite was of the order of magnitude of 2 × 10^{13} ergs each shot. The most energy estimated from any seismic pulse was about 5 % of this.

Another factor shown by Equation 18 is that the amplitude being the same, long wavelengths tend to carry more energy than short wavelengths. Thus, in estimating the energy of a complex-waveform surface wave, short, wavelength energy can be neglected unless it is of large amplitude, but it is less often safe to neglect weak long wavelengths.

The actual seismogram trace is the sum of many frequencies arriving simultaneously, and separation of the energy on the basis of wavelength may be difficult. Fortunately, however, nature helps us here. The earth acts as a filter tending to attenuate high frequencies faster than low frequencies. Figure 4 shows relative amplitude as a function of frequency at different distances as observed by Andrews (1957). Thus at large distances, one frequency or a narrow band of frequencies generally predominates.

Equation 18 was derived for plane waves, and can be expected to represent a good approximation for waves from point sources only at large distances. It may take surface waves several wavelengths of travel to develop their typical characteristics. The importance of this in studying energies is uncertain. Furthermore, at short distances the surface and body waves tend to arrive simultaneously. Indeed it is the incidence of the body waves on the surface which

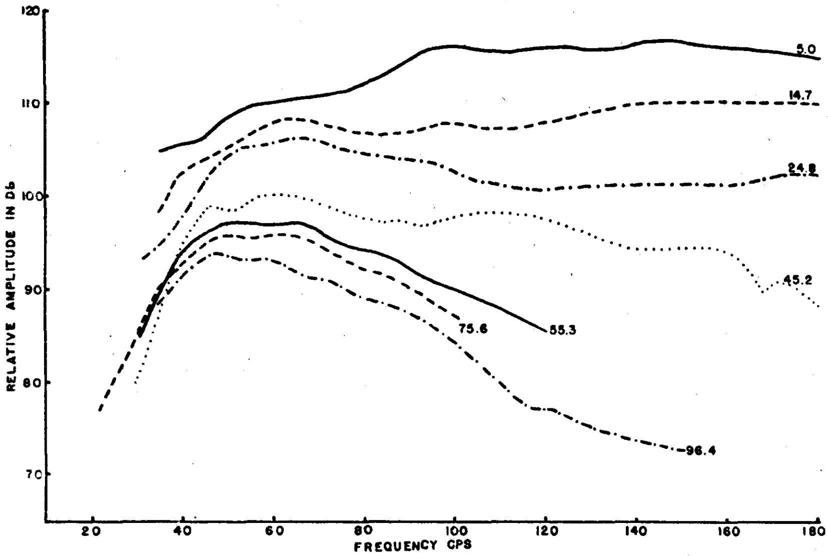

FIGURE 10. FREQUENCY SPECTRA OF VERTICAL COMPONENT RECORDED BY MB4210

4. Frequency spectra of vertical component of ground motion at various distances from a surface impact source.

are presumed to produce the surface waves, and until the two become separated in time, their very existence as separate phenomena is hard to define.

TABLE III.

Observed attenuation constants based on the formula $E = E_0 x^{-A} e^{-ax}$ *where* A *has the value 2 for a body wave, 1 for a surface wave.*

PULSE	AREA	A	*a*
Body waves	Haugh farm	2	.019/FOOT
Coupled waves	Haugh farm	1	.011/FOOT
Pseudo-Rayleigh waves	Haugh farm	1	.0053/FOOT
Total pulse, 0-375 FT.	University Farms	1	.010/FOOT
Refracted pulse, 800-3070 FT.	University Farms	2	.00010/FOOT

Data from Howell and Budenstein (1955) and Howell and Kaukonen (1954).

OTHER SOURCES OF UNCERTAINTY.

Attenuation with distance results from many factors. Absorption appears to be small in the deep interior of the earth, but is large in the soft, near-surface layers (Table III). Loss by reflection and scattering is also of importance. Because of this, energies calculated from (7) are only lower limits of true total energy, and must be increased by appropriate factors. Attenuation factors such as those shown in Table III probably apply only at distances large compared to a wavelength, so do not provide an accurate means of calculating the original energy at the source. However, they have the advantage that they are easily obtained by recording the motion from one source at several distances, and they lump all losses including scattering and viscous losses into two factors, an exponential loss and a radial spreading.

The remaining sources of inaccuracy in calculating seismic energy from (7) probably are less important than those discussed so far. These sources of inaccuracy include the limited frequency spectrum recorded by seismometers, uncertainties as to ground density, and effects of geologic structure on spreading factor. Low frequencies may be missed by seismometers, high frequencies by galvanometers. Accurate corrections for low response can enlarge the useful range only a small amount in most cases. Uncertainties as to the value of density of the ground are generally less than the scatter of most recorded data. The effect of geologic structure on altering the spreading factor is more complex. In general, velocity increase with depth will have a tendency to refract energy upward, and hence near a source may tend in part to compensate for scattering and reflection losses.

In summary, the most that can be expected of measurements of the flow of seismic energy past a point is a rough estimate of the order of magnitude of the energy flux. However, with proper care to evaluate the effects of the factors discussed above, reasonably accurate comparisons of the energy under similar circumstances should be possible. The author has used equation (7) to evaluate total energy particularly in determining attenuation rates of seismic waves in earth materials (Table III; Howell and Budenstein, 1955; Howell and Kaukonen, 1954). Because of high attenuation rates and the complexities of the structure of the earth, pulse shape changes rapidly with transmission. Individual pulses are hard to follow, particularly when dispersion is present. Summation of the total energy of a pulse rather than observation of peak energies is a useful alternative approach.

ACKNOWLEDGMENTS.

Equipment and funds for the conduct of this research were generously provided by the National Science Foundation and the Office of Naval Research, whose support is gratefully acknowledged. The assistance of the various members of the staff of the Department of Geophysics and Geochemistry, especially Mr. A. B. Andrews, Mr. J. A. Ryan and Mr. E. Stengel, who helped gather the data presented above, is sincerely appreciated.

REFERENCES.

ANDREWS (A. B.), 1957 : Frequency dependence of seismic wave attenuation : unpublished Ph. D. thesis, Penna. State Univ.
BYERLY (P.), 1942 : Seismology, Prentice-Hall.
HOWELL (B. F.) Jr., 1949 : Ground vibrations near explosions : Bull. Seis. Soc. Am. 34 : 285-310.
HOWELL (B. F.) Jr.; BUDENSTEIN (D.), 1955 : Energy distribution in explosion-generated seismic pulses : Geophysics 20 : 33-52.
HOWELL (B. F.) Jr.; KAUKONEN (E.), 1954 : Attenuation of seismic waves near an explosion : Bull. Seis. Soc. Am. 44 : 481-492.
KELLER (G. V.), 1955 : Dispersion of seismic waves near a small explosion : Trans. Am. Geoph. Union 36 : 1035-1043.
LEET (L. D.), 1946 : Earth motion from the atomic bomb test : American Scientist 34 : 198-211.
STENGEL (E.), 1954 : The effect of shot depth on the generation of seismic energy : unpublished M. S. thesis, Penna. State Univ.
TIMOSHENKO (S.); GOODIER (J. N.), 1951 : Theory of elasticity, 2nd Ed. : McGraw Hill.

CONTRIBUTION AU PROBLÈME DES MAGNITUDES UNIFIÉES

Par V. KÁRNÍK[1], J. VANĚK[1] et A. ZÁTOPEK[2], Praha (Tchécoslovaquie).

Introduction.

L'importance de la magnitude pour l'étude de la séismicité aussi bien que pour la recherche de l'énergie des séismes et pour la solution des problèmes concernant la structure de la croûte terrestre, a de loin dépassé les limites de son application primitive. En introduisant le rapport des amplitudes et périodes du mouvement réel du sol, on a donné à la magnitude une relation immédiate aux procédés physiques qui se passent dans le foyer et au cours de la propagation des ondes séismiques dans l'intérieur de la Terre.

Au cours des recherches de ces dernières années on a constaté et analysé la divergence des trois étalons utilisés pour la détermination de la magnitude, c'est-à-dire l'échelle originale de Richter [1], puis celle de Gutenberg [2], basée sur les amplitudes maximum des ondes superficielles des téléséismes, et enfin celle qui a été introduite par le même auteur [3, 4] et qui repose sur les amplitudes des ondes préliminaires **P**, **PP** et **S**.

Les récentes analyses faites par Gutenberg et Richter [5, 6, 7] et par Båth [8, 9] nous démontrent que la magnitude **M** représente une fonction compliquée de l'amplitude **A** de l'onde en considération, de sa période **T**, de la distance épicentrale Δ et d'une « fonction d'étalonnage » que nous désignons par β qui, en général, elle-même dépend de la distance épicentrale, de la période et du coefficient d'absorption de l'onde en question. Pour éviter les complications provenant de l'existence de plusieurs échelles différentes, Gutenberg et Richter ont proposé l'introduction d'une magnitude unifiée [6, 7, 10].

La présente communication veut passer en revue les principaux résultats des recherches sur la magnitude entreprises à la station de Praha (50°04′,2 N, 14°26′,0 E). Ensuite, nous présenterons quelques propositions qui se rapportent aux problèmes des magnitudes unifiées et à la prochaine étude de la magnitude en général.

1. Institut de Géophysique de l'Académie Tchécoslovaque des Sciences.
2. Institut de Géophysique de l'Université Charles.

I. Les magnitudes de Praha et leurs corrections.

a) *Généralités.* A la station de Praha, on a déterminé les magnitudes depuis 1949 à l'aide des amplitudes horizontales maximum des ondes superficielles possédant la période de 20 secondes environ et pour les distances entre 15° et 160° (voir [11]). On a analysé aussi les différences entre les valeurs obtenues des magnitudes et les « revised values » de Pasadena et leur distribution régionale. Une année plus tard, on a commencé à déterminer la magnitude des séismes à profondeur normale de foyer aussi pour les ondes préliminaires **P**, **PP** et **S**, en utilisant le rapport **A/T** des amplitudes et des périodes. La communication correspondante [12], comprenant une analyse assez détaillée des résultats obtenus, a été publiée en 1955. En étudiant les amplitudes et périodes des séismes européens depuis 1954, on a étendu l'application du rapport **A/T** aux séismes dont la distance épicentrale varie entre 1° et 30° (voir [13, 14]). On a employé la phase portant le maximum d'énergie, à savoir, suivant la distance épicentrale, l'onde **Sg** ou **L**.

Par conséquent, on dispose à Praha de méthodes qui permettent, au moins pour les séismes à profondeur normale de foyer, de calculer la magnitude pour chacune des distances entre 1° et 160°. Dans la plus grande partie de cet intervalle on peut comparer plusieurs valeurs qui en résultent pour les ondes individuelles. L'erreur probable de la détermination des magnitudes est presque la même pour toutes les ondes utilisées, c'est-à-dire **SgH**, **MH**, **PH**, **PV**, **PPH** et **SH** respectivement, et égale à un quart de l'unité de magnitude.

Dans le dernier temps nous avons unifié les méthodes de détermination de la magnitude, pour toutes les ondes mentionnées. On a défini — avec une précision égale à celle des déterminations précédentes — la magnitude **M** en fonction du rapport **A/T** à l'aide d'une équation générale

$$\mathbf{M} = \log(\mathbf{A/T}) + \beta(\Delta, \mathbf{T}) + \Sigma\delta\mathbf{M}, \tag{1}$$

où les signes se rapportent à l'onde et la composante (horizontale ou verticale) en question. La « fonction d'étalonnage » $\beta(\Delta, \mathbf{T})$ est donnée en forme de tables ou de graphiques pour chaque onde et composante (voir *fig.* 1). La somme $\Sigma\delta\mathbf{M} = \delta\mathbf{M}^s + \delta\mathbf{M}^h + \delta\mathbf{M}^r + \mathbf{D}$ comprend les corrections dont seulement la constante de station $\delta\mathbf{M}^s$ et la correction $\delta\mathbf{M}^h$ pour la profondeur du foyer, s'il s'agit des ondes superficielles, sont impliquées dans les magnitudes publiées dans les bulletins de Praha. Les deux dernières corrections sont plutôt d'un caractère statistique : La correction régionale $\delta\mathbf{M}^r$ se rapporte à la région épicentrale et la correction individuelle **D** est une valeur à l'aide de laquelle on exprime des irrégularités qui ne sont pas comprises dans les corrections précédentes. Elles ne sont utilisées que pendant des recherches spéciales.

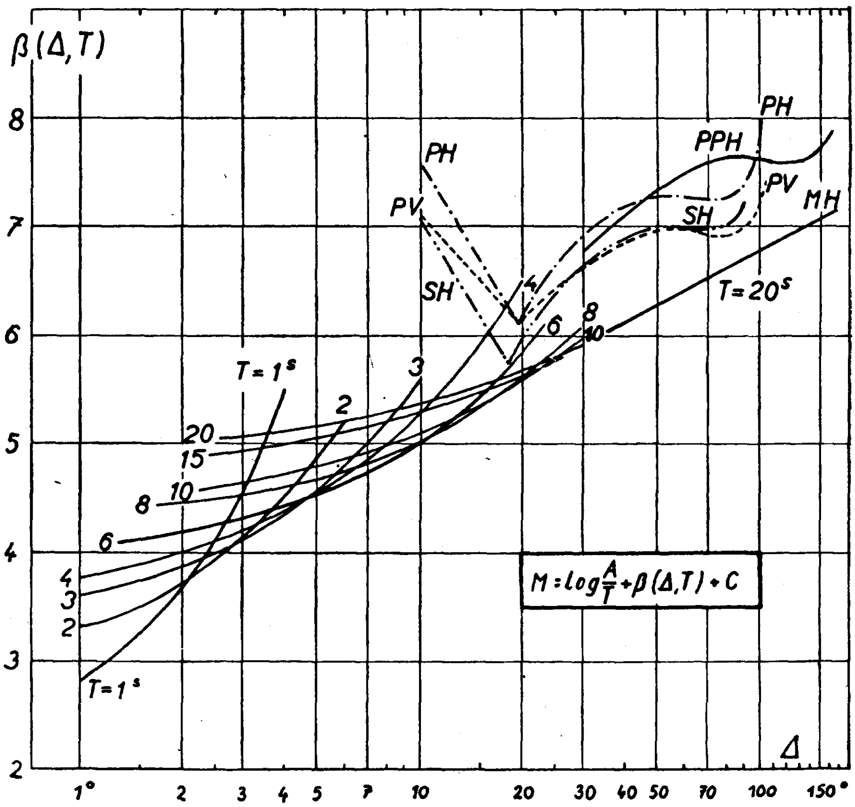

FIG. 1. Les courbes $\beta(\Delta, \mathbf{T})$.

b) *La fonction* β $(\Delta, \mathbf{T})$. La phase portant le maximum d'énergie correspond à l'onde **Sg** quand la distance épicentrale est inférieure à 6° environ. Si $\Delta > 6°$, le maximum d'énergie passe dans la phase **L** (voir [13], p. 405). Pour les deux ondes on a trouvé

$$\beta(\Delta, \mathbf{T}) \;=\; \log(\mathbf{B}_0/\mathbf{T}) + 1/2 \log(\Delta_0/\Delta) - 0{,}434\, \mathbf{k}(\mathbf{T})\, (\Delta - \Delta_0).\; 111{,}1 \qquad (2)$$

où $\mathbf{B}_0/\mathbf{T} = \mathbf{B}(\Delta_0)/\mathbf{T}$, Δ_0 étant une distance d'étalonnage (p.e. 1°), $\mathbf{k}(\mathbf{T})$ représente le coefficient d'absorption en fonction de la période $\mathbf{T}$.

Les valeurs de —log ($\mathbf{B}_o/\mathbf{T}$) pour $\Delta_o = 1°$ sont représentées dans la table 1.

TABLE 1.

T sec	1	2	3	4	6	8	10	15	20
—log ($\mathbf{B}_0/\mathbf{T}$)	(2,65)	(3,16)	3,44	3,62	3,82	4,04	4,22	4,56	4,67

En confrontant les valeurs de **k(T)** publiées par plusieurs auteurs pour diverses périodes **T** on a trouvé une relation approchée

$$-\log \mathbf{k}(\mathbf{T}) = 1{,}42 \log \mathbf{T} + 1{,}78 \qquad (3)$$

Les observations montrent que les périodes de l'onde portant le maximum d'énergie grandissent avec la distance épicentrale. Cet accroissement se produit par sauts; voir [13], p. 450.

Pour les ondes **MH** et les distances entre 15° environ et 160°, les périodes étant voisines de 20 secondes, β devient une fonction d'une seule variable Δ. Dans ce cas-là on tire de l'équation (1) du mémoire [11]

$$\beta(\Delta) = 1{,}66 \log \Delta + 3{,}12 \qquad (4)$$

Remarque : Tenant compte du fait que la correction $\delta\mathbf{M}^s$ pour les ondes superficielles est comprise dans les magnitudes de Praha, on l'a ajoutée dans la fig. 1 à la valeur de la fonction β. On a donc dans la figure, $\delta\mathbf{M}^s$ étant 0,33 pour les ondes **MH**, au lieu de β

$$\beta' = 1{,}66 \log \Delta + 3{,}45 \qquad (4)$$

Une transformation correspondant à la forme de l'équation (1) a été effectuée sur les courbes respectives $\mathbf{B}(\Delta)$ du mémoire [12] (voir [12], pp. 96, 97 et 102, fig. 2, 3, 4 et 8), trouvées pour les ondes **PH, PPH, SH** et **PV** d'après les observations de la station de Praha. On en obtient

$$\beta(\Delta, \mathbf{T}) = \mathrm{B}(\Delta) + 0{,}1\,\mathbf{M}^* \qquad (5)$$

où par **M*** on a désigné une magnitude moyenne déduite de beaucoup d'observations dans un intervalle statistique des Δ qui contient la distance considérée. Les courbes pour **PH** et **PV** sont valables pour les distances 10° à 100° environ. La courbe pour **SH** est applicable entre 10° et 85° environ et celle pour **PPH** entre 20° et 160° environ. Toutes ces courbes ont été étalonnées directement ou indirectement à l'aide des valeurs de magnitude données par GUTENBERG et RICHTER dans le livre « Seismicity of the Earth and Associated Phenomena » [15] et des « revised values », publiées dans les bulletins de Pasadena. Ces valeurs-ci ont été considérées comme un standard d'où on a déduit les valeurs de $\delta\mathbf{M}^s$.

Les courbes $\beta(\Delta, \mathbf{T})$ représentées sur la fig. 1 se rapportent aux séismes à profondeur normale de foyer. On traitera les corrections par rapport à la profondeur dans le paragraphe suivant.

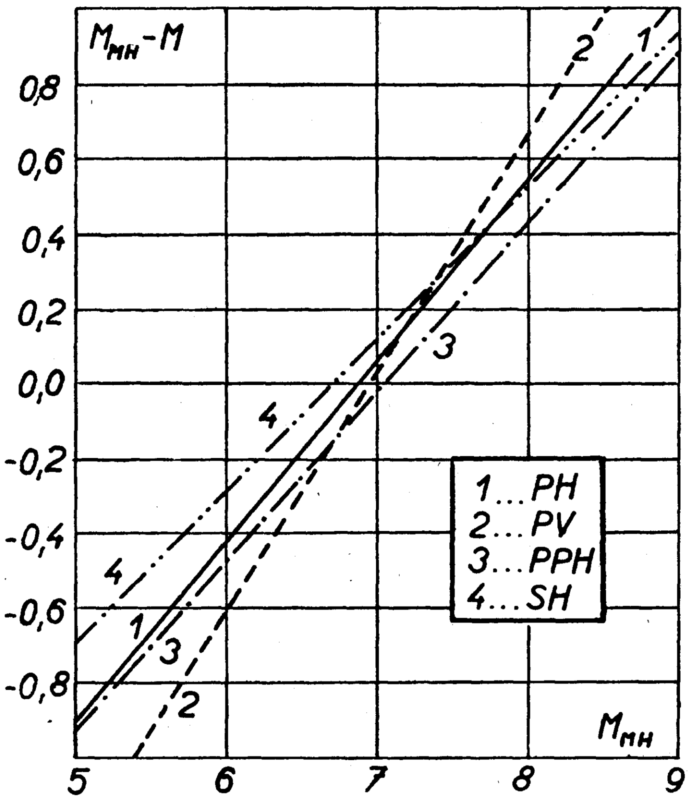

Fig. 2. La relation entre les magnitudes respectives déterminées à l'aide de **PH**, **PV**, **PPH** et **SH** et les magnitudes $\mathbf{M}_{MH}$.

c) Quelques remarques sur les corrections $\delta\mathbf{M}$.

1° La constante de station $\delta\mathbf{M}^s$ (désignée dans la littérature généralement par **C**) caractérise pour chaque onde en question l'effet des conditions locales dans le sous-sol de la station et de son appareillage. A la station de Praha ses valeurs résultent, par rapport au standard choisi, d'un procédé statistique (voir [11, 12, 13]) avec la supposition que les sommes des corrections régionales $\delta\mathbf{M}^r$ et des corrections individuelles **D** donnent zéro pour un nombre de séismes assez élevé. La table 2 présente les valeurs de $\delta\mathbf{M}^s$ pour les ondes utilisées :

TABLE 2.

Onde	SgH et LH	MH	PH	PV	PPH	SH
δM^s	0,26 +	+0,33	+ 0,18	+ 0,07	+ 0,22	+ 0,27

2° Les corrections $\delta \mathbf{M}^h$ pour la profondeur h du foyer ont été trouvées tentativement pour les ondes superficielles et $\mathbf{h} < 200$ km. On a obtenu (voir aussi [13], p. 442)

$$\delta \mathbf{M}^h = 0{,}011\ (\mathbf{h} - 20) \text{ pour } 10° < \Delta < 25° \qquad (6)$$

et

$$\delta \mathbf{M}^h = 0{,}004\ (\mathbf{h} - 20) \text{ pour } \Delta > 50°$$

(**h** en kilomètres).

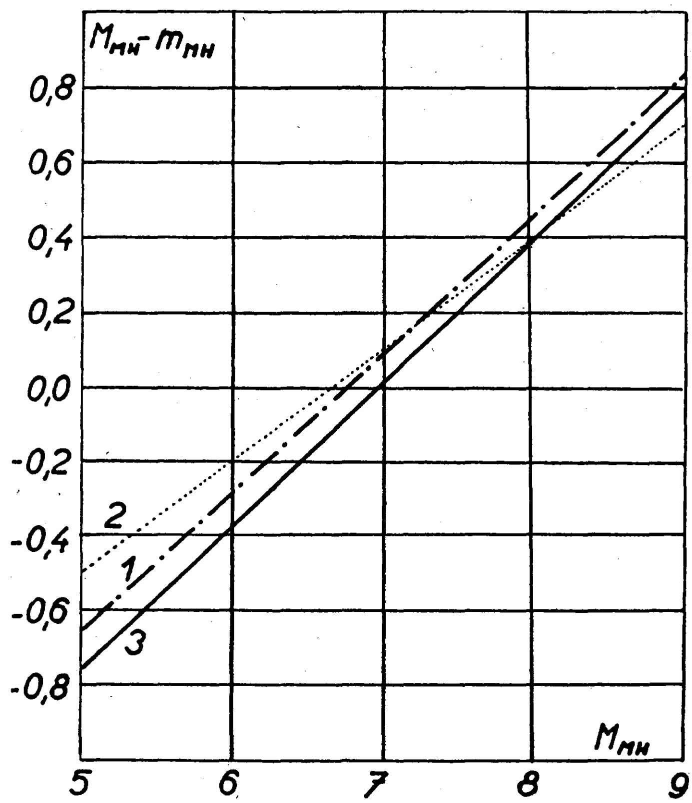

FIG. 3. La relation entre les résidus $\mathbf{M}_{MH} - \mathbf{m}_{MH}$ et la magnitude $\mathbf{M}_{MH}$: *1* la relation de GUTENBERG et RICHTER, 2 ajustement préliminaire et 3 définitif des données de Praha par les auteurs.

Les valeurs déduites de la première équation sont en accord avec celles trouvées par BÅTH [8], mais la deuxième formule donne une correction qui ne fait approximativement qu'une moitié de la valeur déterminée par BÅTH et attendue d'après la théorie. Notre correction est donc limitée à la station de Praha, où elle mène à des valeurs

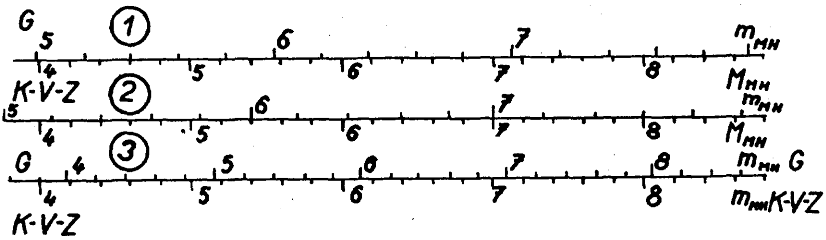

FIG. 4. Les échelles de réduction des $\mathbf{M}_{MH}$ et $\mathbf{m}_{MH}$: *1* (**G**) GUTENBERG et RICHTER, *2* (**K-V-Z**) les présents auteurs, *3* la relation des échelles (**G**) et (**K-V-Z**).

de magnitude bien concordantes avec celles de Pasadena. Les causes de cette anomalie sont probablement dues aux conditions géologiques et sont encore l'objet d'étude. Il en est de même avec les corrections $\delta\mathbf{M}^{h}$ pour les ondes **P**, **PP** et **S** que l'on veut tirer directement des observations faites à la station. Préliminairement on se sert de corrections déduites à l'aide des courbes Q données par GUTENBERG dans le mémoire [7], pp. 5 et 6.

3° Les corrections régionales $\delta\mathbf{M}^{r}$ ont été étudiées de différents aspects par plusieurs auteurs (GUTENBERG [2], PETERSCHMITT [16], ZÁTOPEK et VANEK [11, 12], BÅTH [8] et SOLOVIEV [17]. On a constaté que certaines régions sont caractérisées par des différences systématiques entre les magnitudes de diverses stations. A l'Assemblée générale de l'U.G.G.I. de Bruxelles en 1951 deux de nous ont présenté une analyse de la répartition régionale des différences entre les valeurs des magnitudes $\mathbf{M}_{MH}$ de Praha et les « revised values » de Pasadena et nous avons proposé d'utiliser les différences de ce genre, déterminées dans un réseau convenable de stations et liées à une station considérée comme normale, à l'étude de la structure de l'écorce terrestre. Nous sommes convaincus encore aujourd'hui que l'application de cette méthode pourrait conduire à des résultats intéressants.

4° Dans la correction individuelle **D** nous supposons réunis les effets du mécanisme du tremblement, des anomalies de la distribution azimuthale de l'énergie et d'autres irrégularités pendant la propagation de l'onde en question. On n'a pas encore systématiquement étudié cette correction, mais il est clair que par sa détermination dans un réseau de stations convenablement situées on pourrait gagner des informations précieuses en étudiant les particularités des séismes individuels. Un des problèmes qui se posent est p.e. la distribution de l'énergie d'un séisme dans les diverses phases, mais il y en a beaucoup de cette espèce.

II. La relation des magnitudes déduites des ondes préliminaires avec celles qui ont été déterminées a partir des ondes superficielles.

La divergence des échelles respectives de magnitudes — qui ne coïncident que dans le voisinage du point $\mathbf{M} = 6\ 3/4$ — constatée et étudiée parallèlement par Gutenberg et Richter [5, 6, 7] et Båth [8, 9] a été observée aussi à Praha. En corrélant un ensemble de 196 valeurs $\mathbf{M}_B$ (= magnitudes déterminées à l'aide des ondes préliminaires) avec les valeurs correspondantes $\mathbf{M}_{MH}$, calculées à l'aide des ondes superficielles **MH**, un de nous a trouvé l'expression préliminaire

$$\mathbf{M}_B = 0{,}7\ \mathbf{M}_{MH} + 2 \text{ ou bien } \mathbf{M}_{MH} - \mathbf{M}_B = 0{,}3\ (\mathbf{M}_{MH} - 6.67) \ldots . \quad (7)$$

Cette relation représente une analogie avec l'équation donnée par Gutenberg et Richter [5, 6, 7] qui dans sa forme originale s'écrit [5] dans notre notation

$$\mathbf{M}_{MH} - \mathbf{M}_B = 0{,}4\ (\mathbf{M}_{MH} - 7) \quad (8)$$

et a été révisée plus tard en forme

$$\mathbf{M}_B = 0{,}63\ \mathbf{M}_{MH} + 2{,}5,$$

autrement écrit,

$$\mathbf{M}_{MH} - \mathbf{M}_B = 0{,}37\ (\mathbf{M}_{MH} - 6{,}76). \quad (8a)$$

En ce qui concerne la corrélation des magnitudes respectives $\mathbf{M}_{PH}$, $\mathbf{M}_{PV}$, $\mathbf{M}_{PPH}$ et $\mathbf{M}_{SH}$ avec la magnitude $\mathbf{M}_{MH}$, nous avons trouvé, en bon accord avec Båth, des relations de la forme

$$\mathbf{M}_{MH} - \mathbf{M} = \mathbf{a}\ (\mathbf{M}_{MH} - \mathbf{b}), \quad (9)$$

où, pour l'instant, **M** signifie la magnitude correspondante à l'onde préliminaire considérée; *a* et *b* sont des constantes. La table 3 présente leurs valeurs numériques avec la fréquence *n* de cas étudiés. Les droites correspondantes sont représentées sur la fig. 2. Pour comparaison, la table 3 contient aussi les valeurs de **a** et **b**, publiées par Båth [8] pour les stations suédoises d'Uppsala et de Kiruna.

Table 3.

	PRAHA			UPPSALA			KIRUNA		
Onde	a	b	n	a	b	n	a	b	n
PH	0,494	6,90	137	0,46	6,3	24	0,50	8,5	30
PV	0,647	6,95	70	0,45	6,4	76	0,59	6,2	100
PPH	0,452	7,05	60	—	—	—	—	—	—
SH	0,401	6,71	139	0,23	5,6	71	0,30	6,1	94

En se servant d'un ensemble élargi, formé des 469 paires de magnitudes, on a pu réviser la formule (7). On a obtenu par l'ajustement

$$\mathbf{M}_B = 0{,}611\ \mathbf{M}_{MH} + 2{,}73 \text{ ou } \mathbf{M}_{MH} - \mathbf{M}_B = 0{,}389\ (\mathbf{M}_{MH} - 6{,}98)\ .\ .\ (10)$$

Il faut remarquer que la stabilité statistique de la première constante dans l'équation (10) dépend sensiblement — même pour les ensembles très nombreux — du rapport centésimal dans lequel y sont représentées les magnitudes du type **P** et celles du type **S**. La cause en est que la constante **a** est pour les ondes **SH** notablement inférieure à celle pour les ondes du type **P**.

L'accord de la formule (10) avec la relation (8a) de GUTENBERG et RICHTER est très satisfaisant. Les $\mathbf{M}_B$ calculées suivant l'équation (10) sont un peu supérieures à celles qui ont été déterminées selon (8a); la différence — qui fait 0,13 unités de magnitude $\mathbf{M}_B$ pour $\mathbf{M}_{MH} = 5$ — diminue avec l'accroissement des magnitudes et devient 0,08 pour $\mathbf{M}_{MH} = 8$. L'application d'une constante moyenne $\delta\mathbf{M}'$ qui pour notre ensemble des ondes préliminaires se situe (voir tab. 2) entre 0,1 et 0,2 conduit à une concordance presque absolue des valeurs réduites d'après le procédé de Praha et celles qui ont été calculées d'après GUTENBERG et RICHTER. La fig. 3 montre la relation des valeurs calculées d'après les équations (8a) — (droite 1), (10) — (droite 3) et (7) — (droite 2). La dite corrélation peut être utilisée à une réduction des magnitudes $\mathbf{M}_{MH}$ aux valeurs « équivalentes » (c'est-à-dire à celles des ondes préliminaires) que nous désignerons par $\mathbf{m}_{MH}$ au lieu de $\mathbf{M}_B$. En se servant de la fig. 4 on peut effectuer la dite réduction par voie graphique.

En réduisant les $\mathbf{M}_{MH}$ selon la formule (10) nous éliminons la divergence des échelles pour les ondes préliminaires et les ondes superficielles; nous unifions les deux échelles. Nous avons vu que cette unification est pratiquement égale avec celle d'après la formule (8a) de GUTENBERG et RICHTER; autrement dit on peut unifier les $\mathbf{M}_{MH}$ de la station de Praha à l'aide de cette formule.

III. LES MAGNITUDES UNIFIÉES DE LA STATION DE PRAHA.

D'après la définition de GUTENBERG et RICHTER (p.e. [6, 7].) on calcule la magnitude unifiée *m* en formant le premier moment statistique des valeurs $\mathbf{M}_B$ et $\mathbf{m}_{MH}$, la dernière valeur étant tirée de l'équation (8a).

On a donc dans le cas, si seulement les $\mathbf{M}_B$ sont à la disposition, $\mathbf{m} = \mathbf{m}_B$, où $\mathbf{m}_B$ est la valeur moyenne des $\mathbf{M}_B$ utilisées. Si au contraire on ne dispose que de valeurs $\mathbf{M}_{MH}$, on obtient $\mathbf{m} = \mathbf{m}_{MH}$. Il est naturel que les magnitudes unifiées puissent posséder des poids statistiques différents suivant le nombre des ondes qui ont été prises pour leur calcul.

A Praha, on se sert pour la réduction de $\mathbf{M}_{MH}$ de l'équation (10) au lieu de (8a). Nous avons vu que cette circonstance ne joue pratiquement aucun rôle pendant la réduction de **MH**; si nous disposons en outre de plusieurs valeurs de $\mathbf{M}_B$, les différences des valeurs **m** calculées selon (8a) et (10) ne sont que quelques centièmes de l'unité de magnitude.

Nous avons appliqué le procédé à l'ensemble de 235 tremblements choisis (voir [12]) que nous avons utilisé pour la recherche sur les magnitudes des ondes **P**, **PP** et **S** ([12], pp. 112-130, tables I-III). La figure 5, représentant les résidus correspondants $\mathbf{m}_B - \mathbf{m}$ en

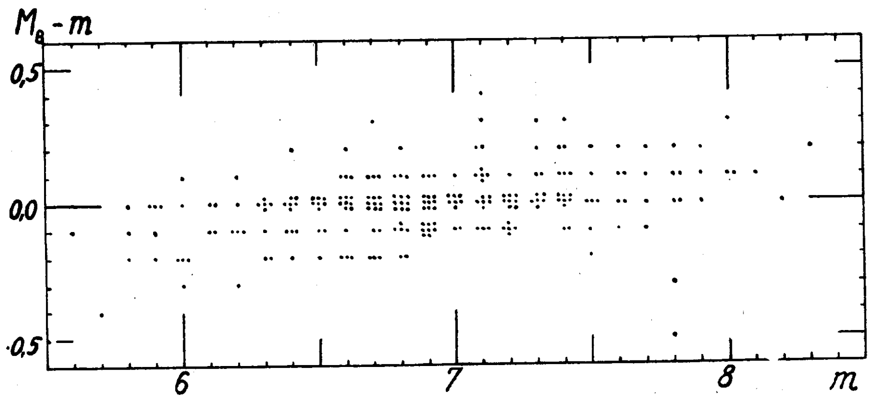

FIG. 5. Les résidus $\mathbf{m}_B - \mathbf{m}$ en corrélation avec les magnitudes unifiées **m**.

corrélation avec les **m**, démontre une coïncidence excellente des valeurs $\mathbf{m}_B$ avec les magnitudes unifiées : 46 % de résidus sont zéros et les résidus possédant les valeurs — 0,1, ± 0,0 et + 0,1 comprennent en tout 82 % de l'ensemble entier. La dispersion des résidus analogues $\mathbf{m}_{MH} - \mathbf{m}$ se montre beaucoup plus considérable : la valeur ± 0,0 n'appartient qu'à 18 % de cas considérés et les résidus — 0,1, ± 0,0 et + 0,1 ne comprennent en tout que 56 % de l'ensemble. C'est, pour la station de Praha, un résultat qui confirme ceux de Pasadena : La consistence des valeurs $\mathbf{m}_B$ est considérablement meilleure que celle de $\mathbf{M}_{MH}$ ou $\mathbf{m}_{MH}$.

GUTENBERG et RICHTER donnent ([7], p. 7, équation (4)) une définition pratique de la magnitude unifiée autant que celle-ci est calculée à l'aide des amplitudes des ondes préliminaires :

$$\mathbf{m} = \mathbf{q} + \mathbf{Q} + \mathbf{s} \tag{11}$$

où, utilisant notre notation, $\mathbf{q} = \log(\mathbf{A}/\mathbf{T})$, $\mathbf{Q} = \beta + \delta\mathbf{M}^h$, $\mathbf{s} = \delta\mathbf{M}^s$. Si nous comparons cette équation avec notre relation (1) et en considérant que les corrections $\delta\mathbf{M}^r$ et $\mathbf{D}$ ne peuvent être déterminées que plus tard, à partir d'un matériel suffisamment riche de la station elle-même et en se basant sur des valeurs considérées comme normales, nous voyons que pratiquement notre équation (1) est équivalente avec l'équation (11). Celle-ci est valable pour les ondes préliminaires, mais (1) se rapporte à toutes les ondes que l'on utilise à Praha pour la détermination des magnitudes. On pourrait s'en servir aussi pour la détermination des magnitudes unifiées en modifiant d'une manière convenable la fonction β. Pour les ondes superficielles cette modification consiste à poser

$$\beta^* = \beta + \delta\beta(\mathbf{M}) \qquad (12)$$

la correction $\delta\beta(\mathbf{M})$ étant calculée suivant l'équation (8a) ou (10). Il n'est pas difficile de compléter la fig. 1 par ces corrections.

L'adaptation des valeurs de $\beta(\Delta, \mathbf{T})$ pour les magnitudes déterminées à l'aide de la phase portant le maximum d'énergie, c'est-à-dire pour de courtes distances épicentrales, exigera encore une étude plus approfondie.

IV. Conclusions et propositions.

Il paraît incontestable que l'introduction des magnitudes unifiées va fournir des matériaux beaucoup plus comparables entre eux qu'il n'en est aujourd'hui, surtout si le nombre des stations qui déterminent régulièrement les magnitudes à partir non seulement des ondes superficielles mais aussi des ondes **P**, **PP** et **S**, augmente. Les magnitudes unifiées seront très importantes dans toutes les recherches qui exigent que chaque tremblement soit caractérisé par une seule valeur numérique. Ce sont p.e. les recherches sur la séismicité de la Terre ou l'étude des relations générales entre la magnitude et l'énergie des séismes.

Mais il y a encore beaucoup de problèmes plus spéciaux, liés surtout à des questions régionales, soit ceux qui concernent la structure plus détaillée de la croûte, soit ceux qui se rapportent au mécanisme dans le foyer et à la distribution de l'énergie dans les diverses phases, soit encore l'étude des anomalies de la propagation des ondes. Dans tous ces cas, on aura besoin d'étudier avec soin toutes les particularités, les magnitudes des ondes individuelles y comprises. Il en sera de même quand on aura à étudier des cas de séismes particuliers ou de leurs groupes. Pour les recherches de ce genre les magnitudes unifiées, où par la méthode de calcul on égalise tous les écarts, sans respect à leur origine et leur caractère, ne seront pas convenables.

Il serait donc très désirable qu'un nombre de station aussi grand que possible soit capable de déterminer les magnitudes pour les ondes préliminaires. Par là, on serait capable d'élever le poids statistique des magnitudes unifiées d'une part, d'autre part on pourrait — avec le temps — accumuler un matériel d'observation pour des recherches spéciales. Les magnitudes individuelles ou — supposant une détermination uniforme — les amplitudes et les périodes respectives — pourraient être publiées dans les bulletins à côté de la magnitude unifiée.

A notre avis toutes les valeurs des magnitudes publiées dans les bulletins devraient être liées à un standard commun. Cela exigerait une description précise des méthodes employées pour la détermination des valeurs normales. Nous recommandons que la station normale soit celle de Pasadena.

Aucune transformation mathématique n'est capable d'élever la valeur interne des données sur lesquelles elle est appliquée. La valeur interne des magnitudes repose substantiellement sur une détermination correcte des amplitudes réelles du sol. On peut commettre des erreurs considérables qui peuvent atteindre plusieurs centaines de pourcents en traitant comme harmoniques les ondes préliminaires de caractère irrégulier [18, 19]. Alors, il faudrait attirer l'attention sur le problème de l'agrandissement dynamique réel des appareils séismiques. Il serait au moins très désirable d'avoir un manuel indiquant une méthode uniforme pour la mesure des amplitudes sur les séismogrammes. Cette question est en relation étroite avec les types des appareils utilisés. A notre avis, il serait possible d'élever la qualité des valeurs de magnitude dans un réseau convenable de stations assez nombreuses, liées à une centrale qui dirigerait leur travail. Pour améliorer l'homogénéité des données d'observation, il serait désirable de réaliser dans le réseau proposé une unification nécessaire de l'appareillage.

Nous proposons enfin d'utiliser une seule formule pour la définition de la magnitude pour toutes les ondes à laquelle on devrait réduire toutes les formules utilisées à présent. D'après nos expériences, une formule correspondant à l'équation (11) de GUTENBERG et RICHTER ou plus généralement notre formule (1) seraient les plus convenables.

RÉSUMÉ.

On décrit d'abord les méthodes dont on se sert à la station de Praha pour déterminer la magnitude des séismes et ses corrections.

On utilise les amplitudes maximum des ondes **SgH**, **LH**, **MH** (**T** = 20 sec), **PH**, **PV**, **PPH** et **SH** respectivement en se basant sur le rapport **A/T**. Ensuite on traite les corrélations entre les magnitudes des ondes respectives à savoir **PH**, **PV**, **PPH**, **SH** et la magnitude déterminée à partir des ondes **MH**. Les résultats obtenus sont semblables à ceux de BÅTH. La réduction des valeurs $\mathbf{M}_{MH}$ aux valeurs équivalentes $\mathbf{m}_{MH}$, déterminées en même temps que les magnitudes M_B conduit à des constantes voisines de celles de GUTENBERG et RICHTER. En accord avec GUTENBERG et RICHTER les magnitudes unifiées **m** sont trouvées généralement très voisines des $\mathbf{m}_B$. L'homogénéité des résultats a confirmé l'importance des magnitudes unifiées dans les cas où il est besoin de caractériser chaque tremblement par une valeur numérique. Pour des recherches spéciales on recommande de publier les magnitudes des ondes individuelles. La prochaine étude devrait être organisée dans un réseau convenable de stations, avec Pasadena comme station centrale.

Praha, Août 1957.

BIBLIOGRAPHIE.

[1] RICHTER (C. F.). An Instrumental Earthquake Magnitude Scale, Bull. Seism. Soc. Am., *25* /1935/, 1.

[2] GUTENBERG (B.). Amplitudes of Surface Waves and Magnitude of Shallow Earthquakes, Bull. Seism. Soc. Am., *35*, /1945/, 3.

[3] GUTENBERG (B.), Amplitudes of P, PP and S and Magnitude of Shallow Earthquakes, Bull. Seism. Soc. Am., *35* /1945/, 57.

[4] GUTENBERG (B.), Magnitude Determination of Deep Focus Earthquakes, Bull. Seism. Soc. Am., *35* /1945/, 117.

[5] GUTENBERG (B.), RICHTER (C. F.), Magnitude and Energy of Earthquakes, Nature *176* /1955/, 195.

[6] GUTENBERG (B.), RICHTER (C. F.), Earthquake Magnitude Intensity, Energy and Acceleration /Second Paper/, Bull. Seism. Soc. Am., *46*, /1956/, 105.

[7] GUTENBERG (B.). RICHTER (C. F.), Magnitude and Energy of Earthquakes, Annali di Geofisica, *9* /1956/, 1.

[8] BÅTH (M.), The Problem of Earthquake Magnitude Determination, Publ. Bureau Central Séism. Intern., Travaux Scientif., A *19* /1956/, 5.

[9] BÅTH (M.), Erdbebenenergie, Bergakademie, *9* /1957/, H. 1, 17.

[10] GUTENBERG (B.), The Energy of Earthquakes, Quart. Journ. Geol. Soc. London, *112* /1956/, 1.

[11] ZÁTOPEK (A.), VANĚK (J.), Les magnitudes de Praha et leur relation avec les revised values de Pasadena, Publ. Bureau Central Séism. Intern., Travaux Scientifiques, A *18* /1952/, 137.

[12] VANĚK (J.), ZÁTOPEK (A.), Magnitudenbestimmung aus den Wellen P, PP und S für die Erdbebenwarte Prag, Travaux de l'Inst. Géophys. de l'Ac. Tchécosl. d. Sc., N° 26 /1955/.

[13] KÁRNÍK (V.), Magnitudenbestimmung europäischer Nahbehen, Travaux de l'Inst. Géophys. de l'Ac. Tchécosl. d. Sc., N° 64, /1956/.

[14] KÁRNÍK (V.), Zur Magnitudenbestimmung der Nahbehen, Studia geophys. et geodaet., *1*, /1957/, 88.

[15] GUTENBERG (B.). RICHTER (C. F.), Seismicity of the Earth and Associated Phenomena, Princeton University Press /1949/.

[16] PETERSCHMITT (E.), Etude de la magnitude des séismes, Annales de l'Inst. de Phys. du Globe, Strasbourg, Nouvelle Série, VI/3, /1950/, 51.

[17] SOLOVIEV (S. L.), Quelques résultats de l'application des magnitudes des séismes aux stations séismologiques de l'U. R. S. S. /en russe/, Studia geophys. et geodaet. /Prague/, 2 (1958), 40.

[18] ZÁTOPEK (A.), L'agrandissement dynamique d'un séismographe excité par un choc de la forme $e^{-\lambda\tau}\tau^3$, Publ. Bureau Central Séism. Int., Tr. Scient., A *18* /1952/, 127.

[19] TOBYÁŠ (V.), Dynamic Magnification of the Galitzin Seismograph Excited by Shock Motion of the Ground, Czechosl. Journ. Phys., *6* /1956/, 22.

STRUCTURE OF THE EARTH'S CRUST IN GEORGIA FROM GEOPHYSICAL EVIDENCE

By B. K. BALAVADZE and G. K. TVALTVADZE

The structure and the physical properties of the Earth's layers in Georgia have been studied for a number of years, mainly by seismic and gravimetric methods in the Geophysical Institute of the USSR Academy of Sciences (Acad. G. A. Gamburtzev, E. A. Koridalin) and the Institute of Geophysics of the Academy of Sciences of the Georgian SSR (B. K. Balavadze and G. K. Tvaltvadze).

The seismic investigations have been carried out in different regions of Georgia by methods of deep sounding of the Earth's crust, by the correlation method of refracted waves from powerful blasts.

Gravity determinations were made all over Georgia and its adjoining regions by means of gravimeters. This work was accompanied by the study of rock density with a hydrostatic method, and of the average density of mountain massifs — by the gravimetric method.

I. Results of seismic investigations.

1. The investigations of the structure and elastic properties of the Earth's crust in Georgia were begun as far back as 1941-1945, when the Seismic laboratory of the Institute of Geophysics of the Academy of Sciences of the Georgian SSR first registered soil oscillations from four powerful industrial blasts (up to two hundred and twenty tons) made in the Borzhomi Valley. Elastic oscillations from these blasts were recorded by field seismic instruments placed in the vicinity of the blasts as well as by regional seismic stations of the republic (1, 2, 3).

The analysis of the seismograms obtained was used in plotting travel-time curves, the interpretation of which made it possible to distinguish three basic layers of the Earth's crust and determine velocities of the elastic waves in these layers (*fig.* 1).

The first layer (a sedimentary complex) is characterized by the following velocities of the propagation of P and S waves, respectively $V_{1p} = 4.4$ km. p. sec., $V_{1s} = 2.6$ km. p. sec.

The thickness of this layer changes from 3.5 to 4.0 km. depending on the region of blasts.

The second layer has the following boundary velocities for P and S waves : $V_{2p} = 5.6$ km. p. sec., $V_{2s} = 3,2$ km. p. sec.

The thickness of this layer is of order of 20 km.

These velocity values are, in general, typical for the granite layer; but geological data of the region and results of seismic investigations in different parts of Georgia give grounds to maintain that the first layer we singled out is only the upper part ot the sedimentary complex, the second one being composed of the lower part of the sedimentary complex and the granite layer. It is evident that elastic properties of rocks composing the lower part of the sedimentary complex are approximately the same as those of the underlying granite layer. It has therefore proved to be impossible to determine the boundary between these two layers.

Boundary velocities in the third (basalt) layer are as follows : $v_{3p} = 6.7$ km. p. sec, $v_{3s} = 4.0$ km. p. sec. To detect diffracted waves from the surface of the substratum proved to be impossible. However, on some seismograms there can be seen some waves which we consider to be reflected waves from the Mohorovicic boundary. This boundary must lie at a depth of 48 km. Hence, the thickness of the basalt layer appears to be about 24 km. (*fig* 1.).

Structure of te Earth's crust in the region of Borzhomi-Akhaltsikhe.

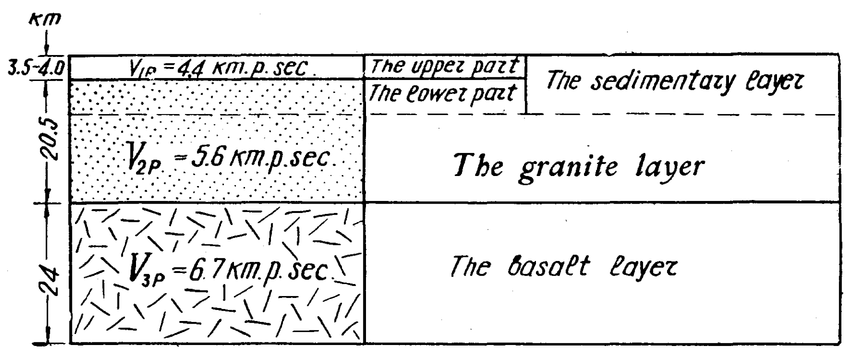

FIG. 1.

2. In 1954 a powerful blast up to forty-five tons was made in the Tkibuli Region (Western Georgia). Soil oscillations from this blast were registered by ten seismic stations in the Caucasus located within a radius of from 60 to 340 km. This blast had a tangible seismic effect due in all probability to the fact that the blasted rock being solid (limestones) favourable conditions had thus been pro-

vided for the formation of intensive elastic waves with a frequency spectrum most suitable for registering them by regional seismic stations in places of their first and subsequent arrivals.

On seismograms of regional seismic stations with epicentral distances from 60 to 140 km. there can be distinguished two arrivals of P waves and two — of S waves, the first arrivals of P and S waves being less intensive than the second ones.

These arrivals correspond to two different waves : waves diffracted from the surface of a crystalline foundation (P_{12} and S_{12}) and direct waves propagating directly in the sedimentary complex (P_{11} and S_{11}).

There are two arrivals to be observed in records of seismic stations located at distances of 144, 160 and 180 km. We consider that the first of them should correspond to waves diffracted from the surface of the basalt layer (P_{13} and S_{13}), the second ones to those diffracted from the surface of the granite layer. It must be noted that the second arrivals are stronger than the first ones.

There are two distinct arrivals seen on a record of a seismic station located at 340 km. from the blast point : the first is a P wave, the second — an S wave. The analysis shows that these arrivals correspond to waves diffracted from the basalt surface. The absence of P_{14} and S_{14} waves can be accounted for by their small intensity. In fact, records of near earthquakes show the intensity of P_{14} waves to be small and the intensity of S_{14} waves to be so small, that the oscillation amplitudes of these waves is less than amplitudes of even P waves of other types.

On the basis of data obtained, travel-time curves were built both for the first and for subsequent arrivals. The travel-time curves having been interpreted, a schematic section of the Earth's crust structure has been given (*fig.* 2).

The first layer (a sedimentary complex) is 7 km. thick and P and S wave velocities are equal to : $v_{1p} = 4.300$ km. p. sec. and $v_{1s} = 2.550$ km. p. sec.

The second layer (granite) is approximately 17 km. thick having velocities : $v_{2p} = 5.600$ km. p. sec. and $v_{2s} = 3.350$ km. p. sec.

The velocities of P and S waves in the third (basalt) layer are equal to : $v_{3p} = 6.500$ km. p. sec and $v_{3s} = 3.900$ km. p. sec.

As has been noted above, there were no arrivals of waves passing from horizons lying under the basalt surface, yet taking into account the results obtained during the study of the Earth's crust structure in other regions of the Transcaucasus, we believe the thickness of the basalt layer to be about 24 km.

Thus, the thickness of the Earth's crust in the Tkibuli region, too, appears to be of the order of 48 km. (*fig.* 2). Velocities in the subs-

Structure of the Earth's crust in the region of Tkibuli.

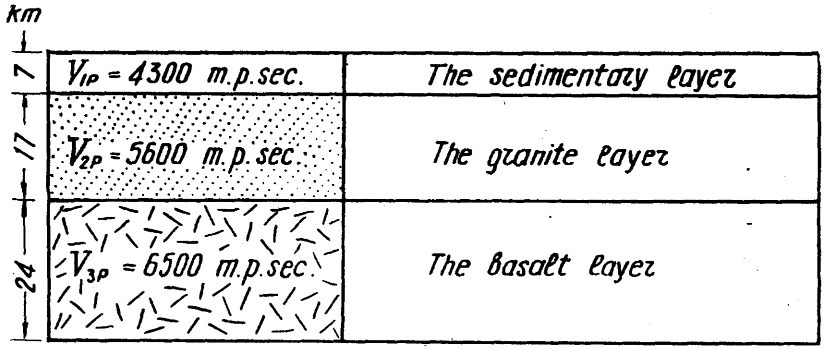

FIG. 2.

tratum, seen on this drawing have been determined by the Caucasuan seismic expedition in the eastern part of the Kura depression by soil oscillations caused by powerful industrial blasts in the area of Kirovobad (the Azerbaijan SSR) (4).

3. To investigate the structure of the sedimentary complex, the morphology of the crystalline foundation surface and the nature of the basic groups of seismic waves in different parts of Georgia (*fig.* 3), explorations were made using seismic methods of prospecting and deep seismic sounding. These following are the main results of these investigations.

Gori-Mukhran Depression (*Eastern Georgia*).

The data recorded show a complex wave picture; a great variety of waves are recorded, the most stable types of seismic waves being those propagating along the surface of the crystalline foundation and Mesozoic depositions. Waves are traced both in the area of the first arrivals and in the area of subsequent arrivals (5, 6, 7).

Reflected waves from the surface of the crystalline foundation differ from those obtained from different horizons of the sedimentary complex in their form and recording intensity. These waves retain their form and intensity and are traced at relatively great distances (12-15 km.) from the source of oscillations.

Waves diffracted from the same surface are characterized by a simple recording form, a comparatively weak intensity and slow damping as against waves diffracted from the basic layers of the sedimentary complex, reflected waves being characterized by a greater intensity than diffracted ones.

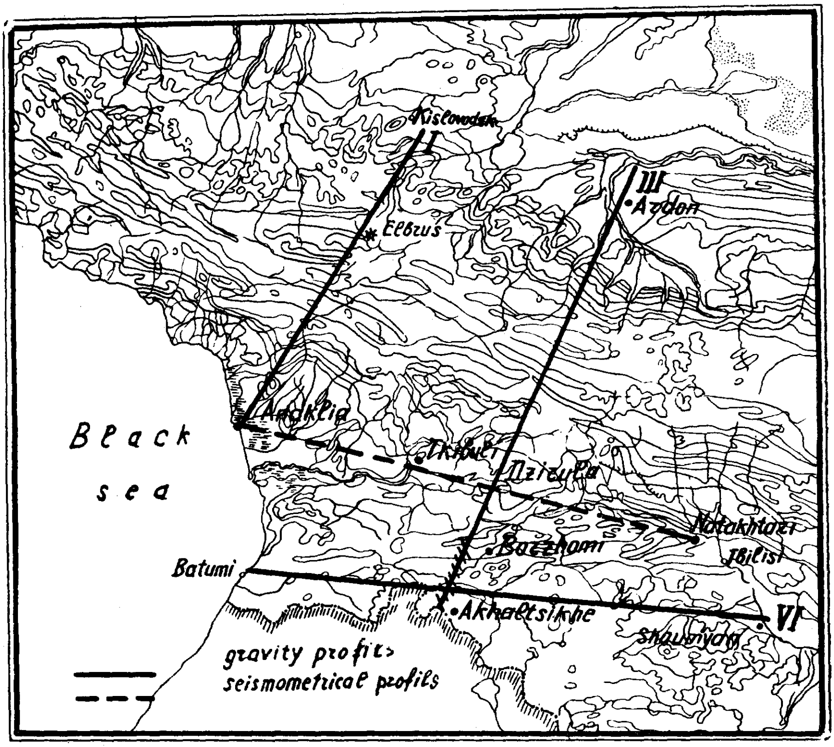

FIG. 3.

According to the analysis of the data obtained, there are in the sedimentary complex of the region three parts to be distinguished (*fig.* 4) :

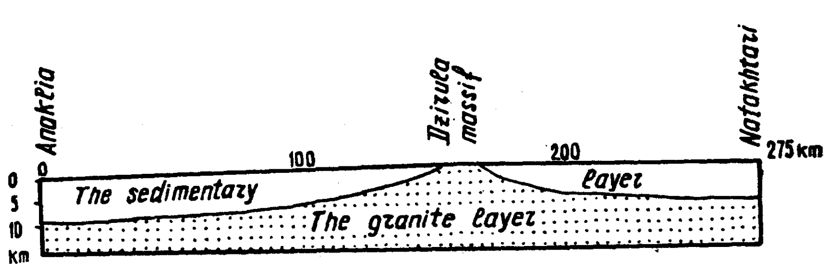

FIG. 4.

1) Post-tertiary depositions, with thicknesses ranging from a few metres to hundreds of metres. Propagation velocities of seismic waves vary in different parts; they range from 1.400 to 2.500 km. p. sec., except in the decay zone.

2) Tertiary depositions with thicknesses from a few metres in the West to a few kilometres in the East. There are several refracting and reflecting horizons to be distinguished in the depositions. Bed velocities range from 2.000 to 4.000 km. p. sec., a small increase being observed in the west-east direction. In the eastern part of the depositions there is to be a noted layer with an increased bed velocity of up to 5.000 km. p. sec.

3) Mesozoic depositions in the region of investigations are composed of Jurassic and Chalk formations with a thickness of about 2 km. except the environs of the Dzirula crystalline massif. Bed velocities of seismic waves there change in the vertical direction from 4.000 to 5.200 km. p. sec.

The boundary velocity for the surface of the crystalline foundation, determined both by two contrary time fields and by a travel-time difference curve, is 5.500-5.700 km. p. sec. Besides, the propagation velocity of seismic waves has been determined directly on natural outcrops of the crystalline foundation on the slope of the Dzirula massif. The obtained result showed it to be of the order of 5.500 or 5.600 m. p. sec. Therefore we assume that the boundary velocity obtained from the travel-time curve of refracted head waves characterizes if not the whole granite layer, then, at least, its upper part.

The surface of the crystalline foundation sinks from West to East. If its depth in the Dzirula massif is only a few metres, in the Natakhtari Valley it reaches 6 or 6.5 km. (*fig.* 4). The sinking is also observed from the South (from Natakhtari) to the North, reaching 8 km. in the Zhinvali region.

Colchidan plain (*Western Georgia*).

Similar work was carried out in the Colchidan Plain in 1948-1949. As a result it was established that the thickness of the sedimentary complex in the region of Anaklia is of the order of 8 or 8.5 km. (8).

The velocity of diffracted waves (P_{12}) from the surface of the crystalline foundation is 6.4 km. p. sec. But inasmuch as the boundary velocity in other regions of Georgia is 5.6 km. p. sec. for the crystalline foundation, it is natural that there must not be a large difference in this value. Therefore, the velocity found for this region is a seeming one. On the basis of these considerations we conclude that the surface of the crystalline foundation has a non-significant uplift from Anaklia to the Dzirula crystalline massif. As one draws nearer to the latter either from the West of from the East, seeming velocities increase, reaching 9.0 or 10.0 km. p. sec., which is indicative of an uplift of the surface of the crystalline foundation in this region (*fig.* 4).

II. Results of gravimetric investigations.

1. The regional gravitation field on the territory of Georgia and the adjoining northern regions has been studied by pendulum and gravimeter observations with sufficient completeness. A map of gravity anomalies with the Bouguer reduction was compiled incorporating corrections due to relief influence within a radius of 200 km., and corrections due to deviations of the geoid from the spheroid (8).

The accuracy of this map of gravity anomalies was estimated by M. S. Molodensky's method of full error of interpolation (9) and by de Graaf Hunter's method full error of representation (10). A mean error proved to be ± 4.2 mgl for plains and ± 8.8 mgl for mountain regions.

The gravimetric map is compiled with due account taken also of anomalousness of the vertical gradient. The gradient value obtained by calculations from the Bouguer anomaly map varies from — 90 to + 30 Eötvös; negative values of the gradient characterizing spheres of regional gravitation minima, while positive — spheres of maxima. These data show that the correction to gravity due to the influence of the vertical gradient anomalousness reaches up to 35 mgl in high mountain regions.

Our investigations prove that by taking account of anomalousness of the vertical gradient a higher standard of precision of the gravity map more is attained.

The gravitation field of Georgia is much disturbed. Large minima of gravity anomalies embracing vast territories are observed in the regions of the central zone of the Greater Caucasus and the Djavakheti Plateau; regional maxima of gravity anomalies found in the regions of the Dzirula and Loki crystalline massifs and as well as Adjaria occur over a vast area; finally, in the Colchidan region an increase of gravity in the direction of the Black Sea is to be observed.

2. To reveal the basic causes determining the general character of changes in gravity anomalies of Georgia, the gravimetric map

was compared with geological and densitometrical maps. It was thus established, that in one case outcrops of Dzirula and Loki crystalline massifs corresponded to maxima of gravity anomalies, while in another case (the central zone of the Greater Caucasus) — to minima, which conflicts with the surface geological structure and density distribution in rocks of the same region. Similarly, a gravity increase in Colchis in the direction of the Black Sea does not tally with a thickness increase of light sedimentary rocks in the same direction. As to the maximum of gravity anomaly in Ajaria, it too, cannot be accounted for on geological and densitometrical maps.

Thus, there are found in the territory of Georgia direct relationships between the regional field with the Bouguer reduction and surface geological structure, on the one hand, and inverse relationships — on the other. It is probable that inverse relationships point to the dominating influence of a deep anomaly mass on gravity.

Should similar analysis be made of the whole orogen of the Caucasus, we shall easily come upon more cases of such relationships and also establish definite laws of their distribution; namely, in the southern and south-eastern part of the Caucasus, as a rule, direct relationships are observed, while in its northern and north-western part- inverse relationships.

The existence of strong anomaly gravitation fields, to our mind, is evidence of a drastic change in the depth of occurence of discontinuities between the main layers of the Earth's crust. According to H. Jeffreys and E. Glennie it may be conjectured that the disturbing masses originate in the sedimentary layer and at foundations of the basalt and granite layers. The presence of large disturbing masses at great distances inside the granite and basalt, in all probability, does not take place (11, 12).

Proceeding from the above statements we take that the structure of the Earth's crust under this or that part of a mountain region may be characterized by one of the diagrams on fig. 5. The drawing shows that cases, *a,b,c,* and *d* cause direct relationships, while cases *e,f,g* and *h* — inverse relationships

3. It is well known that a qualitative interpretation of gravity anomaly meets difficulties of principle when there is no other geophysical and geological evidence. From some seismic data available on the territory in question, we can see that the general thickness of the Earth's crust in Georgia varies from 48 to 60 km., reaching in the Kazbek region about 60 km., in the Lesser Cauca-

sus -50-54 km., in the Kura Depression — about 48 km. (1, 2, 3, 8, 13, 14).

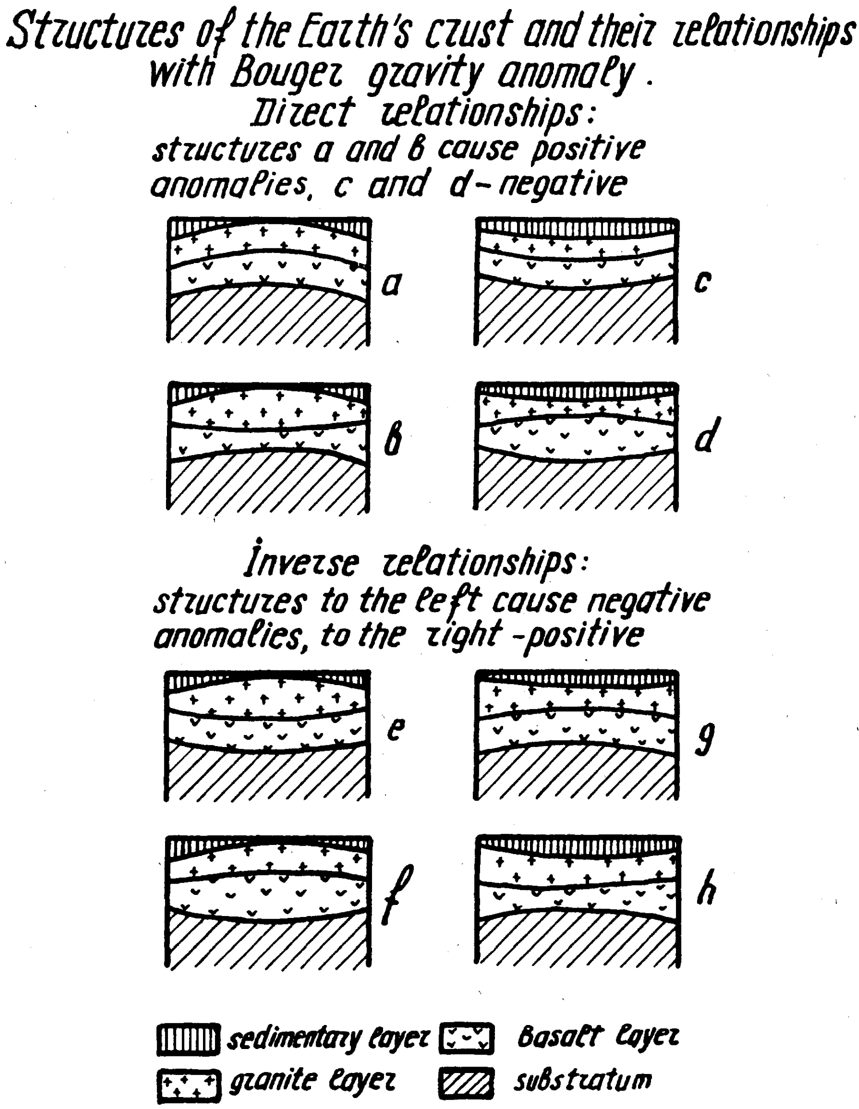

FIG. 5.

Thus, in the high-mountain region of the Greater Caucasus the thickness of the Earth's crust is larger than in a region with a moderate relief; and in the latter it is less than in a considerable intermountain region.

The thickness of the basalt layer in the Borzhomi-Akhaltsikhe region is of the order of 25 km., the granite layer — about 15 km. From seismic data the thickness of the granite layer in the Kazbek region is of the order of 37-46 km., of basalt — 15 km.

There are far richer and more accurate geological and geophysical data on the structure of the sedimentary layer in Georgia than what has been stated above concerning the thickness of crystalline layers of the earth's crust. We have studied density characteristics of rocks in Georgia in sufficient detail. These and the bibliographical data on densities of the granite, basalt and substratum layers give the following results (8, 15, 16) :

1) For the sedimentary complex —

Q	σ_1	$= 1.8 — 2.0$ gr. p. cm^3	
N	σ_2	$= 2.1 — 2.2$	—
P_g	σ_3	$= 2.3 — 2.5$	—
C_r	σ_4	$= 2.60$	—
J	σ_5	$= 2.75$	—

2) For the granite layer — $\sigma_0 = 2.65$ gr. p. cm^3
3) For the basalt layer — $\sigma' = 2.85$ gr. p. cm^3
4) For the substratum $\sigma'' = 3.40$ gr. p. cm^3

By making use of these data we have interpreted curves of gravity anomalies in seven most typical profiles crossing the outcrops of crystalline rocks and patches studied by seismometrical method and by drilling; the profiles also intercross.

While drawing the approximated profile of the Earth's crust the structure of the sedimentary complex and the outcrop bordes of some depositions have been plotted according to geological, drilling and seismic data. Seismogeological discontinuities of layers on diagrams of the Earth's crust structure are shown by short bold lines, while drill holes -by vertical columns.

It is assumed that anomaly masses are located in the sedimentary complex (Ist anomaly layer), at the foot of the granite layer (2nd anomaly layer — one between the plane AA and the granite foundation) and at the basalt layer foundation (3rd anomaly layer, one between plane BB and the basalt foundation) (*fig.* 5). The computation of a gravitation effect of these masses is made on the basis of our equation

$$\Delta g_B = \Sigma\,(\sigma_0 - \sigma_i)\ \ a_i + (\sigma_0 - \sigma')\ b + (\sigma' - \sigma'')\ c + 2\pi f\ (\sigma' - \sigma_0)\ (H_2 - H_1),$$

where the coefficients a_i, b and c are quantities of equal action points which are at the level of traverse profiles of the first, second and third two- dimension anomaly layers respectively.

The computed summary gravitation effect Δg_B was compared with observations of Δg; gravitation effects of separate anomaly layers served for plotting curves which we have named differential curves and have marked on the diagrams as 1, 2, 3 respectively (*fig.* 6).

Let us pass over to the description of some of the section diagrams obtained of the structure of the Earth's crust (*fig.* 4).

Profile I goes from the Black Sea coast through Mount Elbrus to the environs of Kislovodsk (*fig.* 6). A geological profile in this

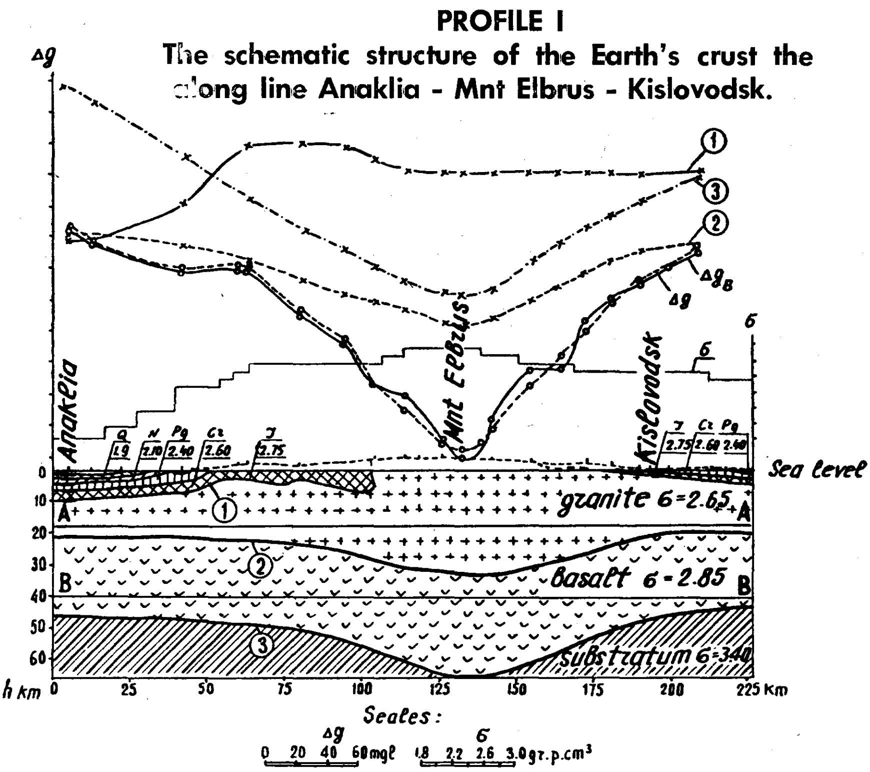

FIG. 6.

direction yields the following picture : a wide band of outcropped crystalline rocks traced along the Main Ridge is observed in the zone of the Greater Caucasus, on either side of the band sedimentary layers occur greatly increasing in thickness especially in the direction of the sea.

As it follows from the diagram a deep regional minimum of gravity is seen which passes over dense crystalline rocks. The main cause of this minimum, as it follows from curves 2 and 3, consists in an increase in the thickness of the Earth's crust under the Greater Caucasus, wich resulted in the replacement of dense Simatic masses by relatively light Sialic masses. The thickness of the granite layer under Mount Elbrus is of the order of 35 km., of basalt — 32 km.

The effect of the sedimentary complex along the profile under consideration is significant only in Colchis, in the area of Khudoni-Anaklia, where a decrease of gravity in the Anaklia region reaches up to 60 mgl. This decrease caused by the presence of light röks in the sedimentary complex is, to a large extent, compensated by a gentle elevation of the substratum under the Colchidan Valley.

Profile III connects the Greater and the Lesser Caucasus, passing through the regions of Akhaltsikhe, Borzhomi, Dzirula, Mamison Pass and Ardon (*fig.* 7). The curve of gravity anomaly consists

PROFILE III

The schematic structure of the Earth's crust along the line Akhaltsikhe - Dzirula - Ardon.

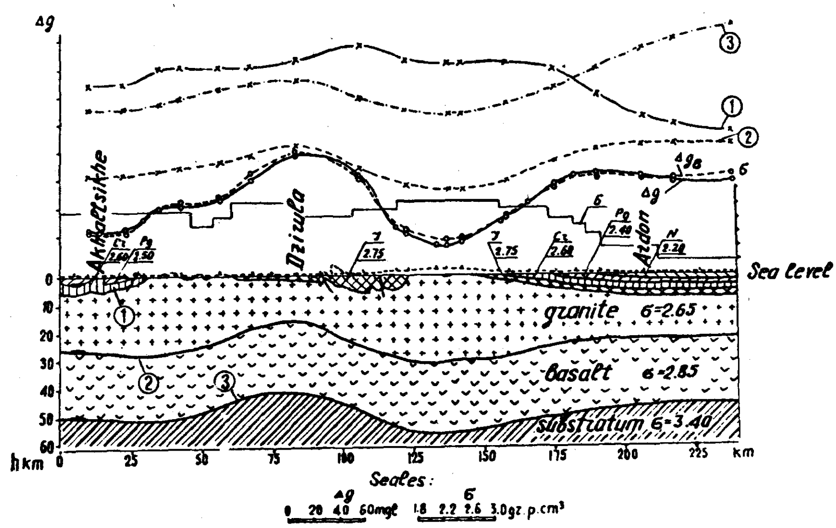

FIG. 7.

of a wide maximum located over the Dzirula crystalline massif and also of a widely extended minimum located in the zone of the Greater Caucasus over the crystalline massif.

The interpretation of gravity has been made with due account of data of deep seismic sounding. The diagram (*fig.* 7) shows that the Earth's crust under the Dzirula massif is thinner than under the Greater Caucasus, which is caused by the warping of the basalt layer. The influence of the defect of masses of the sedimentary complex in the right side of the diagram is completely compensated, largely, by the influence of surplus masses of the substratum.

Profile VI lies in the Lesser Caucasus and passes through the following regions : Batumi, Mount Goderzi, Akhalsikhe, Mount Samsari, Shaumyan (*fig.* 8). Along it a very wide and deep mini-

PROFILE VI

The schematic structure of the Earth's crust along the line Batumi - Akhaltsikhe - Shaumyan.

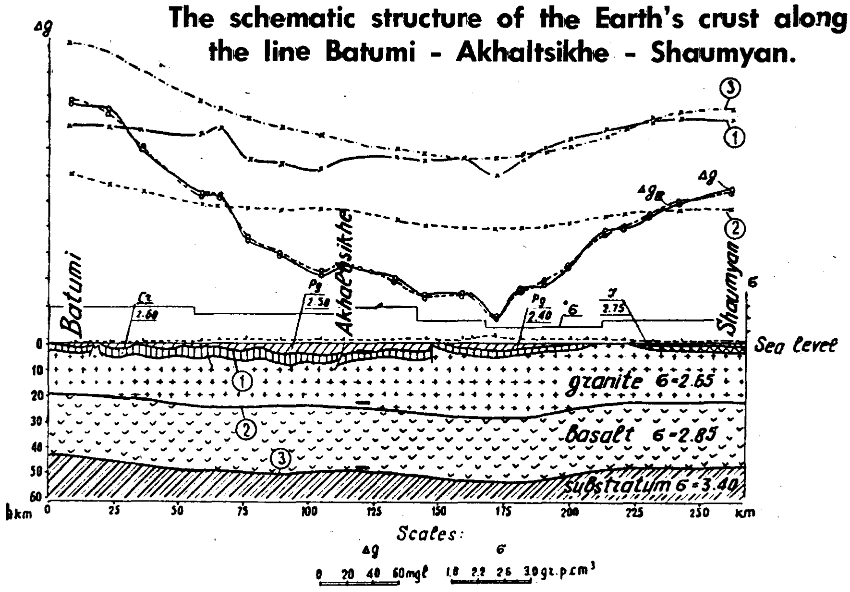

FIG. 8.

mum of gravity anomaly extending over 250 km. is observed. The curve interpretation shows that the gravitation background of the said profile is caused by a general subsidence of the Earth's crust in the Gederzi-Samsari zone, while local anomalies are due to a non-homogeneous structure of the sedimentary layer.

Generalizing the results of the qualitative interpretation of gravity anomaly on the territory of Georgia we come to the following conclusions :

A general nature of gravity anomaly is conditioned thus : in mountain regions — by a change in occurence depth, — largely, of the substratum surface (the Mohorovičić surface), and, to a less degree, of the basalt surface; in low-lying regions, chiefly, by a change in the surfaces of the substratum and the granite (a change of thickness of the sedimentary cover) and to a less degree, of the basalt surface.

Thickness of the Earth's crust in Georgia ranges approximately from 41 to 67 km., the maximum thickness being observed under the central part of the Greater Caucasus (the zone of Elbrus-Kazbek) and the Djavakheti Plateau, the minimum — under the Dzirula Massif and Tsikhisdziri (near Batumi). In Colchis the Earth's crust thickness decreases gradually towards the Black Sea.

Approximate variations of the layer thicknesses in Georgia which compose the Earth's crust are, evidently, as follows : of the sedimentary — from 0 to 8 km., granite — from 14 to 32 km. and basalt — from 22 to 35 km.

4. Non-univalent values of the solution of the inverse problem of gravimetry requires that the question of reliability of the suggested diagrams of the Earth's crust structure be carefully considered. In this connection verification was made of the solution stability of the inverse problem by computing the gravitation effect at extreme values of densities of the basalt layer (2.75 and 2.90) and substratum (3.20 and 3.50); density values of the sedimentary depositions and the granite layer are more reliable and it would be inexpedient to change them.

Gravitation effect computed at these extreme density values for most typical (I, III, VI) schemes yields a displacement of the curves Δg_{B} in both sides respectively in the range of 20-60 mgl. To reduce Δg_{B} curves so obtained to observations Δg it was necessary to get displacement of basalt and substratum to corresponding sides in the average at 1 or 2 km., the planes AA and BB retaining their stable position.

This result shows that if in the choice of density values for basalt and substratum there is an error as against the values of the order of $\pm$ 0.1 gr. p. cm^3 it brings no essential influence to bear on interpretation results. Consequently, under considerable changes of the field the interpretation result undergoes comparatively insignificant changes, which proves the stability of the inverse problem solution.

Let us verify the reliability of the suggested schemes of the structure of the Earth's crust by excluding the less probable schemes. For this purpose, let us admit, in contrast to some seismic results, that a change in the Earth's crust thickness in Georgia takes place, mainly, due to a change not of the granite layer but of the basalt layer, as is the case in the Northern Tien-Shan (17), Sierra Nevada (18) and other places.

The test of this hypothesis along the profiles where gravity anomaly is sharply expressed leads to diagrams of the Earth's crust structure wich seem little probable viz, the basalt layer shows a very deep protrusion into substratum.

Let us consider some hypotheses : 1) the surface of the basalt layer is horizontal, and 2) the basalt layer foundation is horizontal.

In the first case, the interpretation of the curve Δg along profile I yields a quite admissible thickening of the lower basalt. In the second case, to account for a negative gravity anomaly under the parameters adopted above we have to agree to an extreme increase of the granite layer thickness, the basalt layer nearly disappearing and the granite being directly superposed on the substratum and forming a deep root. It is obvious that hardly any arguments can be adduced in favour of such a profile. In our opinion, such a diagram of the Earth's crust structure is unreal.

In summing up we must say that the above diagrams of the Earth's crust structure are the most probable.

Such is the present state of studies of the structure and physical properties of the Earth's crust in Georgia from seismic and gravimetric evidence.

Bibliography.

1. Tvaltvadze (G. K.). Izvestia of the USSR Academy of Sciences geographical and geophysical series, v. Ix, N° 1, 1945, Moscow.
2. Tvaltvadze (G. K.). Communications of the Academy of Sc. of the Georgian SSR, v. IX, N° 8, 1950, Tbilisi.
3. Tvaltvadze (G. K.). Communications of the Ac. of Sc. of Georgia, v. 1, N° 8, 1942, Tbilisi.
4. Koridalin (E. A.). Vestnik of the USSR Ac. of. Sc., N° 3, 1948, p. 114, Moscow,
5. Murusidze (G. Y.). Transactions of the Inst. of Geophysics. Ac. of. Sc. of Georgia, v. XV, 1956, Tbilisi.
6. Ioseliani (M. S.). Transactions of the Inst. of Geophysics. Ac. of Sc. of Georgia, v. XV, 1956, Tbilisi.
7. Tvaltvadze (G. K.), Kosminskaya (I. P.), Murusidze (G. X.), etc. Geophysics, Ac. of Sc. of Georgia, v. XVI, 1957, Tbilisi.
8. Balavadze (B. K.). Gravitation field and structure of the Earth's crust in Georgia. Publ. by the Ac. of. Sc. of Georgia, 1956, Tbilisi.
9. Molodensky (M. S.). Transactions of Tsniigaik, issue 42, 1942, Moscow.
10. De Graaf Hunter. Phil. Trans., ser. A. 234, 1936.
11. Jeffreys (H.). The Earth, 2nd ed., Cambridge, 1939.
12. Glennie (E. A.). Survey of India, Profession paper, No. 27, 1932.
13. Levitskaya (A. Y.). Transactions of the Geophysical Inst., Ac. of Sc., USSR, No. 5 (132), 1950.

14. Bonchkovsky (V. F.). Vestnik of the Moscow University, No. 11, 1948.
15. Birch, Sherer (D.) et Spicer (G.). A reference-book for geologists on physical constants, Translation, Moscow, 1949.
16. Hess (H. H.). Proceed. of the Royal Soc., ser. A., v. 222, No. 1150, 1954.
17. Gamburzev (G. A.), Weizman (P. S.), Tulina (I. V.). Docladi of the USSR Ac. of Sc., v. 105, No. 1, 1955, Moscow.
18. Gutenberg (B.). Bull. of the Geol. Soc. Am., v. 62, May (pp. 427-439), 1951.

NEW DEEP SEISMIC SOUNDING DATA ON THE STRUCTURE OF THE EARTH'S CRUST AND ON MOUNTAIN ROOTS

By

WEIZMAN P. S., KOSMINSKAJA I. P., RISNICHENKO J. V.

A number of the most important geophysical and geological problems, such as the origin of continents and oceans, the connection between large-scale tectonic units, etc. cannot be solved by the study of the upper crustal layers only. Hence the growing attention payed by geophysicists and geologists to the investigation of the earth's crust as a whole, down to its base — the Mohorovicic discontinuity.

The establishment of connections between the surface tectonics, important to mineral prospecting, and the deep crustal structure has lent to the problem of investigating the deep crustal structure, apart from scientific also practical importance.

During the last two decades essential progress was made in the development of methods for investigating the deep crustal structure. Among these are the seismic methods for investigating the earth's crust of continents and oceans developed by scientists of Great Britain and the United States (1-4), and also the special method of a detailed deep seismic sounding « DSS » of the continental crust (in Russian « ГСЗ » — GSZ), proposed by the late academician G. A. Gamburzev (5-9) and developed in the USSR.

The present report contains the results of investigations by the DSS method carried out in 1949-1955 under the guidance of G. A. Gamburzev in the mountain regions of Middle Asia, mainly by the Geophysical Institute (now Institute for Physics of the Earth) of the Academy of Sciences of the USSR.

1. The position of the DSS method among other methods for investigating the earth's crust.

In USSR, as well as in other countries, investigations of the earth's crust are carried out by all the principal geophysical methods : the gravimetric, magnetometric, electrometric and seismometric. The first and the last of these methods proved the most effective, but by the seismic methods can the problem of investigating the crustal structure be solved independently, giving definite numerical results in sufficient detail.

Having obtained seismic data on the deep crustal structure in a number of points or local regions, one can with greater confidence judge on the crustal structure of large areas covered by a gravimetric survey which requires less time and labour. Hence the significance of combining seismic and gravimetric methods for crustal investigations over a large area.

In USSR, as well as in other countries, for the investigation of the earth's crust two principal modifications of the seismic method are used : *a*) methods based on observations of elastic waves from natural sources, such as earthquakes, microseisms and *b*) methods based on recording of explosions. The advantages of the « active » methods of the second group over the « passive » methods of the first one are their operativeness and more accurate and detailed results. Experience has shown however, that in order to obtain complete and accurate data on the crustal structure, one should not neglect the « passive » methods of recording earthquakes. These methods and especially the high resolving power methods of high-frequency seismometry introduced by G. A. Gamburzev, open great possibilities for investigating the crustal structure of seismically active countries from observations of near earthquakes. (10-12.) It is useful to combine these methods with seismic shooting (11-14).

In USSR, as well as in other countries, in the investigations of the earth's crust by seismic shooting *large explosions* had been previously used. Here charges of the order of tens of tons, which are fired from time to time by mining and other industrial organizations had been made use of. The data on the crustal structure obtained from observations of blasts fired in Korkino (in the Ural) (15-16), near Tula (16) and in some regions of Middle Asia (17) are well known. The elastic waves from these blasts were observed by the usual seismological method of observing near earthquakes.

The data on the crustal structure from observations of industrial blasts are more accurate and more reliable than those obtained by the other methods mentioned above. However, as shown by the outstanding progress reached in modern methods of seismic prospecting, the most promising possibilities of the seismic method are in principle far from being exhausted. One of the most important advantages of the methods of seismic prospecting over the methods of observing industrial blasts is the complete control by the geophysicists themselves over the explosions used as sources of vibrations.

The DSS method is free from the limitations and faults of the methods of observing large explosions (6, 18). In its general character this method is close to those of seismic prospecting. Having a high resolving power, the DSS method gives more detailed and more accurate results than all at present known methods for investigating the deep crustal layers.

2. The principal characteristics of the DSS method.

The DSS method was developed under the guidance of G. A. Gamburzev in the Geophysical Institute of the Academy of Sciences of the USSR by G. I. Aksenovitch, P. S. Weizman, E. I. Galperin, N. I. Davidova, M. A. Zajonchkovski, I. P. Kosminskaja, G. G. Michota, J. V. Tulina and oth. (5-9, 18.)

In its present modification the DSS method is close to the correlation seismic refraction method for seismic prospecting (CSRM, in Russian « KMIIB » — KMPV) also proposed by G. A. Gamburzev (19). The difference between the DSS method and CSRM is due to the greater depths investigated in the DSS method and corresponding to the greater shooting distances (up to 300 km. and even more).

The charges used in the DSS method are of the order of 50-300 kg., when fired in water and up to 800 kg. — in bore hole groups. Recording is done on special movable low-frequency (5-15 c/s) multichannel stations similar to those used in seismic prospecting. In order to raise the sensibility of the method not only lower frequencies are used, but also receivers and shot points properly grouped and quiet locations and time of observations chosen (16, 20).

In the DSS method, as well as in seismic prospecting, multichannel recording permits to follow continuously the waves along separate portions of the profiles by the use of « positional » wave correlation. The DSS method is also making use of « azimuthal » correlation of waves observed in separate points on multichannel sets with differently directed axes of the seismic receivers. This permits the investigation of wave polarization and the determination of the type of waves recorded (21, 24). Observations are mostly carried out along continuous lines composed of separate segments; along longitudinal lines with simple, reversed and overlapping time-distance curves; along unlongitudinal lines; on profile systems providing an area survey of the most interesting regions, for instance, with the aim of revealing and tracing deep fault zones. For area surveys in mountain regions short crossed profiles are generally used with a single shot point.

For the interpretation of the DSS data correlational methods of picking out and following waves together with the drawing of sections and maps, mostly developed in CSRM and sometimes only slightly modified are widely used (19). Thus, in the DSS method, in addition to the known principles of phase and wave correlation (25, 26), the principle of wave group correlation (27) was established. Correlation of this kind permits picking out and following separate wave groups in particular those connected with the principal boundaries in the earth's crust, even in cases, when continuous following of separate waves contained in the group cannot for some reasons be carried out.

3. THE PRINCIPAL WAVE GROUPS OBSERVED IN THE DSS METHOD.

Investigations by the DSS method in various regions give different numbers of wave groups of a different origin. The most stable and almost universally observed under continental conditions are the principal groups of longitudinal refracted waves, connected with the three principal boundaries in the earth's crust. These are : the P°-wave group corresponding to the upper boundary of the so called « granitic » layer (the velocity of P°-waves is close to that of P.-waves from shallow earthquakes travelling through the granitic layer), then the P*-waves corresponding to the surface of the « basaltic » layer and finally the P-waves travelling through the subcrustal layer along the Mohorovicic discontinuity. In regions with more less strongly developed sedimentary layer a wave group connected with this layer is observed. In some cases strong waves reflected from the Mohorovicic discontinuity are also recorded.

Fig. 1 represents some samples of records from different parts of the USSR. They show the principal wave groups P°, P* and P in zones preceding (*fig.* 1 *a* and *b*) and following (*c* and *d*) the mutual interference range.

The seismograms in *fig.* 1 *a* were recorded in Northern Tien-Shan on a 12-channel set with the seismographs spaced at 200 m. (along a profile running in the Southern part of Djungar-Ala-Tau, shot point in the Balchash lake, charge Q = 300 kg., shooting distance R = 280,9-285,3 km.). The initial parts of these records show a stretched group of weak P-waves followed by a close group of stronger P*-waves.

The record in fig. 1 *b* is from Northern Pamir (profile in the Ahlie valley, shot point in Kabud-House lake, Q = 300 kg., R = 272,4-274,5 km.). The upper traces of the record correspond to a positional (along a line) distribution of the seismographs and the *8* nether traces — to an azimuthal distribution, the shooting

ТЯНЬ-ШАНЬ ПР долина р.ИЛИ ПВ Балхаш R = 280,9 - 285,3 км

а)

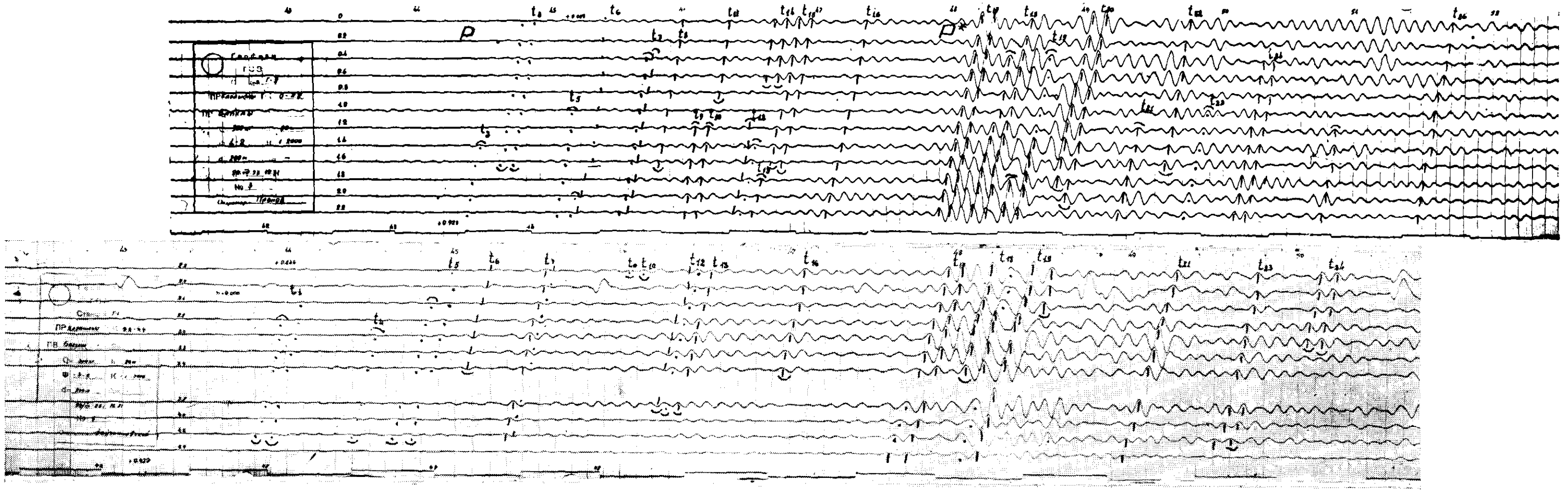

П А М И Р ПР Алайская долина ПВ Кабуд-Хауз R = 272,4 - 274,5 км

в)

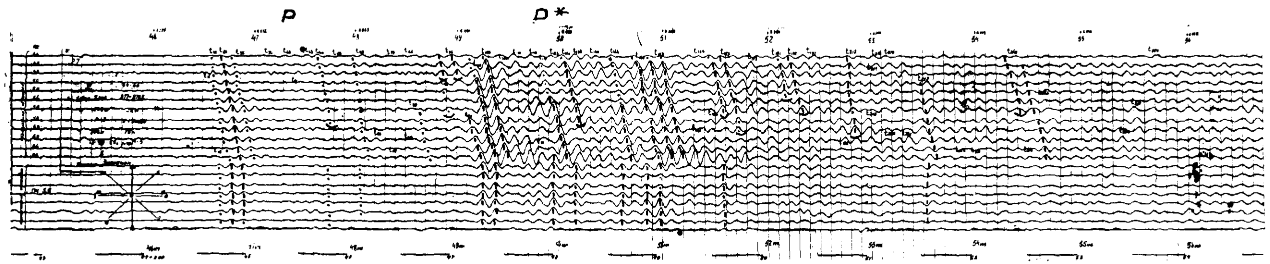

c)

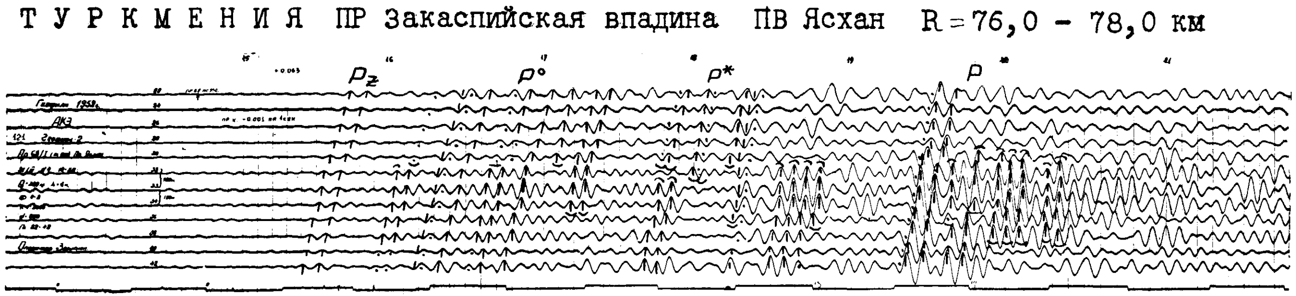

d)

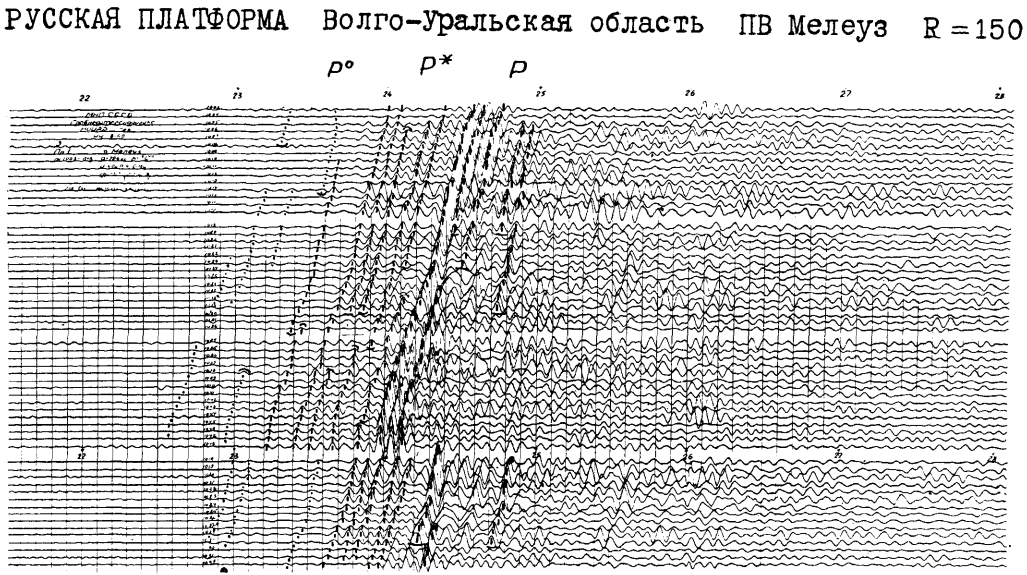

FIG. 1. Samples of records obtained by the DSS method in various regions at various shooting distances.

distance being R = 273,6 km. In the initial part of the record P-waves are seen followed by stronger P*-waves.

The record in fig. 1 *c* was taken in Western Turkmenia (along a profile in the Transcaspian depression, shot point in the Jaschan lake, Q = 300 kg., R = 76-78 km.). The first arrival P_z which is connected with the surface of the Paleozoic basement, is followed by P°, P* and P waves. Here, in the region close to the initial point of the travel time curve for the P-waves, they are the strongest.

Fig. 1 *d* represents a 60-channel record (seismic receivers spaced at 100 m.) taken in the Russian platform of the Volga-Ural district by the Geophysical Research Institute of the USSR Ministry for Oil Industriy under the guidance of J. N. Godin (shot point in Meleus, total charge 798 kg. fired simultaneously in a group of three bore holes 40 m. deep, R = 150-155 km.). The nether group of traces in this record repeats the second group from above but corresponds to a lower frequency filter pass-band. The record shows P°, P* and P waves. The P-waves are the strongest and in this area they are being continuously correlated over a distance above 100 km. In this record the P-waves are clearer and stronger than the P*-waves.

According to observations and computations, the general character and the amplitude ratio of the principal wave groups depend on the shooting distance, the thickness ratio of the principal crustal layers and in particular on the presence or absence of the low-velocity sedimentary layer.

The above records indicate a complex structure of the principal P°, P* and P-wave groups. This structure is still more complicated in areas with a more disturbed crustal structure. Thus, im mountain areas the wave group structure is, as a rule, more complicated, than in plains.

At the present time a numerical interpretation is carried only from the travel time curves for the first waves of each group, which are used for the determination of the position of the principal boundaries in the earth's crust. As regards the nature of the following waves of each group, several assumptions could be made about them. It might be assumed that they are connected with the complex structure of the medium in the zone of transition between the crustal layers, or with the multiple waves on the interface boundaries. Experimental and theoretical investigations of the nature of wave groups have just begun.

4. Results of investigations by the DSS method in Middle Asia.

Observations by the DSS method have been carried out in the following three, seismically most active, areas of Middle Asia : in Northern Tien-Shan, in the Pamiro-Ahlie zone and in Western Turkmenia (*fig.* 2). Such observations were also carried out in the Caucasus and in the Volga-Ural district.

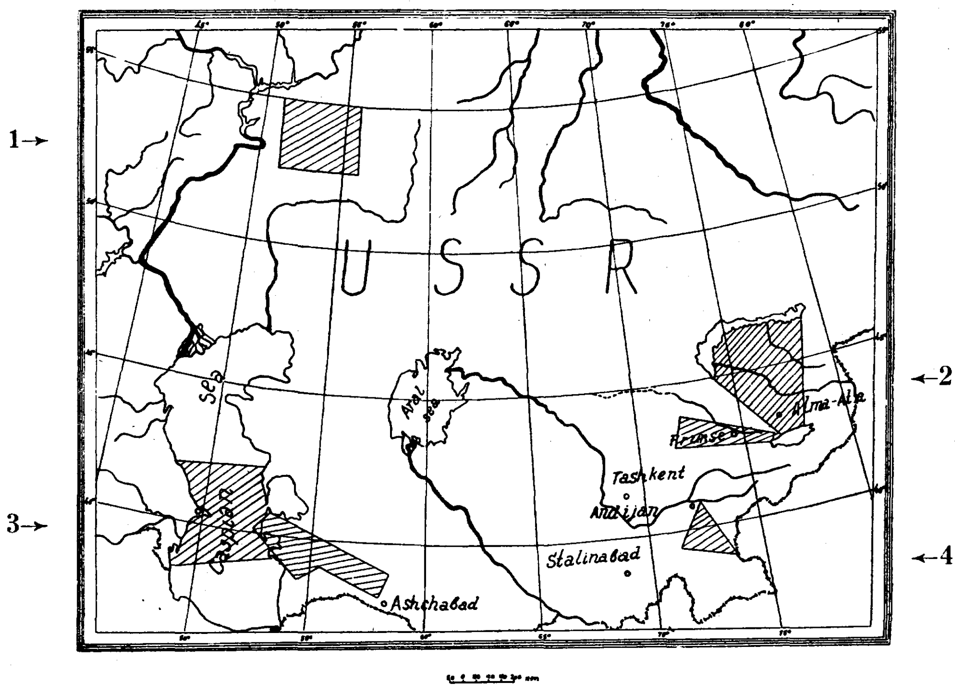

Fig. 2. Regions investigated by the method of deep seismic sounding : 1 — Volga-Ural district (1951, 1955); 2 — Northern Tien-Shan (1949, 1950, 1953); 3 — South-western Turkmenia (1952); 4 — Pamiro-Ahlie zone (1955).

Here only the results of observations in Middle Asia will be discussed. First, the geological structure of the areas under investigation will be recalled in general outline (28, 29).

Northern Tien-Shan represents a Hercynian folding construction in which the main block risings had taken place at the Alpine time. The Pamiro-Ahlie zone belongs to the region joining the Hercynian folding of Southern Tien-Shan and the Alpine folding of the Pamir Northern arcs. Here, the highest mountain peak of the USSR, the Stalin peak, 7.495 m. high is to be found.

In Western Turkmenia two fundamental structural elements are to be distinguished : The Epi-Hercynian platform in the area of the Bolshoi Balchan ridge and the Alpine zone containing the Transcaspian depression and the Kopet-Dag ridge. The presence of a thick (above 10 km.), low-velocity (3-4 km./sec.) loose sedimentary layer is a characteristic feature of this area.

The mountain areas of Middle Asia are characterized by negative Bouguer gravity anomalies. The maximum Bouguer anomalies (about —500 mgl) are observed in the Pamir area and the minimum (about —50 mgl) — in Western Turkmenia. In Northern Tien-Shan the anomalous values of gravity vary between —100 and —250 mgl.

In different regions the DSS observations were carried out on various profiles. The most complete (reversed) profiles providing data for determination of the absolute depths and boundary velocities of seismic waves travelling along the principal crustal boundaries, were followed in Northern Tien-Shan. From the data obtained on the uncomplete profiles of the Pamiro-Ahlie and Western Turkmenia zones only the relief of the deep boundaries could be determined for given boundary velocities, and the absolute depths approximately estimated.

In all three areas the principal wave groups — P°, P* and P — were recorded. In Western Turkmenia, waves corresponding to the paleozoic basement at a depth of 3-13 km. could be also followed.

Crustal sections had been made for the deep boundaries corresponding to the surface of the basaltic layer (horizontal velocity 6,4 km./sec.) and to the Mohorovicic discontinuity (boundary horizontal velocity 8,1 km./sec.) on the assumption that the vertical layer velocities were constant and equal to : 5,5 km./sec. in the granitic layer and 6,4 km./sec. in the basaltic layer.

The sections through the Pamiro-Ahlie zone were drawn from structural maps which in their turn had been made from isochrone maps by methods developed in seismic prospecting (19).

The sections and crustal structure diagrams will be now considered.

Northern Tien-Shan. Here the seismic refraction profiles extend from the Issik-Kul lake in the South to the Balchash lake in the North and from Issik-Kul, along the Kirghiz ridge, to the West. They crossed tectonically differend areas : mountain ridge areas with old Hercynian foldings and present intensive movements of the block type; areas of a platform structure, in particular foothill and intermountain areas.

Fig. 3_I represents a section along one of these profiles made from observations of explosions fired in the Issik-Kul, Kara-Kul (to the South of Issik-Kul) and Balchash lakes. Here a complete system of time-distance curves was obtained (reversed and overlapping). In the section made from seismic data by the method of time fields (19, 26) gravimetric data were also used. In fig. 3_I the boundaries corresponding to the surface d* of the basaltic layer and to the surface d of the Mohorovicic discontinuity are indicated as well as the earthquake foci from the data of E. I. Galperin, A. A. Vogel and I. V. Gorbunova.

According to fig. 3 the earthquake foci in his area are located in the granitic layer.

Crustal sections made from Deep Seismic Sounding data and the corresponding Bouguer anomalies

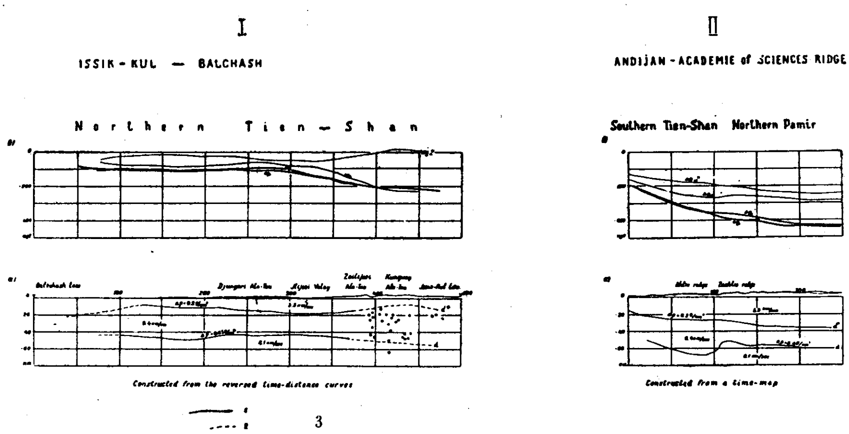

FIG. 3_I. *a*) A crustal section in the direction Issik-Kul-Balchash (eastern shore) made from DSS data with the gravimetric data also taken into account. Here are : d* — the surface of the basaltic layer; d — the Mohorovicic surface. 1 — portions of the d* and d boundaries drawn from reversed time-distance curves; 2 — from unreversed time-distance curves; 3 — earthquake foci.
b) Observed and calculated Bouguer anomaly Δg curves.
FIG. 3_{II}. *a*) A crustal section in the direction Andijan — Academy of Sciences ridge, made from DSS data.
b) Observed and calculated Bouguer anomaly Δg curves.

From this and from other sections drawn from DSS data, follows that over areas of a varied crustal structure the thickness of the crust and the thickness ratio of the principal crustal layers — the granitic, basaltic and sedimentary — may vary to a great extent. What regards Northern Tien-Shan, there we have for the Zailijski Ala-Tau, Kunguey Ala-Tau and Djungar Ala-Tau mountain ridges, corresponding risings of the basaltic layer whose thickness is increased in comparison with that of the depression regions. The Mohorovicic discontinuity, descending slightly under the mountain ridges, forms sloping mountain roots embracing large mountain systems, whereas the basaltic layer surface here repeats to a certain degree the earth's surface relief (*fig.* 3).

The Pamiro-Ahlie zone. In this region the DSS observations were carried out mainly along the Pamir high-way (in the direction leading from the city of Osh to the Kara-Kul lake) and in the Ahlie valley. From the DSS data surface diagrams of the basaltic and subcrustral layers and sections were drawn up (*fig.* 3_{IV}). These diagrams and sections indicate complex surface reliefs of both layers. A general down--buckling of both surfaces from the North to the South and the presence of a deep depression in the region of the highest Pamir mountain peaks (the Academy of Sciences ridge) are clearly outlined.

Fig. 3_{II} represents a crustal section in the meridional direction leading from Andijan to the Academy of Sciences mountain ridge (EL 72°30′) and some gravity curves.

In the crustal section of fig. 3_{II} as well as in other sections made for this region a difference in the crustal structure of Southern Tien-Shan and Northern Pamir is clearly indicated. In Southern Tien-Shan the crustal thickness varies from 45 to 70 km., the thickness of the granitic layer — from 15 to 25 km. and that of the basaltic layer — from 25 to 50 km. In Northern Pamir the crustal thickness is 50-70 km. the thickness of the granitic layer — 30-50 km. and that of the basaltic layer — 20-30 km. The « granitic » layer here includes also the Mezozoic and the Paleozoic metamorphized rocks.

Hence follows that in Southern Tien-Shan belonging to the Hercynian folding zone, the mountain roots are mainly basaltic, similar to those observed in Northern Tien-Shan also belonging to the Hercynian zone. In Northern Pamir of the Alpine folding zone, the mountain roots are on the contrary mainly granitic.

It should be noted that in the Pamiro-Ahlie zone roots of separate mountain ridges are not always delineated by the Mohorovicic surface. Thus, in Northern Pamir, judging from the Mohorovicic surface, the Transahlie ridge seems to have an antiroot. Throughout the Pamiro-ahlie zone the mountain roots are represented by a general down-buckling of the Mohorovicic surface which is complicated by local risings and depressions.

Western Turkmenia. Here the DSS profile lines crossed the zones of transition between the principal structures. They ran across the Kopet-Dag foothill depression and the Balchan and Danatin passages.

Fig. 4 shows a diagram of the crustal thicknesses from the DSS data. The minimum thickness (about 30 km.) was recorded in the

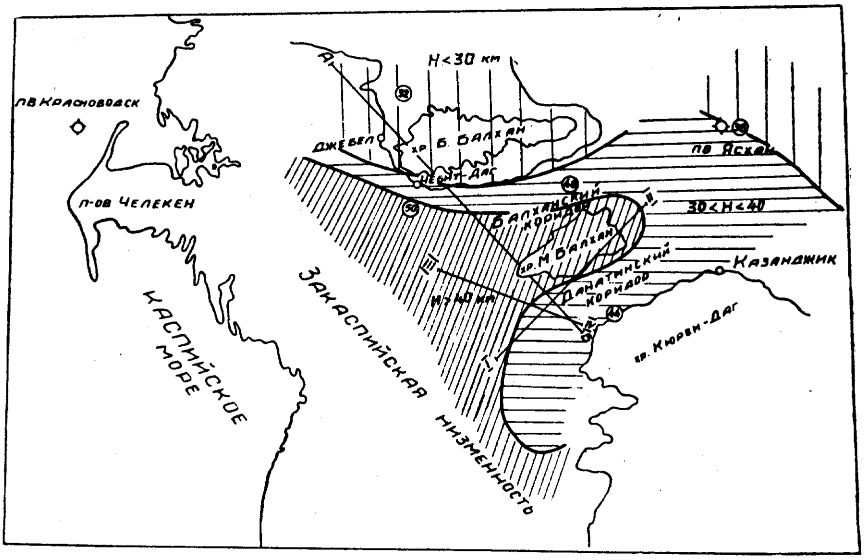

FIG. 4. A diagram of crustal thicknesses H drawn from DSS data for the Western Turkmenia area.

region of the Bolshoi Balchan ridge, which according to the judment of many geologists, belongs to the Epi-Hercynian platform. The maximum thickness was observed in the Transcaspian depression, belonging to the Alpine folding zone. The zone of transition between these regions and also the regions of the Balchan and Danatin passages are distinguished by a crustal thickness of 30-40 km. and by an abrupt descent of the Mohorovicic discontinuity in the direction of the Transcaspian depression.

The behaviour of the mountain roots in this region is rather peculiar. The old Hercynian construction of the Bolshoi Balchan ridge, clearly delineated by the present relief, has no deep roots which seem to have had time to dissolve, whereas under the present flat plain of the Transcaspian depression there are large roots which seem to predetermine a possible future transformation of the plain into mountains.

5. A COMPARISON OF CRUSTAL SECTIONS FOR DIFFERENT REGIONS.

In fig. 5 are represented diagrams of crustal sections from DSS data for different regions of the mountain and foothill areas of Middle Asia and also for the Russian platform and the Volga-Ural district (in Bashkiria), together with the corresponding Bouguer gravity anomalies.

The maximum crustal thickness — above 70 km. — was observed in high-mountain Northern Pamir (column 4). On platforms (columns 1, 2, 8) the crustal thickness was 30-40 km. The columns 5,8 are characteristic for a Hercynian folding. The basaltic layer predominated in this group of sections, the most characteristic of which was section 7 corresponding to the Zailijski Ala-Tau mountain ridge. Here the thickness of the granitic layer was only 10 km. and that of the basaltic — about 45 km. Columns 3 and 4 are characteristic for an Alpine folding. In these columns the granitic layer predominates. Northern Pamir is a striking example of such regions.

The features of the crustal structure in regions of Hercynian and Alpine foldings found in Middle Asia, agree with the well known data on the crustal structure in other regions of the globe. Thus, according to the data of B. Gutenberg and oth. (30, 31), the Appalachian section (a Hercynian folding) shows a thickness ratio of the basaltic and granitic layers similar to that of the Hercynian Tien-Shan; and crustal sections made in the Alps and in the Caucasus (33) (Alpine foldings) are similar to the crustal section of the Alpine Northern Pamir.

6. A COMPARISON OF THE DSS AND THE GRAVIMETRIC DATA.

Sufficiently detailed crustal sections provided by the DSS data have permitted a numerical comparison of the seismic and gravimetric data and a complex interpretation of both. Such a complex interpretation was carried out for regions of Northern Tien-Shan (8), of the Pamiro-Ahlie zone and of Western Turkmenia. For the last area a comparison of the seismic, gravity and magnetic data was carried out by U. N. Godin.

The above comparison has shown that quantitatively the shape of the (Bouguer gravity anomaly) Δg curve was usually close to that of the Mohorovicic surface. However, according to numerical computations, the gravitational effect (wg) depended strongly also on the shape of the basaltic layer surface.

Thus, in Northern Tien-Shan, where the principal boundaries in the earth's crust are not consistent with one another (*fig.* 3), the gravitational effect due to the surface relief of the basaltic layer, compensates to a certain degree the effect caused by the Mohorovicic discontinuity. In mountain areas of this type such compensation brings about a decrease in the gravity anomalies.

In Northern Pamir, where the surfaces of the basaltic layer and the Mohorovicic discontinuity are consistent with one another, the differential gravitational effects caused by both of them, intensify each other.

From the above follows that in trying to give a numerical explanation to the origin of gravity anomalies, one should take into account the influence of both principal layers in the earth's crust. In regions with a thick sedimentary layer, its influence should be also considered.

Modern methods for the determination of the crustal thickness from gravity data, based on the assumption of a so called « averaged » crust, give only a rough estimate of it so that different values of the crustal thickness may be obtained for the same gravity anomaly and vice versa. Thus, columns 3, 5, 6 in fig. 5 give for the crustal thickness very close values about 45-50 km., whereas the gravity anomalies vary from —75 to —260 mgl.

Conclusion.

From experience and from the results of investigations by the DSS method in various areas of Middle Asia — in Northern Tien-Shan, in the Pamiro-Ahlie zone and in Western Turkmenia — and also in other regions of the USSR, the following conclusions may be drawn :

1. In comparison with other known methods for investigating the continental crust, the DSS method, based on a correlational following of refracted longitudinal waves from weak explosions, has a high resolving power and permits to investigate in detail mountain, foothill and platform regions.

2. The investigations, carried out by the DSS method in various regions of the USSR, speak in favour of a layered crustal structure. In all regions under investigation groups of refracted waves were picked out, connected with the boundaries of the « granitic », « basaltic » and « subcrustal » (the Mohorovicic discontinuity) layers. In some regions waves connected with the sedimentary layer were also picked out. The wave groups observed in the DSS method are of a complex structure, indicating a complex nature of the transitions between the deep layers.

3. In the mountain regions of Middle Asia the crustal thickness is as a rule greater than in platforms and in plains : the mountains

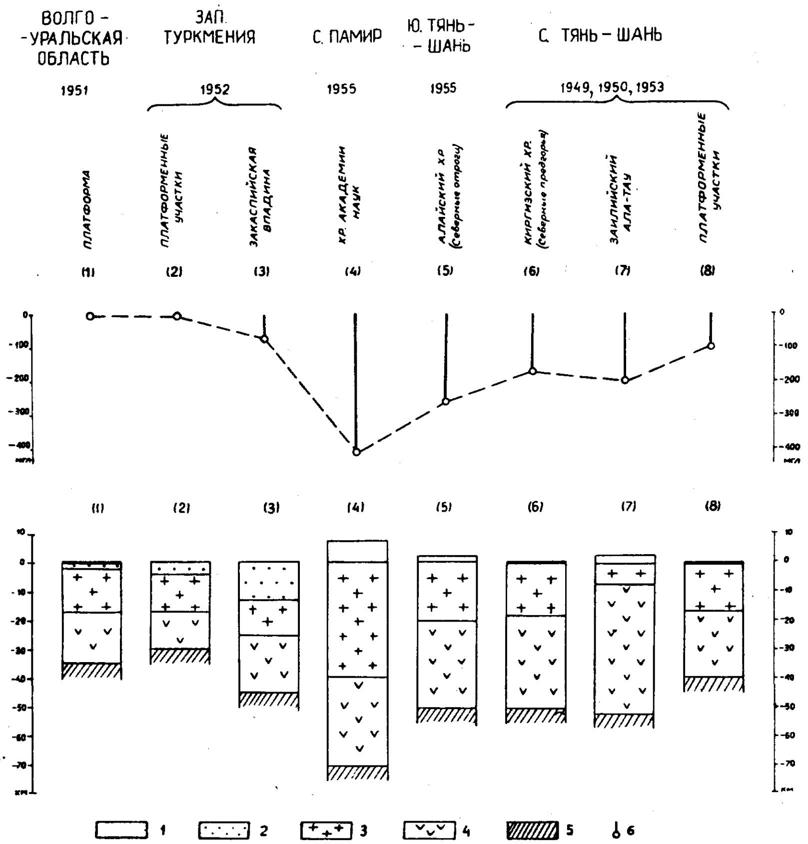

FIG. 5. Crustal structure from DSS data for various regions and the corresponding Bouguer gravity anomalies. 1 — the thickness of rocks lying above sea level; 2 — sediments; 3 — the granitic layer; 4 — the basaltic layer; 5 — the subcrustal layer; 6 — the Bouguer gravity anomalies 6 — a conditional Δg curve.

have roots. Under the large folding systems of Tien-Shan, Pamir and Turkmenia the mountain roots appear as a general down-buckling of the Mohorovicic discontinuity. At the same time this boundary, as well as the surface of the basaltic layer, form local projections and depressions, which do not conform with the present surface relief. In most cases the relief of the deep boundaries is not clearly reflected in such features of the earth's surface relief as separate mountains and valleys.

4. In various moutain regions of Middle Asia different crustal structures are observed, depending on the geologic age of the folding systems. In regions belonging to the Hercynian folding zone, the mountain roots are mainly connected with an increase in the thickness of the basaltic layer; in regions of the Alpine folding zone — with that of the granitic layer. Similar relations seem to exist in other regions of the globe.

5. A comparison of the DSS and gravity data on the shape of the deep boundaries in the earth's crust has shown that the negative gravity anomalies observed in mountain areas (in the Pamir regions the Bouguer anomalies run up to -500 mgl) are mainly due to the depth and shape of the Mohorovicic discontinuity. However, in numerical considerations of the origin of these anomalies, the depth and shape of the surface of the basaltic layer are also of great importance.

6. The DSS method used jointly with the gravimetric method and the high-frequency seismic methods for studying near erthquakes, contributes greatly to the investigation of the earth's crust. These geophysical investigations should be accompanied by geological ones.

It should be noted in conclusion, that in addition to the DSS method for investigating the continental crust, its modification for investigations on sea was also developed. This method is based on the experience gained from the DSS investigations on land and also on the known British and American seismic sea investigations. Investigations by this method were carried out in the central part of the Caspian sea. At present, following the program of the International Geophysical Year, investigations by this method are being carried out in the Ochotsk sea and in the North-western part of the Pacific with the aim of studying the crustal structure in the zone of transition from the continent to the ocean.

References.

1. Hill M. N. Seismic Refraction shooting in an area of the eastern Atlantic. Phil Trans. of the Royal Soc. of London. Series A. N° 890, V. 244, 1952.
2. Raitt R. W. Seismic refraction studies of the Pacific Ocean Basin. Part I : crustal thickness fo the central Equatorial Pacific. Bull. of the Geolog. Soc. Am., V 67, 1956.
3. Officer C. B. A deep-Sea Seismic reflection profile, Geophysics, V. XX, N° 2, 1955.
4. Katz S., Ewing M. Seismic refraction Measurements in the Atlantic Ocean. Part VII : Atlantic Ocean Basin, West of Bermude. Bull. of the Geol. Soc. of Am., V. 67, 1956.

5. ГАМБУРЦЕВ Г.А. Глубинное сейсмическое зондирование земной коры. Доклады АН СССР, т.87, № 6,1952
6. ГАМБУРЦЕВ Г.А. Глубинное сейсмическое зондирование земной коры. Труды Геофиз. ин-та АН СССР, № 25,/152/,1954.
7. ГАМБУРЦЕВ Г.А., ВЕЙЦМАН П.С., ТУЛИНА Ю.В. Строение земной коры в районе Северного Тянь-Шаня по данным глубинного сейсмического зондирования. Доклады АН СССР, т.105, № 1, 1955.
8. ГАМБРУЦЕВ Г.А., ВЕЙЦМАН П.С. Сопоставление данных глубинного сейсмического зондирования земной коры в районе Северного Тянь-Шаня с данными сейсмологии и гравиметрии Известия АН СССР, серия геофиз. № 9, 1956.
9. КОСМИНСКАЯ И.П., МИХОТА Г.Г., ТУЛИНА Ю.В. Опыт применения метода глубинного сейсмического зондирования для изучения строения земной коры в некоторых районах Западной Туркмении. Известия АН СССР. серия геофиз. № 7, 1957.
10. ГАМБУРЦЕВ Г.А. О корреляционных методах изучения землетрясений. Доклады АН. СССР, т.92, № 4, 1953.
11. ГАМБУРЦЕВ Г.А. О высокочастотной сейсмометрии. Доклады АН СССР, т.88, № 5, 1953.
12. ГАМБУРЦЕВ Г.А О новых методах и аппаратуре для регистрации сейсмических явлений. Труды Геоф. ин-та АН СССР, № 25/152/, 1954.
13. РИЗНИЧЕНКО Ю.В. Определение элементов залегания преломляющей границы в предположении, что она плоская лишь в области приема сейсмических волн. Изв. АН СССР, сер. геофиз., № 3, 1951.
14. РИЗНИЧЕНКО Ю.В. О совместной обработке ряда наблюдений головных сейсмических волн. Изв. АН СССР, сер. геофиз., № 1, 1952.
15. КОРИДАЛИН Е.А. Изучение строения земной коры сейсмическими методами. Академиздат, М. 1939.
16. САВАРЕНСКИЙ Е.Ф., КИРНОС Д.П. Элементы сейсмологии и сейсмометрии. Гостехиздат, М., изд. 1-1949, изд. 2 1955.
17. БУНЕ В.И., БУТОВСКАЯ Е.М. О годографе и строении земной коры в Средней Азии по зяписям мощных взрывов. Труды Геофиз. ин-та АН СССР, № 30/157/, 1955.
18. РИЗНИЧЕНКО Ю.В. К изучению строения земной коры в период Третьего Международного Геофизического Года.Изв. АН СССР' Серия геофиз., № 2, 1957.
19. ГАМБУРЦЕВ Г.А, РИЗНИЧЕНКО Ю.В., БЕРЗОН И.С., ЕПИНАТЬЕВА А.М., ПАСЕЧНИК И.П., КОСМИНСКАЯ И.П., КАРУС Е.В. Корреляционный метод преломленных волн. Академиздат., М. 1952.
20. ВЕЙЦМАН П.С. О подборе расстояний между сейсмографами при группировании с целью уменьшения фона помех. Известия АН СССР, Серия Геофиз., № 6, 1952.
21. ГАМБУРЦЕВ Г.А. Об определении азимута на эпицентр при регистрации местных землетрясений. Доклады АН СССР, т.87, № 2, 1952.
22. ГАМБУРЦЕВ Г.А. О новом виде фазовой корреляции при сейсмических наблюдениях. Доклады АН. СССР, т. 87, № 1, 1952.
23. ГАМБУРЦЕВ Г.А., ГАЛЬПЕРИН Е.И. Методика работ по корреляционному методу изучения землетрясений. Изв. АН СССР, сер. геофиз. № 1, 195-1954.
24. ГАЛЬПЕРИН Е.И. Азимутальный метод сейсмических наблюдений Гостоптехиздат, М. 1955.

25. ГАМБУРЦЕВ Г.А., РИЗНИЧЕНКО Ю.В. О фазовой корреляции при сейсморазведке по корреляционному методу преломленных волн. Доклады АН СССР, Новая серия т. 1945.

26. РИЗНИЧЕНКО Ю.В. Геометрическая сейсмика слоистых сред. Труды ИТГ АН СССР, т.П, 1946.

27. Корреляция сейсмических волн при глубинном сейсмическом зондировании земной коры. Известия АН СССР, Серия геофиз. №11,1957.

28. АРХАНГЕЛЬСКИЙ А.Д. Геологическое строение и геологическая история ССС, т. 1 и П. Госгеолиздат, изд. 4, 1947-1948.

29. БЕЛОУСОВ В.В. Основние вопросы геотектоники. Госгеолиздат, М. 1954.

30. REINHARDT H. Steinbruchsprengungen zur Erforschung des tieferen Untergrundes, Freiberger Forschungsheft. Akad. Verl. Berlin, C 15, 1954.

31. GUTENBERG B. Wave velocities in the Earth's crust, Bull. geol. Soc. Am., Special paper v. 62, 1955.

32. GUTENBERG B. Seismological Evidence for Roots of mountains. Bull. geol. Soc. Am., v. 54, 1943.

33. БАЛАВАДЗЕ Б.К. Гравитационное поле и строение земной коры в Грузии. Изд. АН Груз. СССР, Тбилиси 1957.

TRAVEL TIMES AND SOME DYNAMIC CHARACTERISTICS OF SEISMIC WAVES

N. V. KONDORSKAYA.

The present communication consists of two parts :

1. A study of the travel times of seismic waves from earthquakes recorded by the USSR seismic stations for epicentral distances from 2° to 80°.

2. A study of the dynamical features of the seismic waves for the Far East earthquakes.

By studying the travel times of seismic waves we had as a point of departure the well-known Jeffreys-Bullen travel-times curves /I/.

These travel-time curves are average, constructed on the basis of data of the seismological stations all over the globe. As an average these curves are the best and quite applied and justified for the determination of coordinates of the epicentres in different parts of the earth.

However the travel times to separate stations may give systematical deviations from these average curves. Taking into account these systematical deviations one can determine the location of epicentres more precisely. The first part of our communication is devoted to the investigation of these systematical deviations called forth by the peculiarities of the location of seismic stations in the USSR.

1. The travel times were studied in order to obtain the most correct position of the epicentres, for the Far East region in particular.

In this case the positions of the epicentres obtained by means of the data of stations at a short distance from the epicentre, were found different as compared with the positions resulting from the data of the distant stations and the Jeffreys-Bullen travel-time curves (1).

The investigation of the travel times of seismic waves were carried out for great epicentral distances at comparatively short intervals. It may be suggested in this case that the travel-time curves retain the same forms as the J-B ones, the deviations consisting in a parallel displacement of their branches. This leads to linearized conditions of the problem and it may be written :

$$\bar{t} = \mathcal{F}(\Delta) + \frac{\partial t}{\partial \Delta} h$$

The searched deviations are represented by means of additional terms α. The equation of the travel-time curves will thus be of the form :

$$t = \mathcal{F}(\Delta) + \frac{\partial t}{\partial \Delta} h + \alpha$$

The Far East region was studied by us particularly in detail. 22 Far East earthquakes with magnitudes $M \geqslant 6$ and well recorded seismograms of Soviet stations were selected for this purpose. The identification of waves and the determination of the main seismic elements were carried out by means of the following methods independents of the travel-time curves :

a) Methods based on the linearity of the curves and the method of successive approximation were used to determine the location of the epicentres.

b) The determination of the focal depth was carried out by means of the method based on the difference of travel times of sP and P waves at near and distant stations.

As a result of an examination of the dynamical features of the sP waves related with the mechanism of the focus we drew the conclusion that it is possible to distinguish the sP waves on the records of earthquakes with foci in the earths crust /2/.

These sP waves are revealed sufficiently distinctly on the records of the Far East earthquakes for epicentral distances from 2° to 80°. The determination of the focal depths has shown that the earthquakes in the region southeast of the Hokkaido Island and Kamchatka have focal depths of about 30 and 60 km. respectively.

c) The time of the origin was determined by means of the method based on the difference between the travel-times of the longitudinal and transverse waves to the near seismic stations.

The dynamical characteristics of the seismic waves and the focal depths were found different for epicentral regions south-east of the Hokkaido Island and that of Kamchatka. Therefore the travel-time curves of seismic waves had to be studied separately for each of the two above mentioned regions. The observed travel times of the longitudinal and transverse waves were compared with the times obtained from the J-B travel-time curves for the corresponding depths. For epicentral distances up to 10° travel time curves were constructed. It was found that they differ from the curves by Jeffreys-Bullen by their large values of travel times and coincide with the Wadati curves specially constructed for the Far East earthquakes. /3/ The differences between the travel times of P and S waves observed /o/ and calculated /c/ according to the Jeffreys-Bullen travel-time curves were examined for the corresponding depths of foci. These differences are represented in Fig. 1. The curve by

Jeffreys-Bullen was accepted as the zero line. O-C deviations in sec. are plotted along the vertical axis, the epicentral distances along the horizontal axis. Regional peculiarities, depending upon the location of a station are clearly seen from Fig. 1. For two regions

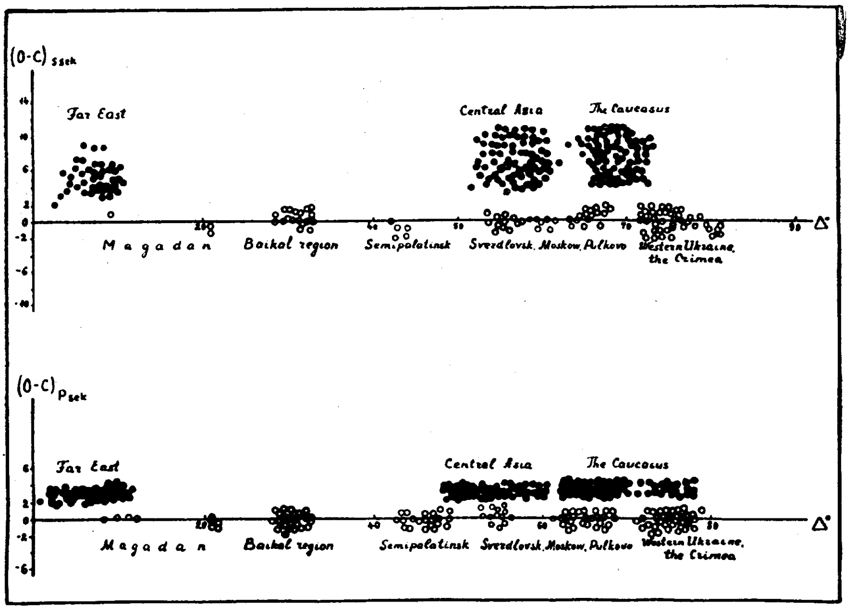

$(O\text{-}C)_{P\,sek}$ and $(O\text{-}C)_{S\,sek}$

FIG. 1.

of the Far East /to the south-east of the Hokkaido island and the Kamchatka region/ the differences $(O\text{-}C)_p$ and $(O\text{-}C)_s$ for seismic stations Moscow, Pulkovo, Sverdlovsk, Semipalatinsk and for stations of the Crimean and the Karpat regions are either negative or zero for P waves and + 2 — 3 sec for S waves. Regular deviations of $(O\text{-}C)_p$ and $(O\text{-}C)_s$ from the J-B travel-time curve are observed in the case of the stations in Central Asia and the Caucasus, situated at the same epicentral distances as the stations Moscow, Pulkovo and Sverdlovsk.

Mean values of the deviations $(O\text{-}C)_p$ and $(O\text{-}C)_s$ were obtained as a result of a statistical averaging by means of the least square method. Thus $(O\text{-}C)_p = +\,(2\text{-}3)$ sec and $(O\text{-}C)_s = +\,(6\text{-}8)$ sec were found by us for P and S waves, respectively. These average values were considered as additional values to the J-B travel-time curves. The deviations which were found may be partially explained by the difference in the structure of the earth's crust in the investigated regions and the average structure of the crust all over the globe. They may also be caused by the difference between the wave velocities on the basalt-ultrabasalt boundary as well as in the layers of the earth's mantle. A study of the $(O\text{-}C)_p$ and $(O\text{-}C)_s$ deviations for the stations of Central Asia and the Caucasus has shown that they did not depend upon Δ and were constant within the regional interval. No relation between the value of these deviations and the azimuth of the stations was established. A study of the local peculiarities of the travel-times of P and S waves was also carried out for four Central Asian and three Turkish earthquakes. The same characteristic features of the travel times were found for the group of stations located in different regions of the USSR. The experimental travel times of seismic waves propagating from the foci in Central Asia and Turkey to the Far East, Central Asia and the Caucasus were found to be greater than the ones calculated by means of the J-B travel-times curves. For longitudinal and transverse waves the differences are 2-3 and 6-8 seconds, correspondingly /4/.

The allowance for the peculiarites of the above mentioned stations permitted to obtain a good agreement between the values of the coordinates of the epicentres determined from the records of near and distant stations and to determine the epicentres more precisely. Experimental corrections of the J-B travel times curves are especially essential for the determination of the epicentres of the Far East earthquakes, since the amount of data obtained at the nearest stations are usually insufficient for correct determinations of the epicentres. These corrections were used by us for the determination of the epicentres of the Kurilo-Kamchatka earthquakes of 1954-1956. The coordinates of the foci of these earthquakes with magnitudes $M \geqslant 4$ were determined by the author and G. A. Postolenko. Seismograms of distant seismic stations were used in the course of this work. It was possible to reveal in these seismograms the sP waves. It was found that on the majority of the Far East records the most intensive were the waves propagating 10-30 seconds after the S wave. According to the kinematic features this seemed to be the sS wave. The detection of these waves was very useful for the determination of the focal depth.

Fig. 2 and 3 represent the chart of earthquakes with different intensities and depths. According to this chart it can be seen that the epicenters of the earthquakes along all the Kurilo-Kamchatka arc are placed in separate groups.

Chart of the Epicenters of Kurilo-Kamchatka earthquakes for the years 1954-1956.

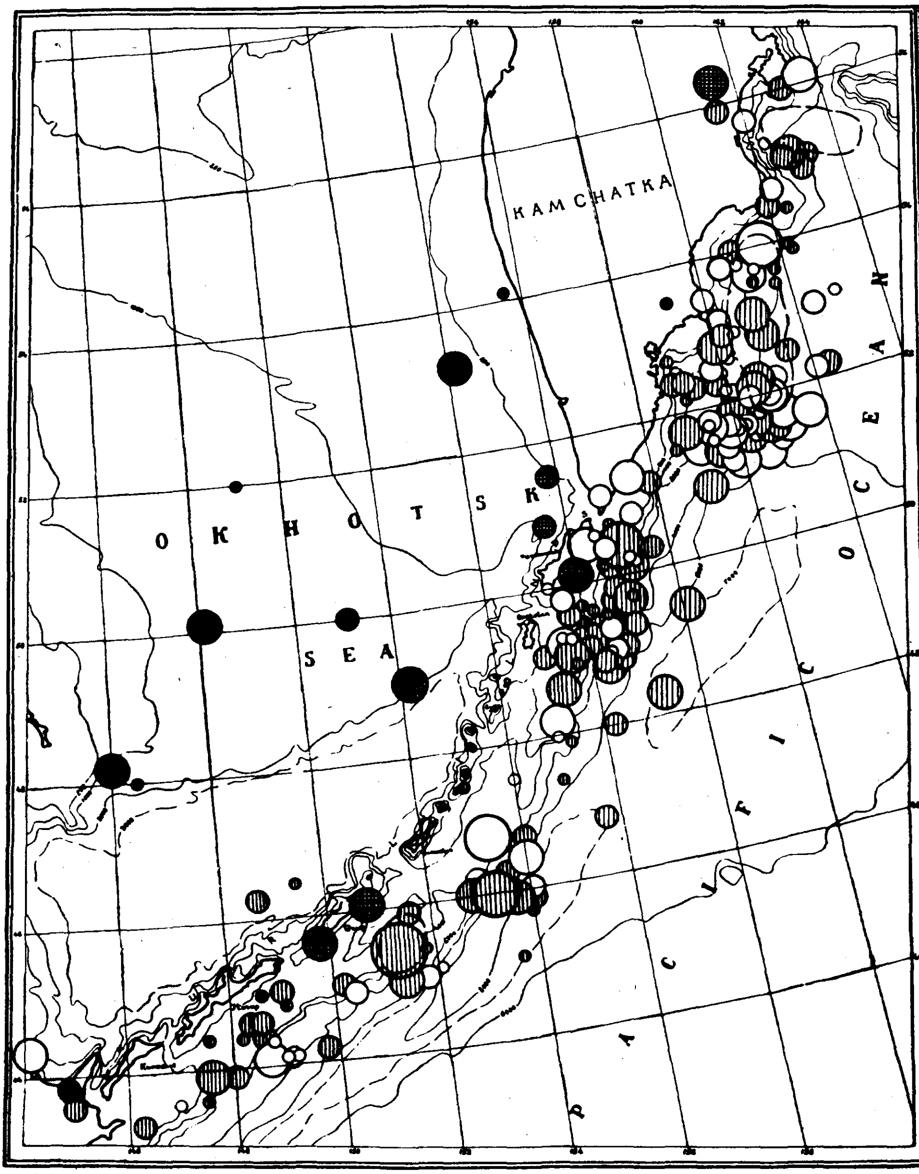

1:5000000

LEGEND

CLASSIFICATION OF EARTHQUAKES ACCORDING TO INTENSITY

- Epicenter of the earthquake M-8
- Epicenters of the earthquakes M-7
- Epicenters of the earthquakes M-6
- Epicenters of the earthquakes M-5
- Epicenters of the earthquakes M = 4

See additional legend note p. 121

CLASSIFICATION OF EARTHQUAKES ACCORDING TO DEPTH

- Epicenters of the earthquakes h-0-50 km
- Epicenters of the earthquakes h-60-100 km
- Epicenters of the earthquakes h-110-300 km
- Epicenters of the earthquakes h>300 km
- Tsunami regions

FIG. 2.

The existence of a group of earthquakes with surface foci seems to be particularly evident. The positions of the epicentres of earthquakes accompanied by tsunamies are given by contour lines. It is clear that these positions lie close or within the region, where the above mentioned surface foci are located.

2. The study of the dynamical features of the Far East earth quakes recorded by the USSR stations.

The study of the amplitudes of longitudinal waves and their dependence upon the epicentral distances was carried out. Attempts were made to obtain the parameters referred to an absorption of the longitudinal waves in the earth mantle on the basis of the decreasing amplitudes of longitudinal waves of the Far East earthquakes.

For the amplitude Ac of longitudinal waves at an epicentral distance Δ and azimuth Az we have :

$$A_e = A_p \sqrt{\frac{\cos e_h \frac{de_h}{d\Delta} T_p e^{-\alpha s}}{\sin \Delta \sin l_0}} f(x, y, e_0, A_z)\, k\, VU_1 \qquad (1)$$

where A_p — is the constant related with the energy emitted by the longitudinal waves,

e_h — angle of emergence from the focus,

e_0 — angle of emergence at the earth plane,

T_p— period of the arrival of the wave,

α — coefficient of absorption,

s — the length of the ray,

f (x, y, e_0, Az) — function taking into account the irregularity in the emission of the earthquake focus, depending upon the orientation of the nodal plane (x, y) and the location of the stations (e_0, A_z),

k — coefficient of reflection at free and inner boundary /5/

VU_1 — magnification of the instrument for the entry P wave.

Equation /1/ may be written :

$$\sqrt{\frac{A_e}{T_p \mathcal{F}(e_h, \Delta, e_0) \quad f(x, y, e_0, A_z)\, k\, VU_1}} = A_p\, e^{-\frac{\alpha}{2} s} = A'_p \qquad (2)$$

For the estimation of the dependence of the right side of equation (2) upon s we determined.

$$VU_1,\ T_p,\ \mathcal{F}(e_h\ \Delta, e_0),\ f(x, y, e_0, A_z) \text{ and } k$$

The question about the magnification of the instrument for the entry waves (VU_1) and the period (T_p) was considered by the author in collaboration with D. P. Kirnos /6/.

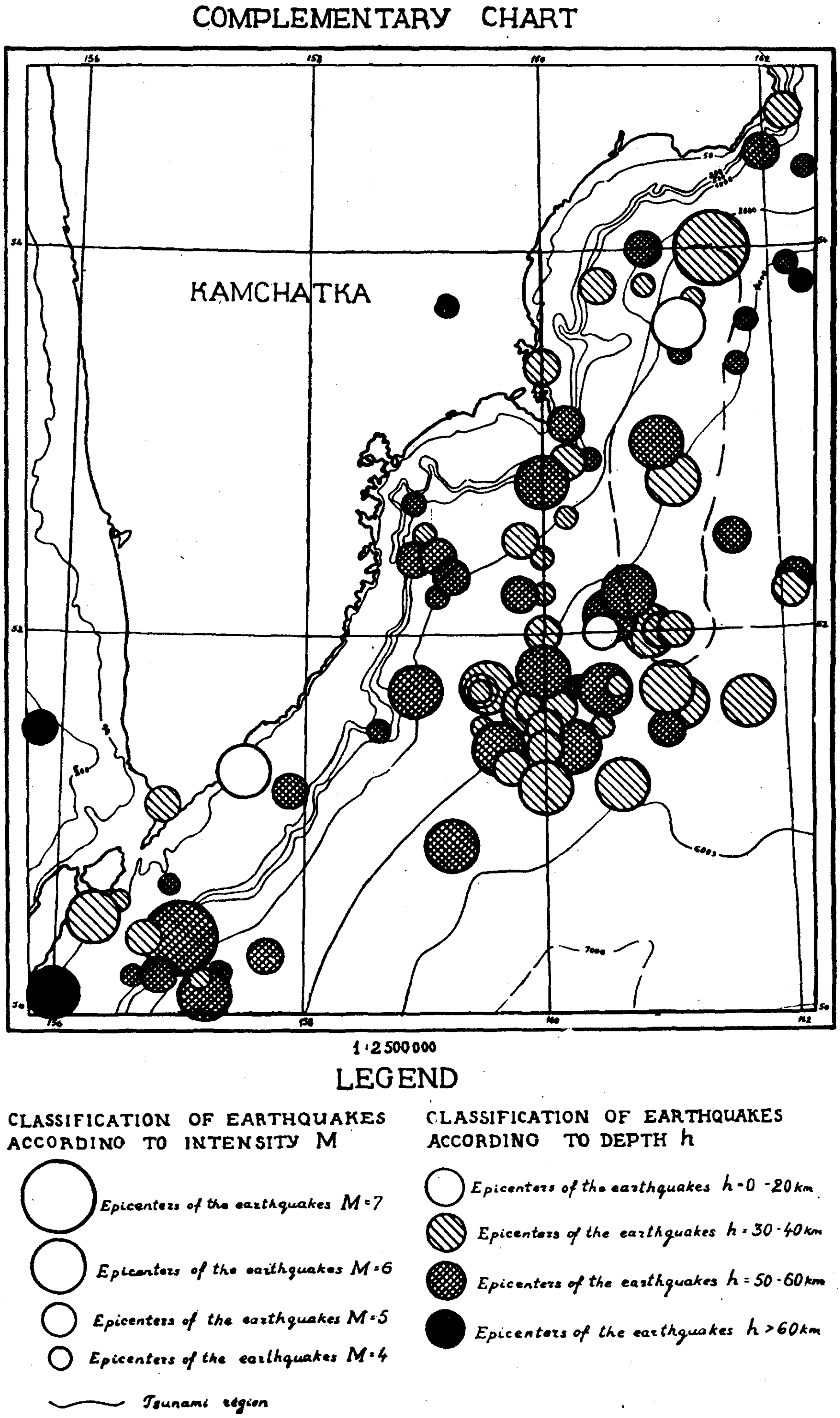

FIG. 3.

See additional legend note p. 121.

The value of f $(x, y, e_0$ $A_z)$ was found assuming the focus to be a dipole with a moment /7/.

The function F (e_h, Δ, e_0) was calculated by means of the method of numerical differentiation of the J-B travel time curve /1/.

The dependences $A'_p = f(s)$ were constructed proceeding from the determination of the values in the left hand side of formula (2).

The dependence $A'_p = f(s)$ for the earthquake 3-1-1957, 12 h., recorded at soviet seismic stations is represented on fig. 4. As can be seen from fig. 4 there is maximum of amplitudes at epicentral distance $\sim$ 40°.

This peculiarity can be explained as follows : 1. The absorption of P waves is different at different depths of the earth's mantle. 2. The absorption of P waves is different for different regions (the maximum of amplitudes has been observed for Central Asia region). However the additional investigations based on experimental data are necessary for the confirmation of the obtained conclusion.

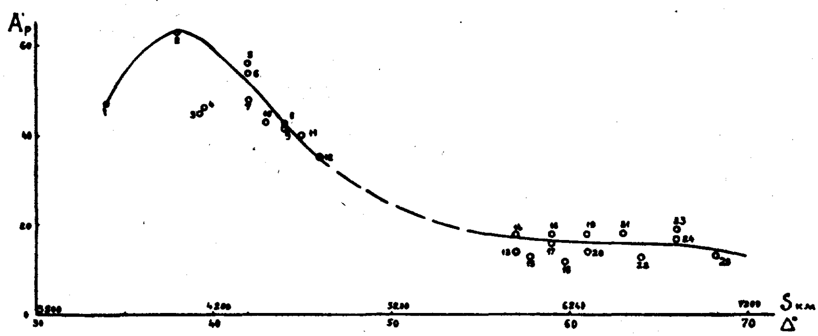

The figures mean the experemental data of the seismic stations of the USSR :

1 Semipalatinsk	9 Horog	17 Pyatigorsk
2 Alma-Ata	10 Chimkent	18 Tbilisi
3 Naryn	11 Kulyab	19 Erevan
4 Frunze	12 Stalinabad	20 Nakhicheran
5 Andijan	13 Moskow	21 Veodosiya
6 Namangan	14 Machatchkala	22 Simverопol
7 Fergana	15 Shemakha	23 Kishinev
8 Sverdlovsk	16 Kirovobad	24 Chernovcy
		25 Ujgorod

FIG. 4.

REFERENCES.

1. JEFFREYS (H.) and BULLEN (K. E.) : « Seismological tables », 1940. British Association for the Advancement of Science. Gray Milne Trust.

2. Kondorskaya (N. V.) : « Application of sP waves with foci in the earth's crust for the determination of focal depths. Publications of the Geophysical Institute of the USSR Acad. of Sciences, N° 36, 1956.
3. Wadati (K.) : « Travel times of P and S waves ». Geophysical Mag. Vol. VII, N° 11, 1933.
4. Kondorskaya (N. V.) : « On the peculiarities of the travel times of seismic waves ». Izvest. Akad. Nauk SSSR, Ser. Geofiz., N° 7, 1957.
5. Kogan (S. D.) : The parameters of the foci of the deep earthquakes ». Publications of the Geophys. Inst. of the USSR Acad. of Sciences, N° 30, 1955.
6. Kirnos (D. P.) Kondorskaya (N. V.) : « On the determination of the amplitudes of first entrances of seismic waves ». Izvest. Akad. Nauk. Ser. Geofig., n° 12, 1958.
7. Keilis-Borok (V. I.) : « The graphical methods of calculations of the earthquake foci parameters ». Izvest. Akad. Nauk SSSR, Ser. Geofiz., N° 6, 1951.

NOTE

Additional Legend for Fig. 2 and Fig. 3

instead of	$M = 8$	read	$M \geqslant 7\,1/2$
	$M = 7$		$6\,1/2 \leqslant M < 7\,1/2$
	$M = 6$		$5\,1/4 \leqslant M < 6\,1/2$
	$M = 5$		$4\,1/4 \leqslant M < 5\,1/4$
	$M = 4$		$M < 4\,1/4$

THE STUDY OF A DECREASE OF P-WAVES AMPLITUDES IN THE SHADOW ZONE ON THE EARTH'S MODEL

L. N. RYKUNOV.

To judge of the waves with the epicentral distances $\Delta > 105°$ it is necessary to solve the problem on seismic waves diffraction by the Earth's core. There is a large number of works devoted to the diffraction problem by the sphere. However there is no satisfactory solution of this problem for the case of seismic waves diffraction.

Similar problem was studied by G. Y. Makarov, G. Y. Petrashen, W. A. Fok, G. Y. Sholte and others. But some simplifications of the principle suppositions (acoustical media, stationary process) do not allow to compare their results with the seismological data. Therefore it is not possible to say anything about these or those mechanical properties of the matter in the core influence on the P-waves diffraction.

In our work this problem was investigated by the seismic model method with an ultrasonic seismoscope developed by prof. Riznichenko and his collaborators (Institute of the Earth's Physics of the USSR Academy of Sciences). Seismic waves were modeled by the ultrasonic pulse. Vibrations of the Earth's model was received by means of piezoelectric cristall and registered with the help of the cathode-tube oscillograph.

Model of the Earth (diameter 38 cm.) was fabricated from paraffino-polyethylenic alloy and represented the sphere with an empty core. This core was filled by matters with different mechanical properties.

The estimation of homogeneousness and absorption of the mantle of the Earth's model made by means of comparison of a theoretical data with experimental ones, for the case of Lamb's problem. This comparison showed that ultrasonic waves periods of which were greater than 12.10^{-6} sec. decreased proportionally to I/r^2, where r is the distance between the source and the receiver. Therefore the obtained results showed that that matter used for model is homogenous and ideally elastic for periods of waves $\tau > 12.10^{-6}$ sec.

To apply the results of modelling to the true Earth it is necessary to execute an requirement of similarity.

Table (for model with paraffino-polyethylenic mantle and gelatinous core) shows that requirements of similarity are satisfied approximately. Criterion of similarity related to the periods of vibrations may be satisfied by some extrapolation.

It was made comparison of the wave pictures in the shadow zone for the case of an empty core (~ Imm. Hg), aerial core and water core (rigidity of core is zero). In this case all round bulk modulus and density of the Earth's model core were significantly changed. All round bulk modulus was equal to 1.4 . 10^6 dn/cm^2 and $.10^{10}$ dn/cm^2; density 1.3 . 10^{-3} g/cm^3 and 1.0g/cm^3, velocity of P-wave — 0.3 .10^5 cm/sec. and 1.5 . 10^5 cm/sec. for aerial and water core respectively. Velocity of P-wave for the mantle of the Earth's model was equal to 2.0 . 10^5 cm/sec.

The results of this comparison show that a change of this parameters does not influence on the P-waves amplitudes decrease (*fig.* 1). The same result takes place for the case of rigidity change

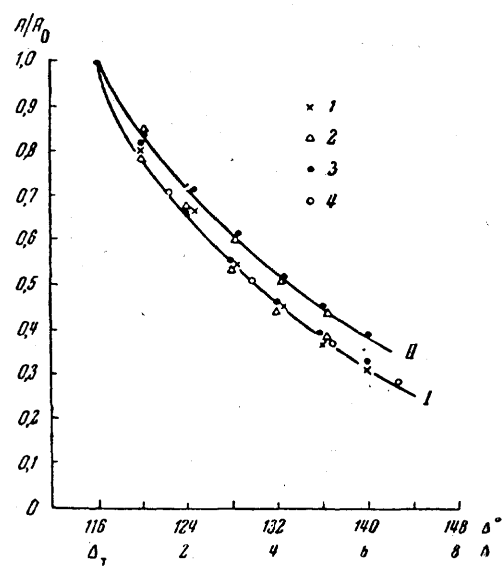

FIG. 1. — Amplitudes of P waves in the shadow zone.
I. $\tau = 14.10^{-6}$ sec.; II. $\tau = 22.10^{-6}$ sec.; 1. « empty » core; 2. aerial core; 3. water core; 4. aerial core and gelatinous mantle.

in the mantle; 10^{10} *dn/cm* (paraffinopolyethylenic alloy) and 10^5 dn/cm^2 (gelatin).

Thus the core of the Earth's model rigidity of which is equal to zero does not influence on P-waves amplitudes in the shadow zone. Therefore it is possible to use acoustical model with an empty core for theoretical conclusions about diffraction of seismic waves on the Earth's core.

2. Some investigations were made to get the estimation of rigidity of the core influence on decrease of P-wave amplitudes in the shadow zone. The rigidity of the Earth's model core was equal to 10^5 *dn/cm* (gelatin) and zero (water), while the rest parameters acquired values near to the similarity demands. The velocity of a decrease of P-wave amplitudes in the shadow zone was found to be essentially dependent on a change in the rigidity of the core (*fig.* 2) /10^5 dn/cm^2 for models is 10^8 dn/cm^2 for the Earth/.

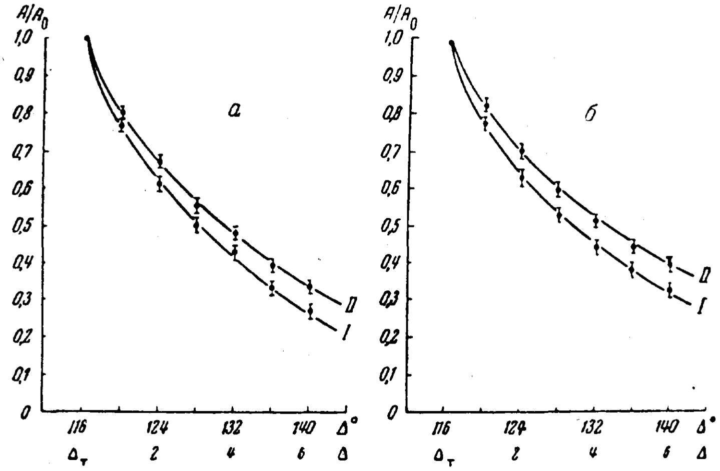

FIG. 2. — Amplitudes of P waves in the shadow zone.
1. $\mu = 10^5\ ^{dn}/_{cm^2}$; II. $\mu = 0$; *a.* $\tau = 14.10^{-6}$ sec.; *b.* $\tau = 22.10^{-6}$ sec.

For our measurements two wave periods equal to 14.10^{-6} sec. and 22.10^{-6} sec. where used. A wave period equal to the requirements of similarity is 2.10^{-6} sec. The character of a decrease of P-wave amplitudes was found to be nearly to exponential low;i.e.

$$A/A_o = e^{-\frac{1}{k(\tau,\ \mu)} \cdot \Delta},$$

where. A is amplitude of P-waves in the shadow zone, A*o* — amplitude of P-waves on the boundary of the shadow zone, Δ -the epicentral distance (Δ °/4°), k (τ, μ) — empirical coefficient characterizing the decrease of P-wave amplitudes, τ -period of P-waves. μ -rigidity of the core. We have that δk (14.10^{-6}) = 0.80. δk (22.10^{-6}) = 1.05 and δk (0) = *o*, where

$$\delta k(\tau) = k(\tau, o) - k(\tau, \mu).$$

Hence the magnitude of δk (2.10^{-6}) is 0.3 approximately. This estimation shows that the change of rigidity of the Earth's core from zero to 10^8 dn/cm^2 changes magnitude of k (τ, μ) to 5 — 10 per cent.

3. From a large number of works on diffraction quantitative results are obtained only by J. G. Sholte, who estimates the velocity of a decrease of P-waves amplitudes with the period of 180 sec. for a stationary process and ideally liquid core. The comparison of the Sholte's results with the seismic data shows that the observed P-waves amplitudes decrease like the computed ones (*fig.* 3).

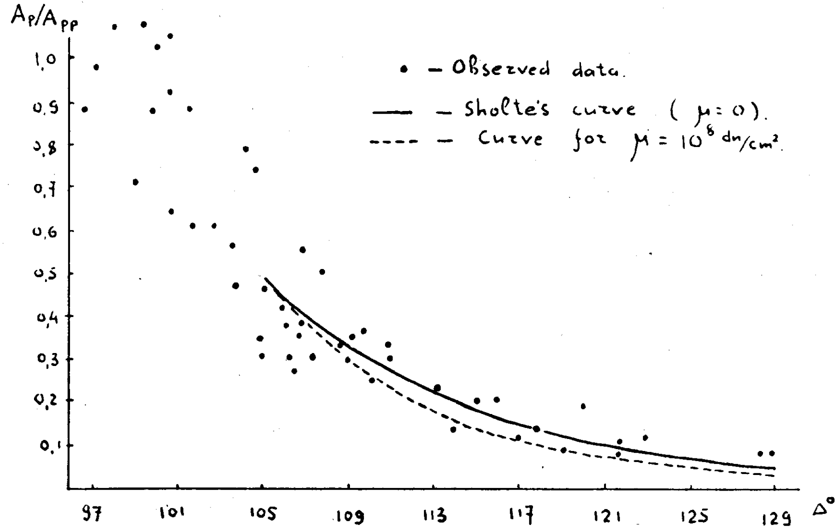

Fig 3.

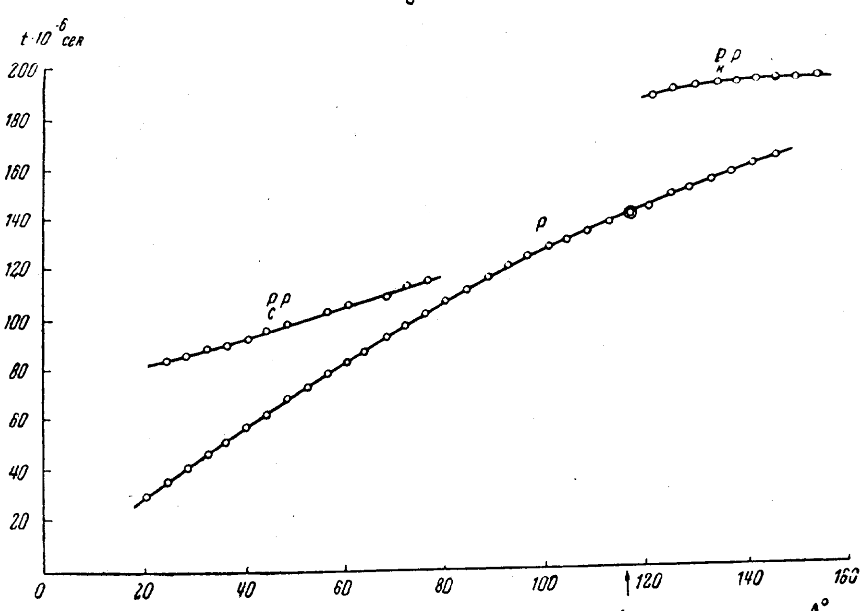

FIG. 4. — Travel time curve for Earth's model.

It is possible to suppose now that the rigidity of the Earth's core is near to zero.

TABLE

Criterion of Similarity	The Earth	The Earth's model
r_2/r_1	0,54	0,54
t/τ	9,50	$1{,}33\ \tau_1 = 14.10^{-6}$ $0{,}86\ \tau_2 = 22.10^{-6}$ $9{,}50\ \tau = 2.10^{-6}$
ρ_2/ρ_1	1,76	1,21
$K_1\tau^2/r^2{}_1\ \rho_1$	$2{,}84.10^{-4}$	$3{,}10.10^{-4}$
$K_2\tau^2/r^2{}_1\ \rho_1$	$2{,}72.10^{-4}$	$3{,}02.10^{-4}$
$\mu_1\tau^2/r^2{}_1\ \rho_1$	$1{,}26.10^{-4}$	$1{,}20.10^{-4}$
$\mu^2\tau^2/r^2{}_1\ \rho_1$	(μ_2)обр $.4{,}35.10^{-15}$	(μ_2) мод $.1{,}16.10^{-12}$

r_1 and r_2 [cm] — radius of the Earth and Earth's core; τ [sec] — period of seismic waves; t [sec] — travel time for $\Delta° - \Delta°_T = 20°$ (Fig. 4); ρ_1 and ρ_2 [gr/cm^3] — density; K_1 and K_2 [dn/cm^2] — all round bulk modulus; μ_1 and μ_2 [dn/cm^2] — rigidity of the mantle and core respectively.

PROPERTIES OF THE EARTH'S MANTLE & THE PHYSICAL NATURE OF THE TRANSITION LAYER (LAYER C.).

V. A. MAGNITSKY et V. A. KALININ

1.

Due to the recent progress in seismology and other branches of geophysics we can safely enough discuss the general character of the structure of the mantle and various properties of its material. The most essential characteristic of the mantle is the fact that it consists of 3 main layers : 1) the upper layer (or B according to Bullen's definition), 2) the transition layer (C), 3) the lower layer (D). It is highly probable that the entire mantle is solid (1, 2, 3). It is only on its uppermost parts that there are some data which may suggest the possibility of a vitrious state existing there (1, 4).

Investigations of the behaviour of the derivative of the incompressibility K with respect to pressure p, $\frac{dK}{dp}$ made by several writers independently have brought to light the fact that B and D layers must, with all certainty, be considered as homogeneous (5, 6, 7, 8).

In solving the problems associated with the structure of the mantle and those concerning the formation and development of the crust, it is of the utmost importance to find out the physico-chemical nature of the transition layer C, i. e. to ascertain nature of the differences between the B- and the D- layers.

The existence of a special transition layer in the mantle was first suggested by B. B. Golitsyn in 1915 (9). Further investigations fully confirmed the idea of a layer possessing somewhat peculiar properties being present in the mantle (1, 3, 10, 11).

The presence and location of the C — layer is revealed by the triplication of the travel — time curves at the epicentral distance of about 20°.

The C — layer rests at the depth of 400-900 kilometers, though some authors suppose it to begin at a lesser depth, there are those who do not believe it to occupy more than the interval between 400-600 km (1). But these differences of opinion do not concern the fundamental characteristics of the transition layer, i. e. the singularly rapid increase in velocities of seismic waves with the depth. Fig. 1 shows both the velocities of longitudinal waves at the depth of 100-1.400 kms according to the widely known Jeffreys &

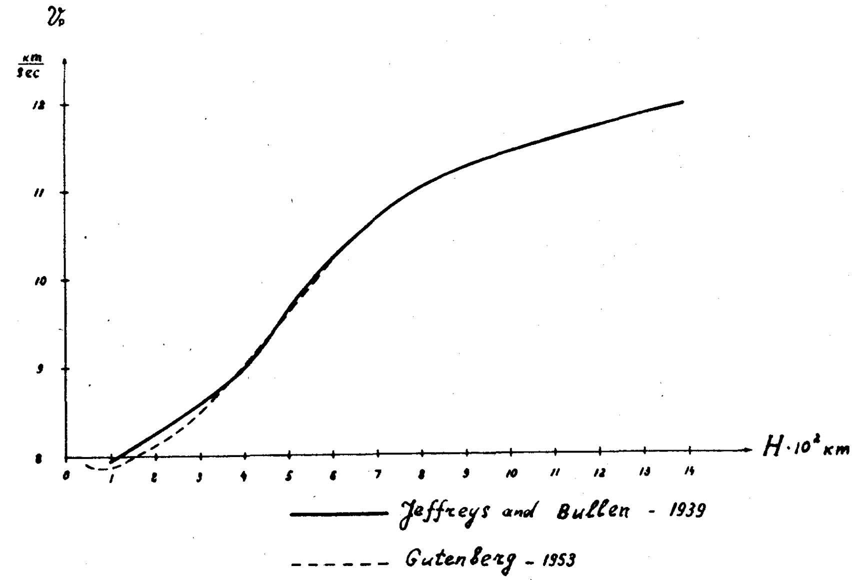

FIG. 1.

Bullen seismological tables (12) and for the sake of comparison the velocities down to 600 kms calculated by Gutenberg, who used an altogether different method (13). The region of rapid velocity increases is easily distinguishable in the diagram. This change in velocity is due to the rapid change in the elasticity coefficients, thus, fig. 2 shows the curve of change in the ratio $\frac{K}{\rho}$ (ρ — density), in which this change of mechanical properties is demonstrated.

Two suggestions have been made as to the nature of the C — layer. The first of them was stated long ago by several investigators, they supposed the unusual properties of the transition layer to be caused by changes in the chemical composition of the mantle. The general concept was that the percentage of heavy atoms, mostly of iron, increased with the depth. However, the increasing of the percent of iron in the olivine, which is considered to be the chief component in the material of the mantle, does not agree with seismological data as the transition from forsterite to fayalite is accompanied with a decrease in velocity and in the ratio $\frac{K}{\rho}$ (5, 14).

An attempt has been made recently to explain the properties of the C- layer on the assumption that the percentage of iron grows only down to the depth of 500 kms, still, even if this is really the case, the properties of the D- layer do not agree with the seismological data, since the ratio $\frac{K}{\rho}$ becomes too small (15).

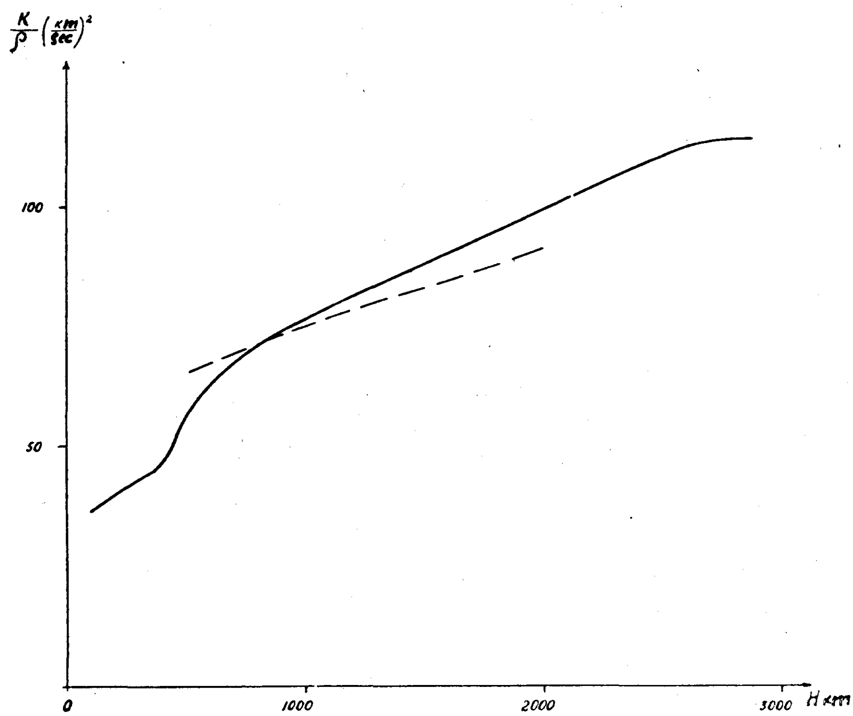

FIG. 2.

In a somewhat better conformance with the seismological data is the suggestion that the D- layer consists of oxides of Mg and Fe, in favour of which V. A. Magnitsky advanced some considerations of thermodynamic character. On the other hand, this suggestion is at variance with our conception of the Earth's chemical composition as based, for instance, on the analysis of meteorites.

The alternative hypothesis as to the nature of the C- layer was advanced by J. Bernal (16). He suggested that at the depth in question a polymorphic transition takes place without any considerable change in chemical composition. This hypothesis, however, gave rise to a controversy : it was pointed out that under a pressure of 2.10^5 atm a mere change in the lattice could hardly be expected to cause a sufficient change in the density of so closely packed structure as olivine. Moreover, such a change must be abrupt, not gradual and taking some hundreds of kilometers (17).

Then Jeffreys pointed out that Bernals hypothesis was based on an analogy that was, seemingly, erroneous (18).

In his well known paper, F. Birch suggested that in layer C there occurs a change in lattice of the different components of the mantle. His idea was criticized by Verhoogen, who, apart from the above mentioned objections, brought out some others based on cristallography (19).

In the same paper Verhoogen drew attention to the fact that the change in different interatom distances under compression must be unequal, and that if it were possible to shorten the distance *Mg* — *O* down to 1.97 Å, instead of the normal 2.10 Å (20), while keeping the distance *Si* — *O* unaltered, the crystals obtained would have sufficient density and incompressibility to conform with the properties of the D- layer in the mantle.

To account for the transition from the B- layer to the D- layer, V. A. Magnitsky suggested that in the C- layer there occurs a change in the type of bond in the olivine : viz. from the prevailing ionic type of bond between *Mg* and *O* in the B- layer to the prevalence of the valence type under pressures existing in the D- layer (21).

2.

The hypothesis which explains the transition from the B- layer to the D- layer by assuming that when pressure reaches the order of 2.10^5 atm, the ionic type of bond is transformed into a valence type, is based on the following considerations.

Considering that the mantle is solid and taking into account the fact that molecular crystals can't affect its structure to any great extent, we must infer that of all types of solids none but ionic crystals and valence crystals should be considered in solving the problem of the structure of the mantle.

The properties of metals are known to approach those of the Earth's core, but in the structure of the mantle the former can play no important part since neither the electroconductivity of the mantle nor its mechanical properties bear any resemblance to these characteristics in the metals.

From the theory of chemical bond (22, 23) as well as from the theory of solids (24) it must be inferred that ionic compounds, valence compounds and metals form a regular sequence, between the typical representatives of these there are many intermediate compounds — the connecting lines that show bonds of mixed character and have intermediate properties. Alkali halides are rather typical of ionic compounds while valence crystals are formed of similar nonmetal atoms such as atoms of Si, Ge, C (diamond). However, among the well defined valence compounds there are many that are formed of atoms of different elements as, for example, pyrite FeS_2, silver iodide.

Gray tin, graphite and indium are typical representatives of intermediate substances that are between metals and valence crystals. Typical as intermediate between ionic and valence crystals is, for example SiO_2, as well as many others : halogenides of silver, for instance, show a whole range of transitionery states from the almost purely ionic AgF to the almost purely valence one AgI. There are well known instances of transition from the metallic type of bond to the valence bond and back taking place in the same substance as a result of changing pressure (white and gray tin, white phosphorus under high pressure is modified to a metallic state). This transition to a metallic phase has received a thorough enough theoretical investigation (24, 25, 26), it was used by Ramsay for explaining the transition from the mantle to the core (27) and in a number of his other works.

The problem of the transition from the ionic type of bond to the valence type as the effect of changing pressure or temperature has hardly been investigated at all, though theoretically its possibility is unquestionable, and it was pointed out long since by Pauling (22). The cause of this problem still remaining practically unexplored experimentally is chiefly due to the difficulty of distinguishing between the normal polymorphic transition that is brought about by high pressure and the one that involves a change in the type of bond. The problem becomes much simpler when the transition to a metallic state is considered, because the characteristics pertaining to the metallic state are easily distinguishable.

The theory of such transition is based on the following assumptions in quantum mechanics (22, 23, 28). Let there be two possible states for a given system, one of these (ionic) having a corresponding wave function ψ_1 and the other (valence) characterized by wave function ψ_2. Then the linear combination of functions

$$C_1 \psi_1 + C_2 \psi_2 \qquad (1)$$

also represents the solution of Schrödinger's equation, and is the wave function of the system. By changing the coefficients of (1), the minimum energy of the system is attained, and the corresponding state of the system will be stable under these particular conditions. If the minimum energy is reached at $\frac{C_2}{C_1} \approx 0$ the ionic state will be stable, if is reached at $\frac{C_1}{C_2} \approx 0$ then the state of valence type of bond will be stable. In most cases the minimum energy is obtained when C_1 and C_2 are just comparable, and so the state of the system is neither purely ionic nor purely one of valence type. Strictly speaking, pure cases are very rarely met. This fact was first pointed out by Heisenberg, and the phenomenon which was given the name of « resonance », found prominent place in the works of Pauling and his collaborators (22, 28). When the inter-atom distance is altered, there occures a change in the ratio of $\frac{C_1}{C_2}$ and, consequently, a change in the relationship of bond type as well. Since valence bond is due to the exchange forces springing up in the process of exchange interaction of valence electrons, it follows that generally speaking, as the distance between the atoms decreases and hence the overlapping of charge clouds of valence electrons is growing, a displacement of the stability point should be expected toward the increase of valence type of bond. The transition may happen in a jump provided it is accompanied by a transition to excited levels, on the other hand, if, as it is usually the case, there is no transition to excited levels, the change from ionic type of bond to valence bond is continuous, though rather rapid, this has been demonstrated by Pauling and, quite recently, by Heitler 29). Fig. 3 represent this kind of transition diagrammatically. Curve I shows the energy of ionic state as a function of volume, curve II does the same for the valence type of bond. Curve I corresponds to function ψ_1, curve II, to function ψ_2. The more general type of wave function (1) will have its correspoding family of curves with differing values of parameters C_1, C_2. The transition from the ionic to the valence curve will follow the envelope of the family (1), shown by dotted line. Fore the sake of simplicity it will be assumed that the transition does not take place continuously, following the dotted curve but is rather abrupt, i. e. occures a jump along the tangent common to both original curves I and II as it would be case if no resonance were present between the states I and II. The pressure at which the jump from curve to curve occurs is evidently determined by the slope of the common tangent *a* — *a*. Accordingly, in our computations a jump in physical characteristics at the depth of 500 kms at the pressure of 176.000 atm is substituted for transition in the C- layer.

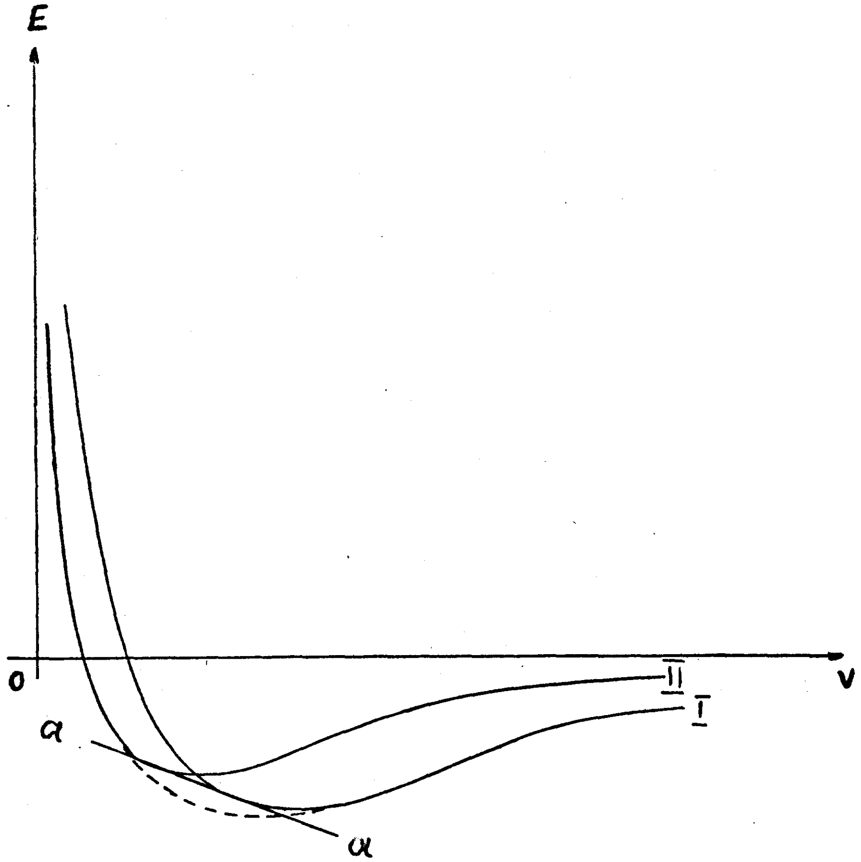

FIG. 3.

3.

In our paper (21) an attempt is made on very rough approximations and assumptions to estimate the conformity of the hypothesis in question with the seismic data. Layer B in the mantle may be considered as consisting mainly of olivine with about 10 % content of Fe and about 90 % of Mg. So, in the first approximation, the upper layer of the mantle may be assumed to consist of Forsterite Mg_2SiO_4 (1, 3, 7). The problem as to the nature of the bonds in $Mg_2\,Si\,O_4$ is rather complex (30), still, in the first approximation, it is possible (as Pauling did) to make use of the values of the electronegativities of atoms O — 3.5; Mg — 1.2; Si — 1.8. From the differences in electronegativities and from the Pauling curve it is found that the *Si* — *O* bond is 5 % valence and 50 % ionic.

while Mg — O is at least 75 % ionic. According to our hypothesis the transition from layer B to layer D must, then, be accounted for by the change in the Mg — O bond from the almost purely ionic to the valence type. The distance Mg — O, computed from valence radii (22) is obtained as 1.95 Å, which agrees with that assumed by Verhoogen and shows an 18 % jump in density*. The same jump is shown in the density value obtained by Bullen for the Earth's model A (11), provided the smooth transition is substituted with a jump at the depth of 500 kms. The jump in density and the pressure at the depth of 500 kms being known, the jump in potential energy can be found readily by using the equation

$$\Delta E = -p\Delta V \tag{2}$$

where V — volume.

Given the jump in energy, the pressure and the jump in density, it is possible to estimate the jump in $\frac{K}{\rho}$, which is obtained as $1.9 \left(\frac{\text{kms}}{\text{sec}}\right)^2$. The jump value arrived at experimentally (see fig. 2) is $1.5 \left(\frac{\text{kms}}{\text{sec}}\right)^2$. Fig. 2 also shows in a dotted line the theoretical $\frac{K}{\rho}$ curve in the D- layer. The discrepancy between the theoretical curve and the experimental is easily accounted for by the roughness of the assumptions on which the theoretical $\frac{K}{\rho}$ curve was deduced (21).

4.

In this paper a somewhat different approach is made to the hypothesis as to the transition from an ionic to a valence type of bond in layer C, no particular theories being advanced concerning the composition of the mantle.

The difficulties arising in the computations of energy according to quantum mechanics and the equations of state of different types of solid bodies at pressures $10^3 - 10^7$ atmospheres (these are the very ones the geophysicist is most concerned with) usually lead to semi-empirical formulae being used. Now in semi-empirical formulae the kind of relationship between the forces of attraction and repulsion and the distances between the atom or ion centres, is established according to the data of quantum mechanics, while the

* Valence radius O was taken for a double bond Pauling's suggestions being taken into account.

values of parameters in the formulae are obtained empirically on experimental data. The deficiency of the latter results makes it necessary to derive formulae in which as few parameters are used as possible, for otherwise the formulae would be unapplicable in practice. These restrictions, however, lead to the use of formulae that are, strictly speaking, but approximations, which is particularly unsafe whenever extrapolation is attempted. In this work we make use of semi-empirical formulae developed by B. I. Davydov (31) for valence and ionic crystals. If temperature correction be neglected, Davydov formulae for energy will be

$$E = \mathcal{A}_1 e^{-B_1 x^{1/3}} - C_1 x^{-1/3} \tag{3}$$

for ionic crystals, and

$$E = (\mathcal{A}_2 x^{-1/3} - C_2) e^{-B_2 x^{1/3}} \tag{4}$$

for valence crystals, where A, B, C are parameters obtained experimentally, ρ_0 — is density at zero pressure, and $x = \frac{V}{V_0}$ is the relative volume.

Using the well known relations

$$p = -\frac{dE}{dV} = -\rho_0 \frac{dE}{dx}; \quad K = -V\frac{dp}{dV} = \rho_0 x \frac{d^2 E}{dx^2} \tag{5}$$

we find for the ionic type of bond

$$E = \frac{3}{\rho_0}\left[\frac{A}{B} e^{-Bx^{1/3}} - Cx^{-1/3}\right] 2{,}34.10^{-5}\,\frac{k\ cal}{g} \tag{6}$$

$$p = \left[Ax^{-2/3} e^{-Bx^{1/3}} - Cx^{-4/3}\right]\frac{kg}{cm^2} \tag{7}$$

$$\frac{K}{\rho} = \frac{1}{3\rho_0}\left[Ax^{2/3}(B+2x^{-1/3})e^{-Bx^{1/3}} - 4\,Cx^{-4/3}\right] 9{,}81.10^{-5}\left(\frac{km}{sec.}\right)^2 \tag{8}$$

and for valence type of bond

$$E = \frac{3}{\rho_0}\left[Ax^{-1/3} - C\right] e^{-Bx^{1/3}}\, 2{,}34.10^{-5}\,\frac{k\ cal}{g} \tag{9}$$

$$p = x^{-2/3}\left[Ax^{-1/3}\left(B + x^{-1/3}\right) - CB\right] e^{-Bx^{1/3}}\,\frac{kg}{cm^2} \tag{10}$$

$$\frac{K}{\rho} = \frac{x^{2/3}}{3\rho_0}\left[Ax^{-1/3}\left(2x^{-1/3} + B\right) - CB\right] e^{-Bx^{1/3}}\left(2x^{-1/3} + B\right).$$

$$9{,}81.10^{-5}\left(\frac{km}{sec}\right)^2 \tag{11}$$

Formulae (7) and (10) are equations of state for both valence and ionic types of compounds.

Fig. 4 represents densities inside the Earth according to Bullen for model A (curve A) and for model B (curve B) (32) as functions

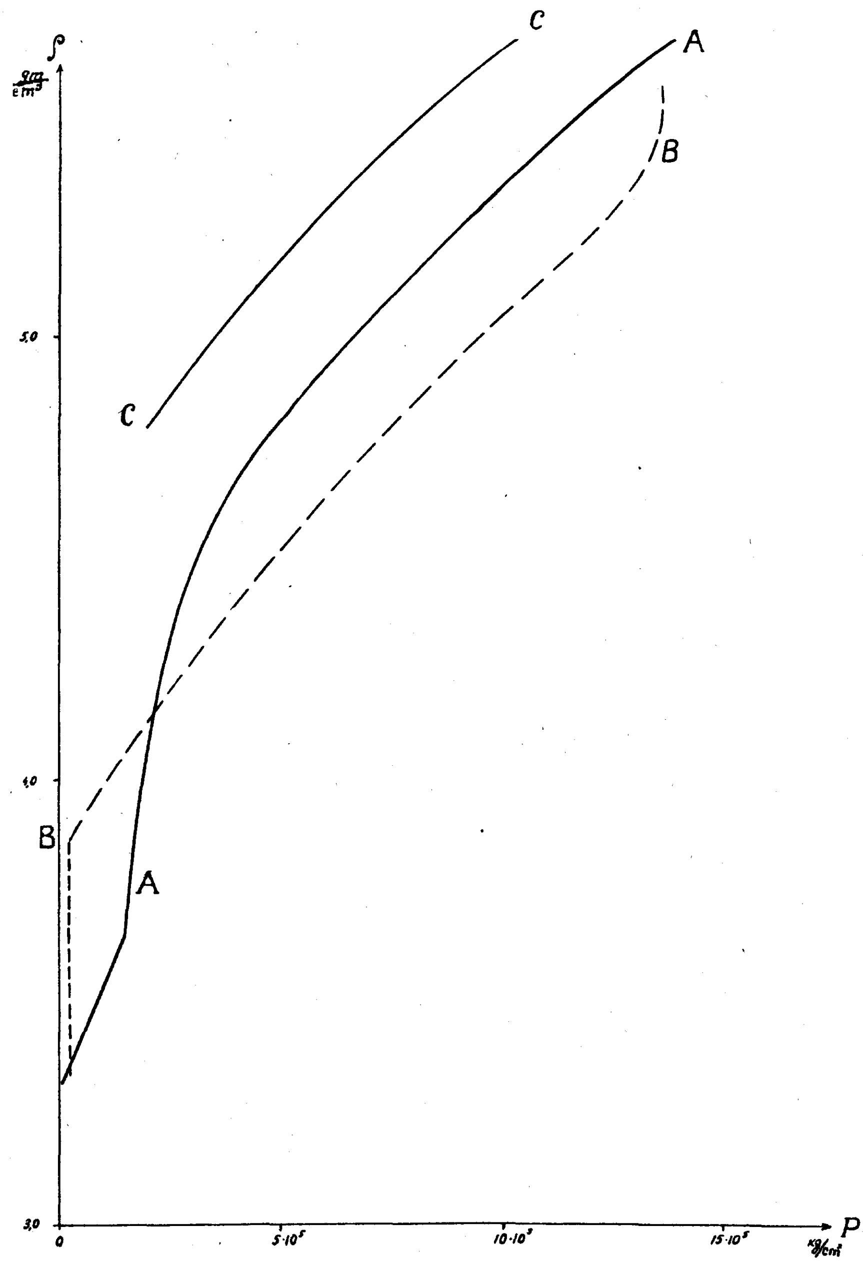

Fig. 4.

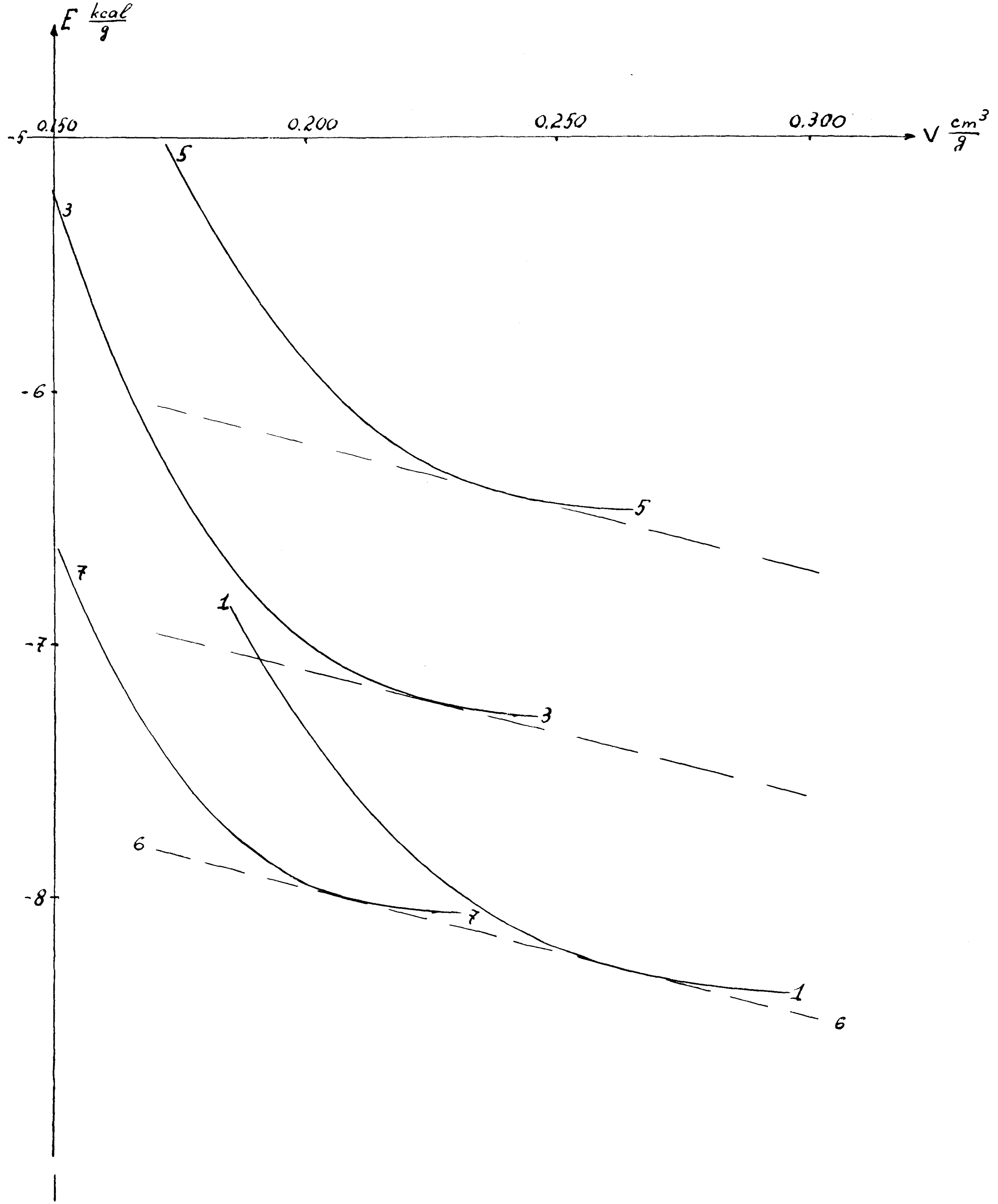

E kcal/g
V cm3/g
0,150
0,200
0,250
0,300
-5
-6
-7
-8
5
3
7
1
6
5
3
7
1
6

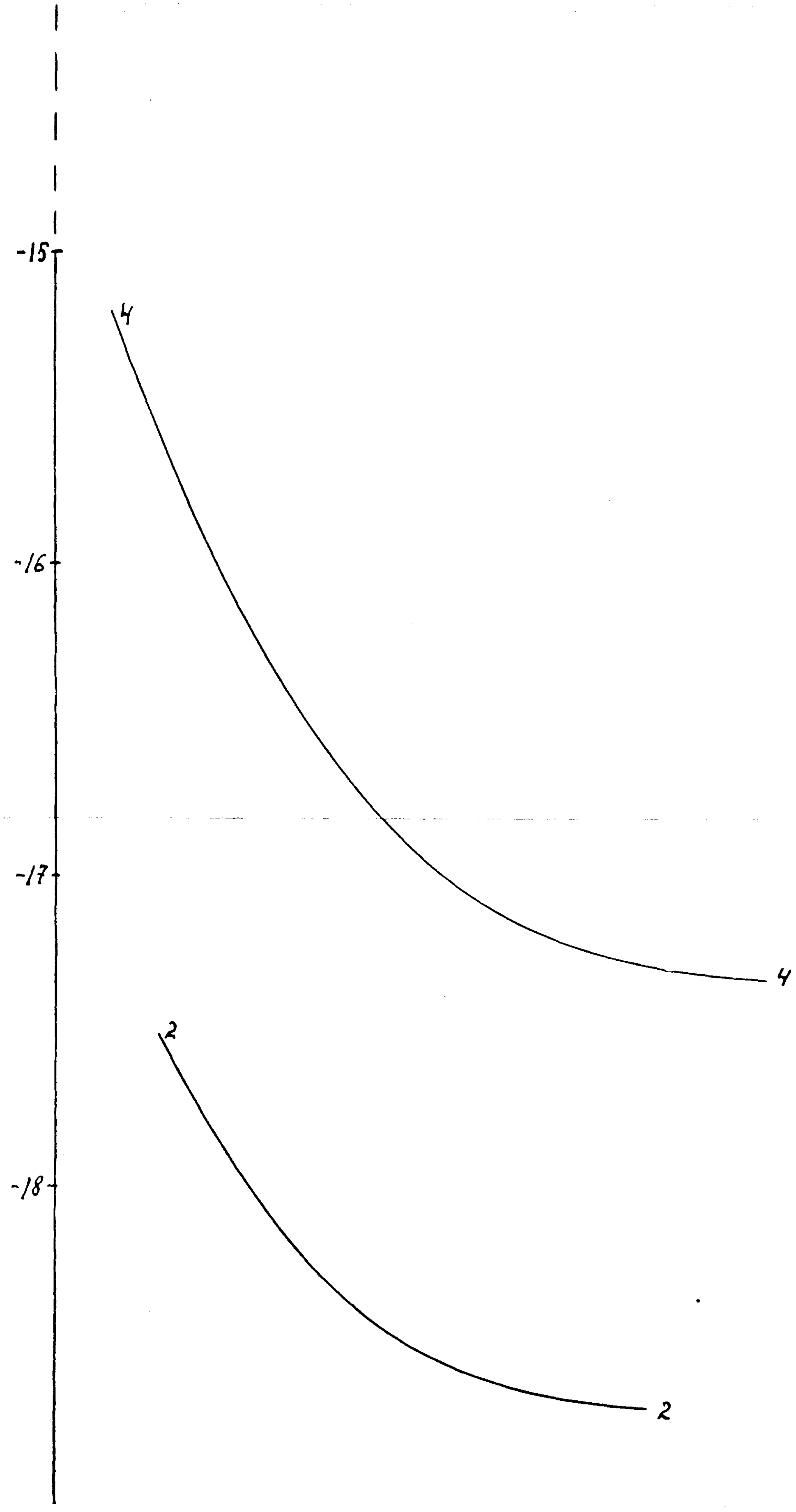

-15
-16
-17
-18
4
4
2
2

of pressure. These curves may, therefore, be regarded as two empirically obtained modifications of the equation of state for the Earth's material in layers B and D. After adding the curve $\frac{K}{\rho}$ in fig. 2, the necessary data are obtained for determining A, B, C in formulae for energy. To find the parameters of the ionic formula in layer B two points were chosen at the depth of 100 and 400 kms. Two more points were also selected at respective depths of 1.000 and 2.400 kms for determining the parameters in both valence and ionic formulae in layer D. The values of parameters obtained are given in tables 1 (ionic bond) and 2 (valence bond). For the sake of comparision, there are also shown parameters of such typically ionic compounds as NaCl and MgO, and of typical valence crystals as Si and Ge, and parameters of a mixed type compounds, in the latter the parts playd by ionic and valence bonds are nearly equal, pyrope and SiO_2 belonging to the latter group.

The fig. 5 shows the curves of energy for the material of the mantle. Curve 1 — 1 for layer B, Bullen's model A, on the assumption of ionic type of bond; curve 2 — 2 for layer D, model A on the assumption of ionic type of bond; curve 3 — 3 for layer D, model A, valence type of bond; curve 4 — 4 for layer D, model B, ionic type of bond; curve 5 — 5 for layer D, model B, valence type of bond. The straight line 6 — 6 is tangent to the curve 1 — 1 at a point at the depth of 500 kms, it is along this line that, according to the hypothesis under consideration, the transition from the ionic to the valence curve must take place.

Bullens models A and B were used for establishing the ways in which permissible variations in the density low may affect the tentative conclusions, since the density curves are somewhat uncertain and are near the lower limit of density as obtained by Molodensky, this may be seen from fig. 6, where density limits are shown by the dotted lines (33), while the curves A and B show the density of Bullen's A and B models. (The curve $\frac{K}{\rho}$ was not based on any hypothesis whatever, and so can't be modified.)

From the analysis of the data in fig. 5, the following conclusions may be drawn :

1. The energy curves, computed for the D- layer on the assumption of an ionic type of bond, are grouped in the region of very low energy values, much lower than the ionic curve for the B- layer, no matter which of the possible versions of density value was assumed (if the upper limit, according Molodensky were chosen,

this would obviously impair the results to a still greater extent). This means that, if the material of layer D were in a state pertaining to ionic type of bond, this state would have to be stable at any pressure considered, including those in the B- layer, but this would imply a density of material in a stable state exceeding 4 at zero pressure, which contradicts with all experimental data and our conception of the earth's composition.

2. Energy curves computed for the D- layer on the assumption of a valence type of bond are grouped about the ionic curve for layer B, passing just above it and crossing with it, which is in good agreement with the hypothesis of the change in the type of bond. The tangent 6 — 6 however plotted at a pressure corresponding to the depth of 500 kms, is not common to any of the valence curves, all of these lying considerable higher. But this is what should be expected as the curves for energy were obtained by integration and must differ by an arbitrary constant, which cannot be determined on the data available. The significance of this constant, from the physical point of view, lies in the fact that the energy of the ionic and the valence curves is measured from different levels : the energy of the ionic curve is measured from the state corresponding to the ions being at infinity, while that of the valence curve is computed from the state of neutral free atoms. Moreover, there may be occasional excited levels involved in this case. For the 6 — 6 to become a common tangent it is necessary to lower the valence curve in model A by 5.6 $\frac{eV}{\text{molec}}$, and that in model B by 11 $\frac{eV}{\text{molec}}$, this value for the arbitrary constant would not be at variance with the ionization potential and the value of affinity with the electron, model A being apparently nearer the truth than model B.

The case of arbitrary constant being zero may be considered as extreme. Here in plotting the curve for layer D, we must accept a displacement of density towards the upper limit of that calculated by Molodensky. The 7 — 7 in fig. 5 gives the valence curve that meets the above condition, the curve C in fig. 4 gives the density in layer D, corresponding to energy in 7 — 7. Since a zero difference in levels is hardly conceivable, density C in fig. 4 may be regarded as limiting, the most probable density in layer D must be somewhere in the neighbourhood of the curve A, possibly between A and C.

Apart from the data supplied in fig. 5, the hypothesis that the material in layer B is in an ionic state while in the D- layer the state corresponds to the valence type of bond is corroborated by the data

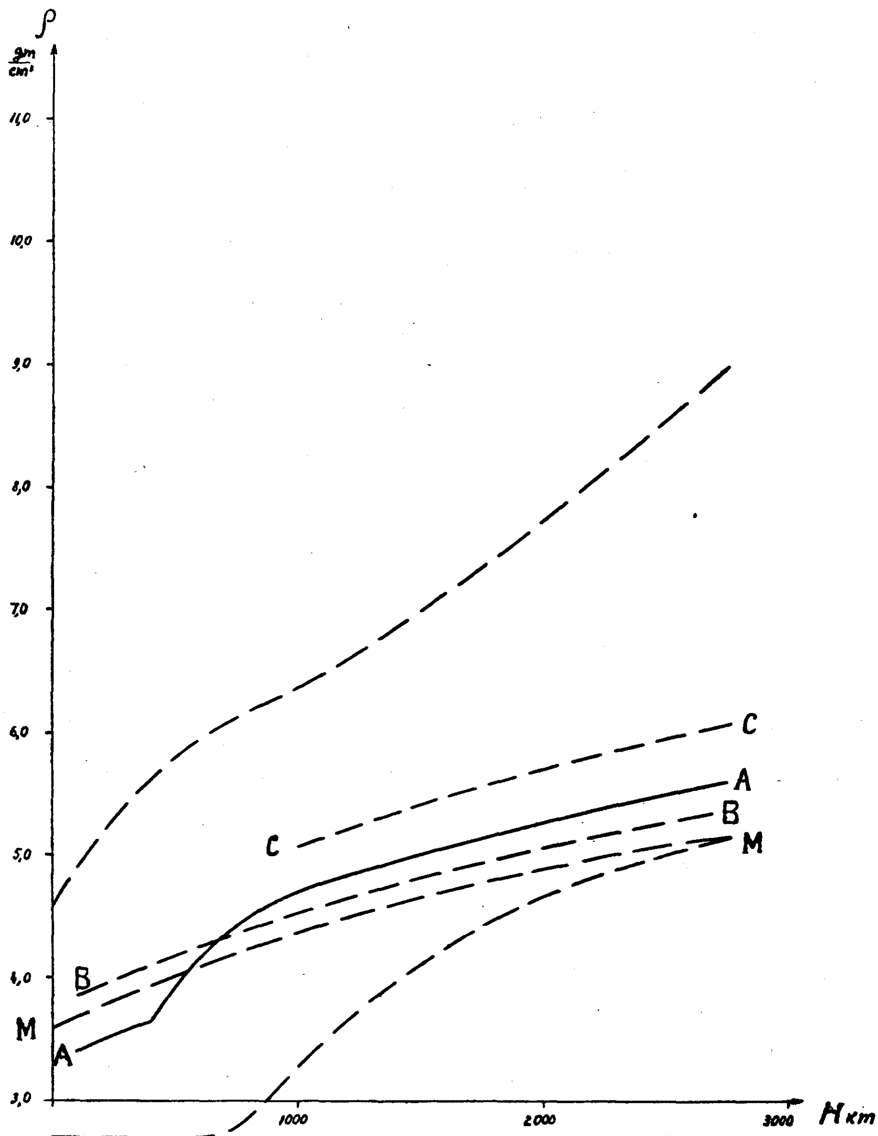

FIG. 6.

in tables 1 and 2. Parameter B (characterizing the type of bond) given by the ionic curve in layer B is very near its value for so typically ionic crystal as NaCl. The same parameter for the valence curve in layer D also nearly coincides with its value for typically valence crystals such as Si and Ge.

On the basis of the hypothesis it is also easy to account for the higher rigidity in the D- layer as compared with layer B since, as a rule, the rigidity of valence crystals is greater.

If this is really the case, the increased electroconductivitv found in layer C may be due to the transition from ionic conductivity to the electronic one of semi-conductors, though so far this is but a hypothesis which calls for special investigations.

Acknowledgements.

We wish to thank B. I. Davydov for valuable advice and attention paid to this work, and V. N. Zharkov for helpful discussion.

TABLE 1.

Ionic type of bond.

Substance \ Parameters	A	B	C	ρ_0
Earth between 100-400 kms, model A	$6{,}876.10^9$	9,663	$4{,}380.10^5$	3,29 g/cm^3
Earth between 1000-2400 kms, Model A	$1{,}562.10^9$	7,122	$1{,}261.10^6$	4,06
Na Cl	$1{,}887.10^9$	9,689	$1{,}073.10^5$	
MgO	$4{,}238.10^8$	5,729	$1{,}384.10^6$	3,60
$Mg_2 SiO_4$	$9{,}689.10^7$	3,871	$2{,}023.10^6$	3,19
α SiO_2*	$15{,}756.10^9$	11,871	$1{,}101.10^5$	2,65
Pyrope	$26{,}582.10^9$	10,661	$6{,}231.10^5$	3,80

Valence type of bond TABLE 2.

Substance \ Parameters	A	B	C	ρ_0
Earth between 1000-2400 kms, Model A	$3{,}033.10^7$	3,062	$4{,}026.10^7$	4,06
Si	$2{,}748.10^7$	3,984	$13{,}736.10^7$	
Ge	$1{,}158.10^7$	3,230	$4{,}915.10^7$	
α SiO_2*	$4{,}234.10^7$	5,704	$13{,}736.10^1$	2,65
Pyrope	$1{,}219.10^8$	5,074	$1{,}459.10^8$	3,80

REFERENCES.

1. САВАРЕНСКИЙ Е.Ф. и КИРНОС Д.П. Элементы сейсмологии и сейсмометрии. Москва, 1955.
2. BULLARD E. The interior of the Earth. The Earth as a planet. Chicago, 1954.
3. JEFFREYS H. The Earth. Cambridge, 1953.
4. GUTENBERG B. Internal constitution of the Earth. N.-Y., 1951.
5. BIRCH F. Journ. Geophys. Res., V. 57, Nu 2, 1952.
6. МАГНИЦКИЙ В. А. К вопросу о плотности и сжимаемости оболочки Земли. Вопросы космогонии, вып 1 1952.
7. МАГНИЦКИЙ В.А. О Физическом состоянии вещества в глубоких частях земного шара. Труды Геофиз. Ин-та АН СССР, № 26, 1955.
8. VALLE P. E. Annali di geofisica, V. 7, N° 1, 1954.
9. ГОЛНЦЫН Б.Б. Известия Постоянной сейсмической комиссии Ак. Наук, т. 7, И° 1, 1955.
10. JEFFREYS H. Mon. Not Roy. Astr. Soc. Geophys. Suppl., V. 3, pp. 401, 1936. V. 4, pp. 13, 1937.
11. BULLEN K. E. Introduction to the theory of seismology. Cambridge, 1953.
12. JEFFREYS H. Mon. Not. Roy. Astr. Soc. Geophys. Suppl., V. 4, N. 7, 1939.
13. GUTENBERG B. Bull. Seismol. Soc. Amer., V: 43, Nu 3, 1953.
14. МАГНИЦКИЙ В.А. Основы физики Земди. Москва, 1953.
15. SHIMAZU Y. Journ. Earth. Sciences. Nagoya Univers., V. 3, Nu 2, 1955.
16. BERNAL J. Observatory, V. 59, p. 268, 1936.
17. KRACHEK F. C. Phase transformations in solids. Symposium. N.-Y., London, 1951.
18. JEFFREYS H. Nature, V. 169, Nu 4294, 1952.
19. VERHOOGEN J. Journ. Geophys. Res., V. 58, Nu 3, 1953.
20. БЕЛОВ Н.В., БЕЛОВА Е.Н., АНДРИАНОВА Н.Н., СМИРНОВА Р.Ф. Доклалы АН СССР, т. 81, № 3, 1951.
21. МАГНИЦКИЙ В.А. Известия АН СССР. серия геофизич. № 6, 1956.
22. PAULING L. The nature of the chemical bond. N.-Y., 1942.
23. EITEL F. The physical chemistry of the silicates. Chicago, 1954.

* Data on SiO_2 given in both tables fit the curve experimentally derived with insufficient accuracy. This discrepancy is due to transition type of bond in SiO_2.

24. Seitz F. Modern theory of solids. N.-Y., 1940.
25. Kronig R., de Boer J., Korringa J. Physica, V. 12, p. 255, 1946.
26. ДАВЫДОВ Б.И. Труды Геофизич. Ин-та АН СССР, № 26, 1955.
27. Ramsey W. H. Mon. Not. Roy. Astr. Soc. Geophys. Suppl., V. 5, Nu 9, 1949.
28. Pauling L., Wilson E. B. Introduction to quantum mechanics with applications to chemistry, N.-Y., 1935.
29. Heitler W. Arkiv för fysik, Bd. 10, H. 2, 1956.
30. Ramberg H. Journ. Geology, V. 60, Nu 4, 1952.
31. ДАВИДОВ Б.И. Известия АН СССР, серия геофизич., № 12, 1956.
32. Bullen K. E. Mon. Not. Roy. Astr. Soc. Geophys. Suppl., V. 6, Nu 1, 1950.
33. МОЛОДЕНСКИЙ М.С. Труды Геофизич. Ин-та АН СССР, № 26, 1955.

ON SOME PECULIARITIES OF THE DISPLACEMENT FIELDS OF THE LONGITUDINAL AND TRANSVERSE WAVES PROPAGATING IN THE EARTH'S MANTLE

VVEDENSKAYA A. V., and BALAKINA L. M.

Studying the Earth's mantle structure by seismic methods is based mainly on the data of velocities of the longitudinal and transverse waves at different depths. The seismic velocities are determined by means of travel time curves. The present paper is an attempt to use the observations on the amplitudes in the longitudinal and transverse waves, propagating into the mantle, for studying the Earth's mantle structure.

Observed amplitude ratios in the first displacements of the longitudinal and transverse waves are compared with the same values in the case of an elastic isotropic media, for which the ratio of seismic velocities is constant. In this way we supposed to find out a departure of the mechanical properties of the Earth's mantle at different depths from the properties of an elastic isotropic body with the constant ratio of bulk modulus to rigidity modulus. In the present paper only the preliminary results of the investigation are described.

The records of 21 earthquakes wit the foci located in the Earth's crust were the material used for the investigation. The earthquakes of Japan, China, Turkey, Greece, Algeria were considered. The initial data were the values of $\frac{U_p}{U_{SV}}$ and $\frac{U_{SV}}{U_{SH}}$, where U_p, U_{SV}, U_{SH} mean the amplitudes of the displacements in the P, SV and SH waves respectively.

In the calculations of these amplitudes the effects due to the reflection at the Earth's surface and the characteristics of the instruments are taken into account. In order to determine the displacement fields of the longitudinal and transverse waves in an elastic isotropic media, the formulae obtained by means of the dislocation theory [1] were used. These formulae describe the displacement fields of P, SV and SH waves propagating in elastic isotropic media in the case of the rupture of finite dimensions at the origin. The rupture is accompanied by slipping in the rupture plane. The ratios of the amplitudes U_p, U_{SV} and U_{SH} are expressed as follows :

$$\frac{U_p}{U_{SH}} = \frac{c^2}{a^2}\,\mathcal{F}_1\,(m, n, l, Az, e), \tag{1}$$

$$\frac{U_{SV}}{U_{SH}} = \mathcal{F}_2\,(m, n, l, Az, e), \tag{2}$$

where a and c are the velocities of the longitudinal and transverse waves respectively; m, n, l are the direction cosines of the tangent to the ray with respect to the axes of the general stresses acting at the origin; Az is the azimuth at the station, e is the angle, which the ray makes with the horizontal plane at the origin. If the rupture in the media coincides with the origin, the functions $\mathcal{F}_1$, and $\mathcal{F}_2$ are determined by these parametres.

To make sure that the formulae (1) and (2) are valid for the present problem, the observed nodal surfaces of P, SV, SH waves with those described by the formulae (6) and (9) from paper [1] were compared using the Wolf stereographic projection. The comparison showed that the position and form of the observed nodal surfaces agreed with those calculated theoretically within the limits of accuracy.

Thus if the Earth's mantle possesses the properties of elastic isotropic media with the constant ratio of the bulk modulus to the rigidity modulus, then the observed amplitudes of the longitudinal and transverse waves propagating in the mantle, must satisfy the equality :

$$\frac{U_p}{U_{SH}} \Big/ \mathcal{F}_1 = \frac{c^2}{a^2} = \text{const.} \tag{3}$$

In order to determine the value of the function $\mathcal{F}_1$, it is necessary to find the direction of the axes of the general stresses acting at the origin. The axes were found by means of the distribution of the signs of the displacements in P and S waves, recorded by seismic stations. Then the ratio (3) was calculated using the observed displacements U_p and U_{SH} and the computed values of the function $\mathcal{F}_1$.

Fig. 1. shows the obtained values of the ratio (3) plotted against epicentral distances and corresponding depths of the penetration of the rays of P -waves. The dependence we are interested in could not be traced at epicentral distances greater than 80°, where SKS waves overlap S -waves.

The plotted curves are preliminary, since they were obtained on the basis of a limited number of observations. Nevertheless, the

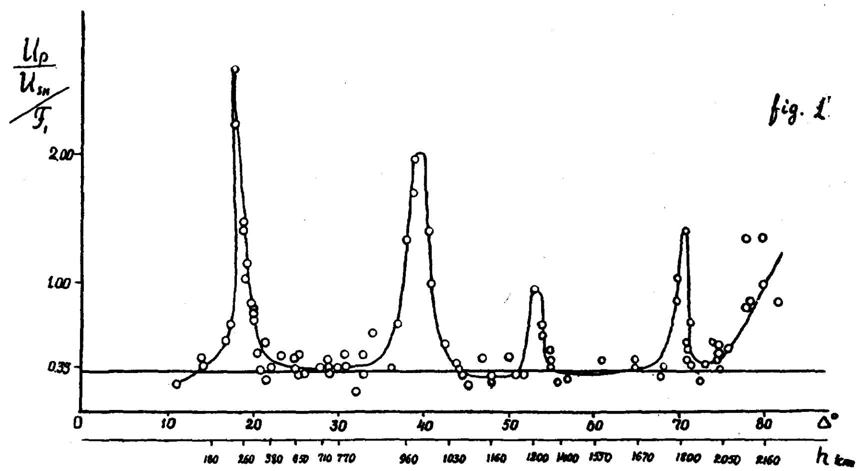

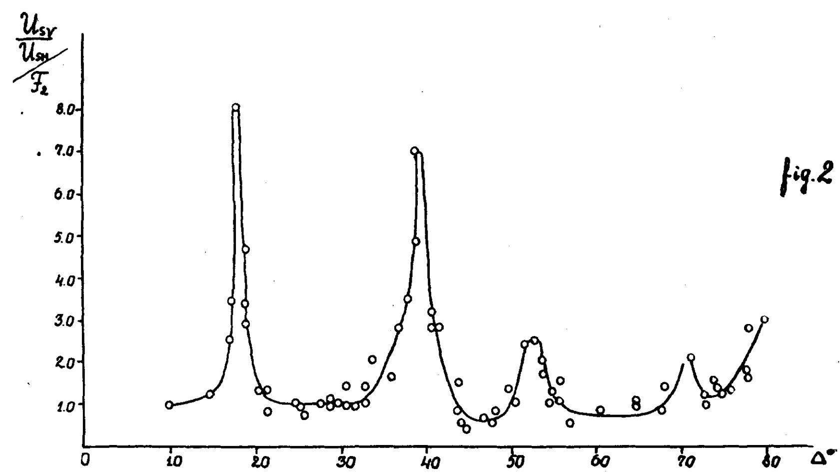

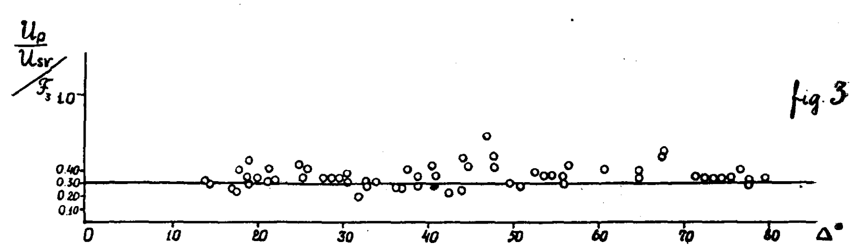

obtained results show that a sharp increase of the ratio $\frac{U_P}{U_{SH}}$ is observed at the depths of the penetration of the rays corresponding to epicentral distances : 18-20°, 35-45°, 52-55°, 68-71° and about 80°. At other epicentral distances the values of $\frac{U_p}{U_{SH}}$ remain constant within the limits of error. The peculiarity of the displacement fields of P and SH waves mentioned above indicates that the mechanical properties of the mantle at depths : 250-500, 900-1000, 1200-1300, 1900-1950 and about 2300 km, differ from those of elastic isotropic media with the constant ratio $\frac{K}{\mu}$.

The discontinuities in the Earth's mantle discovered earlier are related to the same depths. For example, the discontinuity at the depth of about 500 km was first discovered by Galitzin from observations of the angles of emergence [2]. The existence of the discontinuities at the depths of 950, 1200, 1800 and 2150 km was established in papers by Repetti [3], Gutenberg, Richter [4] and others.

It was found also that the observed amplitudes of the displacements in SV and SH waves do not satisfy equations (2) for the intervals of epicentral distances : 18-20°, 35-45°, 52-55°, 68-71° and about 80°. Fig. 2 shows the obtained values of $\frac{U_{SV}}{U_{SH}} / \mathcal{F}_2$ plotted against epicentral distances. One can see from the comparison of Fig. 1 and Fig. 2 that the character of the change of this ratio is the same as for ratio (3). Thus, the values of $\frac{U_p}{U_{SV}} / \mathcal{F}_3$, where $\mathcal{F}_3 = \mathcal{F}_1 / \mathcal{F}_2$, are constant for all the depths of the penetration of the rays. Those are shown in Fig. 3.

It is interesting to compare the obtained values of $\frac{U_p}{U_{SH}} / \mathcal{F}_1$ and $\frac{U_p}{U_{SV}} / \mathcal{F}_3$ with the ratios $\frac{c^2}{a^2}$ determined from the travel time curve [5]. In Fig. 1 and Fig. 3 these ratios are shown by a straight line. It is seen, that the points corresponding to the values of $\frac{U_p}{U_{SV}} / \mathcal{F}_3$ for all epicentral distances and to the values of $\frac{U_p}{U_{SH}} / \mathcal{F}_1$ for the distances, where these ratios are constant, fall along the straight line.

The authors suppose that the observed anomalous behaviour of P. SV and SH waves may be explained by aeolotropy of the media at the depths mentioned above.

References.

1). ВВЕДЕННСКАЯ А. В. Об определении полей смещений при землетрясениях с помощью теории дислокации. Изв. АН СССР, сер. геофизич. № 3, 1956.

2). Galitzin B. B. Sur l'angle d'émergence des rayons sismiques, 1917.

3). Repetti W.C.S.I. New values for some of the discontinuities in the Earth. Manila, 1930.

4). Gutenberg B., Richter C. F. On seismic waves. Gerlands Beitr. Geophysik, 45, 1935.

5). МАГНИЦКИЙ В.А. Основы физики Земли. Москва, 1957.

SEISMIC WORK ON CRUSTAL STRUCTURE IN SOUTH AFRICA

P. G. GANE

Seismic observations were continued using the now well-established radio triggering technique between a master station in Johannesburg and a single mobile field station situated from 50 to 500 km away. The vibrations observed originated from the « earth tremors » which are occasioned by mining on the Witwatersrand and which occur several times a day within a limited epicentral area. A network of eight radio telemetering stations distributed about this area served to locate the epicentres.

Traverses were made to the SSW, E, and NNE of Johannesburg and the results compared with previous work carried out to the west. No significant differences in the thickness of the crustal layer appear to exist in these directions, nor is there any appreciable dip of the Mohorovicic surface. Combination of all the available results from over 400 seismograms gives :

	Depths and Velocities			
	From P phases		*From S phases*	
Superficial layer	1.3 km	(5.40 km/sec)	1.3 km	(3.20 km/sec)
Continental crust	33.8 km	(6.18 km/sec)	32.0 km	(3.66 km/sec)
Top of mantle		8.27 km/sec		4.73 km/sec
Depth of crust	35.1 ±	1.2 km	33.3 ±	1.3 km

Owing mainly to an inability to fix epicentres and focal depths of the rockbursts to an adequate degree of accurary, the residuals of individual reading were found to be of the order of 0.25 sec. Within the degree of accuracy implied by this figure, no curvature of the travel-time graph was evident, and there have been only vague indications of phases corresponding to a layer of intermediate velocity, wherefore it seems that no such layer exists generally, and the crust is on the average uniform for a large proportion of its depth.

On the northern traverse, which lay over the deep basin-like structure of the Bushveld Complex, there was a distinct weakness in the P_n phases, and an almost total loss of the S_n phases, which indicates that in such territory there could well be no Mohorovicic layer at all, in the sense of a plane horizontal interface between crust and mantle. A similar loss of the S — phase has been observed in the crust where the ray path has passed through the deep

Vredefort dome structure. It is evident that local inhomogeneities in velocity occur which can upset the validity of representing continental structure by means of homogeneous layers with plane interfaces.

It is interesting to note that although this work was done on a plateau nearly 2 km above sea-level, the crustal depth here found is not substantially greater than has been found elsewhere.

CRUSTAL STRUCTURE IN THE PUGET SOUND AREA

By Frank NEUMANN

The Puget Sound area contains the greatest gravity anomaly in the United States. Although the prevailing negative character of this anomaly indicates a predominance of the lighter forms of continental layering seismological investigations to date have shed little or no light on the nature of this layering. In 1951 Tatel and Tuve attempted to measure the depth of the Mohorovicic discontinuity from controlled explosions, but their findings were inconclusive. They found near-surface velocities of the compressional P wave ranging from 5.8 to 6.6 km/sec at distances up to 250 km. On Vancouver Island J. H. Hodgson found 6.4 km/sec using a rather similar technique. The writer has noted that along the entire Pacific coastal region P waves apparently do not dip beneath the crustal layers and attain velocities of 8 km/sec or more until epicentral distances reach nearly 2000 km. Epicenters are then near the Mexican border. A recent rare exception was the strong San Francisco earthquake of March 22, 1957 when P traveled from San Francisco to Seattle, about 700 km, at an average speed of 8.0 km/sec. Of significance also is the fact that some investigators, without considering the possibility of an anomalous crustal structure, have designated the University of Washington seismograph station the most unreliable in the United States because of the consistently late arrival of P waves. All of this furnished a strong incentive for learning just what a study of local earthquake data might reveal in the way of deep crustal structure in the Puget Sound area.

Available for such a study were seismographic data from the three Canadian stations at Victoria, Alberni, and Horseshoe Bay (near Vancouver) in British Columbia, and from the station of the University of Washington in Seattle. The writer is deeply indebted to Messrs. W. G. Milne and W. R. H. White of the Astrophysical Observatory at Royal Oak, B. C. for 75 per cent of the data that made this investigation possible. Good impulsive P and S waves are generally registered for light shocks less than 200 km away. Epicentral distances did not exceed 300 km in any of the shocks studied.

In preliminary studies it was found, even before the Tatel-Tuve reports were published, that surface velocities as low as 5.8 km/sec were registered for shocks in certain areas. In other areas a very few approached 8.0 km/sec but never quite reached it. Such variations had to be attributed either to transmission of the P wave through layers having different velocities, to the influence of focal depth on surface velocity, or to both.

Three layer velocities were ultimately adopted. 5.8 km/sec was adopted as the speed in the layer beneath the sediments and was subsequently supported by the published findings of Tatel and Tuve, 6.4 km/sec was adopted as an intermediate layer speed because it was determined directly from explosion tests on Vancouver Island where the 5.8 km/sec layer is obviously missing; and 7.0 km/sec was adopted as the speed in the layer above the Mohorovicic discontinuity because it has been observed in California earthquakes and was provisionally assumed to be common to the Pacific Coast and western mountain area. In further support of these velocities it should be stated that they were the ones that yielded the most consistant results when used in conjunction with the seismographic data in preliminary studies. Other velocities yielded less consistent and even negative results. These preliminary studies took into consideration the effect of focal depth to account for those observed surface velocities that lay between the three layer velocities adopted. At no time was there any evidence that subcrustal velocities (8 km/sec and over) were being registered.

The next step was to determine, if possible, a pattern of crustal layering that would serve as a basis for constructing regional travel-time curves. Hypothetical travel-time curves were constructed for crustal thicknesses of 30, 40, 50 and 60 km using representative average velocities within the crust and a speed of 8.0 km/sec beneath it. The instrumental data were not even remotely consistent with any of these curves nor for curves representing greater crustal thicknesses. Discrepencies between the data and the hypothetical travel-times were of the order of five seconds and over. So far as the instrumental readings were concerned, a Mohorovicic discontinuity did not exist in this region.

Development and discussion of the travel time curves used.

After much experimenting with various types of structures and travel time curves consistent results were obtained only when using three sets of curves that have a purely hypothetical origin, at least as far as their computation is concerned, but could also be considered perfectly legitimate if one were willing to adjust the crustal pattern to suit the curves. These curves are based on an original premise that if we do not know how thick the crustal layers are, and if we assume that P travels most of its path in the layer in which the shock originates (rather than dipping down into higher speed alyers), then the closest approximation to the true travel time for parallel layering (which may or may not be true), is to assume that P travels in a straight line from focus to station at a velocity equal to, or very close to, that in the layer containing the focus.

While neglecting the effect of overlying slower speed layers is theoretically untenable, it will be shown that errors involved are no greater than those involved in the determination of origin time and are therefore acceptable at least as a first approximation. As far as the writer knows no other course is open. By using a slightly lower velocity than the true layer velocity this error could be reduced, but for various reasons this is considered undesirable at least at this stage of the research. Regarding the second assumption no evidence has been found that P waves from light shocks normally dip down into higher velocity crustal layers. P waves of 5.8 km/sec, propagated in a relatively thin layer, were consistently found at epicentral distances far beyond those at which higher velocities should have appeared first on the records if they were to appear at all. If P waves to the more distant stations dipped into a higher speed layer, then travel times to nearby stations representing slower average velocities, would tend (on the higher velocity travel time table) to indicate focal depths slightly deeper than the data from the distant stations. If such a tendency exists, it is too small to stand out above other uncertainties involved in the problem. Since such uncertainties are not amenable to theoretical solution (because the structural patterns and exact origin times are unknown), one is left to judge the validity of the assumptions largely on the apparent validity of the results obtained with them.

On the basis of the above assumptions and findings three sets of travel time curves were constructed for velocities of 5.8, 6.4, and 7.0 km/sec and for various focal depths assuming in each case that these were focus-to-station velocities along straight line paths between focus and station. If such curves provide an acceptable provisional solution to the travel time curve problem, it means that for each earthquake we have an epicenter, a focal depth, and the speed of the P wave at that depth. With a sufficient number of such foci the results would eventually outline in detail the thicknesses of the three layers having these P wave velocities and thus delineate the regional structure provided the foci were widely enough distributed. Results to date indicate that this is a promising possibility even though a certan amount of distortion seems unavoidable.

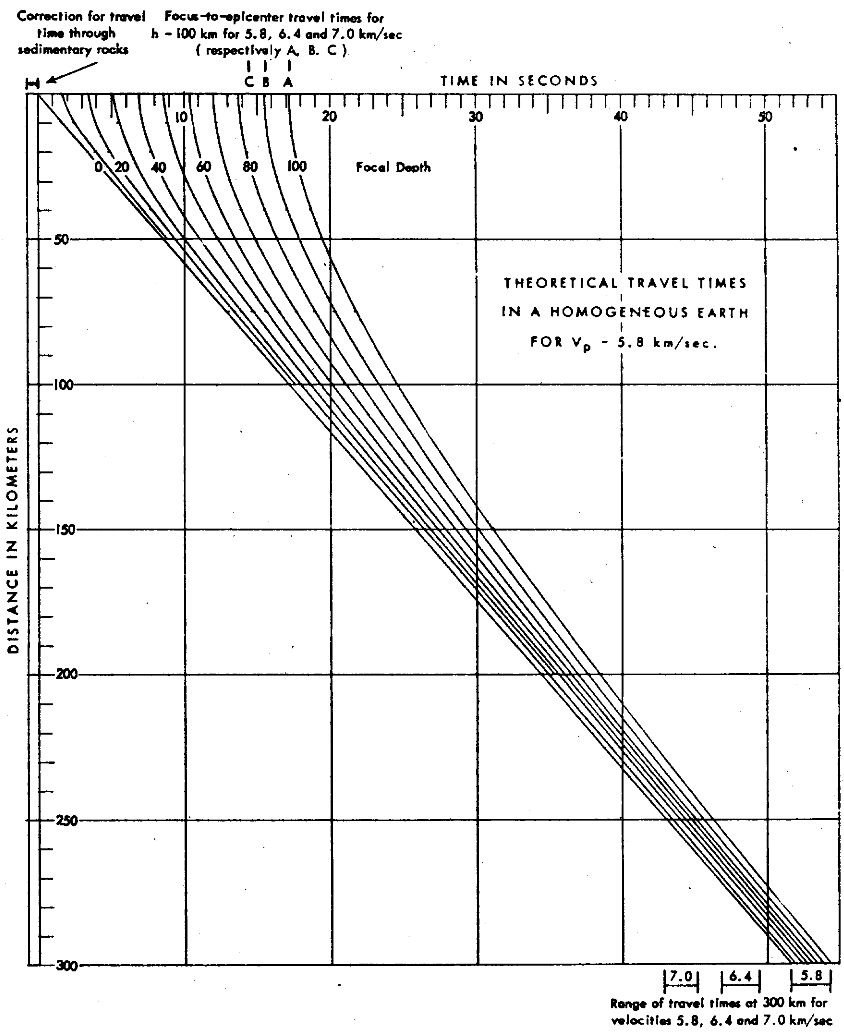

Fig. 1.

Fig. 1 shows the travel time curves for a 5.8 km/sec velocity in a homogeneous, isotropic medium. For comparison there is also shown at zero distance the travel time (focus-to-epicenter) for the velocities 6.4 and 7.0 km/sec for a focal depth of 100 km. These marks serve to show the small percentage error involved in the assumption that at short epicentral distances a constant focus-to-station velocity can be used as a reasonable approximation even though more than one velocity may actually be involved. At 300 km distance on the graph the terminal travel times are shown for 6.4 and 7.0 km/sec. At these greater distances it can be seen how the observed arrival times must fit into relatively straight line patterns and thus determine with little doubt the surface velocity category into which a given earthquake falls. While the slopes of some of these curves may appear in part identical when all three sets of curves are actually drawn, the knowledge of origin time (to be discussed later) eliminates any possibility of confusion and limits an interpretation to only one speed and focal depth.

Similar travel time curves were constructed for the intermediate velocities of 6.0, 6.2, 6.6 and 6.8 km/sec to see if the data would fit such curves equally well. They did not. In only a very few cases of deep foci in the 7.0 km/sec layer did the 6.8 km/sec curves yield better results. One may assume in such cases that large portions of the wave paths were through the lower speed layers thus considerably lowering the average speed. When foci originated in the 5.8 km/sec layer and P waves traveled to Alberni where this layer is absent the Alberni P wave was accelerated and would always fit either the 6.0 or 6.2 km/sec curves better than either the 5.8 or 6.4 km/sec curves. The velocity beneath the sediments on most of Vancouver Island is 6.4 km/sec as previously stated.

One point that may raise some question as to the validity of the adopted travel time curves is that over a range of 250 km epicentral distance the Tatel-Tuve results indicate a maximum velocity of 6.6 km/sec instead of 6.4 km/sec adopted as the P wave velocity in the intermediate layer. See Fig. 2. As 6.4 fits the instrumental data best and has been verified by explosion tests on Vancouver Island, this situation presents an enigma. Perhaps the true speed in the intermediate layer is greater than 6.4 km/sec and 6.4 is merely an average between the higher speeds observed by Tatel and Tuve and the lower speed in the 5.8 km/sec layer which must also be traversed. The difference, however, between 6.4 and 6.6 km/sec is not enough to materially affect the over-all results regardless of what interpretation is placed on this difference.

The Tatel-Tuve results furnish information concerning the sedimentary layering which is incorporated in the travel time curves used in this study. In Fig. 2 the lines defining the limiting surface velocities do not intercept the zero time ordinate at zero distance, but there is a delay of 1.5 seconds. This is interpreted as the additional time required to traverse the sedimentary layering two times — at the firing point and at the recording station. On-half this

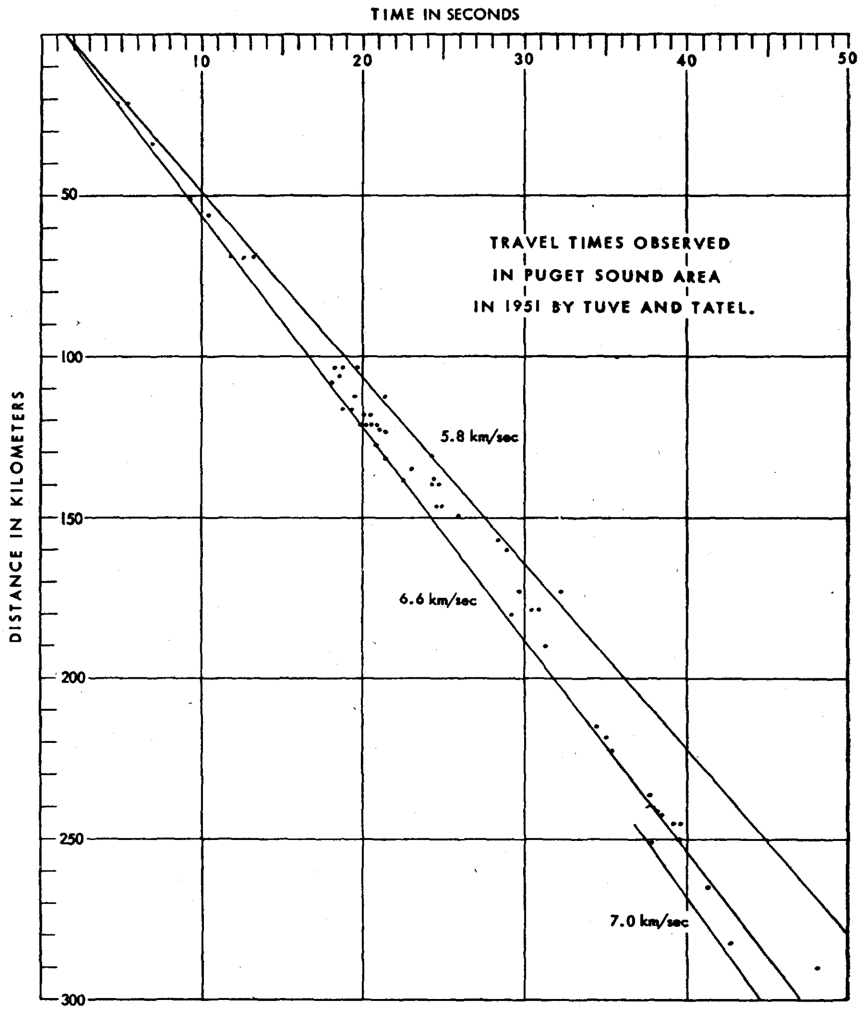

FIG. 2.

time has been added to the theoritical curves used to cover the passage of the P wave through this layer at the recording station.

ANALYSIS OF DATA.

The following procedure was used in analyzing the instrumental data. Origin times at all stations were obtained from the formula :

$$(P - H) = 1.37\ (S - P)$$

This is derived from the equations :

$$\text{Distance} = V_p\ (P - H) = V_s\ (S - H)$$

and

$$V_p = 1.73\ V_s$$

Poisson's ratio is assumed to remain fixed at 0.25.

The origin times thus computed from the (S — P) intervals obtained at the four stations for a particular earthquake generally cover a range of about two seconds. See Table 1. In some shocks it is as low as 0.5 seconds; a few others go as high as four or five seconds. The values used in the epicenter location work were generally within one-half second of the means of the computed values. This much latitude was allowed in the origin time to obtain good fits of the data on the travel time curves.

The use of H eliminated the need for constructing travel time curves for S. S obviously controls the value of H so that epicentral distances can be obtained from (P — H) alone. Ignoring the computed value of H in determining epicentral distances would be equivalent to ignoring S.

In locating epicentres it is found desirable, because of the trial and error method used, to trace the zero ordinate and zero abcissa of the travel time curve on a piece of tracing paper, then draw ordinates completely across the tracing paper diagram to indicate the four P wave arrival times at the four stations; then mark on it the computed origin time, H. These readings are fixed; the epicentral distances are yet to be determined. The next step is to select a probable epicenter location a base map, measure the epicentral distances on this map and plot them on the four time ordinates drawn on the tracing paper. Placing the origin time at zero on the travel time chart, the object is then to see how closely these plotted points align themselves with any of the curves on any one of the three travel time charts. If this is impossible, a new epicenter is selected, new epicentral distances are plotted on the tracing paper and the process is repeated until an alignment on one of the curves is obtained. The curve on which a good fit is ultimately obtained then indicates, according to the assumptions made, the depth of focus and the velocity of P at that depth. In practically all cases the results were such that if the procedure were reversed and epicentral distances were obtained from the selected curve by using only the final value of (P — H), these epicentral distances would always be within one kilometer of those measured on the base map from the adopted epicenter.

Viewing other aspects of the problems, including checks on the epicenter results obtained from a number of intensity distribution maps, it is felt that the instrumental epicenter location error does not exceed a very few kilometers and that focal depths may be off by five or ten kilometers for the shallower depths and perhaps 15 per cent for the greater depths.

The meridians and parallels covering the Puget Sound area and the seismograph stations were accurately drawn on a polyconic projection to a scale of one millimeter to the kilometer so that a millimeter scale could be used for all distance measurements.

Results.

After reviewing all the instrumental data available from the time the British Columbia network began functioning in October, 1951, down to the present there where sufficient data for only 37 reliable epicenters. A large amount of additional data from these stations and Seattle, which were incomplete in one way or another, was rejected although in virtually all cases they tended to support the results presented in this paper.

The epicenters are plotted in Fig. 3, each numeral indicating the

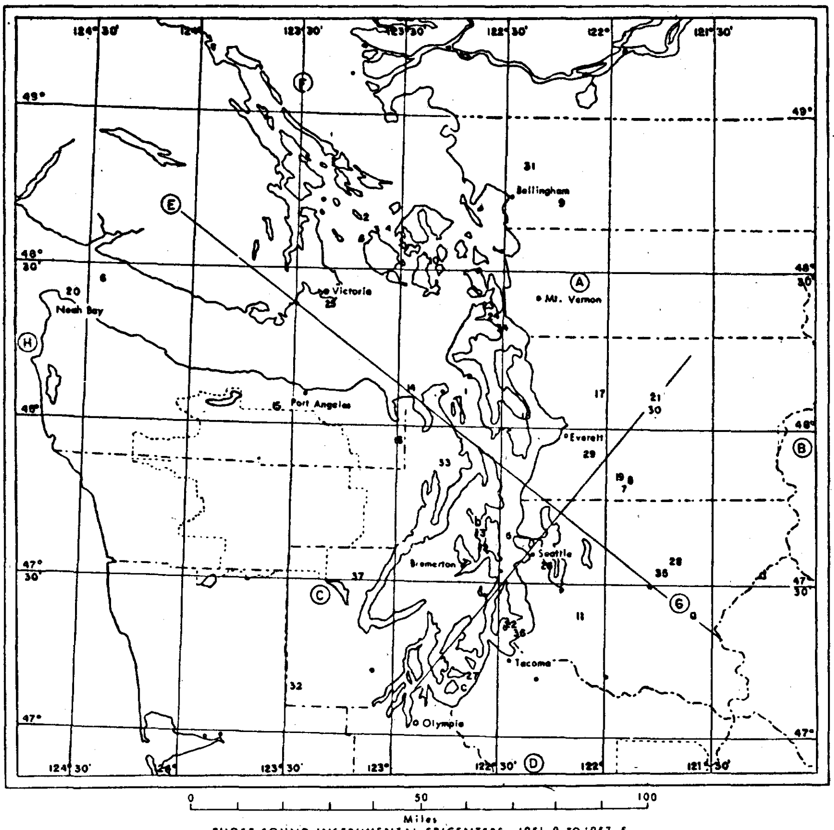

PUGET SOUND INSTRUMENTAL EPICENTERS, 1951.9 TO 1957.5

Fig. 3.

number of an earthquake wich can be identified by date in Table 2. Epicenters marked *a, b,* and *c* were widely felt and damaging shocks that were located with considerable accuracy from intensity information without benefit of supporting instrumental data. At each of the instrumental epicenters, shown again in Fig. 4, the

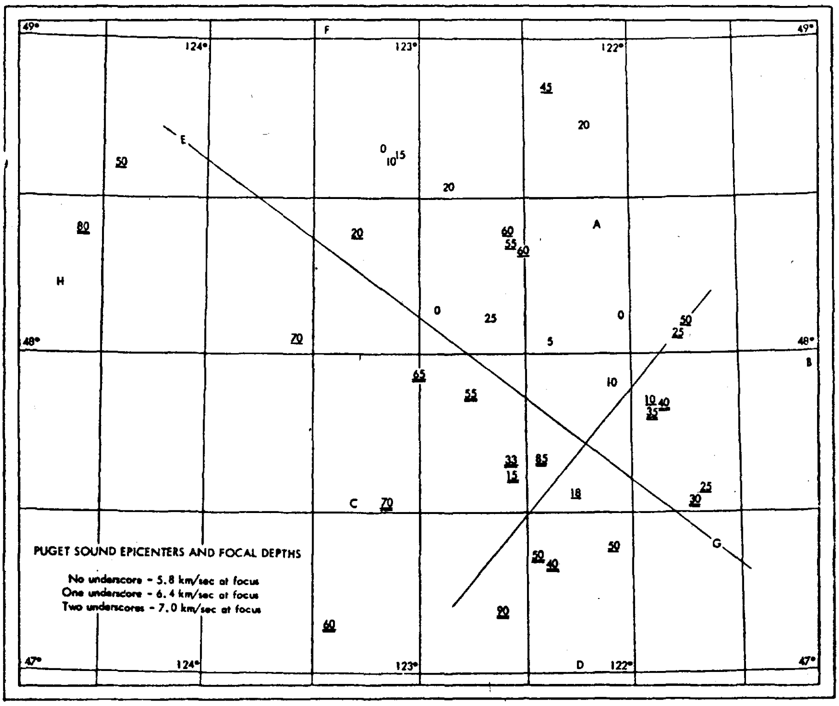

FIG. 4.

depth of focus and the P wave velocity at that depth are indicated so that one can see what type of depth-velocity pattern is evolving from the study. This can be seen better, however, on the three vertical projections in Fig. 5. The top figure shows the projection on a vertical plane of all foci in a 50-mile wide zone extending northeastward from Olympia along the axis AB shown in Fig. 4. The vertical plane is placed 25 miles northwest of axis AB and is parallel to it. The numerals on these projections are the P wave velocities determined from the analysis. Underscores indicate that a focus is in the viewer's or front half of the zone covered; the remainder are in the back half. In a few instances where a low velocity appears to be deeper than a higher velocity the underscore.

or absence of one, shows that they are not in the same geographic area. At the surface are shown the important towns lying within the zone. Also shown are the outstanding features of the gravity anomaly picture. See Fig. 6.

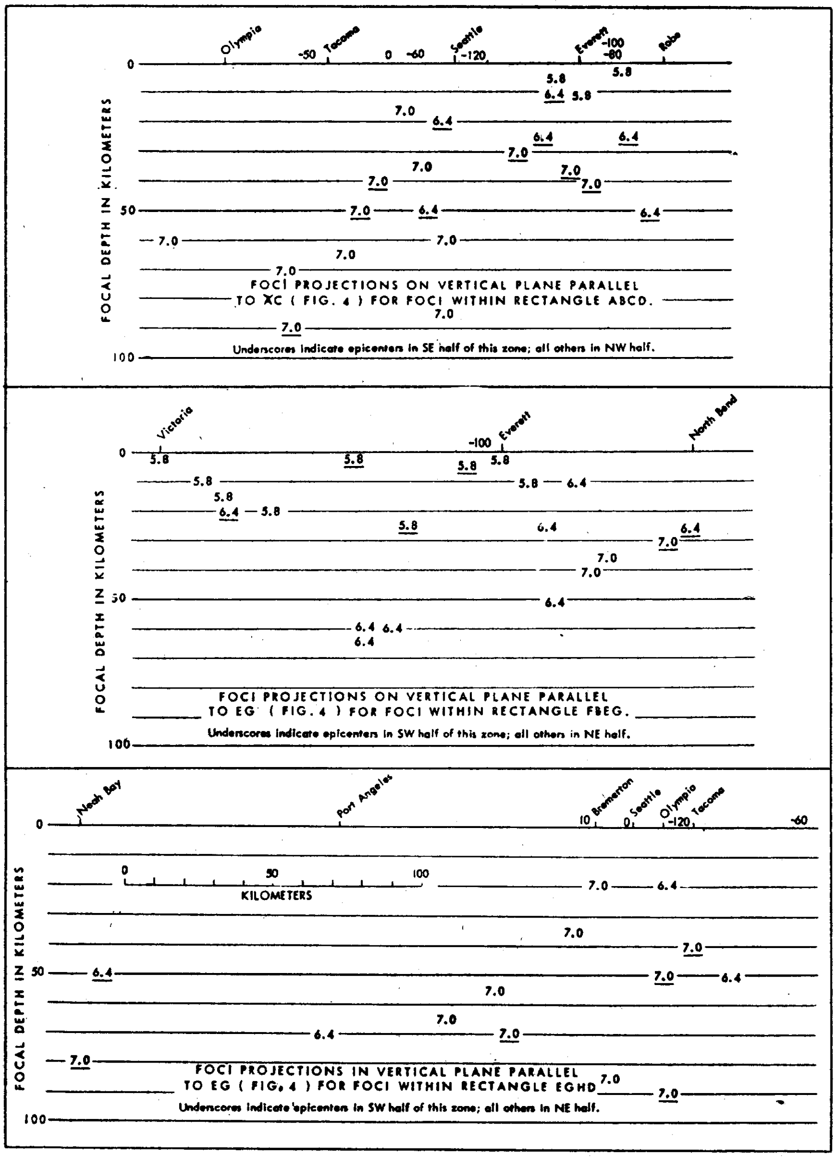

FIG. 5.

An examination of the three projections shown in Fig. 5 reveals that there is no support for the assumption that parallel layering exists in the Puget Sound area. Rock of 6.4 km./sec. speed is often found at lower levels than 7.0 km./sec. rock but always in different

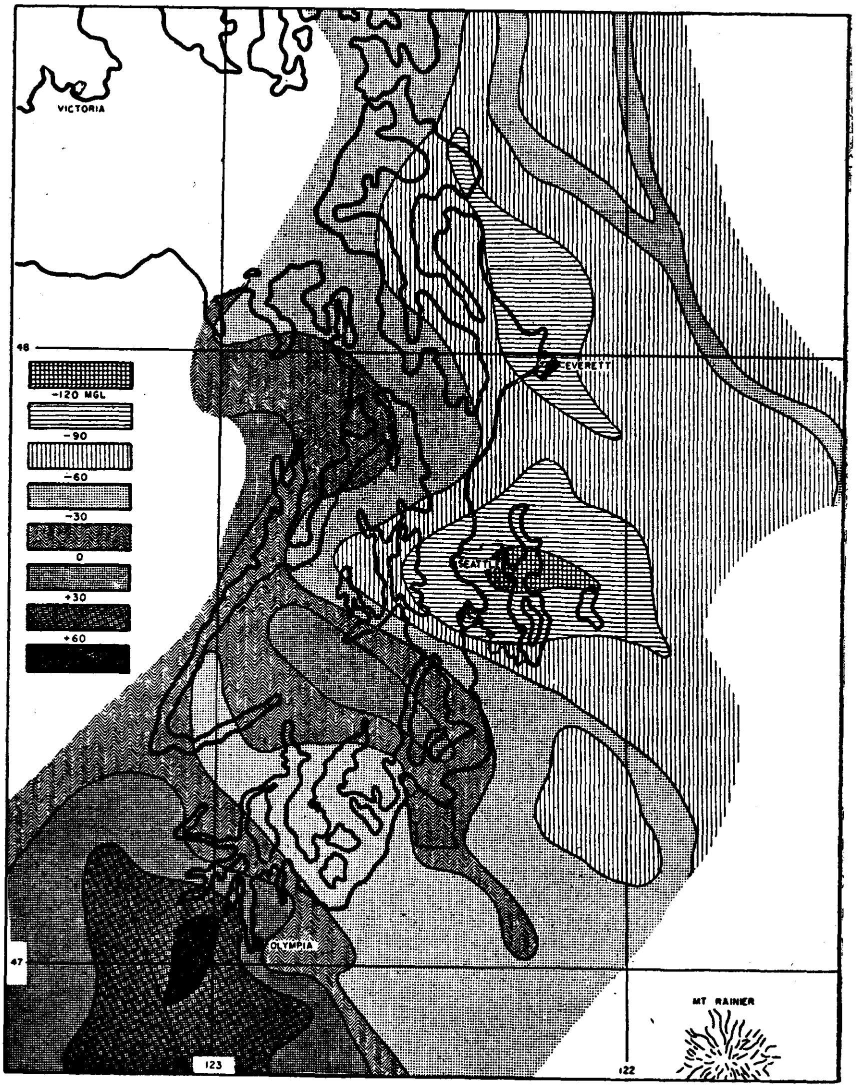

MAP SHOWING FREE-AIR GRAVITY ANOMALIES IN THE PUGET BASIN OF WESTERN WASHINGTON

FIG. 6.

geographic locations. Referring to the gravity anomalies in the top projection it will be seen that the highest level reached by an intrusion of the denser 7.0 km./sec. rock lies close to the highest positive anomaly. Where the lowest negative anomaly appears, a trough of lower speed rock is indicated although it is still poorly outlined. One may interpret such observations as a rough correlation between seismic results and the broader scale features of the gravity picture. It is significant that to date no forceful contradiction has yet appeared in this type of seismic approach. It is significant, too, that in no case has a low velocity layer ever been found directly beneath a higher velocity layer. There are not sufficient foci to indulge in unlimited speculation as to what the figures gathered to date really mean and the reader is free to draw his own conclusions.

The center and lower portions of Fig. 5 are similar projections covering the areas described in the illustrations themselves. Perhaps the most outstanding crustal feature is the basin of 5.8 km./sec. rock that appears in the center figure in the San Juan Islands area. As one moves toward the Cascades a change in structure is indicated. An unexpected feature is the great depth of low velocity rock indicated in the coastal region around Neah Bay. It is generally accepted that continental structure thins out in the coastal areas, but this is contradictory evidence. The proposed installation of a seismograph at Neah Bay will do much to clarify this provisional finding.

In conclusion it is desirable to repeat that while the hypothetical travel time tables used appear to adapt themselves to the observed data as well as any other curves used in seismological practice, a controversial issue arises when one attemps to interpret the curves in terms of structure and wave speeds. More than one combination of structure and wave speed may satisfy any one of the curves within the limits of observational error. The further accumulation of data and additional stations will do much to reveal any serious weaknesses that may exist in the particular interpretation placed on the curves in this paper. In the ultimate solution other types of evidence such as obtained from controlled explosions, geological and gravity investigations will have to be considered along with this earthquake evidence. The technique would in large measure duplicate that used in the geophysical exploration of shallow structure. The current need is for more data to implement such studies.

There has been unexpected delay in establishing a proposed network of auxiliary stations in the Puget Sound area under the sponsorship of the University of Washington, but steps are currently under way to build stations in Mt. Rainier National Park, in Olympia, and at Neah Bay near the entrance to the Strait of Juan de Fuca. The Western Washington College of Education at Bellingam is also planning a station. In another five years sufficient new data should be available to further evaluate the validity of the technique developed in this investigation and perhaps furnish a more authentic picture of the principal features of deep crustal structure in the Puget Sound region.

References.

Tatel (H. E.) and Tuve (M. A.) (1955) : *Seismic Exploration of a Continental Crust,* Geological Society of America, Special Paper 62, pp. 35-50.

Hodgson (J. H.) : Data on P-wave velocity on Vancouver Island obtained from W. G. Milne, Dominion Astrophysical Observatory, Royal Oak, B. C., Canada.

Gutenberg (B.) (1951) : Revised Travel Times in Southern California, Bull. Seis. Soc. of America, Vol. 41, pp. 143-163.

Table 1. — *Instrumental data used in locating epicenters.*
S — Seattle. V — Victoria; H — Horseshoe Bay; A — Alberni
(H) — Origin time at focus. * — iS wave.

Date Time	Sta.	P Sec.	(S-P) Sec.	(H) Sec.	Date Time	Sta.	P Sec.	(S-P) Sec.	(H) Sec.
1951					*1952*				
Oct. 9	S	35.9	8.7	24.0	Sept. 13	V	57.6	15.0	37.1
22^h 59^m	V	38.0	11.5	22.3	22^h 58^m	H	59.8	15.2	39,0
	H	50.5	20.0	23.1		S	62.0	14.3	42.4
	A	57.6	16.5	—		A	74.6	25.4	39.8
1952					Sept. 22	V	52.7	7.0	43.1
Feb. 20	V	13.4	—	—	7^h 21^m	H	62.0	12.8	44.5
19^h 07^m	H	22.8	11.0	07.7		S	63.6	14.8	43.4
	A	31.4	—	—		A	72.5	21.0	43.7
	S	31.7	18.5	13.2	*1954*				
Feb. 22	V	36.7	—	—	March 16	S	28.5	7.0?	19.0?
9^h 39^m	H	46.7	10.4	32.5	15^h 57^m	V	44.0	19.2	17.7
	S	53.2	15.8	31.6		H	55.8	27.5	18.1
	A	54.4	—	—		A	64.0	31.0	22.0
Mar. 14	V	42.6	—	—	May 15	S	20.6	3.6	15.6
14^h 59^m	H	51.5	10.3	37.4	13^h 02^m	V	33.5	15.0?	13.0?
	S	58.6	16.2	36.4		H	45.5	—	—
	A	60.1	—	—		A	52.1	—	—
March 22	S	49.9	9.5	36.9	June 18	S	50.4	4.8	43.8
2^h 01^m	V	58.7	16.8	35.7	15^h 09^m	V	61.9	—	—
	H	68.9	23.9	36.1		H	73.6	21.5	44.2
	A	75.9	—	—		A	80.2	—	—
Apr. 11	V	48.6	2.9	—	Sept. 1	V	24.1	7.0	14.5
9^h 48^m	A	51.3	11.4	35.7	12^h 42^m	S	26.7	9.3	14.0
	H	56.5	15.1	35.8		H	38.7	—	—
	S	63.5	22.1	33.2		A	45.7	16.1	13.7
					1955				
July 27	S	24.0	4.7	17.5	Jan. 11	V	22.4	—	—
19^h 52^m	V	37.3	14.0	18.1	10^h 20^m	S	28.2	14.3	8.6
	H	45.9	22.0	15.6		H	34.4	19.3	8.0
	A	56.1	—	—		A	36.5	17.9	12.0
July 29	S	59.7	5.0	52.9	Feb. 24	S	03.0	10.1	49.2
20^h 13^m	V	72.8	17.0	49.5	10^h 01^m	V	04.3	—	—
	H	81.0	23.0	49.5		H	15.1	18.1	50.3
	A	91.5	29.0	51 8		A	20.2	21.7	50.5

TABLE 1 (Continued)

Date Time	Sta.	P Sec.	(S-P) Sec.	(H) Sec.	Date Time	Sta.	P Sec.	(S-P) Sec.	(H) Sec.
1955					*1956*				
March 26	S	00.3	7.0	50.7	Nov. 8	S	09.9	7.1	00.2
6^h 56^m	V	09 8	14.2	50.4	23^h 13^m	V	25.7	17.4	01 9
	H	19.3	21.1	50.4		H	35.1	25.7	59.9
	A	28.4	29.1	48.7	Nov. 18	S	07.5	5.1	00 5
July 23	S	41.4	5.4	34.0	3^h 57^m	V	21.9	15.1	01.2
19^h 02^m	V	50.1	11.9	33.8		H	32.8	23 7	00 3
	H	61.9	22.4	31.2	Nov. 18	S	14.9*	(7.7)	(56.7)
Aug. 11	S	38.8	4.9	32.1	14^h 43^m	V	17.7	15.7	56 2
6^h 30^m	V	53.4	14.8	33.1		H	25.8	22.1	55.8
	H	63.3	23.0	31.8		A	37.8	29.0	58.0
Sept. 11	V	02.6	9.0?	50 3	Nov. 22	V	53.3	10.5	38.9
0^h 53^m	A	03.7	—	—	0^h 23^m	H	53 8	—	—
	H	09.2	21.7	39.5		S	60.4	17.8	36.0
	S	15.0	21.5	45 5		A	68.0	22.3	37.5
Nov. 2	S	38.9	7.9	28.2	Nov. 26	S	03.7	13 3	45.5
1^h 40^m	V	48.4	13.2	30.3	0^h 00^m	V	10.4	17.6	46.3
	H	55 3	21.5	25.9		H	23.1	27.3	46.7
	A	67.5	27.3	30.1					
1956					*1957*				
Jan. 7	S	45.9	8.3	35.8	Jan. 8	S	22.8	8.8	10.7
4^h 29^m	V	59.0	12 3	43.6	13^h 46^m	V	27.1	11.2	11.8
	H	70.5	26.0	37.5		H	38.1	—	—
	A	76.7	30.4	38.2		A	44.1	22.4	13.4
Feb. 9	V	25.0	—	—	Jan. 26	V	21.1	4.2	—
0^h 57^m	S	27.2	12.5	10 2	1^h 16^m	S	21.7	11.1	06.5
	H	32 6	13.0	13 3		A	39.1	—	—
	A	42.8	22 7	11.7	Feb. 11	S	04.9	5.8	57.0
Feb. 9	V	49.6	—	—	17^h 05^m	V	20.7	23.9	57.9
1^h 28^m	S	51.7	12.4	34.7		H	31.2	26.0	55.6
	H	57.0	14.9	36 6		A	40.7	322	56.5
	A	67.6	22.1	37.4	May 4	S	36.0	6.5	27.1
Apr. 8	S	30.0	13.8	11.1	21^h 09^m	V	50.1	16.4	27.6
22^h 28^m	H	30.2	130	12.4		H	62.5	27.2	25.4
	A	36.0	—	—		A	68.2	28.8	28.7
Apr. 26	S	25.9	3.1	21.7	May 29	S	11.0	10.5	56.6
16^h 48^m	V	43.5	15.7	22.0	9^h 35^m	V	16.5	12.5	59.4
	H	55.8	23 2	24 0		H	28.2	21.8	58.3
July 22	S	29.1	12.1	12.5		A	32.0	22.8	00.8
20^h 52^m	V	39.2	18.4	14.0					
	H	50.8	22 1	20.8					
	A	57.2	29.0	17.4					

TABLE 2. — *Instrumental epicenters in Puget Sound Area.*

Date	No.	Origin Time G. C. T.	Latitude North	Longitude West	Depth	P Wave Velocity	Remarks
1951		h m s	° '	° '	km.	km/sec.	
Oct. 9	1	22 59 24.4	48 07	122 40	25	5.8	Puget Sound, near Port Townsend.
1952							
Feb. 20	2	19 07 08.7	48 40	123 11	0	5.8	Haro Str., Stuart Islands
Feb. 22	3	9 39 31.2	48 37	123 08	10	5.8	Haro Str. N. tip San Juan Is.
Mar. 14	4	14 59 36.4	48 38	123 05	15	5.8	No. end San Juan Channel
Mar. 22	5	2 01 36.2	47 40	122 27	85	7.0	Puget Sound, near Seattle
Apr. 11	6	9 48 34.5	48 27	124 25	50	6.4	Off Neah Bay
July 27	7	19 52 16.1	47 49	121 54	35	7.0	Mt. Si Fault near Monroe
July 29	8	20 13 50.9	47 51	121 53	40	7.0	Mt. Si Fault near Monroe
Sept. 13	9	22 58 41.4	48 44	122 13	20	5.8	East of Bellingham
Sept. 22	10	7 21 44.9	48 32	122 52	20	5.8	Lopez Islands
1954							
Mar. 16	11	15 57 17.7	47 24	122 06	50	6.4	Six miles southeast of Renton
May 15	12	13 02 15.6	47 37	122 34	15	7.0	Bremerton, five mi. N. E.
June 18	13	15 08 44.0	47 40	122 35	33	7.0	Bremerton, eight mi. N. NE.
Sept. 1	14	12 42 14.4	48 08	122 56	0	5.8	Discovery Bay, eight mi. S.W.
1955							
Jan. 11	15	10 20 08.3	48 03	123 35	70	6.4	Port Angeles, 10 mi. S.E.
Feb. 24	16	10 00 50.2	47 57	123.00	65	7.0	Sequim
Mar. 26	17	6 56 50.5	48 07	122 02	0	5.8	South of Arlington
July 23	18	9 02 33.3	48 02	122 23	5	5.8	Whidbey Island, near Langley
Aug. 11	19	6 30 32.0	47 51	121 56	10	6.4	Two miles east of Monroe
Sept. 11	20	0 52 45.5	48 24	124 36	80	7.0	Neah Bay
Nov. 2	21	1 40 26.1	48 06	121 45	50	6.4	Pilchuck Mt., four miles NE.
1956							
Jan. 7	22	4 29 36.0	47 22	122 28	50	7.0	Vashon Is. near Burton
Feb. 9	23	0 57 11.0	48 23	122 35	60	6.4	Skagit Bay, near Whidbey Is.
Feb. 9	24	1 28 35.1	48 21	122 35	55	6.4	Aftershock
Apr. 8	25	22 28 11.8	48 23	123 19	20	6.4	Gonzales Pt. S. E. of Victoria
Apr. 26	26	6 48 21.7	47 34	122 17	18	6.4	Seattle, S. E. section
July 22	27	20 52 12.3	47 12	122 38	90	7.0	Puget Sound off Steilacoom
Nov. 8	28	23 13 00.2	47 35	121 40	25	6.4	Mt. Si Fault, near North Bend
Nov. 18	29	3 57 00.7	47 55	122 06	10	5.8	Snohomish, two mi. N.W.
Nov. 18	30	14 43 56.2	48 04	121 47	25	6.4	Near Pilchuck Mt.
Nov. 22	31	0 23 37.6	48 51	122 23	45	6.4	Bellingham, seven mi. N.E.
Nov. 26	32	0 00 46.2	47 09	123 27	60	7.0	Shelton, 15 mi S.W.
1957							
Jan. 8	33	13 46 12.0	47 53	122 47	55	7.0	Port Townsend, 15 m. S.
Jan. 26	34	1 16 06.0	48 20	122 31	60	6.4	Skagit Bay
Feb. 11	35	17 05 55.6	47 32	121 44	30	7.0	Mt. Si Fault near North Bend
May 4	36	1 09 27.2	47 21	122 24	40	7.0	Puget Sound near Tacoma
May 29	37	9 35 56.6	47 31	123 10	70	7.0	Near Cushman Lake

THE EVOLUTION OF THE GEOPHONE

by T. C. RICHARDS

INTRODUCTION.

It is not surprising that the geophone we know in geophysical exploration owes much of its present high standard of performance to progress in earthquake seismology, the detection of sounds — airborne, underwater or underground while the tremendous advances in metallurgy, electronics and rheology have made their impact.

The earliest known form of seismic detector is accredited to a Chinese named Choko in A. D. 136, but it was not until 1825 that this crude detector was replaced by the mercury seismoscope and, in 1881, by the introduction of Gray's horizontal lever spring seismometer. This seismometer revolutionised seismological measurements and many improved types followed, such as those of Wiechert in 1899 and Milne-Shaw in 1914.

In 1920 Mintrop evolved a pendulum or mechanical vertical seismometer with high magnification for use with explosive charges and the successful application of this seismometer to the discovery of oil fields resulted in a surge of development in the mechanical seismometer for seismic refraction exploration and in the electromagnetic seismometer or geophone for reflection or refraction exploration. Figure 1 shows the Jones (1932) vertical mechanical seismometer, in which magnifications of up to 80,000 and periods up to 0.8 sec. may be achieved by adjustments of two horse-shoe magnets disposed about a suspended soft iron element carried by the helm of the pendulum. This instrument was used with great success in finding many of the great oil bearing limestone anticlines in S. W. Iran.

ELECTROMAGNETIC SEISMOMETERS — GEOPHONES.

The advantages to be gained by devising systems where the mechanical energy received at the detector could be converted to electrical energy and recorded well away from the detector were patent to all geophysicists in the early days of exploration. The principles employed by Bell in 1876 in his moving iron telephone receiver or by Hughes in 1878 in his microphone, were well established while, in 1915, Galitzin appears to have been the first to use the moving coil principle in his vertical earthquake seismometer.

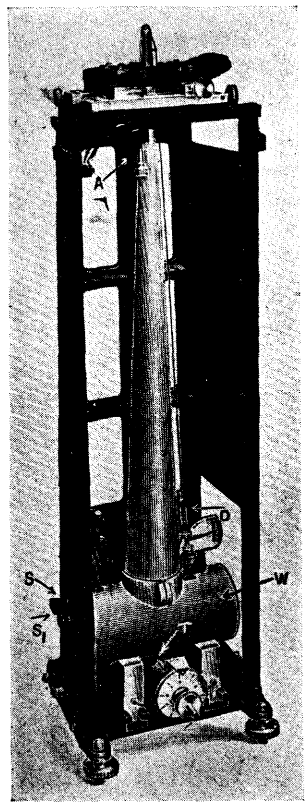

FIG. 1. — The Jones Mechanical Seismometer.

To Karcher, however, belongs the credit for developing the first practical geophone of the moving coil type with electronic magnification, and this geophone was successfully used in discovering several salt domes in the U.S.A. in 1926. This was followed by Benioff's reluctance type (Figure 2) which remained the more popular for both reflection and refraction surveys until 1939 when it gave way almost entirely to the moving coil type. Some manufacturing figures are revealing, for about 8,000 reluctance geophones were made by the leading manufacturers in the period 1930 to 1939 and about a million moving coil geophones from 1939 to 1956, a large fraction of this high output being due to the practice, common in recent years, of using geophones in multiple array at any one observation station.

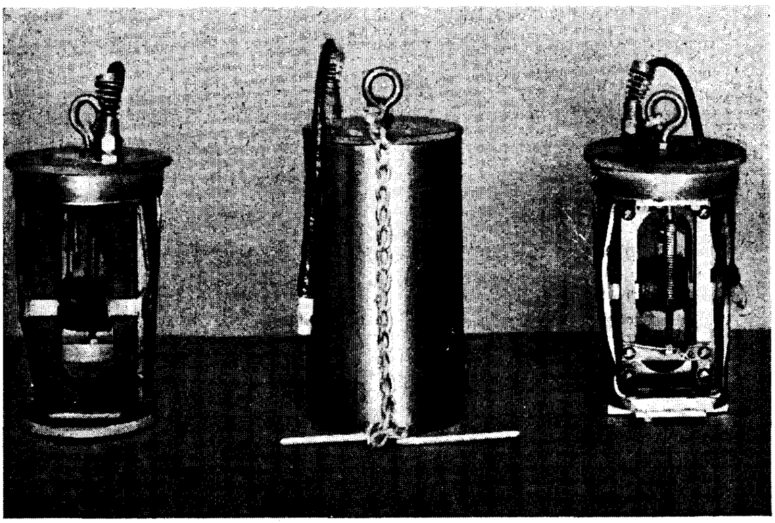

FIG. 2. — The duplex reluctance geophone with 4 air gaps. (Seismograph Service Corp.).

Damping and Sensitivity.

The moving coil or reluctance geophone is essentially a velocity instrument or one in which the emf developed in the coil is proportional to the velocity of ground motion but, if the system is heavily damped, the emf is also proportional to the pressure and independent of the frequency. The geophone then becomes virtually a pressure instrument, but of low sensitivity. If, on the other hand, the geophone has negligible damping and is of low natural frequency, the emf developed is inversely proportional to the applied frequency, while, if the mass is very small in addition, the emf is directly proportional to the applied frequency. By suitable adjustments of the various instrumental parameters, the response of these electrodynamic geophones may be made to vary with frequency in diametrically opposing ways or to be independent of it and such flexibility has proved to be a considerable asset.

In seismic prospecting, high resolution of the signal is desirable, but whereas in those refraction surveys which utilise times to first arrivals on the seismogram, the instrumental requirements are not too stringent, in reflection and late event refraction surveys, certain conditions must be fulfilled. For good resolution, the damping should be ideally critical for all frequencies, but this would diminish the voltage sensitivity of the geophone, especially for the higher frequencies, and a compromise of between 0.5 and 0.7 of critical is normally tolerated although « ringing » at some frequencies may occur. In refraction with first events, a damping coefficient of no more than 0.5 may be used with advantage.

It is obvious that for high voltage sensitivity, the internal impedance of the coil, compared with that of the total load, should be kept as small as possible, and this also has the advantage of minimising unwanted pick-up from power lines and cross channel coupling through earth leakage. On the other hand, the impedance should be high enough to prevent any important mismatching with the amplifier input transformer when varying resistive cable lengths are used, especially in big scale refraction work. Moreover, the sensitivity of the geophone should be such as to magnify the ground motion to a degree higher than the level of the inherent noise in the geophone and the first stage of the amplifier, combined.

Miniature Geophones.

The science of metallurgy was well advanced by the 1930s so that good quality permanent magnets such as Alnico and suspension springs of heat treated berylluim copper to minimise elastic-temperature creep were readily available to the geophone designer. Accompanying these advances was the much improved quality of seismic amplifiers so that it became possible to develop smaller and smaller geophones and, at the same time, to standardise on « utility » types which could be used on dry land, in swamp or shot hole, or floating on water by suitable modifications to the case design or by providing various forms of detachable base.

The construction of miniature geophones introduces special design problems. As the magnetic material becomes less, efficiency falls off to such an extent that the electromagnetic damping becomes almost ineffective but to overcome this, the diameters of the coil and pole pieces are made relatively large. Very careful balancing of the suspension spring system is necessary and one miniature geophone uses one supporting diaphragm spring with a stabilising rod which is fixed to the lower end of the coil, passes through the centre of the magnet and « free » floats in a spider near the base of the instrument. Another miniature type incorporates a coil suspended and centred by three heat-treated flat diaphragm springs as it is claimed that only then is transverse motion effectively prevented. Great care must be taken in suspending these diaphragm springs to minimise « crimping », which may only be revealed by shaking in a mechanical tumbler, a procedure which all geophones must undergo before they are passed as field worthy.

All miniature geophones are filled with a dry inert gas and hermetically sealed in order to eliminate internal moisture condensation and the effects of corrosion, electrical leakage and freezing at low temperatures. The case itself is covered with a suitably coloured plastic jacket to protect the connections from moisture and dirt and to ensure ease of identification. They are available in a range of selected natural frequencies and shunts to provide varying damping coefficients, the coil resistance normally being constant. The sensitivity may be as much as 0.4 Volt/inch/sec at 0.6 critical damping with a coil resistance of about 200 ohms and a frequency of 18 cps. For a geophone weighing less than a pound, these characteristics speak well of technological progress when it is realised that a few years ago the equivalent geophone would weigh ten times as much.

Developments in Very Low Frequency (VLF) Refraction Moving Coil Geophones.

One of the largest moving coil geophones, used for long distance first event refraction surveys in southwest Iran some twenty years ago, weighed 80 pounds or nearly 300 times the weight of the smallest reflection geophone now available (no more than 4 ½ ounces).

A somewhat new principle in VLF design has been described by Dennison and Jones (1955). One leaf spring, equally stressed at all parts of its surface, is alone used. It runs the full width of the instrument and is clamped to angled faces on both the frame and the moving arm which supports the inertia mass and coil and, in so doing, bends the spring into a circular arc. The amount of flexure in the spring and the length of the arm govern the natural frequency which may be as low as 1.8 cps. It has a sensitivity of 1.8 volt/inch/sec and weighs only 14 lbs.

A VLF geophone designed within the last few years employs a double coil hum bucking construction to reduce the effects of external magnetic fields (Figure 3). The coils are series connected to add the seismic signals but act in opposition for magnetic pick-up; with a total coil resistance of 4.000 ohms and a damping resistor of 15.000 ohms, the output is as much as 5 volts/inch/sec at 2 cps and 0.5 critical damping. In weight it is 17 pounds and its cylindrical shape with a diameter of 3 inches allows it to be planted in a small auger hole. Its high resistance necessitates a special

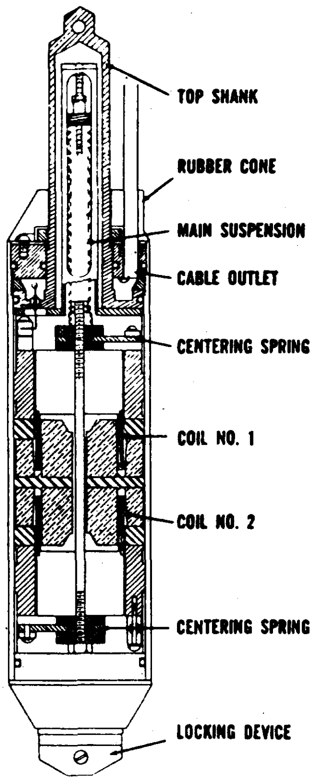

FIG. 3. — The double coil « hum-bucking » refraction gesphone. (Texas Instrument Company.)

refraction amplifier but a modification of the geophone with a 100 ohm coil and 150 ohm damping resistor permits matching to a conventional reflection amplifier, the sensitivity, however, being reduced to one-sixth of its former value, the other parameters remaining unchanged.

Figure 4 shows an assortment of response curves for these VLF geophones and some of the higher frequency reflection geophones.

SWAMP AND MARINE GEOPHONES.

In the early 1940s, adaptations of land geophones were being used for offshore surveys. At first large heavy base plates allowed firm seating on the sea floor but, by 1945, operations were speeded up by attaching the geophone to a paravane and suspending it at selected distances from buoys attached to a steel towing cable which extended the full length of the geophone spread. Another

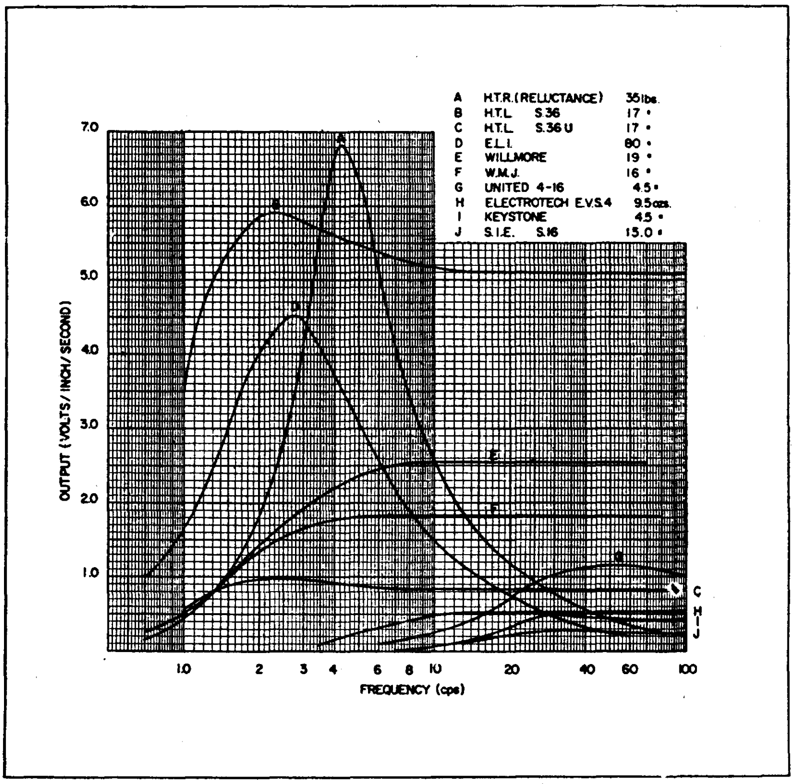

FIG. 4. — Geophone response curves.

semibuoyant adaptation employs a gimbal type of housing, the geophone « floating » a few feet above the cable which is towed along the bottom. The wear and tear on the cable in dragging it along the sea floor, however, is viewed with disfavor by most reflection operators and the floating cable technique is resorted to whenever possible.

Pressure Geophones.

Velocity geophones are less sensitive than pressure geophones of comparable dimensions and thus there has been a tendency to introduce the latter into swamp or marine seismic operations in the last decade. It has been claimed that reliable data have been obtained with these pressure detectors in areas that were previously considered « no-result » prospects and that resolution has been improved. They have the advantage of being relatively unresponsive to wave motion. In one class, the conventional velocity instrument is provided with a diaphragm responsive to pressure variations; excellent mechanical coupling to the transmitting medium is achieved while no impedance matching devices are necessary. Figure 5 shows a double or tandem marine unit weighing only 2 lbs.

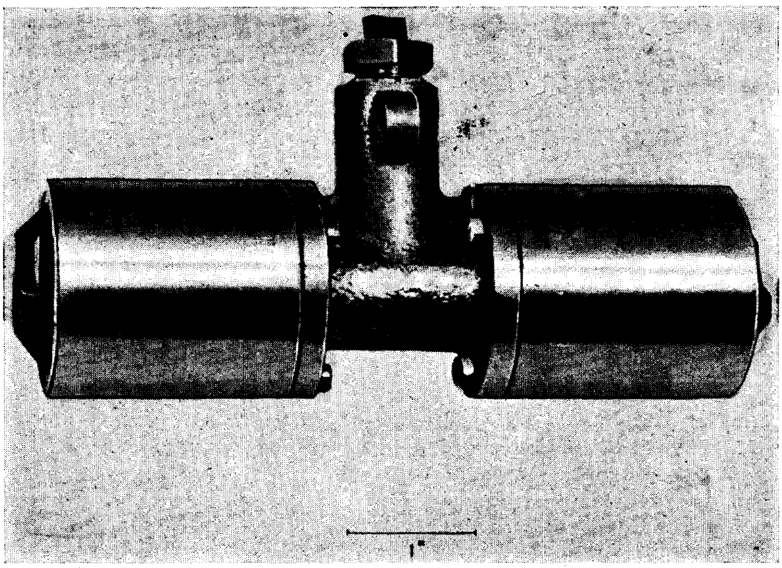

FIG. 5. — Double pressure converted moving coil marine geophone. (Electro-tech International.)

The outputs of the two units are series connected but any important lateral motion is nullified by the opposing reactions of the diaphragms.

Piezo-Electric Geophones.

In the piezo-electric crystal geophone, the absence of moving elements and the extremely linear output give the instrument a certain advantage over the electro-dynamic geophone, but the necessity of using a pre-amplifier and careful impedance matching and of employing special means to eliminate the adverse effects due to humidity have prevented the crystal being developed seriously as the sensitive element in a surface geophone.

The development of the more sensitive ceramic tye of crystal such as barium titanate, has led to the manufacture of a marine geophone using this crystal as the sensitive element, with impedance matching. The element is bonded to an outer rubber cover, protected by a steel cage, and its weight of only 1 lb. makes it ideally suited for use with the floating cable technique which is capable of producing as many as 200 records a day.

The ceramic crystal pick-up is used in the sonoprobe which is having successful application in mapping shallow structures, ancient channels or foundations suitable for drilling platforms below the sea floor.

Borehole Geophones.

Developments of far-reaching importance have taken place in borehole geophones. In the early days, the oil damped reluctance geophone mounted in a water proof steel cylindrical case was used, but today the more sensitive pressure geophone has practically superceded it.

The reluctance diaphragm type shown in Figure 6 is very effective. The detector is relatively insensitive to cable noise and can withstand pressures of more than 10,000 psi. The new lease of life for the reluctance principle is to be noted and this is largely due to the availability of damping fluids with negligible temperature coefficient.

Piezoelectric crystal types have also been used, especially in the « vertical spread » reflection technique for picking up reflected waves at depths below the « weathered » layer. In this technique, barium titanate elements, or « beads » are moulded at intervals of a foot or more into a water tight cable.

Within the past year, however, a very small pressure converted variable reluctance element has been designed to replace the crystal bead. As with the larger reluctance borehole geophone, the disadvantages of pre-amplifiers and high impedance matching are avoided. The element is only a little over 4 inches long, less than an inch in diameter and weighs only 5 ounces. It is interesting to note that the transducer is fixed, the diaphragm movements cutting across the flux circuit as in the case of the Bell telephone. The coil impedance is 500 ohms while a pressure compensating capsule allows reliable readings to be obtained at depths as great as 2,000 ft., where the output available for surface amplification is much greater than in the case of the crystal element.

For detailed borehole logging, the conventional explosive source at the surface is replaced by an impulsive transmitter within the

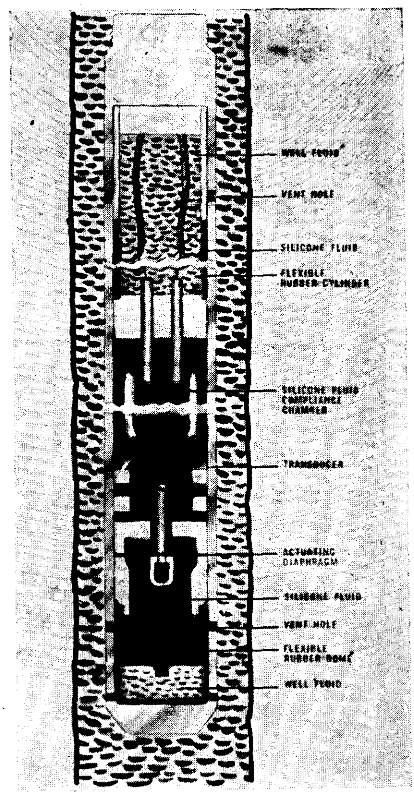

FIG. 6. — The pressure converted reluctance bore hole geophone. (Gulf Research et Development Co.)

geophone housing. In one instrument, described by Summers and Broding (1952), the transmitter is a magnetostriction acoustic pulse generator which emits some twenty pulses per second, the received signal varying in frequency from 10 to 25 kilocycles per second. Special precautions in design are necessary for high impedance matching; they include a coaxial feed to the amplifier and electrostatic shielding. To reduce relatively low frequency hum and noise, high pass filtering is incorporated. Corrections to interval velocities are required for differential travel time in the drilling mud between the case of the instrument and the well bore. To eliminate this correction, another borehole logger (which is activated by a hammer striking an anvil every 6 seconds) uses two crystals spaced 5 or 10 feet apart; in addition the signal amplitude and frequency are faithfully recorded. The logging method discussed by Vogel (1952), also uses a piezo-electric receiver, the transmitting being an electric arc discharged in a liquid at 5 ft intervals down the borehole. A refinement of registration of the receiver output is its continuously photographed display on a CRO and the nature of the waveform acts as a guide in identifying the lithology.

Design trends.

New avenues for more efficient geophones are continually being explored, and some of the present investigations are :

1. The use of more « powerful » magnet materials to allow an increase in output of the miniature geophones thus relatively reducing power line pick-up due to cable leakage; important magnet improvements are not expected, however.
2. Improvements in transducer design for pressure type geophones used off-shore.
3. Improvements in signal/noise ratio may be expected from careful streamlining of geophone cases and investigations into the best means of suspension in floating cable off shore operations.
4. Radio geophones (transistorised) for long range refraction work will become fashionable, while radio signals could be used to turn on and off the amplifiers and recording equipment at unmanned locations. Research is already under way in Germany
   a with a multiplex device with pulse-phase modulation using only two high frequencies for the whole system and,
   b on radio geophones using one separate high frequency for each channel.

   One manufacturer who has been working on the radio geophone concept for some years is doubtful that an effective system can be evolved. In rugged terrain and a wide range of vegetation, the only usable frequencies would be in the low or medium range and these would demand relatively high transmission power and relatively heavy extra equipment which would be economically unfavourable compared with a long land line. These objections do not hold, of course, when a spread of geophones is required to cross a river; small high frequency radios could be most efficient.
5. The development of low frequency geophones with magnetic suspension.
6. Inserting a transistor pre-amplifier into low frequency geophones, to overcome cable resistance.

7. Greater development of transducers with ceramic electrostrictive or self-generating crystal elements in geophones for all types of water or marsh operations.
8. Further miniaturisation to a degree where the detector itself could be enclosed in a land cable eliminating the necessity of individual geophones and geophone planting. The information from the cable would be divided into the smallest practical increments so as to give maximum control at playback from magnetic recording which is fast becoming a standard receiving process.
9. Improvements in methods of geophone placements. The coupling is not always as rigid as it should be, the use of short spikes often being inadequate. More « Pancake » types of geophone housing are anticipated.
10. Low Priced expendable seismometers.

To give a full account of the evolution of the geophone would be a formidable task and in this paper only some of the high lights have been recorded. There is no standing still in the geophone industry. From the artistic and elegant instruments of old, evolution has taken its inexorable course of seeking perfection. Designers have kept pace with the requirements of the prospector which are becoming more and more specific and exacting as the oil bearing structures are becoming increasingly elusive. They have taken miniaturization in their stride, thus making the elimination of ground noise by the use of multiple geophone patterns a practicable field technique. In common with workers in other fields of scientific endeavour, they seek to introduce automation in the detection of the seismic message and so reduce human effort — a process which has already been established in the interpretation of the seismic record. Competition between manufacturers is keen and healthy, and the geophysicist may be assured that no challenge for more efficient instruments will remain unanswered.

Références.

Jones (J. H.) and Jones (D. T.) (1932) : A portable seismograph for recording artificial earthquakes. Journal of Scientific Instruments (London), v. 9, p. 8-16.

Jones (W. M.) and Dennison (A. T.) (1955) : A low frequency refraction geophone : Geophysical Prospecting, vol. 3, pp. 168-176.

Summers (G. C.) and Broding (R. A.) (1952) : Continuous velocity logging. Geophysics, vol. 17, pp. 598-614.

Vogel (C. B.) (1952) : A seismic logging method. Geophysics, vol. 17, pp. 586-597.

DEVELOPMENT OF THE MICROSEISMIC METHOD OF TRACING STORMS AT SEA.

by F. I. Monakhov.

Regular investigations of microseisms in the Soviet Union are conducted since 1951. These investigations are mainly directed by the Academy of Sciences, Moscow University and institutions of the Hydrometeorological Service.

The chief objective of studying microseisms in the USSR is the development of the microseismic method of tracing storms at sea and ocean and making it practically useful, the main stress being laid on methods of determining directions to the sources of microseisms. There are two different methods used to determine the directions of microseisms propagation : by a phase shift in three points (method of a tripartite station) and by the direction of particle oscillations in microseismic waves (method based on the revealing of Rayleigh and Love waves).

A special investigation was undertaken to determine the efficiency of both methods. For this purpose a tripartite and an azimuthal installation were set up in Yalta. The schemes of the tripartite station and the azimuthal installation are shown in fig. 1-2. In fig. 2 the generants of the cones represent the directions of axes of maximum sensitivity of the seismographs. The recording of microseisms by these installations was conducted during the autumn and winter of 1956-1957. Both installations began recording simultaneously. The duration of recording during each period was about 20 minutes. In addition, microseisms were recorded by a vector installation under the Gutenberg scheme (1).

The azimuthal installations was first suggested by G. A. Gamburtsev (2) to determine the direction to earthquake epicentres. However the aspects of its application turned to be much broader (3). It permitted to reveal comparatively easily waves of different types, say Rayleigh and Love waves, on the records. The azimuthal installation permits not only to detect different waves but also to determine the space position of trajectories of particles oscillations in these waves.

The azimuthal installation has an undoubted advantage as against the vector one because the latter records the summary effect of oscillations for a definite period of time without differentiation of waves.

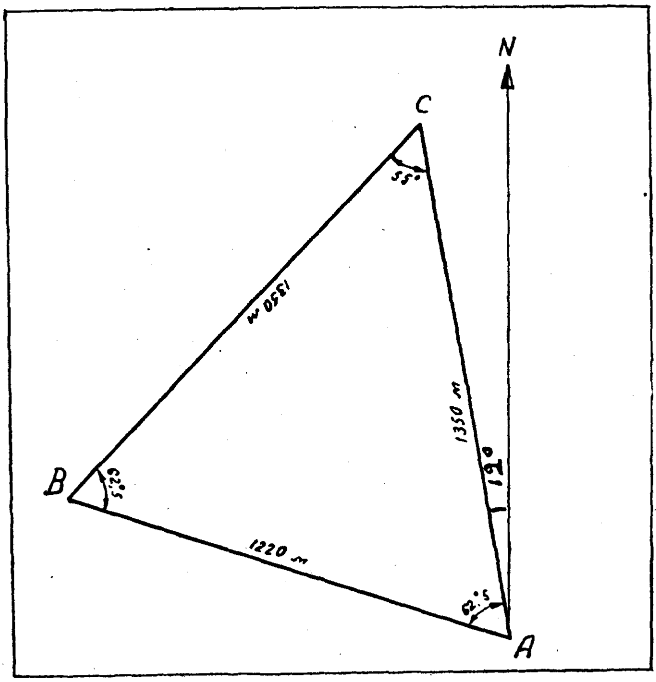

FIG. 1. — The scheme of a tripartite microseismic station.

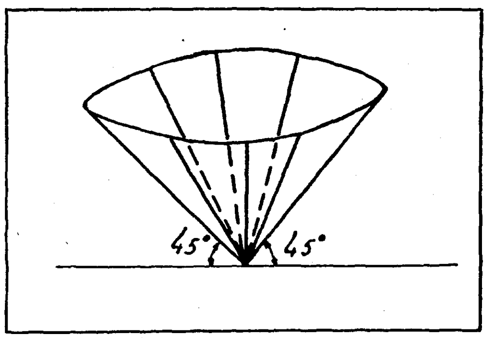

FIG. 2. — The scheme of the azimuthal installation.

The analysis of microseisms recorded by the azimuthal installation has shown that Love waves in the microseisms are absent nearly completely. Rayleigh waves in a pure form i.e. those in which oscillations are polarized elliptically in a vertical plane, are observed to occur both from near and distant sources, but they are seldom to be come across; the oscillation planes are mainly inclined at different angles to the horizon.

From preliminary computations, Rayleigh waves, oscillation planes of which are inclined to the horizon at angles from 60° to 90° make no more than 10 or 15 per cent from the general number of microseismic waves. In the case of near sources (the Black Sea) Rayleigh waves are expressed weaker than in the case of a distant source (the Atlantic Ocean). Besides Rayleigh waves from near sources mostly differ from their normal type. In figures 3-4 the

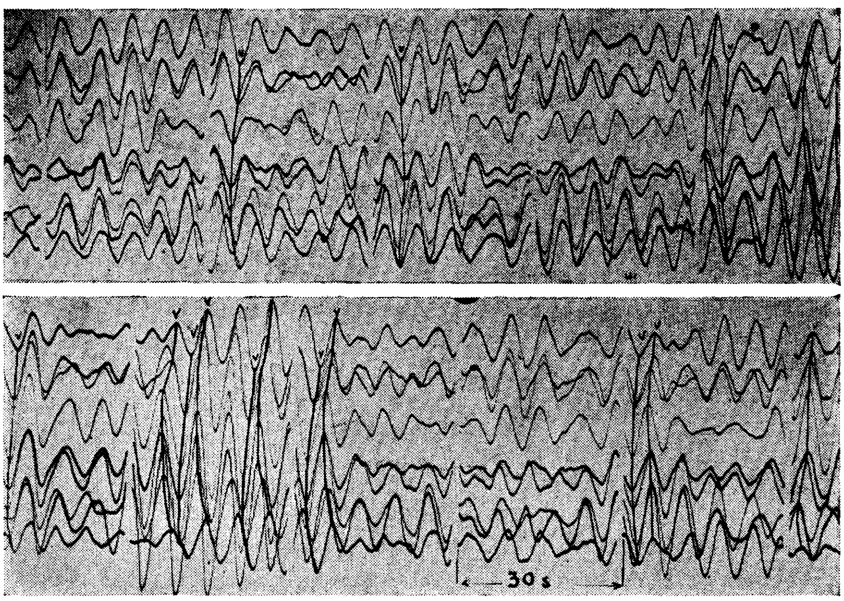

FIG. 3. — Atlantic microseisms recorded by the azimuthal installation.

seismograms with records of storm microseims of the Atlantic and Black Sea origin are shown on which cophasal axes are drawn in Rayleigh waves. It follows from these seismograms that there are Rayleigh waves but a little portion from the general number of waves.

Thus, observations in Yalta prove that in microseismic waves oscillations of a complex nature prevail which differ from oscillations in Rayleigh and Love waves. Hence, the determination of directions to the microseismic sources from observations of the vector installation is not very reliable. This point of view is confirmed by records of storm microseisms obtained by the vector installation.

The observed Rayleigh waves were used to determine the directions of propagation of storm microseisms, the results of determi-

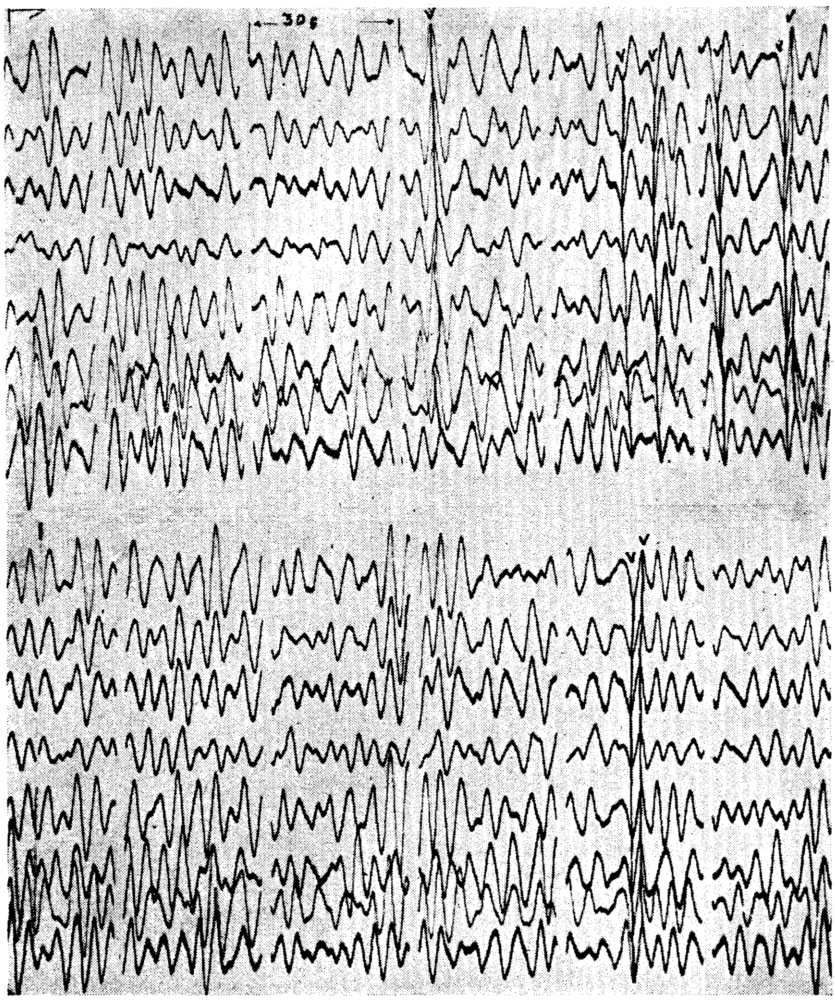

FIG. 4. — The Black Sea microseisms recorded by the azimuthal installation.

nation being compared with observations of the tripartite station. It was found that in the case of the Atlantic microseisms, i. e. when the source was at a considerable distance from the station it was possible to determine the direction to the microseismic source, though its accuracy being lower than from observations at a tripartite station. This can be accounted for mainly by the fact that the number of separate measurements from phase transitions in microseisms is usually much more than from Rayleigh waves during equal periods of time. This can be seen from the comparison of the tripartite station seismogram in fig. 5, where phases suited

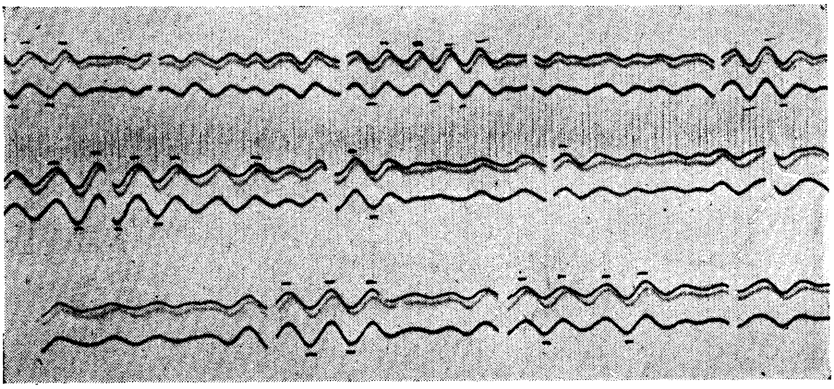

FIG. 5. — Atlantic microseisms recorded by the tripartite station.

for measurements are marked, with the seismogram of the azimuthal installation in fig. 3.

The attempt of using Rayleigh waves to trace the region of exciting microseisms in the Black Sea produced a negative result. In this case oscillation planes in Rayleigh waves took various directions and so the computation of the mean value turned to be impossible. In cases when it is possible, the directions obtained do not correspond to the proposed position of the excitement region of microseisms. Figures 6 and 7 show typical vector diagrams of

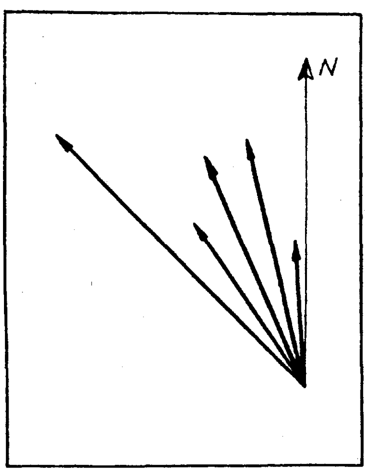

FIG. 6. — Vector diagram of the directions to the Atlantic source of microseisms from observations of the tripartite station.

directions to one and the same source of microseisms locating near Greenland obtained from observations at the tripartite station and

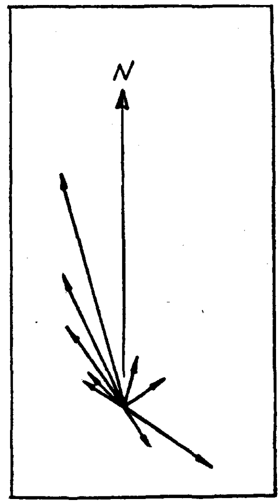

FIG. 7. — Vector diagram of the directions to the Atlantic source of microseisms from observations of the azimuthal installation.

azimuthal installation. The vector length expresses in a certain scale the number of single values of the azimuth corresponding to the given direction. Analogous vector diagrams for the case of a cold front passing over the Black Sea are shown in figures 8 and 9. These diagrams are a sufficiently bright illustration of the conclusion drawn above.

Consequently, from the two methods of determining the direction of microseisms propagation the most efficient for the Yalta region is that based on the measurement of phase shift in microseisms from observations in three points.

Some investigators count that the method of a tripartite station is not suitable for tracing storms at sea because thus obtained direction to the source of microseisms does not coincide with those to the cyclone centre. Observations of microseisms by the method of a tripartite station carried out in different regions of the Soviet Union during many years have proved that the directions to the microseismic source are determined with accuracy of $\pm 10°$, and hence this method can be well applied in practice.

The desire to get the coincidence of directions to the cyclone centre and to the microseismic source mostly failed to achieve the required aim as in the case of a moving cyclone microseisms were excited in its rear, i. e. the region of exciting microseisms lagged behind the cyclone centre. As a result of this the angle between

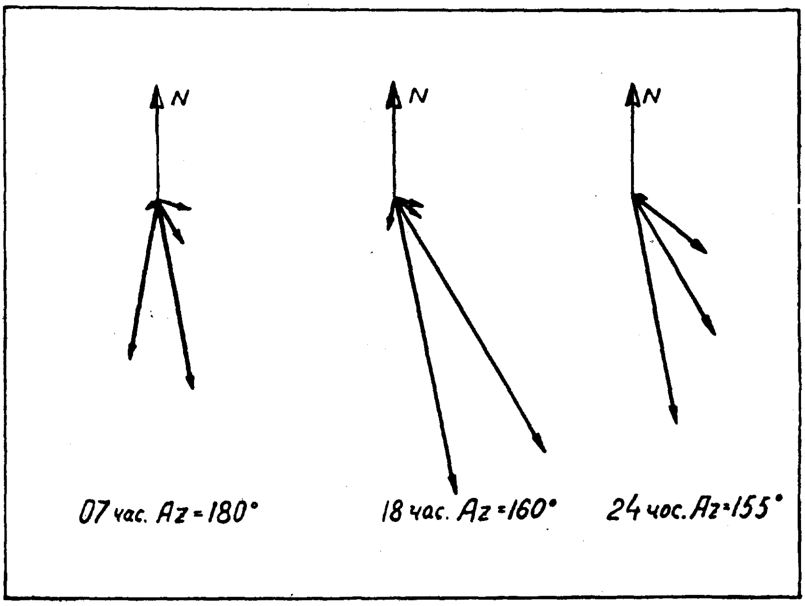

FIG. 8. — Vector diagram of the directions to the Black Sea source of microseisms from observations of the tripartite station on the 19th March 1957.

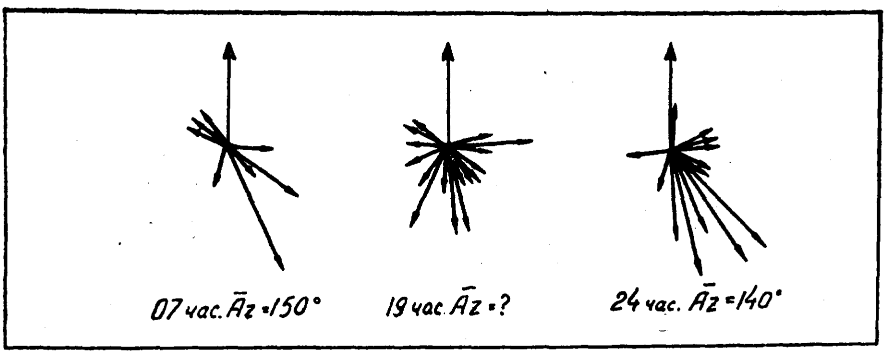

FIG. 9. — Vector diagram of the directions to the Black Sea source of microseisms from observations of the azimuthal installation on the 19th March 1957.

the above directions can reach under specific conditions 180°. The distance between the cyclone centre and source of the dominating microseisms depends on a number of factors, first of all on the velocity of the cyclone motion. This distance is approximately connected with the cyclone velocity (V) by the following ratio :

S = K.V km. The coefficient K has a time's dimension and expresses a lagging of the microseisms development behind the cyclone development. The numerical value of K varied in the range of about 6 to 15 hours.

The excitement of microseisms behind the cyclone centre as well as behind the cold front was noticed by many investigators. From our results in this respect we can give two illustrations. Fig. 10

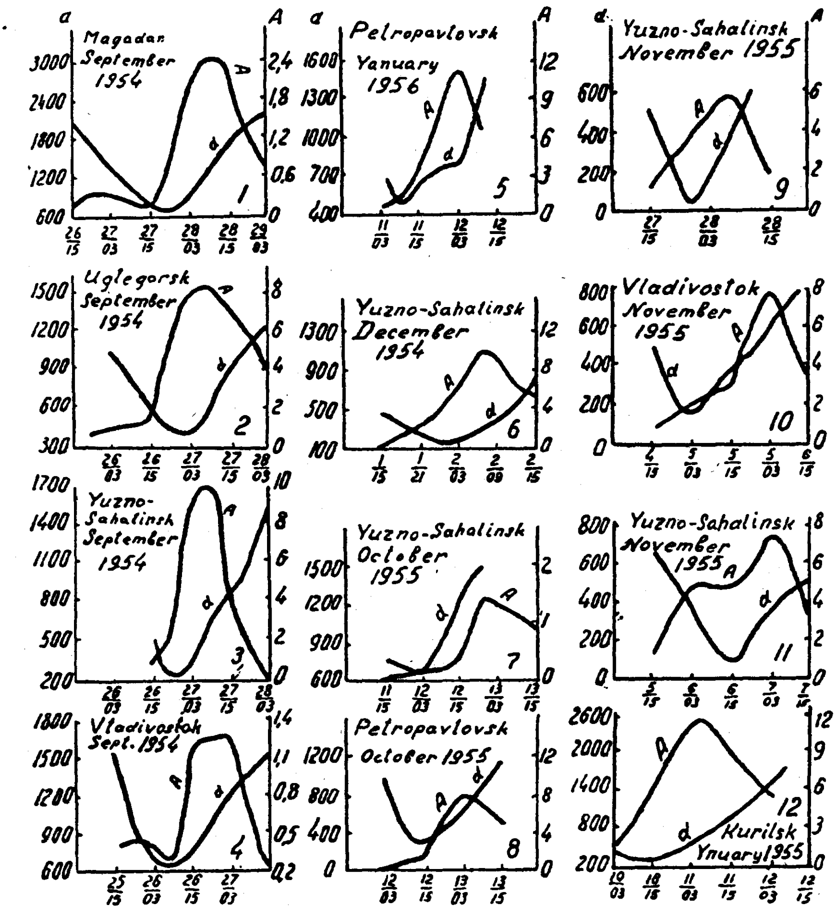

FIG. 10. — Graphs of maximum amplitudes of microseisms (A), distances between the station and the cyclone centre (d).

shows graphs of the microseisms amplitudes and distances between observation points and cyclone centres from observations of the Far East seismic stations. The diagrams show that the maximum amplitudes of microseisms are always observed a few hours later after the cyclone centre passes across the nearest point to the station. That means that the region of exciting maximum microseisms lags behind the cyclone centre. On fig. 11 there are trajec-

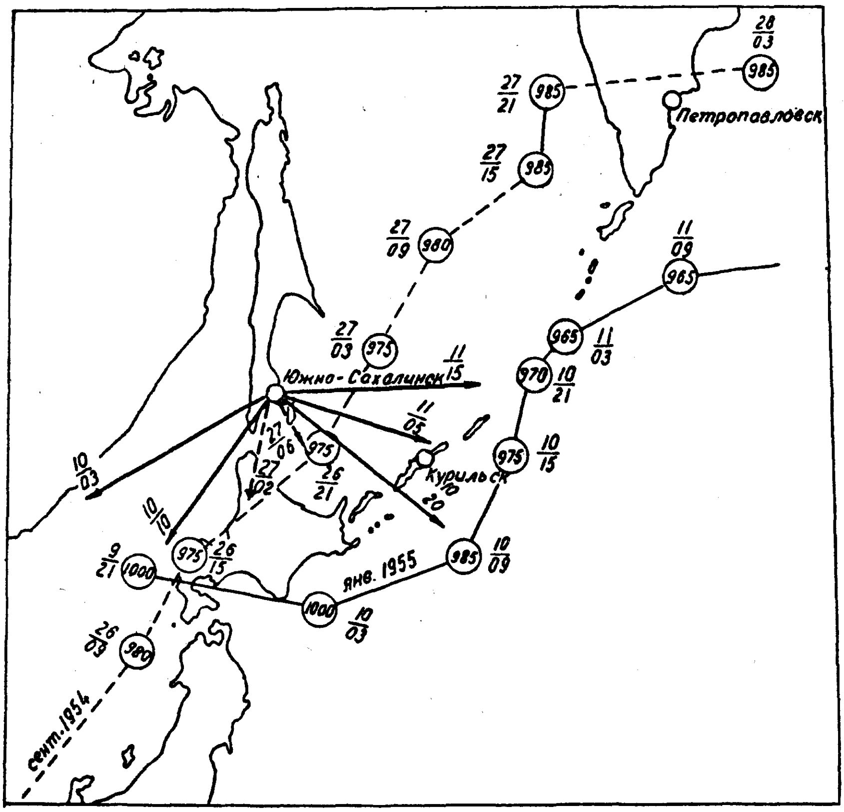

Fig. 11. — Trajectories of the cyclone motion and direction to the region of microseisms excitement from Yuzhno-Sakhalinsk.

tories of two cyclones for which the directions to the region of exciting microseisms have been determined for a few periods by observation data of the tripartite station. These directions are marked by arrows. The maximum amplitudes of microseisms at the Yuzhno-Sakhalinsk and Kurilsk stations during the motion of the cyclones centres along the trajectories sections between the crosses. The conclusion from these directions to the microseismic source is the same as from the diagrams in fig. 10.

The investigation of the microseisms observed in Yalta in the beginning of 1952 has evidenced that at the time of cold fronts passing across the Black Sea from the West to the East or from north-west to the southeast amplitudes of the microseisms reached their maximum a few hours after the cold front had passed by Yalta.

To make an accurate estimate of the method of the tripartite station it is necessary to know the exact directions of the waves propagation. In this respect one can use surface waves of earthquakes and cyclones to be found at considerable distances from the observation point. In many instances we managed to record the surface waves of earthquakes and determine the direction to the epicentres by phase transitions. Besides, the Yalta microseismic station made some determinations of the direction to the sources of the Atlantic microseisms which may be regarded as point sources due to their remoteness from the station. In all cases when definite requirements to the instruments were met the error of determining the directions did not exceed $\pm$ 10°.

The instruments were usually given such a regime under which phase shifts of the recorded waves were brought to the necessary minimum due to the deranging of the instrument parameters. This was chiefly achieved by the introduction of big dampings for pendulums and galvanometers.

The accuracy of the method of the tripartite station much depends on the distance between seismographs of the microseismic station. It is possible that an unsatisfactory result in determining the directions to cyclones from observations of some microseismic stations of the USA is due to small bases between the seimographs. Indeed, at bases of 500 m. the mean value of the phase shift is approximately 0.1 sec. The seismic equipment applied at present does not permit to determine the phase shifts with accuracy more than 0.05 sec. Consequently, at bases up to 500 m. the method of the tripartite station proves to reach very lower accuracy.

The above estimate of accuracy of the tripartite station refers to bases of 1.500-3.000 m. The further most effective increase accuracy of this method consists in the transition from three-point to multi-point stations in order to determine the phase shifts at distances between the seimographs more 3 km. The maximum distances at which it is possible to trace specific phases will be different in regions with different geological structure. For instance, in the Moscow region groups of microseisms are traced at distances of more than 70 km. whereas in the Crimea, between Yalta and Alushta, the correlation of groups is not possible at considerably less distances. In the region of Yuzhno-Sakhalinsk, on the Sakhalin Island, the form of oscillations in microseismic groups with the maximum amplitudes remains quite reliable at distance of 3 km; therefore the measurement of phase shifts in this region can be carried out at distances of more than 3 km. In the USSR the method of large bases is now developed further on.

In connection with the IGY five tripartite stations have been organised in the USSR : three in the East and two in the West of the country. The stations are equipped with the SVK seismographs tuned for the period of 7 sec. and with damping of about 1.5. M-21 galvanometers have the period of 4 sec. and damping about 1.5. The distance between the seismographs is from 2 to 3 km. The recording device admits a smooth regulation of the paper speed. We hope that these stations will make it possible to study the conditions of the microseisms excitement more thoroughly.

BIBLIOGRAPHY.

1. GUTENBERG (B.) : An investigation of microseisms. Pasadena, Calif., 1956.
2. GAMBURTZEV (G. A.), GALPERIN (E. I.) : Izvestia of the USSR Academy of Sciences, Geophysical series, 1954. n° 2.
3. GALPERIN (E. I.) : Azimuthal method of seismic observations. Moscow, Gostoptekhizdat, 1955.

A PROPOSED MECHANISM OF GENERATION OF MICROSEISMS

by S. N. NANDA.

ABSTRACT.

Microseisms produced at sea have been ascribed to various causes, namely, selection of suitable periods from a broad noise band by long oceanic paths, second order pressure effects of standing waves or pounding of surf on steep coast-line. But the observations may point to an all embracing cause involving winds, waves, and special orientation of winds either involving circular wind currents or such winds as will pile up or deplete water near a steep coast-line. Such changes of sea level will pulsate with the auto-correlative periods, if any, in eddy viscosity near the surface of the sea which in turn depends on sea roughness. If there happen to be standing waves, the roughness and, therefore, the eddy viscosity will have a period half that of waves, but in this process standing waves are not necessary for generation of microseisms. In many observed instances the prominent microseisms have less period than half of the period of prevailing sea waves.

While recording microseisms at Cochin Mr. H. M. Iyer of the Indian Naval Physical Laboratory made an interesting observation that during the period 22nd January to 25th January 1956 the microseisms were increasing in intensity from the early hours of the morning and then falling to background level towards afternoon. Eliminating all possible man-made or climatic causes in the neighbourhood, one is led to assign the origin of these microseisms to a hovering cyclone near distant Albatross island in the western Indian Ocean. During these four days a cyclone hovered between the land and the sea at islands to the North of Albatross Island, but on the fifth day it raced towards African coast and the microseisms also did not show any rise later on. Apart from this observation, one observes that microseisms are generated when generating storms are over the ocean, and generation is stopped when the generating storm reaches the land.

From other records at Cochin also, this was clearly visible, e. g., once in February 1956 when a storm starting from a point opposite Bombay, moved north-westwards and then sped over land west of Karachi. The microseisms which were clearly identified at Cochin as coming from North/North-West, vanished when the storm shifted over land. In addition there are instances where frontal disturbances caused microseims when they stepped from land on to the sea. There is, however, some correlation also that wherever waves can exist near steep coast, there is generation of microseisms and there are also many recorded exceptions to this. In addition the are instances of heavy winds over the sea correlating with microseisms. All these phenomena seem apparently to be unrelated, and sometimes it was stated (Nanda (1), that, perhaps, the structure of the earth being different in different places, different modes of origin of microseims may be witnessed in different regions. There is thus scope for some hypothesis which can explain origin of microseisms in all sorts of situations.

There have been two major attempts in recent years in this direction. One was by Press and Ewing (2) relying on the band pass characteristics of oceanic paths treating microseisms as just a noise signal due to disturbed sea at any particular place. The received signal at large distances was modified by the character of the intervening oceanic path and they explained that some of the observed periods were very prominent simply because the intervening path was more congenial to these periods. However, this theory does not throw much light on the mechanism of generation of microseisms at the point of disturbance in the ocean and does really explain why the disturbance must be on the water to give prominent microseims and why prominent periods are observed even when large oceanic paths are not involved.

The second attempt to explain microseisms was made by Longuet Higgins (3) where he used the concept of stationary waves. Though progressive waves will not affect sea bottom over an appreciable area, a standing wave pattern has got a periodic pounding effect on the sea-water, the period being half the period of the waves. This explains the relationship often found to hold approximately between the period of gravity waves and of microseisms. Recent advances in the field of gravity waves prohibit a simple picture of a prominent period in the sea-waves and it is hard to imagine standing waves of a particular period being present in order to generate microseisms. In addition the relationship between period of microseisms and the period of sea-waves is not verified sufficiently for being regarded as a proper justification for this theory. Many times the period of microseims is much less than half of the period of prominent gravity waves observed near the recording station or of waves generated by the storm held responsible. In addition the period of waves under a storm centre is quite hypothetical and has rarely been recorded. Formation of standing waves near a steep coast may be plausible, but microseisms are not invariably generated when waves are high near a steep coast.

The ideas given below are very tentative, theoretical basis being almost impossible to work out with the meagre data on waves and especially on waves under a storm centre. The mechanism of generation is proposed as follows.

Considering first the generation of microseisms under a cyclone, one has to remember that cyclone exists generally in a current of air and that current of air has already disturbed the ocean surface and made it rough. When the curved currents of air blow over the surface of the sea, they are apt to generate surface currents in sea-water at an inclined angle to the direction of the wind. But since the winds are circular, the surface currents are blocked by those generated by the opposite segments of the winds and this tends to raise the surface of water within the eye of the storm. Or the effect may just be an increase of stress over a wide surface under the eye of the storm. If the circular winds are in opposite sense, there will be depletion of water or decrease of stress and corresponding lowering of pressure on the sea bottom under the eye of the storm. The change in water level or change in wind stress will be governed by the roughness of the sea and the wind speed. Assuming the wind speed not to fluctuate, the change in sea level and, therefore, the change in pressure on the sea bottom is governed by the eddy viscosity at the surface of the sea. The cause of any pulsation in the change in pressure over sea bottom is to be found in the behaviour of the eddy viscosity. Unfortunately, there has been very little work on eddy viscosity. Eddy viscosity is known to depend on the roughness of the sea surface. The roughness in turn depends on the instantaneous picture of waves on the surface. If the instantaneous picture is random or composed of uniformly progressing waves, the roughness can be assumed to be uniform and the eddy viscosity will be a constant. It may, however, be guessed that over all eddy viscosity may have an auto-correlative period which is reflected in the variations of piling up of water or wind stress in the eye of the storm. If there happen to be standing waves, eddy viscosity will have a period half that of waves. In the absence of a cyclone, the same effect may be possible if the wind generated currents tend to pile up or deplete water near a coast-line. On this basis, both wind and waves are necessary for producing microseisms, and in addition either the storm should have an eye (circular wind currents) or the storm paths should be suitably oriented near a coast line.

For an empirical justification one may try to obtain a measure of the sea roughness at any place and then to see if this sea roughness has got some auto-correlative periods which approximate to the periods of prevailing microseisms at a nearby station. This can be attempted as follows. A number of pictures can be taken of the glitter over the sea surface by means of a movie camera held on a rigid support, for example, on a jetty projecting into then open sea. Each frame of these movie pictures is then held against a beam of light and the transmitted intensity is measured by means of, say, a photoelectric device. The measured intensity will give an estimate of the sea roughness. A curve can be drawn showing variation of this estimate of roughness with time. An auto-correlative analysis will then show if certain periods exist which correspond with the prevailing periods of microseisms.

The hypothesis is now being put forward for verification or consideration by other workers in this field. In order to explain the beat like structure observed usually in microseisms, one has at present either to think of microseisms to be coming from two distinct directions or coming from two sets of standing waves with slight difference in frequency. Moving source could also explain the beat like structure which is all right in case of travelling cyclonic storm. But the proposed mechanism will easily explain beat like structure in records both for generation by such storms as well as by waves and wind near shore, by the existence of more than one neighbouring frequencies in the periodgram analysis of the sea roughness.

The movie records as suggested above have not yet been completed. In the meanwhile an effort was made by K. Achyuthan at author's suggestion to study roughness of the sea by means of analysis of radar echoes from the sea surface. 10 cm. radar with « A » type scan was used and a small portion of the scan at about 2,000 yards range was photographed by means of a continuously moving film. The deflections on the radar screen corresponded roughly to an area of 200 ft. square calculated from the beam width and the un-blocked portion of range on the screen (at 2,000 yards). The film showed a complicated noise curve which was subjected to an autocorrelogram analysis. In the absence of a suitable computer, amplitudes at 0.4 second interval were read manually and simplified auto-correlogram of successive differences was attempted. Two prominent periods were found to be at 0.8 seconds and 4.8 seconds. There was slight indication of a period at 1.2 seconds. A simultaneous record of microseisms was also subjected to autocorrelogram analysis and a period of 1.5 seconds was observed. The prominent period of 1.5 seconds did not correspond with the period in the sea roughness as shown up by the radar echoes. But similar analysis must be carried out near a better microseismic station since our seismic records were insisting on 1.5-second period even though sometimes it was definite that the period should be higher. For example, a distant earthquake record also came out to be showing 1.5-second period. The microseismic pendulum is placed in the open (with a wooden cover) on an isolated concrete block about one foot thick sunk in soft ground at Willingdon Island at a site which has been retrieved artificially by dumping dredged silt from the sea. There is a strong indication that 1.5 second is a resonant period.

References.

1. Nanda : « A Review of Research on Microseisms » Defence Science Journal, Vol. 4, 19 (1954).
2. Press and Ewing : « A Theory of Microseisms with Geological Applications. » Trans. Amer. Geophysical Union, Vol. 29, 163-174 (1948).
3. Longuet-Higgins : « A Theory of The Origin of Microseisms ». Phil. Trans. Roy. Soc. Vol. 243, 1 (1950).

RELACION ATOMICA — NIOBIO-TANTALO — EN LA PROVINCIA DE LA CORUNA (ESPANA)

Por Juan Manuel LOPEZ DE AZCONA,
Instituto Geológico y Minero (Madrid).

RESUMEN.

Se han efectuado unos estudios detenidos de las reservas de niobio y tántalo de las zonas de Boiro y Noya, de la Provincia de La Coruña. Se ideó una técnica para las valoraciones espectroquímicas de estos elementos y dieron como resultado los valores siguientes : Zona de Boiro en 82 muestras. Relació atómica Nb/Ta = 14,7. Zona de Noya en 83 muestras. Relación atómica Nb/Ta = 11,6.

Durante los años 1955 y 1956 se efectuaron unos estudios detenidos de las reservas de minerales de niobio y tántalo de la Provincia de La Coruña. Como consecuencia de ellos, se puso en evidencia que de las seis zonas que años antes, habiamos descurbierto con formaciones de ambos metales en dicha provincia, las dos mas interesantes son la de Boiro por la riqueza en la concentración de ambos elementos y la de Noya por su extensión.

Los dos metales se presentan bajo la forma de niobitas con contenidos en uranio de hasta el 0,08 % que en algunas ocasiones tienen dimensiones de hasta un par de centímetros. La ubicacion es principalmente en los diques de pegmatitas encajados en los esquistos metamórficos antiguos (supuestos precambrianos) en su facies menos compacta y con preferencia en las inmediaciones de los contactos con las gneises y los granitos. En general dichas pegmatitas son complejas, además de las niobitas mencionadas, contienen casiterita, berilo, turmalina principalmente negra, espodumena, etc.

Las valoraciones de las relaciones atómicas se efectuaron por medio de una técnica espectral original nuestra (2) a partir de los pentaoxidos de ambos metales aislados quimicamente, con la cual se reduce todo lo posible la volatilización fraccionada durante la excitación por arco, de elementos con puntos de ebullición tan diferentes como el niobio y el tántolo que los tienen a 2.900 y 4.000 grados. La técnica que utilizamos consiste en confeccionar una mezcla deflagrante, que se utiliza para todas las muestras, formada a terceras partes en peso de carbón pulverizado puro, cinc y clorato potásico. Una vez homogeneizada la mezcla, se hace un nuevo preparado a base de tres partes de esta mezcla en peso, y una de pentaoxidos.

Para efectuar el análisis se utilizan para esta valoración 0,030 g. de la mezcla ultima que corresponde a 0,0075 g. de pentaoxidos, los cuales se depositan en el cráter practicado en un electrodo de grafito (no hace falta que sea puro) exento de niobio y tántalo que es el inferior y de polaridad positiva. Le excitación utilizada de arco, lo es con corriente contínua a 110 V y 15 A., este circuito tiene montado en paralelo otro de alta frecuencia para el cebado automático y mantenimiento de la excitación mientras dure la nuestra, que suele ser unos cinco segundos.

Efectuamos las valoraciones con la línea de N*b*-3116, 365 A° y la de Ta.-3115,859 A°.

Para el estudio de la relación atómica se seleccionaron 82 muestras de la zona de Boiro y 83 de la de Noya, procurando en todo momento que tuviesen la menor contaminación posible. De unas y otras se efectuaron los correspondientes análisis espectroquímicos.

Las muestras de Boiro dieron como valores extremos 6,6 y 24,7, para la relación atómica N*b*/Ta, con un valor medio de las 82 de 14,7. Los valores extremos de las muestras de Noya fueron 8,6 y 26,4 con une media de relación atómica de 11,6.

Si comparemos estas relaciones con las de otros investigadores como hacemos en el cuadro adjunto, se llega a la conclusión de que los valores que deducimos ahora tienden hacia los que habia fijado Goldschmidt en 1937, o sea a un aumento de la relación con respecto a los valores mas modernos.

AUTOR	AÑO	Atomos Si = 10^6		Relación atómica $\frac{Nb}{Ta}$
		N*b*	T*a*	
Goldschmidt. . . .	1937	6,9	0,40	17,2
Rankama.	1948	26,0	1,20	21,6
Brown.	1949	0,9	0,31	2,9
Urey.	1954	0,8	0,32	2,5
Suess y Urey. . . .	1956	1,00	0,065	15,4
L. de Azcona . .	1955	Zona de Boiro		14,7
L. de Azcona . .	1956	Zona de Noya		11,6

RÉFÉRENCES

(1) BROWN (H. S.). (1949) : A Table of Relative Abundances of Nuclear Species. Rev. of Mod. Phys., XXI, p. 625 á 34.

(2) COMBA (A.) : López de Azcona (J. M.) (1956). Investigación de niobio y Tántalo en la segunda zona reservada de la provincia de La Coruña. Not y Com. del Instituto Geológico y Minero de España, nº 43; ps. 135 a 162.
(3) GOLDSCHMIDT (V. M.) (1937) : Geochemische Verteilungsgesetz der Elemente. IX. Die Mengenverhältnisse der Elemente und der Atom. Arten. — Skrifter Norske Videnskape — Akad. Oslo, I Mat.-natury. Klasse, M. 4.
(4) RANKMA (K.) (1948) : On the geochemistry of niobium. Ann. Acad. Sci. Fennicæ, S. III.
(5) SUESS, HANS (E.), UREY (Y.), HAROLD (C.). (1956) : Abundances of the elements. — Rev. of Mod. Phys. — XXVIII, p. 53 à 74.
(6) UREY (H. C.) (1954) : Estos datos revisados se publicaron en el (5).

RESULTS OF SEISMIC INVESTIGATIONS IN THE USSR

E. F. SAVARENSKY

The results of the work performed by seismologists of the USSR Academy of Sciences and academies of sciences of the Union republics are collected in a Seismicity Atlas of the USSR. This Atlas is based on the conclusions from the observations made by the USSR seismic stations during more than forty years [1].

An essentially new element of the Atlas maps is a uniform principle of dividing earthquakes in their magnitude and accuracy of determining epicentres.

The aim of the work is to compile uniform materials necessary in solving the following basic problems :

1. The study of the causes and conditions of earthquakes occurence.

2. The precising of the map of the USSR seismic intensity.

One of the efficient methods in studying the causes and conditions of earthquake occurence and elucidating the causes of tectonic processes is the correlation of the locations of geological and geomorphological elements and epicentres. Account being taken of the earthquake magnitude. One more important factor here is the analasys of a territorial distribution of earthquake magnitudes which enables to evaluate the field of potential energy of tectonic stresses.

The value of the Atlas in precising the schemes of the USSR seismic regions is that the knowledge of magnitude and a relative energy of earthquakes as well as of the focal depth makes it possible to objectively estimate a relative energy flux to the surface of a medium possessing mechanical properties of the Earth's crust. Such a division into intensity regions provided that proper corrections by geological and local ground conditions are made, will be more reliable than the former.

There are five main intensity groups of earthquakes :

Single, extremely strong, catastrophic under the USSR conditions, earthquakes ($M > 7\ 1/4$) are attributed to the first group.

The second group comprises earthquakes which caused or could be accompanied by serious destructions at a large space ($7\ 1/4 \geqslant$

Explication to fig. 1-7.

Intensity groups and Magnitude

7 1/2 ⩽ M , I group

6 1/2 ⩽ M < 7 1/2, II —

5 1/4 ⩽ M < 6 1/2, III —

4 1/4 ⩽ M < 5 1/4, IV —

M < 4 1/4, V —

Errors and epicentres accuracy classes

error < 25 km, class A

— < 50 km, — B

— > 50 km

error may be more than 2°, doubtful determination

figures denote the noninstrumental epicentre

Depth of focus

inside earth crust

under — —

below 300 km (for map of Pacific Zone)

Seismological stations

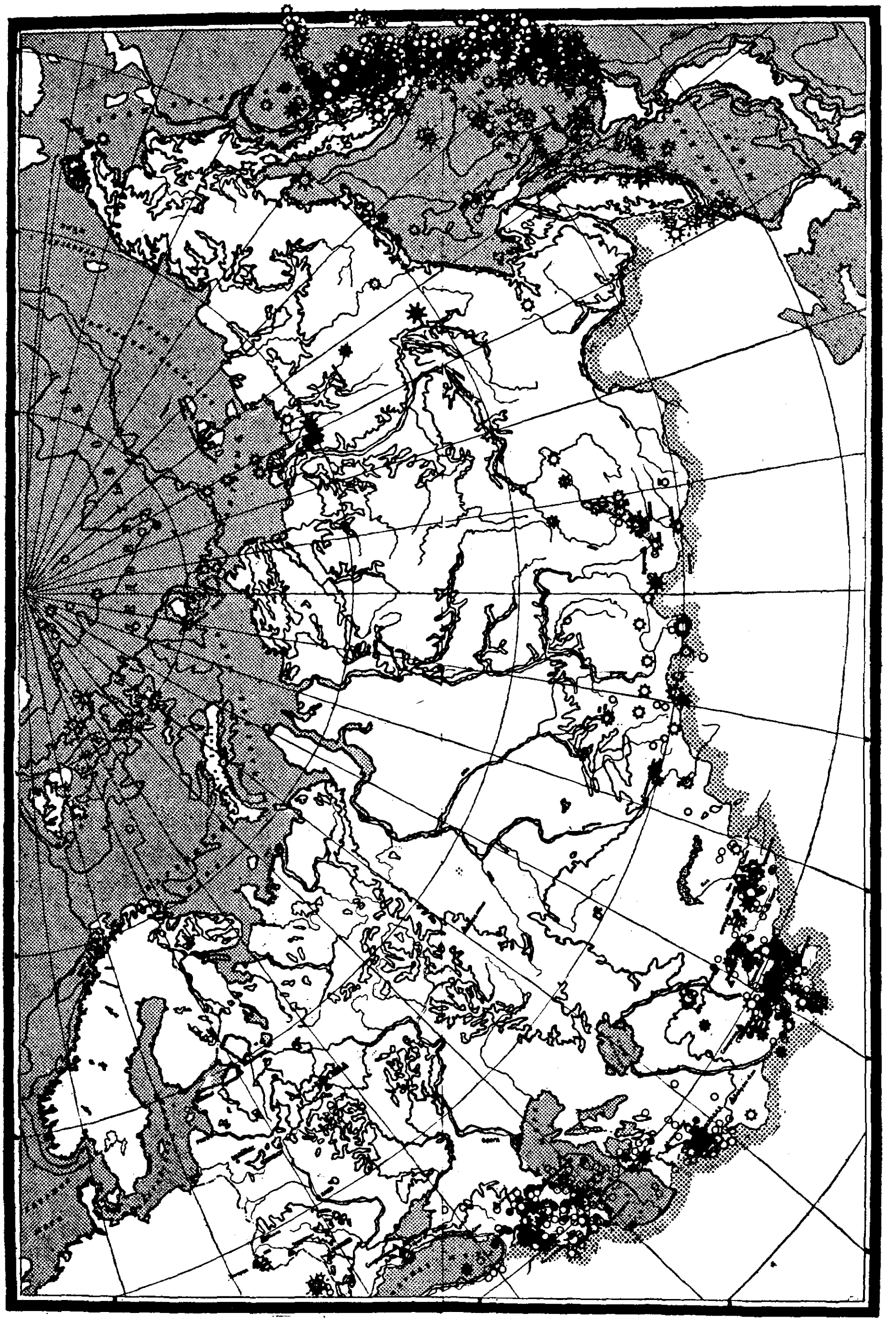

FIG. 1.

M > 6 1/2. If the focus would be in the Earth's crust, earthquake intensity reached 8-9 degrees).

The third group comprises earthquakes which caused or can an cause destructions and damages of buildings (6 1/2 ⩾ M > 5 1/4. With the focus being in the Earth's crust their intensity reached about 7 degrees).

These earthquake groups are of practical value. Deepfocus earthquakes of the same magnitude cannot be always accompanied by destructions.

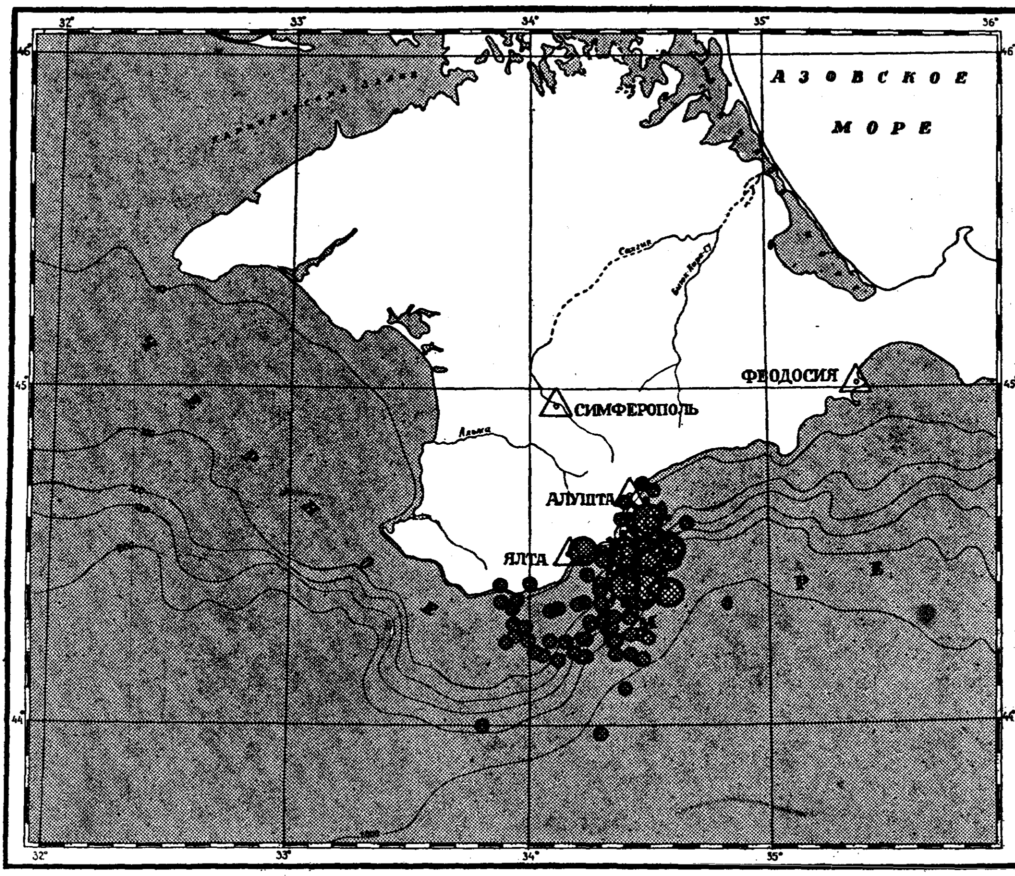

FIG. 2.

The rest two groups, fourth and fifth, embrace, as a rule, non-destructive earthquakes (4 1/4 ⩽ M ⩽ 5 1/4,M ⩽ 4).

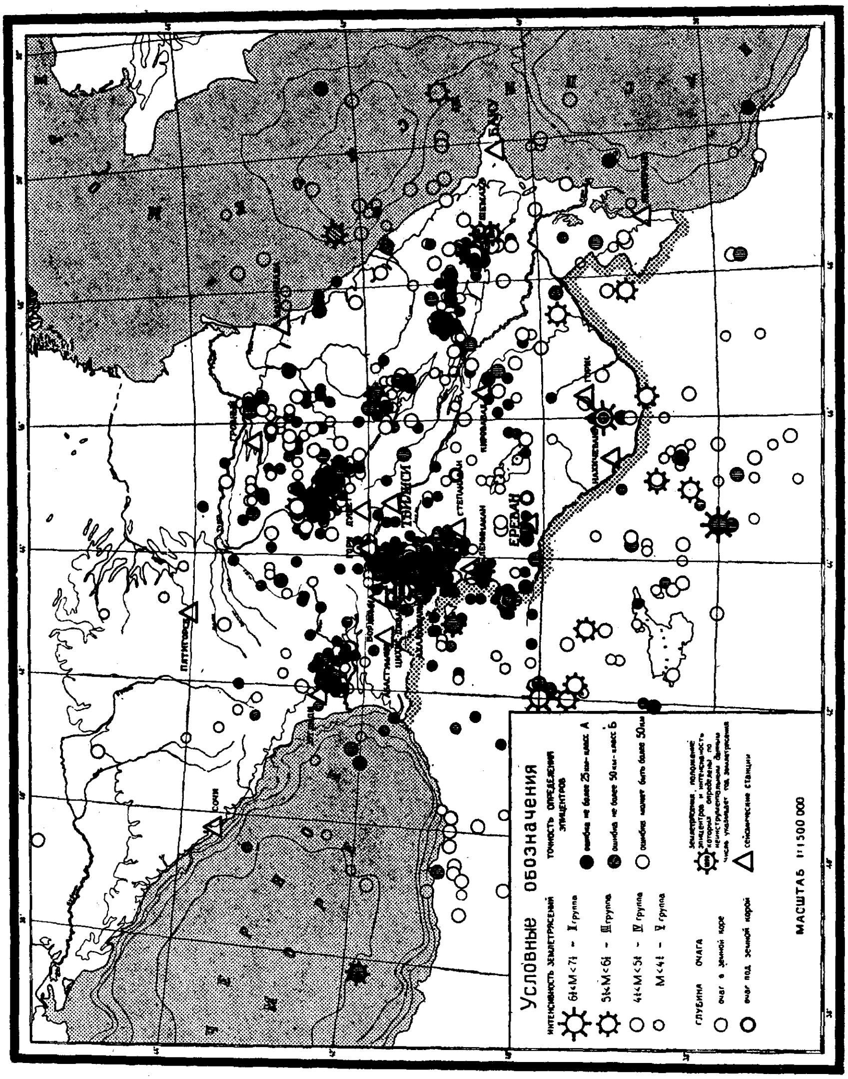

Fig. 3.

The distribution of earthquakes into these groups was made with allowance for the maximum distance in recording earthquakes. Data on weak earthquakes enable to establish genetic relations between strong and weak earthquakes, in particular, to determine the dependence between the earthquake frequency and magnitude.

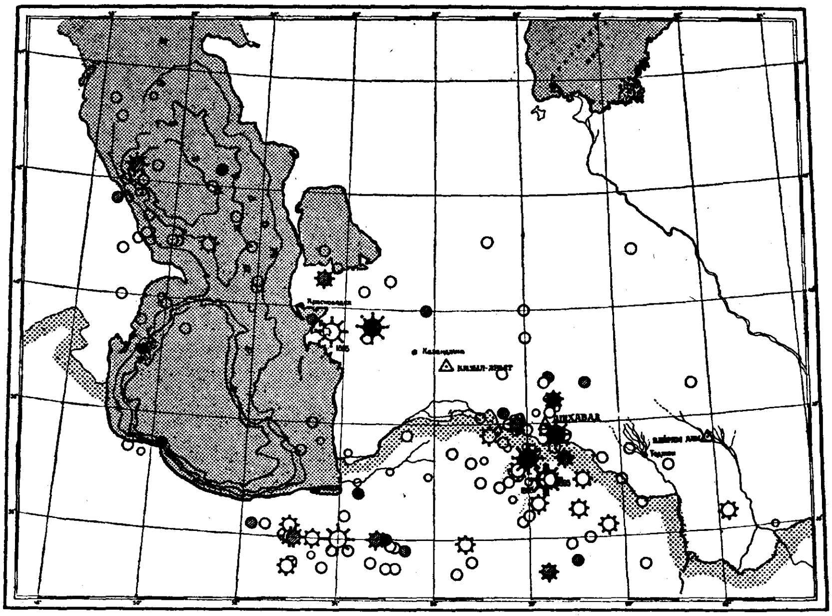

FIG. 4.

Epicentres were classified according to the accuracy of their determination. The first accuracy class (A) comprised epicentres with a possible error in determining the locations not more than 25 km., which was possible if observations were made by the stations next to the epicentres. The second class (B) admitted the error less than 50 km. If the error was not determined the epicentres were considered to be non-class.

In a focal depth earthquakes are divided into those inside the crust earth and under the crust. The latter requires the indication of a focal depth.

Atlas of seismicity contains catalogues and maps of seismicity zones of the USSR :

1. Map of seismicity of USSR.
2. Carpathian Mts.
3. The Crimea.
4. The Caucasis.
5. Copet-Dag.
6. Middle Asia.
7. Altai.
8. The Lake of Baikal.
9. The Far East.
10. The Arctic.

Maps of the atlas are not yet ready, but some examples of the analogous maps are shown in the fig. 1-7, [2], [3], [4], [5], [6], [7], [8], [9].

In total maps of seismicity of USSR include about 10,000 epicentres.

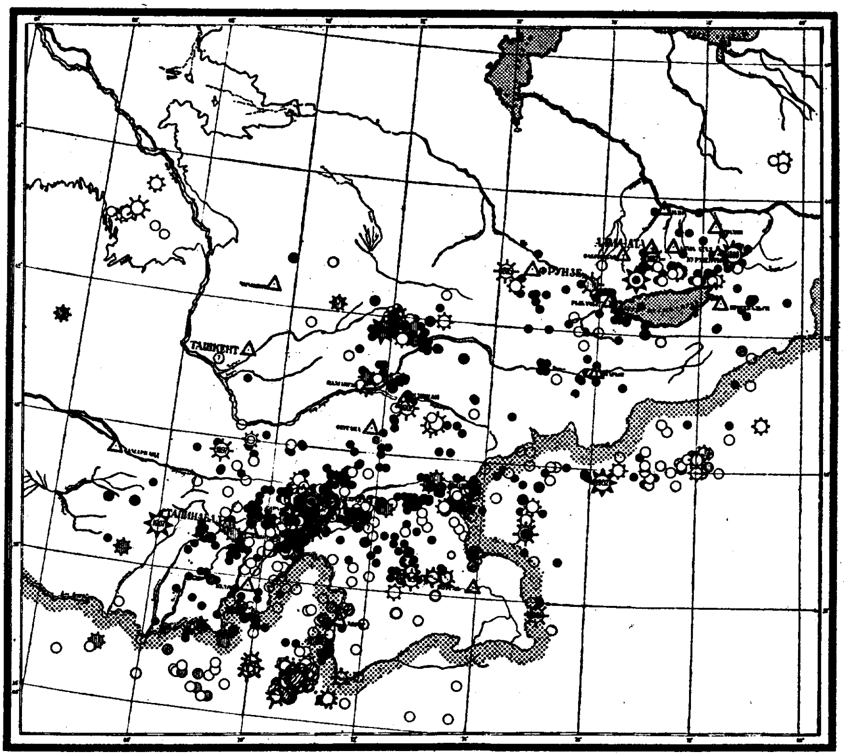

FIG. 5.

It must be noted that there is irregularity in presenting seismicity in time. This refers mostly to weak earthquakes. A gradual increase in their number and frequency is accounted for by an increase of quantity of seismic stations, and increase in sensitivity of instruments.

Investigations have shown that equal seismicity data for the USSR territory can be obtained only by the use of earthquake epicentres with M > 5.

During recent years permanent and temporary seismic stations of high accuracy and equipped with very sensitive instruments have been at work to find the causes of destructive earthquakes in the pleistoseist regions of the strongest earthquakes.

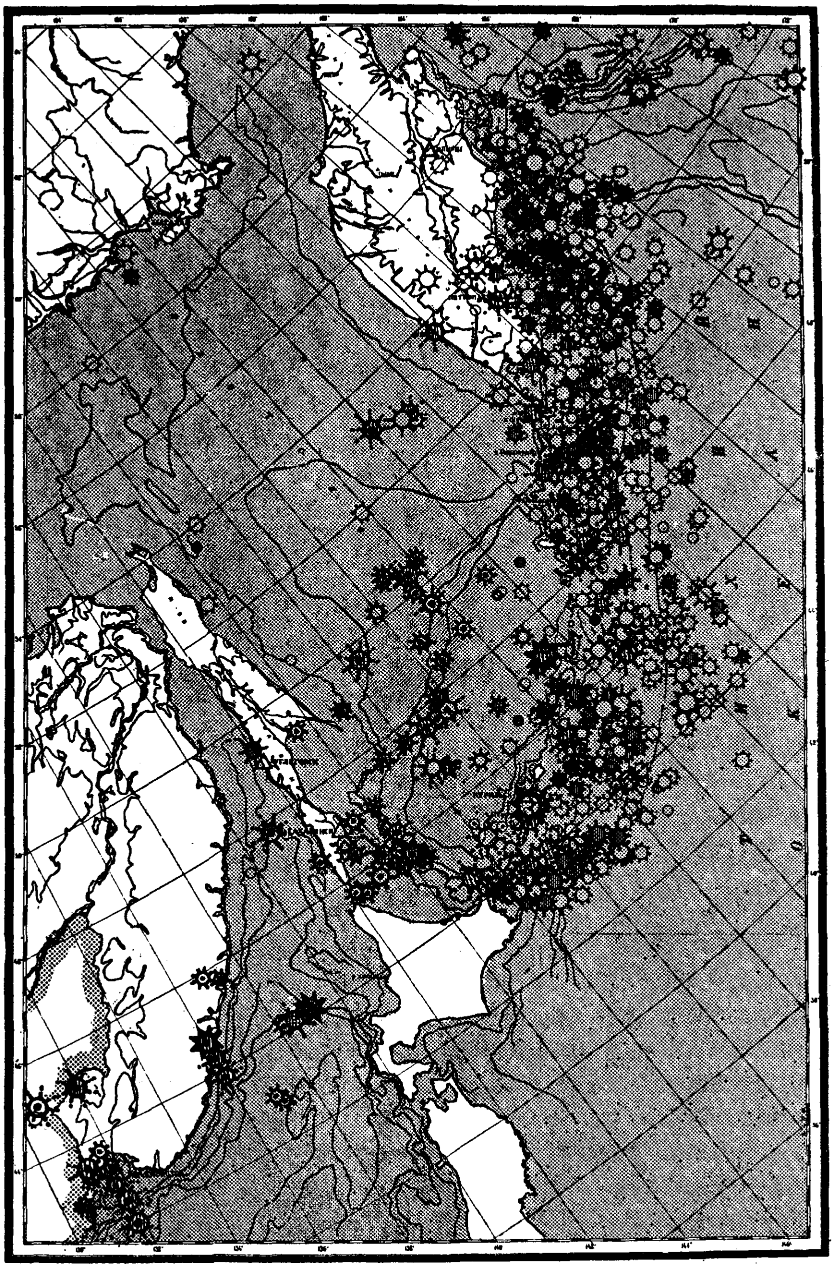

FIG. 6.

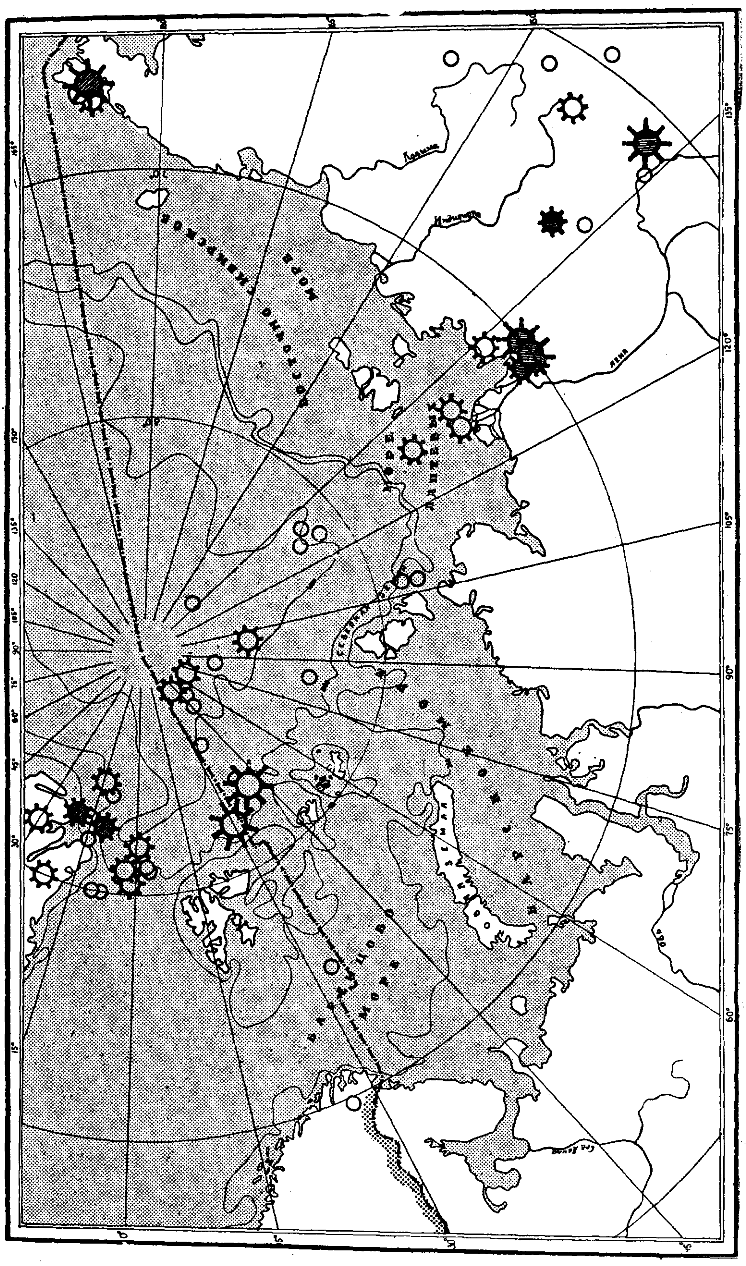

FIG. 7.

This served as the material for compiling additional, more detailed maps of such regions. Maps were compiled for :

1. The Akhalkalakskoye Nagorie.
2. Shemakha region.
3. Ashkhabad region.
4. Western Copet-Dag region.
5. Northern Tien-Shan region.
6. Garm region.

References.

1. Savarensky (E. F.). On the investigation of the seismicity of the USSR. Bull. Seism. Council Akad. Sci. USSR, n° 6, 1957, p. 16.
2. Soloviev (S. L.). Bull. Seism. Council. Akad. Sci. USSR, n° 6, 1957, p. 109.
3. Savarensky (E. F.). Izvestia Acad. Sci. USSR. Ser. Geophys., n° 7, 1956, p. 745-754.
4. Savarensky (E. F.), Linden (N. A.) and Masarsky (S. I.). Izvestia Acad. Sci. USSR, Ser. Geophys., n° 1, 1953, p. 3-16.
5. Savarensky (E. F.). Vestnik Acad. Sci. USSR, n° 5, 1955.
6. Savarensky (E. F.). Vestnik Acad. Sci. USSR, n° 12, 1950.
7. Vedenskaja (N. A.). Izvestia Acad. Sci. USSR, Ser. Geophys., n° 6, 1954, p. 497-514.
8. Savarensky (E. F.) and others. Bull. Seism. Council Acad. Sci. USSR, n° 4, 1958.
9. Savarensky (E. F.). Vestnik Acad. Sci. USSR, n° 6, 1956, p. 78.

ANALYSIS OF EARTHQUAKE INTENSITY DISTRIBUTION MAPS

By Frank NEUMANN.

Several years ago the author made a study of the more important strong motion seismograph records of the U. S. Coast and Geodetic Survey in an effort to correlate instrumentally recorded ground vibrations with earthquake intensity. The results ultimately appeared in a booklet entitled « Earthquake Intensity and Related Ground Motion » published by the University of Washington Press. It is proposed here to present some additional evidence supporting these earlier findings and elaborate somewhat on their use in obtaining more accurate epicenters and further evidence on subterranean structure. The use of instrumental data in explaining the complex nature of intensity phenomena will also be discussed.

One of the more important findings is illustrated in Fig. 1 which

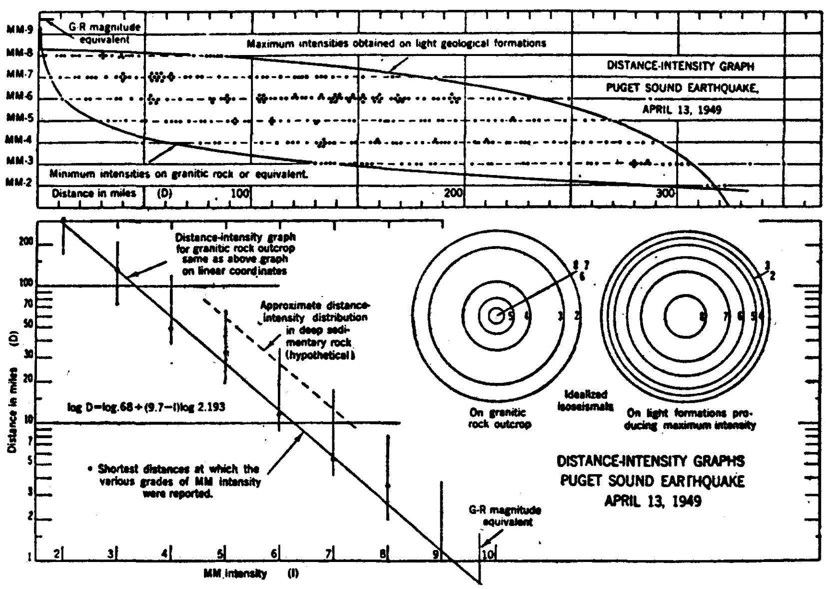

FIG. 1.

shows, in the case of the Puget Sound Earthquake of 1949, the intensity plotted against epicentral distance. The important feature of this illustration is the lower curve or envelope that shows the lowest intensity that can be recorded at any epicentral distance, at least in the Puget Sound area. The places recording these low intensities are considered to be located on or very close to outcrops of basement rock although it is conceivable that other well consolidated formations may react in a similar way to earthquake vibrations. This so-called basement rock intensity attenuation curve was found to be not only exponential in form but similar curves with similar attenuation were found in all earthquakes studied to date. The attenuation is of such form that each time the epicentral distance is doubled, the intensity drops one grade on the Modified Mercalli Intensity Scale of 1931.

The empirical rule thus established is now used to determine epicenters of all Washington earthquakes that are widely felt and well canvassed for descriptive reports. As there is a minimum epicentral distance at which each grade of the intensity scale is found in a given earthquake, and these distances define circles about the epicenter the first problem in analyzing an intensity map is to define the outer circle that represents the minimum distance at which Grade III is found. Since Grade III is sometimes reported as not felt, the zero intensities plotted on the map are also used to locate this circle. In practice a pair of dividers is swung around a number of trial positions in the general epicentral area, using various radii, until a circle can be drawn that excludes all zero and Grade III intensities and includes only intensities of Grade IV and over. This circle is then drawn on a piece of tracing paper and other concentric circles are described with radii equal to one-half, one-quarter, one-eighth, one-sixteenth, etc., the radius of the outer circle. This complies with the attenuation characteristic found in the 1949 Puget Sound shock and in other shocks. It is found that, with some adjustment, the data will fall, with only rare exceptions, within the rings they are expected to. The outside ring will contain only IV's and over, the next inner only V's and over, etc., etc. When zeros occasionally appear in such rings, the original reports show, in the vast majority of cases, that they represent the experience of an individual and not the experience of a community. The center of the circle is a so called « maximum intensity epicenter ».

Fig. 2 shows this technique applied to a Washington earthquake that occurred in 1955. The focus was exceptionally shallow. It will be seen that the intensity epicenter lies only about two miles from the instrumental epicenter.

A 1954 disturbance, Fig. 3, was very unusual in that there were two foci 50 miles apart. The first, near Bremerton, was located from instrumental data; the other and major one was located from inten-

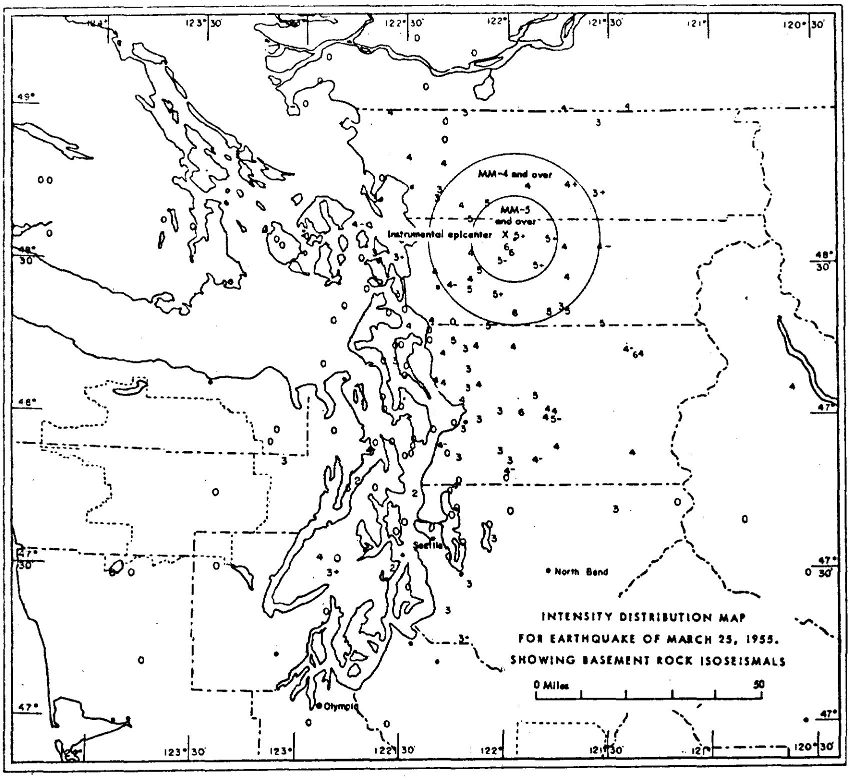

FIG. 2.

sity data exclusively. The Long Beach earthquake of 1933 was a similar type of disturbance because the instrumental epicenter, which undoubtedly always represents the first rupture along a fault, differed from the maximum intensity epicenter and site of the major fault break by 16 miles. Two years after the Washington earthquake of 1954 a University of Washington graduate student, working in his thesis area near the « maximum intensity epicenter » high in the Cascade Mountains, reported the discovery of a major fault within two or three miles of this epicenter. This solution has special significance in that little or no descriptive information was available over a great portion of the epicentral area.

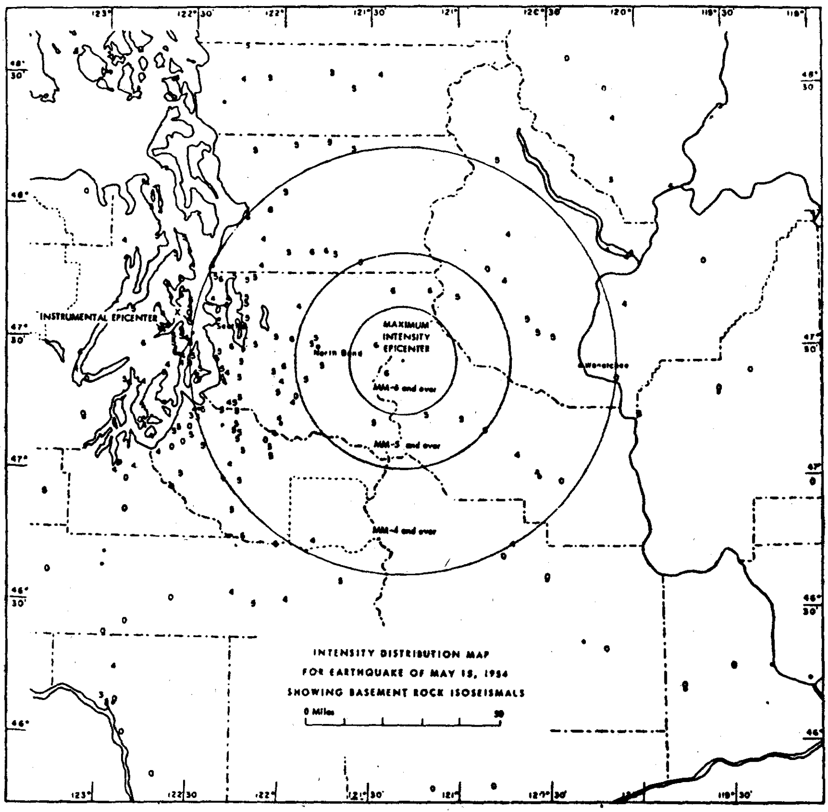

Fig. 3.

Fig. 4, showing a 1957 shock in Washington, is a typical solution of a weak type of shock and one having a deep focus as determined from instrumental data. It is only partially amenable to the rule of basement rock intensity attenuation. It differs from the smaller shock, Fig. 2, in that the focus is 60 km. deep, instead of being shallow, and no intensity exceeds Grade V. An outer ring that excludes all Grade III's can be drawn, but the inner circle which should contain only V's also contains a few IV's. This is typical of weak shocks and as they get still weaker « zeros » (not felt) begin appearing in the epicentral region and the technique can no longer be used.

In this relatively deep shock it seems almost phenomenal that an intensity epicenter can be found that is only about five miles from the instrumental epicenter when the focus is nearly 40 miles deep. This applies also to many other deep shocks in the Puget Sound area. As foci of this order of depth do not seem to materially influence the over-all pattern of intensity distribution, it would appear that the energy at the focus funnels mostly upward along a path of least resistance instead of radiating uniformly about the focus as postulated in various efforts to determine focal depth from the pattern of intensity distribution.

While the State of Washington offers no particular difficulty in pursuing intensity studies of this kind, except for obtaining questionnaire data in sparsely settled mountain areas, other regions may encounter difficulties. Fig. 5, for instance, shows the basement

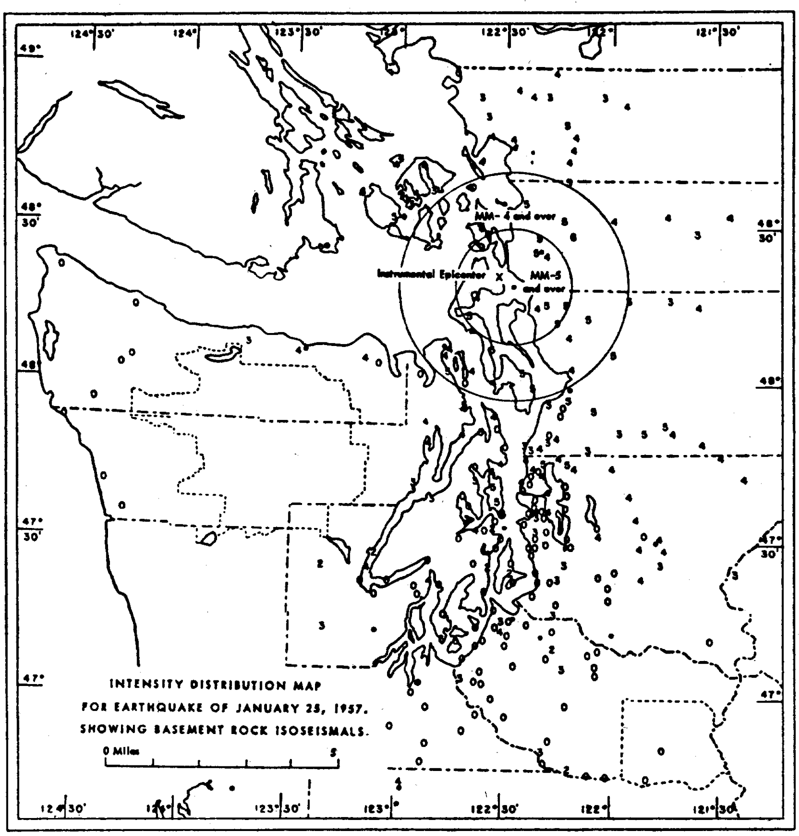

FIG. 4.

rock intensity curve for the Imperial Valley earthquake of 1940. Up to 100 miles epicentral distance the distribution follows a normal pattern, but beyond that, at certain places it definitely drops a whole grade. Since Imperial Valley is in a region designated on tectonic maps as sedimentary, it appears that the sedimentary rock area experiences intensities one grade higher than areas in which a granitic basement is a dominant feature of the near-surface geo-

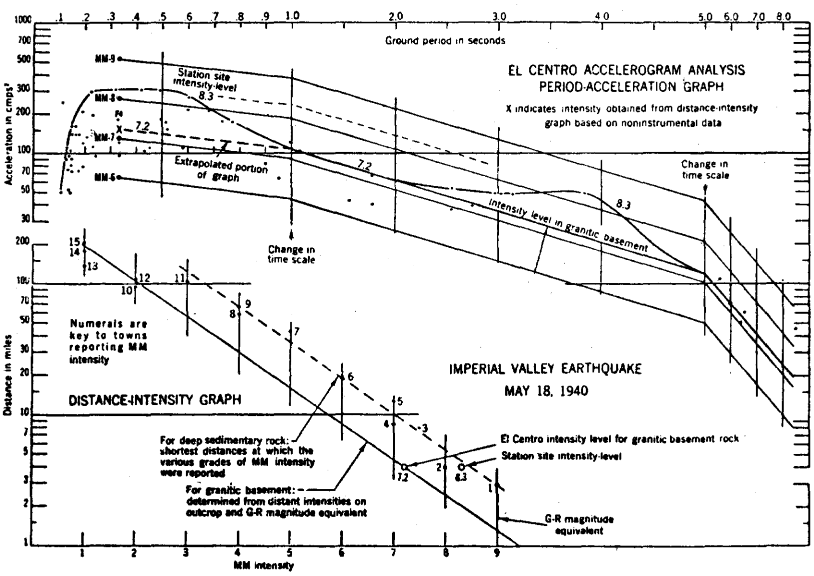

FIG. 5.

logy. Whether or not intensity data can be employed in this way to outline the broader features of basement structures is a question that only further investigation can answer, but it would definitely seem to serve a role of providing contributing evidence.

In some regions like Japan the land area is too limited for studies of this kind, and if there are also complex tectonic features, as in parts of California, such studies may not yield encouraging results. If they do not appear feasible because of inadequate areal coverage, it may still be possible to obtain correlations between intensity and basement rock structure on a piecemeal basis, especially where the tectonic features are well understood. When great land areas have been shaken by destructive shocks anywhere in the world, intensity studies could conceivably lead to new information about the border features of regional tectonics and about epicenter locations, especially when multiple fault breaks have occurred.

Turning to another aspect of intensity analyses, it would seem a simple matter to determine an intensity anomaly for any town or place reporting intensity if the basement rock intensity over the entire shaken area were known as now seems possible. Fig. 1 shows that an increase between four and five grades of intensity could be quite common. No thorough study has yet been made of intensity anomaly patterns, but if results were obtained from a large number of earthquakes there is reason to believe that they would be of real value in determining so-called foundation factors for use by engineers in evaluating earthquake risk and estimating probable earthquake forces on structures. On the basis of instrumental information obtained on different types of soils and rocks (to be discussed further) one could hardly expect the observed anomaly at a given site to repeat itself in different earthquakes because different frequency and amplitude patterns would be imposed on the site. One could not expect geological structures to be any more consistent in their response to complex earthquake motions than engineering structures such as buildings and bridges. It is felt, therefore, that valuable engineering information could be accumulated if records were kept of the intensity anomalies observed at sites and areas of special interest. The highest anomalies would then be expected to represent the maximum susceptibility of a particular site to earthquake vibrations at least as far the record of past earthquakes revealed it.

In order to better understand the nature of intensity anomalies, that is, the increase of vibrational intensity over and above the intensity in adjoining or underlying basement rock, one can examine relevant instrumental data to great advantage. What, for instance, does an increase of four grades of Intensity on the Modified Mercalli Scale mean in terms of actual ground motion? One of the findings in the earlier investigation was that in the central areas of strong shocks a one-grade increase corresponded to a doubling of the acceleration. If this holds true throughout an entire shaken area, as it probably does, an increase of four grades would mean a 16-fold increase in the ground acceleration over that in nearby basement rock. As the actual range is greater than four, amplification factors even higher than this might be expected in widely shaken areas.

In a study of the instrumental records of light shocks in a restricted area of southern California, Gutenberg recently (1957) reported that alluvium-to-rock amplitude ratios may be as great as 10, and estimated (1956) that at some strong motion seismograph stations of the Coast and Geodetic Survey the factor was as high as 8. Some years ago the U. S. Coast and Geodetic Survey actually decreased the sensitivity of certain accelerometer installations to accommodate the greater amplitudes consistently being registered on alluvial formations and on the top floors of tall buildings. In view of the limitations placed on the number of instruments available to obtain quantitative data of this kind, it is believed that the higher values based on practically unlimited numbers of intensity reports are more representative of the maximum amplification factors possible. The higher figures, too, are supported by results obtained in investigations of quarry blasts, and by engineers' estimates of the relative violence of ground motion required to cause the degrees of damage observed on various types of soils and rocks.

Fig. 6 shows the strong motion seismograph records obtained at the time of a damaging earthquake in Los Angeles on October 2,

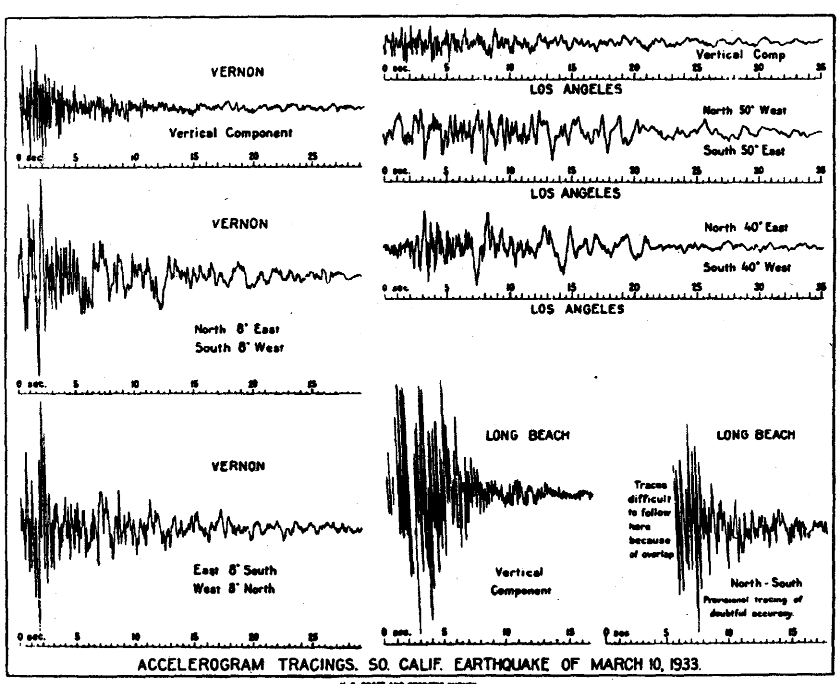

FIG. 6.

1933. The Subway Terminal and Vernon records, obtained at roughly similar epicentral distances, show the same over-all pattern and amplitudes except that when the period at Vernon is 0.7 sec. the amplitude suddenly triples over that registered at the same time in the Subway Terminal Building. The Vernon instrument is on the banks of the Los Angeles River. This is typical of the nature of the increase in ground motion registered when river alluviums are subjected to earthquake vibrations.

The nature of this phenomenon is shown in better detail if period acceleration graphs are constructed for acceleration records of strong shocks as illustrated in Fig. 7. This graph, covering the

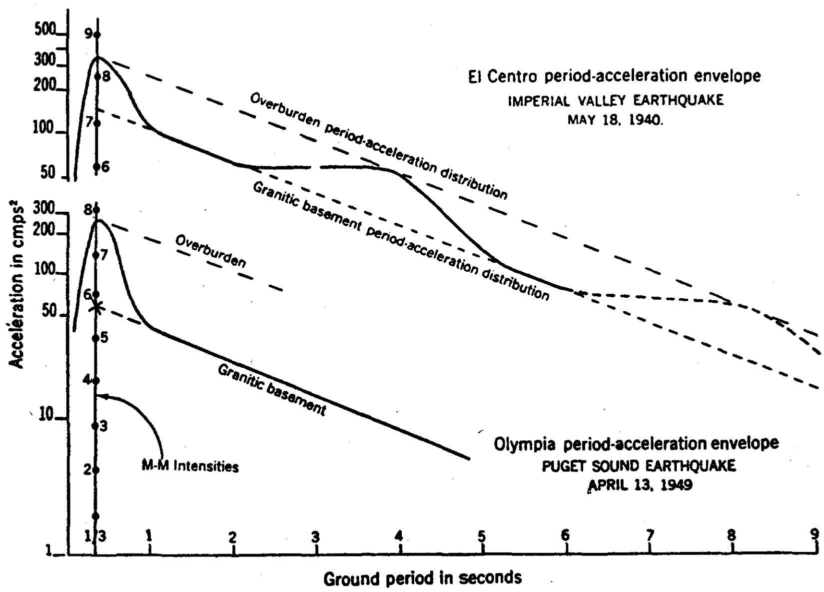

FIG. 7.

Imperial Valley shock of 1940, shows that in certain period zones the acceleration rises to a crest and then subsides to a minimum, or, in the case of many records, certain periods are not registered at all. This pattern of peaks and troughs is different in every record thus far analyzed in this manner. It is undoubtedly a function of local geologic structure, and much more needs to be learned about the various factors that control it.

It was shown in the investigation previously mentioned that the crests and troughs have important significance with respect to intensity. In many records, especially those obtained at the shorter epicentral distances, it is shown that the troughs can be correlated with basement rock intensity, and the peaks with the surface intensity observed at the station site. There thus develops the possibility that intensity may ultimately be measurable in terms of instrumentally recorded ground motion, but work still needs to be done before this technique is fully developed. This means that period-acceleration curves need to be determined for all important earthquake records. It is the writer's experience that they can be developed in sufficient detail only if acceleration records are integrated at least one time. The resulting velocity curve reveals a greater number of clear-cut wave frequencies than either an acceleration or a displacement record, or both of them together.

In conclusion it is felt that earthquake intensity data can be put to much more productive use than they have been in the past especially after their true relation to ground motion has been more thoroughly established. Progress has been made in correlating intensity with acceleration within a limited epicentral area, and more recent studies have indicated that a broader interpretation may correlate intensity with energy, not necessarily the energy of the ground motion, but the energy represented in maximum building motions. Intensity by definition is measured by the effect of an earthquake disturbance on people and things, including buildings, and not on ground motion alone.

While some of these relationships are still in a formative stage, it is clear that the important thing to be done now to advance research in this field is to improve the efficiency of our earthquake information services, especially questionnaire programs. It would seem that the time is ripe for a re-evaluation of the effectiveness of our questionnaire forms. The time also seems overdue for a broad-scale statistical analysis of our questionnaire card and the results being obtained with it; and to correct any inconsistencies that such an analysis might reveal. If this is done, it is felt that future intensity investigations may be considered comparable in potential importance with instrumental investigations.

References.

Neumann (F.) (1954). *Earthquake Intensity and Related Ground Motion,* University of Washington Press, Seattle, Washington.

Gutenberg (B.) (1957). *Effects of Ground on Earthquake Motion,* Bulletin, Seismological Society of America, Vol. 47, pp. 221-250.

— (1956). *Effects of Ground on Shaking in Earthquakes,* Trans. American Geophysical Union, Vol. 37, No. 6, pp. 757-760.

ABNORMAL DISTRIBUTION OF SEISMIC INTENSITY OBSERVED IN JAPAN

by Kiyoo WADATI, Takuzo HIRONO.

1. Introduction.

In 1918, a pretty strong shock was felt by human bodies in the zone along the Pacific Coast of north Japan. There were already 38 seismological stations in Japan then. According to Mr. K. Hasegawa's investigation in the records obtained at these stations, the epicenter of this earthquake was located in the Japan Sea, opposite direction to the Pacific. Strange as it may seem, the shocks were not felt along the Japan Sea side which is closer to the epicenter. (*Fig.* 1). Since then, such phenomenon has frequently been obser-

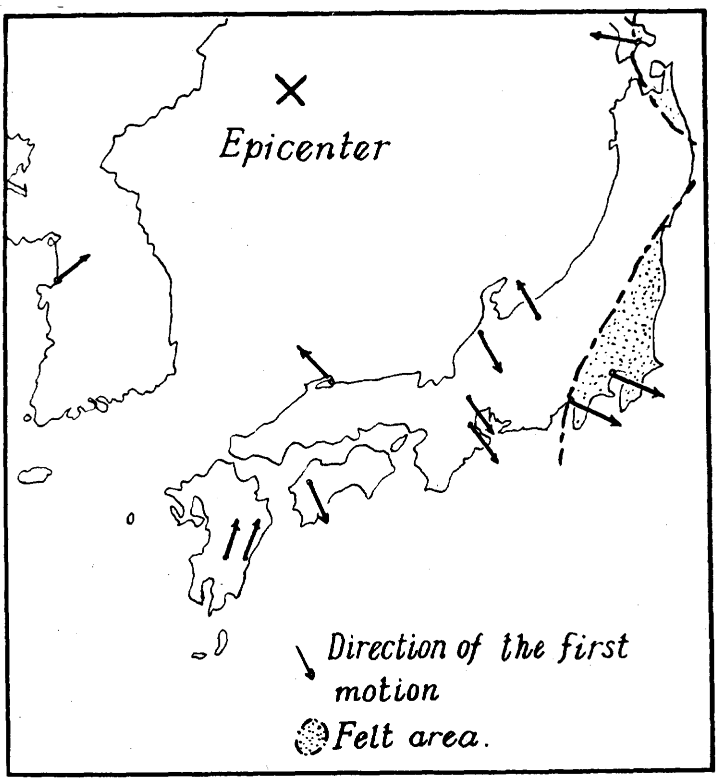

Fig. 1. — « Area of abnormal perceptibility » reported by Mr. Hasegawa in 1918.

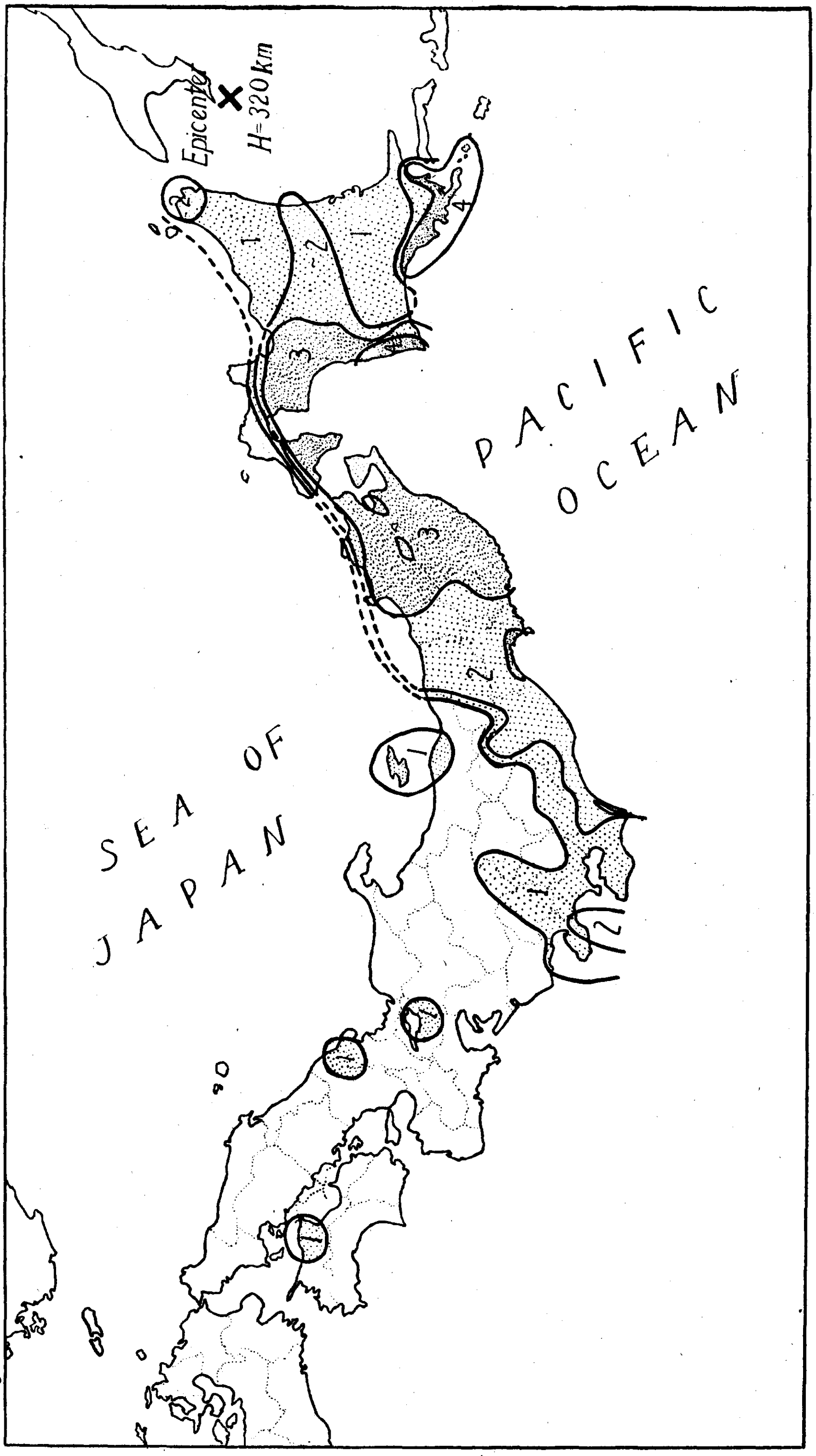

Fig. 2.

A typical Example of the area of abnormal perceptibility caused by a Deep-focus Earthquake originated in the Okhotsk Sea.

ved and called as « abnormal distribution of seismic intensity » or « area of abnormal perceptibility ». This phenomenon happened to lead one of the authors to the discovery of the existence of deep-focus earthquakes.

Today, it is well known that such « area of abnormal perceptibility » is a striking characteristics observed at the occurrence of deep-focus earthquakes wherever the epicenters may be located.

Fig. 2 and 3 show typical examples of « area of abnormal perceptibility » observed in Japan.

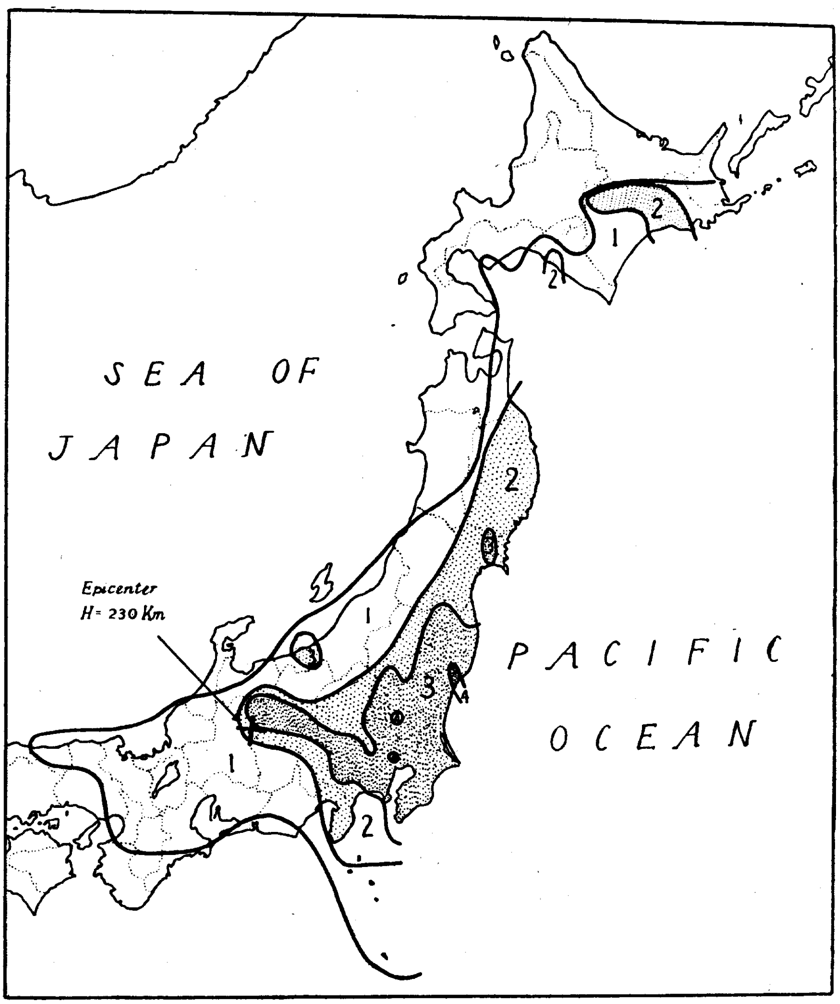

FIG. 3. — A Typical Example of the area abnormal perceptibility happened at the Deep-Focus Earthquake originated in the Central Part of Japan.

This phenomenon is considered to be caused chiefly by the structure of the earth's crust and to form a problem of great interest from the geophysical stand-point. The present investigation is based on the reports from the seismological Observatories of the Japan Meteorological Agency (J.M.A.) and other local weather stations where non-instrumental seismological observation are made. The scale of seismic intensity used by J.M.A. is shown below.

JMA Scale	0	I	II	III	IV	V	VI	VII
Accel. (gal)	< 0.8	0.8-2.5	2.5-8.0	8.0-25	25-80	80-250	250-400	400 <
Mercalli Scale	0~1	I~III	III~IV	IV~VI	VI~VII	VII~IX	IX	IX~X

2. « Area of Abnormal Perceptibility ».

Abnormal distribution of seismic intensity is also observed to a certain degree at the occurrence of shallow earthquakes, but the deeper the epicenter, the more conspicuously it is observed.

Now the authors have divided intermediate and deep-focus earthquakes which occurred during recent 30 years into six groups according to the locations of epicenters as follows :

1. The Pacific off East Hokkaido and the Kuriles.
2. The Sea of Okhotsk.
3. North Japan Sea.
4. Mid-Japan Sea.
5. The Pacific off the coast of mid-Honshu.
6. Area of South-West Islands.

Fig. 4-9 shows the observed number of earthquakes felt by human bodies in each group. As seen in these figures, the « area of abnormal perceptibility » is always noticed almost in the same area, irrespective of the position of the epicenter : i.e. south-east coast of Hokkaido, and east coast of North-east Honshu and Kanto district.

Of course, there is a tendency that seismic intensity is comparatively higher at places nearer to the epicenter, but the regularity that isoseismal lines form concentric circles, as is usually believed, has scarcely been noticed.

In the case of destructive earthquakes which occurred in land, it is natural that the intensity is maximum in the vicinity of the epicenter and its intensity distribution is nearly regular. If any irregularity is found, the intensity is not always specifically high in the habitual « areas of abnormal perceptibility ». However, the phenomenon of « abnormal perceptibility » is occasionally observed to a certain degree, depending on the location of epicenter, even in

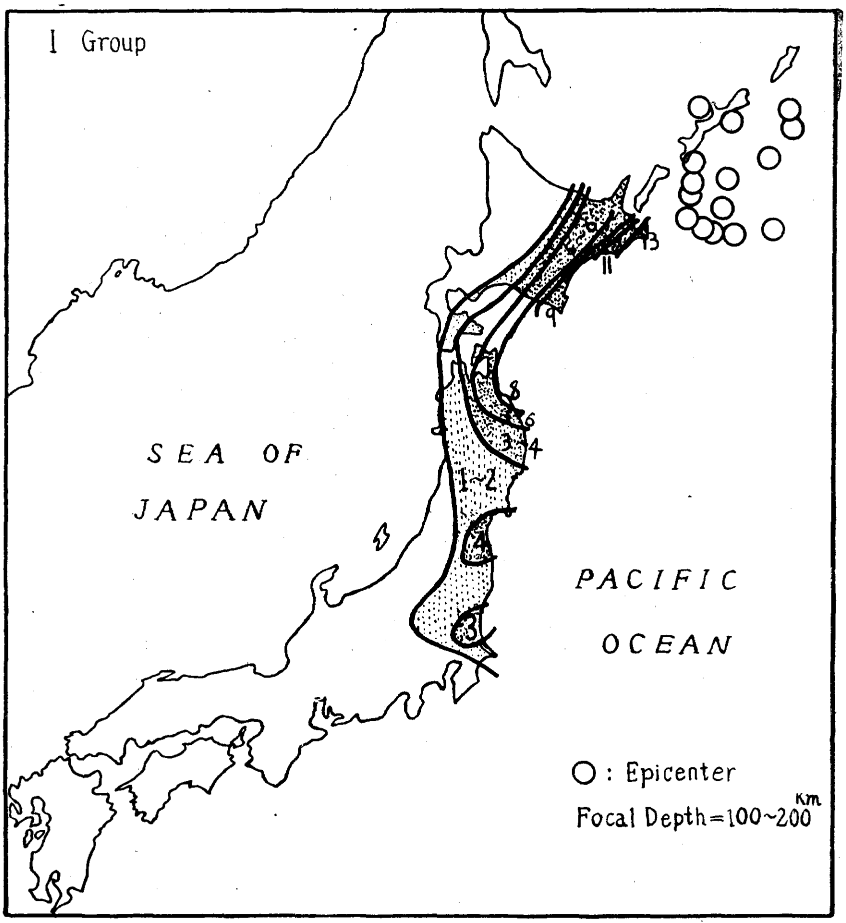

FIG. 4. — Observed Number of shocks (non-instrumentally) at seismological stations for the Earthquakes of Group 1.

the case of shallow earthquakes. The earthquakes which occur in the Pacific off the coast of North-east Japan come under this category. Fig. 10 shows the « areas of abnormal perceptibility » which was observed at the occurrence of the earthquakes on Mar. 4th, 1952 off south coast of Hokkaido. This earthquakes, followed by Tsunami, inflicted some damage. Earthquakes of 6th group are all intermediate. Some anomaly is recognized in the intensity distribution for this group, but not so conspicuously as seen in the other 5 groups.

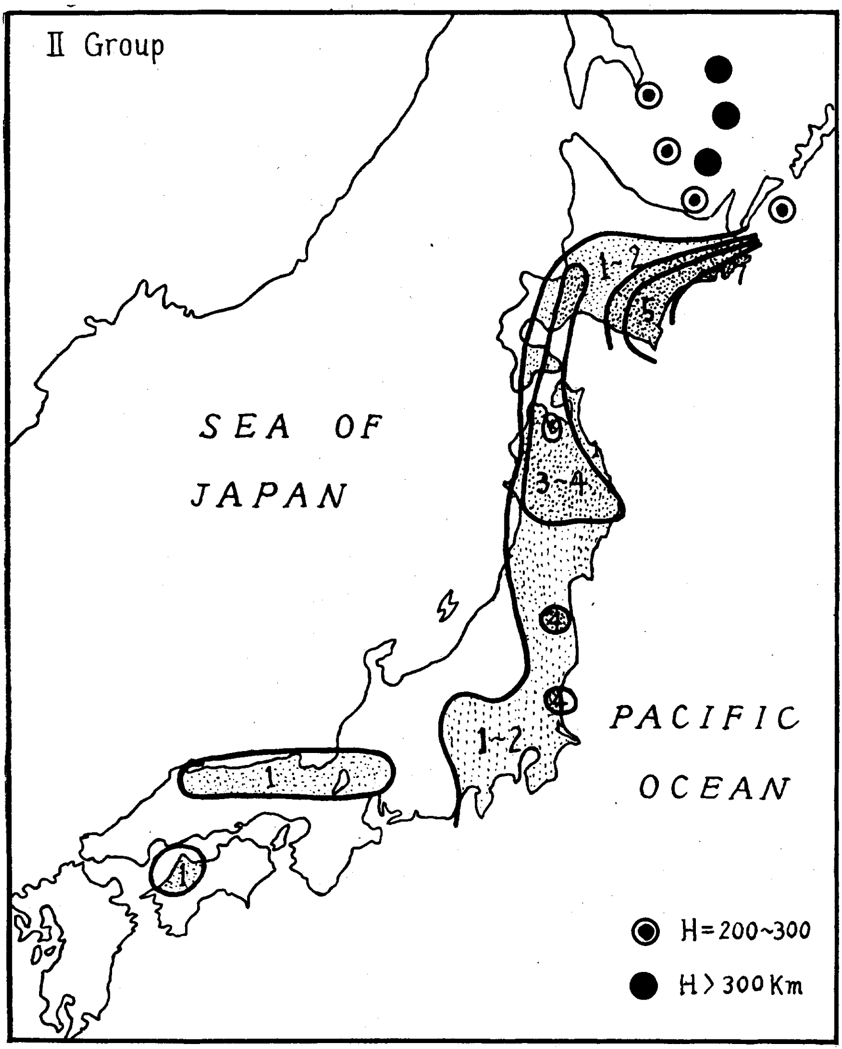

FIG. 5. — Observed number of shocks (non instrumentally) at seismological stations for the Earthquakes of Group 2.

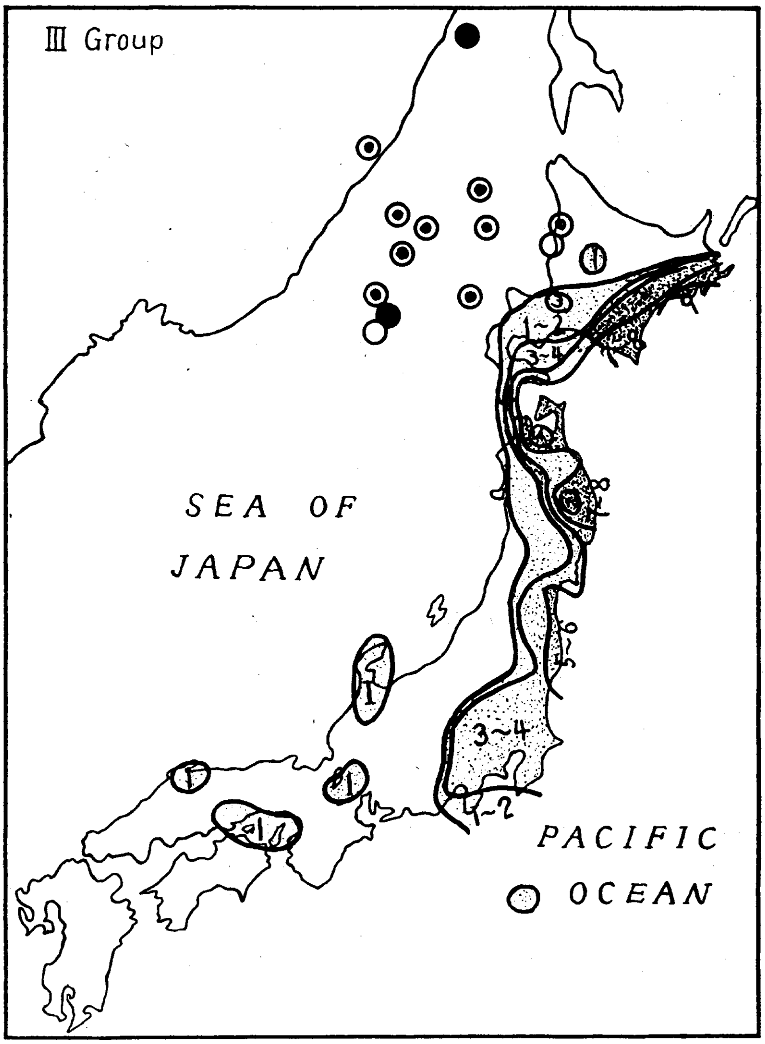

FIG. 6. — Observed number of shocks (non instrumentally) at seismological stations for the Earthquakes of Group 3.

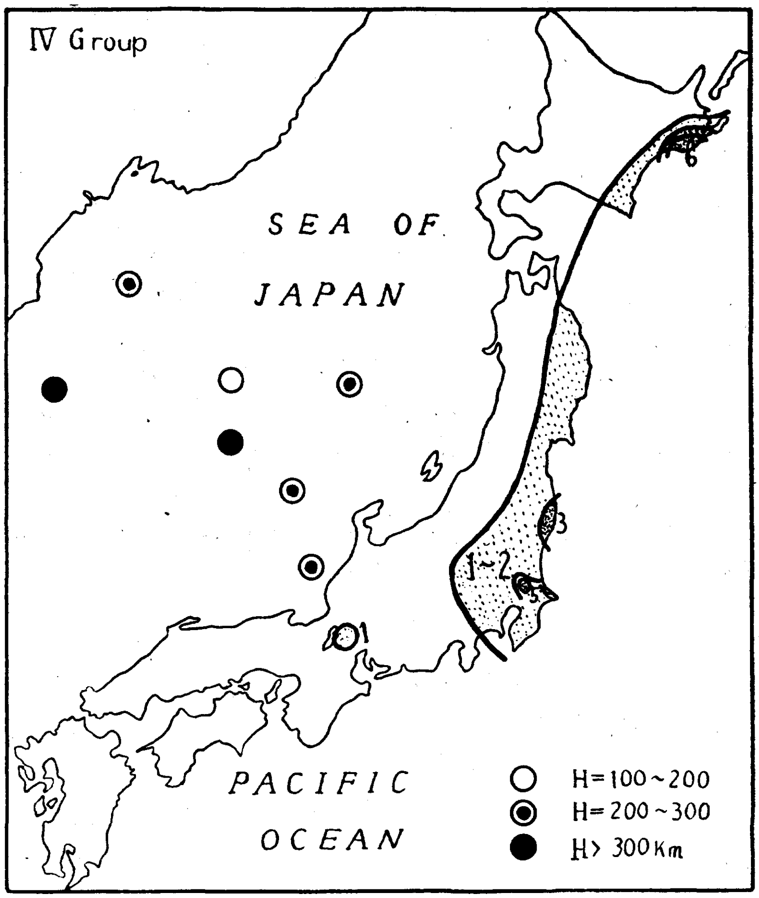

FIG. 7. — Observed number of shocks (non-instrumentally) at seismological stations for the Earthquakes of Group 4.

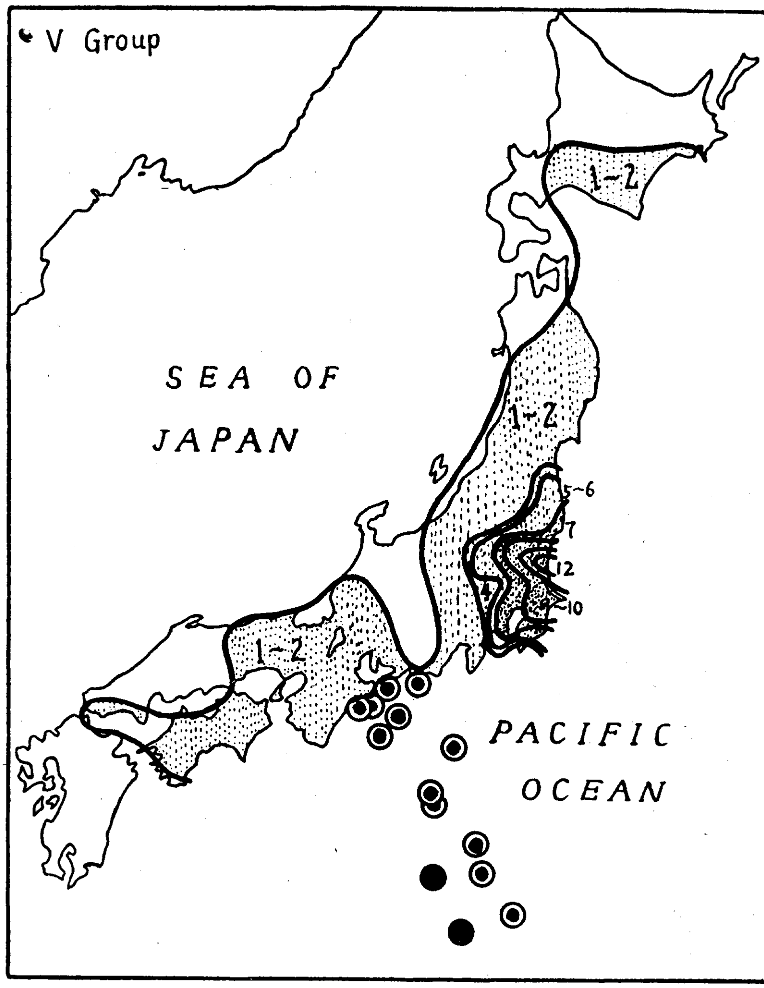

FIG. 8. — Observed Number of shocks (non-instrumentally) at seismological stations for the Earthquakes of Group 5.

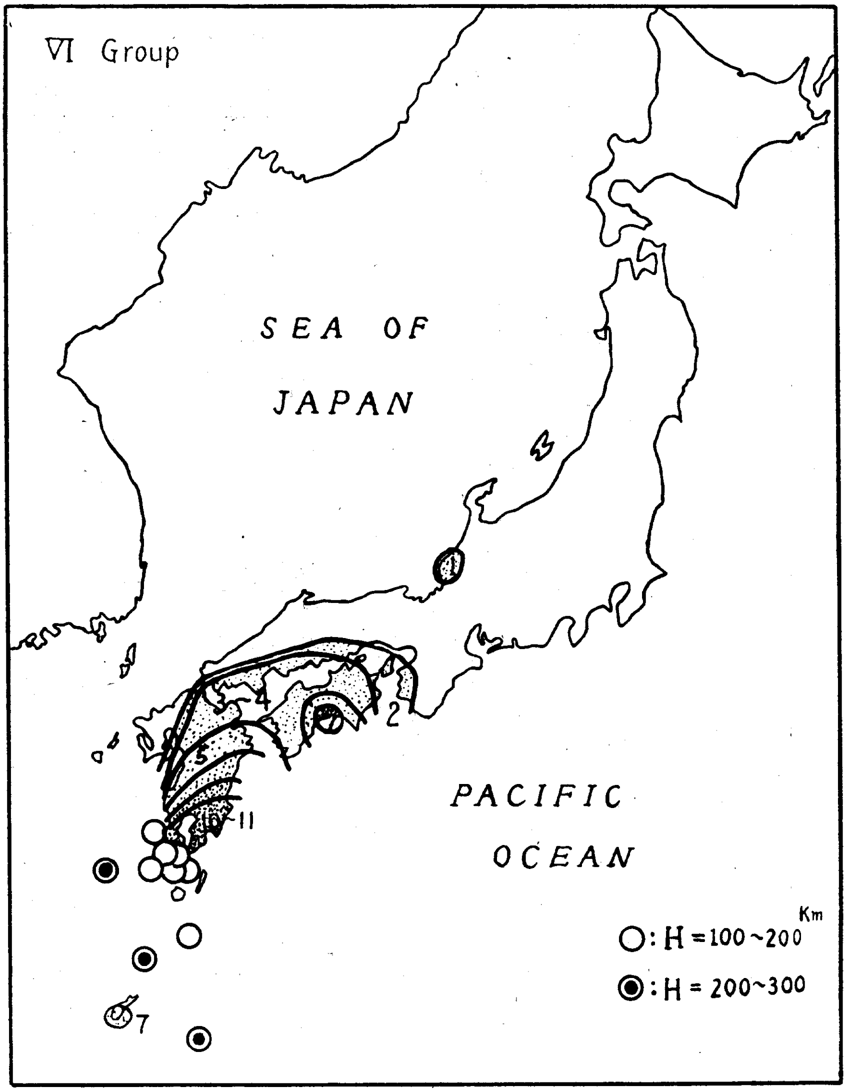

Fig. 9. — Observed Number of shocks (non-instrumentally) at seismological stations for the Earthquakes of Group 6.

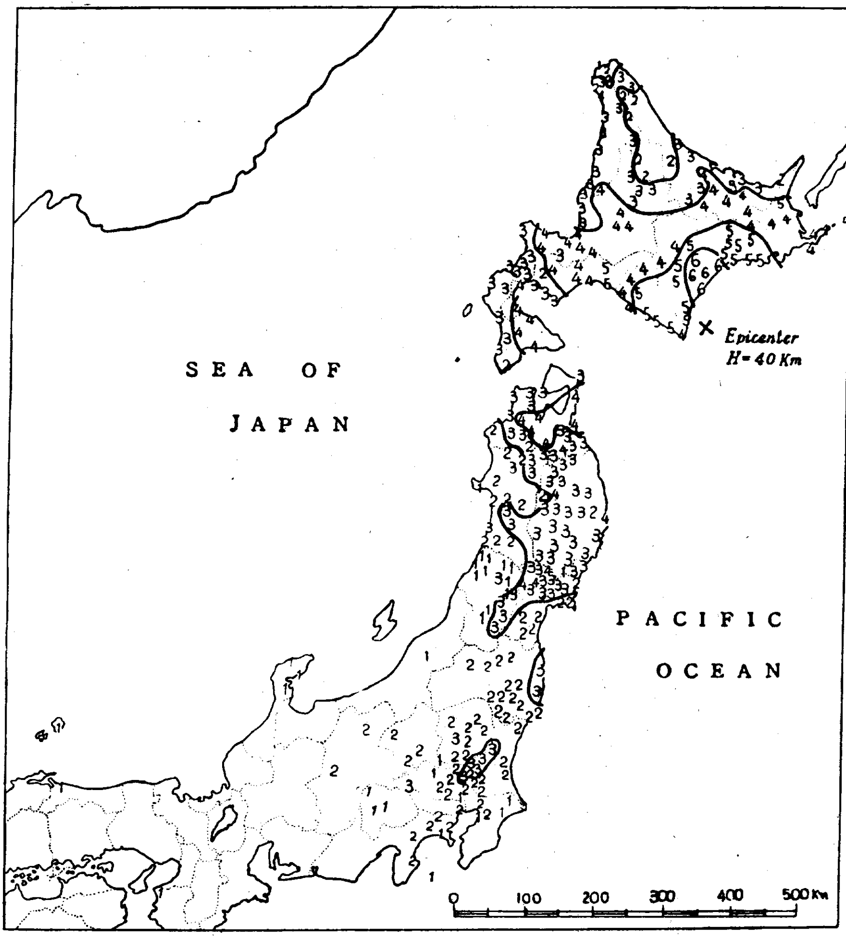

FIG. 10. — Distribution of seismic Intensity for the shallow-focus Earthquakes of March. 4 1952.

3. Acceleration of Seismic Motions Observed in the « Area of Abnormal Perceptibility ».

Acceleration of seismic motions is larger in the region of the « area of abnormal perceptibility » rather than in other regions. From the seismograms at some stations in Japan which recorded deep-focus earthquake which occurred in the north-east area of China, (44°8 N, 130°6 E, $h = 500$ km), we calculated the accelerations of seismic ground motions. Since the epicenter is situated approximately at the center of the arc of Japan Islands, the distance to the epicenter from each seismological station was nearly the same. From the records at each station, we measured the amplitude and period of vibration which is shorter than 5 seconds. Then we calculated the acceleration and prepared the diagrams showing their relations.

In Fig. 11 and 12, are shown only two instances of these diagrams. (Fig. 11) denotes the result obtained from the observa-

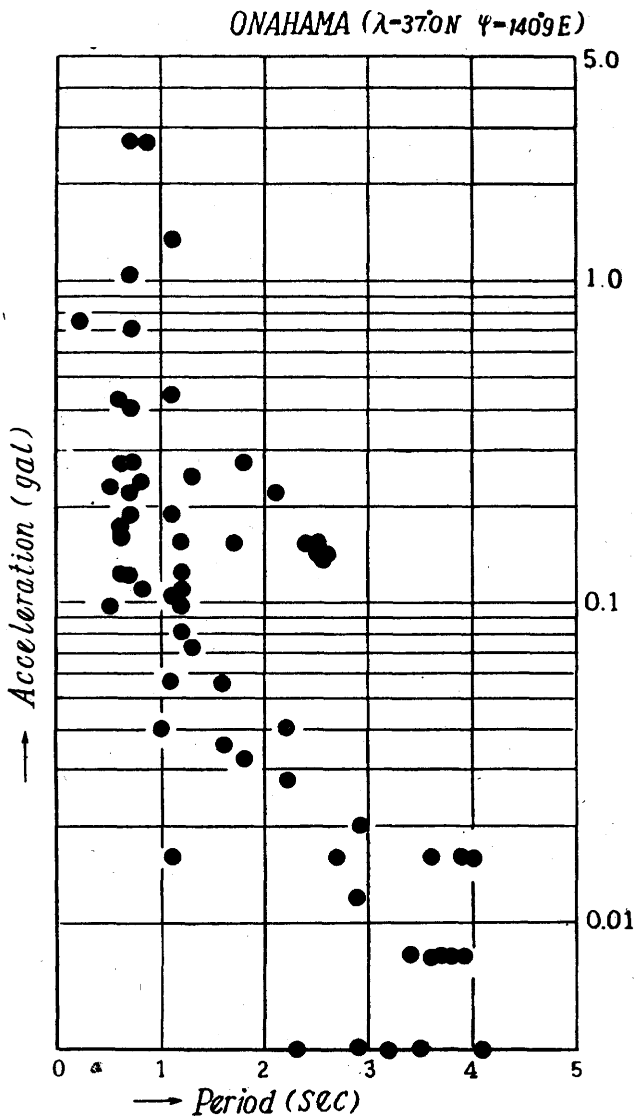

FIG. 11. — Acceleration — Period Diagram of seismic oscillations observed at Onahama in the « Area of abnormal perceptibility ».

tion made in the « area of perceptibility » and fig. 12 in the « area of non-perceptibility ».

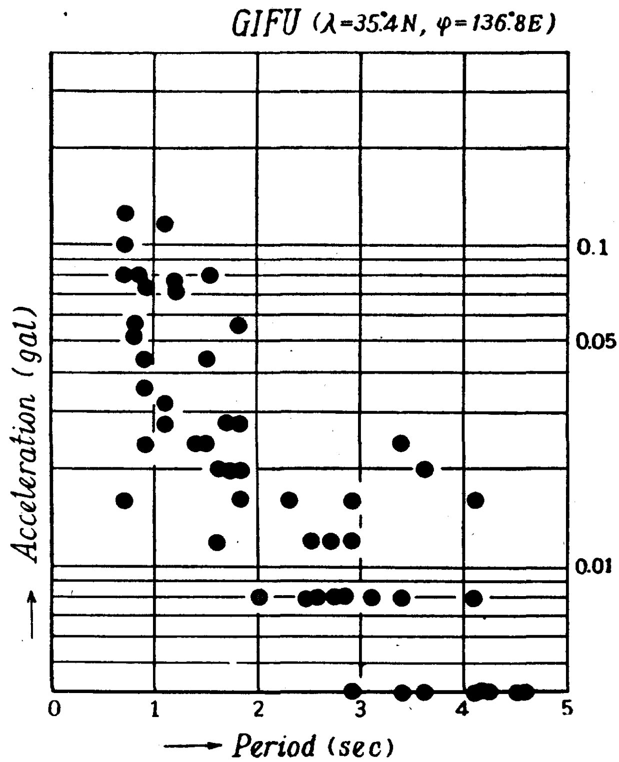

FIG. 12. — Acceleration — Period Diagram of seismic oscillations observed at Gifu in the « Area of non perceptibility ».

As is seen in Fig. 11 and 12, large accelerations appear when the period is short in both cases. But it is clear that the acceleration is larger in the « area of perceptibility », especially when the period is under 1.0 second. This indicates that short period oscillations predominate in the « area of abnormal perceptibility » rather than in other regions. As regards the part of comparatively longer period of oscillation, the acceleration is generally larger in the « area of abnormal perceptibility ».

4. THE « AREA OF ABNORMAL PERCEPTIBILITY » AND THE STRUCTURE OF EARTH'S CRUST.

Fig. 13 shows the maximum amplitude of the said earthquake in China observed at each station. Not much difference is noticed at stations in the areas of abnormal and non-abnormal perceptibility.

We know the values of the so-called ground coefficient for all seismological observatories belonging to J.M.A. As long as the

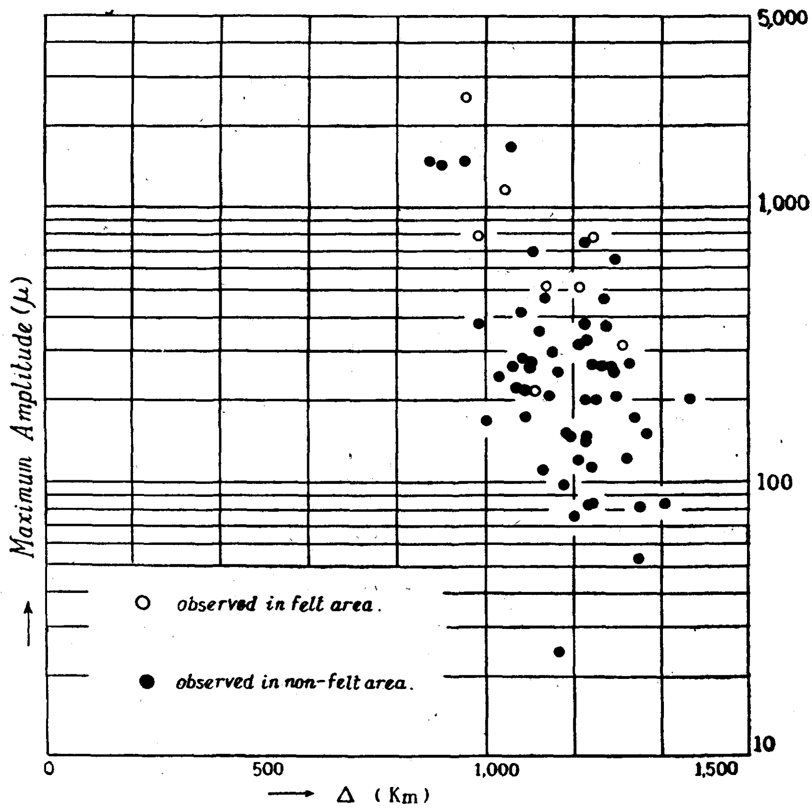

FIG. 13. — A-Δ Diagram for the deep-focus Earthquake of July 10, 1940.

coefficient distribution goes, the area of hard ground coincides with the « area of abnormal perceptibility » to some degree, but not always exactly, especially in West Japan. This shows that the fundamental cause of the « abnormal perceptibility » does not lie in geology of the surface, but in the comparatively deep layers.

When an earthquake occurs, such waves of short period must be emitted from the hypocenter to all directions. Consequently they reach the « area of abnormal perceptibility » without being absorbed in the medium through which they travel while the reverse is the case in other regions.

If there is no fundamental cause found in geology near the earth's surface, the structure of Mohorovičić layer, or the crust, comes in notice. Since the anomaly of gravity is considered to be much affected by the complex structure of the crust, the authors have compared the distribution of the areas of abnormal perceptibility with the map of gravity anomaly in Japan, prepared by Dr, Tsuboi (Fig. 14). It is distinctly recognized that the said « area

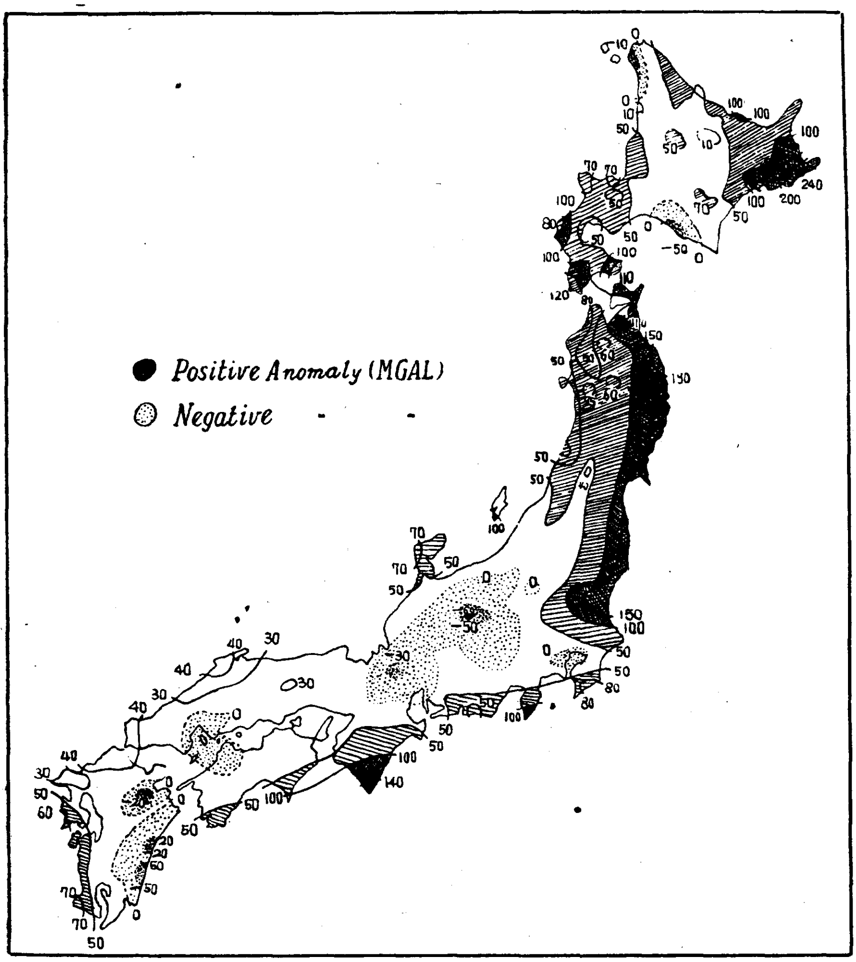

FIG. 14. — Bouguer Anomalies of Gravity by Dr. Tsuboi.

of abnormal perceptibility » well coincides with the zone of positive anomaly of gravity. However, this fact cannot explain the detailed mechanism of this phenomenon.

The structure of the earth's crust in Japan has been studied by means of artificial earthquakes[1], and propagation of natural seismic waves[2], but the authors have not yet been able to obtain precise data in the greater part of Japan. The full discussions of this problem will be made in the next opportunity.

1. Research Group for Explosion Seismology : The Explosion Seismic Observations carried out in North-eastern Japan, Bull. Earthq. Res. Inst., Vol. 33, p. 699, 1955.
2. Itsuo Tamaki : The Crustal Structure of Japan derived from Observed Travel Time Curves of Shallow Earthquakes, ZISIN, Vol. 7, p. 1, 1954.

LES PRINCIPES MÉTHODIQUES ET ESSAI DE RÉPARTITION DE LA SÉISMICITÉ EN URSS

S. V. Medvedev, B. A. Petrouchevsky.

Dans les régions séismiques, situées le long des frontières méridionales et orientales de l'URSS, on trouve un grand nombre d'agglomérations parmi lesquelles il y a des villes importantes. L'appréciation des différences d'efforts sur les constructions lors de l'élaboration des projets de ces constructions se fait en URSS d'après les cartes de répartition de la séismicité. La carte de répartition de la séismicité en URSS à l'échelle 1/5.000.000e, utilisée jusque-là, avait été approuvée en 1951 et était jointe à l'Instruction réglementant les travaux de construction dans les régions séismiques. Actuellement on vient de terminer la révision et la préparation d'une nouvelle Instruction; en même temps on a effectué des retouches à la carte de répartition de la séismicité en URSS.

La légende de la carte n'a pas été modifiée; on y a figuré les divisions territoriales d'après l'intensité des secousses, appréciées en degrés et rapportées aux conditions de constitution du sol moyennes. Sur la carte sont indiquées les zones d'intensité séismique du 6e, 7e, 8e et 9e degrés; dans cette dernière zone des intensités supérieures au 9e degré peuvent être enregistrées, mais les territoires correspondants n'ont pas été différenciés.

Lors des travaux de précision de la carte de répartition de la séismicité on a utilisé les données suivantes :

1. L'Atlas séismique de l'URSS, ainsi que les catalogues séismiques pour les trois dernières années.
2. Les données de la géologie séismologique.
3. Les comptes rendus des observations des tremblements de terre importants et les rapports des ingénieurs séismologues.

Examinons plus en détails ces renseignements.

***

L'Atlas séismique de l'URSS a été établi par un groupe de séismologues de l'Académie des sciences de l'URSS et des Académies des sciences de différentes républiques de l'Union. Cet atlas contient les résultats des observations du réseau des stations séismiques de l'URSS pour la période 1911-1953, les résultats d'investigations sur le terrain, ainsi que les comptes rendus des observations sur les tremblements de terre importants depuis 1850. La différence essentielle entre les nouvelles cartes séismiques et les cartes du passé

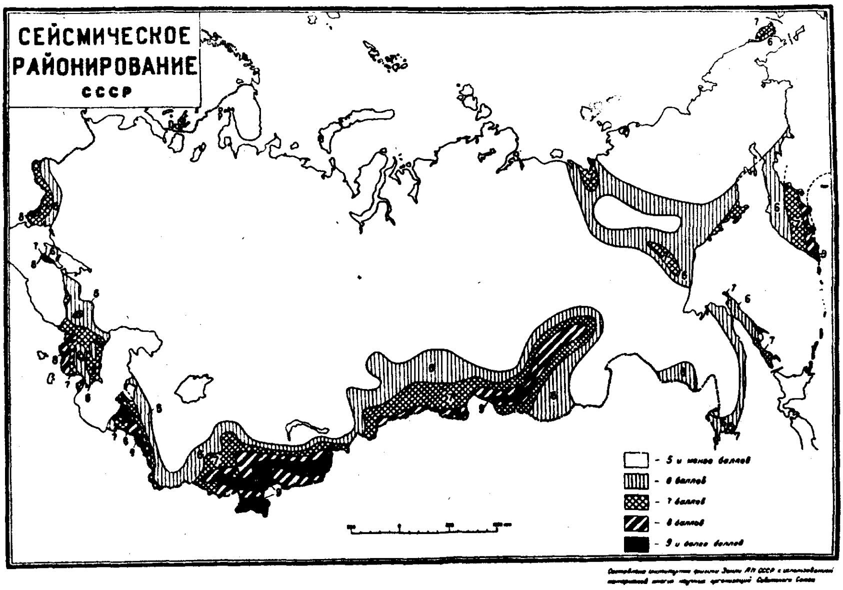

FIG. 1.

réside dans l'établissement d'une classification d'après l'intensité des secousses et la précision attachée à la détermination de l'épicentre.

Tous les tremblements de terre figurant sur les cartes des épicentres sont groupés d'après leurs intensités. L'intensité du tremblement de terre au foyer est exprimée au moyen de la valeur M. Suivant la profondeur du foyer l'intensité à la surface extérieure peut atteindre un degré différent.

Les groupes de tremblements de terre	Intensité de la secousse au foyer (M)	Degré d'intensité à la surface suivant la profondeur (H) du foyer		
		H 5 km.	H-20 km.	H-40 km.
I	7 1/2	—	9-10	8-9
II	6 1/2 - 7 1/4	10-11	8-9	7-8
III	5 1/4 - 6 1/4	8-9	7-8	5-6
IV	4 1/4 - 5	7-8	5-6	—

Un exemple de tremblement de terre du groupe I nous est fourni par le séisme de Khait en 1949 et celui de Quebin en 1911.

Un exemple de tremblement de terre du IIe groupe nous est fourni par le séisme d'Achkhabade en 1948 et celui de Guarm en 1941.

Le degré de précision dans la détermination de la position de l'épicentre est variable suivant le cas considéré, c'est pourquoi les épicentres sont rangés en trois classes suivant le degré de précision de leur détermination :

Classe A ± 25 km.
Classe B ± 50 km.
Hors classe plus de 50 km.

Suivant la profondeur du foyer les tremblements de terre sont divisés en deux catégories :

a) foyers localisés dans l'écorce terrestre,
b) foyers localisés sous l'écorce.

Lors de la précision de la carte de répartition de la séismicité en URSS l'atlas a permis l'utilisation plus poussée qu'auparavant des observations instrumentales; ceci a une grande importance pour toutes les régions de l'URSS et particulièrement pour les territoires à population clairsemée où les études instrumentales étaient rares. La connaissance de l'intensité ou de l'énergie relative des séismes, ainsi que de la profondeur du foyer permet d'apprécier objectivement le flux d'énergie et de comparer l'intensité au foyer avec l'effort exercé à la surface extérieure. L'établissement des lois de la répartition des foyers d'intensité différente permet d'utiliser lors du dressement des cartes de répartition de la séismicité non seulement les comptes rendus sur les tremblements de terre importants mais aussi les observations sur les microséismes.

Les renseignements sur les tremblements de terre enregistrés ces dernières années (1954-1956), nécessaires à l'établissement des cartes de répartition de la séismicité, ont été pour la grande part puisés dans les catalogues séismiques groupant les données fournies par le réseau des stations séismiques de l'URSS. On a également utilisé certains comptes rendus des effets des tremblements de terre importants.

***

Durant les quinquénats écoulés on a effectué de grands travaux de recherche dans le domaine de la géologie séismologique (particulièrement à l'Institut de physique du Globe de l'Académie des

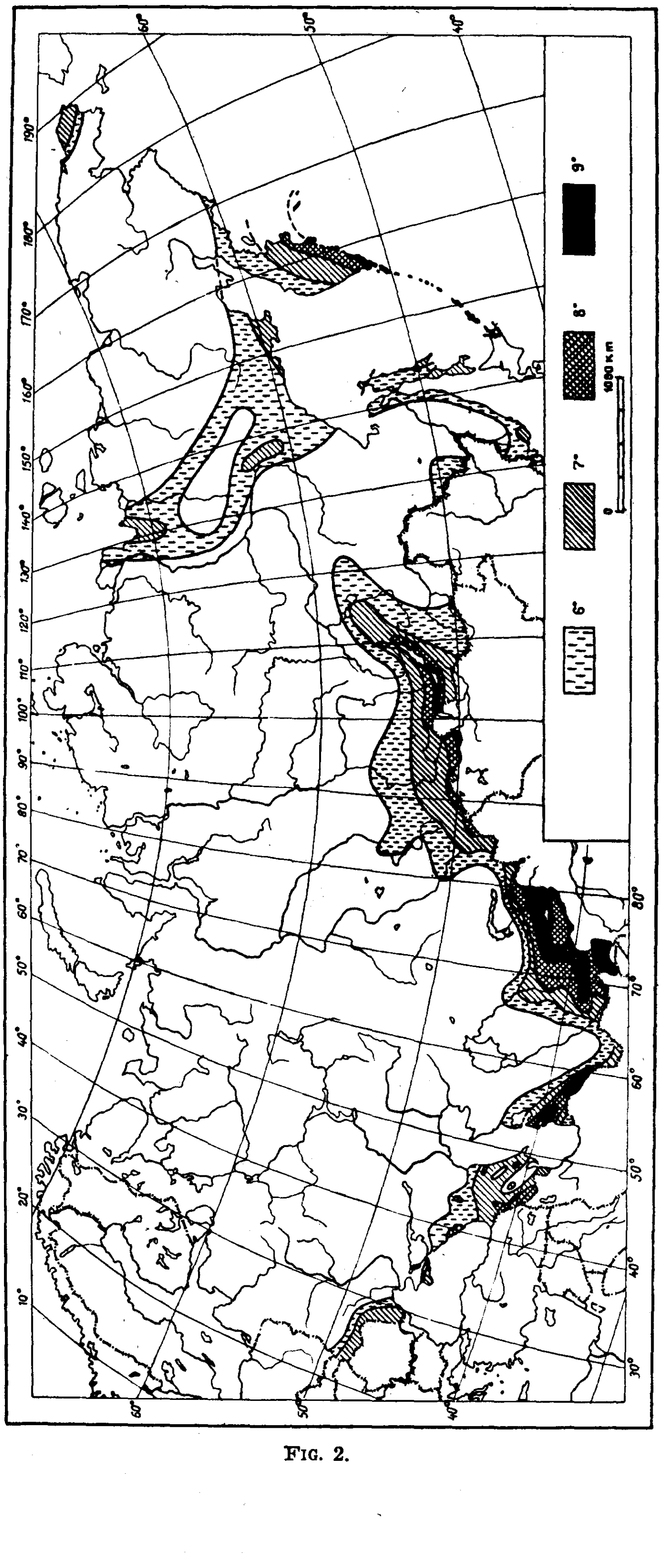

FIG. 2.

sciences de l'URSS). Ces recherches ont permis de formuler un certain nombre de principes, qui ont beaucoup contribué à préciser la carte de répartition de la séismicité.

Les grands mouvements du sol dont l'impulsion est ressentie dans l'écorce terrestre sont provoqués, ainsi que les tremblements de terre, par des mouvements internes. La nature et les causes de ces mouvements ne sont pas encore précisées, mais on peut considérer comme établi que la profondeur atteinte par ces mouvements dépasse au maximum des centaines de kilomètres, ce qui est confirmé par la présence à ces grandes profondeurs de foyers de séismes.

Toutefois la grande majorité des tremblements de terre est causée par des mouvements localisés à des moindres profondeurs — soit dans l'écorce terrestre, soit à proximité de celle-ci.

L'hypothèse la plus répandue sur l'origine des tremblements de terre consiste à les considérer comme la conséquence des ruptures de continuité de la matière à l'intérieur du Globe, provoquées par l'accroissement progressif de l'énergie potentielle, c'est-à-dire de l'énergie de déformation. On suppose que la cause de ces concentration de l'énergie élastique réside dans les phénomènes internes du Globe, conditionnés par les changements de températures et les passages de la matière d'un état dans un autre.

On peut distinguer sur le territoire de l'URSS plusieurs zones séismiques de grande intensité.

La première zone se situe à la limite des aires continentales et des cuvettes océaniques. Il est opportun de mentionner ici la bande séismique qui traverse le Kamtchatka, les îles Kouriles et se dirige vers le sud par le Japon.

La seconde zone se rattache aux régions du géosynclinal alpin. Sur le territoire de l'Union Soviétique cette zone comprend les Carpathes, le Caucase, le Kopet Dagh et le Pamir.

La troisième zone se rapporte aux architectures tabulaires des aires continentales, qui ont été dès la fin du tertiaire sujettes à de forts mouvements du sol. Des exemples de cette zone nous sont fournis par les régions de Tian Chan et du Baïkal.

Ainsi on constate que des régions de structure géologique différente et dont l'histoire géologique est dissemblable sont sujettes à des séismes intenses. Cette constatation rend difficile la compréhension des rapports entre les secousses et la géologie. Cependant en partant de l'idée de dépendance des tremblements de terre et de l'orogénie des mouvements internes on arrive à établir des rapports plus ou moins nets entre ces phénomènes.

Sous ce rapport le fait que superficiellement l'orogénie due à des mouvements internes, affecte la forme de grands complexes structuraux ou d'ensembles tectoniques apparus à des différentes phases de l'évolution de l'écorce terrestre et qui peuvent être groupés en des systèmes géologiques acquiert une grande importance. On ne peut prendre en considération que de grands complexes, coïncidant avec des terrains d'un seul bloc de structure géologique homogène, car il n'est pas possible d'étudier chaque pli du relief comme une conséquence directe des mouvements compliqués produits à des dizaines de kilomètres de profondeur.

Nous devons remarquer que quand on considère les phénomènes séismiques on doit les étudier en rapport avec les mouvements internes actuels, tandis que dans le cas de grands complexes structuraux ce sont les mouvements de grande durée géologique qui doivent être envisagés. Cette grande durée témoigne d'une grande stabilité dans le temps de telle ou telle particularité d'évolution de fragments importants de l'écorce terrestre. En se basant sur ces considérations on peut assimiler en général les mouvements de fond actuels, qui conditionnent le régime séismique envisagé, aux manifestations des tendances propres aux régions étudiées durant la longue période antérieure.

Un rapport génétique s'établit donc entre les phénomènes séismiques, causés par des mouvements tectoniques actuels, et les grands complexes structuraux de la surface extérieure, dus aussi à des mouvements tectoniques mais de durée beaucoup plus longue. Il est entendu que ces conséquences, considérées du point de vue du temps de leurs apparitions, sont différentes. En général les complexes structuraux se forment d'abord dans l'écorce terrestre. Puis à mesure qu'ils se développent ils se compliquent, sont disséqués à des profondeurs variées par des failles qui sont la cause immédiate des secousses séismiques. C'est pourquoi ces dernières sont généralement classées dans le groupe des effets secondaires quant à leur temps d'apparition.

L'existence de rapports ainsi conçus entre les grands systèmes géologiques et les phénomènes séismiques permet de tirer certaines conclusions quant aux effets de l'activité séismique dans les différentes régions. Il est évident vu la complexité et la multiplicité des mouvements tectoniques que les rapports entre les secousses et la géologie sont aussi très compliqués et variés.

Sans pouvoir entrer dans le détail de tous les phénomènes géologiques qui peuvent être rattachés à une activité séismique élevée (et qui pour cause peuvent être identifiés à des indices géologiques de la séismicité) nous indiquerons que ces rapports, entrevus entre les phénomènes séismiques et la géologie peuvent être classés en quelques grands groupes qu'on est arrivé à distinguer sur le territoire de l'URSS. Ces rapports acquièrent un caractère différent dans : *a*) les zones de plissements récents (alpins) ; *b*) les zones de plate-formes rajeunies (à soubassement primaire plissé) ; *c*) les fragments de plate-forme sujets à des modifications dues aux mouvements tectoniques de grandes amplitudes; et enfin *d*) les régions de contact entre le continent asiatique et l'océan Pacifique.

a) Les régions de la zone géosynclinale (c'est la zone des plissements alpins qui se sont formés au tertiaire dans le sud de l'URSS) sont essentiellement caractérisées par un régime de transformations structurales. Elles ont donné lieu à de multiples successions d'affaissements et de bombements affectant un même terrain, à des plissements répétées, à des nouveaux mouvements de faille ainsi qu'à des rajeunissements de failles anciennes, etc...

Utilisant une expression imagée on peut dire que les zones géosynclinales sont le siège d'une orogénie toujours « vivante » et dont la durée peut être très longue. Il est naturel de voir un lien entre ces manifestations et une forte activité séismique; le nombre de séismes qui affectent ces régions est très élevé, certains atteignant jusqu'à 9 degrés d'intensité. Un exemple de ces régions nous est fourni par le Caucase où une activité particulièrement forte de la séismicité s'observe dans la Transcaucasie, de construction plus récente que la chaîne principale du Caucase. Les mêmes conditions s'observent aussi dans le Kopet Dagh, partie septentrionale des plissements alpins de la Turkmenie et de la Khorossan.

b) A l'inverse des régions de plissements récents, dans les régions de plate-forme la structure ne subit pas de transformation sous l'action d'efforts orogéniques, mais évolue lentement dans un sens durant plusieurs âges géologiques. Pour les plate-formes relativement récentes à soubassements plissés primaires un rôle important est joué par l'évolution passé du territoire, caractérisée par les adaptations de la couverture sédimentaire d'âge secondaire et cénozoïque à l'orogénie du soubassement.

Ces héritages du passé sont les plus sensibles dans les aires les plus récentes de plissement du soubassement (la fin du primaire), qui se caractérisent par des discordances de structure très marquées durant le stade tabulaire de l'évolution. C'est dans ces régions que l'activité séismique est la plus intense, cependant le degré d'intensité des tremblements de terre n'est pas très élevé (de 5-6, au maximum 7 degrés).

Ainsi donc dans les zones de plate-forme, l'activité séismique a pour origine les processus commencés dans ces régions depuis fort longtemps et se manifestant actuellement sous une forme atténuée. C'est le phénomène de « réminiscence » d'une mobilité géosynclinale depuis fort longtemps résolue à travers le stade tabulaire de l'évolution, d'une mobilité en général très faible.

En qualité d'exemples de ces régions séismiques nous pouvons citer l'Oural, le Kisil-Koum et la région de Karabouguase en Turkménie. Peut-être il faudrait rattacher à ce type de régions certains territoires séismiques du nord-est de la Sibérie, en particulier le Verkhoianié et la Haute Kolima.

c) Dans les terrains de plate-forme dont la structure a subi des transformations ou bien est en train de se transformer, ayant été introduits dans le cycle des mouvements récents et vigoureux, on observe des rapports plus compliqués entre l'activité séismique et la géologie. Les phénomènes de « réminiscence » de la mobilité géosynclinale se manifestent aussi ici, provoquant un très grand nombre de tremblements de terre dans les régions à soubassement plissé de la fin du primaire (le Tian Chan occidental). Cependant vu la grande mobilité de ces terrains, l'intensité maximum des tremblements de terre est plus élevée que dans les zones de plate-forme correspondante et atteint 9 degrés et même quelquefois davantage.

Dans les terrains de la plate-forme en transformation, dont la stabilisation au stade géosynclinal s'est effectuée depuis fort longtemps et qui durant l'ère secondaire et cénozoïque étaient caractérisés par une très faible mobilité, le rôle de facteurs principaux incombe tout d'abord aux mouvements tectoniques actuels. Quand ils ont pour conséquences à la surface des soulèvements des blocs relativement peu importants suivis d'affaissement correspondants, l'activité séismique augmente brusquement. C'est probablement dans ces régions qu'apparaissent les séismes les plus importants (de 9 degrés et davantage), mais toutefois à des intervalles espacés. Ceci peut sans doute être expliqué par le fait que durant la transformation de ces terrains particulièrement rigides et très stables, il aurait dû se produire des dislocations et des fractures très fortes.

En même temps les régions de plate-forme subissant des mouvements du sol unilatéraux pouvant conduire à des soulèvements de grandes amplitudes sont le siège de séismes manifestement moins intenses. Parmi les exemples de terrains où l'activité séismique s'observe dans les zones de plate-formes transformées (ou en transformation) il faut tout d'abord mentionner le Tian Chan. Sa partie centrale et orientale ayant été plissée puis stabilisée durant la première moitié de l'ère primaire, c'est-à-dire deux périodes géologiques avant que ne l'a été le Tian Chan occidental, sont affectés par un nombre de séismes moins grand que ce dernier; toutefois leurs intensités dépassent les ébranlements les plus forts enregistrés dans le Tian Chan occidental (le tremblement de terre de Tchilik en 1889 et de Quebin en 1911). On doit aussi rattacher à ces régions séismiques la zone du Baikal, ainsi que de nombreux terrains de l'Asie Centrale ne faisant pas partie de l'URSS.

d) Il est vraisemblable que les rapports entre les séismes et la géologie en Extrême-Orient sont d'un (ou de plusieurs) types différents. Ces régions séismiques se caractérisent par des tremblements de terre de surface (foyers localisés dans l'écorce) et de tremblements de terre internes (foyers localisés à de grandes profondeurs). Le problème de ces séismes est encore insuffisamment étudié et il est vain de prétendre fixer les lois de leur répartition. Remarquons toutefois que nous sommes ici en présence de conditions de structure profondément différentes de celles observées dans les autres groupes de régions. Il ne fait pas de doute que le contact entre des fragments de l'écorce terrestre d'une architecture différente, telle le continent asiatique et l'océan Pacifique, peut être suivi sur une grande profondeur à l'intérieur du Globe. C'est pourquoi il n'est pas étonnant d'y rencontrer des tremblements de terre dont le foyer se trouve à des grandes profondeurs, ainsi que des séismes à foyer localisé près de l'écorce ou même dans l'écorce, car les mouvements du sol actuels se produisent certainement le long de toute la zone de contact, de haut en bas, entre ces deux grands complexes structuraux.

Nous devons souligner que les critériums géologiques qu'on vient de dégager peuvent être pris en considération seulement comme une première approche, lors de l'investigation des causes des tremblements de terre. La signification concrète de ces critériums, formulant telle ou telle incidence géologique d'après leur manifestation à la surface extérieure, peut être très différente même pour un seul groupe de régions.

Il n'est pas difficile de voir que l'emploi d'une telle méthode permet en général de formuler des jugements sur l'activité séismique de diverses régions, ce qui est d'une grande importance pour les études de répartition de la séismicité.

La méthode d'étude des rapports entre les séismes et la géologie régionale se ramène donc à l'analyse de l'évolution de la structure. Cette dernière consiste dans l'étude historique de l'évolution géologique de la contrée, étude englobant un laps de temps important et un espace étendu en attachant une attention particulière aux rapports entre les grands complexes structuraux dégagés actuellement. Cette analyse doit être effectuée en considération de toutes les données de la statistique séismique disponible. L'absence de ces données rend en général erronées toutes les conditions concernant les rapports des séismes avec la géologie.

Il est évident que les frontières entre les grandes unités structurales ne peuvent être tracées qu'approximativement.

Des erreurs peuvent être aussi commises dans la détermination des épicentres des tremblements de terre. Ces considérations nous amènent à conclure que les études de géologie séismologique ne peuvent fournir des données sur l'activité séismique qui ne sont valables que pour le dressement des cartes de répartition de la séismicité à de petites échelles. Les résultats des travaux menés en U.R.S.S. dans les différentes régions séismiques ont conduit à la conclusion que l'échelle maximum utilisable est de 1 : 1.000.000 ou 1 : 2.000.000. Pour les terrains insuffisamment étudiés au point de vue de la géologie séismique, il faut choisir une échelle plus réduite de l'ordre de 1 : 5.000.000.

***

Lors de la représentation cartographique de la répartition de la séismicité — en utilisant les données de la séismologie statistique ainsi que ceux de la géologie séismique — on délimite les frontières des zones séismiques et on établit l'intensité des secousses en degrés d'après les renseignement fournis par les ingénieurs séismologues.

Pendant les travaux de précision de la carte de répartition de la séismicité en U. R. S. S. on a fait appel aux renseignements fournis par les missions d'étude des séismes importants aussi bien actuels que de ceux qui ont eu lieu autrefois. On a également envoyé des missions d'étude dans les zones séismiques où on a installé des stations séismiques temporaires et des instruments très sensibles.

Une importance particulière était attachée à l'appréciation de l'intensité des tremblements de terre.

Des missions séismiques ont été envoyées en Turkménie en 1949, 1951, 1952 et 1953. On y a étudié la distribution des foyers des microséismes en délimitant les frontières des régions sujettes aux tremblements de terre. L'étude de l'influence de la constitution des sols sur l'intensité des oscillations séismiques a été effectuée par ces missions à l'aide de stations séismiques spéciales. Des études analogues avec installation d'un réseau de stations séismiques temporaires ont aussi été effectuées durant les cinq dernières années dans les régions de Guarm (R.S.S. de Tadjikie), dans le Tian Chan septentrional et dans un grand nombre de régions du Caucase : Krasnaia Poliana, Chemakha, la zone d'Akhalkalak.

Sur la carte de répartition de la séismicité en U. R. S. S. on a figuré des régions d'inégale intensité des tremblements de terre, exprimées en degrés de l'échelle séismique. Une nouvelle échelle d'intensité a été élaborée en 1952 à l'Institut de physique du Globe de l'Académie des sciences de l'U. R. S. S. Cette échelle comprend 12 degrés; les caractéristiques descriptives de cette échelle peuvent être comparées à celles de Mercalli-Cancani-Sieberg utilisées dans certains pays d'Europe, ainsi qu'à celles de l'échelle de Wood-Neumann — échelle MM — utilisée en U.S.A. et de la nouvelle échelle proposée dans la République Populaire de Chine.

Le problème de l'appréciation de l'intensité des tremblements de terre est un vieux problème de la séismologie. A la fin du XVIII^e^ et au début du XIX^e^ siècle différentes échelles d'intensité des séismes ont été proposées. Durant le XIX^e^ et le XX^e^ siècle on a imaginé plusieurs dizaines d'échelles.

Dans la nouvelle échelle d'intensité de l'Institut de physique du Globe de l'Académie des sciences de l'U. R. S. S. le degré d'intensité est tout d'abord déterminé à l'aide des observations instrumentales, puis sont données les appréciations des effets des tremblements de terre.

D'après cette échelle l'intensité de la secousse est exprimée à l'aide de la valeur X_0 qui équivaut au maximum de déviation du pendule sphérique dont la période d'oscillation propre est T_0 = 0,25 sec. et le décrément logarithmique de l'amortissement $\lambda = 0.50$.

Dans l'échelle d'intensité les valeurs des déviations sont données du 5^e^ au 10^e^ degré. Ceci permet d'utiliser l'instrument pour les mesures de l'amplitude des déviations dans la zone la plus importante du spectre des oscillations séismiques. Cette amplitude joue le rôle de paramètre pour le spectre entier. L'amplitude de déviation pour les pendules à période T_i et de décrément d'amortissement des oscillations λ_i est calculée à l'aide des coefficients de transition. La valeur de ces coefficients a été établie après analyse des accélérogrammes et séismogrammes.

Les degrés de l'échelle sont fixés pour les valeurs suivantes de X_0 exprimé en mm. :

5 degrés : 0,5 — 1,0 mm.
6 degrés : 1,1 — 2,0 mm.
7 degrés : 2,1 — 4,0 mm.

8 degrés : 4,1 — 8,0 mm.
9 degrés : 8,1 — 16,0 mm.
10 degrés : 16,1 — 32,0 mm.

Il est important de noter que les spectres des oscillations séismiques varient énormément suivant les tremblements de terre. On peut affirmer qu'il n'y a pas deux tremblements de terre ayant des spectres identiques. C'est pourquoi les valeurs des coefficients spectraux ne sont que des valeurs moyennes. Ces moyennes ont été calculées après l'analyse de 80 enregistrements d'oscillations séismiques. Les moyennes quadratiques des écarts de cette courbe moyenne du coefficient spectral ont atteint sur certains terrains près de 100 %. De tels écarts sont conditionnés par diverses causes : a) la consistance physique des sols; b) la structure et les propriétés du milieu de propagation des ondes; c) la distance au foyer; d) la direction des secousses; e) l'intensité de la secousse au foyer.

La nouvelle échelle permet d'obtenir des données numériques utilisables pour le calcul des constructions antiséismiques.

L'effort essentiel des ingénieurs-séismologues doit porter sur l'étude de détails de la répartition de la séismicité. La solution de ce problème est intimement liée aux questions de recherche d'une méthode nouvelle d'étude de la répartition générale de la séismicité.

Sous ce rapport un intérêt particulier s'attache aux estimations des moyennes spectrales des oscillations séismiques, considérées comme des étalons à partir desquelles il est possible de calculer les anomalies des spectres régionaux. Ceci nous montre que le problème de microdivision territoriale doit être résolu par des méthodes différentes de celles employées auparavant. Il s'agit d'une étude détaillée de la répartition de la séismicité tenant compte non seulement des changements de signification des différents degrés de l'échelle d'intensité, mais aussi d'une étude et de l'appréciation des spectres d'oscillation séismique. Les spectres d'oscillation ne sont pas les mêmes dans les différentes zones. C'est pourquoi la tâche des études ultérieures en matière de microdivision territoriale doit consister dans un travail de mesure et d'investigation des particularités des spectres des régions considérées.

On est en train d'effectuer de semblables mesures en U. R. S. S., cependant cette branche d'étude de la répartition détaillée de la séismicité, si importante pour l'appréciation des efforts séismiques sur les constructions, n'est qu'à ses débuts.

Avant que les résultats pratiques de ces recherches soient obtenus, les problèmes de répartition détaillée de la séismicité ne peuvent être résolus que grâce à l'utilisation des renseignements sur l'influence de l'élasticité des roches sur l'intensité séismique fournis par les ingénieurs-géologues, c'est vers une solution analogue qu'on se tourne quand on veut résoudre numériquement le problème posé par le changement du degré d'intensité des séismes.

Les renseignements fournis par les études des effets des tremblements de terre permettent de déterminer les rapports existant entre le degré d'intensité et la constitution des sols. Le dépouillement des résultats des observations a permis d'évaluer les accroissements du degré dus aux différents types de roches. Cet accroissement du degré d'intensité est apprécié par commodité en fonction d'un étalon de référence dont le rôle est joué par le granite.

Les observations recueillies sont confrontées avec les propriétés physiques des roches. On a ainsi constaté que l'une des propriétés physiques des roches, jouant un rôle important dans l'appréciation de leur influence sur les phénomènes séismiques, est ce qu'on peut appeler la rigidité séismique qui est définie par le produit de la vitesse de propagation des ondes séismiques longitudinales par la densité des roches.

Les conditions du drainage du sol ont aussi leur influence sur le degré d'intensité.

Les résultats de ces études ont été utilisés lors des recherches détaillées sur la répartition de la séismicité dans nombre de grandes villes : Achkhabad, Alma-Ata, Frounzé, Stalinabad, Tbilissi et autres agglomérations.

Sur la carte de la répartition générale de la séismicité le degré d'intensité est évalué en tenant compte de l'élasticité moyenne des roches. La majorité des agglomérations et des localités sont situées sur des sols dont les conditions d'élasticité sont moyennes, c'est pourquoi sur la carte de répartition générale de la séismicité les points du canevas de base côtés « zéro » correspondent aux terrains les plus répandus. Généralement ces terrains sont composés de sédiments sableux et limoneux. Cependant la solution de ce problème exige encore des efforts ultérieurs de la part des investigateurs.

Il est important pour l'étude de répartition de la séismicité de tenir compte des dimensions des aires des fortes secousses. Les dimensions de la zone affectée par les secousses dépendent de la profondeur du foyer. Ainsi lors du tremblement de terre d'Achkhabad en 1948 qui a atteint 9 degrés d'intensité la surface de la région ébranlée par des secousses du 8e degré a atteint 3.000 km², tandis que lors du tremblement de terre de Tchatkal en 1946, dont l'intensité était aussi de 9 degrés, la surface de la région ébranlée par des chocs du 8e degré a couvert 35.000 km². Des études ont été faites afin de déterminer un rapport numérique entre la profondeur du foyer et les dimensions de la surface ébranlée par des secousses d'un degré donné. Ces travaux ont fourni des renseignements nécessaires à la détermination de la largeur de la bande séparant deux isoséistes lors du dressement des cartes de répartition de la séismicité.

***

En guise de conclusion notons que les études de répartition de la séismicité sur le territoire de l'U.R.S.S. entreprises durant les 10-15 dernières années ont clairement montré que cette tâche ne peut être menée à bien que grâce à une étude complexe du phénomène, avec l'utilisation des méthodes de la géophysique et de la géologie et le contrôle de l'une par l'autre. Ni les séismologues, ni les géologues ne peuvent séparément trouver une solution juste au problème. Les renseignements recueillis par ces études permettent de dresser des cartes de répartition de la séismicité très générales c'est-à-dire à petite échelle. Pour les cartes de grande échelle — pour l'étude détaillée de la répartition de la séismicité — Il est indispensable d'utiliser les travaux des ingénieurs-séismologues.

Les questions de division territoriale de l'U. R. S. S. d'après la répartition de la séismicité ont été longuement discutées en U. R. S. S. Les méthodes et les expériences de division territoriale ont été exposées dans un grand nombre de rapports publiés dans les revues soviétiques. On est arrivé à la conclusion que pour l'élaboration de bases solides à ces divisions territoriales il faut encore effectuer des études plus approfondies et que la principale difficulté consiste à trouver une méthode nouvelle de division territoriale. C'est pourquoi on a inséré dans le plan des travaux de l'Institut de physique du Globe de l'Académie des sciences de l'U. R. S. S. l'étude de ces problèmes importants sous la rubrique « recherche de la répartition de la séismicité et investigations des tremblements de terre ».

RÉFÉRENCES.

1. BELOUSSOV (V. V.) : Les problèmes de division territoriale en matière séismique. Izv. de l'Acad. des sciences de l'U.R.S.S. Série géophysique N° 3, 1954.

2. Beloussov (V. V.) et Gzovsky (M. V.) : Les conditions tectoniques et le mécanisme des tremblements de terre. Les trav. de l'Institut de géophysique de l'Acad. des sciences de l'U.R.S.S., N° 25, /1927 1954.
3. Beloussov (V. V.), Kirilova (I. V.), Sorsky (A. A.) : Etude sommaire de la séismicité et de la tectonique du Caucase. Izv. de l'Acad. des sciences de l'U. R. S. S. Série géophysique, N° 5, 1952.
4. Gorchkov (G. P.), Kostenko (N. P.) : Les méthodes d'investigation des mouvements tectoniques récents en rapport avec l'activité séismique. Revue de l'Université de Moscou, N° 10, 1953.
5. Kirilova (I. V.) : L'activité séismique dans les hauts pays d'Akalkalak. Izv. de l'Acad. des sciences de l'U. R. S. S., série géophysique, N° 1, 1952.
6. Kirilova (I. V.) : Le problème de la généralisation des cartes des épicentres dans le Caucase. Trav. de l'Institut de géophysique de l'Acad. des sciences de l'U. R. S. S. N° 30, /157/, 1955.
7. Krestnikov (V. N.) : Confrontation de l'activité séismique avec la structure géologique de la partie centrale du Caucase. Rapports de l'Acad. des sciences de l'U. R. S. S. V. 85, N° 5, 1952.
8. Krestnikov (V. N.) : L'évolution de la structure et la séismicité au Tian Chan. Izv. de l'Acad. des sciences de l'U.R.S.S. Série géologique. N° 3, 1954.
9. Medvedev (S. V.) : L'évaluation du degré d'intensité suivant l'élasticité des roches. Trav. de l'Institut de géophysique de l'Acad. des sciences de l'U. R. S. S. N° 14, /141/, 1952.
10. Medvedev (S. V.) : La nouvelle échelle d'intensité. Trav. de l'Institut de géophysique de l'Acad. des sciences de l'U. R. S. S. N° 21, /148/, 1953.
11. Medvedev (S. N.) : La dépendance des efforts séismiques de la période propre d'oscillation des constructions. Trav. de l'Institut de géophysique de l'Acad. des sciences de l'U. R. S. S. N° 36, /163/, 1956.
12. Nersessov (I. L.), Rastvorova (V.A.). : Le tremblement de terre de Vartachen en 1953. Izv. de l'Acad. des sciences de l'U. R. S. S. Série géophysique, N° 3, 1955.
13. Petrouchevsky (B. A.) : Le rôle de la géologie pour l'étude de la répartition de la séismicité. Trav. de l'Institut de géophysique de l'Acad. des sciences de l'U. R. S. S. N° 28, /155/, 1955.
14. Petrouchevsky (B. A.) : La plate-forme posthercynienne de l'Oural et de la Sibérie et le Tian Chan; l'évolution durant les ères Mésozoique et Cénozoique et l'activité séismique.
Les éditions de l'Acad. des sciences de l'U. R. S. S., 1955.
15. Petrouchevsky (B. A.), Resanov (I. A.), Rastvorova (V. A.) : Les conditions de la géologie séismique en Tourkménie. Izv. de l'Acad. des sciences de l'U. R. S. S. Série géophysique, N° 2, 1954.
16. Popov (V. V.), Resanov (I. A.) : Les mouvements tectoniques récents au Tian Chan et ses rapports avec l'activité séismique. Les problèmes de Géologie de l'Asie, v. 2, 1954.
17. Resanov (I. A.) : Le tremblement de terre de Kasandjik. Izv. Acad. des sciences de l'U. R. S. S. Série géophysique. N° 5, 1955.
18. Sorsky (A. A.) : L'activité séismique dans la région de Chemakha dans la Transcaucasie Orientale. Izv. de l'Acad. des sciences de l'U. R. S. S. Série géophysique. N° 3, 1955.

RESEARCHES ON THE NUTATION IN CONNECTION WITH SOME PROBLEMS OF THE CONSTITUTION OF THE EARTH

E. P. FEDOROV.

The present paper is intended to show that some conclusions about the interaction between the Earth's core and shell can be drawn from an investigation of the nutation.

It is to be reminded that equations of the nutation govern the motion of the Earth's angular momentum $\overline{G}$. They express the nutation in longitude (ψ) and that in obliquity ($\varepsilon - \varepsilon_0$) in functions of time :

$$\psi = f(t), \qquad \varepsilon - \varepsilon_0 = f'(t) \tag{1}$$

where ε_0 is the mean obliquity of the (fixed) ecliptic.

Since $\overline{G}$ is a vector laying in the equatorial plane XOY, it may be put under the form of a complex number, as follows

$$\dot{\overline{G}} = G(\sin \varepsilon\dot{\psi} + i\dot{\varepsilon}). \tag{2}$$

We confine ourselves to the discussion of the main and fortnightly terms in the nutation. For these we have the following theoretical expressions :

$$\begin{aligned} \sin \varepsilon\psi &= -6''869 \ \sin \Omega - 0''0812 \ \sin 2 \,☾, \\ \varepsilon - \varepsilon_0 &= +9''220 \ \cos \Omega + 0''0884 \cos 2 \,☾, \end{aligned} \tag{3}$$

in which Ω = the longitude of the ascending node of the Moon's orbit;

☾ = the Moon's mean longitude.

The computation of the coefficients in the above formulae have been made assuming the theoretical value for the constant of the nutation N, namely, that found by the equation

$$N = 231981''8 \, H \frac{\mu}{1+\mu}, \tag{4}$$

in which H is the Earth's dynamical ellipticity and μ the ratio of the Moon's mass to that of the Earth. The formulæ (3) and (4) were first obtained on the assumption that the Earth is rigid, but they are legitimate to all reasonable hypothesis of Earth's mechanical properties.

Observatories' positions are definite places on the Earth's surface. Since an observer is thus always attached to the shell so are the data obtained from astronomical observations relevant to the motion of the shell alone, but not of the Earth as a whole. It follows that with a view to comparison with observations we must take equations governing the motion of the angular momentum of the Earth's shell.

Let $\overline{L}$ be the couple arising from the attraction of the Moon and Sun on the shell. It can be easily shown that

$$\overline{L} = h\,G_s\ (\sin \varepsilon\dot{\psi} + i\dot{\varepsilon}) \tag{5}$$

where h is the ratio of dynamical ellipticity of the shell to that of the Earth as a whole.

Since we deal now with the shell, effect of the core regardless of its nature, should be considered as an action of some external forces. Denoting the moment of these forces by $\overline{M}$, we shall write the equation of motion, as follows

$$\dot{\overline{G}}_s = \overline{L} + \overline{M}. \tag{6}$$

The couple $\overline{M}$ transferes the angular momentum between the shell and the core, but does not affect the momentum of the Earth as a whole.

Let ψ_a and $\varepsilon_a - \varepsilon_0$ be the nutation in longitude and obliquity as obtained from astronomical observations. We have then

$$\dot{\overline{G}} = G\ (\sin \varepsilon\dot{\psi}_a + i\dot{\varepsilon}_a) \tag{7}$$

Let us put

$$\overline{M} = X + iY. \tag{8}$$

Substituting (5), (7), and (8) in (6), we have

$$X + iY = G_s[\sin \varepsilon(\dot{\psi}_a - h\dot{\psi}) + i(\dot{\varepsilon}_a - h\dot{\varepsilon})] \tag{9}$$

Now, it is interesting to compare this expression for $\overline{M}$ with that obtained on the assumption that no motion of the core relative to the shell is possible, as would be if the core is rigid. For this special case we denote the couple araising from a mutual action between the core and shell by

$$\overline{M}' = X' + iY'$$

and the angular momentum of the shell by $\overline{G}'_s$. The direction of the latter is practically the same as that of the vector $\overline{G}$, and consequently, its motion is governed by the equation

$$\dot{\overline{G}}'_s = G_s\ (\sin \varepsilon\dot{\psi} + i\dot{\varepsilon}) \tag{10}$$

where ψ and ε are also the same as in (2).

Substituting the values of $\overline{G}'_s$ and $\overline{L}$ given by (10) and (5) in the equation

$$\overline{M'} = \dot{\overline{G'}} - \overline{L},$$

we find

$$X' + iY' = G_s (1 - h) (\sin \varepsilon \dot{\psi} + i \dot{\varepsilon}) \quad (11)$$

Let A_c be the equatorial moment of inertia of the core, A that of the Earth as a whole and H_c the dynamical ellipticity of the core. According to Bullen [1]

$$\frac{A_c}{A} = 0.112, \quad H_c = 0.0026.$$

Then

$$h = 1.027.$$

Let n be the Earth's angular velocity. We have

$$\Omega = \alpha t, \quad (\alpha = -0.000146\, n),$$

$$2 \,☾ = \beta t, \quad (\beta = +0.013\, n).$$

Substition of (3) in (11) leads to the following equation

$$X' + iY' = (\overline{U}_1 + \overline{U}_2) + (\overline{V}_1 + \overline{V}_2) \quad (12)$$

where

$$\overline{V}_1 = 0''.217\, \alpha\, G_s\, e^{i\alpha t}, \qquad \overline{V}_2 = -0''.032\, \alpha\, G_s\, e^{-i\alpha t}$$
$$\overline{V}_1 = 0''.0023\, \beta\, G_s\, e^{i\alpha t}, \qquad \overline{V}_2 = -0''.0001\, \beta\, G_s\, e^{-i\alpha t}. \quad (13)$$

The meaning which has to be attached to (12) is then that in vector representation the couple acting on the shell consists of two components, one is due to the main term in the nutation and another to the fortnightly term. Each of them in turn can be resolved into two vectors rotating in space in opposite directions. However, relative to the Earth itself all the vectors are rotating clockwise, but with different angular velocities. Such is the theoretical expression of the action between the shell and core obtained under the assumption that no relative motion of the latter with regard to the former is possible.

Let us consider now the actual motion of the momentum $\overline{G}_s$. The equation of this motion must, naturally, result from astronomical observations. Therefore, it should be a present task for us to obtain the expressions for ψ_a and $\varepsilon_a - \varepsilon_0$. Only the most extended series of astronomical observations suit this task and, first of all, latitude observations.

The expression for the main term in the nutation has been derived using the observations at Carloforte, Mizusava and Ukiah from 1900 till 1934 [2]. The total of about 135000 observations has been turn to account. The same materials have been used for the fortnightly term, but in addition I have availed miself of the results obtained by H. R. Morgan [3] from the observations with the

P.Z.T. at Washington from 1931 till 1951 and those obtained by A. J. Orlov from latitude observations at Pulkovo from 1915 till 1928 [4]. Thus, the amount of the observations that have been used to derive the expression for the fortnightly term totals 230000.

The results thereby obtained are as follows

$$\begin{aligned} \sin \varepsilon\, \psi_a &= -6.''853 \sin \Omega + 0.''008 \cos \Omega - 0.''0866 \sin 2 ☾ + 0.''0019 \cos 2 ☾ \\ \varepsilon_a\text{-}\varepsilon_o &= +9.''198 \cos \Omega - 0.''001 \sin \Omega + 0.''0894 \cos 2 ☾ + 0.''0019 \sin 2 ☾ \end{aligned} \qquad (15)$$

As to the details of calculation, I do not dwell on them, for they are given in the previous papers [5, 6].

These values of $\sin \varepsilon\, \psi_a$ and $\varepsilon_a\text{-}\varepsilon_o$ substituted in (9) give

$$X + iY = (1.09 + 0.02\, i)\, \overline{U}_1 + (1.09 + 0.13\, i)\, \overline{U}_2 + (-0.43 + 0.83\, i)\, \overline{V}_1 + 24\, \overline{V}_2. \qquad (15)$$

Having regard to the uncertainties of some observed values, as well as the computed values of N and h, it is not easy to say to what extend the result can be trusted. Nevertheless, some of the conclusions that can be drawn from the equation (12) are likely to diserve credit. We note especially three of them.

1. The actual magnitude of the vector $\overline{U}_1$ as inferred from observational data is larger than that for the rigid core.

2. The actual direction of the vector $\overline{V}_1$ is opposite to that for the rigid core.

3. Both vectors ($\overline{U}_1$ and $\overline{U}_2$) that are due to the main term in the nutation are turned clockwise, that is in the direction of the rotation of these vectors relative to the Earth.

At the first sight the results (1) and (2) seem to contradict one another. However this contradiction evaporates under more close consideration. The theory of the dynamical effects of the liquid core developed by F. A. Sludsky [7], H. Poincaré [8] and H. Jeffreys [9] offers a possible explanation of the results (1) and (2) : the observed changes of the vectors $\overline{U}_1$ and $\overline{V}_1$ agree in sight with what would be expected on this theory.

The result (3) appears to be attributable to dissipation of energy due to the friction on the boundary of the core or to some similar phenomena.

The quantitative comparison makes no sense, for the theory is yet incomplete and observational data lack accuracy. For such a comparison to be possible much theoretical work needs to be done and new results of astronomical observations to be worked up.

RÉFÉRENCES.

1. BULLEN (K.) : M. N. R. A. S. Geoph. Suppl. *3*, 5 (1936).
2. FEDOROV (E. P.) : Astr. Circ. of the USSR, N. 164 (1955).
3. MORGAN (H. R.) : Astr. Journ. *57*, 232 (1952).
4. ORLOV (A. J.) : Astr. Circ. of the USSR, N. 126 (1952).
5. FEDOROV (E. P.) : Comptes rendus, Acad. des Sc. URSS, *91*, 759 (1953).
6. FEDOROV (E. P.) : Astr. Circ. of the USSR, N. 148 (1954).
7. SLUDSKY (F.) : Bull. de la Société des Natur. de Moscou, n. 2 (1895).
8. POINCARÉ (H.) : Bull. astr., *27*, 321 (1910).
9. JEFFREYS (H.) : M. N. R. A. S., *109*, 670 (1949).

SECULAR CRUSTAL MOVEMENTS OF THE EAST-EUROPEAN PLAIN AND ASSOCIATED PROBLEMS

J. A. MESCHERIKOV (U.S.S.R.).

INTRODUCTION. METHODS OF RESEARCH.

Crustal movements which are taking place at the present time are subdivided into two groups. The first consists of fast or seismic movements; the second — of slow movements called also secular movements.

Beginning with 1950 the Geographical Institute of the USSR Academy of Sciences and the Central Scientific-Research Institute of Geodesy, Airsurvey and Cartography are carrying out a systematic study of secular tectonic movements on the territory of the Soviet Union. A characteristic feature of the researches conducted under the direction of Academician I. P. Gerasimov and Prof. J. V. Filippov is a strictly complex approach. To study secular movements three methods are being used simultaneously : (A) precise levelling; (B) tide-gauge observations and (C) geological and geomorphological researches. The compilation of a map of secular movements for the West of the European part of USSR (fig. 1) was the first stage of this work.

The map is based on a network of precise levellings with a total length of about 20 000 km. The first levelling was done during the period between 1913 and 1932, the second — between 1945 and 1950. Precise levelling data were coordinated with foot gauges on the coasts of the Baltic, Azov and Black seas[1]. As a result absolute values were calculated for crustal movements rates (in mm per year) for 250 points.

Geological and physiographic researches included : (1) study of bench-marks, datums and foot-gauge readings in order to calculate their stability and exclude points subjected to local displacements of a non-tectonic character and due to landslides, heavings and swellings of the ground; (2) analysis of neotectonics and especially of Postglacial (Holocene) movements. To establish young movements a study was carried out of the morphology of river and sea terraces as well as of the thickness and composition of various depo-

1. Methods of analyses and treatment of geodetic and tide-gauge data are dealt with in the report by M. I. Siniagina, submitted to the present Assembly of the International Geodetic and Geophysical Union.

sits (particularly of flood plain alluvium). Comparison of geological and physiographic data with geodetic materials served to check the

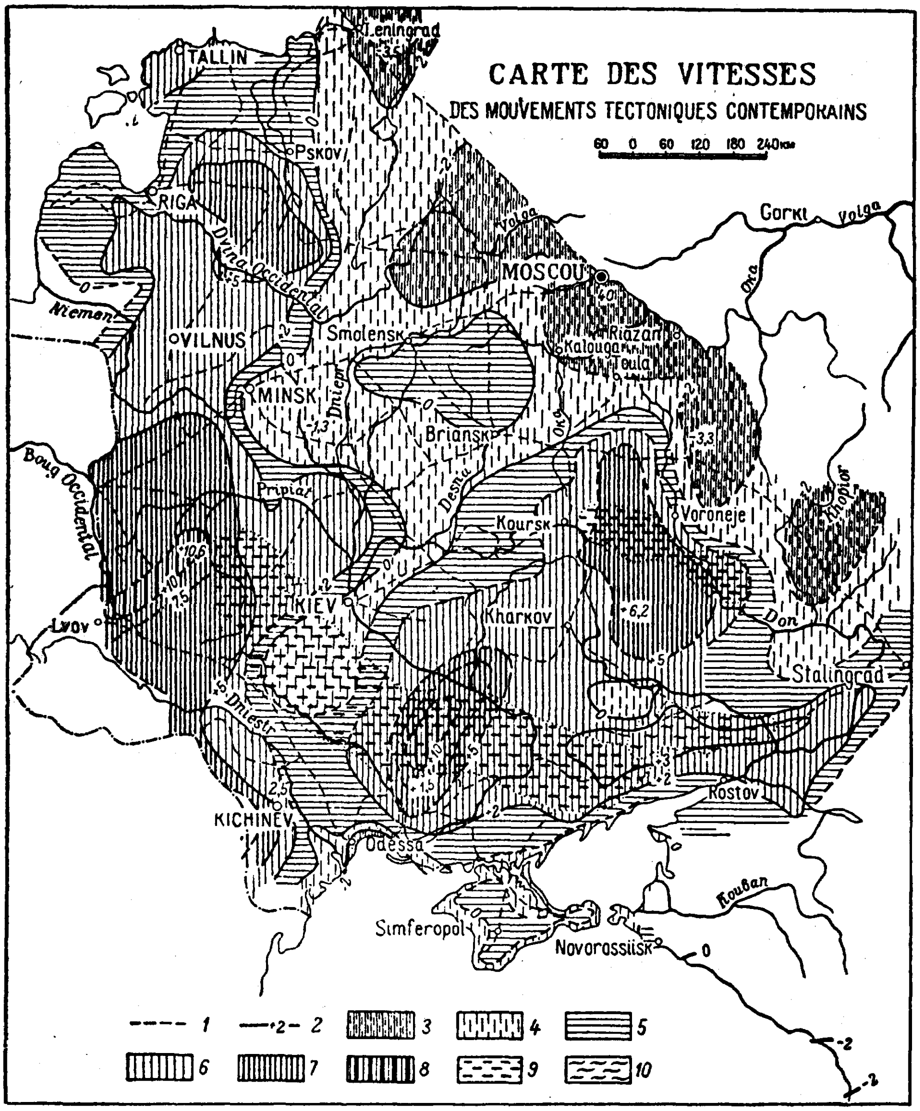

FIG. 1. *Map of secular movements in the Western half of the European part of USSR.* Compiled by M. I. Siniagina, L. G. Kamanin, J. A. Mescherikov, V. A. Zenin, A. W. Zhivago. Edit. Academician I. P. Gerasimov.

1. — Lines of precise levelling.
2. — Rate of present tectonic movements (mm. per year).
3-4. — Subsidences.
5-8. — Uplifts.
9. — Uplifted blocks of the crystalline basement.
10. — Outcrops of folded Paleozoic rock (Donetz basin).

latter and provided sufficiently reliable and fully substantiated conclusions on secular movements.

Results.

Within the studied territory of the East-European plain several large zones of elevation have been established separated by zones of absolute or relative subsidence.

Two *zones of uplift* are of special interest. (A) The Esthonian-Carpathian zone which includes the Southern slope of the Baltic shield, the Belorussian-Lithuanian uplifted block of the basement, the « Polessie bridge » and the Western part of the Ukrainian crystalline massive. This zone can be regarded as a prolongation of the contemporary uplift of Fennoscandia. The establishment of a big present uplift within the East-European plain, extending from the Baltic sea coast and up to the foothills of the Carpathian mountains was among the most interesting and unexpected results of the investigation, because until then it was thought that the uplift dies out somewhere within the borders of Esthonia.

(B) The Middle-Russian zone of uplift is associated with the Voronezh block of the crystalline basement and includes as well the area of the Donetz ridge, the Azov massive and the Krivoi Rog structure of the Ukranian massive.

Among the zones of subsidence four territories have been studied with more details : (1) Ilmen-Dnieper zone, separating the Esthonian-Carpathian uplift from the Middle-Russian zone of elevation. This zone of an absolute and relative subsidence stretches from the Finnish Bay up to the Black sea; it includes the Western part of the Moscow and Dnieper-Don sedimentary basins. East of the Middle-Russian uplift the Tambov-Kuban subsidence zone is found (II). An independent area of subsidence (III) is attached to the Black sea — Azov sea depression. Outlines of the Baltic zone of subsidence (IV) have been traced embracing the Western part of Lithuania.

Some points within the studied territory are characterized by the following intensities of secular movements.

The average values of uplifts and subsidences of the East-European plain can be estimated at 2-4 mm. per year. Maximum intensities of movement (uplift) come to 7-10 mm. per year. It is characteristic that the transition from the zone of uplift to the zone of subsidence often happens in a comparatively narrow stretch of a linear orientation and looks like a flexure bend.

Largest contemporary flexures of that type form the Eastern boundary of the Esthonian-Carpathian and Middle-Russian uplifts.

Station	Secular movement (mm/year)	Probable error (mm/year)
Tallinn	+ 2.3	
Rezekne	+ 5.3	±1.7
Vilnus	+ 3.8	
Baranovichi	+ 5.5	±2.1
Sarny	+ 9.5	
Vitebsk	— 1.4	
Moscow	— 3.7	±2.3
Odessa	— 5.1	
Kursk	+ 3.6	
Kharkov	+ 3.9	
Stalingrad	+ 1.3	±1.9
Krivoi Rog district	+10.8	
Donetz basin	+ 3.7	±1.1

Generally speaking, present deformations of the Earth's crust in the European part of the USSR have an appearance of big waves with a predominant meridional trend.

Discussion.

Scarcity of factual data available on secular movements resulted in a rather poor knowledge of the laws which govern them. There are different and often contradictory opinions on all questions regarding the origin of secular movements, their relations to the structural elements of the Earth's crust and various processes which take place in its depths as well as on its surface. Abundant material on secular movements of the East-European plain permits to express a number of well founded views on these subjects and give a critical appreciation of existing theories. Comparing secular movements of the East-European plain with movements in other territories (fig. 2, 4, 5), we will attempt to establish certain common features and local specific characteristics of secular movements. In doing so we will try everywhere to draw a line between sufficiently studied points and the problems which are not clear yet and demand a further study.

Relation of secular movements to geological structure and to the phenomena of isostasy. In studying the East-European plain it has been established that throughout the entire territory from the Baltic sea to the Black sea there is not a single substantial stretch of land where secular movements would be absent. Experience shows that present movements of a certain sign and rate are to be found everywhere where their study is being started. Apparently, secular movements are a most universal form of present tectonic manifestations. They embrace both mountain areas and flats, continents and sea bottoms. That is why ideas regarding the existence somewhere of « stable » sections of the crust devoid of secular movements should be considered as absolutely unfounded. In particular, it is necessary to discard completely as an obsolete notion the idea of a tectonic passivity or immobility of plain-platform regions during the Quaternary period and at the present time.

Slow crustal movements in platform regions are often explained by the phenomena of glacio-isostasy. According to his theory, regions of Quaternary glaciation, after the melting of ice caps, experience an uplift, while extraglacial regions are stable or subside. To what extent is this point of view confirmed by data accumulated on the Russian plain and in other territories? As figure 1 shows, a number of uplifts has been found in the extra-glacial area of the European part of the Soviet Union and their rate is no less than the intensity of uplifts in the center of glacia-tion in Fennoscandia. For instance, the uplift in the district of Krivoi Rog amounts to 10 mm. per year, the uplift of the Middle Russian highland — to 6 mm. per year. Intense uplifts have also been discovered on the islands of Japan, in the Indus-Ganges plain and other extraglacial regions (fig. 2). Thus, the theory of isostasy can not fully explain the distribution of present areas of subsidence and uplift.

In comparing the map of secular movements with tectonic maps it becomes evident that the sign of present movements is to a great extent determined by the geological structure. The East-European platform is represented by positive structures — the basement blocks experience an uplift (Voronezh block, Ukrainian massive, etc.), while the sedimentary basins (Moscow, Dnieper and others) are mostly sinking. Analyses of detailed structural and geophysi-cal maps compiled during the prospecting for oil on the Russian platform, show that very often even the details of present move-ments are determined by deep-seated structures (fig. 3). Depen-dence of secular movements upon geological structures has been established also for other territories — both platforms and oroge-nic ones. For the territory of the Netherlands which has been studied in details, a great similarity has been recorded between the map of secular movements and the structure of Tertiary rocks

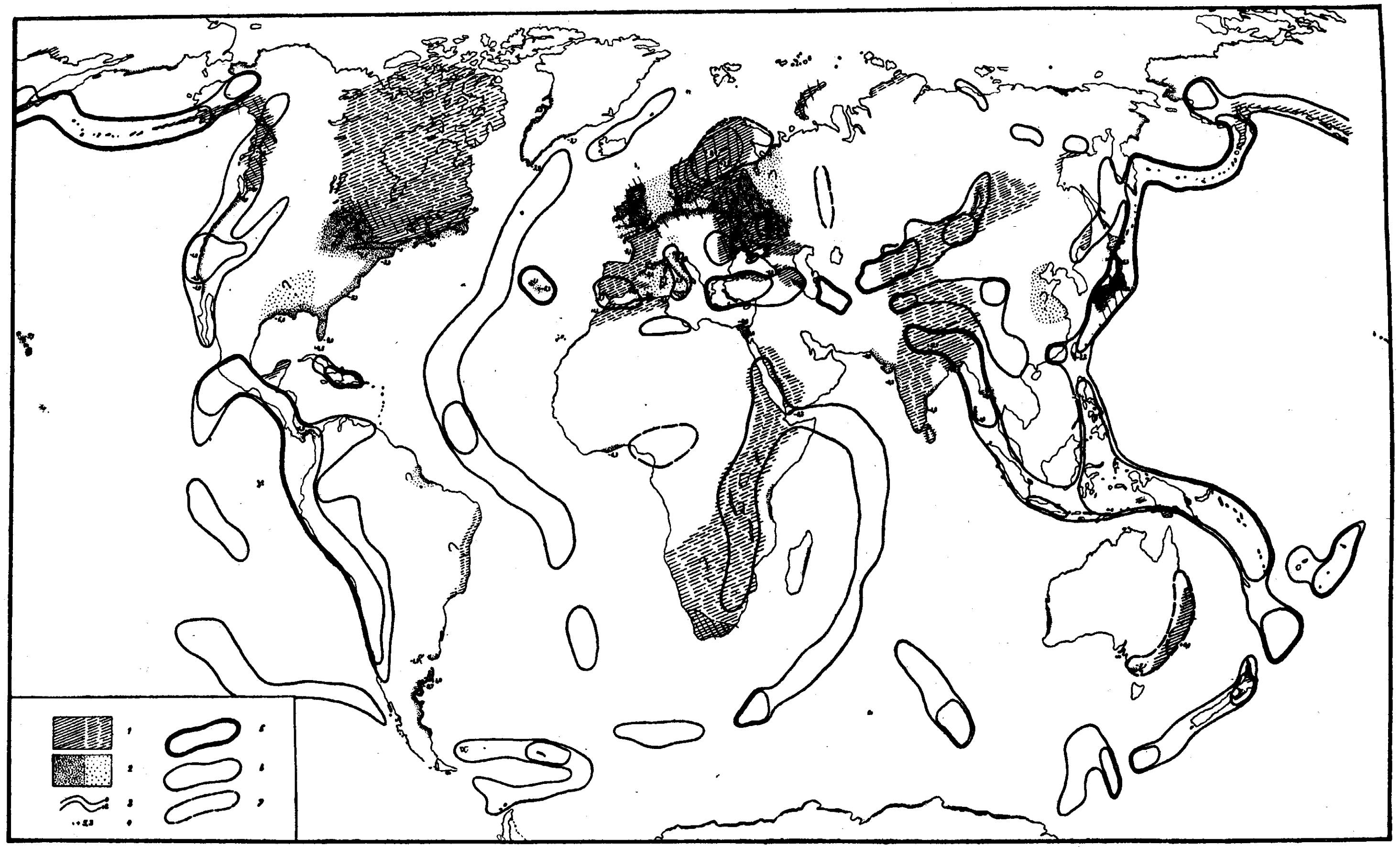

FIG. 2. *Sketch of present tectonic movements of the Earth.* Compiled by J. A. Mescherikov. Data used : Association d'Océanographie physique (1954), M. I. Siniagina & oth. (1956), G. P. Gorshkov (1952), H. Valentin (1952, 1954), Sh. Moore (1948), E. Kääriäinen (1953), T. Nakano (1954) and others.

Slow (*secular*) *movements.*

1. Regions of present uplift (established and supposed); 2. Regions of present subsidence (established and supposed); 3. Isolines of secular movements; 4. Rate of secular movements (mm per year).

Fast (*seismic*) *movements.*

5. Regions of intense and frequent earthquakes; 6. Regions of more moderate and sporadic earthquakes; 7. Separate

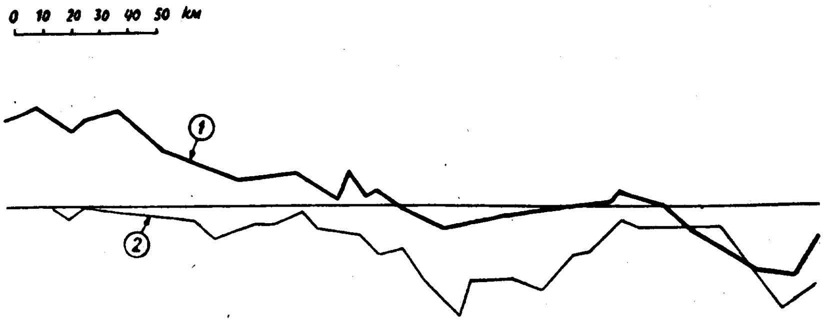

FIG. 3. *Curve of present tectonic movements* (1) and *geophysical profile* (2) *in a district of Northern Caucasus* (Rostov-Armavir).

(fig. 4). The correlation ratio between the intensities of present movements « v » and depths of the Tertiary deposits bottom « H » is, according to our estimates, $r = 0{,}82$. On the islands of Japan

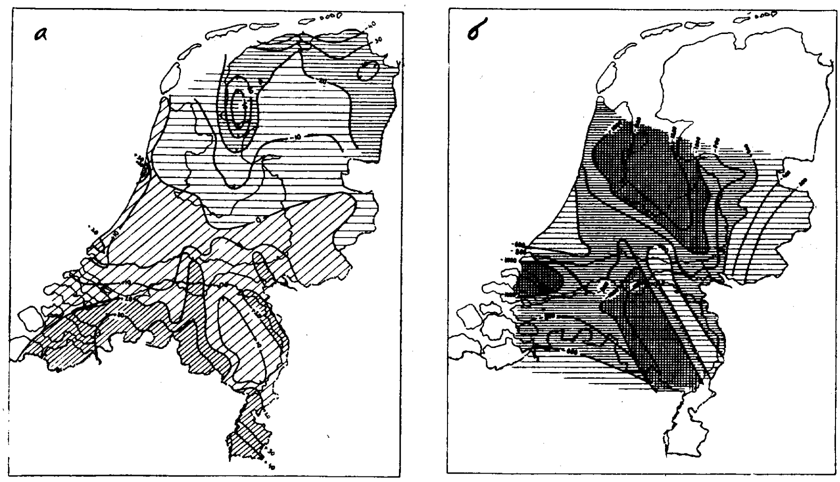

FIG. 4. *Comparison of present tectonic movements and the geological structure of the Netherlands* (after T. Edelman, 1954, and A. J. Pannekoek, 1954).

a) Values of secular movements (in relation to Amsterdam for the period from 1875-87 up to 1926-40).

b) Bottom relief of Tertiary deposits.

present uplifts and subsidences coincide with transversal zones of young undulations which have been pointed out on the basis of geological and geomorphological data by F. Ruellan (1932), (fig. 5). Compared to the platform regions, the orogenic part of the Japanese islands is characterized by a greater differentiation of secular movements and increased values of movement gradients. Consequently, present tectonic manifestations should be regarded as a regular continuation of those tendencies in the development of the Earth's crust which have been taking place throughout the entire

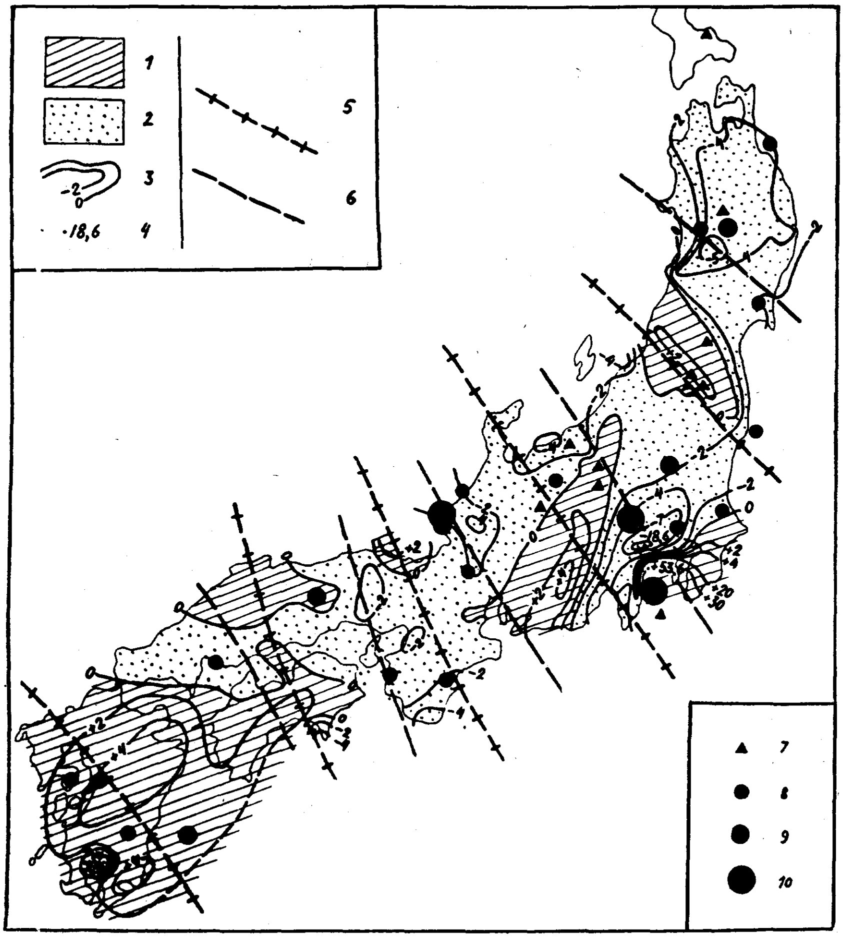

FIG. 5. *Present tectonic movements of Japanese islands for 1900-1928* (after T. Nakano, 1954).

1. Regions of uplift.
2. Regions of subsidence.
3. Isolines of presents movements.
4. Movement intensities (in mm. per year).
5. Transversal uplifts.
6. Transversal downwarps (5 & 6 after F. Ruellan, 1932).
7. Manifestations of present volcanism.
8. 10. Earthquake epicenters of varying intensity.

geological history and have found their expression in geological structures and large relief features[2].

Though present movements to a great extent repeat the features of ancient movements, they also have a number of peculiar aspects which it would be wrong to disregard. Data on the Russian platform not only proves coincidences of secular movements with geological structures, but also facts of discrepancies between them. It happens that vast zones of present uplifts include not only positive, but also some negative structural elements. For instance, the Esthonian-Carpathian uplift zone includes along with anticlinal structural elements, also some negative structures like the so-called Latvian basin and Carpathian marginal basin. Separate large structural elements of the basement are unlike in their sign of present tectonic movements. For instance, the axial line of the Ukrainian massive undergoes an undulation at the present time : the Eastern and Western parts of the massive are subjected to a rise, while the middle part is sinking.

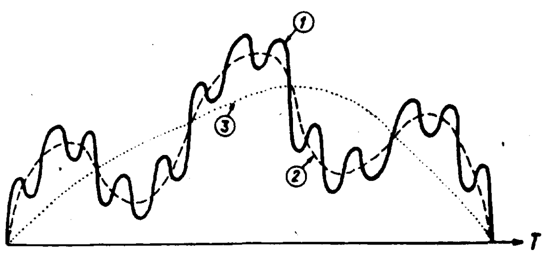

FIG. 6. *Combination of oscillation movement of different orders* (after N. I Nikolaev, 1949).

1. Movements detected by precise levelling.
2, 3. Movements detected by geological and geomorphological methods.

For the time being we can not work out any laws governing the spatial distribution of secular uplifts and subsidences with any

2. From this point of view it seems necessary to reconsider the traditional viewpoint upon the nature of contemporary uplift of Fennoscandia and the Canadian shield in order to avoid an over-estimation of the isostatic factor. Investigating these territories with a sufficiently wide historical background, it is possible to state that their most characteristic feature is a tendency of an uplift which became manifest long before the Glaciation period. In Postglacial time, owing to a release from the load of ice, the uplift of the Baltic and Canadion shields, was, probably, greatly intensified. However, by the present time, the isostatic factor has been exhausted, which is proven by a « retardation of land uplift » of the Baltic shield during the last six or eight thousands of years (Kääriäinen, 1953). That is why the present uplift of the Baltic and Canadian shields, which in its intensity practically does not differ from uplifts in extraglacial regions, should also be ascribed to the influence of endogenetic process, associated, apparently, with the migration of subcrustal masses (Magnitsky 1953).

degree of precision and can formulate in this respect only our surmises and hypothesis. In the author's opinion the picture of secular movements of the East-European plain can be most satisfactorily interpreted along the lines of ideas expressed by A. P. Karpinsky (1894) in his paper on the tectonics of the Russian platform. According to Karpinsky during each moment of its geological history the platform was experiencing movements of two types : (A) directed movements of separate blocks of the basement, mainly along fractures; and (B) smooth undulating movements of a tangential origin. The undulating movements of the Russian platform had an interchanging meridional (« Ural ») and latitudinal (« Caucasian ») trend. For the Quaternary period Karpinsky suggested a predominance of oscillations of a meridional trend, which is in full accord with data on present tectonics.

The existence of present meridional « waves » superimposed on block movements of separate masses is confirmed not only by analyses of events on the Russian platform but also by data, even if, unfortunately, scanty ones, on other territories. There are reasons to suggest a meridional « wave » in Western Europe, parallel to the Esthonian-Carpathian uplift and including the uplift of the British Isles, France and Iberian peninsula. The big role of meridional trends in present tectonic life of the Earth becomes obvious from analyses of seismicity (*fig.* 2). In this connection it should be pointed out that the present uplift of the Baltic shield and the Esthonian--Carpathian zone are, probably, not by accident located on a sort of prolongation of active seismic zones of the Balkan peninsula and East Africa (*fig.* 2).

In such a way the spatial distribution of secular uplifts and subsidences can not be satisfactorily explained from the positions of the glacio-isostatic theory. Both in the geological past and during present times slow crustal movements were determined mainly by endogenetic processes, associated, apparently, with displacements of subcrustal masses and possibly with the changes in the volume of the planet. However, the establishment of laws governing the distribution of secular movements of different signs remains still, to a great extent, a problem of the future.

Intensity of present movements. It can be taken for an established fact that slow movements of the Earth's crust are measured everywhere in values of several millimeters per year. Average intensities in platform regions with a plain topography and those in mobile, orogenic zones do not differ so strongly as it could be expected. For instance, on the Japanese islands the rates of movements usually do not exceed 4-5 mm. per year (*fig.* 5). However, in some points of orogenic regions these intensities amount to 20-50 mm. per year (Kanto region in Japan and possibly South-Eastern Caucasus) — such intensities for platform regions are unknown of. Maximum intensities within platforms do not exceed 10-11 mm. per year.

If the spatial distribution of regions of present uplifts and subsidences is dependent to a great extent upon the distribution of anticlinal and synclinal zones, the intensities of present and ancient movements are values of a completely different order. As geological and geomorphologica data show, by estimating the thickness of deposits and the deformations of erosion surfaces intensities of movements are being estimated expressed not in whole millimeters per year, but only in tenths or even hundredths of millimeters per year.

What explanation could be offered for this contradiction? There are two possible solutions : (A) The intensity of movements had sharply increased during the very recent time; (B) crustal movements are of a complex oscillatory character and the sign of the movements can change in the course of time. During the lengthy period of geological time a sort of a mean movement is being worked out. Geodetic methods display elementary oscillations — sort of « microstructure » of movements, while geological and geomorphological methods permit to establish more general tendencies of movements — so to say their « macrostructures ».

In our opinion suggestion (B) is better founded. Changes in signs of young movements are established by many data. For instance, analyses of geomorphological features of the North-West of the Russian plain has shown that subsidence in the district of lake Ilmen occured not earlier than 3-5 thousand years ago; previously this area was subjected to an uplift which could have been intensified by an isostatic « floating ». Certain indications of changes in signs of present movements are provided by numerous levellings in Japan and by some lengthy tide-gauge observations. However, the question of periods in present crustal movements is yet quite unclear. It is possible only to suppose that secular movements, as their name suggests, keep their sign for at least a few centuries [3].

3. Actual secular movements are, apparently, superimposed by oscillations with a very short period and large amplitudes. These oscillations, indicated by some geodesists, are, in all probability, of a non-tectonic origin. It is possible to assume that with a sufficiently long time interval between levellings (not less than 20 years), oscillations of this type are somewhat compensated and their influence is excluded.

Relations between secular movements and seismicity and their influence on the course of exogenetic processes. Slow — secular and fast — seismic movements are, undoubtedly, mutually connected. The dependence between the intensity and gradients of secular movements and the location of earthquake epicenters has been outlined for the Japanese islands (Nakano, 1954). Such a dependence takes place on platforms as well. It has been established now that the viewpoint of regarding platforms as absolutely aseismic areas is incorrect. In particular, during the past 150 years 76 slight earthquakes took place on the Russian platform (Andreev, 1956). A comparison of the map of secular movements and the map of epicenters on the Russian platform permits to speak about a certain correlation between them. The majority of strongest earthquakes is attached to flexure-like tracks separating sections of present uplifts and subsidences. It has also been observed that epicenters have more tendency to be associated with regions of uplifts than with territories of subsidences. Such a connection between seismic and secular movements testifies to their genetic association and serves as an additional confirmation of the fact that secular movements are controlled by endogenetic processes taking place in the interior of the Earth's crust.

Until recently the absence of reliable quantitative data on secular movements made it impossible to consider their influence upon present process of landscape-making and continental sedimentation. That is probably why an impression was created that this influence is most insignificant and especially so in « quiet » areas of platforms. A study of secular movements of the East-European plain permits to establish many new facts demonstrating the great influence which secular movements exercise upon various exogenetic processes. It was proven, for instance, that in the Baltic provinces the distribution and thickness of peat bogs is largely controlled by secular movements. The thickest deposits of peat (« peat basins » of M. N. Nikonov) are associated with regions of subsidence. Prof. K. K. Orviku (Tartu) has established, among other things, that in the North-West of Esthonia, where an uplift is taking place and the level of underground waters is gradually falling, the thickness of peat deposits does not exceed 1 m. In the South-East of Esthonia, where the uplift proceeds at a slackened rate and the water level is rising, the thickness of peat bogs comes to 6-7 m. Under different morphoclimatic conditions like in the zone of South-Russian steppes, the influence of tectonic movements on gully erosion has been registered. Young uplifts are characterized by increased intensity of gully development.

Exceptionally great is the influence of secular movements on the work of rivers. This is demonstrated by the morphology of stream valleys and by specific features of alluvial deposits. For instance, during a traverse of the Esthonian-Carpathian uplift a deformation of terraces has been observed in the valley of Zapadnaia Dvina (*fig.* 7); the flood plain deposits here are very thin and

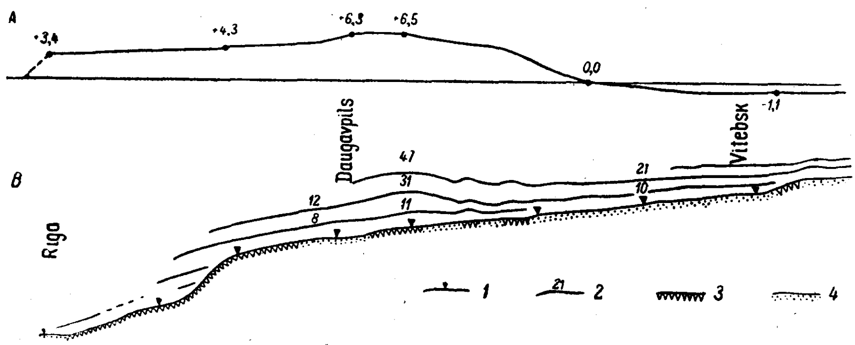

FIG. 7. *Sections along the valley of the river Zapadnaia Dvina.* Compiled by J. A. Mescherikov.

A — Curve of present tectonic movements (figures of uplifts and subsidences in mm. per year) .

B — Geomorphological section of the valley.

1. Longitudinal section of the river.
2. Longitudinal sections of terraces.
3. River bed in bedrock.
4. River bed in Quaternary deposits.

the river bed cuts into the bedrock. On the other hand, in the regions of present subsidence the terraces are often submerged, the thickness of river deposits is increasing and an accumulation of alluvium is taking place. On the basis of logging records and field observations a map showing thickness of present (Holocene) river deposits (*fig.* 8) has been compiled for the North-West of the European part of the USSR. A comparison of this map with a map of secular movements permits to find an explanation of many specific features of present erosional processes.

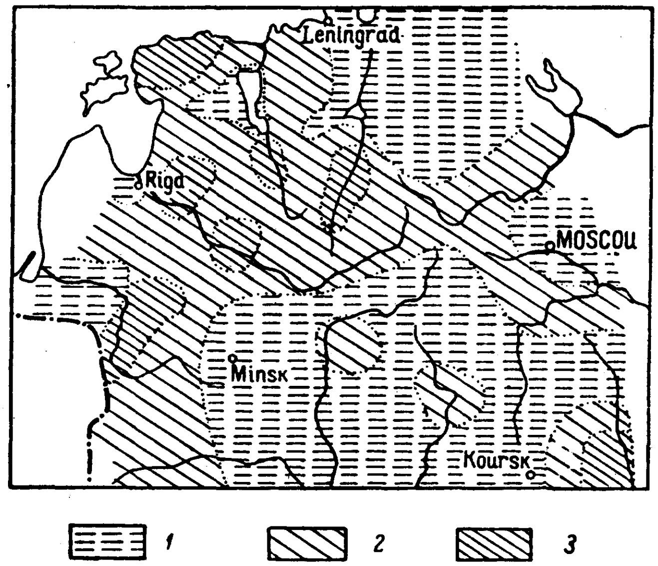

FIG. 8. *Sketch of alluvium thickness in the Nort-West of the European part of USSR.* Compiled by J. A. Mescherikov.

1. Regions with a predominance of accumulation, with increased thicknesses of flood plain deposits.
2. Regions with a predominance of erosion, with decreased thicknesses of flood plain deposits.
3. Regions of the most intense erosion, with thin flood plain alluvium.

J. MESCHERIKOV.

REFERENCES.

ANDREEV S.S. (АНДРЕЕВ С.С.) О сейсмической характеристике Русской платформы.-Изв. Акад. наук СССР, сер. геофиз., № 12, 1956.

BELOUSOV V. V. (БЕЛОУСОВ В.В.) Основные вопросы геотектоники. М., 1954.

EDELMAN T. Tectonic movements as resulting from the comparison of two precision levellings. Geologie en Mijnbow, N° 6, 1954.

GERASIMOV I.P. (ГЕРАСИМОВ И.П.)Современные движения и новейшая тектоника.-Проблемы физич. географии, т. ХУ, 1950.

GORSHKOV G.P. (ГОРШКОВ Г.П.) Карта сейсмичности Земли.—Большая Советокая энциклопедия. 2 изд., т. 16, 1952.

GUTENBERG B. Changes in sea level, postglacial uplift and mobility of the earth's interior. Bull. Geol. Soc. America, V. 52, N° 5, 1941.

KAARIAINEN E. On the recent uplift of the earth's crust in Finland. — Veröffentlichungen des Finnischen Geodät. Inst., N° 42, 1953.

KARPINSKY A. P. (КАРПИНСКИЙ А.П.) Общий характер колебаний емной коры в пределах Европейской России. — Изв. Акад. наук, серия, № 1, 1894.

KUKKAMAKI T. J. Secular movements of the earth's surface observed in the world. — Comptes rendus des séances de travail de la section des nivellements de l'Assoc. Intern. de Géodésie. — Bull. geod., Suppl. N° 34, 1954.

MAGNITZKY V.A. (МАГНИЦКИЙ) В.А. Основы физики Земли. М. 1953..

MESCHERIKOV J. A. et SINYAGUINA M. I. Les mouvements contemporains de l'écorce terrestre et les méthodes de leur étude. Essais de Géographie. Recueil des articles pour le XVIII[e] Congrès International Géographique, Moscou, 1956.

MIYABE N. Vertical earth movements in Japan as deduced from the results of rerunning the precise levels. — Bull. of the Earthquake Research Institute, XXX, part. 2, 1952.

MOORE Sh. Crustal movement in the Great Lakes area. — Bull. Geol. Soc. of America, V. 59, N° 7, 1948.

NAKANO T. Crustal movement and shoreline development along the Pacific coast of Japan since Holocene period. A report on the geomorphological studies of lowlands of Japan. — Bull. of the Geographical Survey Institute, vol. IV, part 1, 1954.

NIKOLAEV N.I. НИКОЛАЕВ Н.И. Новейшая тектоника СССР. Труды комиссии по изучению четвергичного периода Акад. наук СССР, т. 8, 1949.

PANNEKOCK A. J. Tertiary and Quaternary subsidence in the Netherlands. Geologie en Mijnbow, N° 6, 1954.

RUELLAN F. Relief et structure du Japon du Sud-ouest. — Annales de Géographie, 1932.

Secular variation of sea-level. Association d'Océanographie physique. Union Géodésique et Géophysique Internationale. Publication scientifique, N° 13, 1954.

VALENTIN H. Die Küsten der Erde. Ergänzungsheft N° 246 zu 1952 Peterm. Geogr. Mitt., 2 Aufl. 1954.

VALENTIN H. Gegenwärtige Niveauredänderungen im Nordseeraum. — Peterm. Geogr. Mitteilungen, 2 Quartalsheft, 1954.

ZHIVAGO A.V., ZENIN V.A., KAMANIN L.G. MESÇHERIKOV J.A. and SINIAGINA M.И. (ЖИВАГО А.В., ЗЕНИН В.А., КАМАНИН Л.Г., МЕЩЕРЯКОВ Ю.А. и СИНЯГИНА М.И.) Некоторые итоги изучения современных тектонических движений в западной половине Европейской части СССР.—Изв. Акад. наук СССР, сер. Географ., № 1, 1956.

AN INVESTIGATION OF ELASTIC PROPERTIES OF ROCKS AT HIGH PRESSURES

by M. P. VOLAROVICH, D. B. BALASHOV and Z. I. STAKHOVSKAYA.

The study of the physical-mechanical properties of rocks at high pressures is of great interest for geophysics as well as for the geological sciences /1/. However, investigations of this kind are not numerous. Thus the geologist's Handbook of Physical Constants /2/ contains a considerable amount of data on the elastic properties of rocks at atmospheric pressure, but gives very few results of experiments at high pressures. In particular, the elastic moduli of rocks at high pressures have not been measured so far by the static method.

The papers by J. R. Balsley /3/, J. Handin /4/, D. T. Griggs and collaborators /5/ and E. C. Robertson /6/ who studied the deformations as well as the strength of rocks at high pressures, give no numerical data concerning elasticity moduli. Nor was the shear modulus calculated in investigations carried out after the method of torsion of thin rock plates under uniaxial pressures of up to several tens of thousands of kg/cm^2 /7, 8/. Only recently D. S. Hugues and H. J. Jones /9/ carried out a direct measurement of the velocity of elastic ultrasonic waves in several rock specimens at pressures of several thousands kg. per cm^2, while U. V. Riznichenko and collaborators /10/ studied the influence of uniaxial pressure on the velocity of longitudinal and transverse waves in rock specimens. In connection with these we undertook an investigation of the velocity of elastic waves, as well as Young's modulus of rocks under a confining pressure of up to 5.000 kg/cm^2.

Measurements of the velocity of longitudinal waves in rock specimens were carried out by the pulse method at a frequency of about 100,000 c. p. s. in a special high-pressure apparatus /11/. The rock specimen 4 (see *Fig.* 1) 30 to 12 cm long was placed inside the body 1 of a high-pressure bomb in special holders 2 and 3 . The top of the bomb was capped with the body 7 of an four conductor electric lead-in; the body was kept in place by means of a threaded plug 8. The bomb body had an aperture in its bottom for a union 9 which was held in place by threaded plug 10. The purpose of this union was to allow the pressure carrying medium, nitrogen, to enter the bomb. Seals 11 and 12 are based on the principle of unsupported area (after Bridgman) /12/. Nitrogen was pumped into the bomb through a thick-walled steel pipe connected to the union, by means of a 5.000 kg/cm² L. Vereshchagin and V. Ivanov type gas compressor /13/.

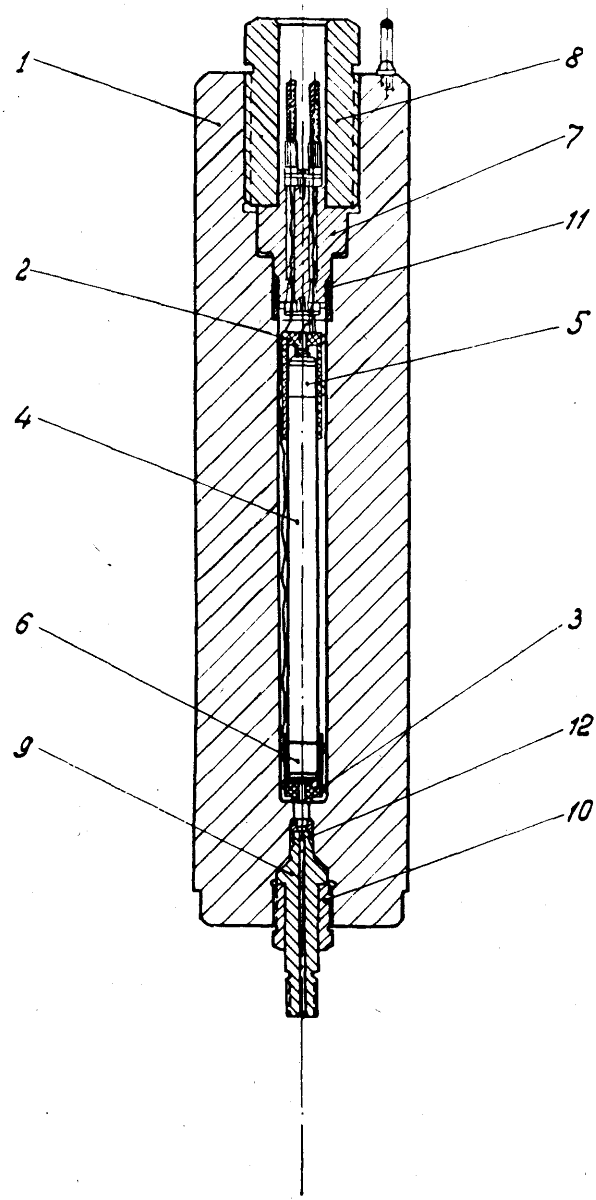

FIG. 1. Diagram of apparatus for measuring the velocities of propagation of elastic waves in rock samples under pressures up to 5.000 kg/cm².

The ultrasonic vibrations are excited and received by means of piezoelectric transmitters 5 and 6. Such transmitters prepared of ammonium dihydrophosphate crystals gave sufficiently stable performance at confining pressures of up to 5.000 kg/cm^2. The velocities of the longitudinal waves in the rock specimens were measured by means of an ultrasonic seismoscope of the U. V. Riznichenko, B. N. Ivakin and V. P. Bugrov type /14/. The electric pulses from the seismoscope generator are converted by piezocrystal transmitter 5 into mechanical vibrations which are propagated as a longitudinal elastic wave through the specimen under test. At the moment the pulse is delivered to the transmitter a conventional signal appears on the cathode oscillograph screen. After passing through the specimen the elastic wave in the form of a pulse is converted by the piezoelectric receiver 6 back into an electrical pulse, which is amplified and also gives a signal on the oscillograph screen. These signals are photographed on an oscillogram which records also the time marks from alternating current of 500, 250 or 100 kc frequency. Thus the oscillogram makes it possible to determine the time of travel of the elastic waves through the rock specimen. The velocity of the longitudinal waves is found as the quotient of the length of the specimen divided by the time of travel of the wave. The compressive deformation of the specimens under the action of high pressures was not taken into account, as the relative shortening of rocks under a confining pressure of 5.000 kg/cm^2 does not exceed 0.5 to 0.8 p. c. On the other hand, the error of determination of the time of travel of the elastic wave through the rock sample, and therefore that of the velocity of the elastic wave, amounts to several per cent.

Owing to the fact that upon penetrating the pores of the rock the medium transmitting the pressure (nitrogen) may change the structure of the specimen, the latter should be enclosed in a thin shell of some kind /2/. For this the rock cylinder was soldered into a shell of copper foil 0.1 mm. thick. This covering protects the rocks sufficiently well from the penetration of gas into their pores at high pressures.

The results of the experiments are presented in Figs 2 and 3 as v vs. p curves, v being the velocity of the longitudinal waves, and p, the confining pressure, for basalt N° 21 and syenite N° 42. The arrows near the curves indicate the order in which the experiments were carried out : increasing and subsequent decreasing of the pressure. It can be seen that rock specimens enclosed in thin copper shells display a slight hysteresis.

Curves 1 and 2 in Fig. 2 are the results of tests performed on

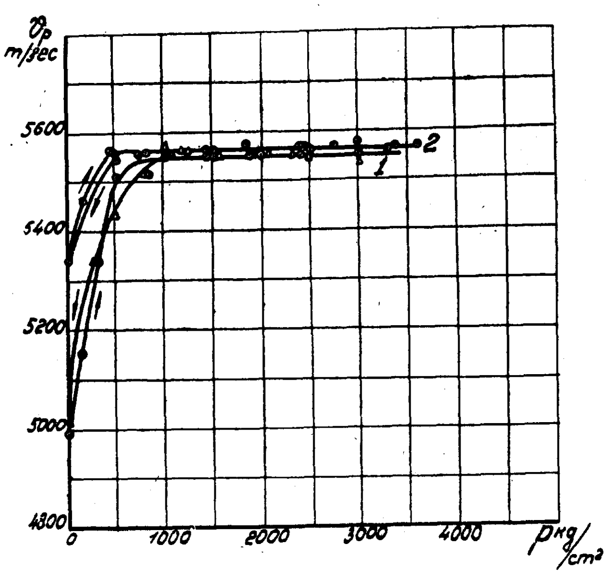

FIG. 2. Velocity of longitudinal waves plotted against pressure for two samples of basalt N° 21.

two different samples of the same basalt N° 21. The values of their wave velocities at atmospheric pressure differ by 6 per cent, which is quite natural, owing to the heterogeneity of the rocks. But the nature of the $v = f(p)$ curves for the two samples is quite identical. An examination of Figures 2 and 3 shows that the velocity of elastic waves in rocks grows abruptly (by 10 to 12 per cent) upon increase of the pressure to 500 or 1.000 kg/cm². Further increase of the pressure to 4.000 kg/cm² hardly increases the velocity any further. Table 1 gives the interpolated velocities of elastic waves in basalt, syenite and dolomite at high pressures. These results are discussed below, after a description of the experiments for determining the elastic moduli of rocks.

TABLE 1.

Variation of the velocity of longitudinal waves with pressure in rock samples.

Pressure (kg/cm²)	Depth (km)	Velocity (m/sec)		
		Basalt	Syenite	Dolomite
1	0	5000	4480	4150
500	1,2	5500	5050	4280
1000	3,7	5550	5270	4350
1500	5,5	5550	5310	4400
2000	7,4	5550	5330	4430
3000	11,1	5550	5370	4470
4000	14,8	5550	5410	4500
5000	18,6	5550	5460	4530

A diagram of the apparatus for measuring Young's modulus for rock specimens at high pressures by the static bending method is

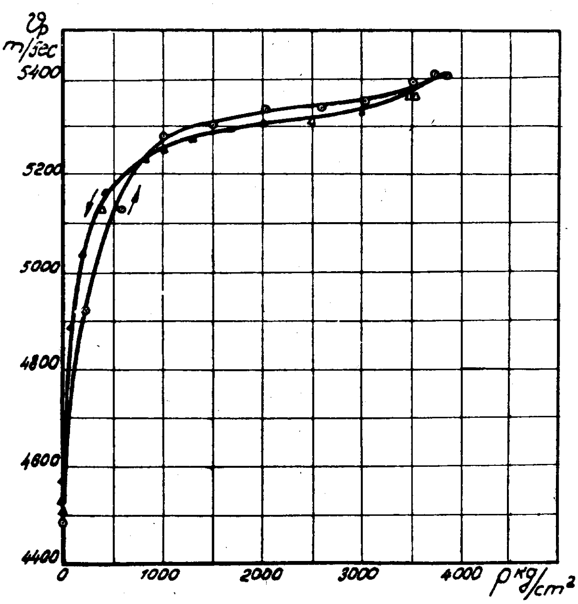

FIG. 3. Velocity of longitudinal waves plotted against pressure for syenite sample N° 42.

shown in Fig. 4. The rock specimen 1, in the shape of a rod 21 or 17

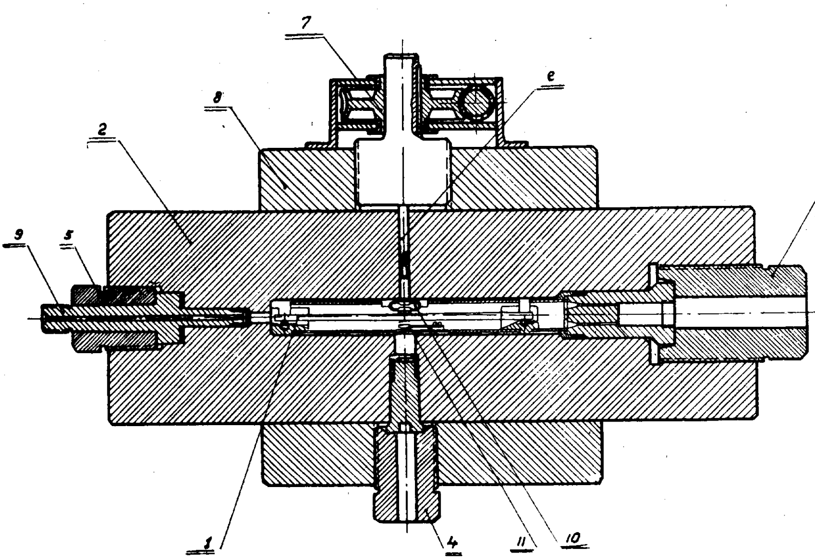

FIG. 4. Diagram of apparatus for measuring Young's modulus for rock samples by the method of bending under pressure up to 5.000 kg/cm².

cm. long and 0.5×1.5 or 0.9×0.9 cm. in cross-section was placed horizontally on two supports (with free ends) inside a steel thick-walled body 2. This body had four holes three of which were closed by plugs 3,4 and 5, held in place by threaded bushings. The fourth hole carried a piston 6 which caused a concentrated stress on the centre of the rock rod. The piston and plugs 3 and 4 were sealed with gaskets after the Bridgman unsupported area type. The piston was advanced into the bomb body by means of a specially designed reducing gear 7, fixed to steel ring 8. The desired force could be applied to the specimen smoothly within a range of 0.1 to 30 kg. by rotating the handwheel of the reducing gear. A confining pressure of up to 5.000 kg/cm^2 could be obtained from the gas compressor mentioned above which pumped nitrogen into the bomb through a thick-walled steel piping connected with union 9. The pressure was measured, like in the apparatus for determining the velocity of elastic waves, by means of a Borden type spring gauge with a scale graduated up to 10,000 kg/cm^2.

The force on the rock specimen as well as its strain (deflection), was measured by means of a dynamometer 10 and a deformometer 11. The dynamometer was a very rigid elliptical steel ring. The force on it was determined by its deformation by means of wire tensimetric transmitters cemented to it. The deformometer was a thin flat steel spring, the bend of which was also recorded by means of transmitters cemented to it. The transmitters were connected to form a Wheatstone Bridge with two transmitters inside the bomb. With this circuit the influence of the pressure and temperature of the electrical resistance on the transmitter wires was compensated. The debalance of the bridges caused by the thrust applied to the dynanometer and by the bend of the deformometer were measured by means of a sensitive galvanometer. The dynanometer and deformometer were tared at atmospheric pressure. A verification of the taring curves at high confining pressures showed that they could be used at high pressures also, by introducing a definite correction. Thus varying the current, the force could be determined directly by the galvanometer scale with an accuracy of 4 per cent for loads up to 1 kg. and of 2 to 1.3 per cent for larger loads. The accuracy of determination of the deformation (deflection) was between 1.5 and 5 per cent.

The following rocks were studied by the above method : basalts from three different deposits, gabbro, labradorie, syenite, marble and two sandstones. As in the case of the velocity measurements of elastic waves in rocks at high pressures, the rock samples were encased in thin copper foil, which, as experiments show, did not influence the Young modulus of the specimen under test perceptibly.

Fig. 5 shows, as an example, the curves of dependence of the deformation f mm. (deflection) of gabbro specimen N° 15-5 on the

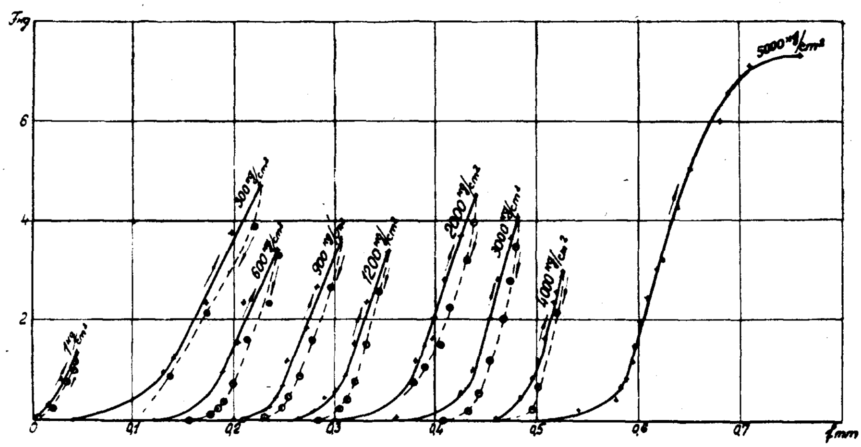

FIG. 5. Dependence of deflection f (mm) on the bending force F (kg) for gabbro sample N° 15-1.

bending force F kg. at various pressures up to 5.100 kg/cm². The arrows next to the curves indicate the order in which the experiments were carried out : increase and subsequent decrease of the bending force. As can be seen from this figure, elastic hysteresis is observed in this case. The load-up branches of the hysteresis loop, represented by solid lines are with few exceptions close to straight lines within a load range of 1 to 4 kg. For this section of the curves Young's modulus was calculated after the usual formula for the bend of a beam with free ends loaded in the middle with a concentrated force.

Fig. 6 presents the curve showing the dependence of Young's modulus on the confining pressure for a number of rock samples encased in copper shells. As in the case of the velocity of elastic waves (*Fig.* 2 and 3) the sharpest increase of Young's modulus is observed when the pressure is raised to 500-1.000 kg/cm². Thus, when the confining pressure was raised to 900 kg/cm², Young's modulus increased 30 to 70 per cent for the basalt samples, 40 to 110 per cent for the gabbro samples 35 to 46 per cent for labradorite, 25 to 50 per cent for marble, and 30 to 40 per cent for sandstone. Further increase of the pressure, however, up to 5.000

kg/cm², causes a less intensive increase in Young's modulus for the rock specimens tested : it increases another 10 to 30 per cent.

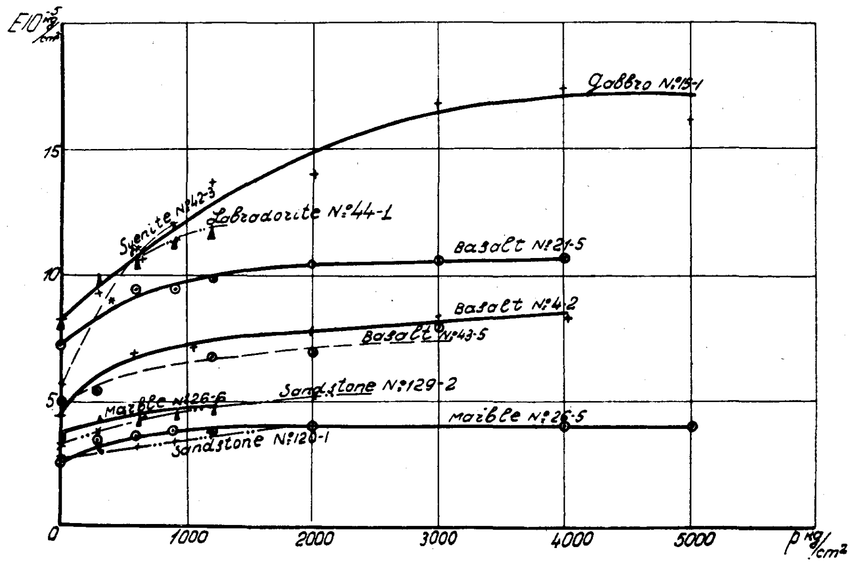

FIG. 6. Yo'ing's modulus vs. pressure for samples of various rocks.

Only for gabbro was this increase as high as 110 per cent in this range also. It is as yet impossible to carry out an exact comparison of the experimental values of the elastic longitudinal wave velocities and for Young's modulus for rocks on the basis of the well-known formula of the theory of elasticity. However, there is a qualitative agreement, inasmuch as the velocity of the elastic waves increases less than Young's modulus with rising pressure the ratio being approximately that of the square root.

It should be noted that when the rock samples are not encased in copper shells Young's modulus increases when the pressure rises to 500 or 600 kg/cm²; then at higher pressures it falls off, amounting at 5.000 kg/cm² to about 75 or 50 p. c. of its initial value. Besides, both in measuring Young's modulus and in determining the velocity of elastic waves, considerable hysteresis is observed for specimens not enclosed in shells.

The above regularities of the variation of the elastic parameters of rocks as a function of the pressure can be explained as follows. In the absence of the shells the deformation of the specimens under pressure is of a somewhat different nature than in conditions of occurence of rocks in the depths of the Earth's crust. The confining pressure in such experiments acts only on the structural elements of the specimen, i.e. the minerals. But the total bulk deformation of the specimen is then apparently smaller than in the case of the action of pressure only on the surface of the specimen through a copper foil shell. In the absence of a shell, owing to penetration of the medium transmitting the pressure (nitrogen) into the pores of the specimen, the latter cannot be closed when the pressure rises and the forces of elastic interaction in the contacts between the mineral grains constituting the rock cannot increase appreciably.

Other phenomena, similar to those occuring in the Earth's crust, are observed when the rock samples are studied in shells. In this case pressures up to 500-1.000 kg/cm² apparently lead mainly to closure of the rock pores and to increase of their density; besides, owing to compression, the elastic forces in the contacts between the individual grains of the rock-forming minerals increase considerably; this is due to an increase in the number and area of such contacts. The aggregate of minerals constituting the rock acquires the properties of a continuous elastic medium to a considerable degree, resulting in a sharp increase of the elastic parameters of the rock in this pressure range. The comparatively slight increase in Young's modulus upon further rise of the pressure up to 5.000 kg/cm² is due to the further growth of the potential energy of confining compression. But as the density thereupon also increases somewhat, the velocity of the elastic waves increases insignificantly and in the case of basalt N° 21 (see *Fig.* 2), remains practically constant.

Besides Young's modulus, the strength of some of the rocks was also determined at a high confining pressure after the bending method. According to the data of various authors, in compression tests where the confining pressure is raised the strength increase substantially (by several times). But in tension tests the increase in strength with rising pressure is much smaller than in compression experiments. In our experiments most of the samples failed in bending tests under high confining pressures with stresses just a little higher than at atmospheric pressure. Only four samples (gabbro, labradorite and syenite) could be loaded to stresses exceeding the ultimate stresses at atmospheric pressure about ten-fold.

As a pressure of 5.000 kg/cm² corresponds to a depth of the order of 20 kilometres in the Earth's crust, the data obtained for the mechanical properties of rocks at high confining pressures bear an interest for seismology and particularly for problems of earthquakes physics, as it is known that the centres of the most destructive earthquakes are located at depths of between 10 and 40 kilometres. The Young's modulus values for rocks at high pressures may find application in the examination of a number of geological problems, in geotectonics, particularly in modelling geo-dynamic processes. These data may be used also in seismic exploration, which is employed at present for depths of about 10 kilometres.

Credit is due to laboratory assistants V. A. Pavlogradsky, A. T. Bondarenko and N. P. Semyonova for their great aid in carrying out the experimental part of this study.

References.

1. Volarovich (M. P.). On Experiments at High Pressures in Geology and Geophysics, Bull. Acad. Sci. USSR, Chem. Ser., No. 6, 985, 1940.
2. Birch (Fr.), Schainer (J. F.) a. Spicer (H. C.). Handbook of Physical Constants, Geol. Soc. of Amer., 1942.
3. Balsley (J. R.). Deformation of Marble under Tension at High Pressure, Trans. Amer. Geophys. Union, 11, 519, 1941.
4. Handin (J.). An Application of High Pressure in Geophysics : Experimental Rock Deformation, Trans. Amer. Soc. Mech. Engrs, 75, N 3, 315, 1953.
5. Griggs (D. T.) a. Miller (W. B.). Compression and Extension Experiments on Dry Yule Marble at 10000 at. Conflning Pressure, Room Temperature, Bull. Geol. Soc. Amer., 62, 853, 1955.
6. Robertson (E. C.). Experimental Study of the Strength of Rocks, Bull. Geol. Soc. Amer., 66, 1275, 1955.
7. Bridgman (P. W.). Shearing Phenomena at High Pressure of Possible Importance of Geology, Journ. of Geol., 44, N 6, 635, 1936; Larsen (E. S.) a. Bridgman. Shearing Experiments on some Selected Minerals and Mineral Combinations, Amer. Journ. Sci., 36, 81, 1938.
8. Volarovich (M. P.), Gorazdovski (T. J.) a. Parkhomenko (E. I.). An Investigation of Shear in Thin Rock Plates under Conditions of Torsion and Uniaxial Pressure, Trans. 4th Confer. Experim. Mineral. a. Petrogr., 2,230, 1953; Volarovich (M. P.) a. Parkhomenko (E. I.). Reproduction of Spontaneous Ejections of Coal during Compression with Simultaneous Torsion of Thin Coal Plates, Trans. Geophys. Inst. Acad. Sci. USSR, No. 34 (16), 193, 1956. An Investigation of Rupture on Torsion of Thin Rock Plates under Uniaxial Pressure, Bull. Acad. Sci. USSR, Geophys. Ser., No. 2, 190, 1957.
9. Hughes (D. S.) a. Jones (H. J.). Variation of Elastic Moduli of Igneous Rocks with Pressure and Temperature, Bull. Geol. Soc. Amer., 61, N 8, 842, 1950.
10. Riznichenko (U. V.), Silayeva (O. I.), Shamina (O. G.), Myachkin (V. I.), Gluhov (V. A.) a. Vinogradov (S. D.). Seismo-Acoustic Methods of Studying Stresses in Rocks on Test Samples and in situ, Trans. Geophys. Inst. Acad. Sci. USSR, N° 34 (161), 74, 1956.
11. Volarovich (M. P.) a. Balashov (D. B.). An Investigation of the Velocities of Elastic Waves in Coal Samples under Pressures up to 1000 kg/cm², Trans. Geophys. Inst. Acad. Sci. USSR, No. 34 (161), 164, 1956; Investigation of the Velocities of Elastic Waves in Rock Samples under Pressures up to 5000 kg/cm², Bull. Acad. Sci. USSR, Geophys. Ser., No. 3, 319, 1957.

12. Bridgman (P. W.). The Physics of High Pressure, London, 1931.
13. Bridgman (P. W.). Recent Work in the Field of High Pressures, Rev. of Modern Phys., 18, N 1, 1946 (Russian Edition, Moscow, 1948).
14. Riznichenko (U. V.), Ivakin (B. N.) a. Bugrov (V. R.). Seismic Waves Modelling with Ultrasonic Pulses, Bull. Acad. Sci. USSR, Geophys. Ser., N 3, 58, 1952.

PIEZOELECTRIC EFFECT OF ROCKS

by M. P. VOLAROVICH and E. I. PARKHOMENKO.

According to present day views on earthquakes the great majority of them, including catastrophical earthquakes, are due mainly to growth of mechanical tensions in the tectonically active regions of the earth crust (1). Besides, a number of cases are known where magnetic and electrical disturbances were apparently related to earthquakes (2).

In studying the relationship between seismic and electromagnetic phenomena it is interesting to investigate the influence of mechanical tensions on the electrical and magnetic properties of rocks. At present several papers are known dealing with the study of the influence of mechanical action on the magnetic parameters of magnetite and several other rocks (3). But laboratory investigations of electrical phenomena in rocks depending on mechanical tensions have not been described as yet in the literature. The only papers known so far are devoted to a study of the appearance of a difference of electrical potentials in rocks upon the passage of elastic waves through them under field conditions, i. e., to the study of the seismoelectric effect $\mathcal{E}$. The latter phenomenon, which is of considerable interest for geophysics, was discovered by A. G. Ivanov (4) and is attributed to the presence of a liquid phase in the rocks, accounting for the entire complex of electrokinetic phenomena.

In connection with the search for other phenomena of the electrization of rocks under the influence of mechanical action it was important to establish whether the piezoelectric effect is observed in rocks, no such effect having been known previously to exist in them. A. V. Shubnikov proved theoretically that a substance containing piezoelectric crystals which possesses acentricity and one of the textures of the types ∞; $\infty.m$; $\infty : 2$ may manifest piezoelectric properties (5).

Owing to the fact that a number of rocks, quite abundant in the Earth's crust, contain quartz and other piezoelectrics and often have an oriented texture (banded, fluidal, taxitic, etc., in gneisses, granites and quartzites), it was natural to assume the existence of piezoelectric properties in such rocks and to undertake an investigation of them. For this purpose the pulse-type ultrasonic seismoscope designed in the Institute of the Physics of the Earth of the

USSR Academy of Sciences was used to model seismic wave processes (6). This seismoscope made it possible to detect a piezoelectric effect in rock specimens by the dynamic method and to carry out a relative comparison of the piezoelectric effect of various rocks (7).

The seismoscope consists of a bank of generators, a bank of amplifiers, cathode-ray tubes (cathode oscillograph) and two piezoelectric transducers of Rochelle salt cut at 45° x and operating at resonance frequencies of the order of 100 to 50 kilocycles per second. In our experiments we left only one of the Rochelle salt transducers, namely the transmitter, the other being replaced by the test rock specimen. In some cases, however, the rock specimen played the part of the transmitter while the Rochelle salt crystal served as the receiver.

Electric pulses (peaks) delivered by the generator bank entered the piezotransmitter causing elastic (ultrasonic) vibrations in it. These elastic vibrations passed through an acoustic retarder into the test rock specimen and were transformed, when the specimen possessed a piezoelectric effect into electrical vibrations which were transferred to the amplifier and then to the cathode-ray tube. The acoustic retarder was employed to obtain a more distinct initial entrance of the electrical vibrations radiated by the rock specimen and to avoid electrical interference from the transmitter.

The amplitude of the electrical vibrations observed on the screen of the tube depends on the tension developed by the specimen, i.e. on the piezoelectric characteristics of the specimen. The piezoelectric effect was estimated as regards amplitude with maximum amplification of the seismoscope. The amplitude scale was such that 1 mm on the oscillogram corresponded to three microvolts. The rock specimen was enclosed in a metal chamber which served as an interference screen. To make a second movable electrode which would enable carrying out experiments with the specimen without specially applied electrodes, tin foil was glued to a rubber gasket and the gasket to a brass plate with a screw.

The rock specimens were prepared as rectangular parallelopipeds 2,5 × 2,5 × 2,5 cm. The following igneous, metamorphosed and sedimentary rocks were studied : gabbro, diabase, diorite, syenite, granites, quartzites, gneiss, jasper, marble, sandstones, dolomite, limestone, etc.

Fig. 1 gives some of the oscillograms of the rock specimens studied, obtained by the method described above. Arrow *a* on one of the oscillograms shows the electrical pulse delivered simultaneously to the transmitter and to the cathode-ray tube to mark the moment of transmission. Arrow *b* shows the moment the front

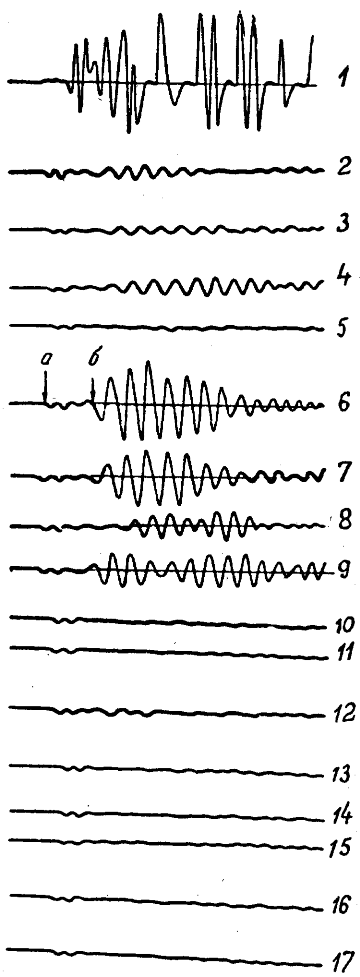

FIG. 1 : Oscillograms of rocks obtained with ultrasonic seismoscope; a — moment of emission of a mechanical pulse / for granite N° 49 /; b — moment of arrival of the elastic wave front to the surface of the rock sample. 1 — quartz plate, 2 — quartzite N° 22, 3 — quartzite N° 18, 4 — sandstone N° 48, 5 — sandstone N° 8, 6 — granite N° 49, 7 — granite N° 50, 8 — granite N° 10, 9 — gneiss N° 51, 10 — jasper N° 23, 11 — gabbro N° 15, 12 — diorite N° 16, 13 — skarn N° 17, 14 — syenite N° 31, 15 — marble N° 26, 16 — limestone N° 27, 17 — dolomite N° 9.

of the elastic wave reaches the rock specimen. At this moment the elastic vibrations are converted in the specimen into electrical vibrations.

It can be seen from the oscillograms presented that some rock specimens show distinct piezoelectric properties (quartzites, sandstone n° 48, granites, gneisses) : but not all the rocks possess these properties. Piezoelectric effect is manifested by rocks which contain quartz (and tourmaline) grains. Of the rocks studied the highest piezoelectric effect was observed in granites; that of gneiss, sandstone n° 48 (coarse-grained) and quartzites was somewhat smaller. Rocks such as jasper, syenite, gabbro, skarn, marble, dolomite and limestone do not manifest piezoelectric properties.

Fig. 1 shows the oscillogram of a quartz monocrystal, made at a lower amplification than the oscillogram of all the rest of the rock specimens. For this reason the amplitude on these oscillograms cannot be used to compare the relative piezoeffect of quartz with that of other rocks.

To confirm the piezoelectric nature of the effect observed in the rock specimens it was necessary to establish the presence of polarity. To ascertain this the charges were removed from one surface and then the specimen was rotated through 180° and an oscillogram was again made. Thus in the second case the charges were removed from the other surface of the specimen. It was found that if upon the entrance of an elastic wave in the first case the first oscillation is directed downwards on the record (Fig. 2) the

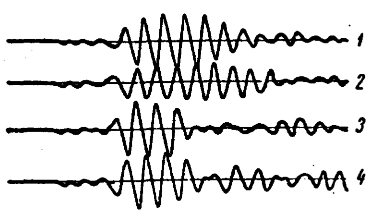

FIG. 2 : Polarity effect in rocks which exhibit piezoelectric effect; 1 — granite N° 50; 2 — Ds., turned through 180°; 3 — granite N° 50, 2nd plane; 4 — Do.; turned through 180°.

course of this curve on the oscillogram after turning the specimen through 180° was the reverse, as it should be in the case of the piezoelectric effect.

It should be noted that the seismoelectric effect $\mathfrak{E}$, as A. G. Ivanov's experiments in field conditions have shown, should be characterized by absence of polarity (4). To prove this experiments were carried out also with a view to reproducing the seismoelectric effect $\mathfrak{E}$ in artificially moistened specimens of the rocks which did not manifest piezoelectric properties in the previous experiments.

The experimental procedure with the ultrasonic seismoscope was the same as described above. It was established (see Fig. 3) that

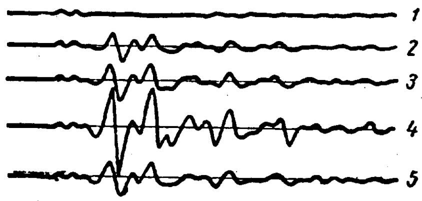

FIG. 3 : Effect of moisture on the electrization of dolomite — seismoelectric effect $\mathcal{E}$; 1 — Ist plane before moistening; 2 — Do., after moistening; 3 — the same sample turned through 180°; 4 — the same sample, 2nd plane after moistening; 5 — Do., turned through 180°.

before artificial moistening a dolomite specimen, in agreement with the above, manifested no electrization and gave a straight line on the oscillogram. After the dolomite sample was moistened the passage of an elastic wave led to the appearance of a potential on its faces. However, the sign of the charge in this case did not depend on the face of the specimen the charges were removed from, as can be seen in Fig. 3. These experiments confirm, to our opinion, A. G. Ivanov's conclusion (4) that the seismoelectric effect $\mathcal{E}$ observed by him in field conditions is due to the presence of solid and liquid phases in the rocks. It should be noted that drying quartz-containing rocks which manifest the piezoelectric effect in order to drive off the moisture contained in them, did not lower the piezoeffect.

It could be assumed that the effect we observed in rocks belonged to the class of contact phenomena and is connected for instance with the so-called Rabek effect (8). However, the above mentioned polarity of the phenomenon observed by us shows that it is not due to the Rabek effect. Besides the effect was observed in special experiments where the mobile electrode was set up at some distance (1-3 mm.) from the test rock sample, though the amplitude became smaller and smaller as the distance was increased. This eliminates the possibility of any contact effect in our experiments and confirms the piezoelectric nature of the phenomenon.

After the discovery of the piezoelectric effect in rocks was undertaken a theoretical investigation of ideal piezoelectric quartz textures and textures of quartz-containing rocks (9). In agreement with A. V. Shubnikov's theory (5,10) it was shown that if the quartz texture is made up of one form of quartz (right or left) and all the quartz grains are orientated in the texture so that the like terminals of their electrical axes are pointing in the same direction, we get a ∞ type texture. On the basis of the piezoelectric tensor of this texture the piezoelectric moduli d_{ik} of such an ideal texture were calculated by the piezoelectric moduli δ_{ik} of a quartz monocrystal. It was thus established that

$$d_{33} = \delta_{11}\,;\; d_{31} = -\frac{1}{2}\delta_{11},\quad d_{14} = \frac{1}{2}\delta_{14} \text{ and } \quad d_{15} = -\delta_{11}.$$

When the optical axes of the quartz grains in the texture are arranged parallelly a $\infty : 2$ texture results. The only piezoelectric modulus d_{14} of this texture equals the piezoelectric modulus of a quartz monocrystal ∂_{14}.

If, on the other hand, the texture includes right — and left — quartz in statistically equal quantities and all the quartz grains are orientated so that the like terminals of their electrical axes are pointing in the same direction, the result is a piezoelectric symmetry texture $\infty \,.\, m$. The piezoelectric effect of this texture is described by the followed tensor :

$$\begin{array}{ccccccc} & t_{11} & t_{22} & t_{33} & t_{23} & t_{31} & t_{12} \\ \mathfrak{J}_1 & 0 & 0 & 0 & 0 & d_{15} & 0 \\ \mathfrak{J}_2 & 0 & 0 & 0 & d_{14} & 0 & 0 \\ \mathfrak{J}_3 & d_{31} & d_{31} & d_{33} & 0 & 0 & 0 \end{array}$$

Here t_{11}, t_{22}, t_{33} are the normal tensions and t_{23}, t_{31}, t_{12} the tangent tensions of the mechanical tension tensor; $\mathfrak{J}_1$, $\mathfrak{J}_2$, $\mathfrak{J}_3$, are the components of the electrical polarization intensity vector and d with subscripts are the piezoelectric moduli of the texture. Expressed as the piezoelectric moduli δ_{ik} of quartz, these piezomoduli have the following values : $d_{33} = \delta_{11}$, $d_{31} = -\frac{1}{2}\delta_{11}$ and $d_{15} = -\partial_{11}$.

A considerable number of rocks containing quartz should be classed as having real piezoquartz textures. These are gneisses, quartzites, granites, quartz porphyries, granite porphyries, sandstones etc. According to the literature right — and left — quartz is present in rocks in statistically equal quantities. Therefore, with linear orientation of the optical axes of the quartz grains in the rock in the absence of orientation of their electrical axes a piezoelectrically neutral texture will result. But with plane or linear orientation of the optical axes of the quartz grains and orientation of the electrical axes in one direction only the symmetry texture $\infty \,.\, m$ is possible.

As rocks almost always contain other rocks forming minerals besides quartz, rocks should be regarded as multi-component textures. The above indicated piezoelectric moduli of three symmetry groups are applicable only to monomineral textures with ideal quartz grain orientation. In order to use these formulae for computation of the piezoelectric moduli of rocks they must be supplied with coefficients allowing for the degree of orientation of the quartz grains, as well as the concentration of quartz in the texture. This can be done, for instance, according to I. S. Zheludyov's formula /10/ in the case of mixed piezoelectrics textures.

In connection with the above it was interesting to carry out quantitative estimations of the piezoelectric moduli of rocks by the static method. For this purpose an apparatus was developed /11/ for measuring the difference of potentials appearing on rock specimens under the action of a static mechanical force. The pressure was applied by means of a hydraulic press, optimal results being obtained with a rate of loading equal to 2 cm. per minute.

The rock specimens were prepared in the form of right parallelepipeds of various sizes with volumes ranging from 8 to 830 cm³. The parallelitly of the faces had to be very accurate / deviation not over ± 0.01 mm /. Before the test the specimens were degreased and washed with alcohol and dried for from 8 to 32 hours, depending on the size of the specimen. The quality of drying and the cleanness of the surface were of prime importance for obtaining reproduceable results, as moisture and contamination increase the bolk and surface electroconductivity and make it impossible to measure the difference of potentials due to piezoelectric effect.

Fig. 4 shows by way of example the curve of dependence of the

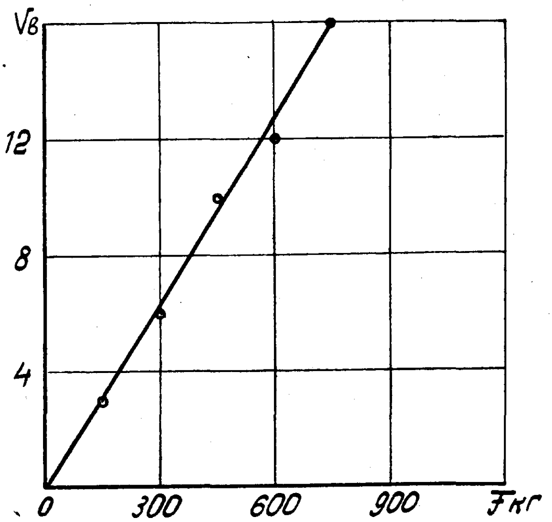

FIG. 4 : Potential difference plotted against the force F kg / piezoelectric effect for granite sample N° 5/.

difference of potentials due to the longitudinal piezoeffect on the mechanical force for granite specimen N° 5 $2 \times 2 \times 2$ cm. in size. In this figure the force $\mathcal{F}$ in kilograms is plotted along the abscissa axis and the difference of potentials in volts along the ordinate axis. As can be seen, the dependence between these two values is linear in agreement with the theory of the piezoelectric effect. Analogous results were obtained also for other rock specimens.

The results of these experiments showed that the piezoelectric moduli of small rock specimens of the order of $2 \times 2 \times 2$ cm. depend on the size of the quartz grains. The piezomodulus values for the longitudinal piezoeffect for such specimens of granites, quartzites and sandstones consisting of mineral grains 1 to 3 mm. in size is 0.6 to 1.4 per cent and for small grain rocks with grains 0.1 to 0.7 mm. large it is 0.08 to 0.12 per cent of the piezomodulus of an X-cut quartz monocrystal. Besides it was established that the piezoeffect is observed in all three perpendicular directions and, furthermore, for a number of samples the piezomoduli were almost equal in all three directions. These facts suggested that the piezoeffect in small rock samples should not be attributed to the texture, but to presence of uncompensated large quartz grains.

Increasing the size of the rock samples decreases their piezomoduli, but when the volume of the sample exceeds 150-200 cm³ they remain constant. Table 1 presents the piezomoduli of the

TABLE 1.

Piezoelectric Moduli of Granites for Longitudinal Piezoeffect.

Name and Origin of Rock	Size of Specimen in cm.	Volume of specimen in cm³	Piezoelectric moduli (CGSE-units) d'_{33}	d'_{22}	d'_{11}
Granite 69	$4.8 \times 4.7 \times 4.7$	108	0.7	0.6	0
Karlakhti, coarse-grained	$8.9 \times 6.5 \times 4.8$	274	2.3	0.9	0.5
Granite 131 Orekhov, coarse-grained	$11.1 \times 9.9 \times 8.4$	830	0.6	0.4	0.2
Granite 130 fine-grained	$7.0 \times 4.7 \times 4.9$	137	0.7	0.4	0.2
	$6.8 \times 5.0 \times 9.8$	334	0.6	0.4	0.1
Granite 67 from Valaam Island, middle-grained	$7.4 \times 5.4 \times 5.0$	200	1.6	1.5	1.2
Granite 65 Leznikov middle-grained	$9.9 \times 9.8 \times 5.1$	501	0.5	0.2	0.1

Besides granites the piezoelectric moduli were measured for samples of vein quartz (No. 90 and No. 174). The piezomoduli for two such rocks (No. 90 and No. 174) are given in Table 2.

TABLE 2.

Piezoelectric Moduli of Vein Quartz Samples.

Name of Rock	Size of Specimen in cm.	Volume of specimen in cm³	Piezoelectric moduli (CGSE-units) d'_{33}	d'_{22}	d'_{11}
Vein Quartz No. 90	3.4 × 3.3 × 3.9	44	36.7	2.4	2.1
Vein Quartz No. 174	3.6 × 4.0 × 18	26	22.4	3.9	1.5

largest samples of a number of granites. The last three columns contain the values of the piezoelectric moduli for longitudinal piezoeffect on three mutually perpendicular faces. The moduli are given in an arbitrary coordinate system. It should be remembered that the piezomodulus of quartz is $\partial_{11} = 6.8 \times 10^{-8}$.

The granites studied by us were mainly very slightly deformed

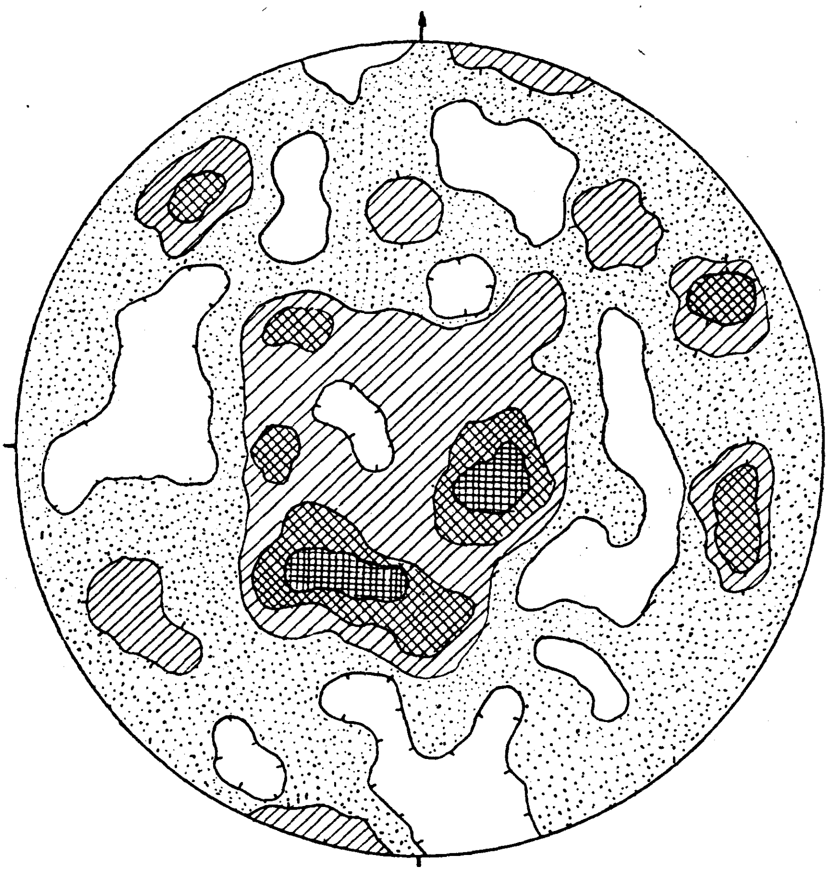

FIG. 5 : Diagram of orientation of optical axes of quartz grains for granite N° 130.

rocks. A study of polished sections under the microscope and diagrams plotted after Sander with a Fyodorov table showed that the optical axes of the quartz grains in these granites have no distinct orientation. By way of example Fig. 5 shows a detailed diagram for granite N° 130 plotted for us by N. E. Galdin. But as a piezoelectric effect, though very small in value / of the order of 0.2 per cent of the piezoeffect of an X-cut quartz monocrystal / is observed in these samples this may be regarded as evidence of some orientation of quartz grains with respect to their electric axes.

Of greatest interest are the vein quartz samples. As can be seen from Table 2 the piezoelectric effect in these samples is considerably greater in one direction / 10 to 15 times / than the two others. This shows that they were cut from a piece of rock with an insignificant deviation from the infinite order axis of the $\infty . m$ texture. It should also be pointed out that three specimens 11, 22

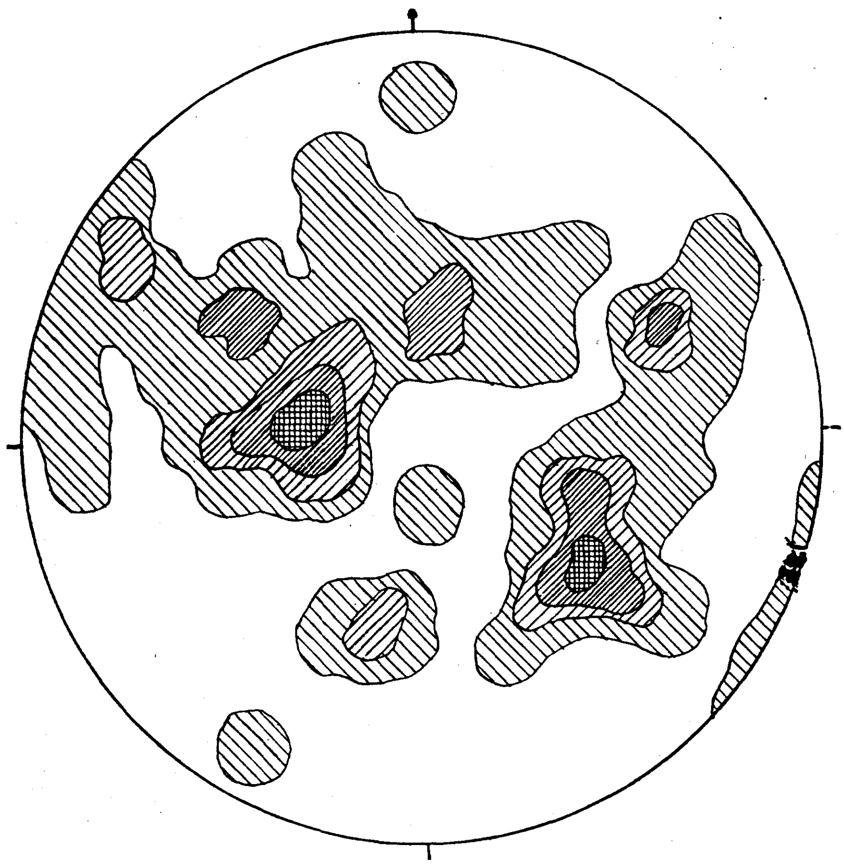

Fig. 6 : Diagram of orientation of optical axes of quartz grains for vein quartz N° 90.

and 44 cm³ in volume cut from vein quartz N° 90, despite the large size their grains / 5 mm. on the average /, showed almost identical piezoelectric moduli independent of the size of the specimens. An orientation diagram built after Sander on the basis of seventy measures of the positions of the optical axes / see Fig. 6 / indicates a certain tendency towards condensation of axis exits in the central part of the diagram.

Contrary to the above described sample, vein quartz N° 174 is a fine-grained aggregate having a grain size of 0.02 mm. with a distinct optical axis maximum on the diagram. However, the maximum exit of optical axes is not normal to the specimen face, but at an angle of about 15° to it as can be seen on the block diagram in Fig. 7. Therefore in this sample of vein quartz N° 174 the piezoeffect is observed in the other two directions as well. The piezomoduli d'_{33} of vein quartz N°s 90 and 174 equal 5 and 3 per cent respectively of the piezomoduli of an X-cut quartz monocrystal.

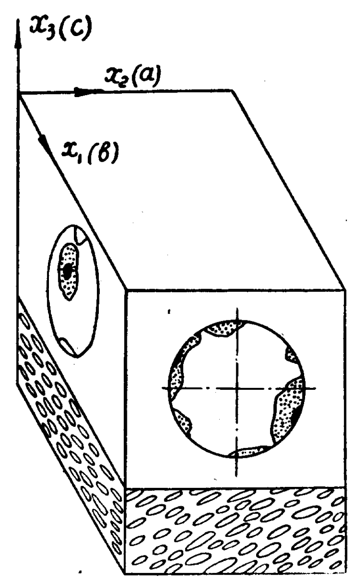

FIG. 7. : Diagram showing the preferential direction of the optical axes of quartz grain with respect to simple faces / vein quartz N° 174/.

To confirm our assumption as to the possibility of applying this new property, namely, the piezoelectric effect, of quartz-containing rocks for practical purposes in geophysics qualitative model experiments were carried out. The models were blocks of granites N^{os} 1 and 2, 34 × 18 × 12 and 25 × 5,5 × 5 cm. in size respectively. Besides, one model was made of a block of granite of smaller size with a piece of marble 21 × 90 × 5,5 cm. ground to it. Modelling was carried out by means of the supersonic seismoscope briefly described above. It consisted in the application of an elastic pulse at one point of the model surface by means of a seignette-electric piezo-transducer connected with the seismoscope, this pulse conventionally representing an « explosion » or « earthquake centre ». At some distance from this spot a receiving seignette-electric transducer or just an electrode of copper foil was set up. The picture of elastic vibrations and oscillations of the electromagnetic field was recorded on the screen of a cathode-ray tube.

As a result of the passage of the longitudinal profile along the surface of the granite 1 block and passage of the profile with the transmitter set up on one of the surfaces of the granite 2 block with an electrode and receiver on the opposite side / See Fig. 8 /

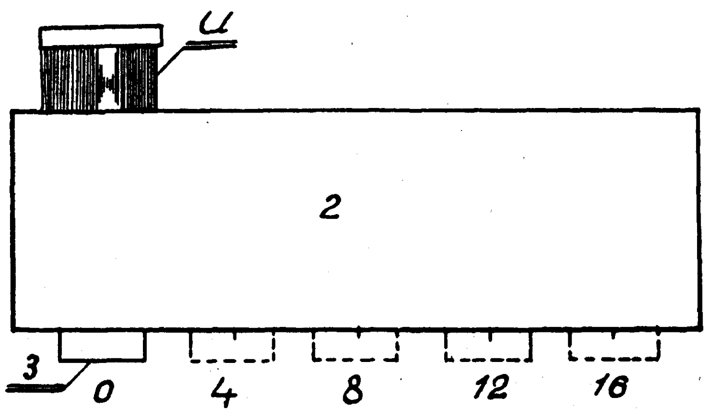

Fig. 8 : Diagram of arrangement of piezoelctric oscilator and receiver / and electrode / on granite block No. 2 in modelling experiments; *u* — oscillator, 2 —granite block, 3 — receiver.

the presence of, one might say, two types of electromagnetic waves was established, in both cases.

The corresponding oscillogram of N° 2 block is shown in Fig. 9. In this oscillogram four points of the profile are given with a pitch of 4 cm. / See Fig. 8 /, three recordings being given for each point. The upper recording (1) for each point represents the picture of electric vibrations obtained with the electrode, and the two other recordings (2 and 3) show the picture of elastic vibrations registered with the piezoelectric transducer at two different degrees of

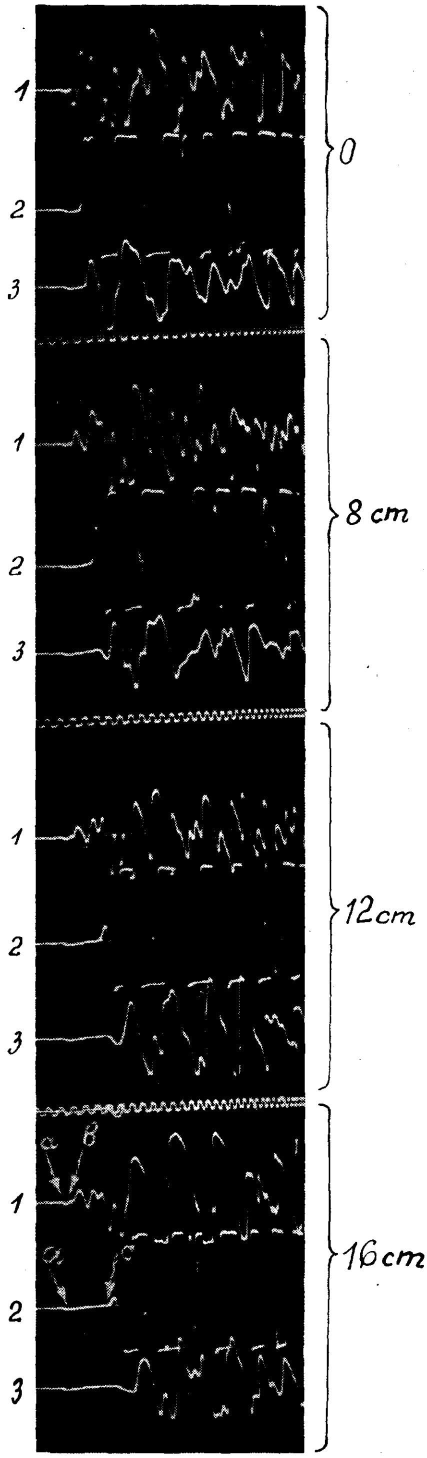

FIG. 9. Oscillogram obtained in modelling experiments with 4 cm. spacing for granite block N° 2 according to diagram in Fig. 8.

amplification. For the point of the 16 cm. profile arrows *a* indicate the moment of emission of the elastic pulse into the rock, arrow *b* the entrance of the electromagnetic wave registered by the electrode and arrows *c* the entrance of the elastic waves registered by the piezoelectric transducers. As can be seen from the arrangement of the upper record of each point of the profile, the entrance of the electromagnetic wave practically coincides with the moment of emission. But the distance between the moment of emission and the entrance of the elastic wave increases as the receiver is moved away from the emitter. No electromagnetic waves were observed in the case of rock blocks which did not exhibit the piezoelectric effect / marble, labradorite, etc./.

Upon passage of the profile over a distance of 15 cm. on the composite granite and marble model the same wave were observed, the amplitude of the first electromagnetic wave upon passage of the entire profile being almost the same. This is evidently related to the low absorption of the energy of the electromagnetic wave in the marble.

The existence of the described piezoelectric effect in rocks may prove useful in studying the physics of earthquakes and may also be of some importance in developing new geophysical methods of exploration, particularly for the study of geological sections.

Conclusions.

1. The piezoelectric effect has been detected in samples of quartz-containing rocks, namely granites, quartzites, sandstones, gneisses, etc.

2. No piezoelectric effect was observed in such rocks as dolomite, limestone, marble, syenite, diabase, gabbro, jasper, etc.

3. The first experiments were carried out by the dynamic method with the aid of the pulse ultrasonic seismoscope developed by the Laboratory of Modelling of the Institute of the Physics of the Earth of the USSR Academy of Sciences. The rock specimens which manifested piezoelectric effect were used as transducers / ultrasonic receivers or transmitters / instead of quartz or Rochelle salt piezocrystals.

4. The difference of the piezoeffect in rocks from the seismoelectric effect $\mathfrak{E}$ established by A. G. Ivanov has been confirmed by our experiments. The nature of the effect $\mathfrak{E}$ arises when the rock / dolomite, limestone / is moistened and disappears when it is dried. When granite is dried its piezoelectric effect does not decrease.

5. On the basis of an analysis of ideal piezo-quartz textures of quartz it has been established, in accordance with A. V. Shubnikov's theory, that quartz-containing rocks may belong to piezoelectric texture of the type $\infty . m$.

6. The piezoelectric moduli of the ideal texture have been calculated from the piezoelectric moduli of a quartz monocrystal. In the case of rocks allowance should be made, in accordance with I. A. Zheludyov'a formula, for the presence of piezoelectrically neutral components and the imperfection of orientation of the quartz grains.

7. Qualitative measurements of the piezoelectric moduli of rocks, carried out by the static method have shown that in small size samples / 8 to 10 cm^3 / the piezoeffect may be due to uncompensated quartz grains.

8. It has been established by measurement of the piezoelectric moduli of rock specimens of various sizes that in the case of large specimens /300 cm^3 and larger /, the piezoeffect is due to the piezoquartz texture.

9. The piezoelectric moduli of granites are 0.1 to 0.2 per cent and for some samples of vein quartz 3 to 5 per cent of the piezo-modulus of a quartz monocrystal.

10. Modelling on granite blocks showed that besides the elastic wave on the passage of a profile an electromagnetic were is also observed due to the piezoelectric effect.

References.

1. Savarensky (E. P.) a. Kirnos (D. P.). Elements of Seismology and Seismometry, Moscow, 1949 (in Russian).
2. Orlov (A. P.). Earthquakes and their Relationships with Other Natural Phenomena, Kazan, 1887 (in Russian); Chernyavsky (E. A.). Atmospheric, Electric and Electrotelluric Phenomena During Earthquakes, Socialisticheskaya Nauka i Tekhnika, No. 12, 1936; Gutenberg (B.). Fundamentals of Seismology, translated from the German, Moscow, Leningrad, 1936; Problems of Earthquake Prediction, Trans. Geophys. Inst. Acad. Sci. USSR No. 15 (150).
3. Grabovsky (M. A.) a. Parkhomenko. On changes in the Magnetic Properties of Magnetites Under the Influence of Large Compressing Streases, Bull. Acad. Sci. USSR, Geophys. Ser., No. 5, 1953; Kalashnikov (A. G.) a. Kapitsa (C. P.). Magnetic Susceptibility of Rocks Under Elastic Tension, Compte Rendu (Doklady) Acad. Sci. USSR, 86, No. 3, 1952 .
4. Ivanov (A. G.). Seismoelectric Effect of the Second Kind, Bull. Acad. Sci. USSR, Geograph. and Geophys. Ser. No. 5, 1940; Effect of Electrization of Earth Layers on the Passage of Elastic Waves through them, Compte Rendu (Doklady) Acad. Sci. USSR, 24, No. 1, 1950; On the Seismoelectric Effect of the First Kind in the Region adjacent to the Electrode, Compte Rendu (Doklady) Acad. Sci. USSR, 68, No. 1, 1949.

5. SHUBNIKOV (A. V.). Piezoelectric Textures, Moscow, 1946. (in Russian); Quartz and Its Uses, Moscow, 1940 (in Russian).
6. RIZNICHENKO (Y. V.), IVAKIN (B. N.) a. BUGROV (V. D.). An Ultrasonic Pulse Seismoscope, Bull. Acad. Sci. USSR, Geophys. Ser. No. 1, 1953.
7. VOLAROVICH (M. P.) a. PARKHOMENKO (E. I.). Piezoelectric Effect in Rocks, Compte Rendu (Doklady) Acad. Sci. USSR, 99, No. 2, 1954; Bull. Acad. Sci. USSR, Geophys. Ser., No. 3, 1955.
8. SMIRNOV (N. A.). The Rabek Effect. Trans. Bauman Mechanical and Machine-Building Institute No. 47 (48) 1938 (in Russian).
9. PARKHOMENKO (E. I.). Piezoelectric Texture of Quartz and Quartz-Containing Rocks, Bull. Acad. Sci. USSR, Geophys. Ser. No. 3, 1956.
10. SHUBNIKOV (A. V.), ZHELUDYOV (I. S.), KONSTANTINOVA (V. F.) a. SILVESTROVA (I. M.). Investigations of Piezoelectric Textures, Moscow, 1955.
11. PARKHOMENKO (E. I.). Measurement of the Piezoelectric Moduli of Rocks by the Static Method, Bull. Acad. Sci. USSR, Geophys. Ser. No. 4, 1957.

ON THE APPLICATION OF THE ULTRASONIC PULSE METHOD TO SEISMOLOGICAL PROBLEMS

By J. V. RISNICHENKO.

1. Ultrasound here means vibrations — dilatational, shear, or other — taking place in solid, liquid or gaseous media, their dominant frequency being of the order of about 10^4 c/s or more. In seismology and in adjacent fields the ultrasonic pulse method was used to study the earth crust and the Earth as a whole, as well as earthquakes and also in seismic prospecting. The use of the ultrasonic pulse method in these fields had such definite objects in view : a) modelling of seismic waves processes; b) studying the elastic properties of rocks on samples and under natural bedding conditions; c) observations under laboratory and mine condition of elastic waves in rocks put to a growing stress up to its breaking value. Investigations in all these directions were carried out during the last decade in the Institute for Physics of the Earth of the Ac. of Sci. of the USSR (formerly the Geophysical Institute of the Ac. of Sci. of the USSR — « GIAS ») in our laboratory with the participation of B. N. Ivankin, O. J. Silajeva, O. G. Shamina, V. I. Mjachkin as well as a number of other persons and institutions.

2. In the first works of the GIAS the ultrasonic pulse method was applied to modelling seismic waves. For this purpose in 1947 a special apparatus was developed, the so called ultrasonic pulse seismoscope, identical with the ultrasonic pulse defectoscope which had been developed in 1934 by professor S. J. Sokolov and is since widely used in industry. The « seismoscope » is a radioelectric system generating short electric pulses which are applied to a piezoelectric radiator of ultrasonic vibrations, excited in the model of the medium under investigation. The elastic waves travelling through the model are received by a piezoelectric « microseismograph ». A seismogram is obtained by photographing the stationary pattern appearing on the screen of the electron - beam tube of the seismoscope. Three- and two-dimension models were made of liquids (usually of water) or of solid materials (metals or plastics).

Later on, different types of the seismoscope based on the same principle were built for various purposes.

In the USSR at the present time the seismoscope is widely used for modelling seismic waves in a number of Higher Schools and Industrial Research Institutes dealing with geophysical problems. As far as we know from literature, similar work is being done since about 1953 also in USA.

3. Similarity in modelling seismic waves is discussed in detail in the works by S. J. Chubarova and B. N. Ivankin. The principal condition for similarity is the maintainance in separate parts of the model of the same wavelength to linear dimensions and also of dilational and shear velocities to densities ratios as in the prototype. In the presence of absorption of elastic waves, the principal requirement to be satisfied, is the realization in the model of the same absorption decrement (for a given wavelength) as in the prototype.

4. The following problems were studied by the above mentioned method of modelling : of direct and surface waves in a two-dimension semispace with the « earthquake source » located at various depths; of refracted head waves connected with the boundary of the semispace (in connection with the study of the Mohorovicic discontinuity) ; of head waves connected with the wave-guiding layers having a higher velocity of propagation of seismic waves; of refracted, diffracted, multiple and other waves. All these problems are of interest to seismic prospecting. In other institutions (in Moscow University, the works guided by prof. E. F. Savarensky) the seismoscope was used for modelling waves in the earth crust and in spherical Earth with a central core and also waves from earthquake sources in the form of a dipole possessing a moment.

5. For the investigation on samples of the elastic properties of rocks and for a study of seismological problems the ultrasonic pulse method proved more effective than that of continuous vibrations. In order to obtain correct values of the elastic constants, special investigations were carried out with the aim to determine the required relation between the dimensions of samples in the form of cylinders and rods and the dominant frequency in the pulse. Simultaneously important features of the wave processes in cylinders and rods were discovered which had previously escaped the attention of experimentalists and theorists.

6. In the USSR the ultrasonic pulse method was first applied to seismic logging of bore holes in 1954-1955, its object having been a detailed investigation of the elastic properties of rocks under natural bedding conditions. For this purpose a special seismos-

cope was constructed in GIAS. This method permits a determination of the velocities of propagation of dilational, shear and some other waves and also a judgement on their absorption with a detailness tens of times exceeding that of the known method of seismic logging used in prospecting. It should be noted that in USA the use of the ultrasonic pulse method for seismic logging started before (C. B. Vogel and oth., 1951-1952).

7. By means of the ultrasonic seismoscope special investigations were carried out in order to study the dependence on pressure of the velocity of propagation of elastic waves in samples of rocks : in our laboratory — with a unidirectional pressure and in the laboratory of prof M. P. Volarovich — with a confining pressure. Such investigations for sand were made in Moscow University. Similar investigations were also carried out by prof. W. Buchheim in German Democratic Republic.

From our observations follows that under reasonable pressures (of the order of 1.000 kg/cm² and more) the velocities of elastic waves depend essentially on pressure, so that this should be taken into account in geologic interpretation of seismic investigations of the earth crust. This dependence might perhaps be used for a study of the stresses in the earth leading to earthquakes (for shallow earthquakes).

8. For mining purposes the ultrasonic pulse method was first used in 1953 in a study of rock pressure in connection with the sudden coal and gas blow-outs in pits, and later on also for a study of rock bursts. From observations by this method of the elastic pulses travelling through the coal beds in the pit, it is possible to judge on the stresses exerted on the beds and even follow the changes in these stresses arising in process of mining.

In the study of rock bursts the ultrasonic pulse method was used in combination with the « acoustic » method consisting in observation of the elastic pulses arising spontaneously in rocks under rock pressure. The investigations of rocks bursts were carried out not only for mining purposes, but also for a study of processes similar to those taking place in sources of tectonic earthquakes.

References.

1. Risnichenko (J. V.), Ivakin (B. N.), Bugrov (V. P.). Modelling of seismic waves. Izv. A. N. SSSR, ser. geophys., N° 5, 1951.
2. Risnichenko (J. V.). Modelling of seismic phenomena. Viestnik A. N. SSSR, N° 5, 1952.

3. Risnichenko (J. V.). A study of the laws governing the propagation of seismic waves in real geologic media and in models. Viestnik A. N. SSSR, N° 4, 1946.
4. Risnichenko (J. V.). On propagation of seismic waves in discrete and heterogenous media. Izv. A. N. SSSR, ser. geogr. i geophys., N° 2, 1949.
5. Ivakin (B. N.). Elastic waves in one- and two-dimensional meshed models of continuous media. Trudi Geophys. In-ta A. N. SSSR, N° 9 (136), 1950.
6. Risnichenko (J. V.), Ivakin (B. N.), Bugrov (V. P.). The ultrasonic pulse seismoscope. Izv. A. N. SSSR, ser. geophys., N° 1, 1956.
7. Risnichenko (J. V.), Ivakin (B. N.), Bugrov (V. P.). Modelling of seismic waves by means of ultrasonic pulses. Izv. A. N. SSSR, ser. geophys., N° 3, 1953.
8. Ivakin (B. N.). Head, penetrating refracted and other waves in case of a thin solid sheet floating in a liquid. Trudi Geophys. In-ta A. N. SSSR, N° 35 (162), 1956.
9. Risnichenko (J. V.). On divergence and absorption of seismic waves. Trudi Geophys. In-ta A. N. SSSR, N° 35 (162), 1956.
10. Risnichenko (J. V.), Shamina (O. G.). On elastic waves in a solid stratified medium from investigations on two-dimensional models. Izv. A. N. SSSR, ser. geophys., N° 7, 1957.
11. Northwood (T. D.), Anderson (D. V.). Model seismology. Bull. Seism. Soc. Am., 43, N° 3, 1953.
12. Howes (E.), Tejada-Flores, Lee (R.). Seismic model study. Journ. Acoust. Soc. Am., 25, N° 5, 1953.
13. Oliver (J.), Press (F.), Ewing (M.). Two-dimensional model seismology. Geophysics, 19, N° 2, 1954.
14. Chubarova (S. I.). Model study of the propagation of seismic waves. Kand. dissert., Moscow University, 1954.
15. Ivakin (B. N.). Similarity of elastic wave phenomena. Izv. A. N. SSSR, ser. geophys., I-N° 11, II-12, 1956.
16. Risnichenko (J. V.), Silajeva (O. I.). Determination of the dependence on a directional pressure of the velocities of propagation of elastic waves in samples of rocks. Izv. A. N. SSSR, ser. geophys., N° 3, 1955.
17. Ozierskaja (M. L.). Trial laboratory measurements of the elastic properties of rocks., Prikladnaja Geofisika, 12, Gostoptechizdat, M, 1955.
18. Risnichenko (J. V.), Gluchov (V. A.). A seismic ultrasonic pulse logging method. Izv. A. N. SSSR, ser. geophys., N° 11, 1956.
19. Vogel (C. B.). A seismic velocity logging method. Geophysics, 17, N° 3, 1952.
20. Summers (G. C.), Broding (R. A.). Continuous velocity logging. Geophysics, 17, N° 3, 1952.
21. Denton (E. R.). Continuous velocity logging supplements seismic data. Oil in Canada, 7, N° 17, 1955.
22. Risnichenko (J. V.). Seismoacoustic methods of studying the strained state of rocks. Izv. A. N. SSSR, ser. Geophys., N° 6, 1955.
23. Risnichenko (J. V.), Silajeva (O. I.), Shamina (O. G.), Mjachkin (V. I.), Gluchov (V. A.), Vinogradov (C. D.). Seismoacoustic methods of studying the strained state of rocks on samples and under natural conditions. Trudi Geophys. In-ta A. N. SSSR, N° 34 (161), 1956.
24. Volarovich (M. P.), Balashov (D. B.). A study of the dependence on a confining pressure up to 1000 kgr/cm² of the velocities of propagation of elastic waves in coal samples. Trudi Geophys. In-ta A. N. SSSR, N° 34 (161), 1956.
25. Buchheim (W.). Zum Probleme der Drucksondierung in Gesteinen auf akustischer Basis. Freiberger Forschungshefte, Bergakademie, Heft 7, 1953.

26. RISNICHENKO (J. V.), MJACHKIN (V. I.). Seismic pulse method of studying rock pressure, Dokladi A. N. SSSR, N° 3, 1955.
27. SHAMINA (O. G.). Elastic pulses arising in the destruction of rock samples. Izv. A. N. SSSR, ser. geophys., N° 5, 1956.
28. SHAMINA (O. G.). A frequency analysis of seismic vibrations. Izv. A. N. SSSR, ser. geophys., N° 8, 1956.
29. VINOGRADOV (C. D.). Acoustic observations in pits of the Kizelov coal basin. Izv. A. N. SSSR, ser. geophys., N° 6, 1957.

ORIGIN AND COMPOSITION OF THE EARTH *

by O. J. SCHMIDT[1] and B. J. LEVIN.

Over 99 per cent of the Earth's matter is inaccessible for direct investigation. Therefore all studies of the chemical composition of the Earth as a whole (Tchirvinsky, 1919; Clark, 1924; Link, 1924; Washington, 1925; Niggli, 1928; Saslavsky, 1931, 1932; Fersman, 1932) are based not only on geophysical and geochimical, but also on cosmochemical data. In doing it these authors use in some or other way the ideas on the origin, evolution and present constitu tion of the Earth. Data on the chemical composition of the meteorites are widely used, but this is not in all cases based upon mutually correlating hypotheses on the origin of the Earth and meteorites (Levin, 1955).

1. The modern cosmogonical investigations of various authors are concerned with the formation of planets from a cold gas-dust cloud. However, proceeding from the same initial state of planetary matter these investigations diverge markedly in the suggested process of planet formation.

In 1943-44 appeared almost simultaneously the hypotheses by Weizsäcker and by Schmidt, in which a gradual growth of the Earth by means of a sweeping up of the surrounding diffuse matter is supposed. In subsequent investigations by Schmidt and his collaborators the main idea of the Earth's gradual growth was defined and developed (Schmidt, 1955 b). The formation of the Earth by means of accumulation of solid matter was suggested later by Edgeworth (1949), Hoyle (1955), Gold (1957) and also by Urey.

In his investigations of the origin of the solar system, begun from about 1949, Kuiper considered the formation of the Earth and other planets as a gradual dissipation of massive protoplanets, which were formed ,as he thought, during the first stage of evolution of the cloud. But in recent years Kuipers views began to change and now he suggest that Mercury and Mars and probably Venus and Earth also were formed by means of a gradual growth (Kuiper,

1. Prof. O. J. Schmidt died Sept. 7, 1956. The present paper had to be prepared by B. J. Levin alone.

* The russian version of this paper was published in the « Bulletin of Ac. Sci. USSR, ser. geophys. », N 11, 1957. This Bulletin is published in English by Pergamon Press. The translation of the mentioned paper contained serios errors. For instance in the table 1 and in the accompaning text is written « core » instead of « crust ».

1956). Kuiper discusses mainly the astronomical aspect of the problem, without an analysis of the detailed chemical data and of the thermal history of the Earth.

Urey in his investigations, based mainly on the chemical evidences, first took Kuiper's hypothesis as the astronomical basis. But in the course of his work he had to reject it. The formation of the Earth from a massive proto-earth can explain some chemical evidences only, but the analysis of their totality shows that such protoplanets did not exist and that the formation of the Earth began in the form of an accumulation of cold solid particles (Urey, 1952, 1956). Moreover, it has been shown by Shklovsky (1951) that the dissipation in which hydrogen and helium are lost and other gases are retained, must be very slow and requires unreasonably long intervals of time of the order of $10^{10} - 10^{11}$ years. In spite of this, Fessenkov, who accepted in 1951 the hypothesis of planet formation from a gas-dust cloud, admits up to the present a process similar to that suggested by Kuiper and claims that the Earth originated as an incandescent body (Fessenkov, 1957).

2. The chemical composition of the Earth is discussed in the present paper proceeding from the cosmogonical theory, developed on the basis of Prof. Schmidt's ideas. It is impossible to review in a short communication the evolution of this theory, or to give a detailed cross-examination of the actual data, which should be necessary to give the reasons why a given process of Earth's formation is preferred to any other processes. It will only be noted that the analysis of the main regularities of planetary motions gives evidences of the formation of planets from a swarm of bodies, which moved along different orbits, and an analysis of the regularity in the chemical composition of planets permits to penetrate further into the past and to establish that a still earlier state of planetary matter was a gas-dust cloud, surrounding the Sun.

Prof. Schmidt advanced a hypothesis that this cloud was captured by the Sun. This hypothesis, also expressed later by Edgeworth, permits to explain the distribution of the angular momentums between the Sun and the planets. Other investigators (Weizsäcker, Kuiper, Fessenkov) suppose that the protoplanetary cloud originated in the process of formation of the Sun. But these authors do not give any description of this process and do not solve therefore the problem of the momentæ, thus leaving it for the future.

Intense turbulent motions existed probably in a cloud during its first stages and particularly in the case of its capture. However, Safronov and Ruscol (1956) had shown that this motion must be rapidly damped, because of the absence of energy sources for their maintenance. Therefore, in the study of the subsequent evolution of the cloud, independently of the point of view of its origin, we can suppose that it was first in a quiet laminar rotation around the Sun.

The gaseous component of the cloud, owing to great thermal velocities of molecules, was distributed over a moderately flattened spheroidal volume. But solid particles whose chaotic velocities were damped by gaseous friction and by inelastic collisions, must have been accumulated in a central plane of the cloud, forming a dense and flat disk. At a certain stage of flattening the density of the disk attained Roche's critical value, gravitational instability has set in and the disk broke up into a multitude of condensations, whose internal gravitational forces exceeded the tidal forces of the Sun. The masses of condensations depended upon their distances from the Sun, but they were everywhere many times less, than the masses of the contemporary planets (L. Gurevitch and A. Lebedinsky, 1950).

Condensations mainly consisting from dust were formed at first. Afterwards they collapsed into bodies of some tens and hundreds of kilometres in diameter. The formation of such asteroidal type bodies by means of a sticking of small particles is a less probable process, because particular physico-chemical conditions are required for it. But after the formation of sufficiently great bodies, the possibility of their further growth as a result of a sweeping up of the surrounding diffuse matter is beyond doubts. At first the asteroidal bodies collected the remainder of the « primordial » particles and then mainly the debries formed by the fragmentation of some bodies, in their collisions. Those few bodies the growth of which became more rapid has finally developed into modern planets. During the last stages even the fall of asteroidal bodies on their surface was a part of the process of their growth and not lead to their destruction and fragmentation.

The gravitational interaction of asteroidal bodies, which increased with their mass, transformed the initially circular and complanar orbits of these bodies into differently inclined elliptic orbits. But in the course of accumulation of a multitude of bodies into planets the individual properties of motions were averaged and therefore the planetary orbits are nearly circular and complanar.

Prof. Schmidt (1946) had shown that the process of growth by means of a sweeping up of the surrounding matter contains the mechanism which regulates the distances between the orbits of neighbouring growing bodies. This lead finally to a regularity in the planetary distances from the Sun. The simultaneous application of the laws of conservation of the energy and of angular momentum to a process of planet accumulation gives an explanation of the direct axial rotation of planets (Schmidt, 1950). Thus such process of the formation of the planetary system explains its main astronomical properties. It gives also an explanation of the masses and chemical properties of planets.

3. The formation of a dust disk was accompanied by the appearance of zonal differences in the chemical composition and the total mass of solid particles (L. Gurevitch and A. Lebedinsky, 1950). When the dust was mixed with gas and distributed over a great volume the space around the Sun was transparent enough, the temperature of the particles was comparatively great and therefore they were composed of refractory, non-volatile substances only. But in the course of dust collection the forming disk became more and more opaque and the temperature of its outer parts became gradually more and more low. Only the inner part of the disk remained heated by the Sun and only there the composition of particles remained unaltered. But in the outer parts owing to the lowering temperature the molecules of different volatile substances present in a gaseous component of a protoplanetary cloud became frozen to the particles. From the cosmic abundances of elements it follows that excluding H_2 the most abundant molecules were H_2O, NH_3, CH_4, CO_2. Obviously the freezing of not only the stable molecules, but also of radicals must be considered (Donn and Urey, 1956, Urey and Donn, 1956).

As the matter of a dust disk passing through the stage of a swarm of asteroidal bodies, were accumulated into planets, these zonal differences in the amount and composition of solid particles became zonal differences in the masses and composition of planets. The refractory stony particles of the inner zone formed small dense terrestrial planets, while the particles of the outer zone congelated by volatile substances formed the giant planets of low densities. Neglecting the changes of the temperature during this process, it can be said, that the composition of planets (and of comets, asteroids and satellites also) depends upon the temperature, which existed at the place and time of their formation. It is not correct to suggest Jupiter to contain abundant light elements because of its large mass, which prevented their dissipation. On the contrary the mass of Jupiter is so large, because its formation was going on under conditions, which permitted to incorporate light elements, which are cosmically very abundant.

Chemical data are of course especially complete for the Earth (and for meteorites) and their analysis confirms the process of planet formation described above (Levin, 1949, 1953, 1955, 1957; Urey, 1951, 1952, 1954 a, b, c, 1956). Indeed the problem of the composition of the Earth's core is of great importance in this connection. If it is adopted that it consists from silicates transformed into metallic state under the action of high pressure (Lodotchnikov, 1939; Ramsey, 1948, 1949), the analysis of the mean densities of terrestrial planets and of the Moon shows that they have the same composition (except Mercury, which is the nearest to the Sun) (Ramsey, 1949, Koslowskaya, 1953). It is namely what should be expected, when accumulation of solid particles present in the heated part of the dust disk is considered[2]).

If the earlier hypothesis of the iron core of the Earth is retained, as it is done by Urey, the difference in the densities of the terrestrial planets must be explained by a different content of metallic iron. Some process must be searched for in this case, owing to which this differences have originated. It was the aim of Urey's attempts to modify Kuiper's ideas about massive protoplanets. He suggested that asteroidal type bodies were imbedded into protoplanets, where they underwent surface heating, during which a separation of metal and silicates and a partial evaporation of the latter took place. But in a recent paper Urey (1956) concluded that such protoplanets had never existed. The different content of metallic iron in the terrestrial planets, suggested by Urey, he attempts to explain now by a very complicated process of solar system formation, some stages of which do not agree with the modern astronomical data.

But it must be stressed once more that all these attempts and complications may be rejected, if Ramsey's hypothesis is accepted.

4. Even at the times when the meteorites were believed to be strangers arriving from the interstellar space, the data about their composition were used in the study of the composition of the Earth. This was then motivated by the simple reason that both are the result of evolution of the silicate matter. Now it is known that meteorites are the debries of asteroids, i.e. of bodies, which belong same as the Earth to the inner zone of the planetary system. The

---

2. The high density of Mercury is due, obviously, to its formation from the most intensely heated and therefore most dense particles or, perhaps, from particles which had condensed from the gas at higher temperatures.

identity of isotopic composition of several elements in the Earth and in the meteorites indicates a good mixing of the protoplanetary matter at least in the inner zone. Indeed, the asteroids were formed at the junction of the zones of the terrestrial and giant planets. The substantial variation of the external conditions over the zone of asteroids, can be the cause of the differences in their composition, manifested in the composition of meteorites. Some years ago Urey and Craig (1953) distinguished two groups of meteorites, which they connected with two parent asteroids. Later five groups of such kind, differing mainly in their iron content were revealed by Javnel (1955, 1956). The fall on the Earth of meteorites belonging to a few groups only indicates that the fragmentation of the respective parent asteroids take place not earlier than some hundred million years ago. Therefore, even if we could find the true mean composition of the meteorites, corrected for their evaporation and destruction in the atmosphere, and for the incompleteness of their collection, this composition would be referred to the present moment and could not reflect exactly the composition of the Earth as a whole.

It is clear that the composition of meteorites can characterize the abundance of only such elements in the Earth, which form compounds non-volatile at temperatures about O°C. The origin of the atmosphere and hydrosphere of the Earth is connected not only with the sorption of gases by solid particles, but also with a past fall on the Earth of icy bodies, similar to cometary nuclei. This process remains yet uninvestigated.

At the present stage of knowledge we prefer to use the meteorite analysis to determine the mean composition of stony and metallic parts of meteoritic matter and to accept the same composition of these parts in the Earth. The ratio of these parts must be determined separately. In a paper by Levin (1955) it was supposed from some indirect evidences that the massratio of stone to metal is 6 : 1. We prefer now Bullen's hypothesis that the inner core consist from nickel-iron and is due to a differentiation of the core (in the mantle silicate and metal remain in a mixed state). But the density and therefore the mass of the inner core are known but poorly. The mass of the inner core is about 8 per cent of that of the whole core. Computing the composition of the Earth we adopt this percentage for the metallic part.

In table I the abundances of stony and metallic parts of the meteoritic matter are given for 78 chemical elements (each of these parts is considered including troilite, contained in it). They differ somewhat from the data published earlier (Levin, 1955; Levin, Kozlowskaja and Starkova, 1956) because they were revised by S. Kozlowskaya on the basis of the newly published analyses. The mean composition of the whole Earth (colum 5) is calculated, supposing as mentioned above the percentage of metal to be 8. The data of columns 3 and 4 permit to recalculate it easily for any other percentage of metal. This will change the data only for a dozen of most abundant elements and for a dozen of siderophyllic elements, contained only in the metal. The majority of elements is concentrated in the silicate part and therefore the various suppositions on the metal percentage affect only slightly their mean abundances.

A comparison with the data by Vinogradov (1956) on the composition of the Earth's crust, given in column 6, permits to reveal the elements, which were concentrated in the crust during its formation or vice versa remained in the mantle. According to the ratios « crust/Earth », given in column 7, the following 25 elements were concentrated in the crust : Li, Be, B, N, F, Al, K, Ti, Rb, Sr, Zr, Nb, Cs, Ba, La, Ce, Pr, Nd, Ta, Hg, Tl, Pb, Ra, Th, U. (for them the ratio crust/Earth $\geqslant 5$). The following 19 elements were found to be deficient in the crust : Mg, S, Cr, Fe, Co, Ni, Ge, Se, Ru, Rh, Pd, Cd, Te, W, Re, Os, Ir, Pt, Au (for them we have the ratio crust/Earth $\leqslant 0{,}2$).

5. The abundance of radioactive elements in the Earth is of a special interest. It is needed for a study of the Earth's thermal history. Recently Urey (1955) has calculated the mean concentration of radioactive elements in the Earth, supposing that owing to the existence of convective currents the total heat generation is equal to the heat flow through the surface. However, the viscosity of the silicate substance of the mantle is probably so great that convection does not occur in spite of a temperature gradient exceeding probably the adiabatic gradient. Therefore a method used by Urey, giving a right order of magnitude, can easily give a concentration, which will be for 2-3 times in error.

Last year Urey turned to an evaluation of the concentration of radioactive elements in the Earth, using the data about their concentration in meteorites (1955 b). This is namely the procedure used already for several years in our department of the Institute of physics of the Earth (Lubimova, 1952, Levin, 1955).

For K, U and Th the mean values, obtained by Starkova (1955) are adopted in table I. Although they are based on a small number of analyzes they seem to be approximately correct. According to the calculations by Lubimova (1956) they give a heat flow through the Earth's surface close to the observed flow. Starick and Shaz (1956) received a five times greater concentration of U in the silicate part of meteorites, i.e. 20.10^{-8} g/g. If such a great concentration is adopted for the silicate matter of the Earth, the heat flow must be several times greater that observed. On the other hand if a low value of 1.10^{-8} g/g is accepted, as it is done by Urey (1956 c), the total generation of heat in the Earth becomes 1,5 times less than the heat loss and it is impossible to collect sufficient amount of U from the whole Earth to explain its actual content in the Earth's crust.

According to the contents of radioactive elements given in Table I, the generation of heat in the Earth exceeds the heat loss. The inner parts of the Earth remain to be heated.

Practically all the heat of the Earth is of a radiogenic origin. The main part of the Earth's formation (the accumulation of 95-97 per cent of the mass) has taken 1 — 2.10^{8} years. Therefore the heat liberated on the surface by the impacts of particles had time enough to be radiated in the space, heating the Earth only slightly.

The central parts of the Earth were formed 100-200 millions of years earlier, than the outer parts and were heated for a longer time by the radiogenic sources. This lead to a temperature gradient and consequently to a heat flow from the core through the mantle. If Bullen's explanation of the inner core is correct, much heat must be generated in its formation and the heat flow from the core must become stronger. This makes possible to explain the convective motions in the core, which are assumed to be the cause of the magnetic field of the Earth. The substance of the outer parts of the core, being in metallic state, can in spite of the enormous pressure possess a viscosity, which is too small to prevent convection.

6. The formation of the cold Earth, which is later on gradually heated by the radiogenic sources, described above, leads to the idea about a continuous formation of the crust, as a result of physico-chemical and gravitational differentiation of matter in the outer layers of the Earth (Levin, 1953, Schmidt, 1955 a). In the course of heating, when the temperature of these layers becomes large enough, a partial melting has set in, i.e. the melting of less refractory compounds. After having accumulated in sufficient quantities and being of a lesser density, they rose to and on the surface.

As it had been said in § 4, we take the mean composition of the whole Earth to be almost the same as that for meteorites. The possibility of a melting out of the meteoritic substance of some parts, having the same composition as the crust, was noted long ago. For example Goldschmidt (1938), after a comparison of the composition of the meteorites and of the crust, wrote :

« Man wird derart zu der Auffassung geführt, dass solche Silikatmeteoriten etwa ein Analogon des Ausgangsmaterials der irdischen Silikatgesteine bilden könnten, in der Weise, dass unsere irdische Lithosphäre als Ganzes eine ähnliche Zusammensetzung aufweisen könnte wie die Chondriten, dass aber durch fraktionierte Kristallisation in den uns zugänglichen obersten Teilen der Lithosphäre die Restmagmen und Mutterlaugen einer solchen fraktionierten Kristallisation angereichert worden sind. Solche Restmagmen, wie etwa die Magmen granitischer und nephelinsyenitischer Gesteine, besitzen ein viel niedrigeres spezifisches Gewicht als die Silikate der Chondriten und müssen sich daher im Laufe der geologischen Geschichte in den alleroberstenTeilen der Lithosphäre vorzugsweise ansammeln. »

Somewhat further Goldschmidt wrote again :

« Das Ergebnis des Vergleiches zwischen den Stoffbeständen des Silikat-Anteiles der Meteoriten und der irdischen Gesteine, auch in Bezug auf seltene Elemente ist also vereinbar mit der Hypothese, dass die uns zugänglichen Gesteine der Erdoberfläche durch fraktionierte Kristallisation aus einem Magma stammen, dessen Zusammensetzung etwa den Silikatmeteoriten entspricht. »

Goldschmidt supposed the formation of the Earth from a hot gaseous condensation and therefore he does not connect the appearance of the crust with the heating of the Earth from cold initial state.

The idea of a gradual formation of the crust was suggested some years ago by Wilson on the ground of some geological evidence. This idea is being successfully developed by him (Wilson, 1957). It is confirmed by the evidences about the continuous growth of the continents, based on the age measurements.

Modern concept of a gradual formation of the atmosphere and hydrosphere by means of a storage of gases and vapours emanated from the internal parts of the Earth (see for instance Rubey, 1951) also agrees with the cosmogonical concept of the cold accumulation of the Earth and its subsequent heating.

7. Last year B. Gutenberg (1956) pointed out that « Eine zunehmende Zahl von Astrophysikern und Geophysikern halt es für wahrscheinlich, dass die Erde durch allmähliche Anhäufung von kaltem Material entstanden war, und mehrere Geologen haben die Ansicht ausgesprochen, dass die Erde nie vollig geschmolzen war (ZB. Rubey, 1951, S. 1117) ».

As can be seen from the present paper, its author belongs to the group of soviet scientists developing this point of view on the origin and evolution of the Earth, because it seems to them to be the true one. It opens the possibility for a progress in the geophysical and geochemical studies of our planet.

REFERENCES.

BULLEN (K. E.). 1957, M. N., Geoph. suppl. *7*, 271.
CLARK (F. W.). 1924, U. S. Geol. Survey, Prof. Paper, N° 132-D, 76.
DONN (B.) and UREY (H. C.). 1956, ApJ *123*, 339.
EDGEWORTH (K. E.). 1949, M. N. *109*, 600.
FERSMAN (A. E.). 1932, Geochemistry, *1*, Moscow.
FESSENKOV (V. G.). 1957, A. J. USSR, *34*, 105.
GOLD (T.). 1956, Report on the Geophysical discussion, See Nature, *179*, 121, 1957.
GOLDSCHMIDT (V. M.). 1938, Geochemische Verteilungsgesetze der Elemente, IX, Oslo.
GUREVITCH (L. E.) and LEBEDINSKY (A. I.). 1950, Bull. Acad. Sci. USSR, sér. phys., *14*, 765; (see also C. R. Acad. Sci. USSR, *74*, 673, 905, 1061, 1950).
GUTENBERG (B.). 1956, Geol. Rundschau, *45*, 342.
HOYLE (F.). 1955, Frontiers of Astronomy, London.
JAVNEL (A. A.). 1955, C. R. Acad. Sci. USSR, *102*, 477.
— 1956, Geochemistry (USSR), N° 2, 78.
KOZLOVSKAYA (S. V.). 1953, C. R. Acad. Sci. USSR, *92*, 903.
LEVIN (B. J.). 1949, Nature (USSR), N° 10, 3.
— 1953, Bull. Acad. Sci. USSR, sér. géophys. N° 4, 289.
— 1955, Publ. Geophys. Inst. N° 26 (153), 11.
— 1957, Mém. Soc. R. Sci. Liège, *18*, 186.
LEVIN (B. J.), KOZLOVSKAYA (S. V.), STARKOVA (A. G.). 1956, Meteoritics (USSR), *14*, 38.
LINK (G.). 1924, Aufbau des Erdballs, Jena.
LODOTCHNIKOV (V. N.). 1939, Mem. Mineralog. Soc. USSR, *64*, 207.
LUBIMOVA (E. A.). 1952, Bull. Acad. Sci. USSR, sér. géophys. N° 2, 3.
LUBIMOVA (E. A.). 1956, C. R. Acad. Sci. USSR, *107*, 55
NIGGLI (P.). 1928, Fennia, *50*, 1.
RAMSEY (W.). 1948, M. N., *108*, 406.
— 1949, M. N., Geophys. suppl. *5*, 409.
RUBEY (W. W.). 1951, Bull. Geol. Soc. Amer., *62*, 1111.
SAFRONOV (V. S.) and RUSCOL (E. L.). 1956, C. R. Acad. Sci. USSR, *108*, 413.
SASLAVSKY (I. I.). 1931, Nature (USSR), 20, 754.
— 1932, Mineralog. und Petrograph. Mitt., *43*, 144.
SHKLOVSKY (I. S.). 1951, A. J. USSR, *28*, 234 (see also C. R. Acad. Sci. USSR, *76*, 193, 1951).
SCHMIDT (O. J.). 1946, C. R. Acad. Sci. USSR, *52*, 673.
— 1950, Bull. Acad. Sci. USSR, sér. phys. *14*, 29; Publ. Geophys. Inst. N° 11 (138), 3.
— 1955 a. Publ. Geophys. Inst. N° 26 (153), 5.
— 1955 b. Mém. Soc. R. Sci. Liège, *15*, 638.
STARIK (I. E.) and SHATZ (M. M.). 1956, Geochemistry (USSR), N° 2, 19.
STARKOVA (A. G.). 1955, Meteoritics (USSR), *13*, 9.
TCHIRVINSKY (P. N.). 1919, Bull. of the Donskoy Polytechnical Inst. *7*, Part 2, 94.
UREY (H. C.). 1951, Geochim. Cosmochim. Acta, *1*, 209.
— 1952, The Planets, New Haven.
— 1954, XIII, Int. Congr. Appl. Pure Chem. 1953, 188, Uppsala.
— 1954 b. ApJ Suppl. *1*, 147.
— 1954 c. Nuclear geology, ed. by H. Faul, 355, Ch. X.
— 1955, Proc. Nat. Acad. Sc. *41*, 127.
— 1956 a. ApJ *124*, 623.
— 1956 b. Proc. Nat. Acad. Sci. *42*, 889.
UREY (H. C.) and CRAIG (H.). 1953, Geochim. Cosmochim. Acta, *4*, 36.
UREY (H. C.) and DONN (B.). 1956, ApJ *124*, 307.
VINOGRADOV (A. P.). 1956, Geochemistry (USSR), N° 1, 6.
WASHINGTON (H. S.). 1925, Amer. J. Sci. *9*, 351.
WILSON (J. T.). 1957, Nature, *179*, 228.

TABLE 1

Atomic number	Element	Stony part of the meteoritic matter	Metallic part of the meteoritic matter	Earth as a whole	Earth's crust	Crust/Earth
3	Li	$2,7.10^{-4}$		$2,5.10^{-4}$	3.10^{-3}	10
4	Be	1.10^{-4}		1.10^{-4}	$4,2.10^{-4}$	5
5	B	$2,5.10^{-4}$		$2,3.10^{-4}$	$1,3.10^{-3}$	6
6	C	0,034	0,10	0,04	0,023	0,6
7	N	0	1.10^{-3}	1.10^{-4}	0,01	100
8	O	40,5		37,3	47,2	1,3
9	F	$2,8.10^{-3}$		$2,6.10^{-3}$	0,066	25
11	Na	0,67		0,62	2,50	4
12	Mg	16.3	0,032	15,0	1,70	0,1
13	Al	1.69	0,004	1,6	8,08	5
14	Si	20,8	0,004	19,1	29,0	1,5
15	P	0,16	0,20	0,16	0,09	0,6
16	S	2,22	0,50	2,1	0,09	0,04
17	Cl	0,05		0,05	0,02	0,4
19	K	0,085		0,08	2,50	30
20	Ca	1,81	0,05	1,7	3,30	2
21	Sc	6.10^{-4}	4.10^{-5}	5.10^{-4}	$1,3.10^{-4}$	2
22	Ti	0,08	0,01	0,07	0,44	6
23	V	0,007	$6,5.10^{-4}$	0,007	0,009	1,4
24	Cr	0,29	0,03	0,27	0,012	0,04
25	Mn	0,23	0,031	0,21	0,09	0,4
26	Fe	15,1	88,8	21,0	4,63	0,2
27	Co	$/6.10^{-4}/$	0,65	0,05	0,0018	0,03
28	Ni	$/6.10^{-3}/$	9,46	0,8	0,01	0,01
29	Cu	$/1,6.10^{-4}/$	0,03	3.10^{-3}	0,007	3
30	Zn	$/10^{-3}/$	0,014	0,002	0,004	2
31	Ga	$3,2.10^{-4}$	$1,5.10^{-3}$	4.10^{-4}	0,0015	4
32	Ge	9.10^{-4}	0,02	2.10^{-4}	2.10^{-4}	0,1
33	As	$/3.10^{-5}/$	$1,2.10^{-3}$	1.10^{-4}	2.10^{-4}	2
34	Se	$1,3.10^{-3}$	4.10^{-4}	0,001	$/10^{-6}/$	10^{-3}
35	Br	6.10^{-4}	1.10^{-4}	6.10^{-4}	$1,8.10^{-4}$	0,3
37	Rb	$5,5.10^{-4}$	0	5.10^{-4}	0,03	60
38	Sr	2.10^{-3}		2.10^{-3}	0,035	20
39	Y	7.10^{-4}	3.10^{-5}	6.10^{-4}	0,002	3
40	Zr	$3,3.10^{-3}$	8.10^{-4}	3.10^{-3}	0,02	6
41	Nb	5.10^{-5}	2.10^{-5}	5.10^{-5}	0,001	20
42	Mo	6.10^{-5}	8.10^{-4}	1.10^{-4}	1.10^{-4}	1
44	Ru	0	1.10^{-3}	1.10^{-4}	$/10^{-8}/$	10^{-4}
45	Rh	0	5.10^{-4}	4.10^{-5}	1.10^{-7}	0,0025
46	Pd	0	$3,6.10^{-4}$	3.10^{-5}	4.10^{-7}	0,007
47	Ag	0	$4,2.10^{-4}$	3.10^{-5}	$/2.10^{-5}/$	0,6
48	Cd	$/1.10^{-3}/$	$8,3.10^{-4}$	1.10^{-3}	$1,3.10^{-5}$	0,01
49	In	2.10^{-5}	5.10^{-5}	2.10^{-5}	1.10^{-5}	0,5
50	Sn	1.10^{-4}	5.10^{-4}	1.10^{-4}	2.10^{-4}	2
51	Sb	1.10^{-5}	5.10^{-5}	1.10^{-5}	2.10^{-5}	2
52	Te	1.10^{-5}	$2,3.10^{-5}$	1.10^{-5}	$/10^{-7}/$	0,01
53	J	$1,2.10^{-4}$	6.10^{-5}	1.10^{-4}	3.10^{-5}	0,25
55	Cs	1.10^{-6}		1.10^{-6}	1.10^{-4}	100
56	Ba	8.10^{-4}		7.10^{-4}	0,06	80
57	La	2.10^{-4}	6.10^{-6}	2.10^{-4}	4.10^{-3}	20
58	Ce	$2,3.10^{-4}$	7.10^{-6}	2.10^{-4}	4.10^{-3}	10
59	Pr	$1,10^{-4}$	2.10^{-6}	1.10^{-4}	7.10^{-4}	8
60	Nd	$3,4.10^{-4}$	8.10^{-6}	3.10^{-4}	3.10^{-3}	10
62	Sm	$1,2.10^{-4}$	3.10^{-6}	1.10^{-4}	$/4.10^{-4}/$	4
63	Eu	3.10^{-5}		3.10^{-5}	$/1.10^{-4}/$	4
64	Gd	$1,8.10^{-4}$	6.10^{-6}	2.10^{-4}	$/7.10^{-4}/$	4
65	Tb	$5,8.10^{-5}$	[illegible]	5.10^{-5}	$/1.10^{-4}/$	2

Atomic number	Element	Stony part of the meteoritic matter	Metallic part of the meteoritic matter	Earth as a whole	Earth's crust	Crust/Earth
66	Dy	$2,3.10^{-4}$	7.10^{-6}	2.10^{-4}	$4,5.10^{-4}$	2
67	Ho	$6,6.10^{-5}$		6.10^{-5}	$1,3.10^{-4}$	2
68	Er	$1,9.10^{-4}$	6.10^{-6}	2.10^{-4}	2.10^{-4}	1
69	Tu	$3,4.10^{-5}$		3.10^{-5}	$/1.10^{-4}/$	3
70	Yb	$1,8.10^{-4}$	6.10^{-6}	2.10^{-4}	2.10^{-4}	1
71	Cp(Lu)	6.10^{-5}		6.10^{-5}	1.10^{-4}	2
72	Hf	1.10^{-4}		1.10^{-4}	$3,2.10^{-4}$	4
73	Ta	$3,8.10^{-5}$	6.10^{-6}	4.10^{-5}	$2,1.10^{-4}$	6
74	W	$1,6.10^{-3}$	8.10^{-4}	1.10^{-3}	1.10^{-4}	0,06
75	Re	2.10^{-7}	$/1.10^{-4}/$	$/7.10^{-6}/$	1.10^{-7}	0,01
76	Os	0	8.10^{-4}	6.10^{-5}	$/10^{-8}/$	10^{-4}
77	Ir	0	4.10^{-4}	3.10^{-5}	10^{-7}	0,003
78	Pt	8.10^{-6}	2.10^{-3}	$1,7.10^{-4}$	$/5.10^{-7}/$	0,003
79	Au	0	$1,6.10^{-4}$	1.10^{-5}	2.10^{-7}	0,01
80	Hg	$/1.10^{-6}/$	3.10^{-7}	$/1.10^{-6}/$	6.10^{-6}	6
81	Tl	$1,5.10^{-5}$	4.10^{-7}	$1,4.10^{-5}$	3.10^{-4}	20
82	Pb	2.10^{-4}	$1,8.10^{-4}$	2.10^{-4}	$1,6.10^{-3}$	8
83	Bi	1.10^{-5}	5.10^{-5}	1.10^{-5}	2.10^{-5}	1.5
88	Ra	2.10^{-12}	$1,6.10^{-13}$	$1,8.10^{-12}$	9.10^{-11}	50
90	Th	$2,4.10^{-5}$	$1,8.10^{-6}$	2.10^{-5}	$1,3.10^{-3}$	60
92	U	6.10^{-6}	$4,8.10^{-7}$	6.10^{-6}	3.10^{-4}	54

PHYSICAL PROPERTIES OF SOLIDS AT HIGH PRESSURES

By B. I. DAVYDOV

ABSTRACT.

Approximate expressions for the free energy of typical crystalline solids (ionic, valence, molecular crystals and metals) have been derived from the quantum theory of solids. These expressions enable to obtain in the usual manner the equation of state, as well as the compessibility and thermal expansion coefficient as functions of the pressure and temperature. The constants appearing in the formulae can be determined from the experimental data relating to low pressures. The resulting equations are valid up to a pressure at which some phase transition is taking place. Theoretical curves for several substances of interest for geophysics (NaCl, MgO, Fe_3O_4, $(Mg, Fe)_2SiO_4$, Si, Ge, Fe) agree well with the observational data at experimentally attainable pressures.

General theoretical expressions for ionic electric conductivity of non-metallic solids depending on pressure and temperature are given. Ionic conductivity increases rapidly with growing temperature, but it must fall with increasing pressure. It may therefore be supposed that electric conductivity is not ionic, but electronic in the deeper layers of the Earth mantle. Conductivity of electronic semi-conductors may either increase or decrease with pressure.

1. EQUATION OF STATE, COMPRESSIBILITY AND THERMAL EXPANSION.

The equation of state of solids at high pressures, their compressibility and thermal expansion belong to the most essential problems for the physics of the Earth.

Formulae based on the theory of finite deformations developed by Brillouin, Murnagan and oth. [1] are being used by some geophysicists during the recent years. In addition to the quadratic terms in the expression for the potential energy of a solid leading to the linear dependence of the stress from the strain components, terms of higher order are taken into account. The third-order terms are means practically.

The resulting expressions may, of course, be applied only to such cases when the deviations from the linearity are not large. For larger deviations the third-order terms were insufficient even at a formal convergence of the whole expansion. A great number of the expansion terms should be taken into account, which is practically non-realizable.

Actually, as it is seen from the experimental data, the deviations from the linear dependence cannot be considered as small, even at pressures of the order of 10^5 atm. This concerns still more the region of the order of 10^6 atm. important for geophysics. The formal method in which the peculiarities of the molecular structure of various solids are not taken into account cannot be used at such pressures and it becomes necessary to apply the modern theory of the structure of matter.

In the quantum theory of solids an approximate dependence of the energy of a macroscopic body from its volume, which determines its physical properties, may be already given on the ground of the general properties of electronic wave functions. Indeed, in the pressure range of interest to geophysics only the interaction between the outer electronic shells of atoms or ions of the considered solid is essential. The general exponential character of their wave functions leads to the characteristic exponential form of the corresponding terms in the expression for the energy. The slowly changing pre-exponential factors are inessential and can be replaced by constants. The expression for the total energy of a given body will contain several constants, which may be easily determined according to experimental data concerning experimentally accessible pressures. The dependences obtained in such a way will be valid until a phase transition causing an essential change of the curves will take place.

The equation of state of different solids being of interest to us, their compressibility and the thermal expansion coefficient can be expressed by means of the free energy of a mass unit F(V,T), where V is the specific volume and T is the temperature. For temperatures higher than the Debye temperature Θ, namely exceeding some hundred degrees abs, it can be written :

$$F = E + N \upsilon k T \left(3 \, ln \frac{\Theta}{T} - 1\right) \tag{1}$$

where

$$\Theta = \frac{hc}{k} \left(\frac{6\pi^2 N\upsilon}{V}\right)^{1/3} \tag{2}$$

Here N is the number of molecules in a mass unit, ν is the number of atoms in a molecule, k is Boltzmann's constant, and h is the Planck constant divided by 2π; c is some mean sound velocity :

$$\frac{1}{c^3} = \frac{1}{3}\left[\frac{1}{c_l^3} + \frac{2}{c_t^3}\right], \tag{3}$$

c_l and c_t are the velocities of the longitudinal and transverse elastic waves respectively. If the compressibility β is introduced, then

$$c_l = \sqrt{\frac{3V}{\beta}\frac{1-\sigma}{1+\sigma}} \qquad c_t = \sqrt{\frac{3V}{2\beta}\frac{1-2\sigma}{1+\sigma}}$$

where σ is Poissons's coefficient. Its changes with pressure and temperature are small and σ can be considered as nearly constant.

Knowing the free energy $F(V,T)$ we shall find pressure P, i.e. the equation of state, the volume compressibility β and the thermal expansion coefficient α by means of the usual formulae :

$$P = -\frac{\partial F}{\partial V} \cdot \frac{1}{\beta} = V\frac{\partial^2 F}{\partial V^2}, \ \alpha = \frac{1}{V}\left(\frac{\partial V}{\partial T}\right)_P = -\beta\frac{\partial^2 F}{\partial T\,\partial V} \tag{4}$$

Thus the problem is reduced to the determination of the dependence of the energy at absolute zero upon the volume. We shall show approximately this dependence for the main types of the crystalline solids.

a) *Ionic crystals.*

Among the non-metallic solids the ionic crystals had been studied in particular details. The energy of such a crystal may be represented in the form : [2]

$$E = A_1 e^{-B_1 a} - \frac{C_1}{a} = Ae^{BV^{1/3}} - CV^{-1/3} \tag{5}$$

where a is the lattice constant. A, B and C are the constants. The second term represents here the Coulomb attraction between the ions. The first term accounts the mutual repulsion of electronic shells of ions. The exponential form of it follows from the general exponential character of the electronic wave functions.

From equations (1), (4) and (5) the equation of state of the ionic crystals is obtained :

$$P = K_1 x^{-2/3} e^{-bx^{1/3}} - K_2 x^{-4/3} + K_T \tag{6}$$

Here x is the ratio between the specific volume and the specific volume V_0 at zero pressure : $x = V/V_0$, constants

$$K_1 = \frac{1}{3}ABV_0^{-2/3}, \ K_2 = \frac{1}{3}CV_0^{4/3}, \ b = BV_0^{1/3} \tag{7}$$

K_T is the temperature correction resulting from the second term of the expression (1) for the free energy. This correction is not large at moderate temperature and does not depend much on the volume. It can be calculated by means of the above equations.

The energy of electrostatic attraction of crystal ions was calculated by Born, Madelung and oth. As to the coefficients A and B it is better to determine them empirically. Thus for example, one may proceed from the values of the specific volume and compressibility related to the pressure $P = 0$.

The values of the coefficients A, B and C may be found in the first approximation neglecting the temperature dependence, i.e. taking $T = 0$ in (1). The temperature correction may then be calculated with these approximate values. Substracting the correction from the experimental data the values of the coefficients can be found then in the second approximation.

Coefficients K_1, K_2 and K_T (for $T = 300_o K$) and b, as also the Debye temperature Θ for some ionic crystals — rocksalt, periclase, magnetite, olivine (Mg_2SiO_4 with admixtures of Fe_2SiO_4) — are summarized in Table I. We proceeded from the experimental data of Bridgman [3]. It should be pointed out that for such a comparatively complex crystalline structure as the olivine lattice, a more complicated expression for the energy should possibly be applied.

If the mean atomic volume is introduced

$$V_a = \mu V / N \nu$$

where μ is the molecular weight, ν is the number of atoms in a molecule, it may be taken

$$B V^{1/3} = V_a^{1/3} / a \tag{8}$$

Values of the coefficient a(cm) are also given in Table I.

Theoretical curves $P(V_a)$ for pressures up to 2.10^6 atm (for $T = 0°K$) are plotted in Fig. 1. As it is seen all these curves are closely approaching at high pressures.

b) *Valence crystals.*

We pass now to the crystals consisting of neutral atoms with covalent cohesive forces between them. The energy of such a crystal is composed, on the one hand, by the negative energy of covalent attractive forces, which depends exponentially on the distance between the atoms and may be represented by the expression $- Ae^{-BV^{1/3}}$. On the other hand, it contains positive energy of electrostatic repulsion between the ionic cores of atoms, i.e. between atoms without their outer, valence electronic shells. The Coulomb

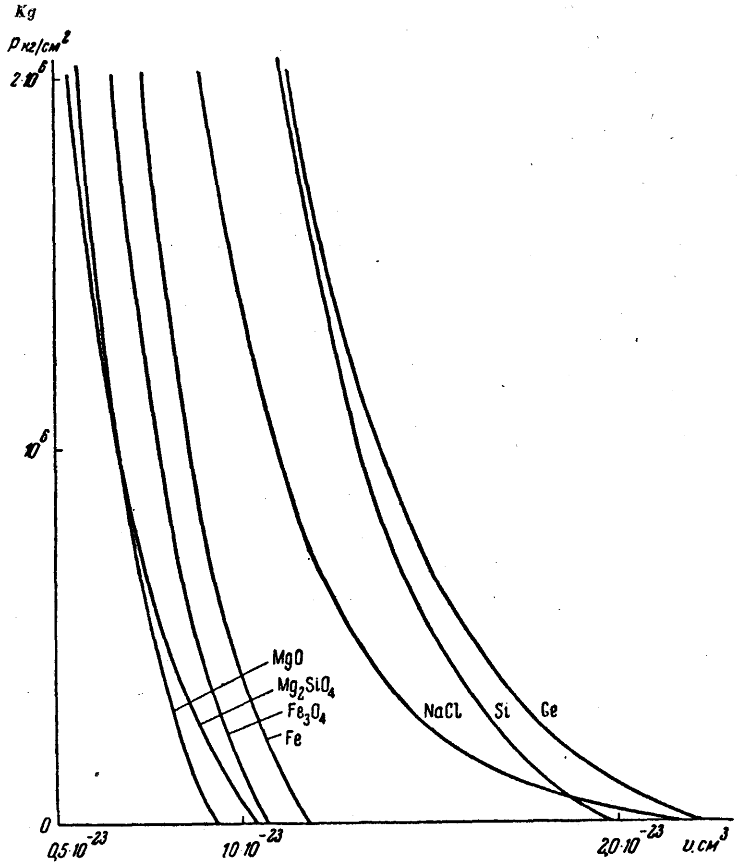
Kg
P кг/см²
2·10⁶
10⁶
0
0,5·10⁻²³
10·10⁻²³
2,0·10⁻²³
υ,см³
MgO
Mg₂SiO₄
Fe₃O₄
Fe
NaCl
Si
Ge

FIG. 1.

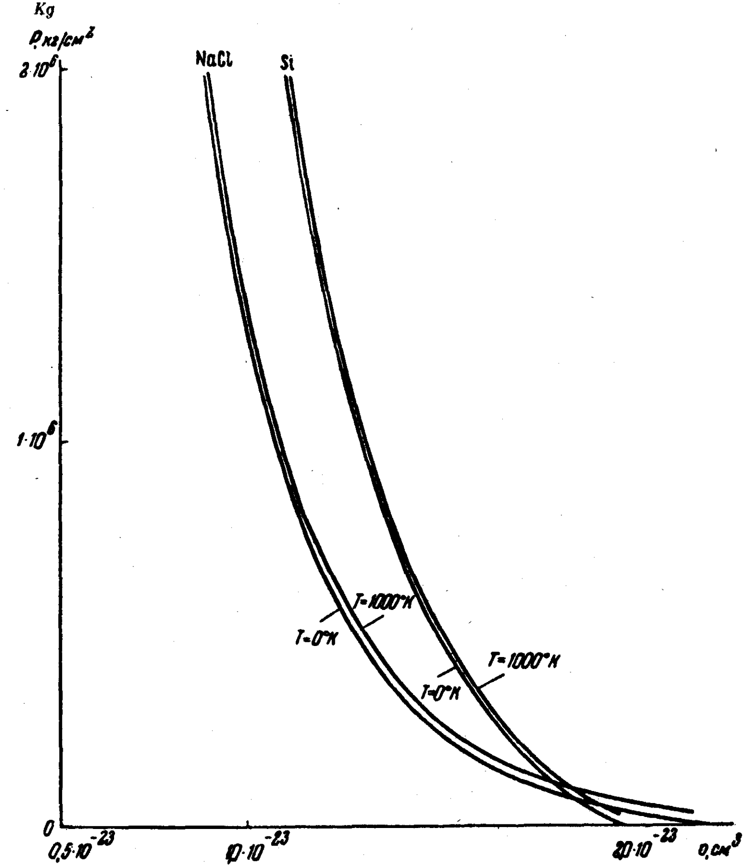
Kg
P,кг/см²
2·10⁶
1·10⁶
0
0,5·10⁻²³
1,0·10⁻²³
2,0·10⁻²³
υ,см³
NaCl
Si
T=1000°K
T=0°K
T=1000°K
T=0°K

FIG. 2.

repulsion between the ionic cores, which may be approximately regarded as the positive point charges, gives a crystal energy term, which is inversely proportional to the lattice constant, i.e. proportional to $V^{-1/3}$ It is screened by an exponentially distributed negative charge of the outer electronic shells and the corresponding term of the energy expression may be written as $CV^{-1/3}e^{-BV^{1/3}}$. The coefficient B in the exponent must be here the same as in the covalent term, since the exponential factors are in both cases due to the same external electronic shells. As a result the total energy of a valence crystal acquires the form :

$$E = (CV^{-1/3} - A)\, e^{-BV^{1/3}} \tag{9}$$

This gives according to formulae (1) and (4) the equation of state

$$P = [K_1 (x^{-4/3} + bx^{-1}) - K_2\, x^{-2/3}]\, e^{-bx^{1/3}} + K_T \tag{10}$$

where

$$K_1 = \frac{1}{3} CV_0^{-4/3}, \quad K_2 = \frac{1}{3} b\, AV_0^{-1}, \; b = BV_0^{1/3} \tag{11}$$

K_T is as before the temperature correction.

Values of the coefficients of Eq (10) for two typical valence crystals — silicium and germanium are given in Table 2. To determine the three independent coefficients K_1, K_2 and b we used the value of the normal density and two points on the experimental curves obtained by Bridgman. Corresponding curves are also represented in Fig. 1. Fig. 2 represents two isoterms for NaCl and *Si* for $T = 0°$ and $T = 1000°K$. As it is seen, the temperature dependence is appreciable only at moderate pressures.

c) *Molecular crystals.*

The formula for the energy of molecular crystals, the cohesion forces of which are connected with the van der Waals attraction, must differ from formula (5) for the ionic crystals by the replacement of the electrostatic energy — $CV^{-1/3}$ by the van der Waals energy proportional to the inverse sixth power of the lattice constant, i.e. the square of the specific volume. This gives :

$$E = Ae^{-BV^{1/3}} - CV^{-2} \tag{12}$$

The first term connected with the repulsion of electronic shells remains unchanged. The equation of state acquires the form :

$$P = K_1\, x^{-2/3}\, e^{-bx^{1/3}} - K_2\, x^{-4/3} + K_T \tag{13}$$

where $K_2 = 2\, CV_0^{-3}$.

There are in the literature calculations of the sublimation energy of molecular crystals, based on the formula (12).

d) *Metals.*

A great number of papers is devoted to calculations of the cohesive energy of metals. The energy of a metallic crystal may be represented with sufficient degree of precision in the form :

$$E = Ae^{-BV^{1/3}} - CV^{-1/3} + DV^{-2/3} \tag{14}$$

from which we obtain according to the general formulae the equation of state :

$$P = K_1 x^{-2/3} e^{-bx^{1/3}} - K_2 x^{-4/3} + K_3 x^{-5/3} + K_T \tag{15}$$

Here

$$K_1 = \frac{1}{3} ABV_0^{-2/3}, \quad K_2 = \frac{1}{3} CV_0^{-4/3}, \quad K_3 = \frac{2}{3} DV_0^{-5/3} \tag{16}$$

The second term of Eq. (14) and (15) is connected with the electrostatic attraction between the free electrons and the positive ionic cores. The third term represents the Fermi kinetic energy of free electrons.

The first term proceeds from the electrostatic repulsion of internal electronic shells. In alkaline metals it is seemingly of no importance. In other metals this repulsion is, on the contrary very important, it being possible to neglect the third term as compared with it. The transition from the body-centered crystalline lattice of alkaline metals to the close packing of the majority of other metals is probably connected with this.

Formulae (14) and (15) will not differ from corresponding Eq. (5)and (6) for ionic crystals, if the third term is neglected in them. The values of the coefficients of such simplified formulae for iron based upon Bridgman's data are also given in Table 1. The corresponding curve is given in Fig. 1.

We have written above only the equation of state, i.e. the expression for P for the simplest types of crystalline lattices. The compressibility β and the thermal expansion coefficient α are obtained from the corresponding energy expressions according to the general equations (1) and (4).

II. Electric conductivity.

Leaving aside the metal core of the Earth let us discuss the electric conductivity of non-metallic solid bodies similar to those constituting its mantle.

a) *Crystalline bodies with ionic conductivity.*

At comparatively high temperatures and pressures corresponding to the upper layer of the Earth mantle the ionic crystals must apparently possess ionic conductivity. If n is the number of free ions per unit volume and u is their mobility the electric conductivity will then be $\sigma = e\, n\, u$.

Both n and u depend exponentially on temperature and pressure. Neglecting the weaker and therefore inessential dependence of the pre-exponential factors we may write as usually : [4]

$$n = n_0\, e^{-E_n/2kT}, \quad u = u_0\, e^{-E_u/kT} \tag{17}$$

Thus,

$$\sigma = \sigma_0\, e^{-E_\sigma/kT}$$

where $E_\sigma = \frac{1}{2} E_n + E_u$.

Writing the number of free ions in the form (17) we mean the ions connected with the Frenkel lattice defects, i.e. the ions thrown into anomalous positions by the thermal motion, as also the lattice points remaining consequently free, which play the role of free ions of opposite sign.

Lattice defects of other kind — the Shottky defects, — can hardly be of significance at high pressures, because their formation is accompanied by the increase of the crystal volume, which is very unfavourable from the energetic point of view at high pressures. As concerns random ions of foreign admixtures, their number does not depend on the temperature. They are of importance at low temperatures only. We shall not take them into account at all.

The energy E_n can be written in the first aproximation in the form, which is similar to (5), the electrostatic energy being here added :

$$E_n = A_n\, e^{-B_n V^{1/3}} + C_n\, V^{-1/3}. \tag{19}$$

Estimates show that at the pressure $P = 0$, i.e. at $V = V_0$, the two terms are usually of the same order of magnitude, usually ~ 1 eV. With increasing pressure the first term increases, naturally, stronger than the second.

The mobility of the ions is cumbered mainly by the exponential repulsion, hence the energy

$$E_u = A_u\, e^{-B_u V^{1/3}}$$

Here usually $E_u < E_n$, but B_u must be near to B_n. They are both somewhat less than B in (5). Therefore in (18) with sufficient accuracy may be written :

$$E_\sigma = A_\sigma\, e^{-B_\sigma V^{1/3}} + A_n\, V^{-1/3} \tag{21}$$

If the equation of state is known it is not difficult to determine the dependence of E_σ on pressure.

According to the order of magnitude [4] :

$$\sigma_0 \sim \frac{e^2 \Theta}{h \tau} \left(\frac{N}{V}\right)^{1/3} \tag{22}$$

where e is the elementary charge.

As it is seen from (18), (21) the ionic conductivity decreases strongly at high pressures. Therefore in deeper layers of the Earth mantle the most important part is played by the electronic and not the ionic conductivity.

b) *Electronic semi-conductors.*

The conductivity of electronic semi-conductors may also be written in the form similar to (18). We are not interested in the electric conductivity of semi-conductors connected with random admixtures, important only at lower temperatures, but in their proper conductivity. For the latter

$$\sigma = \sigma_0 \, e^{-E_e/2kT} \tag{23}$$

where E_0 is the width of the forbidden band of the energy levels of electrons in the crystal. Here again the dependence of σ on pressure is determined mainly by the dependence of E_e. The influence of the pressure and temperature on σ_0 is considerably weaker and may be neglected.

The value of E_e may be easily determined for the alkalihalides. For them we have with sufficient accuracy [2] :

$$E_e = E_- - E_+ + CV^{-1/3} - A_1 e^{-B_1 V^{1/3}} - A_2 e^{-B_2 V^{1/3}} \tag{24}$$

Here E_- is the electron affinity of a haloid atom, E_+ is the ionisation energy of a metal atom, the third term is the electrostatic energy, which must be spend for the transition of an electron from the haloid ion, surrounded by positive ions, to the metal ion surrounded by negative ions. The fourth and the fifth terms represent the half-width of the conductivity band and of the filled band of levels respectively. The latter not being large it may be neglected in the first approximation.

These exponential terms increase comparatively rapidly with the pressure. This leads to a decrease of E_e, i.e. to an increase of electric conductivity.

It is difficult to express by such a clear formula the width of the forbidden band for other semi-conductors. With decreasing volume the permitted level bands in them may become superimposed, but a forbidden band can appear in them again afterwards. Therefore the width of the forbidden band can either increase, or decrease with increasing pressure. Usually it can still be expressed in some interval by means of an expression similar to (23) with empirically chosen coefficients. A_1 and A_2 can in this case either be positive, or negative.

An electrostatic term cannot, of course, appear in valence and molecular crystals. It must be remembered that valence crystals with their nonfilled shells must be metals with at very large V (exceeding the normal volume V_0). Therefore the forbidden band appears in them only with decreasing V. It is quite natural in consequence to expect in this case an increase of E_e, i.e. the decrease of electric conductivity with the decrease of V. It is observed actually, as for instance in the case of germanium.

TABLE 1.

	$K_1\,10^{-7}$	$K_2\,10^{-5}$	$K_T\,10^{-3}$	b	Θ°K	$a.10^8$
NaCl	159	1,07	9,0	9,69	299	0,291
MgO	42,4	13,8	6,8	5,73	829	0,367
Fe^3O^4	29,1	18,2	0,44	5,07	692	0,434
$(Mg, Fe)_2\,SiO_4$	9,69	20,2	5,1	3.87	726	0,565
Fe	78,7	11,5	8,8	6,53	521	0,348

TABLE 2.

	$K_1\,10^{-7}$	$K_2\,10^{-7}$	$K_T\,10^{-3}$	b	Θ°K	$a.10^8$
Si	2,75	13,7	7,2	3,98	613	0,354
Ge	1,16	4,92	6,2	3,23	348	0,872

REFERENCES.

1. BIRCH (F. J.), Geophys. Res., *57*, 227 (1952).
2. SEITZ (F.), Modern Theory of Solids, McGraw-Hill (1940).
3. BRIDGMAN (P. W.), Am. J. Sci. 10, 483 (1925), Proc. Am. Acad. Arts et Sci. *67*, 345 (1932); ibid. *76*, 1 (1945); ibid. *76*, 71 (1948); Rev. Mod. Phys. *18*, 1 (1946).
4. MOTT (N. F.) a. GURNEY (R. W.), Electronic Processes in Ionic Crystals, Oxford (1948).

AGE OF THE PEGMATITE OF KISHENGARH, RAJASTHAN, INDIA

By U. ASWATHANARAYANA

ABSTRACT.

Samples of microline and a radioactive mineral (tentatively identified to be samarskite on the basis of spectrochemical and X-ray data) drawn from a pegmatite mine near Kishengarh, Rajasthan, India, were analysed in the laboratory. The concentrations of uranium and lead and the isotopic composition of lead isolated from samarskite were determined and the data were used to compute Pb^{206}/U^{238} (586 m.y.) Pb^{207}/U^{235} (578 m.y.) and Pb^{207}/Pb^{206} (580 m.y.) ages. Samarskite has thus given an unusually closely-spaced age spread, and an age of 580 $\pm$ 20 m.y. can be assigned to it with confidence. The lead-lead ages from the felspar were anomalous. Apparently when the felspar crystallized 580 m.y. ago, it drew into its lattice an « abnormal » lead which subsequently remained « frozen ». This « abnormal » lead may have evolved in a region which, for long periods in the past, contained abnormally high concentrations of thorium and low concentrations of uranium relative to lead.

The age of samarskite indicates that the Kishengarh pegmatite is younger than the pegmatite of Bisundni, Rajasthan, dated by Holmes. This finding is consistent with geological evidence.

INTRODUCTION.

The province of Rajasthan, India, has a complex orogenic history and the age levels of the numerous pegmatites dotting this region are not precisely known, except in a few cases. The present investigation was initiated with the objective of dating one of the pegmatites from at least two of its constituent minerals.

An open-cast pegmatite mine, locally known as Bajrang mine, is located (75°2′; 26°36′) at a distance of 13 miles east of Kishengarh town along the Kishengarh-Jaipur road. The mine (about $100' \times 40' \times 20'$) was formerly worked by M/S Ratanlal Kamdar for monazite, samarskite, beryl and mica, but at the time of the author's visit, it was not in production. The author collected specimens of microline from the pit. M/S Ratanlal Kamdar gave to the writer specimens of samarskite and monazite collected from the same pegmatite before the production was discontinued. The present paper pertains to the laboratory work done on the felspar and samarskite, and constitutes an extension of the studies earlier reported by the author (1956).

ACKNOWLEDGMENTS.

I am deeply grateful to Dr. Claire Patterson under whose supervision this work was carried out. Dr. T. J. Chow and Judith Kawafuchi have been of immense help to me in doing my laboratory work. I wish to thank Prof. Harrison Brown and Prof. Robert Sharp who kindly permitted me to work in the laboratories of the Geological Division. The financial assistance of the State Department of the U.S.A. and the Andhra University, India, which enabled me to work at the California Institute of Technology for a short period, is thankfully acknowledged.

GEOLOGIC SETTING.

The Pre-Vindhyan (Pre-Keweenawan?) succession of central Rajasthan together with the tentative North American time equivalents of geological formations, as given by Heron (1953, p. 5, 27) is summarized below :

North America	Rajasthan, India		
	Malani Series	Rhyolites, tuffs	Granite and ultra-basic rocks. Erinpura granite, pegmatite and aplite, Epidiorites and hornblende schists.
Animikie (Algonkian)	Delhi system	Phyllites, limestones, calc-gneisses and schists, quartzites, conglomerates grits, etc.	
			Aplogranite, epidorites and hornblende schists, ultrabasics

Huronian	Aravalli System	Limestones, quartzites, composite gneisses, etc.	
Laurentian (granites, etc.) Keewatin (basic igneous) Greenville and Coutchiching (sediments)	Banded Gneissic Complex	Schists, gneisses and quartzites, etc.	Pegmatites granites, aplites and basic rocks.

(Though it is inadmissible to correlate geologic formations of such widely separated areas as India and North America, the correlation table is nevertheless given to help ready recognition of the age levels of the Rajasthan formations.)

There are three orogenic belts in Rajasthan — the Gneissic complex, the Arvalli orogenic belt and the Delhi orogenic belt. « Each of the three orogenic cycles of Rajputana ends with a display of pegmatites and, since the younger pegmatites also occur in the older rocks, it is not always easy to assign its proper age to any particular occurrence » (Holmes et al, 1949). Apparently there are marked differences in the characteristics of Pre-Delhi and Post-Delhi pegmatites. The former are medium-grained, often foliated and disturbed by later movements. They contain hardly any radioactive minerals. The Post-Delhi pegmatites, on the other hand, are coarse-grained, massive and unfoliated and have yielded radioactive minerals. Holmes et al (1949) determined the ages of uraninite from Bisundni (735 ±5 m.y.) and monazite from Soniana (700-865 m.y.) in Rajasthan.

The Kishengarh pegmatite is inferred to be of Post-Delhi age as it is coarse-grained and massive and contains radioactive minerals like other Post-Delhi pegmatites. It has a strike direction of N 110° E and dips 70° N. It consists of quartz, pink felspar, usually microline, muscovite, beryl and radioactive minerals. The felspar does not occur in conspicuously large crystal. There is no evidence for the segregation of minerals in any particular zone.

Laboratory Studies.

A. *Description :* The felspar is of the microline variety and has a pale brown to cream yellow color. It has an excellent cleavage. A double series of fine lamellae nearly at right angles to each other (presumably due to polysynthetic twinning according to the albite and pericline laws) have resulted in the characteristic grating structure on the basal sections. The felspar shows slight alteration to kaolin and limonite in the peripheral zones.

The samarskite specimen has a velvet black color and is massive. Cleavage is indistinct. The mineral has a conchoidal, brittle fracture and the luster on the fracture is vitreous. The mineral has an earthy coating outside. Alteration is spreading into the mineral along the fractures and the altered zones have a dull luster and brown color.

B. *Identification :* The radioactive mineral was tentatively identified in the field as samarskite but it was impossible to be certain about it since it is not easy to distinguish it from several other Columbate-tantalates, on the basis of its megascopic characteristics alone. Hence spectrochemical and X-ray analyses have been made to help in the identification of the mineral.

The following is the spectrochemical data in terms of the elements and their concentration in ppm :

Ba — 145; Ce — 4250; Co — 240; Cr — 29; Cu — 40; La — 440; Mn — 630; Nd — 2000; Pb — 2000; Sc — 215; Th — 18500; Zr — 2650; Sr — 320; V — 121.

Y and Yb are present as minor elements. While the spectrochemical analysis certainly narrowed the range of mineral species to which the mineral under study could belong, it was not conclusive. X-ray diffraction analysis using goniometric set-up clearly indicated that the mineral is non-crystalline and metamict. This observation coupled with the data on the *d* spacing of the x-ray powder pattern suggests that the mineral is samarskite.

C. *Powdering Procedure :* Elaborate precautions were taken to avoid contamination in the process of powdering. In the case of felspar, the diamond mortar and pestle, hammer and chisel and stainless steel sieve were first cleaned with triple-distilled water, immersed fully in nitric acid, rinsed with quadruple distilled water and tested for the absence of acidity. The crushing is done in a dust-free room and on a table top vacuum-cleaned and covered with plenty of clean paper.

The core of the mineral is separated from the rest, untouched by hand, crushed and sieved with a 60 mesh sieve. The-60 mesh powder is used in the investigation.

The powdering and subsequent treatment of samarskite with its large quantities of lead posed a real problem as special care was taken all along to keep the lead contamination in the laboratory at an absolute minimum (Tilton et al, 1955). The samarskite was first broken into bits in an ordinary mineral chemistry laboratory by pounding it gently with a clean hammer. Small lustrous pieces, free of visible alterations and fractures, were hand-picked and crushed in an agate mortar to an extremely fine powder. The steel hammer and tongs and agate mortar and pestle used in this operation were thoroughly cleaned according to the procedure explained in the previous case.

D. *Chemical Procedures :* The precautions described by Tilton et al (1955) to avoid contamination from reagents, apparatus and laboratory air have been scrupulously followed. Whenever possible, lead-free teflon beakers and hoods have been used in preference to pyrex glassware and this step is hoped to have contributed to the accuracy of the data. The nature of the laboratory studies undertaken are given in the following schematic arrangement :

Felspar < Unwashed-Dissolution [Isotopic Composition / Total lead concentration } Two aliquots from the same solution
Felspar < Washed-Dissolution... Isotopic Composition

Samarskite < Dissolution [U concentration / Pb concentration } Two aliquots from the same solution
Samarskite < Dissolution... Pb isotopic composition

The concentrations of uranium and lead in samarskite and the concentration of lead in the felspar were determined by using isotope dilution techniques (Tilton et al, 1955). 30 μg of Pb^{206} was used to estimate the lead concentration in felspar, while 60 μg of shelf lead and 20 μg of U^{235} were used to determine the lead and uranium concentrations in samarskite. The techniques of chemical analysis used for the isolation of lead and uranium are substantially the same as those described by Tilton et al (1955).

Isolation of lead. — The techniques of isolation of lead from minerals have been described by Tilton et al (1955).

The samarskite and the felspar were dissolved by heating with hydrofluoric and perchloric acids. Lead was isolated from these solutions by complexing interfering ions with citrate and extracting lead dithizonate in chloroform at a pH of 9.5. The chemical procedure used for unspiked and spiked samples were substantially the same; only the quantities of reagents used were changed suitably.

The actual steps of analysis are given below :

(a) Felspar :

1. 10 gms. of unwashed felspar powder was weighed out into a platinum crucible and treated thrice with 50 gms. of HF and 20 gms.

of $HClO_4$ each time, evaporating the material slowly to a moist cake in the first two operations at a temperature of 90°C and to dryness in the third operation at a temperature of 200°C. About 50 ml. of $HClO_4$ were added and evaporated to dryness. The evaporated material was taken up in about 50 ml. of 6.5 M HCl, transferred into a pyrex beaker and evaporated to dryness. The solids were redissolved in 100 ml. of 6.5 M HCl and made up to 500 ml. with water. A 100 ml. aliquot of this was spiked with Pb^{206}.

2. Both aliquots were evaporated to dryness. The larger unspiked sample was dissolved in 100 ml. of 6.5 M HCl and extracted with equal volume of di-ethyl ether. The aqueous layer was evaporated to about 30 ml. and then diluted to 100 ml. with water.

3. 300 ml. of 25 % ammonium citrate solution were added to the solution. Ammonium hydroxide was then slowly added until the pH is 8-9. This solution was shaken in a liter separating funnel reagent until the chloroform turned violet. The chloroform layer was drained into a 250 ml. separating funnel and shaken up with 20-30 ml. of 1-2 % (by weight) of nitric acid (the final pH is about 1). The aqueous layer was rinsed with 5-10 ml. of pure chloroform and the chloroform was drained off. 5 ml. of KCN solution (1 gm. of KCN dissolved in 100 ml. of 10 % NH_4OH) were added. The pH was adjusted to 9.5 with NH_4OH. This was shaken first with 5 ml. of standard dithizone chloroform (one ml. of solution corresponds to 2 micrograms of lead), and later small quantities of the same reagent until the chloroform turned violet. The chloroform layer was drained out, evaporated to reduce the volume, transferred into a 5 ml. beaker containing 1 ml. of conc. HNO_3 and 1 ml. of conc. $HClO_4$ and evaporated to dryness at 225°C.

4. About 10 mg. of ammonium nitrate was added to a 1 ml. centrifuge tube and filled half-way with water. This solution (with a pH of 3 to 4) was taken up in a micropippette and used to rinse the evapored material out of the 5 ml. beaker. This solution was put back in the centrifuge tube, H_2S was passed into it and the resulting PhS was loaded on the tantalum filament for isotopic analysis.

This same chemical procedure was adopted for isolating lead from the washed felspar (the felspar powder was washed by swirling four times for several minutes with 40 ml. of 20 % hot HNO_3 each time and then rinsing repeatedly with water until no acidity was left. This procedure dissolves traces of galena more or less completely and partly dissolves traces of pyrite).

(b) Samarskite :

Because of the large quantities of lead that this mineral contains, about a milligram only of the sample was used for the analysis. The sample was first spiked with shelf lead and U^{235} and created with hydrofluoric and perchloric acids as in the previous case. 5 ml. of HNO_3 was then added and evaporated to dryness again. The evaporated material was redissolved in 5 ml. of hot HNO_3, then diluted with water to 20 ml. Two equal aliquots were taken from this solution for estimating U and Pb concentrations. The Pb concentration was determined in the same way as has been described earlier. Lead for isotopic analysis was isolated from a 60 mg. sample. The procedure for the isolation of lead has already been explained in the previous cases.

Isolation of uranium. — The samarskite sample was treated with hydrofluoric acid and after that, the insoluble fluorides were dissolved by fuming with perchloric acid. The uranium was purified by treatment with ammonium carbonate — the carbonate ion has the ability to hold uranium in solution by complex ion formation. The remaining impurities were got rid of by employing hexone extraction of a nearly saturated solution of nitrate salts (Tilton et al, 1955).

The analytical procedure employed for the extraction of uranium from samarskite is given below :

Ammonium hydroxide was added drop-wise to the uranium aliquot until a precipitate just formed. Conc. HNO_3 was added dropwise until the precipitate just dissolved. This left the pH at 1. The solution was transferred to a 50 ml. pyrex centrifuge tube and 20 ml. of 1 : 4 amm. carbonate was added. The centrifuge tube was then set in a beaker of distilled water at 90°C for 30 minutes and the contents were centrifuged. The precipate was acidified with HNO_3, evaporated to dryness and baked at high heat until all the ammonium salts disappeared. 20 ml. of conc. HNO_3 was added to the baked material and set in cracked ice. Ammonia gas was passed in until the pH was 2. Water was added drop-wise until the excess of amm. nitrate just dissolved. Then the liquid was extracted with equal volumes of hexone thrice. The pH of the aqueous solution throughout this operation must be kept at about 2. The hexone layers were then combined and extracted three times with 1 % HNO_3. The aqueous solution was evaporated to dryness, dissolved in 5 μl of HNO_3 and loaded on the tantalum filament for isotopic analysis.

E. *Mass-spectrometric Procedures :* The mass-spectrometric procedures employed by Tilton et al (1955) for the isotopic analysis of uranium and lead have been utilized in the present investigation too. The isotopic composition of lead was computed from about 40 sets of peaks in each case. The concentrations of lead and uranium were calculated from about 25 sets of peaks. The limits for the acceptable data were the following : *i*) 3×10^{-11} amps. in ion beam for more than about two hours, with less than about one-half % of intensity change per minute and *ii*) the deflection on the data chart above 50 % of full scale (Chow and Patterson, unpublished). The probable absolute accuracy is $\sim \pm 0.5$ % for Pb^{206}/Pb^{204} ratio, $\sim \pm 0.2$ % for Pb^{206}/Pb^{207} ratio and $\sim \pm 0.3$ % for Pb^{206}/Pb^{208} ratio.

RESULTS :

TABLE I.

Samarskite-lead and uranium.

Isotopic Composition of total lead	*Concentration of* Pb^{206}	*Concentration of total uranium*
Pb^{206}/Pb^{204} = 5,942 Pb^{206}/Pb^{207} = 16,28 Pb^{206}/Pb^{208} = 22,65	9.694 μg. per 1.2 mg. of sample	119.2 μg. per 1.2 mg. of sample

The atomic percentages of Pb^{206}, Pb^{207}, Pb^{208} and Pb^{204} were computed from the ratios in Table I and corrected for non-radiogenic Pb^{206} and Pb^{207}. The non-radiogenic lead ratios in the unwashed felspar lead (Table III) (Pb^{206}/Pb^{204} = 16.47; Pb^{207}/Pb^{204} = 15.58) were used in the calculations. The isotopic composition of non-radiogenic lead is not critical, however. The non-radiogenic lead ratios (Pb^{206}/Pb^{204} = 17.43; Pb^{207}/Pb^{204} = 15.54) read from the curves given by Faul (1954, p. 299), assuming an age of 700 m. y. which is roughly the age calculated without the correction, can be used and it is found that this does not change the ages at all. This is so because Pb^{204} atomic percent is extremely low. The corrected atomic percents were then converted into weights (Table II) using the Pb^{206} content of the sample, as estimated by the use of isotope dilution technique.

TABLE II.

Atomic percentages of isotopes.

Isotope	Total Atomic %	Atomic % non-radiogenic contribution	Atomic % corrected radiogenic	Microgram sample
Pb^{206}	90.4388	0.2503	90.1885	9.667
Pb^{207}	5.5535	0.2368	5.3167	0.5704

Ages can be computed from the following equations :

$$Pb^{206}\,(\text{now}) = U^{238}\,(\text{now})\,(e^{\lambda_{238}t_m} - 1)$$
$$Pb^{207}\,(\text{now}) = U^{235}\,(\text{now})\,(e^{\lambda_{235}t_m} - 1)$$
$$\frac{N^{207}}{N^{206}} = \frac{1}{K}\left[\frac{e^{\lambda_{238}t_m} - 1}{e^{\lambda_{235}t_m} - 1}\right]$$

where N^{207}/N^{206} is the atom ratio of Pb^{207}/Pb^{206} and t_m, the age of the mineral.

The following constants have been used in the calculations :

$\lambda_{238} = 0.1537 \times 10^{-9}\,yr^{-1}$; $\lambda_{235} = 0.972 \times 10^{-9}\,yr^{-1}$; $K = 137.8$

The age spread is given below :

Pb^{207}/Pb^{206} age = 579 m. y.
Pb^{206}/U^{238} age = 587 m. y.
Pb^{207}/U^{235} age = 578 m. y.

TABLE III.
Felspar Lead
Isotopic Composition (atomic ratios)

Sample	Pb^{206}/Pb^{204}	Pb^{206}/Pb^{207}	Pb^{206}/Pb^{208}	Total lead conc. in ppm.
Washed felspar	16.58	1.055	0.4267	N. D.
Unwashed felspar	16.47	1.057	0.4285	68.3

The data in Table III can be used to calculate the hypothetical time at which the lead was isolated from its uranium and thorium environment and was introduced into the felspar lattice. Assuming that the lead in the felspar had a normal evolutionary history, one can either calculate the time required to go from a normal lead today back into time into the felspar lead or one can calculate the time required to go from the primordial earth lead to the felspar lead. In the first calculation the following expressions due to Collins et al (1953) can be used :

$$t_m = \frac{1}{\lambda}\log_e \frac{a - x_m}{v} + 1$$

$$t'_m = \frac{1}{\lambda''}\log_e \frac{c - z_m}{w} + 1$$

where x_m and z_m are abundances of Pb^{206} and Pb^{208} relative to Pb^{204} at time t_m a and c are corresponding relative abundances of Pb^{206} and Pb^{208} in the earth's crust in the present time. V and

W are the present relative abundances of U^{238} and Th^{232} relative to Pb^{204} in the earth's crust. λ and λ'' are the decay constants of U^{238} and Th^{232} respectively.

T. J. Chow (unpublished) provided the following constants : a = 18.69; c = 38.82. Constants for V = 9.84 and W = 38.2 were given by Collins, Russell and Farquhar (1953).

In the second calculation, the following expression given by Patterson (1956) can be used :

$$\frac{R_1a - R_1b}{R_2a - R_2b} = \frac{1}{K}\left[\frac{e^{\lambda_1 t_0} - e^{\lambda_1 t''_m}}{e^{\lambda_2 t_0} - e^{\lambda_2 t''_m}}\right]$$

where R_1a and R_2a are the abundances of Pb^{207} and Pb^{206} relative to Pb^{204} at time t_m and R_1b and R_2b are the corresponding ratios in the primordial earth lead. t_o and t_m are the ages of the earth and the felspar respectively. λ_1 and λ_2 are the decay constants of U^{235} and U^{238} respectively. K is the present ratio of U^{238} to U^{235}.

While the constants for λ_1, λ_2 and K used in this equation are the same as those given above, $t_o = 4.55 \times 10^9$ yr., $R_1b = 10.36$, $R_2b = 9.50$ (Patterson, 1956).

The calculated ages were as follows :

$$t_m = 1300 \text{ m.y.}; \; t'_m = 200 \text{ m.y.}; \; t''_m = 1400 \text{ m.y.}$$

Discussion.

A. *Samarskite :* Samarskite has given an unusually closely-spaced age spread and hence an age of 580 ±20 m.y. can be given with confidence to samarskite. It is believed that the errors in chemical determinations define the errors in the ages. Eckelmann and Kulp (1957, p. 1121) listed lead isotopic data on five samarskites. The low abundance of Pb^{204} in the present sample is of interest as it is among the lowest concentrations reported, if not the lowest.

Eckelmann, W. R., and Kulp, J. L., 1957 uranium-lead method of age determination, pt II, Geol. Soc. Amer. Bull., v. 68, p. 1117-1140 (introduce as Ref. 3).

B. *Samarskite and felspar :* The original purpose in studying the lead in the felspar was to obtain a check on the samarskite age. The gross discrepancy among the felspar lead ages and the samarskite age can be best explained in the following way : The lead contained in the felspar is abnormal in the sense that its isotopic composition does not correspond to that of ore lead of the same age. The abnormality consists in its having marked deficiency in Pb^{206} and marked excess of Pb^{208}.

The similarity in the isotopic composition of lead obtained from the acid-washed and unwashed felspars indicates that neither leaching subsequent to the formation of the felspar nor the presence of trace quantities of galena could have modified the isotopic composition of felspar lead. The unwashed felspar was found to be inactive when radiometrically assayed but, considering the statistical fluctuations in the background, it was computed that the sample could (but need not necessarily) contain a maximum of 1 ppm. of U or 3 ppm. of Th. Thus, even if it is assumed that the sample is radioactive and the activity is due to thorium, the concentration of thorium is still about 15 times less than that required to account for the excess of Pb^{208}.

Data on the isotopic composition of lead isolated from three felspars, drawn from three distinct environments, are available. Tilton et al (1955) reported that, while the felspar component of the granite they analyzed has an abnormal excess of radiogenic Pb^{206} and Pb^{208}, the felspar in the pegmatite which intruded into the granite has an isotopic composition which corresponds to that of « normal » ore lead of the same age. Patterson (unpublished) found « normal » lead in the Southern California batholith granite of Cretaceous age. The lead in the felspar under study with its deficiency of Pb^{206} and excess of Pb^{208} apparently constitutes a new and distinct type.

The age data, given earlier, permit two possible explanations : (*i*) Both samarskite and felspar crystallized 580 m.y. ago. The felspar, however, drew into lattice lead evolved in a region which, for long periods in the past, contained abnormally high concentrations of thorium and low concentration of uranium, relative to lead. It remained « frozen » with this abnormal lead as there was practically no subsequent contribution of lead from the negligible amounts of U and/or Th contained in the felspar. (*ii*) The felspar composing the pegmatite crystallized 1400 m.y. ago but the samarskite was introduced much later, about 580 m.y. ago.

The second possibility would mean that the samarskite-bearing massive pegmatite of Kishengarh is of pre-Delhi age and hence runs counter to the observation cited by Holmes et al (1949) that most of the pre-Delhi pegmatites are neither massive nor mineralized. The first explanation is thus apparently more probable of the two.

This conclusion accords well with the interesting, though not very specific, observation of Farquhar and Russell (unpublished) who found that, in Canada, anomalous lead is characteristic of rocks of proterozic type while the lead occuring in the Archaean basement type rocks is « ordinary ».

Conclusions.

The age of the samarskite indicates that the Kishengarh pegmatite is very young Precambrian or earliest Palaeozic in its age; it is younger than that of Bisundni, Ajmer-Merwara dated by Holmes et al (1949) and Holmes (1955). This finding is consistent with geological evidence as it is not necessary to suppose that pegmatites intruded at the same time all along immense synclinorium (Heron, 1953, p. 368).

It will be interesting to study the lead isotopic composition of minerals in the various pegmatites in Central Rajasthan. This may lead to a better understanding of the general geochemistry of uranium and thorium in this region.

References.

Aswathanarayana (U.). 1956, Absolute ages of the Archaen orogenic cycles of India : Amer. Jour. Sci., v. 254, pp. 19-31.

Collins (C. B.), Russell (R. D.) and Farquhar (R. M.). 1953, The maximum age of the elements and the age of the earth's crust : Can. Jour. Physics, v. 31, pp. 402-418.

Eckelmann (W. R.) and Kulp (J. L.). 1957, Uranium — lead method of age determination, pt. II, Geol. Soc. Amer. Bull., v. 68, pp. 1117-1140.

Faul (H.). 1954, Nuclear Geology, John Wiley, New York, pp. 1-414.

Kulp (J. L.), Bate (G. L.) and Gilletti (B. J.). 1955, New age determinations by the lead method : Proc. Geol. Assn. of Canada, v. 7, part II, pp. 15-24.

Heron (A. M.). 1953, The geology of Central Rajputana : Mem. Geol. Surv. Ind., v. 79, 1-389.

Holmes (A.), Smales (A. A.), Leland (W. T.), and Nier (A. O.). 1949, The age of uraninite and monazite from the post-Delhi pegmatites of Rajputana : Geol. Mag., v. 86, pp. 288-302.

Holmes (A.). 1955, Dating the Precambrian of Peninsular India and Ceylon : Proc. Geol. Assn. of Canada, v. 7, part II, pp. 81-106.

Patterson (C. C.). 1956, Age of meteorites and the earth : Geochim. et Cosmochim. Acta, v. 10, pp. 230-237.

Tilton (G. R.), Patterson (C.), Brown (H.), Inghram (M.), Hayden (R.), Hess (D.), and Larsen (Jr. E.). 1955, Isotopic composition and distribution of lead, uranium and thorium in a Precambrian granite : Bull. Geol. Soc. Amer., v. 66, pp. 1131-1148.

Division of Geological Sciences, California Institute of Technology, Pasadena, California.

THERMAL HISTORY OF THE EARTH AND THE THERMAL CONDUCTIVITY OF ITS MANTLE

By H. A. LUBIMOVA.

Two methods for the estimation of the temperature inside the Earth exist at present : the possibility to determine the temperature from the degree of the variation of some physical parameters with depth and from the equation of the thermal conductivity. However, only the study of the latter with calculation of the time can give an ansver to the question whether the Earth is undergoing the process of cooling or heating. A number of problems of the Earth's evolution are connected with this question.

Experimental data about the heat flow lost in the space, the Earth's age, density distribution in it, content of radioactive elements in the rocks, thermal conductivity and thermal capacity of the rocks are used for the study of the thermal history of the Earth on the basis of the heat conduction equation. Moreover, definite suggestions regarding the initial distribution of temperature and the function of the distribution of the heat sources H (r, t) in the Earth are also introduced.

The temperature of fusion, or of the solidification of the Earth's matter is most frequently accepted as $T_0(r)$. At this assumption however any heat generation inside the Earth, where no heat is escaping, should be exclused. Otherwise the Earth's temperature would exceed now the melting point and the Earth could never become solid[1].

There is no reason to believe that the mantle is quite free from radioactivity at present. The data about the flow on the oceanic and continental areas, having granite-basalt layers of different thickness [1] gives a direct indication that such sources are present deep inside the Earth's mantle. The increased amount of data concerning the content of U, Th., K in various rocks and meteorites, leads to the conclusion that radioactive elements are spread all over the Earth [2, 3]. Even in the iron meteorites, with the composition of which the core of the Earth is usually identified, a quite definite concentration [4, 5, 27] of them was discovered. In addition to that the amount of iron in the Earth's core is accepted now to be much less, than it was believed earlier. According to

1. Heat transfer is assumed to take place mainly by conduction. Under the low of rocks [Lomnitz] the convection currents are not likely to exist in the mantle [Jeffreys].

Lodotchnikov [7] and Ramsey [8] hypothesis the composition of the Earth's core differs very little from the silicates one. Therefore, we cannot intirely exclude radioactive elements even from the Earth's core, and assume $T_o(r) = T_{melting}$.

Cosmogonical ideas represent one of the foundations for conclusions about the initial temperature and the distribution of radioactive elements. According to modern ideas the Earth and the planets had been formed as a result of an accumulation of particles of a gas-dust protoplanetary cloud. The most complete explanation of the main features of the structure of solar system from the point of view of this hypothesis is given in the papers by O. Yu. Schmidt and his collaborators [9], [10]. These papers also lead to the conclusion that $T_o(r)$ was less than $T_{melting}$. The initial temperature of the Earth was caused by the following three processes : *a*) impacts of particles against the surface of the growing Earth; *b*) compression of the matter inside the Earth under the pressure of the growing outer layers; *c*) radioactive heat, which could accumulate during the process of Earth's formation, if this process was not very short.

Effect *a*) was estimated by V. S. Safronov [11 a, b] for two limiting schemes of the Earth's growth :

1) at the expense of large particles; which are not mutually colliding, 2) at the expense of small in-elastically colliding particles. If the variations in the velocity of particles motion is not taken into account the maximum increase of temperature is about 200° in the case of the first scheme and about 1200° in the second scheme at a distance of about 0,8 R from the Earth's centre.

Taking the variation of the velocity of particles, in the first case which is most probable, into account, the maximum temperature increase will only constitute 50-100°. Approximate period of the formation of the greatest part of the Earth (about 97 per cent of its mass) equals $0{,}2.10^9$ years [11 b]. A correction for radioactive heating for this period is about 700° (if the Earth's age is about 5.10^9 years). The temperature rise due to the increased pressure in the process of Earth's growth can be estimated from the formula [12 a].

$$T_{''} = T'_0 \, exp. \ \frac{1}{2a} \left[\frac{1}{\rho_0^2} - \frac{1}{\rho^2} \right] \tag{1}$$

where T' — the temperature of the matter before its compression, *a* — the coefficient characterizing the dependence of Gruneisen's constant on the volume. If all three effects are taken into account the maximum temperature rise in the process of Earth's formation is about 1000° K in its centre :

Curves of the distribution of the initial temperature $T_0(r)$ are given in fig. 1. The hatched and the dotted curves were calculated

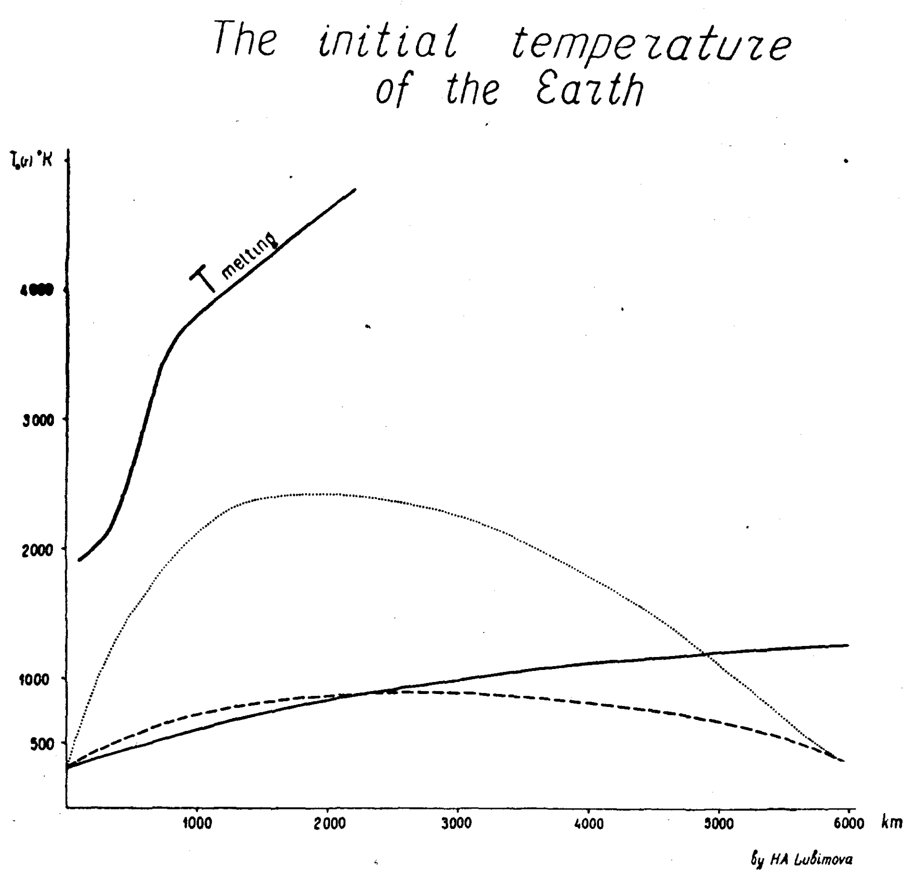

FIG. 1. Distribution of the initial temperature $T_0(r)$ in the Earth formed as a result of accumulation of gas-dust particles of protoplanetary cloud.

without taking the variations of the velocity of particles into account and neglecting the radiogenic heat in the period of the Earths' growth (the hatched curve corresponds to scheme 1) of the Earth's growth; the dotted — the scheme 2). These corrections were taken into account in the preparation of the continuous curve. As it is seen from fig. 1, $T_0(r)$ is much less than the temperature of fusion (thick line), taken according to Uffen [13]. Thus the Earth formed as a result of an accumulation of particles of the gas-dust proto-planetary cloud did not become fused.

The distribution of the radioactive elements in the Earth is usually accepted, when the thermal regime of the Earth is investigated, as unchangeable in the process of Earth's evolution (Tychonoff [16], Slichter [15], Magnitsky [17 a], Urry [18], Jacobs and Allan [19]).

However, the modern geological ideas lead to the conclusion about the permanent formation of the Earth crust, the gradual growth of the continents by means of a partial remelting of an initially uniform meteoritic mantle and carring of the easily fusible sialic constituents from the inside to the surface of the Earth, as a result of which the distribution of the radioactive elements should have been changed (Rubey [20], Wilson [21], Jeffreys [14]).

From this point of view the equality of the heat flow on the oceans and the continents may be understood. The total amount of sources must be the same in these parts of the Earth, but underneath the oceans the matter is less differentiated, the heat sources being distributed more uniformly, than in the continental regions.

The suggestion about the uniform distribution of the radioactive sources of heat during the initial stage of Earth's evolution follows naturally from the hypothesis of its origin as a result of an accumulation of protoplanetary cloud's particles. In the process of the Earth's evolution there had been a gradual passage from the uniform distribution of sources to the modern layer distribution of the latter.

The period of the existence of the uniform distribution of sources can be approximately assumed equal to the difference between the values of the age of the Earth as a planet ($4\text{-}5.10^9$ years) and of the age of the Earth's crust ($\sim 3.10^9$ years).

A solution of the equation of heat conduction, containing the function of sources $H(r, t)$ at constant $\mathcal{K}$, c, ρ was obtained by means of Green's function; using the reflection method [12 b, c, d] for its construction. This method, developed in the mathematical papers of A. Tychonoff [16, 22] leads to a rapid convergence of series. After some transformations an expression for the temperature inside a spherical body is obtained in the form of a difference of two items having a simple meaning. The first depends upon the time and represents the temperature resulting from the heat generated in a given volume. The second — in the form of a rapidly converging series and characterizes the influence of heat escape towards the surface on the temperature[2]. For the thermal diffusivity of rocks $K = \frac{\mathcal{K}}{c\rho} = 0{,}01\ cm^2/sec$ ($\mathcal{K}$ — thermal conductivity). For time intervals less than 6.10^9 years it is sufficient to take the first term of the series, if the body radius is greater than 1600 km (for the Earth and the Moon in particular). From 4 to 16 terms are taken into account [49] for the radii of 200, 100, 50 km (the dimensions of the largest asteroids).

The temperature inside the Earth at a uniform distribution of the sources and of the zero initial[3] and the surface temperature is given by the formula [12 b, c]

$$T(r,t) = \frac{1}{c\rho}\int_0^t H(\tau)\,d\tau - \frac{R}{r\,c\rho}\int_0^t H(\tau).\,\bar{\Phi}\left[\frac{R-r}{\sqrt{4K(t-\tau)}}\right]d\tau \quad (2)$$

$$H(t) = \sum H_a(t_0)\,exp\,(-\lambda_a t)\ ;\ \bar{\Phi} = 1 - \Phi(x)\,; \quad (3)$$

where $\varphi(x)$ — integral of errors, λ_a — the decay constant of the element a, $H_a(t_o)$ its heat generation t_o a billion of years ago. From formula (2) it follows that the region of heat escape towards the surface and the inner region, where all the emitted heat is spent on heating, may be distinguished in the temperature field of the Earth. In the internal region $r < R - \beta\sqrt{Kt}$ the second item is zero, the temperature being determined by the first item,, increasing with the rise of t.

In the surface layer ($r > R - \beta\sqrt{Kt}$) the second item becomes comparable with the first one. Some portion of heat flows from this region towards the surface. The depth of the region of escape is proportional to $\sqrt{Kt}$. At a usually accepted value of $k = 0{,}01\ cm^2/sec$ it equals about 1000 km and may reach the centre after 10 billion years only. A conclusion follows that the cooling of the Earth as a whole cannot begin earlier than after 10.10^9 years. At $k = 0{,}1$ the region of heat escape will exceed 2900 km already after 2.10^9 years after the Earth's formation [12 f]. Heat generation below the

2. The obviously applied Laplace transformation method [23] or of the division of variables [24] led to the extremely slowly converging series. Their summing up has become possible only after the electronic computers were introduced [19]. It may be shown, that the method of automodel solutions leads to the same slowly converging series.

3. The influence of the initial temperature $T_n(r)$ can be taken into account separately by means of an additional item presenting the solution of a homogeneous equation of thermal conductivity for the cooling globe, deprived of internal sources of heat : $\frac{1}{r}\int_0^r T_0(r).\,\mathcal{G}(r, t, r', o)\,dr'$

where $\mathcal{G}(r, t, r'\ \tau)$ is the Green's function.

4. β — is the coefficient depending upon $\sum\limits_a H_a(t_n)$.

region of heat escape, as well as the changes of the physical properties of matter, which are going on there, do not influence the heat flow observed at the earth's surface.

The obtained solution permits to calculate the thermal flow $q = \mathcal{K} \left.\frac{\partial T}{\partial r}\right|_{R=r}$ lost by the Earth. Results of a calculation of q for various values of the mean concentration of the radioactive sources and of the different values of age are given in fig. 2. Content

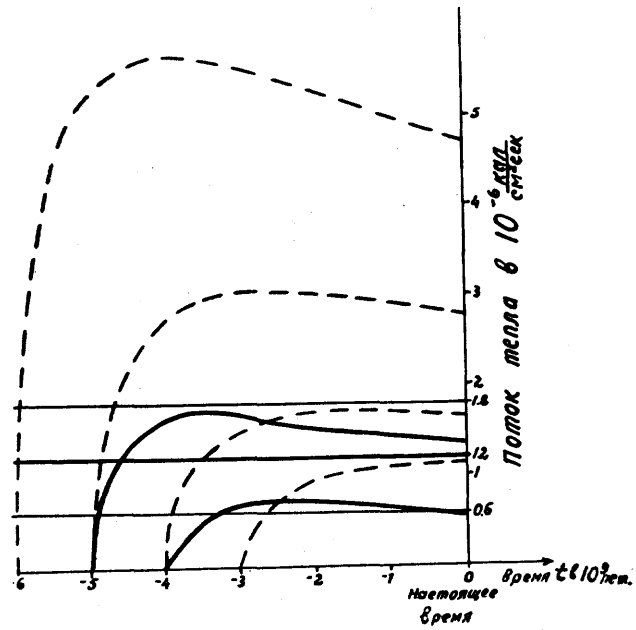

FIG. 2. Surface flow of heat.
A — minimum content of radioactive elements.
B — the maximum.
Straight lines *a* and *b* are the boundary of the interval of observed values.

of U, T*h* and K in the Earth was taken equal to their mean abundances in the meteorites. According to the two values obtained earlier : A — the minimum and B — the maximum one [12 b][5]. We see

5. According to the value A one gram of the Earth contains $0{,}93.10^{-8}$ *g* U, $0.67.10^{-10}$*g* of AcU, $2{,}8.10^{-8}$ *g* Th and $1.95.10^{-7}$ *g* of K^{40}. According to the value B : 1.10^{-7} *g* of U, $0{,}72.10^{-9}$ *g* of AcU, 3.10^{-7} *g* of Th, $1{,}95.10^{-7}$ *g* of K^{40}. A new value of C is obtained from recent data [25] : $5{,}2.10^{-8}$ *g* U, $3{,}7.10^{-10}$ *g* AcU, 21.10^{-8} *g* Th, $0{,}9.10^{-7}$ *g* K^{40}. This value give the curve of heat generation, which differs very little from the curve of variant A for the last 2.10^{9} years and practically coincides with it in the more remote past [12 d]. All these values are within the intervals limiting on the one hand the minimum value introduced recently by Urey [26] and on the other hand a maximum value, which may be deduced from the new data by Starik and Shaz [27].

that the surface heat flow had decreased during the recent $(2\text{-}3).10^9$ years. However conclusions about the cooling of the Earth as a whole, as it was supposed by Urry [18], are not correct. The Earth interior which is below the region of the heat escape is getting heated. Only the surface layers are cooling.

The concentration of radioactive elements, the age of the Earth and the lost heat flow are mutually connected. The calculated values of the flow q are within the range of the measured values $(1{,}2 \pm 0{,}6).10^{-6}$ cal/cm^2 sec, if concentration A and the Earth age of $(4\text{-}5).10^9$ years are accepted (see *fig.* 2).

Formulae obtained for the temperature at a uniform distribution of heat sources are applicable to the description of the thermal regime of bodies having, much smaller masses, than the Earth, as for example the Moon and the asteroids. A differentiation of the matter of these bodies may be neglected. It may be considered in some approximation that these formulae describe also the thermal regime of the Earth below the oceans, where there is a very low differentiation of matter.

The features of the thermal field and of the heat flow of the Earth pointed out above are maintained as it will be shown below, both at a non-uniform distribution of heat sources, as well as at a variable coefficient of thermal conductivity.

We suggested that the change from a uniform distribution of heat sources to their layer distribution took place 3.10^9 years ago. The temperature distribution established by the moment of differentiation was accepted as the initial one. The total content of U, AcU, T*h*, K in the Earth corresponded to the variant A. The process of redistribution of sources is supposed to be going on only in the mantle and the crust of the Earth; the region of the core was not involved. As a result of this the heat generation in the 20 km crust increased for ten times, while in the mantle up to the depth of 2900 km it has correspondingly diminished for 8 per cent (see curves of fig. 3 of heat generation before and after the differentiation).

The solution of the equation of heat conductivity for layer distribution of heat sources was also obtained by means of the Green function method with the aid of reflections [12 d]. Curves calculated from these formulae are given in figs. 4 and 5. The history, which took place before the differentiation, was not taken into account in the curves of fig. 4. Curves of fig. 5 give the resulting

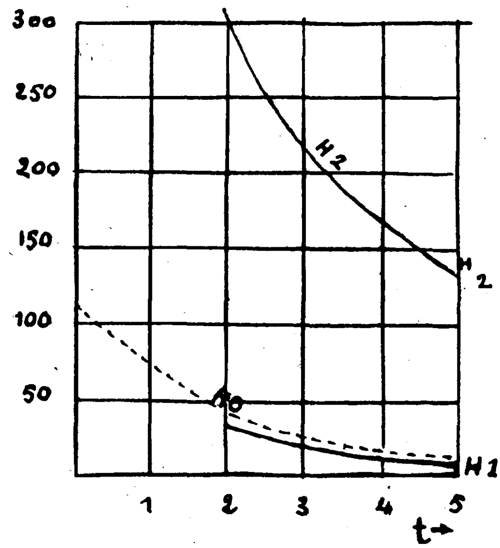

FIG. 3. Heat generation after the redistribution of sources : $H_2(t)$ — in the earth crust, $H_1(t)$ — in the mantle, $H_0(t)$ in the core assuming the hypothesis of its silicate composition.

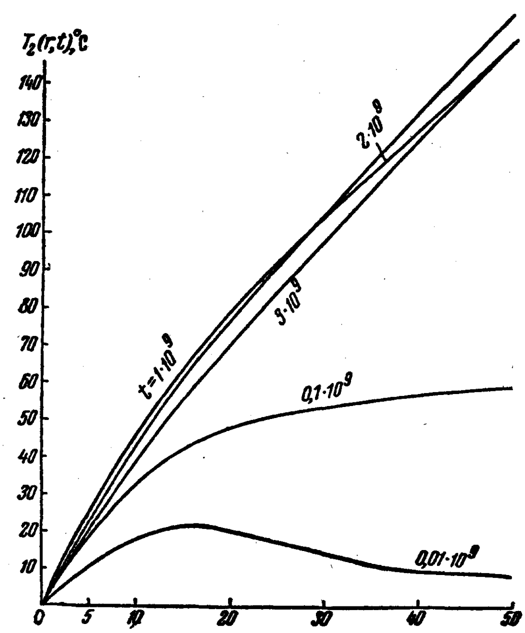

FIG. 4. Temperature distribution near the surface of layered Earth.

---

6. For the calculation of the curves of fig. 5 the content of the radioactive elements was taken according to the variant A, the Earth's age equal to 4.10^9 years and the initial temperature $T_0(r)$ in accordance with the dotted line of fig. 1.

temperature distribution[6] in which the influence of the heat discharged in the stage of the Earth formation and the stage of uniform distribution of radioactive sources were taken into account. From these curves it is seen that the temperature of the earth's crust has never reached the melting point. The high concentration of the sources in the Earth's crust cause but an insignificant increase of its temperature, because the largest part of the heat generated in the crust was rapidly lost in space. The increase of heat flow q was 20-30 per cent as compared with the flow at a uniform distribution of sources. At present the heat flow equals $1.26.10^{-6}$ cal. per cm^2/sec, which is close to the observed one. A comparatively small increase of q is explained by the fact that the dimension of the region of heat escape exceeds the thickness of the earth crust for many times. We see that about 2.10^9 years ago the heat escape to the surface began to exceed the total amount of heat generated in the crust and carried out from the deeper layers. A lowering of the temperature of the upper layers has begun as a result of this[7].

Curves of fig. 5 confirm the conclusion that the thermal history of the upper and internal layers of the Earth are different, which was arrived from the simple instance of a uniform distribution of the heat sources. An accumulation of heat inside the Earth continues even at present. The temperature of the basin of the mantle increase for about 200° for the last billion of years. The temperature of the mantle in this place is about 4000° C at present. Thus the thermal history of the Earth may be represented as a secular heating of its interiors; but not its secular cooling.

Another property of the temperature field of the Earth is the cooling of the upper layers, which are inside the zone of the heat escape. The resulting compression of the surface layers lying on the expanding bedding may be one of the causes of the deep-focus earthquakes.

The above conclusions depend essentially upon the thermal conductivity of the Earth; which determines the rate of the losses of heat by the Earth. Let us discuss this question.

According to its conducting properties the mantle of the Earth resembles most closely dielectrics. The thermal conductivity of dielectrics is determined by the vibrations of their crystal lattice. Therefore the estimates of the changes of thermal conductivity $\mathcal{H}$,

7. In the paper [12d] we have considered the case of the continuous redistribution of heat sources also. But there is not meaning to adduce this here as we do not know the true rate of differentiation of the mantle.

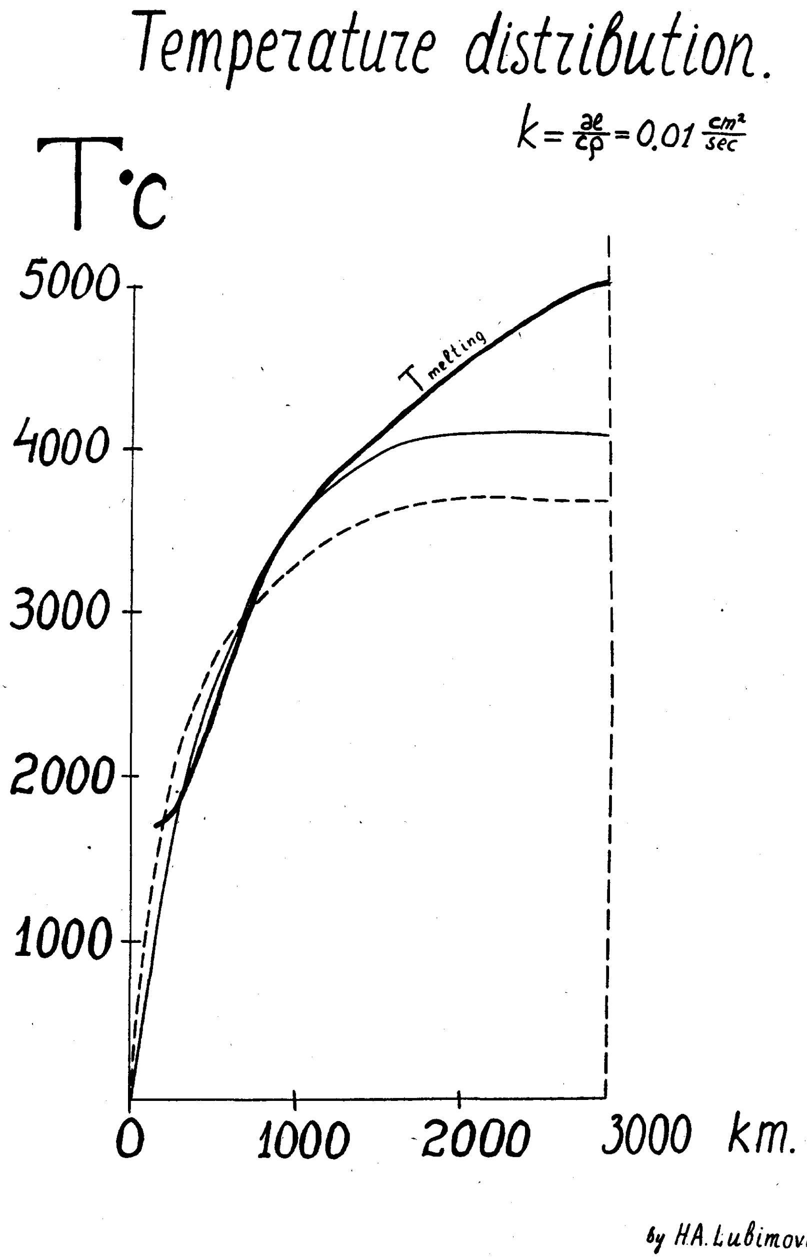

FIG. 5. Temperature distribution in the Earth calculated at the assumption of constant coefficient of thermal diffusivity. K = 0,01 cm^2/sec. a — at present; b — 1.10^9 years ago; c — 2.10^9 years ago; d — T melting according to Uffen.

obtained according to the data about electric conductivity (McNish [28]; are sensible proceeding from the Wiedemann-Franz's law, only in the region of the metallic core of the Earth.

In order to obtain a more grounded estimate of the thermal conductivity one should proceed from the lattice theory of thermal conductivity of solids. Debye [29] has shown that the main property of crystal lattice leading to its final thermal conductivity is the anharmonicity of vibrations of its atoms. The thermal motion of atoms must be represented as a totality of mutually interacting plate waves (phonons).

The theory of Debye was applied by Uffen [30] to the calculation of the thermal conductivity.

Peierls [31 a, b] investigated this question from the point of view of quantum mechanics, taking the discrete character of the crystal lattice into account. Only the collisions of the phonons of a discrete lattice lead to a finite thermal conductivity, as a result of which the summary wave vector is changing; this change is equal to a period of the inverse lattice. These are the so-called « Umklapp » processes. At high temperature, T $\gg$ θ (θ — the Debye temperature) the « Umklapp » processes are as frequent as the ordinary collisions. At low temperatures T $\ll$ θ the probability of such processes is small, the free path of the phonons being large; therefore the scattering of the phonons on the lattice defects, impurities, or mosaic blocks has a considerable influence on the thermal conductivity of dielectrics. In the present paper high temperature case is of interest, when such effects are not appreciable and the thermal conductivity is determined by the anharmonic terms. Debye and Peierls took the third order terms into account in the expansion of the potential energy in a power series with respect to the displacement of atoms from their equilibrium positions. A similar dependence $\mathcal{K} \sim \frac{1}{T}$ was obtained by them in the high temperature region $T > \theta$. The same dependence was obtained according to approximate estimates by Leibfried u. Schlömann [32] and Dugdall [33], who also restricted with cubic anharmonius approximation only.

The important contribution in the further development of phonon thermal conductivity theory was made by Pomeranchuk [34 a, b]. He has shown that the anharmonicity alone can give no thermal resistance, if the dispersion of the velocity of thermal vibrations is absent and this velocity does not depend upon the direction of the propagation in a body. The anharmonicity of third order determines the thermal conductivity for selected bodies only, in which sound velocity is a function of the angles, only. For all other bodies the integral determining the thermal conductivity[8]

$$\mathcal{K} \simeq \int c_f\, u_f\, l_f \frac{d\vec{f}}{8\pi^3 h^3} \tag{4}$$

will converge in the case, if fourth order terms will be attributed in the expansion of the potential energy, according to the powers of the displacement of the atoms from equilibrium positions, namely the collisions in which four phonons are participating will be examined.

The peculiarities of such collisions had been examined by Pomeranchuk [34 a, b], who obtained a solution of the kinetic equation for this case.

The following expression was obtained for $\mathcal{K}$:

$$\mathcal{K} \sim k.\, \mathrm{N}.\, u.\, a \left(\frac{\mathrm{M}u^2}{\mathrm{T}}\right)^{5/4} \tag{5}$$

where N — the number of elementary cells in 1 cm^3, k — Boltzmann constant, M — the mass of a cell, a — lattice constant, u — some mean sound velocity, which is determined from the velocity of the longitudinal elastic waves, u_l and the velocity of the transverse elastic waves u_c.

The dependence of the thermal conductivity from pressures is determined according to formula (5) by means of values of u and a.

The matter of the possess isotropic velocities of sound its temperature is higher, than the Debye temperature. This gives grounds to suppose that formula (5) may be applied for a description of the phonon component of thermal conductivity of the mantle. Zharkow [35] proposed to use Leibfried's formulae for $\mathcal{K}$. However the numeral differentiation of the Debye temperature over the volume must be execute for this and it introduces an additional unnecessary error. Apart from the ordinary conduction by means of lattice vibrations, the radiative transfer of heat, due to the scattering of electromagnetic waves, is possible in dielectrics at a very high temperature.

It was established experimentally that the thermal conductivity of ceramic materials of the MgO, Al_2O_3, BeO type [36] decreases as $1/T^n$, where $n \sim 1$, at temperatures $T < 1500$-$1800°$ K. However

8. The symbols in formulae (4) are : l_f — the free path of a phonon, C_f — the specific heat of a phonon, U_f — its group velocity, $d\vec{f} = df_x\, df_y\, df_z$, $\vec{f}/h$ — its the wave vector.

at T > 1500-1800° it begins to rise rapidly. The same was established for glasses. At these temperatures along with the usual molecular thermal conductivity the radiative transfer is introduced.

Since the mantle of the earth consists of substances, similar to ceramics and glasses the role of the radiative transfer of heat inside the Earth must be taken into account (Clark [37], Preston [38]). Indeed the investigations of the olivine spectra ([39, 40]) show that the maximum radiation at temperatures prevailing in the Earth will take place in the interval of respective transparency.

As it was shown by Van-der-Held [41] the effect of radiative transfer in solid may be taken into account by introducing the coefficient consisting of the sum $\bar{\mathcal{H}} = \mathcal{H} + \mathcal{H}'$ into the equation of thermal conductivity, instead of the usual coefficient of thermal conductivity, where taking the radiative transfer of heat into account $\mathcal{H}'$ is

$$\mathcal{H}' = \frac{16}{3} \cdot \frac{n^2 \sigma T^3}{\varepsilon} \tag{6}$$

ε is the coefficient of the extinction of the material, n — the index of refraction, σ — the Stefan-Boltzmann constant. Such method of account follows from the transformation of the usual equations of radiative transfer in a grey body, providing a considerable absorption coefficient which the solids are possessing : There are grounds to consider the matter from which the Earth is consisting as a grey body, because of a high spreading of olivine spectra.

As a whole the thermal conductivity of the Earth's mantle must be determined by the sum of phonon and radiative thermal conductivity[9]

$$\bar{\mathcal{H}} = \mathcal{H} + \mathcal{H}' = B\, \rho^{2/3} \frac{u^3\, u'^{1/2}}{T^{5/4}} + \frac{16}{3} \frac{n^2 \sigma T^3}{\varepsilon} \tag{7}$$

As it is seen from formula (7) the first term is decreasing with the rise of temperature, while the second term is increasing. This circumstance is very essential for the study of the thermal history of the Earth.

Clark found that with decreasing coefficient of extinction from $\varepsilon = \infty$ to $\varepsilon = 100\text{-}10\ \mathrm{cm}^{-1}$ the temperature of the Earth's interior must fall for 3 times. However the decrease of the molecular thermal conductivity with temperature, which takes place in the upper

9. The coefficient of proportionality of B in (7) was determined by us from the condition that the molekular thermal conductivity must be equal to the normal thermal conductivity of rocks on the Earth's surface. The value $\mathcal{H}_0 = B\rho^{2/3} u^3\, u^{1/2}$ is given in the table 1.

layers and prevents considerable amounts of heat to be carried out from the earth's interior (owing to which no rapid cooling of the Earth can take place [12 g]) was neglected by him.

The interest calculation by Clark was carried out at the assumption that temperature distribution is stationary in the Earth. In consequence of this he was obliged to take a 100 time lesser radioactive heat generation in the Earth, in order to satisfy the heat flow observed at the surface.

The non-stationary equation of thermal conductivity

$$c\rho \frac{\partial T}{\partial t} = \frac{1}{r}\frac{\partial}{\partial r}\left[(\mathcal{H}+\mathcal{H}')\, r^2 \frac{\partial T}{\partial r}\right] + \sum H_a e^{-\lambda at} \qquad (8)$$

becomes nonlinear when the changes of the coefficient of thermal conductivity $\overline{\mathcal{H}} = \mathcal{H} + \mathcal{H}'$ and of density $\rho(r)$ is taken into account. The method of hydraulic analogies was used for the solution of this equation with the aid of V. S. Lukjanov's hydrointegrator [42]. This apparatus permits to model the process of thermal conductivity for variables $\mathcal{H}$, c, ρ in one, two and three-dimensional space. The change of the amount of heat in an elementary volume V_k cm^3 per time unit equal to $dQ_K/dt = c\rho V_K \, dT_K/dt$, is being modelled by changing the water amount $dQ_k/d\tau = \omega_K \frac{dA_K}{d\tau}$ where A_k — is the level of water in a volume $\overline{V}_k$; ω_K — the area of its cross-section in cm^2.

In our case the elementary volumes are the volumes of the spherical layers.

Similar analogy is established for the heat flow $q = \mathcal{H}(T_k - T_{k-1})$ from volume V_k to V_{k-1} and the water flow $\overline{q} = r_{k,k-1}(A_k - A_{k-1})$ between $\overline{V}_k$ and $\overline{V}_{k-1}$. $\mathcal{H}$ and $r_{k,k-1}$ — are the coefficients of exchange, which are the values reverse to the resistance : the thermal value $R_{k,k-1} = \frac{1}{K} = \frac{d_{k,k-1}}{\mathcal{H} F}$ ($\mathcal{H}$ — thermal conductivity, F — section of the area crossed by the heat flow q, $d_{k,k-1}$ — the distance between the volume centres) and the hydraulic value : $1/\rho_{k,k-1} = r_{k,k-1}$. If the method of dimensions is used, the criterium of similitude is obtained, from which the scale of time m_τ and the modelling of heat generation follows from the formulae

$$m_\tau = \frac{c\rho\, R_{k,k-1}}{\omega_K\, \rho_{K,K-1}} \; ; \quad \hat{\rho}_{K,K-1} = \frac{c\rho\, m_a\, m_H}{\omega_K\, m_\tau}$$

where $\hat{\rho}_{K,K-1}$ is the hydraulic resistance determining the water flow, which models the heat generation; m_a and m_H — are the scale of temperature and the scale of intensities of the internal sources respectively.

The heat flow is calculated by us from the volume of water outflowing at the exit of the hydro-model. In our calculations the error did not exceed 7 per cent.

The calculation of the thermal history of the Earth, taking the variation of the thermal conductivity according to the depth into account, was carried out according to the scheme of its evolution given in the first part of the present paper. But the thickness of the earth crust was accepted as equal to 40 km. The mean heat generation in the Earth's crust was calculated according to the data on the content of U, Th, K in the granities and basalts given by Birch [2] which coincide approximately with that given by Bullard [43]. The ratio of granites and basalts in the crust was taken as 1:2. The initial temperature $T_0(r)$ was taken in correspondance with the continuous curve of Fig. 1 deduced on the ground of recent and more precise estimates. The mean abundance of radioactive elements was as well taken from more precise data according to the estimate of C (see the footnote on page 350). The age of the Earth was taken equal to $4.5.10^9$ years [44][10]. The redistribution of radioactive sources of heat was supposed to take place about $3{,}0.10^9$ years ago (more exactly $2{,}9.10^9$ years ago).

According to the data of a comparative analysis of the density distribution in the Earth and other planets of the same chemical composition ([45], [46]) the differentiation of the matter in the Earth affects only the upper part of the mantle. We supposed in this connection that the carrying out of the sources into the earth crust took place in the upper part of the mantle to a depth of about 1400 km. The concentration of radioactive elements in the impoverished thickness of the mantle will correspond to a dunite. Below 1400 km including the region of the core the source content was supposed as similar to what it had been before the differentiation, corresponding namely to the mean their content in the iron and stone meteorites.

The phase transition on the boundary of the core must have been going on when the mass of the Earth reached 0,8 of its present mass (8). We believed therefore that metal conductivity was possessed by the core already in the stage of uniform distribution of sources. Thermal conductivity of the Earth's core was calculated according to the law of Wiedemann-Franz

$$\mathcal{H} = 3\left(\frac{k}{e}\right)^2 \mathrm{T}.\ \lambda$$

10. If the period of the Earth's formation include the age of the Earth is equal to about $4{,}7.10^9$ years.

(k = Boltzmann constant, e — electron charge, λ — electric conductivity) equal to 0,5 cals/grad per sec. g; As the change of λ in metals is reversely proportional to the temperature, thermal conductivity of the core does not depend upon T. The radiative transfer must be of a very small effect in the earth's core, as the absorption of radiative energy in metals is very great : ε reaches 10^5 cm_{-1}. Besides the absorption changes very little along the spectrum and does not depend consequently upon the temperature and pressure.

The most uncertain value is the coefficient of absorption ε, which is very sensitive to the increase of T and the radiation frequency. The lowest value of it given by Clark is $\varepsilon = 10$ cm_{-1} for olivine at room temperature at wavelengths of 0,8 μ. As it may be judged from the data for semiconductors [47] the coefficient of absorption increases with temperature. For T close to 600° K the coefficient of absorption in Si and Ge reaches $\varepsilon = 100$ cm^{-1}.

We took $\varepsilon = 200$ cm^{-1} [in[12 g] and $\varepsilon = 10$ cm^{-1} in present paper. The index of refraction was taken $n^2 = 3$ (about the value for olivine or MgO in the visible part of the spectrum).

Results of temperature calculations and the corresponding thermal conductivity distribution are given in figs 6 and 7. We see that for all the moments of time thermal conductivity is decreasing at first with the growth of the depth, rapidly increasing afterwards. The effective conductivity $\overline{\mathcal{K}}$ at the base of the earth's mantle is four times larger than the ordinary conductivity of rocks *at* ε = 200 $cm.^{-1}$ and 15 times at $\varepsilon = 10$ cm^{-1}. Inside the earth, whence no heat is escaping, the temperature rises rapidly with time, while in the first upper hundred kilometres, out of which the heat escapes to the surface, a much more gradual temperature change is taking place. Radiative transfer is going on only very deeply inside the Earth. The thermal conductivity of the upper layers is determined by the molecular component $\mathcal{K}$, owing to which thermal conductivity at a depth of 50-100 km. has minimum. The value $\overline{\mathcal{K}}$ decreases at this depth for 1.5-2 times as compared with the normal thermal conductivity of the surface rocks. This decrease of thermal conductivity is followed by a number of peculiarities in temperature distribution. On the background of the general decrease of the temperature gradient with the approximation to the centre some interval of depths (see table 1) may be chosen, where there is an increase of the gradient.

The low thermal conductivity of the upper layers prevents considerable heat escape from the inside of the earth. As a result the heating of the interior of the Earth is continued up to the present moment. Thus the conclusion made earlier is confirmed : the region of heat escape to the surface and the internal part which is heated may as before be separated. Although in the thermal field of the Earth the thermal conductivity of the internal layers of the Earth is considerably higher than that of the surface layers (it equals 0,03 cals per cm. °C sec. at a depth of 1.000 km.) no considerable heat escape takes place from the depths exceeding 500 km., as the temperature gradient there, caused by the initial distribution of T_0 (r) and the nonuniform distribution of sources is much less than the gradient in the upper layers.

The depth of the region of heat escape is about 500 km. The temperature inside it is nearly constant during of the recent billion years, and has a tendence to decrease.

We shall compare the temperature rate at various depths with the Uffen's curve of fusion (see *Fig.* 6). The temperature of the

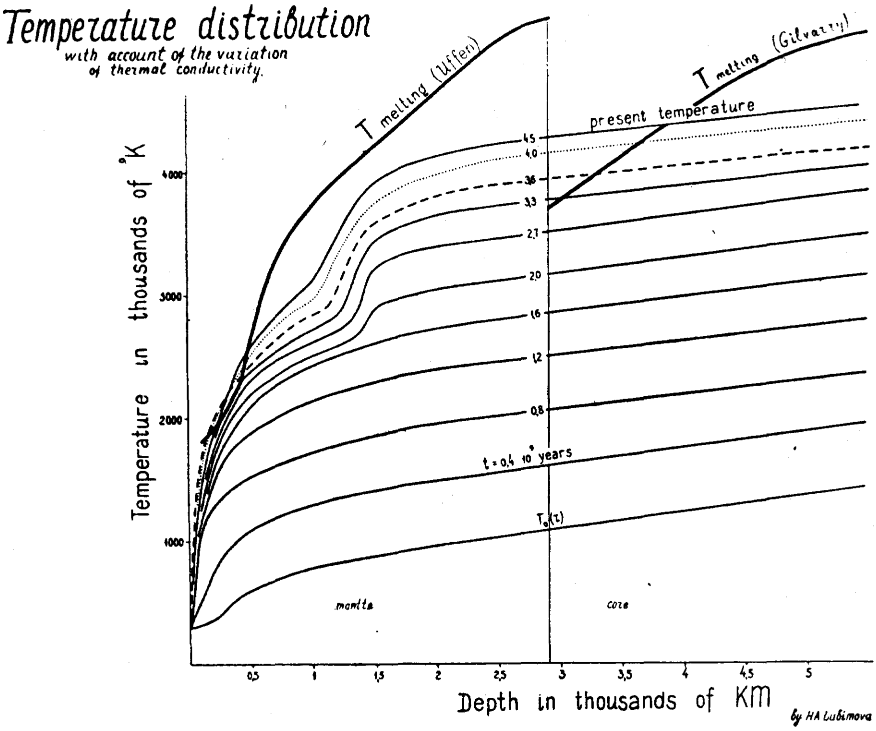

FIG. 6. Temperature distribution in the Earth for different moments of time with account of the variation of thermal conductivity with depth.

Earth increases rapidly in the upper layers after which its rise is lessened; in the region of the core the temperature had time to smooth to its adiabatic gradient.

Contrariwise, the fusion temperature of the Earth rises slowly in the upper layers, in which the pressure is not large and rapidly in the interior. This leads to a tendency to fusion in the upper part of the Earth's mantle. This tendency can also be noticed in the curves of Fig. 5. This does not mean the appearance of an entirely melted gurdle in it, as the physical properties of matter in the earth's mantle are practically inhomogeneous, but permits to suggest that individual magmatic hearths or pockets may possibly originate in it. Volcanic activity can obviously be connected with it. As it is seen from figures 5 and 6 the zone of the hearths is displaced with time towards the inside of the Earth. Its limiting depth is 500-700 km. for the present. This is also the limiting depth for deepfocus earthquakes.

The Earth as a whole could not melt in the process of its evolution : complete melting is only possible for bodies of much lesser mass, than the mass of the Earth, as the Moon for example[11] [48]. However, in the case of smaller bodies like the asteroids the melting could take place only in the centre [49]. If the melting temperature for the metallic state of silicates is supposed to be close to that of iron, estimated by Simon-Gilvarry [50] for the pressures in the Earth's centre, then, as it is seen from fig. 6, the outer parts of the core must be in a melted state, while the internal core must be solid. This agrees with the hypothesis of Jacobs [51] about the hardness of the internal core.

Maximum value of the heat flow reached $3{,}4.10^{-6}$ cals/cm^2 per sec. and had taken place $2{,}5.10^9$ years ago. The modern value equals $2{,}3.10^{-6}$ cals/cm^2 per sec., which exceeds twice the observed mean value $1{,}2.10^{-6}$ cals per cm^2/sec. This value was recently obtained by Clark and Nibblett [52] for the region of Alpine railroad tunnels. This is explained by very great thickness taken for the crust (40 km.) in particularly for the granitic layer. This leads to a suggestion that the uppermost layer of the Earth cannot consist of a continued granite massive only. The selection of the correct heat generation in the uppermost layer of the Earth is connected with the problem of granite distribution. This note was, also, advanced by Birch [2 *b*] from other data recently.

11. It is possible that the volcano eruption observed on the Moon is a consequence of its previous melting state.

The fact of the minimum of the thermal conductivity in the upper layers can be apply to the explanation of the phenomenon of the low velocity layer at the depth about 100 km. without an additional supposition about the special physical state of this layer. For the decrease of the seismic velocities the temperature gradient in dunitic mantle should be exceed 10 grad. per km. for P-waves and 7 grad. per km. for S-waves [53, 54]. In the table 1 we give the values of the thermal conductivity $\mathcal{H}$, temperature T°C, and temperature gradient l in grad. per km. for the continental type of the crust. We took the heat generation equaled to 53.10^{-14} cal. per cm^3/sec. — for the granitic layer [10 km.], 15.10^{-14} — for the basaltic layer (20 km.) and $0,4.10^{-14}$ — for the dunitic mantle. We see, that the temperature gradient l increases at the depth 50-100 km. where it exceeds the limit values. But for 150 km. the value of l decreases up to 9 grad. per km. Therefore the low velocity layer for P-waves should be narrower then for the S-waves. This corresponds to the observations. The similar calculations for the oceanic basalt crust (10 km.) shows, that the maximum of l is equal $\sim$ 6 grad. per km. on the depth of 50 km. in the case of the meteoritic composition of the mantle under Mohorovicic discontinuity and the maximum of l is equal to about 14 grad. per km. at the depth 30 km. in the case of the eclogitic mantle. Thus there are not any low velocity layers under the oceanic crust, this will be show the probability of the meteoritic composition of the mantle under the oceans.

TABLE 1.

km	20	30	40	50	80	100	150	200	250
$\mathcal{H}_0$	9	12	14	15	17	18	19	21	22
$\bar{\mathcal{H}}$	0.004	0.004	0.003	0.003	0.002	0.002	0.004	0.008	0.011
T°C	300	340	400	520	970	1300	1700	1950	2070
l	11	4	6	12	16	17	9	4	2.5

Thus our calculations carried out in a wide interval of initial data concerning the age of the Earth $(4\text{-}5).10^9$ years), the concentration of the radioactive elements (A,B,C), thermal conductivity $\mathcal{H}(r, t)$ and initial temperature $T_0(r)$ (2500 — 1.000° max.) show that the limits, in which possible variations of these data are going

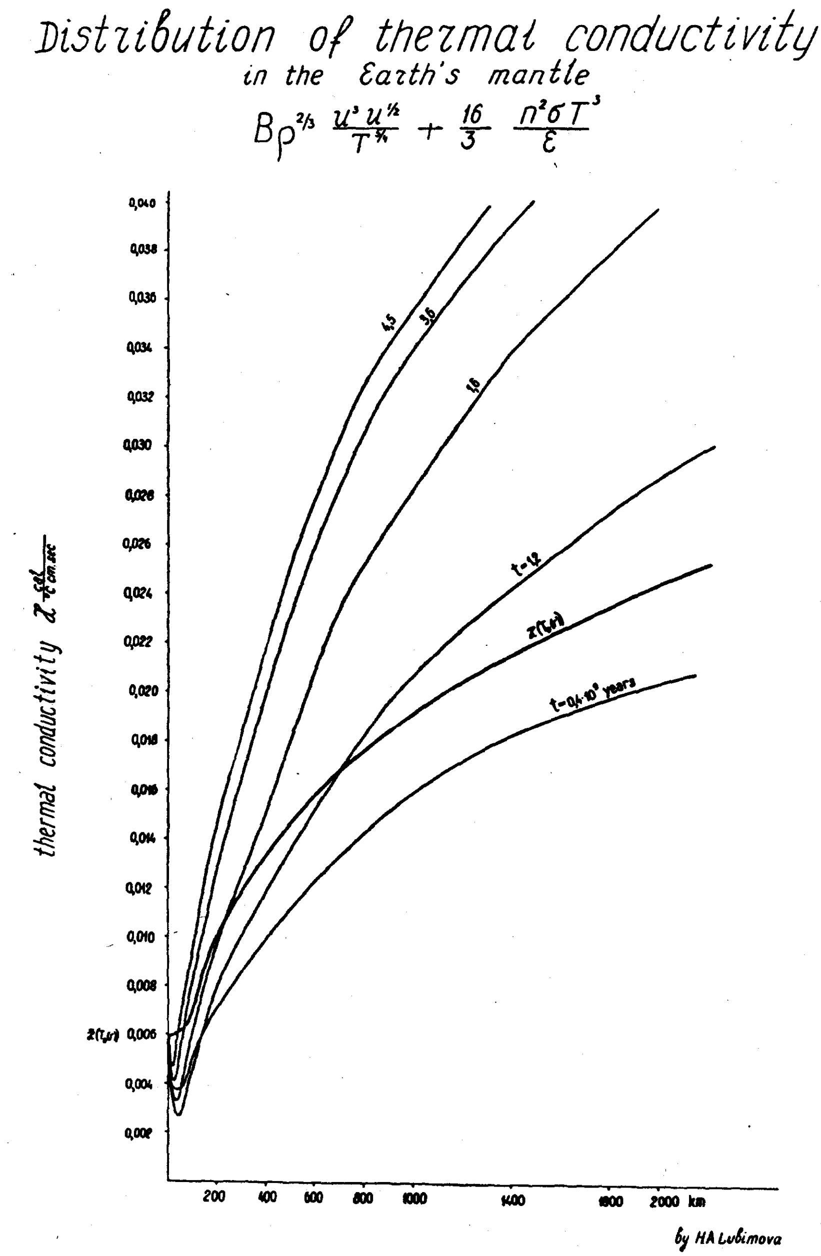

FIG. 7. Distribution of thermal conductivity H (r, t) in the Earth's mantle for $\varepsilon = 10$ cm-1; $n = 1{,}7$.

on, do not change the main conclusions about the secular course of the temperature of the Earth, formed from cold particles of gas-dust protoplanetary cloud. The obtained regularities of the thermal field and its changes with time differ from regularities following from the ideas about the secular cooling Earth. This gives new grounds for the explanation of a number of geophysical and geological phenomena.

We made an attempt to ascertain the correspondence between our temperature distribution and the electrical conductivity distribution determined from the electromagnetic variations [56]. We used the formulae of Davydov for the activation energy of ionic conductivity [55]. The coefficients A and B in this formulae were determined by us from the experimental data about the electrical conductivity of the olivine at high pressure and temperature [57]. It was shown that the ionic mechanism of the electroconductivity can explain the observating increase of the conductivity in the mantle up to the depth 500 km. only. But at the great depth the mobility of ions decreases with pressure very strongly. Therefore at the depth about 1000 km. ionic conductivity is 10^{-2} of its observed value and it begins to decrease with depth from 2000 km. on the contrary to the observing data.

In order to study the nature of the conductivity in lower part of the mantle we considered the variation of the activation energy of the intrinsic semiconductors (« the energy gap ») with temperature and pressure. The interaction between electrons and phonons leads to the increase of the intrinsic electron conductivity. This interaction modifies the states of the electrons. In consequence of this the permitted levels of the electron energies begin to spread and the energy gap begins to narrow. The temperature effect narrows the gap in all semiconductors and does not depend on its structure. The pressure may both narrow and widen the gap. The formulae for the gap is :

$$E_g = E^0_g + p\, \partial E_g/\partial p - \alpha\, K\, T \frac{\partial E_g}{\partial p} - \beta T$$

where E^0_g — the energy gap at the normal pressure and temperature, α — the coefficient of the thermal expantion, K — the incompressibility; β — parameter, determinated the electron-phonon interaction. We took $E^0_g = 3{,}3$ ev, $\frac{\partial E_g}{\partial p} = -2.10^{-6}$ ev per dyne-cm², $\beta = 3.10^{-4}$ ev per grad. The calculated values of electroconductivity agrees pretty well with its observated values. It is mean, that the temperature distribution does not contradict to the electromagnetic data.

REFERENCES.

1. REVELLE (R.), MAXWELL (A. E.). Heat flow through the floor of the Eastern North Pacific Ocean. Nature 170, N° 4318, 1952.
2. BIRCH (F.). *a*) Radiogenic heat. chap. 5, in « Nuclear Geology », 1956. N. Y., London.
b) Physics of the Crust. Geol. Soc. of Am., sp. paper 62, 1955.
3. VERHOOGEN (J.). Temperatures within the Earth. Ch. 2 in Physics and Chemistry of the Earth, 1956, London.
4. DAVIS (G. L.). Radium content of ultramafic igneous rocks. Am. Journ. Sci., *245*, 677, 1957; *248*, 2, 1950.
5. PANETH (F. A.), ARROLL (W. J.), JACOBI (R. B.). Meteorites and the age of the Solar system, Nature *149*, N° 5774, 235, 1942.
6. BULLEN (K. E.). On the constitution of Mars. M.N.R.A.S. Geoph. Suppl. 7, N° 5, 271, 1957.
7. LODOTCHNIKOV (V. N.). Some general questions : connected with the magna producing basalt rocks. Transactions of the Russian Min. Soc. Part 68, N° 2, 1939.
8. RAMSEY (W. H.). On the nature of the Earth's Core, M.N.R.A.S. Geophys. Suppl. *109*, N° 3, 9, 1949.
9. SCHMIDT (O.). Rôle des particules solides dans la cosmogonie planétaire. Les particules solides dans les astres, 1955, 638-649 (Colloque à Liège, 1954).
10. SCHMIDT (O. J.). A theory of Earth's origin 3 ed. For. Lang. Publ. House Moscow, USSR, 1958.
11. SAFRONOV (V. S.). *a*) On the growth of planets in protoplanetary cloud. A. J. USSR, N° 6, 1954.
b) On the initial temperature of the Earth. Bull. of the USSR Acad. of Sci., geoph. ser., 1959, N° 1.
12. LUBIMOVA (H. A.). *a*) On the heating of the earth's inside in the process of its formation. Bull. Acad. Sci. USSR, geoph. ser., N° 5, 1955.
b) On the influence of radioactive decay upon the thermal regime of the earth. Bull. of the USSR Acad. Sci. USSR, Geoph. ser., 2, 1952.
c) On the thermal history of the Earth and its geophysical consequences. Comptes rendus de l'Acad. Sc. de l'URSS, 107, N° 1, 1956.
d) On the influence of radioactive element redistribution upon the thermal history of the earth. Bull. de l'Acad. Sc. de l'URSS, N° 10, 1956.
e) On the thermal regime of the earth. Publ. Geoph. Institute of the Academy of Sc. of the USSR, *26* (153), 1955.
f) Role of thermal conductivity in the thermal regime of the earth. Bull. USSR Acad. of Sc., N° 6, 1953.
g) On the role of radiative transfer in the thermal regime of the earth. Bull. of the Acad. of Sc. USSR, N° 5, 1957.
13. UFFEN (R. J.). A method of estimating the melting point gradient in the Earth's Mantle. Trans. Am. Geoph. Un., *33*, 6, 1952.
14. JEFFREYS (H.). The Earth's thermal history. M. N. R. A. S. *116*, 231, 1956.
15. SLICHTER (L. B.). Cooling of the Earth. Bull. Geol. Soc. Am., *52*, 4, 1941.
16. TYCHONOFF (A. N.). On the influence of radioactive decay upon the temperature of the earth's crust. Bull. Acad. Sc. de l'URSS, ser. Geophys. and geogr., N° 3, 1937.
17. MAGNITSKY (V. A.). *a*) Foundations of the physics of the Earth. 1953, Geod. Publ. House, Moscow.
18. URRY (W. D.). Significance of radioactivity in Geophysics. Thermal history of the Earth. Trans. Am. Geophys. Union., *30*, 171-180, 1949.

19. JACOBS (J. A.), ALLAN (D. W.). Temperature and heat flow within the Earth. Trans. Roy. Soc. Canada, *48*, ser. III, 1954.
20. RUBEY (W. W.). Geologic history of sea water. Bull. Geol. Soc. Am., *62*, IIII, 1951.
21. WILSON (Y. T.). The development and Structure of the Crust. Ch. 4. The Earth as a planet, ed. by G. P. Kuiper, Chicago, 1954.
22. TYCHONOFF (A. N.) and SAMARSKY (A. A.). Equations of mathematical physics. Moscow-Leningrad, 1951.
23. LOWAN (A. N.). On cooling of a radioactive sphere. Phys. Rev., *44*, 769, 1933.
24. ALLAN (D. W.). Heat in the Earth. Advancement Sci., *12*, N° 45, 1955.
25. STARKOVA (A. G.). Content of radioactive elements in meteorites. Meteoritics, N° 13, 1955.
26. UREY (H. C.). The cosmic abundances of Potassium, Uranium and Thorium and the Heat Balances of the Earth, the Moon and Mars. Proc. Nat. Acad. of Sci., *42*, N° 12, 1956.
27. STARIK (I. E.) and SHATZ (M. M.). Determination of Uranium in Stone and Iron Meteorites. Geochemistry, N° 2, 1956.
28. MCNISH (A. G.). The Earth's interior as inferred from terrestrial magnetism. Trans. Geophys. Union 1937, Nat. Res. Council, 43-50.
29. DEBYE (P.). Vortrage uber die Kinetische Theorie. Ets. Teubner, 1914.
30. UFFEN (R. J.). Thesis. Univ. of Western Ontario.
31. PEIERLS (R. E.). *a)* Ann. d. Phys., 5, 3, 1055, 1929.
b) Quantum theory of Solids. Oxford, 1955.
32. LEIBFRIED J. u. SCHLOMANN E. Wärmeleitung in elektrisch isolierenden Kristallen, Akad. Wissen. Göttingen, Math.-physik. Klasse II a, N° 4, 1954.
33. DUGDALL (J. S.), MACDONALD. Lattice Thermal Conductivity. Phys. Rev., *98*, N° 6, 1955.
34. POMERANCHUK (J.). *a)* Heat conductivity of dielectrics at high temperatures. Journ. of Phys. USSR, *7*, N° 5, 1943.
b) Journ. of Phys. USSR, *4*, 259, 1941.
35. ZHARKOW (W. N.). On coefficient of thermal conductivity of the Earth's mantle. Bull. of the USSR Acad. Sci. USSR Geoph. Ser., N° 11, 1958.
36. MCQUARRIE (M.). Analysis of variation of conductivity with temperature for Al_2O_3, BeO, MgO. J. Am. Ceramic Soc., *37*, N° 2, 1954.
37. CLARK (S. P.). Effect of radiative transfer on temperature in the Earth, Bull. Geol. Soc. Am., *67*, 1123, 1956. Trans. Am. Geoph. Union *38*, N° 6, 1957.
38. PRESTON (F. W.). Thermal conductivity in the depths of the Earth. Am. J. Sc., *254*, 754, 1956.
39. KELLER (W. D.), SPOTTS (J. H.), BIGGS (D. L.). Infrared Spectra of Some Rock-forming Minerals. Am. Journ. of Sc., 250, N° 6, 1952.
40. RUNCORN (S. K.). Experiments on the Displacement of the Ultra-violet Absorption Edge of olivine at High Pressures. J. App. Phys., *27*, N° 6, 1956.
41. VAN DER HELD (E. F. M.). The contribution of radiation to conduction of heat. App. Sc. Res. sec. A, *3*, N° 3, 237, 1952.
42. LUKJANOV (V. S.). Hydraulic analogy as a new means for the solution of technical problems. Bull. l'Acad. des Sc. de l'URSS, ser. techn., N° 3, 1938.
43. BULLARD (E.). The Interior of the Earth. Ch. 3. The Earth as a planet ed. by Kuiper, Chicago, 1954.
44. PATTERSON (C.), BROWN (H.), TILTON (G.) and INGHRAM (M.). Concentration of Uranium... Phys. Rev., *92*, 1234, 1953.
45. KOSLOVSKAYA (S. V.). Comparative analysis of the internal structure and composition of planets and satellites, C. R. Acad. Sc. de l'URSS, *92*, N° 5, 1953.
46. LEVIN (B. J.). Composition of the Earth. Publ. Geoph. Inst., N° 26 (153), 1955.
47. FAN (H. Y.). Infrared absorption in semiconductors. Reports on Progress in Physics, *29*, 1956.

48. LEVIN (B. J.), LUBIMOVA (H. A.). Thermal history of the Moon. Nature (USSR), n° 10, 1955.
49. LUBIMOVA (H. A.), STARKOVA (A. G.). On the radioactive heating of large asteroids and meteorite structure. A. J. USSR, N° 5, 1954.
50. GILVARRY (J. J.). Temperatures in the Earth's interior. Journ. Atmosph. Terrestr. Phys., *10,* 84-95, 1957.
51. JACOBS (J. A.). Temperature distribution within the Earth's core. Nature, *173*, 258, 1954.
52. CLARK (S. P.), NIBLETT (E. R.). Terrestrial heat flow in the Swis Alps. M. N. R. A. S. Geoph. Suppl., *7,* N° 4, 195, 1956.
53. VALLE (P.). Sul gradiente di temperatura necessario per la formazione di « low velocity layers » Ann. Geofisica *9,* N° 3, 1956.
54. MAGNITZKY (B. A.). On the low velocity layers in the crust and under the crust. Bull. Moscow Soc. expl. nature, ser. geol. *33,* N° 4, 1958.
55. DAVYDOV (B. J.). Physical properties of solid at high pressures. This volume.
56. MCDONALD (K. L.). Penetration of the geomagnetic secular field through a mantle with variable conductivity. J. Geoph. Res. *62.* N° 1, 1957.
57. HUGHES (H.). The pressure effect on the electrical conductivity of peridot. J. Geoph. Res. *60,* N° 2, 1955.

FUNDAMENTAL FEATURES OF THE STRUCTURE AND DEVELOPMENT OF GEOSYNCLINES

By V. V. BELOUSSOV

In this paper the author has endeavoured to give a brief summary of his views on the nature of geosynclines — views that are developed in greater detail in a number of his publications /2,3,4,5/.

The division of the earth's crust, or at least the continental part, into geosynclines and platforms is characteristic of a long period of geologic history — from the Proterozoic to the Tertiary inclusively. Our conceptions of the Archaezoic, are vague. It is possible that at that remote time the entire crust of the earth behaved like one immense geosyncline. But it is no less probable that during the Archaezoic Era the crust was characterized by some particular condition to which the concept of geosynclines and platforms is inapplicable.

In the same way we do not know whether this division of the earth's crust into geosynclines and platforms will be preserved in future. As a consequence of the gradual growth of platforms at the expense of geosynclines, it came about that by the Quaternary geosynclines seemed to be disappearing from the continents, and geologists seek modern geosynclines, for the most part, on the sea bottom. Besides this, the latest geologic time / the end of the Tertiary, and the Quaternary / is marked by a new tectonic phenomenon — the activization of former platforms, something particularly noticeable in Central Asia / the Tien Shan, the Kuenlun, Tibet and others /. This would indicate the transition of the earth's crust to new forms of development, and it is very probable that « classic » geosynclines and platforms will not exist in the near geologic future.

Since the division of the earth's crust into geosynclines and platforms was apparent during the entire period of which the geologist actually has any knowledge, we are inclined to make this division absolute and regard it as « eternal ». The division unquestionably did exist for about five hundred million years, i. e. approximately one-eighth the time the earth has been in existence. But if there are no geosynclines in the future, then their historical importance during the next geologic era will steadily decline. Phenomena of larger categories, such as continents and oceans, will undoubtedly play a considerably more important role from the standpoint of geologic history as a whole, although up to now structural geologists have occupied themselves much more with geosynclines and platforms than with the question of the origin and development of continents and oceans.

What has been said, however, by no means signifies that the question of geosynclines and platforms has lost its importance. It remains one of the fundamental problems of modern geotectonics.

***

When an attempt is made to differentiate geosynclines and platforms, a large number of characteristics are usually cited, among them the intensity of the vertical / oscillatory / movements of the earth's crust, folding, magmatism and metamorphism. In order to give a more precise definition it is extremely important to choose some one of these heterogeneous characteristics as fundamental. To our mind such a characteristic is the regime of oscillatory movements of the terrestial crust. When it comes to magmatism, it is a fact in individual geosynclines it differs considerably in intensity and character. Folding, of course, is characteristic of geosynclines, but it too is manifested quite differently in various geosynclinal areas. The character of oscillatory movements, however, always distinguishes a typical geosyncline from a typical platform.

Characteristic of geosynclines is a great diversity in the oscillations of the earth's crust : the geosyncline is always divided into zones of intensive subsidence and elevation, zones that are situated in close proximity and sharply opposed one to the other. It may be said that steep gradients of oscillations are typical of geosynclines, especially in a direction perpendicular to their trend. Since the amplitude of the sinking of the earth's crust is indicated with sufficient exactness by the thickness of the sedimentary deposits, geosynclines are characterized by steep gradients of thickness of these beds — rapid variations in this thickness from one place to another, particularly in a direction perpendicular to the trend of the geosyncline.

Some authors hold the view that geosynclines may be characterized as areas of intense subsidence of the earth's crust. All geological evidence shows that this definition is not only insufficient but grossly distorts the facts : the thing most characteristic of any geosynclinal area is the sharp differentiation of the terrestial crust into narrow zones of elevation and subsidence, elevation at all stages in the development of the geosyncline being no less pronounced

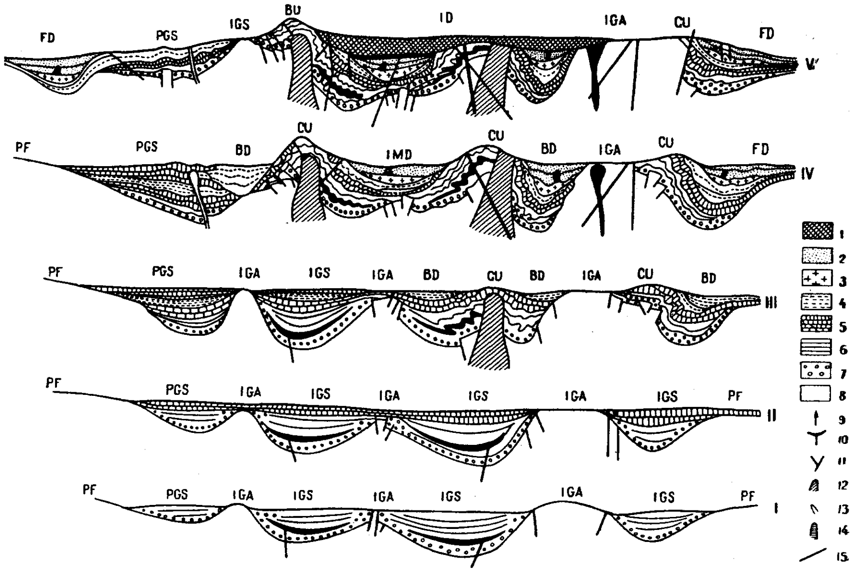

FIGURE 1.

PF — platform.
IGS — intrageosyncline.
IGA — intrageoanticline.
PGS — parageosyncline.
FD — fore-deep.
BD — border-deep.
IMD — intermontanedeep.
ID — interior deep.
CU — central uplift.
BU — border uplift.
1 — formation of the interior deeps.
2 — molassic formation.
3 — salt, gyps (Lagoonal formation).
4 — flysh, coal-bearing and oil bearing formations.
5 — limestones (limestone formation).
6 — sandstone and shale deposits (lower terrigenous formation).
7 — coarse-grained deposits.
8 — formations of the previous tectonic cycles.
9 — volcanoes.
10 — effusive rocks and sills.
11 — dikes.
12 — batholites.
13 — minor intrusions.
14 — diapiric structures.
15 — faults.

than subsidence. The latter, however, is more easily detected in the structure of the earth's crust in the form of sedimentary layers of great thickness, and therefore attracts more attention. I use the terms intrageosyncline and intrageanticline to signify these zones of sinking and uplift within the geosyncline.

Platforms are characterized by a gentler regime of oscillatory movements. They are also divided into areas of subsidence / *syneclise* or subgeosynclines / and elevation / *anteclise* or subgeanticlines /, but the contrasts between them are by no means so great : each area of subsidence or elevation occupies a large territory and goes over very smoothly and gradually into the neighbouring area of opposite movement. The gradients of thickness of sedimentary layers, are here small.

It follows from this definition of geosynclines and platforms that their development should be considered first of all on the basis of the sequence of oscillatory movements, comparing the latter with other tectonic and magmatic processes.

Two categories of oscillatory movements of the earth's crust are to be considered. Stille, for example, divided oscillations into what he called undation and undulation /10/. The author distinguishes « general oscillations » and « undulatory oscillations ». The formation of intrageosynclines, intrageanticlines, *syneclise* and *anteclise* is caused by undulatory oscillations. These movements bring about the division of the earth's crust into zones or areas where there is a long development of the processes of subsidence or elevation, which either preserve their situation or gradually migrate, changing their dimension and form. A geological record of these movements is preserved in the arrangement of thicknesses, as well as the litho-facies of sedimentary deposits.

General oscillations give rise to subsidences and elevations simultaneously affecting large areas, far beyond the boundary of one geosyncline. Such general subsidences and elevations are manifested in the transgressions and regressions of seas, and in interruptions in the process of sedimentation. They are characterized by reversibility / subsidence and elevation follow one another on one and the same territory /, and complexity / the mutual superimposing of oscillations of different orders and periods/. General oscillations of very great magnitude are known, manifested in the almost universal and simultaneous development of very great transgressions and regressions. Such oscillations determine what is known as geotectonic cycles or stages. Each cycle or stage begins with the predominance of the elevation of the earth's crust, develops first in the direction of an ever-greater subsidence and transgression, and ends with the reverse process of increasing elevation. The length of the cycle / Caledonian, Hercynian or Alpine / apparently averages 150 million years.

On these major cycles, are imposed cycles of increasingly higher order, corresponding to the length of the geological Period / 30-40 million years /, the Epoch /15-20 million years/, the division and so on, down to the smallest quasi-periodic oscillations which determine, for example, the rhythm of deposition in « flysch » or coal-bearing layers. In this paper we shall consider only the largest cycles.

In their development, geosynclines are always subordinated to the cyclic nature of the general oscillations. In accordance with this one can distinguish two stages in the development of geosynclines, « active » within the bounds of a big geotectonic cycle : the first stage is characterized by increasing subsidence and its growing predominance over elevation, the second stage, on the contrary, is characterized by ever-greater predominance of elevation over subsidence. I call the transition from one stage to another the general inversion of the geotectonic regime.

The Caledonian cycle begins everywhere with transgression at the end of the Proterozoic or in the Cambrian and ends with regression and extensive elevation at the end of the Gotlandian or the beginning of the Devonian. The Hercynian cycle begins with transgression in the Devonian and ends with the regression in the Permian. During the development of the Alpine cycle certain differences are observed between the so-called « Atlantic » and « Pacific » zones : in the Atlantic zone / in Western Europe, for example /, subsidence began to increase at the expense of elevation at the end of the Permian or the beginning of the Triassic while general inversion, after which elevation became predominant, occured at the end of the Cretaceous or in the Paleogene; in the Pacific zone / China and the Cordilleras /, subsidence developed in the Triassic or the beginning of the Jurassic, while the predominance of elevation is noticeable from the end of the Jurassic. Thus general inversion in the latter zone occured earlier.

The development of undulatory oscillations in geosynclines is somewhat more complex. On the basis of the development of geosynclines in the USSR and some other localities the author worked out a scheme for the development of undulatory oscillations in geosynclines similar to the scheme proposed by Van Bemmelen on the basis of other geosynclines /9/.

The fundamental principle is that at a certain stage of development of the geosyncline, new uplifts / central elevations / occur within the zones of subsidence, i.e. the intrageosynclines. This marks the beginning of an undulatory process : the central elevation develops vertically and laterally, while the residual subsidences alongside are shifted outwards, gradually overlaping onto the neighbouring zones of elevation (intrageanticlines). If this process proceeds to the end, and the neighbouring intrageanticlines are narrow, there is complete inversion in the zones of subsidence and elevation : a zone of elevation is formed in place of the former intrageosyncline, and zones of subsidence in place of the former neighbouring intrageanticlines (intramontane deep). If the intrageosyncline is peripheral, one of the subsidences formed at the foot of the central elevation overlaps the edge of the platform, forming a foredeep.

I use the term « local inversion » to describe the formation of central elevations in intrageosynclines and the replacement of the latter by the former, intrageanticlines being replaced by intramontane deeps. But although this constitutes a most important stage in the development of geosynclines, there are actually a number of complications affecting the scheme just expounded. Local inversion does not take place in all intrageosynclines within the limits of the given geosyncline, but only in part of them or even in just one (the principal one). Once the central elevation has formed, it does not always develop to such an extent as to replace the entire intrageosyncline. In some cases it only complicates the structure of the intrageosyncline but does not destroy it completely. If the intrageanticline is broad, the down-folding encroaching upon it from the neighbouring intrageosyncline involves only its edge, while the central part is preserved as a stable zone of elevation. Examples of such diversity in development were described in an earlier work (2). For those geosynclinal areas where partial inversion is not observed or occurs in a weakened form, I proposed the use of the term parageosyncline.

There is undoubtedly some connection between the development of undulatory oscillations in geosynclines and « cycles » governed by general oscillations. In the majority of cases the scheme laid down for the development of undulatory oscillations is contained in one geotectonic cycle, and local inversion coincides with general inversion. In these cases the transition from predominating subsidence to predominating elevation coincides with the inversion of the zones of elevation and subsidence within the geosyncline, and at the end of the cycle mountains are formed where the deepest intrageosynclines were situated. An example of such development is the Great Caucasus where the general and partial inversion took place in the Oligocene.

But in other cases the connection between cycles and the development of undulatory oscillations appears to be less binding. In the Lesser Caucasus during the Alpine cycle, for example, or in the Ural during the Hercynian, local inversion took place earlier than general inversion. As a result the central elevations formed were again involved in subsidence for a certain time and sediments accumulated on their surfaces; only later did they again begin rising and widening intensively. In the Lesser Caucasus the central elevations began to appear as far back as the Jurassic, while general inversion took place only in the Paleogene. Up till then the central elevations were small lowlying islands in a geosynclinal sea. After general inversion they developed into large mountainous elevations that ran together.

Cases are also known where the complex of undulatory oscillations was not completed within one geotectonic cycle but covered several cycles. The development of the Ural was of this type. During the whole Caledonian cycle subsidence was developing in the Ural geosyncline at the expense of elevation. This process continued into the beginning of the Hercynian cycle. It was only in the middle of the Hercynian cycle (in the Early Carboniferous) that central elevations were formed and the geosyncline entered on the second stage of its development. An analogous « two-cycle » development is to be seen in the southern Tien Shan. So far as it is possible to judge by the data published the Himalayas are developing in three cycles : subsidence began during the Caledonian cycle, while elevation became predominant only at the end of the Alpine cycle.

At the same time, there are geosynclines which are active during several successive cycles, and in each of them they exhibit a complete development. In such cases the intramontane subsidences formed as the result of local inversion during one cycle, play the role of intrageosynclines during the next. The North American Cordilleras are an example.

From what has been said it is apparent that the development of undulatory oscillations in geosynclines is subject to subtle laws and proves to be rather complicated. And if a definite scheme for the development of these oscillations is to be detected in all geosynclines, still each of them is distinguished by certain individual characteristics, and even within a single geosyncline, there are zones in which development proceeds in several different ways.

All these complications and niceties in the development of oscillations categorically cannot be packed into simplified, purely mechanical schemes based on a concept of an external lateral compression of the geosyncline, no matter what its source — no matter whether it be connected with the shrinking of the earth, the drifting of continents or local lateral displacements of separate blocks of the earth's crust. The causes determining the development of undulatory oscillations in geosynclines must be within the geosyncline itself, not exterior to it. Evidently they should be beneath the earth's crust — directly under the geosynclines — and the forces exerted on the crust must be directed vertically.

The last conclusion is not contradicted by the need to explain folding. Moreover, in the very phenomenon of folding in geosynclines there are features which themselves testify to the predominant role of vertical tectonic forces acting in geosynclines.

Ampferer pointed out that the complicated form of many geosynclines, broken up as they are into separate ovals, and the bow-shaped contours of a number of folded mountain chains contradict the idea of lateral pressure being exerted on geosynclines from neighbouring platforms (6). In the latter case, the Russian platform should have exerted pressure on the various parts of the Carpathians simultaneously from south to north, from east to west, and from north to south.

A study of the history of folding in geosynclines shows that the folding originates in the sunken parts of the intrageosynclines (at the spot where the central elevation is formed) and from there extends to their peripheries. If the folding were caused by lateral pressure from without, then one would expect a reverse development — from the periphery inwards, i. e. away from the zones nearest the source of pressure. One would likewise expect the folding to be most intense at the edge of the platform exerting the pressure, and considerably less in the internal regions of the geosynclines. Actually, the reverse is to be observed : folding in the sunken parts of the intrageosynclines is the most complex and the most intense, whereas in the peripheral regions it not only decreases in intensity but changes in form : holomorphic (linear, strongly compressed) folding gives way to comb folding (narrow anticlines alternating with broad, flat synclines) and idiomorphic folding (isolated brachi-folds or domes).

The author is convinced that no room has been left now for doubt that folding results from the horizontal redistribution of the material of the earth's crust within the limits of the geosyncline or even its separate zones. During this process the material flows from some places and accumulates in others where it is crumpled into folds. This horizontal flowing of material is a secondary process taking place against the background of the primary oscillations. The author has set forth his views on the genesis of folding in another paper to be presented at this symposium. On this point also the author's view's are now rather close to those of Van Bemmelen (8), though the author is inclined to add some other modes of fold formation to the gravitational mechanism, and he also hopes that he has been able to consider the whole problem of folding somewhat more fully than has been done before.

When it comes to explaining the origin of vertical tectonic forces, the only *geological* data available are those obtained through the study of the development of magmatic phenomena in geosynclines. As is well known these are distinguished by great intensity and considerable diversity. The general principle is that the outpouring of basic volcanic lavas is associated with subsidence in geosynclines, while acid (mostly granitic) intrusions are associated with elevation. It is known that ophiolithic formations are characteristic of the first stage in the development of a geosyncline, when subsidence is predominant; these consist of basic (mostly basaltic) lavas, and sills formed very close to the surface. Then as the geosyncline matures and elevation begins to gain the ascendancy, the time arrives for the formation of enormous granite batholiths.

This principle is also evident in small-scale structures. It is not difficult to find examples where alongside a growing elevation in which granite intrusions are already forming, there is a residual subsidence in which the outpouring of basic lavas is continuing. The magmatic emanations in intrageosynclines and intrageanticlines are different in composition. The real picture is of course more complicated than this simple sketch but the principle outlined may be considered as an approximation that is fundamentally true.

It is a very interesting fact that in a given zone a change in the direction of the vertical movements is accompanied by a corresponding change in the composition of the magmatic emanations.

I am of the opinion that these correlations are convincing evidence that undulatory oscillations in geosynclines are most closely associated with the differentiation of the abyssal material. One may suppose that the differentiation of substances within the depths of the earth is the main source of tectonic energy. Geosynclines are the areas where this process is most active. The mechanics of the differentiation process are still not quite clear but it is evident that the process results in the accumulation of basic material under some zones of the geosynclines and these zones sink; there is an accumulation of acid material under other zones, and in these areas an uplift takes place.

Another general principle to be seen is that alongside zones of intense uplift within a geosyncline, we find zones of subsidence that are equally intense. Conversely, alongside zones of weak uplift, there are corresponding zones of relatively weak subsidence. Thus there is a tendency toward mutual compensation of elevation and subsidence, i. e. a tendency toward a conservation of volume which is in accordance with the assumption that there is a connection between oscillations in geosynclines and differentiation of the abyssal material.

In the course of time, every geosyncline that has ever existed from the Proterozoic to the Tertiary inclusively has been transformed into a platform. Such transformations have always coincided with the end of one or another geotectonic cycle. Platforms are accordingly classified on the basis of the period at which they were formed as epi-Proterozoic, epi-Caledonian and epi-Hercynian. What will become of the Alpine geosynclines is still not clear, due to the short time that has elapsed since the end of the Alpine geotectonic cycle, but it is very probable that many of them will give way to platforms.

The transition from a geosynclinal to a platform state indicates a moderation of the undulatory oscillations — a diminution in speed, amplitude and intensity. The young platform at first preserves « memories » of the preceding geosyncline and inherits the areas of elevation and subsidence characteristic of the former geosyncline at the final stage of its development, though much less pronounced. But in the course of time the arrangement of *syneclise* and *anteclise* changes : they become larger in area, rounder and less strongly pronounced. The structure of ancient platforms with pre-Cambrian basements is in this respect quite different from that of young platforms, e. g. the epi-Hercynian platforms.

I have advanced the suggestion that undulatory oscillations in geosynclines and platforms reflect the processes of differentiation of material taking place at different depths within the earth (5). The way I picture it, changes in composition and in conditions with depth bring it about that the process of material differentiation is « multi-storeyed » and proceeds with different speed at the various « floors » or levels. It is natural to assume that at the upper level, thanks to the lesser viscosity of the material and the more intense fluctuations of conditions, the differentiation develops the most energetically. This is manifested at the surface in intense movements of the earth's crust of geosynclinal style.

At the lower level, the considerably more moderate and slower differentiation causes the undulatory oscillations of platform style.

While differentiation takes place at both upper and lower levels, the more intense differentiation at the upper level masks what is going on below, and on the surface we are aware of geosynclinal conditions. Nevertheless, I have called attention to certain cases where it is possible to detect in geosynclines movements that are more general in character and embrace larger areas — movements that would seem to be visible through the intense and split up, genuinely geosynclinal movements.

The more rapid differentiation at the upper level should naturally run its course more quickly. It should become weaker as the distribution of material at this level according to density approaches a state of equilibrium, and should at last cease almost entirely. This marks the transition from the geosynclinal to the platform state : the effect of the differentiation at the upper level is removed and the slow and vast flows of substance arising from differentiation at the lower level begin to make themselves felt at the surface. The fact that young platforms are distinguished from older ones by a greater splitting up of movements shows that the damping of differentiation at the upper level does not take place at once but over a certain length of time, during which the platform retains, though in a greatly weakened form, certain elements of « geosynclinal style ».

I have also attempted to show that the assumption of a gradation of differentiation according to levels gives an approach for explaining the activization of platforms, a phenomenon that occurred in Central Asia at the end of the Tertiary.

The last question I should like to touch on here is that of the relationship between geosynclines, and continents and oceans. It is sometimes assumed that geosynclines are phenomena of the same order as continents and oceans, and represent moreover an intermediate stage in the evolution of the earth's crust from the oceanic to the continental state. Adherents of this view consider the earth's crust beneath the ocean to be primary in character. Then the geosynclinal stage of differentiation sets in, and as a result a granitic continental crust is formed.

It seems to me that this point of view is fundamentally erroneous. Continents and oceans as structural elements are much more general in character than geosynclines and platforms. Geosynclines and platforms are traced not only on the continents but in many cases on the ocean bottom as well. The ocean shoreline often cuts off continental structures, both geosynclines and platforms, and under circumstances that leave no room for doubt that they continue on the ocean bed, or continued there earlier. There is much convincing evidence that many areas of the ocean have formed on the site of former continents. In such instances the earth's crust not only subsided but became more basic in composition (1). This process, which is the opposite of granitization, undoubtedly exists and is manifested over vast territories, although its nature is still not fully understandable. Geosynclines situated today along the edge of the ocean bottom, as in Indonesia and other island-arcs in the western part of the Pacific, represent zones which have subsided in the recent past. They have been flooded by the ocean, which has bitten off a large territory from the Asian continent, and by no means represent zones where the ocean is beginning to be transformed into a continent. All the geological evidence categorically disproves this assumption.

I have set forth some conclusions on the structure and development of geosynclines drawn from the geological data. I have purposely not touched upon geophysical data and considerations. Today many geophysicists are interesting themselves in the causes of tectonic movements, and in the tectonic development of the earth as a whole. Among other things they are manifesting an interest in the origin and development of geosynclines. This is extremely gratifying since a theory for the processes taking place within the depths of the earth can be built only on a geophysical foundation. At the same time it would be dangerous to ignore geological facts. They must be taken into account in such a theory, which consequently should not be merely geophysical but rather geological-geophysical.

References.

1. Beloussov (V. V.). On the geological structure and development of oceanic basins. Izvestia USSR, Acad. of Sciences, Geol. Ser., 1955, N° 3 (Russian).
2. Beloussov (V. V.). Fundamental questions of geotectonics. 606 p., Moscow, 1954 (Russian).
3. Beloussov (V. V.). Fundamental principles of the geotectonic process. Izvestia USSR, Acad. of Sciences, Geol. Ser., 1948, N° 5 (Russian).
4. Beloussov (V. V.). Problems of general tectonics. Soviet Geology, collected papers 41, 1954 (Russian).
5. Beloussov (V. V.). Problems of the internal structure and development of the earth. Izvestia USSR, Acad. of Sciences, Geoph. Ser., 1951, N°s 1 and 2 (Russian).

6. AMPFERER (O.). Uber das Bewegungsbildung von Faltengebirgen. J. d. k. k. Geol. Reichsanstalt. Wien, Bd. 56, 1906.
7. BELOUSSOV (V. V.). Grundfragen der allemeinen Geotektonik. Geol. Rundschau, Bd. 45, H. 2, 1956.
8. BEMMELEN (R. W. V.). Tectogénèse par gravité. Bull. Soc. de Géologie, t. LXIV, fasc. 1, 1955.
9. BEMMELEN (R. W. V.). The undation theory... Rep. XVI Sess. Int. Geol. Congr., USA, 1933, vol. II, 1936.
10. STILLE (H.) Grundfragen der vergleichenden Tektonik, 1924.

METHOD OF MODELLING IN TECTONOPHYSICS

by M. V. GZOVSKY

We consider that tectonophysics is a science on the mechanism of the development of tectonical deformations and faults in the Earth's crust. The object of investigation is tectonical (geological). The problems and the methods of its solution are tectonical (field observations) as physical (laboratory experiments, modelling, theoretical analysis). The study of tectonic faults is necessary for the elucidation of the regularities of the development of the earth's crust and is of great practical importance as it may help to find places favourable for mineralization and to judge the influence of faults on the quality of cal and oil deposits traversed by them as well as in solving the problems of hydrogeology and engineering geology. It is also necessary for the development of methods of earthquake forecasts which is considered one of the importants tasks of Soviet science. Leading role in the study of tectonic deformations and faults is played by field geological observations. Laboratory tests are very important.

The method of modelling of tectonical deformations and faults developing in the Earth's crust must be an essential addition to the field tectonical investigations. Despite the fact that the modelling method has been used in the course of the whole history of geology, its main statements require some more work.

The results of testing models can be applied in considering natural geological phenomena only in the case if the models meet the similarity conditions. According to the theory of physical modelling developed in the USSR by the Kirpichevs, father and son, A. A. Gukhman and L. S. Eigenson and to avoid mistakes and unnecessary complications one derive similarity conditions from differential equations which describe the fields of physical variable values characteristic of the process under study.

To describe tectonic deformations one can use the wellknown system of equations of equilibrium and motion suggested by Cauchy and Maxwell's equation :

Velocity of growth of general deformation | Velocity of growth of elastic deformation | Velocity of growth of plastic deformation

$$\frac{d\gamma_i}{dt} = \frac{1}{2G} \cdot \frac{d\tau_i}{dt} \cdot + \frac{1}{2\eta_{III}} \cdot \tau_i \qquad (1)$$

where : t is time;

$$\gamma_i = \sqrt{\frac{1}{6}\left[(\varepsilon_1 - \varepsilon_2)^2 + (\varepsilon_2 - \varepsilon_3)^2 + (\varepsilon_3 - \varepsilon_1)^2\right]}$$

is expressed by three main relative elongations ε_1, ε_2 and ε_3 characterised the form changes of each elementary volume;

$$\tau_i = \sqrt{\frac{2}{3}(\tau_1^2 + \tau_2^2 + \tau_3^2)}$$

is the general characteristic of three main tangential stresses together; G — equilibrium modulus of full elastic shear deformation; η_{III} — is coefficient of effective viscousity attached to plastic deformation.

The elastic afterworking is selected from the conventionally momentary elastic deformation in the well-known equation :

$$\gamma_i = \frac{\tau_i}{2G_I} + \frac{\tau_i}{2\,G_{II}}\left(1 - 2{,}7^{-t\frac{G_{II}}{\eta_{II}}}\right) + \frac{\tau_i}{2\eta_{III}}\cdot t \tag{2}$$

where : G_I — modulus of the conventionally momentary elastic shear deformation; G_{II} — modulus of the elastic afterworking shear deformation; η_{II} — viscousity of elastic afterworking.

A number of scientists determined important changes of G_I, G_{II}, η_{II}, η_{III}, for various materials depending on all-round pressure (confining pressure) σ_m temperature T and the intensity of tangential stresses τ_i [1, 2, 6, 17, 20, 21, 25, 26, 28, 53]. The principal dependences are expressed in equations :

$$\eta_{III} = \eta_0\, 2{,}7^{\frac{u - a\,\sigma_m}{kT}} \tag{3}$$

$$\eta_{III} = \eta_{III\,min} + (\eta_{III\,max} - \eta_{III\,min})\frac{\frac{\tau_i}{P_\eta}}{sh\,\frac{\tau_i}{P_\eta}} \tag{4}$$

where : η_0, $\eta_{III\,min}$, $\eta_{III\,max}$ u, a, P_η — are constants; K — Boltsman's constant. According the results of tests with rocks the rock viscousity is a function of σ_m and τ_i like (3) and (4).

In rocks as well as in metals and many other materials there are two kinds of breaking : expansion and shearing. Expansion result from the action of tension normal stresses and shearing — from tangential stresses. Accordingly each material has two resistances to breaking, i. e. two strengths. The breaking either by expansion or by shearing depends upon the ratio between the material strengths, and normal and tangential stresses acting in the material [3, 12, 15, 27, 28].

The data obtained from any tests together with the molecular theory of strength [3, 12, 15, 17, 28, 41, 54] make it posible to consider that in time range from 0,0001 sec. till tens of millions of years the value of fracturing stresses P_{∂} is a linear function of duration ∂ logarithm of their action. This dependence can be given in the form of various versions of the same equation :

$$P_{\partial} = P_1 - \zeta \ln \frac{\partial}{\partial_1} \tag{5}$$

$$\partial = \frac{\delta}{2{,}7^{P\delta/\zeta}}$$

where : P_1, ζ, δ are constants characterizing the properties of the material; P_1 denotes the strength at stress duration of about 1 sec.

Rock strengths received in laboratories are close to conventionally momentary ones but still somewhat below them as stress intensification often took a little more time.

Rock strengths at definite duration of stress action are not constants. They are reduced with a rise of temperature and they increase when all-round pressure grows [12, 17, 28, 45, 50, 57]. It is expressed for the conventionally momentary shear strength $P_{1\tau}$ in the equation of O. Mohr's hypotesis :

$$P_{1\tau} = P_{0\tau} - q\,\sigma$$

where : q is the coefficient whose value in the small interval of the values of normal stresses σ can be considered constant. This coefficient also determines the shearing angle α :

$$tg\, 2\alpha = \frac{1}{q} \tag{7}$$

$P_{0\tau}$ — is conventionally momentary shear strength at $\sigma = 0$.

The values of many coefficients and moduli from (1)-(7) for the rocks have been known already approximately (Table 1). Their sistematic determination for all rocks is important problem of further laboratory research. They may be determinated with the help of he curves of durable strain of the rocks at action of the constant stresses (Fig. 1).

The follow general conditions of similarity are mathematically derived from (1) — (7) :

$$C_G = C_{\rho}\, C_g\, C_l \tag{8}$$

$$C_{\tau_r} = C_{\tau}\, C_t \tag{9}$$

TABLE 1. — *Mechanical properties of rocks and equivalent materials.*

Property characteristics C. G. S.	Rocks	Equivalent materials					
		C_l from 10^{-4} till 10^{-5}; C_t from 10^{-11} till 10^{-13}				$C_l = 10^{-5}$; $C_t = 10^{0}$	
		Theoretical necessary values	Clays moisture 40-50 %	Petro-latum	30 % ethyl cellulose solutions	Theoretical necessary values	25 % gelatin gels
G_I and E_I	10^{11}-10^{12}	10^6-10^8 usually 10^6	10^5-10^6	10^6	10^5	10^6-10^7	10^5-10^6
G_{II} and E_{II}	10^{11}-10^{12}	10^6-10^8 usually 10^6	10^5-10^6	10^6	10^4-10^5	10^6-10^7	10^5-10^6
θ_{II}	10^3-10^4	10^{-10}-10^{-7}	10^1-10^2	10^0-10^1	10^0-10^1	10^3-10^4	10^3-10^4
η_{III}	10^{18}-10^{23}	10^0-10^8 usually 10^4-10^6	10^4-10^6	10^3-10^4 at 20°C	10^5-10^6 at 20°C	10^{13}-10^{18}	approxim. 10^{10} ?
$P_{o\tau}$	10^8-10^9	10^3-10^5 usually 10^3	10^2-10^3	10^5		10^3-10^4	approxim. 10^7-10^8 ?
$P_{1\sigma}$	10^7-10^8	10^2-10^4 usually 10^2-10^3	10^2-10^3			10^2-10^3	10^6-10^7
q	0-2	0-2	0-0,6			0-2	

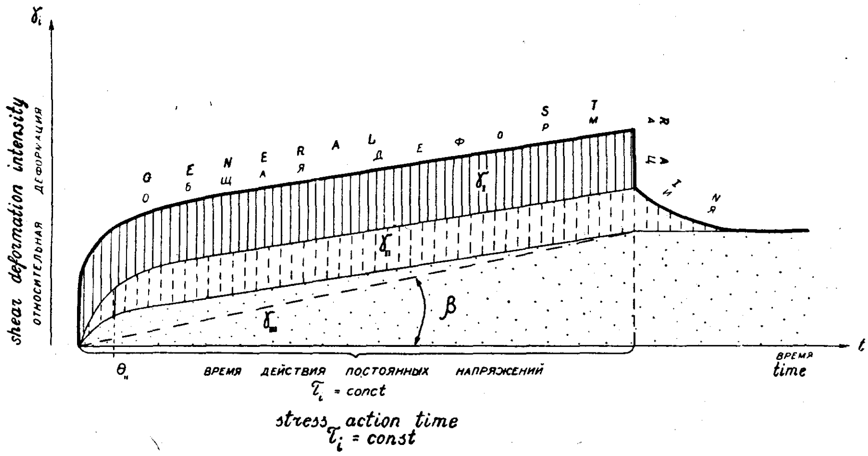

$G_I = \dfrac{\tau_i}{2\gamma_I}$	$G_{II} = \dfrac{\tau_i}{2\gamma_{II}}$	$\eta_{II} = G_{II}\,\theta_{II}$	$\eta_{III} = \dfrac{\tau_i}{2\,tg\beta}$

FIG. 1.The interpretation scheme of the rocks deformation curves, at constant stress intensity τ_i; γ_I — conventionally momentary elastic shear deformation. γ_{II} — elastic afterworking; γ_{III} plastic deformation; θ_{II} — time, when 0,63 γ_{II} is reached; t — time.

Besides it is required that

$$C_G = C_\tau = C_E = C_\sigma = C_P \qquad (10)$$

The similarity of boundary and initial conditions should be also observed [11, 16,30].

Here the corresponding factors of similarity are : for equilibrium moduli of full elasticity at shear and elongation :

$$C_G = \frac{G \text{ of model}}{G \text{ of object}} \quad \text{and } C_E = \frac{E \text{ of model}}{E \text{ of object}} ;$$

for tangential and normal stresses : $C_\tau = \dfrac{\tau \text{ of model}}{\tau \text{ of object}}$ and

$C_\sigma = \dfrac{\sigma \text{ of model}}{\sigma \text{ of object}}$; for viscosity : $C_\eta = \dfrac{\eta \text{ of model}}{\eta \text{ of object}}$;

for strength : $C_P = \dfrac{P \text{ of model}}{P \text{ of obj ct}}$; for time : $C_t = \dfrac{t \text{ of model}}{t \text{ of object}}$;

for gravity acceleration : $C_g = \dfrac{g \text{ of model}}{g \text{ of object}}$;

for distances : $C_l = \dfrac{l \text{ of model}}{l \text{ of object}}$; for density : $C_\rho = \dfrac{\rho \text{ of model}}{\rho \text{ of object}}$

While modelling faults it is necessary to establish similarity between the stress fields and the values characterizing the strength properties of the material. The similarity of the stress fields is provided by conditions (8), (9), and (10). The derivation of the similarity conditions of the destruction process from equations (5) shows that factors of similarity C_{P_1} and C_ζ of strength characteristics with the stress dimension about ζ from (5) and strength values $P_{1\tau}$ and $P_{1\sigma}$ should equal to :

$$C_{P_1} = C_\zeta = C_P = C_G = C_E = C_\tau = C_\sigma \tag{11}$$

Other characteristics δ from (5) having time dimension should submit to the factor C_δ of similarity which is equal to :

$$C_\delta = C_t \tag{12}$$

As the mechanical properties of rocks have been studied very insufficiently, it is not possible now to calculate the properties of the model accurately enough. The results of approximate calculations [11, 19, 29, 39, 45, 46, 51, 52] are summarized in table 1.

The properties of the equivalent materials for model preparation should coincide with those which are calculated according to the conditions of similarity. The instruments necessary for the investigation of the properties of equivalent materials are being developed in the USSR. Figure 2 shows the curves received on this instruments indicating G_I G_{II} η_{II} η_{III} P_1 of some equivalent materials. This curves are similar to the curves of rocks.

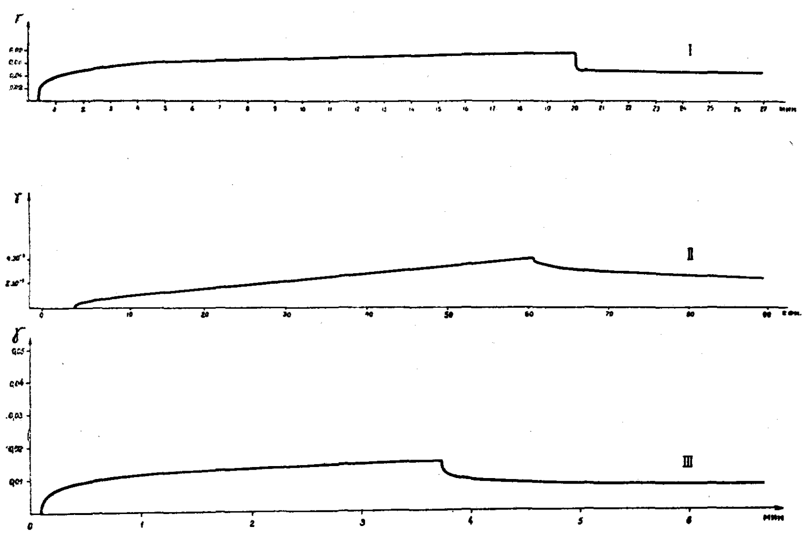

FIG. 2. Deformation curves of the equivalent materials. I — clay (moisture 43 %); II — bakinish petrolatum; III — 30 % ethyl cellulose solution. Automatically recorded on instruments designed by V. P. Pavlov (I and III) and N. V. Mikhailov (II).

The values of the main mechanical property characteristics of moist clays, petrolatum and some other materials coincide in general with those properties which the models should have according to the conditions of similarity (8), (9), (10) and (11) if the factor of the geometric similarity $C_l = 10^{-5}$ (i.e. 1 : 100.000) and the factor of the time similarity $C_t = 2.10^{-12}$ where one minute of the experiment corresponds approximately to 10^6 years in the natural process.

To solve many tectonophysical problems a serious importance should be attached not only to deformations and fractures but also to the stress state of models which had not been investigated until that time [9 ,10, 12, 13, 24, 43, 58]. The study of the stress state of models of geological objects has been begun by us with an optical method [9, 11]. Its application in tectonophysics was made more complicated by the fact that only elastic optically active materials for making models were known while the necessary plastic materials were absent. At present we have at our disposal plastic optically active materials and special instruments for determining their mechanical and optical properties [14, 23].

From 1952 we applied the method of testing models made of gelatin gels. This allowed quality models of momentary stress fields to be made, i.e. those appearing at a certain moment of time. The models for this were prepared according to the only satisfied condition of similarity (8). The deformation of such a model reproduces only the elastic part of the general deformation where as its plastic part is rendered by the initial form of the model. The model under stress is affected by polarized light on an instrument similar to a petrographical microscope (*Fig.* 3). The relative value of the maximum tangential stresses in the model is determined either by means of an optical compensator or directly by the interference colouring of the screen image of the model. While studying laminated models and solving some problems connected with earthquake forecasts it is necessary to know the absolute value of the stresses in every isochromatic bend. In this case the material undergoes special preliminary testing.

D. N. Osokina [22] who worked under the direction of the author has proved that in gelatin gels the phase difference (relative retardation in the passing light) R is connected with the whole of the elastic part of the general deformation and not with the stress which is the generally accepted opinion. As the second part of the elastic deformation (afterworking) keeps on increasing for more

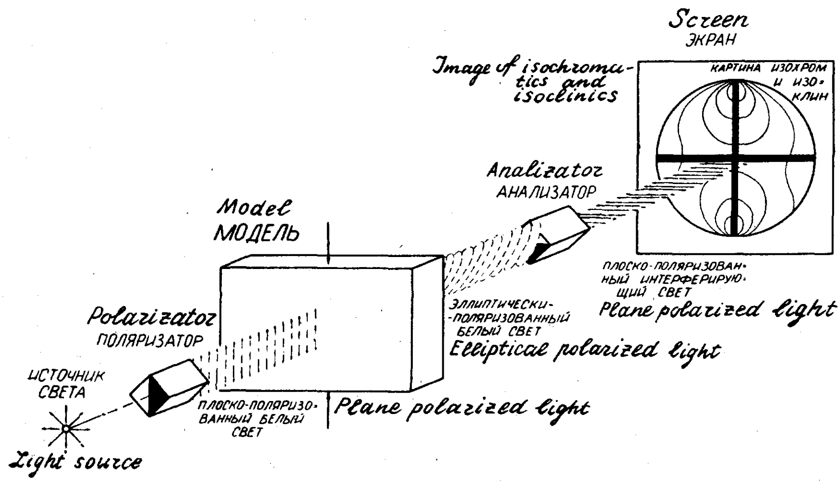

FIG. 3. Scheme of an optical polarization installation for studying stresses in transparent models.

than forty hours the phase difference in the model is continually growing with the flow of time in spite of the constanstancy of stresses.

The value of the maximum tangential stresses τ_{max} in any point of the model is determined by the following equation :

$$\tau_{max} = \frac{R_t}{B_t\, d} \cdot 10^{-7}\ g/cm^2 \qquad (13)$$

where : R_t is the phase difference at a given moment of time; B_t is the optical ratio of the stresses which characterizes the material of the model and is the function of the duration t of the experiment; d is the thickness of the model in cm [22].

When applying formula (8) moduli G and E of a gelatin gel have to be replaced by G_t or E_t because of the duration of the development of the second part of elastic deformation. They are considered time functions. Thus the method we use for the study of models made of gelatin gels differs from the methods applied in engineering. G, E, B, R in engineering are considered constants.

The orientation of the stress axes is fixed in any point of the model owing to the fact that the light ceases to pass through them as soon as the polarization planes of the crossed nicols are parallel to the stress axes. The lines which are locuses of the points with the same orientation of the stress axes are called isoclinics and form black lines on the screen (*Fig.* 3).

Working with gelatin gels one must always keep in mind that their strengths are too high. Therefore the general elastic deformation may go up to tens of per cent (whereas in rocks it never exceeds one per cent).

The development of an optical method of studing stresses in models undergoing considerable plastic deformation was an important improvement. It satisfied two conditions of similarity (8) and (9). The mutual work of physical chemist G. V. Vinogradov, physicists V. P. Pavlov and D. N. Osokina and the author (geologist) showed that one of suitable and optically active materials for tectonic modelling are concentrated solutions of ethyl cellulose in benzil alcohol [23]. The value of the phase difference R observed in them is directly proportional to the general value of the elastic part of the deformation. If the stresses are constant it appears to be directly proportional to the maximum tangential stresses after a short time (several seconds). Therefore

$$\tau_{max} = \frac{R}{Bd} \cdot 10^{-7}\ g/cm^2 \qquad (14)$$

The optical ratio of the stresses B is very high and reach 6.10^{-6} cm^2/g. The phase difference does not depend on the value of plastic deformation and can be correlated only with the velocity of the plastic deformation which is determined by the value of the stresses as well as the elastic part of the deformation.

The difference of the mechanical and the optical properties of ethyl cellulose solutions from those of gelatin gels is shown on Figure 4. The mechanical properties of ethyl cellulose solutions in

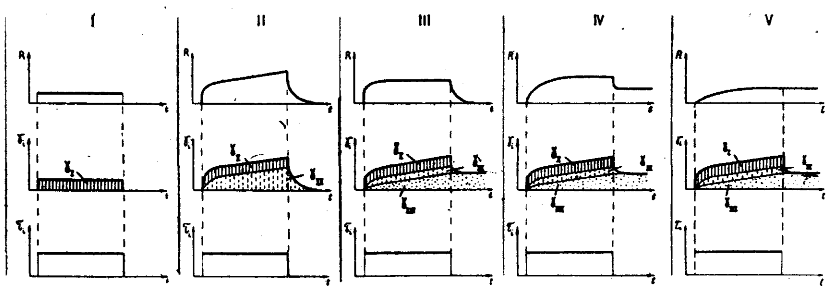

FIG. 4. The comparison of the phase differences (relative retardation) R, shear intensity γ_i and tangential stress intensity τ_i; t — time; I — bakelites; II — gelatin gels; III — ethyl cellulose solutions; IV — transparent soap; V — plastical greases (IV and V after G. V. Vinogradov — 5). R is connected with : only the elastic part ($\gamma_I + \gamma_{II}$) of the general deformation in I, II and III; both elastic ($\gamma_I + \gamma_{II}$) and plastic (γ_{III} parts of the general deformation in IV; only the plastic (γ_{III}) part of the general deformation in V.

benzil alcohol are more similar to those of rocks; the phase difference is correlated very well just with the value of the stresses.

The most important task of future work is to create an optically active plastic material which would furnish the condition of similarity for strength.

The method of modelling was used in tectonophysics successfully many times [4, 18, 32, 34-39, 47-49, 51, 55, 56, 59]. The main importance of this method is ability to determine by the experiment the physical conditions of the development of strains and ruptures investigated. Besides it is able to fix important additional facts which cannot be noticed during the field geological observations. There are three examples :

1. The ascertainment of the physical conditions of the development of folds of longitudinal bending and longitudinal thickening. There are two types of fold's arising in the Earth's crust under the pressure of longitudinal active force. The first type folds are the folds of longitudinal bending. In this folds the thickness of beds is invariable, and the process of deformation is the totality of longitudinal pressure and plastic bending. The second type is presented by the longitudinal thickening folds, in which the thickness of beds alters very much, and the process may be regarded as a local thickening with a small bending at the same beds (Fig. 5). The

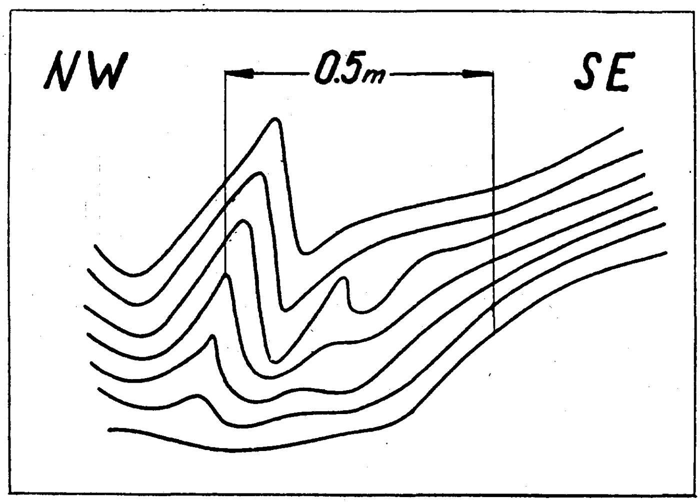

FIG. 5. Longitudinal bending (to the left) and longitudinal thickening (to the right) folds in palaeozoic limestones (vertical outcrop, Karatau range).

folds of those two types accompanied by the definite complex of faults. That is why the knowledge of the conditions of arising of the definite folds is much important. The theoretical investigation of one layers deformation gives us the following hypothesis. The folds of longitudinal bending at the definite duration ∂ of action of the active longitudinal pressure force $\mathfrak{L}$ arises only when the size and duration of active forces are in the definite correlations with the mechanical properties of the bed and three conditions are satisfied.

The first of them — the longitudinal force $\mathfrak{L}$ must be more than $\mathfrak{L}_K$ depended on : bed's viscousity η_{III}; tangential stress on the bed's surface f, duration of the experiment ∂; extent of the bed on the strike d; thickness of the bed m :

$$\mathfrak{L} > \mathfrak{L}_K . \quad \mathfrak{L}_K = K_I \frac{f^{2/3} \eta_{III}{}^{1/3} md}{\partial^{1/3}} \tag{15}$$

When instead of the force $\mathfrak{L}$ we examine the longitudinal stress p excited by it, the condition of the arising of the longitudinal bending folds will be

$$p > p_K ; \quad p_K = K_I \frac{f^{2/3} \eta_{III}{}^{1/3}}{\partial^{1/3}} \tag{16}$$

Where : K_I — is constant numeral coefficient, with empirically determined value.

The second condition — longitudinal pressing stress p is to be less than doubled longtime strength of the bed for shearing $P_{\partial\tau}$ conforming to the duration of the stress action ∂ :

$$p < 2P_{\partial\tau} \tag{17}$$

The third condition — the normal stress of the bed's surfaces s is to be less some value proportional to the tangential stress f on the surface of the bed. This is an empiric coefficient K_{III}

$$s < K_{III} f \tag{18}$$

The first problem of the modelling is to control pointed origin conditions of the folds of longitudinal bending in the separate homogeneous layer.

In simple case, when in the same time one homogeneous layer with the viscousity η_{III} is deformed, the least value of the p_K which is needed for the origin of the fold of longitudinal bending depends only on the tangential stress f on the foot of the bed. Accordingly to (16)

$$p_K = K' . f^{2/3} \tag{19}$$

where K' is constant coefficient. The stress f depends on the bed's weight and on the coefficient of friction Kf between the bed and it's bottom. The thickness m of the bed influences on the origin of the bending by the weight of the bed, which defines the value of the stress f. Conditions II and III are the same.

I. M. Kuznetsova and author have made many experiments in order to control the ability (19) to get the folds of longitudinal bending or longitudinal thickening because of changing only two factors — longitudinal normal stress p and tangential stress f. Our calculations of the properties of models were based on the conditions of similarity (8), (9) and (10); where $C_l = 10^{-4} = 1 : 10000$; $C_t = 10^{-12}$; $Cg = 1$; $C_\rho = 1/2$; $C_\gamma = 10^{-16}$; $Cp = 10^{-4}$.

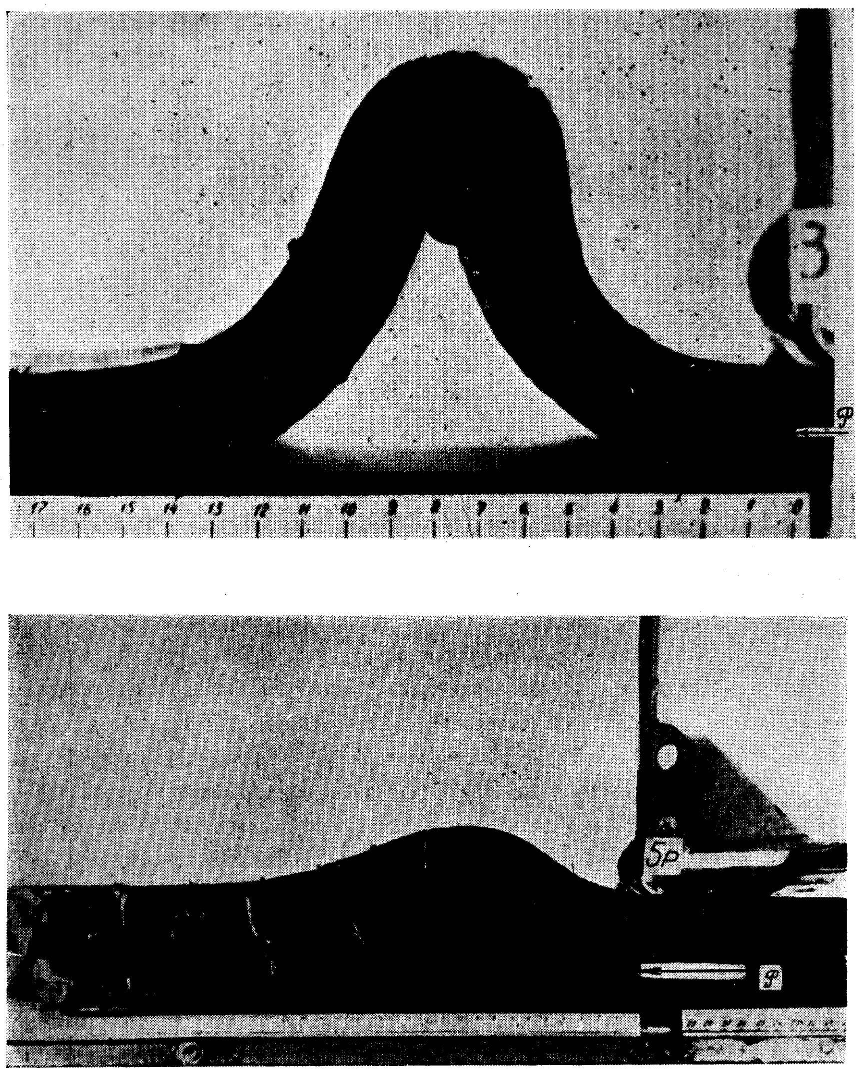

FIG. 6. Longitudinal bending (at the top) and longitudinal thickening (below) folds in homogeneous models. $\mathfrak{P}$ — longitudinal active force. Linear scale in cm

The satisfaction of the conditions of the similarity for the moduli of elasticity is not obligatory because these moduli don't enclose in (15-19). There were taken for the rocks η_{III} approximately 10^{19}-10^{20} puas; $P_{1\tau}$ — 10^9 dyna/cm². Accordingly the models were to have η_{III} approximately 10^4-10^3 and $P_{1\tau}$ about 10^5. One sort of petrolatum (bakinish) has such properties.

Many experiments confirm that there may be in homogeneous bed as the fold of longitudinal thickening and so longitudinal bending depending on value *f* or *p* (Fig. 6).

The main result of the experiments consist in this fact that the position of the dots in the diagrams (Fig. 7) correspond to the equation (19).

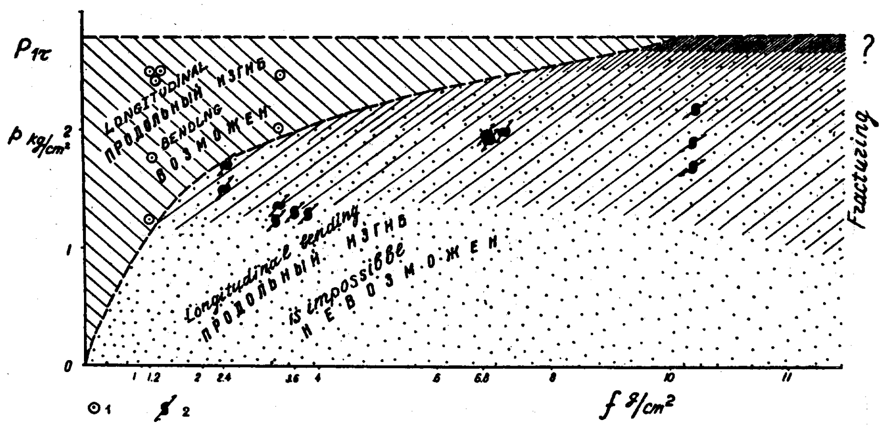

FIG. 7. Scheme of the physical conditions of different folds origin in homogeneous layer (after M. V. Gzovsky and I. M. Kuznetsova). $P_{1\tau}$ — conventionally momentary shear strength; $\mathfrak{L}$ — longitudinal active force; *f* — tangential reactive stress at the surfaces of the layer; 1 — longitudinal bending folds were recorded; 2 — longitudinal thickening folds complicated by shear faults were recorded.

It is important to determine the fisical conditions of the origin of the folds of longitudinal bending and longitudinal thickening not only in one bed, but in stratified bodies. To determine it theoretically is very difficult. The second problem which is solved by the modelling method consists in the determination of ability to spread the conditions of deformation of one bed over stratified models. The most important special features of the stratified models are the thickness *m* of separate beds and coefficient of friction K_f. It is clear from (15) that the different folds are arising in one bed depending on the correlation between its thickness *m* and coefficient of friction K_f on its bottom and upper surface. The condition of the longitudinal bending is.

$$m < \frac{K''}{K_f^{2/3}} \tag{20}$$

where K″ is a coefficient depending on the viscousity of the material, experiment's duration and the value of the force $\mathfrak{L}$. In order to control the application (20) for the stratified models I. M. Kuznetsova and author had tested models with many layers.

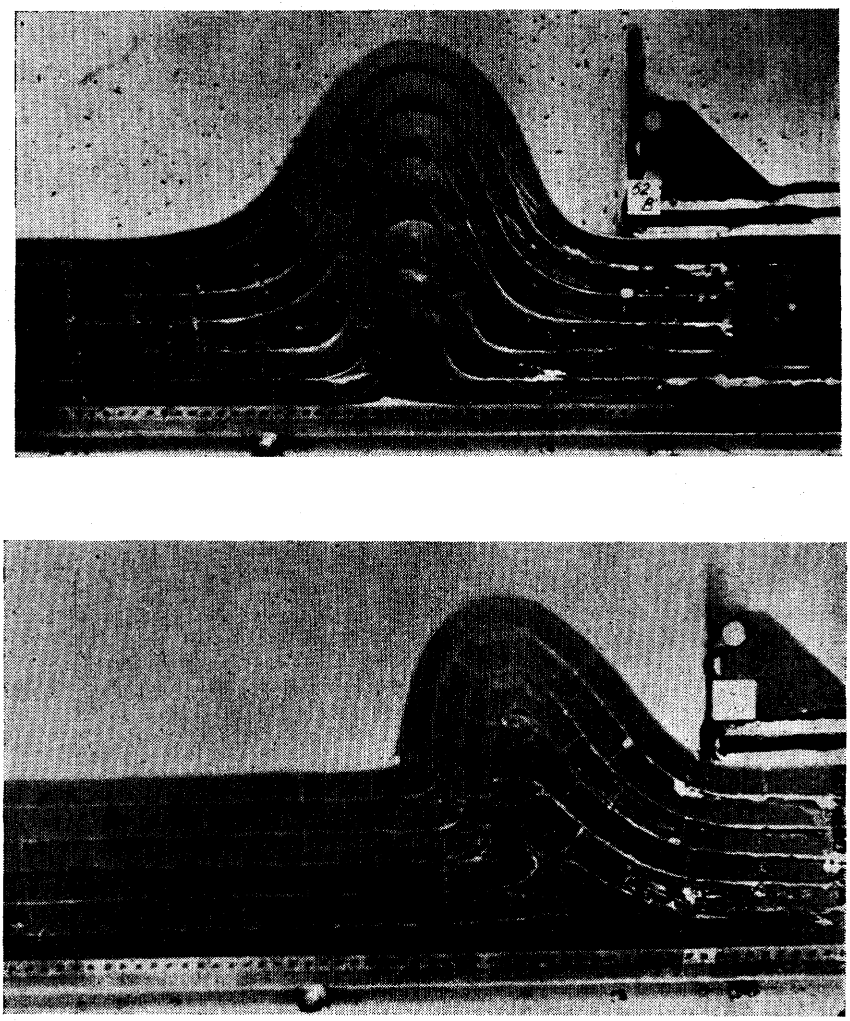

FIG. 8. Longitudinal bending (at the top) and longitudinal thickening (below) folds in stratified models. $\mathfrak{L}$ — longitudinal active force. Linear scale in cm.

Model ratio were the same as for the model with one layer. There was used petrolatum. The friction ration K_f between the beds depended on the properties of the lubricant which covered separate beds.

It was established with the help of experiments that the change of thickness *m* and coefficient of friction between beds K_f was the cause of origin of the folds of two pointed types. All other factors (summary thickness of model, longitudinal force $\mathfrak{L}$ and etc) are constant (*Fig.* 8).

It is also important that the dots in the diagrams for the stratified models (*Fig.* 9) correspond to the equation (20). The different folds

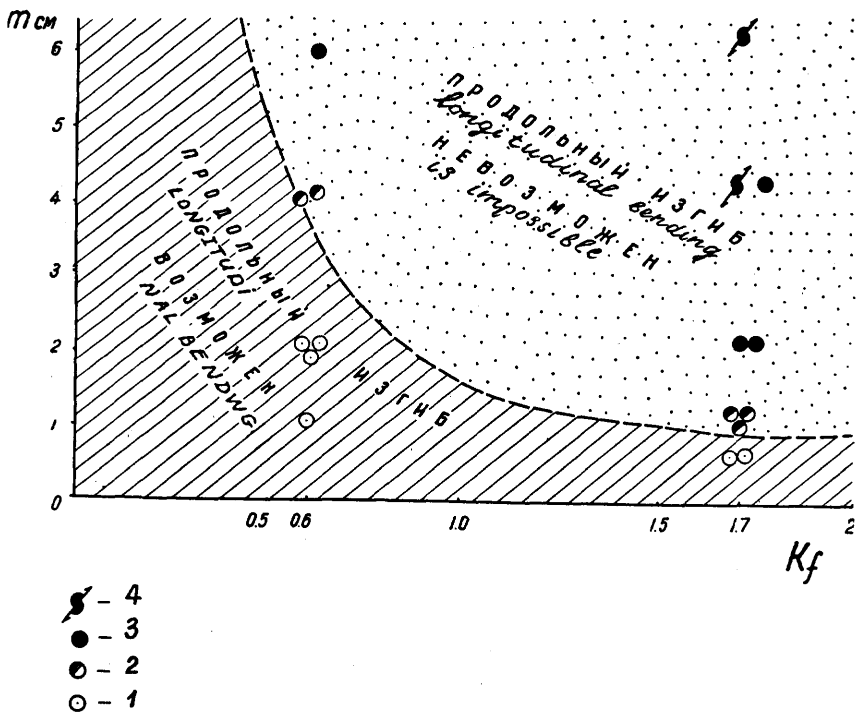

FIG. 9. — Scheme of the physical conditions of different folds origin in stratified models (after M. V. Gzovsky and I. M. Kuznetsova). m — original thickness of separate beds; K_f — coefficient of friction, 1 — longitudinal bending folds were recorded; 2 — complex deformation folds were recorded; 3 — longitudinal thickening folds were recorded; 4 — longitudinal thickening folds complicated by shear faults were recorded.

were resulted accordingly to (15) in models with many layers depended on the material's viscousity η_{III} also.

Thus it was made clear by the method of modelling that the equation (15) may be used for the investigation of the physical conditions of arising folds of the longitudinal bending and longitudinal thickening in the stratified formations.

2. *The development of notions about distribution of tectonic faults in space and time.* Model test under controlled conditions makes it possible to ascertain the way how tectonical faults are distributed in space and what their succession in time is if a certain deformation of the Earth's crust takes place. Many brachy-anticlinal folds had studied by us in one ore region. The brachy-anticlinal folds cut in their domes by longitudinal normal faults and in the limbs by longitudinal reverse faults getting less steep in the upper parts. For solving the question of the possibility of simultaneous development of both these types of faults and for clarifying the origin of the folds the stress field was reconstructed [10]. The same field can be observed in plastical models of uplifts caused by the action of vertical forces (*Fig.* 10). That is why we connect the formation of the given natural anticlines with the action of vertical forces.

In all cases the stress fields in transparent models showed that normal faults and reverse faults should originate generally simultaneously but they should develop in opposite directions : normal faults should grow from the earth's surface downwards and reverse faults upwards. Just this development of faults can be observed in plastic models made of moist clay [11]. The practical importance of such a conclusion is evident. It is important for directing search and prospecting work of both hydrothermal ore deposits and oil deposits. It also plays some role in connection with the determination of seismic regions. The small normal faults outcropping in the dome and disappearing in the depth caused by the action of slight stresses should by seismically less dangerous than larger reverse faults developing more deeply in the uplifts limbs [13]. It is very important that the latter most dangerous faults may be not observed on the surface.

The threedimensional models of brachy-anticlines made of moist clay clearly show that after the formation of the above mentioned longitudinal normal faults and reverse faults later transverse faults appear. This is caused by the fact that the existence of longitudinal disturbances changes the original stress field and excludes the possibility of considerable tension stresses across the axis of the uplift [10]. The field investigations and seismic data on the character of earthquake foci in Central Asia and the Caucasus show that the crosswise faults in uplifts occur often in natural conditions and

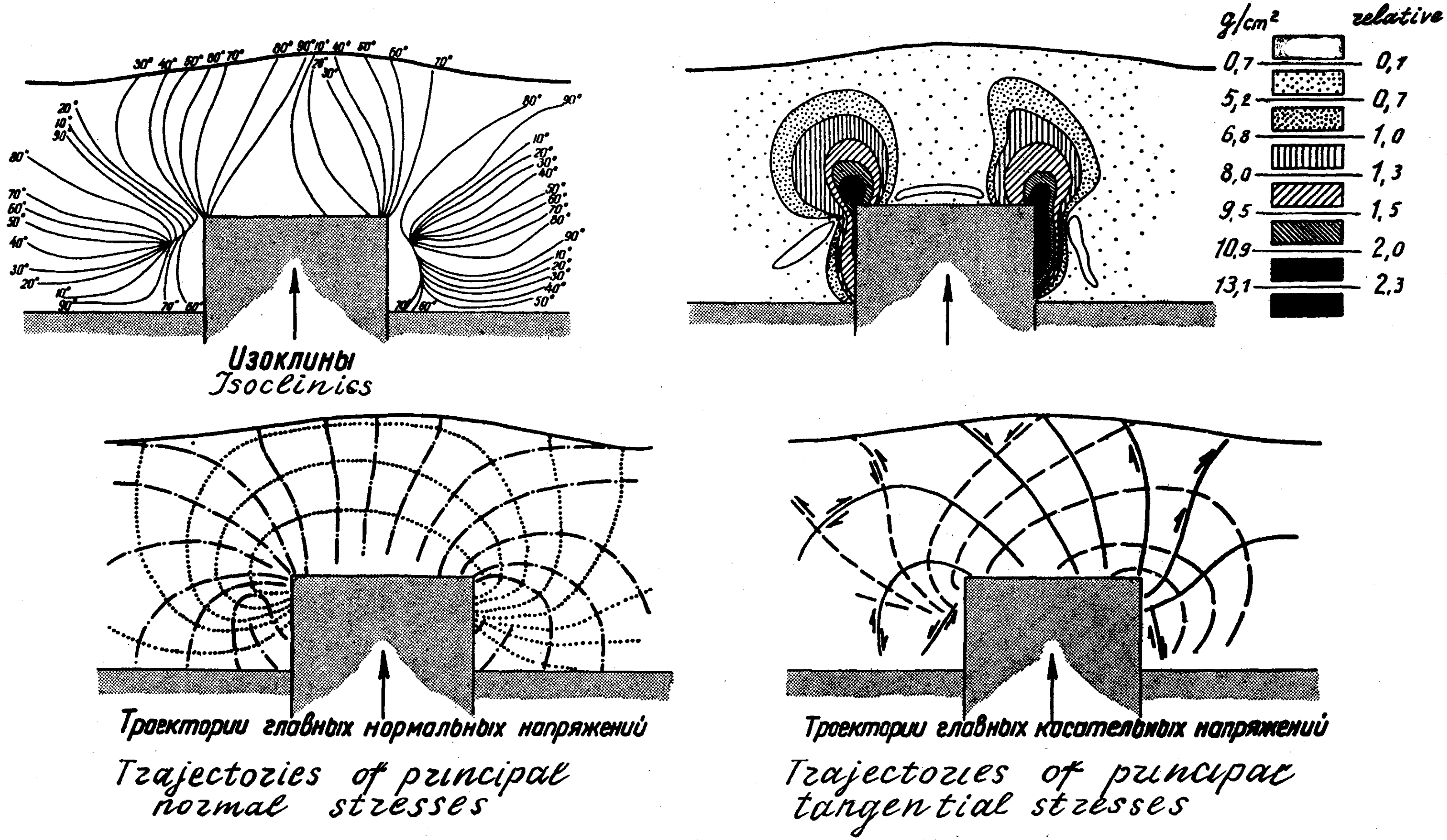

FIG. 10. — Distribution of stresses in an plastical model of transversal bending anticline (value of τ_{max} — to the right at the top). 30 % ethyl cellulose solution in benzil alcohol, C_l from 10^{-6} till 10^{-5}, $C_t = 10^{-13}$; C_c from 10^{-6} till 10^{-5}; C_{τ} from 10^{-19} till 10^{-18}; C_n is not observed. (After M. V. Gzovsky, I. M. Kuznetsova and D. N. Osokina).

appear generally after longitudinal ones. That is why it is probable that transverse faults in ore-deposit regions often prove to be post-mineralizing ones.

3. The development of hypothesis about earthquake foci. In 1955 we began to use models for the investigation of the seismogeological problems.

The connection of earthquakes with tectonic faults is now firmly established. According from the dependence of strength on time reflected on the first approximation by (5) one may consider that tectonic faults and earthquakes arise at different intensity of stresses τ_i acting in the earth's crust or under it. The magnitude of an earthquake in the epicentre depends on the depth of the hypocentre, the structure of the earth's crust in its neighbourhood and on the total kinetic energy of seismic waves U_S composing a certain portion from ΔU_I — the energy of focus. Developing further the ideas of H. Benioff [31] G. A. Gamburtsev [7, 8] and K. E. Bullen [33] one should regard ΔU_I to be equal to that decrease of potential energy U_I of the elastic conventionally momentary change of the form, which is caused by the appearance of a tectonic fault. The energy of the earthquake can be correlated with the length l of the tectonic fault along the strike and with the intensity of the stress τ_i :

$$U_s = \frac{\omega\, n\, \lambda}{2} \frac{\tau_i^2}{G_I} l^3 \tag{21}$$

Here : G_I — modulus of the conventionally momentary shear; ω, n and λ are coefficients showing respectively : ω — what portion of the general energy U_I breake loose during the formation of the fault; n — what part of the free energy ΔU_I transforms into U_S; λ — what the proportion is between the volume of the earthquake focus and l^3.

As it follows from (1) that value τ_i can be correlated with the velocity of a prolonged deformation of the earth's crust $\frac{d\gamma_i}{dt}$ and that, besides this, this velocity is approximately proportional to the gradient value of the velocity (V) of tectonic vertical movements of the earth surface: $\frac{d\gamma_i}{dt} \approx \Phi \mid \text{grad } V \mid$. It is possible to derive from (21) the following approximate equation :

$$U_s \approx \Psi \frac{\eta_{III}^2}{G_I} l^3 \mid \text{grad } V \mid^2 \quad (22) \qquad\qquad \Psi = 2\, \omega\, n\, \lambda\, \Phi^2 \quad (23)$$

Thus it is possible to connect the general energy of seismic waves U_S with : a) coefficient Ψ determined on the type of the tectonic fault and depending on : *a*) how the appearance of the fault changes the original stress field, what portion of ΔU_I is U_S and what the relation is between the volume of the earthquake focus and l^3; *b*) the viscousity coefficient η_{III} to the second power and the modulus of conventionally momentary shear G_I; *c*) the length *l* of the tectonic fault that appeared, in the third power; *d*) the value of velocity gradient | grad V | of the vertical tectonic movements of the earth's surface in the second power.

Admitting that equation (5) in the first approximation holds for both expansion faults and shearing faults it should be applied for solving the question of the time of the appearance of earthquakes. It can be transformed into :

$$\partial_s \approx \frac{\delta}{2{,}7\,\dfrac{2\,\Phi\,\eta_{III}}{\zeta}\cdot|\text{grad V}|} \tag{24}$$

where : ∂_s is the time period from the beginning of tectonic movements with constant value of velocity gradient | grad V | to the appearance of a fault and an earthquake.

Equations (22) and (24) generalize our notions of the geological criteria of seismicity and are their tectonophysical basis.

Proceeding from the above considerations the focus of the earthquake should be considered not the surface of the fault but the volume in which the conventionally momentary change of stresses takes place, caused by the appearance of a new fault or by renewing a previously existing tectonic fault.

We use plastical models to study by the optical method the ratio of value of velocity gradient on the upper surface in a deformed part of the Earth's crust to the magnitude of tangential stresses inside it, in the region of earthquake foci. The coefficient Φ to our plastical model of transversal bending folds were approximately from 2 till 3,5. (*Fig.* 10).

In the elastic gelatin models can be observed the short-time (quick) processes of stress field changes in the moment of fault appearance. In such models we study the influence of a type of tectonic deformation and fault magnitude on the shape and volume of an earthquake focus and on the value of energy emissing from it. The coefficient λ to uplifts, like one on the fig. 10 and 11, is approximately from 2 till 0.1 and coefficient ω — is from 0.01 till 0.3.

In models it is possible to see a change in the character of earthquake foci with time in the cause of the development of tectonic faults.

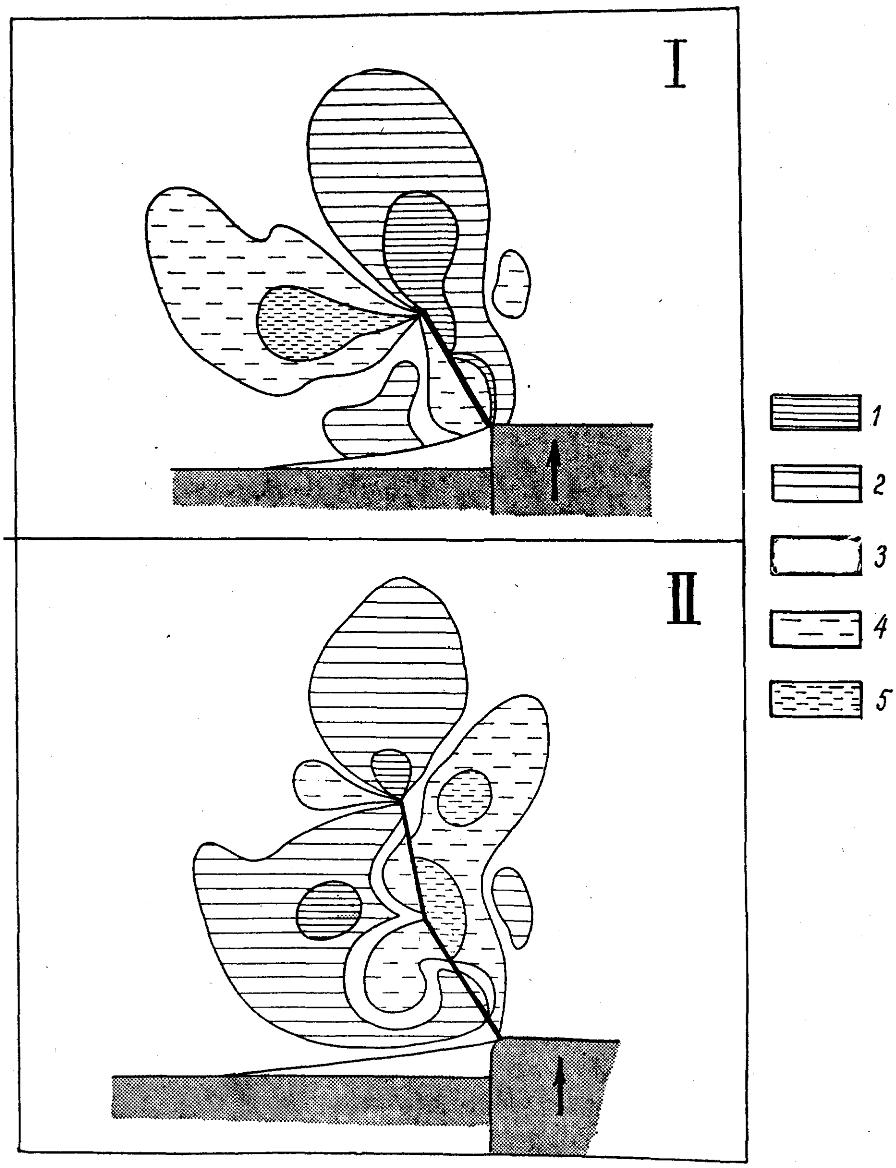

FIG. 11. — Models of earthquake foci connected with transversal bending anticlines (after M. V. Gzovsky and T. A. Tikhomirova). Gelatin gel, $C_I = 10^{-6}$; $C_{II} = 10^{-6}$. I — first stage of fault development; II — second stage of fault development. Stress $\tau_{max.}$ changes after fault origin : 1 — heavily increase (mean by 1,7), 2 — weakly increase (mean by 1,3), 3 — invariable stresses, 4 — weakly decrease (mean by 0,8), 5 — heavily decrease (mean by 0,6).

All these data cannot be obtained by the investigations of only natural objects. Therefore even approximated information on the models facilitates the development of geological criteria of seismicity.

There we shall enumerate the main thesis of this article :

a) It is possible with the help of theory of scale models and data about mechanical properties of the rocks to define the model's properties similar to the natural geological objects.

Thus *method of the modelling of tectonic deformations and faults in the Earth's crust is well grounded theoretically.*

b) There are instruments which may be used for the definition such mechanical properties of models which are present in the condition of similarity. Some materials with corresponding properties are known a long time. New materials with definite properties have been done. It mean that *the method of the modelling can be practicaly used.*

c) It was established new facts by the experiments which were difficult or impossible to investigate at the natural geological objects. First of all it concerns the details of structure of the Earth's crust till the big depth; investigation of the evolution of the deformations and faults during long time; the investigation of the stress in Earth's crust and physical conditions of arising of the deformations and faults of definite types. It means that *the modelling method may be used for the settling different geological and geophysical problems.*

Institute of the Physics of the Earth, Academy of Science USSR, Moskow.

REFERENCES.

1. АБДУРАГИМОВА Л.А., РЕБИНДЕР П.А, СЕРБ-СЕРБИНА Н.Н. Упруго-вязкостные свойства тиксотропных структур в водных суспензиях бентонитовых глин. Колл. журн., 17, № 3, 1955.
2. АЛЕКСАНДРОВ А. П. Морозостойкость высокополимерных соединений Тр. I и II конфер. высокомолекул. соединений Изд. АН СССР, 1945.
3. БАРТЕНЕВ Г.М. О временной и температурной зависимости прочности твердых тел. Изв. АН СССР, отд. техн. наук, № 9, 1955.
4. БЕЛОУСОВ В.В. Основные вопросы геотектоники. Госгеолтехиздат, 1954
5. ВИНОГРАДОВ Г.В. Строение, оптические и механические свойства псевдогелей мыл (смазок). Тр. Всесоюз. конфер. по колл. химии, стр. 249, изд. АН УССР, Киев, 1952.
6. ВОЛАРОВИЧ М.П. и БАЛАШОВ Д.Б. Исследования скоростей упругих волн в образных горных пород при давлении до 500 кг/см 2. Изв. АН СССР, сер. Геофиз., № 3, 1957.
7. ГАМБУРЦЕВ Г.А. Состояние и перкспективы работ в области прогноза землетрясений. Бюлл. совета по сейсмологии, № ,1 1955.

8. ГАМБУРЦЕВ Г.А. Краткое содержание доклада "О прогнозе землетрясений" в хронике Известий АН СССР, сер. геофиз. № 3, 1955.

9. ГЗОВСКИЙ М.В. О задачах и содержании тектонофизики. Изв. АН СССР, еер. геофиз. № 3, 1954.

10. ГЗОВСКИЙ М.В. Тектонические поля напряжений. Изв. АН СССР, сер. геофиз., № 5, 1954.

11. ГЗОВСКИЙ М.В. Моделирование тектонических полей напряжений и разрывов. Изв. АН СССР, сер. геофиз., № 6, 1954.

12. ГЗОВСКИЙ М.В. Соотношения между тектоническими разрывами и напряжениями в земной коре. Разведка и охрана недр, № 11' 1956.

13. ГЗОВСКИЙ М.В. Тектонофизическое обоснование геологических критериев сейсмичности. Изв. АН СССР, сер. геофиз., № 2 и 3, 1957.

14. ГЗОВСКИЙ М.В. Совещание по тектонофизике. Хроника. Изв. АН СССР, сер. геофиз., № 7, 1957.

15. ЖУРКОВ С.Н. и НАРЗУЛЛАЕВ Б.Н. Временная зависимость прочности твердых тед. ЖТФ, 23, № 10, 1953.

16. КИРПИЧЕВ М.В. Теория подобия. М., изд-во АН СССР, 1953.

17. КУЗНЕЦОВ Г.Н. Механические свойства горных пород. М., Углетехиздат, 1947.

18. ЛЕБЕДЕВА Н.Б. Моделирование процесса образования диапировых куполов. Сов. геология, Сб. 54, 1956.

19. ЛЮСТИХ Е.Н. Условия подобия при моделеровании тектонических. процессов. ДАН СССР, XIУ, № 5, 1949.

20. МИХАЙЛОВ Н.В. Упруго-пластические свойства нефтяных битумов Колл. журн. 17, № 3, 1955.

21. МИХАЙЛОВ Н.Б., ЛИХТГЕЙМ А.М. Исследование полных реологических кривых и формулы для расчета эффективной вязкости структурированных жидкостей с молекулярно-кинетической интерпретацией входящих в них членов. 17, № 5, 1955.

22. ОСОКИНА Д.Н. Изучение желатино-глицериновых студней как материала для оптического метода исследования напряжений. Хроника. Изв. АН СССР, сер. геофиз., № 4. 1955.

23. ОСОКИНА Д.Н., ПАВЛОВ В.П., ВИНОГРАДОВ Г.В., ГЗОВСКИЙ М.В. Реологическое и поляризационно-оптическое исследованне растворов и гелей этилцеллюлозы. Тезисы докладов IX конф. по общим вопросам химии и физики высокомолекулярных соединений. Стр. 124. Изд. АН СССР, М., 1956.

24. РИЗНИЧЕНКО Ю.В. Сейсмоакустические методы изучения напраженного состояния горных пород. Изв. АН СССР, сер геофиз., № 6, 1955.

25. СИНИЦЫН В.В., ВИНОГРАДОВ Г.В. Вязкостные свойства углеводородных смазок. Колл. журн. 17, № 3, 1955.

26. ФРЕНКЕЛЬ Я.И. Кинетическая теория жидкостей. Изд. АН СССР, 1945.

27. ФРИДМАН Я.Б. Единая теория прочности материалов. Оборонгиз, 1943

28. ФРИДМАН Я.Б. Механические свойства металлов, Изд. 2-ое, 1952.

29. ШНЕЕРСОН Б.Л. О применении теории подобия при тектоническом, моделировании. Тр. Инст. Теорет. Геофиз. АН СССР, т. 3, 1947.

30. ЭЙГЕНСОН Л. С. Моделирование. Гос. издат. "Сов. наука". Москва 1952.

31. Benioff (H.) : Earthquakes and rock creep. Bull. Seismol. Soc. Am., vol. 41, N. 1, 1951.

32. Bucher (W.) : Role of gravity in orogenesis. Bull. Geol. Soc. Am., vol. 67, pp. 1295-1318, oct. 1956.

33. BULLEN (K. E.) : On the size of the strained region prior to an extreme earthquake. Bull. Seismological Soc. Am., vol. 45, N. 1, 1955.

34. CHANG (W. G.) : Adaptation as a Mode of Development of Fractures and its Relation to Geological Phenomena. Contrib. Nat Res. Inst. of Geol. Academia Sinica N. 8, 1948.

35. CLOOS (E.) : Experimental analysis of fracture patterns. Bul. Geol. Soc. Am., vol. 66, N. 3, 1955.

36. CLOOS (H.) : Experimente zur inneren Tektonik. Zentralbl. f. Min., v. 12, p. 609-621, 1928.

37. CLOOS (H.) : Zur experimentellen Tektonik, Brûche und Falten. Naturwissenschaften, 19 th Jarhb., H. II, p. 242-247, 1931.

38. DAUBRÉE (A.) : Etudes synthétiques de géologie expérimentale. Paris, 1879.

39. DOBRIN (M. B.) : Some quantitative experiments on a fluid salt-dome model and their geological implications. Transact. Nat. Research Council Am. Geol. Union, Part. II, 1941.

40. GRIGGS (D. T.) : Deformation of rocks under high confining pressures Journ. Geol., vol. 44, N. 5, 1936.

41. GRIGGS (D. T.) : Creep of Rocks. Journ. Geol., vol. 47, N. 3, 1939.

42. GRIGGS (D. T.) : Experimental flow of rocks under conditions favouring recrystallization. Bull. Geol., Soc. Am., vol. 51, N. 7, 1940.

43. HAFNER (W.) : Stress distributions and faulting. Bull. Geol. Soc. Am. vol. 62, N. 4, 1951.

44. HUBBERT (M. K.) : Theory of scale models as applied to the study geological structures. Bull. Geol. Soc. Am., vol. 48, pp. 1459-1520, 1937.

45. KARMAN (T.) : Festigkeitversuche unter allseitigem Druck. Zeit. des Ver. Deut. Ing., 5, s, 1749-1757, 1911.

46. KOENIGSBERGER (G.), MORATH (O.) : Theoretische Grundlagen der experimentellen Tektonik. Zeit. der Deutsch. Geol. Gesellschaft, vol. 65, pp. 65-86, 1913.

47. LEE (I. S.), CHEN (C. H.), LEE (M. T.) : Experiments with clay on shear Fractures. Bull. Geol. Soc. China, vol. 28, N. 1-2, 1948.

48. LI SZU-KUANG : Vortex structure and other problems relating to the compounding of geotectonic systems of North-Western China. Academia Sinica, 1955.

49. LINK (T. A.) : The origin and significance of « epianticlinal » faults as revealed by experiments. Bull. Am. Ass. Petr. Geol., vol. 11, N. 8. 1927.

50. MOHR (O.) : Ueber die Darstellung des Spannungszustandes und des Deformationszustandes eines Kôrperselements und ûber die Anwendung derselben in der Festigkeitslehre. Der Civilingenieur, H. 2 u 3, 1882.

51. NETTLETON (L. L.) : Recent experimental and geophysical evidence of mechanics of salt dome formation. Bull. Am. Ass. Petr. Geol., vol. 27, N. 1, 1943.

52. PARKER (T. J.), McDOWELL (A. N.) : Model studies of salt-dome tectonics. Bull. Am. Ass. Petr. Geol., vol. 39, N. 12, 1955.

53. PHILIPPOFF (W.) : Zur Theorien der Structurviskousitât. Kolloid-Zeitschrift. Band. 71, Heft 1, April, 1935.

54. PHILLIPS (D. S.) : Tectonics of mining. Colliery Engineering, June-okt., 1948.

55. RAMBERG (H.) : Natural and experimental boudinage and pinch-and-swele structures. Journ. Geol., vol. 63, N. 6, 1955.

56. Reier (E.) : Geologische und Geographische Experimente. Heft 1-Falten, Heft II — Vulkanische und Massen Eruptionen, H. III-Rupturen, H. IV-Methoden und Apparate. Leipzig, 1892-1894.

57. Robertson (E. C.) : Experimental study of the strength of rocks. Bull. Geol. Soc. Am., vol. 66, pp. 1275-1314, 1955.

58. Wallace (R.) : Geometry of shearing stress and relation to faulting. Journ. Geol., vol. 59, N. 2, 1951.

59. Willis (B.) : The mechanics of Appalachian structure. U. S. Geol. survey, 13, Annual Report, pt. 2, p. 211-281, 1893.

ON SEISMIC REGIONING OF ASIAN COUNTRIES

by G. P. GORSHKOV.

The most complicated problem of natural science — the problem of earthquake forecast involves the following three phenomena : the prediction of *place* of the future earthquake, its *magnitude* and *time* of origin. The location of the future earthquakes and determination of their magnitudes is the subject matter of seismic regioning. Seismic regioning therefore is aimed at receiving data concerning the capacity of danger which seismic activity represents for any point of the Earth's surface.

The problem of seismic regioning in the practice of seismic research work in the USSR is being solved by combined analyses of both, seismic and geological data. The statistical registration of earthquakes supplies information about their location and magnitude; the study of geological conditions of the origin of earthquakes makes it possible to draw definite lines of seismotectonic interdependance. Extrapolation of data based on comparative analysis of tectonic movements furnishes the material which permits to draw a chart of theoretical distribution of seismic force even for those regions which either lack seismic statistics or it is incomplete.

Earthquake is the result of tectonic activity of the Earth. Strictly speaking, earthquakes are associated with the regions within the limits of which intensive and differentiated tectonic movements take place at any given moment.

Intensive tectonic movements of the recent epoch are common, first of all, to the Alpine folded zones. The last stage of development of geosynclines in the Tertiary system-such as Tetis-is the origin of folded zones in the areas previously occupied by geosynclines. Movements common to the Alpine stage of folding, remain the same in the Quaternary period and modern epoch. Hence, Alpine folded zones are *a-priori* seismic in character and the exceptions to this rule are few.

But not only such areas of the crust are seismic. During the Quaternary period tectonic movements of great force were known to be registered not only in the zones of Tertiary geosynclines but also in many other places : within the confines of long ago consolidated areas of Cimmerian, Hercynian and Caledonian foldings and even in the areas of Precambrian crystal blocks. To such rejuvenated mountains pertain the Tien-Shan, the Altai and southern region of the Baikal. Tectonic movements in these areas take the shape of « block tectonics », i. e. the shape of folds of « Germanic type » (H. Stille). Earthquakes in these areas are rather rare comparing with the folded zones, but their magnitude comes to the highest level. The Tien-Shan earthquake of 1911 the intensity of which was estimated as 12 grades supplies a good example to this statement.

Thus, when estimating the capacity of seismic danger it is necessary to take into consideration, on the one hand, the whole geological history of the area in question, and, on the other, the recent movements which play a decisive role in the incitement of seismic activity.

The above mentioned considerations were taken as a basis when drawing up the map of seismic regioning of the USSR territory. The first map of such a type was issued in 1937 (2). From that time on this map underwent a number of improvements which were due to new data and advanced methods of research (e. g. (3).

The network of seismic stations has considerably increased during the last decade and by now there are about 70 of them on the territory of the USSR. The stations are equipped with modern instruments constructed according to D. P. Kirnos and D. A. Kharin system (some stations still have B. B. Galitzin instruments). As a result of all this, new and important data on seismic regime in the Causacus, Turkmenia, Middle Asia, Far East and other seismic regions were received.

Those data were used as a basis for charting the latest map of seismic regioning of the USSR territory (7); the map was charted by the Institute of the Earth's Physics of the Academy of Sciences of the USSR in 1957 (fig. 1).

It can be seen (fig. 1) that the following regions of the USSR territory make themselves conspicuous (though to a various degree) for their high seismicity : the Carpathian region, the southern part of the Crimea, the Caucasus, South Turkmenia (particularly Copet-Dag), Middle Asia (Pamir, Tien-Shan) the whole belt of mountains beginning from Tien-Shan to the Baikal region, Kuril Islands and eastern part of Kamchatka. Weak and rare earthquakes were also registered in the Urals, Karelia, the Arctic and some other places.

An analoguous map of seismic regioning was also made up for the territory of China in 1956. It was made up by the geologists of the Chinese People's Republic under the direction of Prof.

Li-Shen-Pan and on the consultations of the author of this article (5, 10).

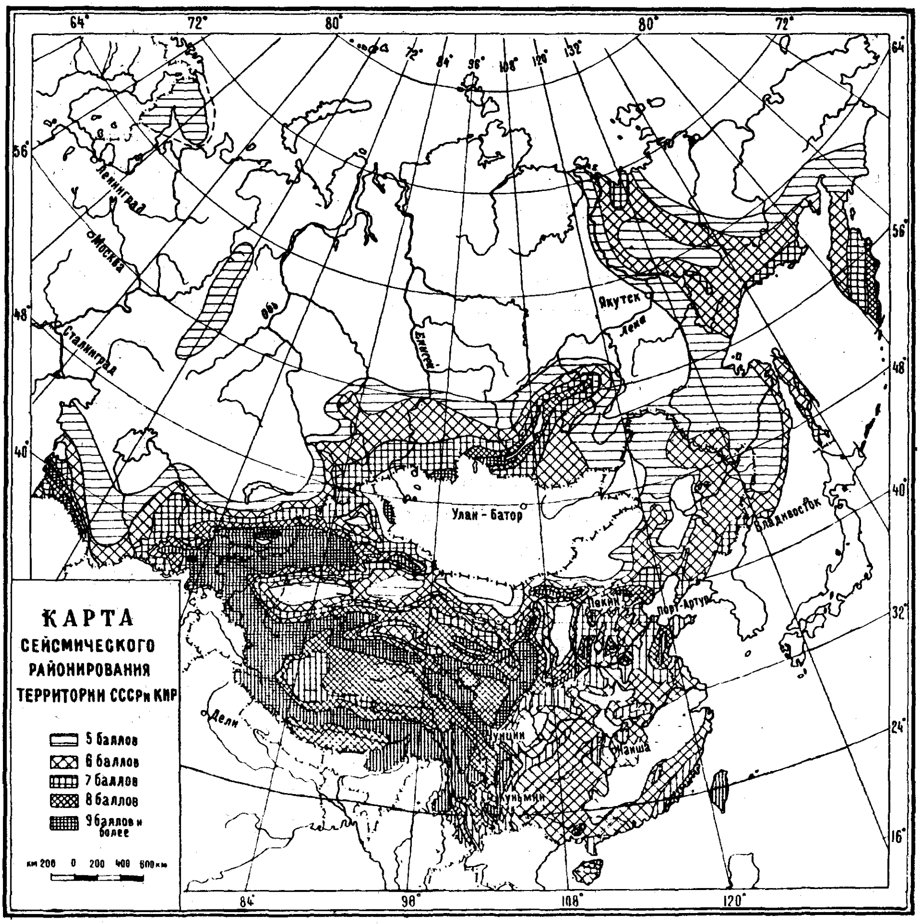

FIG. 1.

Various documents of the History of China contain data on many thousands of earthquakes registered within the period of three thousand years (4). Nearly 800 of them were of destructive force. Some earthquakes which took place in 1556, 1668, 1920 and 1927 are to be considered as the greatest seismic catastrophies in the world. The study of data on these numerous earthquakes made it possible to draw a chart of epicentres and an aggregate map of isoseisms. Geological peculiarities of Chinese earthquakes were then studied in the first proximity. The association of seismic regions with the areas of the newest and recent tectonic movements has displayed itself here with particular distinctness. The neotectonic movements associated with Quaternary deposits have reached, in a number of places in China great intensity and differentiated themselves quite effectively (6). The neotectonic movements differentiated themselves in the way of folding and disruptive deformations of layers of Quaternary deposits, in bends and inclined terraces, in deformations of denudated surfaces, in the plan of river. network and structure of river valleys, etc. And, as a rule, the areas of intensive and differentiated movements are highly seismic.

To such areas of high seismicity on the territory of China belong[1] :

1. Alpine (Himalayan) folded zones : Himalayas, Caracorum-Transhimalayas, Burmese extension of Himalayas, Taivan.

2. More ancient folded structures rejuvenated in Quaternary period :

a) Precambrian massives : Shan-Dun, Inshan, Tsinlin and others.

b) Caledonian folded zones : Mufushan, Tzulinshan, the coast of Taivan strait, Hainan and others.

c) Hercynian folded zones : Mongolian Altai, Tien-Shan, Kuenlun-Altintag, Nanshan, Tchanquantsai ridge and others.

d) Cimmerian (Janshan) folded zones : Tibet, Junnan, Western coast of Sitchuan basin, Liubanshan, Hollanshan, Liulanshan, Taikhanshan, Sishan, Janshan and others.

The rest of the regions are of weak seismicity : Djungaria, Tarim, Tsaidam, Ordos, Alanshan, Inner Mongolia Plateau, Manchuria, North-China and Uchan depressions.

All the above mentioned considerations were taken as a basis for the map of seismic regioning of the territory of China.

Thus, if we deal with the Asia mainland, there exist maps of seismic regioning (m. 1/10.000.000^{e}) for the asian part of the USSR and China. And quite naturally the idea of possibility and necessity of making up analoguous maps for other Asian countries makes itself felt. We know of such sort of experience in Japan and India (9, 11). In both those countries they made use of their own particular methods, although the final aim is one and the same : it is the estimation of force of the future earthquakes. The statistical data on earthquakes accumulated to this day, especially in the last 50 years (e. g. 8, 13) and the results of geological research made during the same period of time permit, as it seems to us, to make an attempt to compile maps of seismic regioning for all the

1. Tectonic subdivisions are made according to Huan Ti-Tsin, 1925.

countries of Asia with the above mentioned ratio. They may turn out to be of different precision but there is every reason to believe that it will be much higher of that which the seismic maps published by A. Sieberg (12) possess.

We believe that the organisation of research work on seismic regioning in the countries of Asia may be carried out by the Section of Seismology of the International Geodetic and Geophysical Union.

References.

1. Атлас сейсмичности СССР. Совет по сейсмологии Академии наук СССР, рукопись, 1957, Москва.
2. ГОРШКОВ Г.П. и др. Сейсмическая карта СССР. Большой Советский Атлас Мира, т.1, карта № 93, 1937, Москва.
3. ГОРШКОВ Г.П. О новой карте сейсмического районирования территории СССР. Труды Геофизического института Академии наук СССР № 1 (128), 1948. Москва.
4. Каталог землетрясений Китая т.1 и П, 1956, Пекин на китайском языке.
5. ЛИ ШАН-ПАН. Сейсмические карты Китая и их описание. Журнал Китайского геофизического общества, 1957 (на китайском яз.)
6. Неотектоника Китая. 1957, Пекин (на китайском языке).
7. Нормы и правила строительства в сейсмических районах, СН-8-57, 1957, Стройиздат. Москва
8. Gutenberg B. and Richter C. F., Seismicity of the Earth and associated phenomena, 1949, London.
9. Indian Concrete Journal, 15 oct. 1954.
10. Lee S. P. Seismological maps of China, Science Records, New. Ser., V. 1, N° 5, 1957.
11. Omori F. On the earthquake zones in Central Japan, Bull. Imp. Earthq. Inv. Comm,, V. 1, N° 3, 1907.
12. Sieberg A. Erdbebengeographie, Handbuch der Geophysik, B. IV, L. 3, 1932, Berlin.
13. The International Seismological Summary, 1931-1948, Oxford.

EVOLUTION OF THE CRUST AND ITS ROCK ASSOCIATIONS GEOPHYSICS AND CONTINENTAL GROWTH

by J. TUZO WILSON

Modern theories of the origin of the solar system suggest that the planets have descended from larger protoplanets by the loss of gaseous elements. Comparisons between the composition of stars and that of atmosphere and hydrosphere support this view and suggest that the present gaseous and liquid envelopes of the earth are not relics of a primitive atmosphere but that they have been entirely generated during the earth's history by the escape of material trapped within the solid earth. Among the leading exponents of these arguments are von Weizächer, a physicist, Kuiper, an astronomer, Urey, a chemist and Rubey, a geologist.

The obvious channels by which gases escape from within the earth are volcanoes, and in spite of some difficulties it does seem possible for volcanic activity to have produced steam and other gases in the right amounts to have created air and oceans; but volcanoes also produce lava and this must therefore be accumulating on the surface.

When the active volcanoes are examined they are found to fall into two principal classes. The majority lie along island arcs and young mountains and produce lavas of intermediate silica content, generically called andesites, together with some more basic basalts, while a minority rise from mid-ocean ridges and produce basalts almost exclusively.

At this point it is useful to combine the classifications made by Turner and Verhoogen of the igneous rocks and those made by Kyrnine and Pettijohn of the sedimentary rocks in such a way as to suggest that different geological environments exist, each occupied by a characteristic association of rocks. For example, continental platforms of granodioritic gneiss are overlain by sediments which have been well sorted into sandstones, shales and limestones. Island arcs are built up of andesites and related volcanic rocks with the products of their rapid erosion — greywackes and micaceous shales — whereas mid-ocean ridges are chiefly basalt lavas crowned by coral limestone. (See Table 1.)

The last two of these associations are now being formed along two systems of mobile belts about the earth, which are volcanically and seismically active. The geophysicists Heezen and Ewing have suggested that the one which we will call the mid-ocean fracture system extends the length of the Atlantic Ocean, passes south of Africa across the Indian Ocean and enters the Pacific Ocean south of Australia to join most of the ridges there. They believe that the topographic ridges lie along a continuous system of fractures which earthquakes show to be shallow, that is, not deeper than 70 kilometers. Presumably these fractures have scarcely moved during the earth's history, for few abandoned ridges exist and it may be that it has taken the greater part of that vast time for outpourings of basalt to have built up this system of ridges. The required rate of volcanism is reasonable but unfortunately it is impossible to make precise quantitative estimates because neither the rate of oceanic volcanism nor the extent of the roots below the ridges is accurately known.

The second, or continental, fracture systems forms two belts meeting in Indonesia and extending from the Mediterranean to New Zealand and around the margin of the Pacific Ocean respectively. These belts are more active. The location of earthquake foci shows that beneath them fractures extend to as much as 700 kilometers, suggesting that the andesites rise from greater depths in the mantle than do the basalts. Both kinds of lava presumably arise by partial melting or differentiation of more siliceous components which have lower melting points than the ultra-basic mantle as a whole.

These continental belts are made up of two series of elements, frequently arcuate, which seem to evolve with time and grow to larger forms — from small arcs to great mountains. The primary arcs first appear off coasts and give rise as they grow to secondary ranges on the continental side, marked by a different rock association. Thus the Rocky Mountains of North America are considered to be a series of secondary arcs corresponding to the Coast Ranges which are primary. In the past at long intervals, the belts migrated, often one part at a time, so that elements of different ages have been combined in the belts, just as short-cuts in a highway may have been constructed later than other parts.

When belts move the abandoned mountains become inactive and are slowly eroded away, but the roots of even the oldest systems can be traced in continents by studies of geology coupled with isotopic age determinations. It appears that all continents are made up of old mountain roots and that the rocks called Archean and Proterozoic are the scars of former primary and secondary arcs respectively and not, as was long supposed, rocks of different ages.

Consideration of the rates of andesitic volcanism and of the volumes of various rock associations suggest that the entire crust has grown during geological time and that its base, the seismologists' Mohorovičič discontinuity, is the original surface of the earth. This being so, ores as well as rocks must have risen from the mantle. Many of them never moved far from major fault systems to which they can be seen to be related, and by which they can be assumed to have risen. There are differences in the radioactive content of crustal rocks and of the mantle which lead to change in the isotopic constitution of those lead ores which have migrated far through the crustal rocks. A study of these differences is assisting in the reconstruction of the history of some ore bodies.

In recent decades two theories of mountain building have arisen to challenge the older contraction theory. The theory of continental drift lacks a mechanism; it has never been extended to explain the events of the greater, Precambrian, part of geologic time; and most if not all of the evidence favouring it is readily explained in other ways. The idea that convection currents cause mountain building has been stated in many ways, some of which are contradictory, so that it can be said that no complete theory of the mechanism exists. There is no direct evidence of the existence of the supposed currents. None of the suggestions yet made has explained the arcuate pattern and other features of mountain belts. It is not apparent why flow should create the deep fractures on which earthquakes occur.

On the other hand, a number of recent developments have strengthened the contraction theory. There has been the recent realization that mountains and ocean ridges are due to two systems of world wide fractures which so interlock that they could allow the earth as a whole to contract. The theoretical physicist, Scheidegger has given at least a partial explanation of how the observed patterns of mountain belts could have been formed. It is clear that the escape from inside the earth of sufficient matter to form the whole crust would greatly augment the amount of contraction of the surface possible from cooling alone. These developments all suggest that the contraction theory remains the most satisfactory yet put forward. It can be combined with the suggestion recently made that wandering of the poles has occurred because the earth as a whole has in the past slowly rotated relative to its axis of rotation.

These new developments have greatly changed our outlook upon

Association	Location	Igneous rock kindreds	Sedimentary rock facies	Extent of metamorphism
Oceanic	mid-ocean ridges, ocean basins	olivine basalt	reef limestone or abyssal muds	local
Borderland	continental shelves secondary mountains	negligible	sand and shale	negligible
Island arc	Islands arcs	Andesites, ultrabasic and spilite	greywacke and shale	important
Primary Mountain	Primary mountains	Plutonic rocks, ultrabasics and post-orogenic andesite	(erosion, no deposition)	very important
Piedmont	intermontane ? late secondary mountains	quartz and olivine basalt	arkose	local
Continental	Covered shields secondary mountains	minor alkaline volcanics	sandstone, shale and limestone	local

the earth sciences. Mapping, which reveals the details of that quarter of the earth's surface upon which we live and which can be likened to a study of surface anatomy, was at one time the chief work of geologists. Now geophysical investigations of the ocean floors and of the hidden interior, consideration of rates of growth and chemical and isotopic studies of composition are enabling studies of the internal structure and of the behaviour or physiology of the earth to be undertaken. The result is that modern investigations in the earth sciences (and modern prospecting practices also) depend as much upon physical, chemical and even astronomical and theoretical studies of the earth as upon the visual observation and mapping which was at one time all that was possible. Earth science is in fact continuing the process of graduating from the mere collection of surface data to a mature physical science. To make progress in these studies a combination of geophysics with geology is needed.

« STATISTICS OF NON-FOLDED BASINS »

by RHODES W. FAIRBRIDGE
(Columbia University, New York, 27.)

ABSTRACT.

A series of maps covering every continent (or major subcontinental unit) have been prepared, on which the fundamental structural divisions of shield, fold belt, and basin have been delineated.

« Non-folded basins » are taken to be those free from « alpinotype » folding and metamorphism. Folds of lesser order, such as those due to basement faulting or minor gravitational adjustment, may be present, but metamorphism is absent and a clear interpretation of the sedimentary characteristics, notably facies and thickness, may be obtained.

A distinction is made for the « platform » as a subdivision of the shield category, being a unit of rigid basement but covered by thin sheets of sediment generally not exceeding about 300 m. but locally reaching 1.000 m.

Statistical treatment shows that basins of each broad category tend to repeat the same dimensional characteristics. Categories identified in this way correspond fairly well to the « parageosynclines » (of Stille) and the subdivisions of this class recognized by Kay. It is suggested that each category corresponds to an underlying crust of specific thickness and mobility characteristics.

CONTENTS

Introduction.

For a long time, the geophysicists in general and the students of the physics of the Earth's interior in particular, have demanded that the geologists provide them with certain parameters that are essential to any mathematical treatment of the lithosphere.

They have often asked in vain. Indeed it is frequently difficult to derive a precise figure or formula with which to express an object or process in the world of nature. A figure can be given, but the question arises as to whether it presents a true picture or not; it may present a dangerous half-truth. One may measure the cranial capacity of a man and an ape and say that this ratio represents an essential difference between the two. This is partly true, but surely it would not be a universally acceptable criterion of distinction between these two species of mammal!

For the structure of the earth's crust, it is necessary to derive a series of criteria, of formulae, which may serve as a first approximation in the organized and mathematical description of this immense and confusingly varied subject.

For the purposes of this paper, we are studying only the continents and the continental shelves in any detail. Within this realm, we recognize the following major structural entities :

A. *Shields.*
B. *Fold belts.*
C. *Basins.*

Shields may be further subdivided into bare, sediment-free structural blocks, domes, etc. and into areas with a strong foundation of crystalline rocks, but with a superficial veneer of sediments or extensive volcanic flows (e. g.« plateau basalts »). These veneered areas are referred to here as « platforms » because they are generally broad and flat; the basement crystalline rocks often project above the surrounding sediments, which generally do not exceed some 300 m. in thickness, but occasionally reach 1.000 m. Platform sediments consist often of alluvium, eolian or glacial deposits, and are generally free from marine sediments, except those brought in by exceptionally high eustatic rises. These regions are sometimes included in « basins », which is a misleading procedure, since the latter are characterized by varying degrees of basement mobility and thus have sediment thicknesses often greatly exceeding 300 m. Many sections of the present-day continental shelf are in fact platforms, while only specific sections are actual sites of major sediment accumulations (thus « basins », see below).

The fold belts, for their part, may be regarded geotectonically as on the way to becoming shields, but they are younger and less universally consolidated. Only certain sections consist of igneous and highly crystalline metamorphics. Many parts consist of heavy folded and thrust sediments (« Alpinotype » tectonics of Hans Stille). However, in these zones (« eugeosynclines ») it is not easy to determine exactly the former thicknesses and dimensions of basins, and accordingly they have been omitted for the present series of statistics. A special subcategory of fold belt displays rows of volcanic cones or linear accumulations of volcanic accumulations.

We are left with the third category : Basins. These represent those parts of the semi-rigid cratons that have subsided sufficiently to permit the accumulation of sediments in large amounts. Marginally, these may overlap onto the semi-rigid structures of the deep ocean floor (« thalasso-cratons », Fairbridge, 1955).

Basins located on continental regions, possessing a semi-rigid basement of crystalline rocks (the « Hedreocratons » of Kay, 1951), display a great longevity in geological time, and many will probably never be folded, except for local adjustment to basement faulting, buried hills, and gravitational processes. They never become granitized or act as hosts to major magmatic intrusions. Volcanic activity is generally somewhat rare. These are therefore regions of paramount interest to oil geologists.

Basins superimposed on the hedreocraton are those characterized as « parageosynclines » by Stille (1935) and subdivided by Kay (1951) as « paraliageosynclines », « auto- », « zeugo- », « taphro- », and « epieugeosynclines ». Some observers have suggested that there is such a continuous gradation between these types that no useful purpose is served by distinguishing them. One of the interesting results of this research is the conclusion that these types, although admittedly gradational, are in fact rather distinctive and may be expressed so by formulation.

Average dimensions of world basins.

Numbers and Area.

There are approximately 310 recognized basins in the world. Extremely small basins, especially of an intramontane type, are ignored. A number of the basins here recognized are groups of basins, that is, they lie in a linear or parallel sequence and are unified by a former hydrologic continuity, so that they may have been originally single basins of sedimentation and are only now separated by structural accidents and erosion. A number of uniform-looking basins mask a heterogeneity at depth (e. g., West Texas Basin) owing to the presence of several partly truncated troughs there, but they are now unified by a subsequent, broad basinal development over the whole area. In most cases dealt with in this paper, an endeavour has been made to classify accordig to the latest (and generally most extensive) phase of basin development. As shown by Kay (1951) over the course of a long evolution, the character of a basin may alter progressively.

The area covered by these basins slightly exceeds 21 million square miles (55×10^6 km^2), which makes the average size for a basin some 66,000 square miles (170,000 km^2). Our figure for total area indicates a significantly different approach from that of Weeks (1952), who has given the total as 15 million square miles (or 39×10^6 km^2).

Numbers and mean areas of basins in the various categories may be expressed in percentages as follows :

	Number	*Area Percentage*	*Mean Area (Sq. miles)*	*Mean Area (sq. km.)*
Stable Region :				
Paraliageosynclines. . . . (« Stable Coastal Basins »)	34 %	28 %	54,500	141,000
Taphrogeosynclines. . . . (« Graben Basins »)	17 %	11 %	43,500	112,700
Exogeosynclines. . . . . . (« Foreland Shelf Basins»)	16 %	17 %	72,000	186,500
Autogeosynclines. . . . . . (« Interior Basins »)	13 %	37 %	200,000	520,000
Mobile Belts :				
Epieugeosynclines. . . . (« Intermontane Basins »)	12 %	3 %	19,000	49,000
Zeugogeosynclines. . . . (« Median Mass Basins »)	8 %	5 %	44,000	114,000

For convenience, the approximate equivalents to Kay's terms, employed by Weeks (1952) have been added in parentheses.

From this analysis it may be seen that by far the most numerous basins are the paraliageosynclines, which are also second greatest in area. Autogeosynclines cover the greatest area, but with relatively few units.

The Shape Constant.

The figures for mean area by itself are not so illuminating as an shape constant, simply derived by taking the ratio of width to length, thus a shape constant in the horizontal plane. Here again, autogeosynclines show up as the most distinctive with a ratio of about 1 : 2.5 . Taphrogeosynclines on the other hand represent marked linearity, long narrow grabens, marked by a mean shape ratio of 1 : 7 and ranging up to 1 : 25.

Since the classification of a basin is in the first place based on such features as sedimentary character, shape and location, it may be suspected that any gross divergence from the mean shape constant may indicate a primary error of classification. Here, however, we must be careful to avoid constructing a « Deus ex machina », a classification that possesses only crude mathematical parameters and which lacks real value; it could fail if it were not founded on interrelated criteria of fundamental natural science.

The proof of the reality and utility of the Shape K may be found in testing the order of the various types of basin against other characteristics : thickness, lithology, etc. A distinctive order and pattern *is*, in fact, found, ranging from autogeosynclines at one end to taphrogeosynclines at the other, a continuing demonstration of the usefulness of the method.

Thickness.

Thickness of sediments in any basin is a difficult factor to express with accuracy. From an accumulation of maximum formation thicknesses based on measured sections scattered around the basin, we may well obtain a figure that far exceeds the maximum vertical section in any one place, such as might be obtained by drilling a well in the deepest part of the basin. This disparity is due, of course, to the uneven accumulation, variation in the locus of maximum deposition, and foresetting of beds on slopes. As closely as possible, we have attempted to state a thickness which corresponds to the maximum depth of the basin floor .

Thicknesses vary more sharply from region to region than do most factors, depending on such local conditions as relief, climate, and so on. However, a distinctive trend still appears; the autogeosynclines are generally the shallowest, with 10-15 % of the total for each continent, while epieu — and exogeosynclines loom high, with 20 % or more. Average thicknesses for any basin type are particularly striking. The most common of all basins, paraliageosyncline, averages 3,500 m. (12,000 ft.), compared with 5,200 m. (17,000 ft.) for the exogeosynclines, and 3,100 m. (10,000 ft.) for autogeosynclines.

The average thickness of sediments over the whole land surface area (plus basin-shelves) is 1,840 m. (6.000 ft.), which is interesting to compare with the 1.000 m. average for the deep oceans. Since the continental sediments are contained in basins, however the average for all of these is rather more significant : 5.100 m. (17,500 ft.).

Broken down into continents, it is striking that the larger masses all show rather similar low averages (Eurasia — 1.645 m., North America — 1.296 m., Africa — 1.050 m.), while the smaller continents show greater averages (South America — 2,075 m., Australia — 2,515 m.). Antarctica is insufficiently known to be included. The same trend is apparent when these figures are taken on the basis of average thickness for basin area : the larger consolidated units have the thinner basins (Eurasia — 4.700 m., North America — 3.600 m., Africa — 2.800 m.) and the smaller units the thicker basins (South America — 5.300 m., Australia — 5.100 m.).

Thickness (Area) Shape Relations.

The total measured thickness for the world basins is 1,480,000 m. (5,000,000 ft.). This is not a tremendously significant figure but it does provide an interesting basis for Thickness/Area relations. Thus, in the metric system (meters to sq. km.), T/A = 1,480,000 : 55,200,000, thus 1:38; in terms of feet to square miles, it would be 5,000,000:21,262,000 thus 1:4.25.

The ratio for specific regions reflects the trend mentioned above, that the larger the unit the smaller (proportionally) the thickness. Taken on a basis of specific basin type, the ratio points up their peculiarities very well. Thus (in metric system), the autogeosyncline shows the lowest T/A ratio as follows : 123,000 m. : 20,000,000 sq. km (1 m : 163 km^2); in contrast, the epieugeosyncline is the largest, 1:11, and so on. Respectively, in ft./sq. miles, these are 1:19 and 1:5. Thus again, the broad basin is distinctly shallower for its area than the narrow, downfolded intramontane basin.

Since the shape of any basin (in plan) is distinctively expressed by the shape K (ratio of width to length), this constant is used to illustrate relations of thickness to shape in basins. Here again, it is found that a characteristic ordering of basin types emerge : autogeosynclines, the most rounded (shape K: 2.5), are also the shallowest; epieugeosynclines, very elongate and narrow, are also proportionally the deepest. The fault-controlled taphrogeosynclines represent a rather special case : most elongate, but relatively shallow.

Distribution of basins.

It is apparent that, within any category of basin (distinguished on characteristics mainly of a sedimentary nature), there must be recognized a certain spread of dimensions. There are, however, *average* sizes and shapes which differ markedly from the averages of each other category. The question arises now : is there an identifiable structural control of basin dimensions ? This may emerge from studying the distribution of basins.

Location of Basins on Continents.

In recent studies of world geotectonic patterns, geologists are gradually accepting the thesis, founded in part on the evidence of Africa by Krenkel (1925) and Cloos (1937), that the earth's crust is made up of a mosaic of blocks (« tessarae » of Brock, 1956), some high, some low (« anticlise » and « syneclise » of Russian geologists), separated by narrow, sometime mobile belts and fault zones. Sonder (1956) has applied the scheme to the ocean floors and the world generally. These mosaic blocks are suspected of falling into a definite geometric pattern, the first-order boundaries corresponding to great circles (according to Vening Meinesz, 1947), the intersections coinciding with specific vertices or nodes of mountain-building or other such geotectonic foci. Vertices are geometrically placed, according to Brock (1956), and commonly separated by angles of 45°, 72°, and 90° (from the earth's center); structural units so bounded provide continental-sized areas (long axis often about 5.000 miles).

Second-order features (according to Sollas, 1903; Boutakoff, 1952) correspond to small circles, sectors of which match recognized tectonic arcs and are integrated into the great-circle lineaments. Brock found that the radii of these belts, measured in angles of arc subtended at the earth's center, show a preference for aliquot-angles of a quadrant, e. g., 7 1/2°, 10°, 12 1/2°, 15°, 18°, 22 1/2°, etc. The post-Cambrian mosaic of structural blocks in Africa show a preference for 15° long axes (about 1,600 km. or 1,000 miles), while the late Pre-Cambrian mosaic prefers 5 to 7 1/2 (about 530-800 km. or 300-500 miles), which suggests perhaps a progressive welding together of the older units.

The idea that the Pre-Cambrian « grain » of continents has a mosaic pattern has also been propounded by Hills (1946) with Australia particularly in mind; the order of magnitude of the blocks is the same as in Africa and the other shields. Hills suggested that this mosaic is related to an original « pantectogenesis » of the earth's sialic crust, which tended to nuclear arrangement, around or over which subsequent basin or trough-like geosynclines evolved. This interpretation is different from that of Sonder, Vening Meinesz, Brock, and others who visualized the mosaic pattern as based on fracture patterns, while Hills saw in it the outlines of primary crushed nuclei. The two hypotheses are not necessarily incompatible, since the fracturing may be a logical follow-up from the junction to dismemberment of the primary nuclei.

Let us consider the evolution of such groups of units. Brock noted that in Africa in post-Cambrian times the tendency was toward larger units, combinations of two or three Pre-Cambrian tessarae. While the primary patterns may well have been in polygons, the eventual outline tended toward an oval. In preparing a geotectonic map of Australia, the writer (Fairbridge, 1950) has adapted the Hills concept and added the successively younger crustal belts (« Paleo-, Meso-, and Neo-Australia », using the terminology of Stille; see Kölbel, 1945). If the map showing the pattern of non-folded basins is super-imposed on the geotectonic base, it will be seen that two main tendencies emerge :

a) Old, Pre-Cambrian shield areas give rise to broad, ovoid type of basins : these are auto- or paralia-geosynclines.

b) Successively younger continental accretions, once welded onto the old shield, favor the smaller and more linear depressions : thus taphro-, epieu-, and exogeosynclines.

Extending this type of observation to other continents, one observes, for example, Europe. Here the great bulk of the continent, outside of Scandinavia and Russia, consists of a series of younger folded and consolidated basement rocks : « Paleo-, Meso-, and Neo-Europa », to borrow from Stille, the regions welded onto the Fenno-Sarmatian shield in the Caledonian, Hercynian, or Alpine orogenies. Here again we find that the younger superimposed basins are all small, mostly of the taphro-, epieu-, and exogeosynclinal types. On the other hand, as we go back into the shield regions of European Russia and Siberia, the basin sizes grow much larger and the types are mainly auto- or zeugogeosynclinal.

The same picture is true of the Americas; the regions with old, Pre-Cambrian basements are normally marked by the larger basins, normally 250.000 to 1.000.000 sq. km. (100.000 to 400.000 square miles), while the basins superimposed on the younger basement are normally small and of rather different character.

A general rule then emerges : (Ia) The younger the consolidation of the basement, the smaller (areally) the superimposed basins; they are generally of narrow, linear types and frequently carry much thicker sequence of sediments than the older consolidated regions, which follow the converse of this rule (Ib), in that their superimposed basins are ovoid, broad, and shallow.

A second rule emerges for the shield areas : (IIa) As the original nuclei become welded together, the size of superimposed basins increases. However (IIb), along specific zones, e. g., « young » continental margins, and along the East African and South Australian rift belts, a youthful fracturing of the great shield areas may occur, resulting in the introduction and elongate, narrow sedimentary basins of taphrogeosynclinal character.

Continental Shelves.

Measurement of the length of the continental shelves of the world have been carefully rechecked on large scale maps, using the 200 m. (110 fathom) contour as the mean shelf edge, except for certain glaciated regions such as Antarctica, Greenland, and the adjacent Canadian Arctic, where about 1000 m. (or 550 fm.) most often approximates the break in slope that indicates the true shelf edge. Large continental-type islands have been included in the survey, but small oceanic-type islands have been excluded. The final figure of 352,000 km. (218,000 miles) must represent a fairly close approximation of the total length of the continental shelves. Of this, 102,000 km. (63,400 miles) marks the seaward extension of paraliageosynclines, which is close to 34 % of the total.

Kossinna (1921) gave the area of the world's continental shelves (to 200 m.) as somewhat over 7 % of the total ocean area. Our own figure coincides closely. The seaward areas of paraliageosynclines now coinciding with the shelf amount to 8 million square kilometers (3.1 million square miles), or 30 % of the total shelf. If the areas of land plus total shelves is 175×10^6 km^2, and if the total cratonic basins (that is to say, the non-folded sedimentary basins outside of the deep sea and continental slopes) is $55{,}2 \times 10^6$ km^2, then the latter represents 32 % of the former.

A residue of 70 % of shelf area is underlain by rocky shelves or shelves covered by only a thin veneer of recent sediment. This is shown in places by the presence of basement rocks in outlying islands of the shelf, or, in rare cases, by seismic or gravity surveys. Therefore, the « standard » definition of a continental shelf as an apron (lens) of sediment spread out over the continental margin is invalid if taken on a universal basis and only applies to certain areas — the paraliageosynclines of today. Areas without that apron (i. e., little, if any, sediment) require the hypothesis that the shelves (a) are of recent origin, (b) were recently drowned, (c) were cut off by a major faulting or down-warping, and (d) that the adjacent ocean floor has been recently depressed by at least 12.000 feet.

Relation of Basins to World Areas.

If the area of continental land in the world is 150 × 10^6 km^2 (× 0.386 = 59 × 10^6 $miles^2$) and the total area of non-folded basins is 55 × 10^6 km^2 (21 × 10^6 $miles^2$), this comes to about 36 % of the land area. A correction, however, must be allowed, because certain basins overlap the continental shelf; if this amount is taken as 8 million square kilometers, 32 % of the land area corresponds to non-folded basins.

The balance of the land areas are occupied by fold belts, crystalline shields, and platforms (i. e., shields with a thin veneer of sediments). The sediments of platforms add an appreciable fraction to the surface area covered by sediments but very little as to volume, since (by definition) platforms are taken as extensive areas of less than 1.000 m. (3.000 ft.) sedimentary thickness, and usually it is much less.

The distribution of basins on the continents is interesting : the great land masses of the northern hemisphere (including Africa) all have basins covering about 35 % of their area, while the smaller southern continents, South American and Australia, show 50 % and 49 % respectively. Antarctica cannot be included as yet, because of inadequate information.

SÉDIMENTATION OVER THE EARTH AND SEDIMENTARY EUSTASY.

Some 30 % of the Earth is continental, 70 % ocean, but of the latter, 30 % again is continental shelf, terrace, and slope, with pericontinental basins and tranches receiving terrigenous sediments. Using the hypsometric curve in Kuenen (1950, based on Kossinna's statistics of 1921), the area of the Earth's crust between sea level and 3.000 m. (: 1.83 = 1.640 fathoms) is 16 % of the total; the area between 0 and 4.000 m. (2.200 fm.) is 30 % of the total : this last figure is the best approximation of the base of the continental slope and the limit of large-scale terrigenous sedimentation.

Pelagic Sedimentation.

A residue of somewhat less than 40 % of the Earth's total area is occupied by deep oceanic basins (not trenches) which are isolated by distance or by pericontinental trenches from most of the terrigenous material. The sedimentation here today is organogenic pelagic detritus, passing to volcanic or the finest terrigenous material. If the average sediment thickness over this area is taken as approximately 1 km. (3.000 feet), thus expressing the total pelagic sedimentation of all geologic time (say 5×10^9 years), the average rate of pelagic accumulation may be calculated as 1 mm. per 5.000 years. Even if the deep sea thickness is somewhat greater (Kuenen, 1946, says 1 to 5 km. thick) the sedimentation rate is still extremely slow.

Observed rates of mid-Atlantic globigerina ooze accumulation suggest 1 to 3 cm. per 1.000 years is the *present* average; this is 50 to 150 times the over all average and may be explained in part by the element of compaction in the 1.000 m. total and in part by the appearance of worldwide foraminifera in Cretaceous times. However, by allowing only 1 cm. per millenium (to represent compacted thickness) for the last 100 million years (back to mid-Cretaceous), we have the full total of 1.000 m. of sediment. Thus, the acceleration in pelagic supply during the last 100 million years could account for the total figure. It may therefore be necessary to conclude that the present rate of supply is grossly in excess of the past norm.

Since the area of the ocean is 361×10^6 km², and 149×10^6 km² is the area of the shelf and other basins at present being filled with terrigenous sediment, the residue (40 % of the total earth's area of 510×10^6 km²) is 204×10^6 km², the area of the earth's pelagic sedimentation. If the mean thickness of the latter is taken as 1 km., the *total volume of pelagic sediments* accumulated in 5×10^9 years is 204×10^6 km³. Kuenen's calculations (1946) suggest the same order of magnitude but somewhat higher (6 to 8×10^8 km³), which may be explained in part by Kuenen's assumption of a larger area of the ocean as « deep sea ».

Our calculated rate would correspond to 1 km³ in 25 years, or 40×10^6 m³ per year; one could say 40 million metric tons of sea water are displaced per year.

Thus : 40×10^{15} mm³ is added over an area of 360×10^{18} mm² per year; this will result in a eustatic rise of $\frac{40 \times 10^{15}}{360 \times 10^{18}}$ mm. per year $= \frac{1}{9000}$ mm. per year or 1 mm. per 9.000 years. This is a secular eustatic rise of sea level due to pelagic sedimentation alone. If the pericontinental sedimentation were to be entirely compensated by isostatic subsidence, then no further eustatic rise due to sedimentation could be accounted for; at this stage, glacio-eustatic movements and tectonically controlled changes are not being considered.

This rate would be equivalent to a 50 m. rise of sea level since the Cambrian (say 450 million years ago). There seems to be no doubt, however, that far greater oscillations of sea level have occurred from time to time, both positive and negative swings, so that pelagic sedimentation, which can only account for positive movements in any case, is of no great over all significance. This is contrary to the general conclusion of Suess (1888; see English ed., 1904-24).

However, with respect to sedimentation *since* the Cretaceous, the rate may have been notably greater, as observed above. If we allow 1.000 m. (which seems grossly excessive) as the total pelagic accumulation in the last 100 million years, it would result in a rise of sea level corresponding to the fraction 4/7 of the sediment added, this being the ratio of pelagic to total ocean area. The Post-Cretaceous rise would thus be nearly 600 m. Explanations for this rather extreme figure may be found in several ways : the globigerina ooze accumulation rate is clearly far in excess of the radiolarian ooze rate, but again it seems that contemporary accumulation (after the climatic oscillations of the Pleistocene) must be abnormally high.

Neritic Sedimentation.

The quantities of terrigenous sediments transported and laid down in the neritic zone within any period of time is considerably greater than in the pelagic. Moderate quantities are transported further by gravitational processes into deeper water. However, owing to oscillations of sea-level, isostatic uplift and other tectonic disturbances, high proportions of these sediments are eventually re-incorporated in folded mountain belts or otherwise emerge above sea level; they are thus exposed once more to erosion and a process of recycling.

Taking the area of the world's basins as 55×10^6 km^2 and the average thickness as 5.100 m., *the total volume of neritic sediments* (relatively unfolded today) is 2.8×10^8 km^3. This compares closely with a calculation made by Kuenen (1946, 1950) of 2×10^8 km^3. The above figure includes shelf basins, which may account for the discrepancy. In any case, about half of this amount probably stands below sea level, since the total volume of the world's land above sea level is only 1.3×10^8 km^3 (Kossinna, 1933).

With respect to eustatic rises related to sedimentation other than pelagic, it has been argued that the rate of sedimentation is compensated by the rate of isostatic subsidence of the basin, so that the net eustatic rise of sea level would be nil. It is now shown that isostatic subsidence is NOT sufficiently rapid, indeed by a factor at least 3 times. Young (1953) has estimated that, on the basis of the post-glacial Scandinavian isostatic recovery, compensation proceeds at only one-third the rate of sea-level rise over the last 10,000 years. The rate was initially much greater than today and seems likely to taper off over an extended period.

Applying this analogy to a typical sedimentary basin, it seems likely that, under conditions of heavy infilling, the basin would rapidly fill up, resulting in displacement of water and a eustatic rise. Isostatic compensation would operate more slowly, permitting continued but progressively reduced sedimentation; this gradual attenuation would, however, be modified by two factors : the eustatic rise would raise the relative sea level, and compaction would increase the local depth. The interplay of these three forces will result in a rhythmic alternation in depth and ecologic conditions, resulting in the well-known rhythmic sedimentary sequences characteristic of paralic and epicontinental basins.

The total for the present mass of neritic sediments in non-folded basins, together with marginal shelf and (by gravitational transport) adjacent bathyal regions, is 2.8×10^8 km^3 for material of all ages. Since the total area of the oceans is 361×10^6 km^2, that amount of marine sedimentation would correspond to a worldwide eustatic rise of 780 m. if uncompensated isostatically. It may be possible to exclude, for the moment, the mobile belts, since subsidence there may exceed rates of sedimentation.

It would not be unreasonable to take, perhaps for the sake of a hypothetical model, a figure of 50 % of the known neritic mass as having accumulated in the 60 million years since the Cretaceous. If this were so, we should have :

$$\frac{280 \times 10^6}{361 \times 10^6} \times \frac{50}{100} = 0.39 \text{ km. in } 60 \times 10^6 \text{ years}$$

$$= 7 \text{ mm. in 1000 years, thus 1 mm. in 150 years,}$$

as the mean rate of eustatic rise over the last 60 million years. This is not even of the same order of magnitude as the present rise, determined by means of tide gauges (Gutenberg, 1941).

The conclusion is clear therefore that neritic sedimentation in the non-orogenic basins does not seem to be of the right order to explain even normal eustatic rises of sea level. Abnormally rapid rises can be explained by periodical (but relatively rare) glacial melting and major geotectonic deformation. Eustatic fall of sea level requires either glaciation of tectonic subsidence of major proportions, topics which will not be considered further at this juncture.

SEDIMENTATION AND ISOSTASY.

Glacial Loading and Sediment Loading.

The analogy between glacial loading and sediment loading does not seem entirely too far-fetched. The Greenland ice cap is 1.65×10^6 km² ($\times$ 0.386 = 640.000 square miles), about 3 times the size of the *average* autogeosyncline, but examples nearly of this size exist in Africa. During the Pleistocene glaciations, the Scandinavian ice was three times as much again. The North American ice was even larger, however — almost as great as Antarctica today (13×10^6 km² or 5 million square miles). Niskanen (1939, 1943) calculates the Scandinavian ice to have had a maximum thickness of about 2.650 m. (8.700 ft.), which is approaching the same order of loading as in some autogeosynclines of the same dimensions (even allowing for the reduced specific gravity of the ice).

Taking the rate of isostatic adjustment to be in line with the recovery of Scandinavia since the last glacial period, we have the evidence of fairly accurate data calculated by Niskanen as follows : a total updoming of 520 m. has occurred, 250 being over the last 8750 years; 270 m. is still to go. This gives an average rate of 3.5 m. per century. A gradual diminution of uplift is observed, but the mean rate is sufficient.

This compares with a rate of 24 cm. per century (over the last 5,000 years) of observed subsidence near New Orleans in the inner part of the Mississippi delta, as determined by the writer from recent radiocarbon dating. A much higher rate is observed in the outer parts of the delta and may exceed one meter per century. The factor of compaction has not yet been separated from tectonic subsidence.

In the geological past, rates of subsidence of the same order can be calculated for certain restricted types of geosyncline only, e. g., the Alpine-Himalayan foredeeps, exogeosynclines; the Siwalik series of India were formed in a trough that subsided at least 10,000 m. in 3 million years — thus a mean rate of 0.3 m. per century.

Obviously, at times it would have accelerated, say to 1 m. per century, alternating with periods of deceleration. For the autogeosynclines and others of the more gently deformed basin types, rates would be far less.

It has been observed that the rate of adjustment in Scandinavia is far behind the rate of deglaciation. In fact, the ice has been entirely gone for over 5.000 years; the mean rate of compensation is probably slower than the rate of unloading by a factor of at least 3. It seems reasonable to postulate that the rate of loading in the Mississippi delta (see Fisk and McFarlan, 1955) exceeds the rate of the reaction-subsidence by something of the same order. The fact that it is greater is self-evident, since the delta has reached up to sea level over broad areas, even keeping pace with the rising eustatic level in addition. The *primary* subsidence that may be postulated as having initiated the development of the Gulf Coast Geosyncline back in early Mesozoic times (say 200×10^6 years ago), may well be still in progress, but it must certainly have a nature and quite distinct from the subsidence here considered, the isostatic reaction-subsidence.

It seems likely therefore that in the geological past isostatic reaction can never account for the primary subsidence of basins. Even provided with an initial basin, the sediment poured into it will arrive at such a rate that the isostatic subsidence rate of the basin will not be adequate to maintain the basin form (as a sedimentary receptical), so that the depression will become rapidly filled unless an additional factor of subsidence is operative. Isostasy and compaction will both help to maintain sedimentation in a given basin after the major tectonic subsidence has slowed down, but at a greatly reduced rate.

Transfer of Loads.

If we calculate the area of any specific type of basin of sedimentation selected from contemporary examples and compare this with the area of the drainage basin or basins that feed it, we can derive a ratio of *Area of Loading* to *Area of Unloading.*

Each of these can be refined by circumscribing the areas of maximum loading (largely a matter of depth, related to proximity to rivermouths) and areas of maximum unloading. The fulcrum is asymmetric because the area of maximum erosion is almost always greater than the area of maximum deposition. Therefore the area to be uplifted is greater than the area to subside, and therefore the amount of absolute uplift is likely to be much less than the amount of subsidence.

Actual mass transfer of material must take place at considerable depth beneath the crust. This is an asymmetric, one-sided lateral migration of material. Relatively little transfer takes place to seaward (toward the thalassocraton), since there is no unloading in this direction; only a low ridge will form (not rising even to sea level), as seen, for example, immediately south of the Java Trench in the Indian Ocean.

Because of the small area of loading and large area of unloading (large drainage basins of major rivers) there will be a dissimilar spread of matter set in motion by the isostatic reaction. The tendency will be toward an elevation over broad platforms and a subsidence along narrow, elongate belts. The ratio between these areas is at least 3 : 1 and may exceed 10 : 1.

Rate of Subcrustal Flow.

By taking individual cases of ancient basins, one by one, it should eventually be possible to determine, from a study of the stratigraphic record, both a volume of mass transfer and a rate of transfer. From these figures it should be simple to determine the rate and volume of subcrustal flowage required for the formation and maintenance of any particular basin type (see, for example, Heaps, 1953).

Correlation between basin types and crustal thickness is also a project for the future, and it would be acceptable as a working hypothesis that the shallowest basins will correspond to the thickest (strongest) crust, and vice versa. Earthquake seismology may thus provide a clue to the prediction of basin depths in relatively unexplored regions.

SEDIMENTARY STATISTICS AND PETROLEUM.

It is inevitable that a survey of world sedimentary basins should lead to some conclusions of deep significance to the economic question of petroleum.

Our figure of 55×10^6 km², representing the area of the world's sedimentary basins, including continental shelves of basin-like character, is notably higher than the 39×10^6 km² of Weeks (1952), but the shelf basins were not included in the latter figure. This gives us a total volume of 2.8×10^8 km³ for the non-pelagic sediments of the world, outside of the heavily folded belts. Clearly, this is the absolute finite ceiling of potential oil-bearing strata.

However, this figure must be severely curtailed. An appreciable area near the continental shelf margins and slope is not a present commercially drillable. Another enormous segment belongs to non-marine, continental basins almost totally devoid of oil. Certain basins have sediments of little or no porosity; others have too much — that is to say, no imprevious traps; others have too many breaks in the stratigraphic succession or excessive faulting, so that hydrocarbons have long ago been lost. In short, there is much evidence to support the statement of Weeks (1952) that « fully 80 % of the commercially recoverable hydrocarbons in the world » lie in pools scattered through only 20 % of the total basin area.

Unlimited Oil Reserves ?

There is a sanguine view prevalent among some oil men that, because petroleum reserves have been constantly rising over the last half century, directly in proportion to demand and exploration effort, those reserves will continue to expand into the foreseeable future. This concept is now held to be unsound. There is a finite limit to the potentially petroliferous sediments on the earth's crust.

The significant problem for oil economists and geologists to decide is just where is that limit. Capitalization of new oil ventures will not be justified if we are shortly approaching that end-point. On the other hand, if the present abundance will last for, say 30 to 40 years, then capitalization to that end will be justified.

In fact, as increasing depths have to be drilled and more dry holes must be written off, costs will rise considerably, so consumption will tend to taper off as customers seek alternative and less costly fuel sources.

According to the latest calculations of oil economists, the total oil reserves of the world (outside of U. S. S. R.) now stand at 200 billion barrels, of which 70 % lie in the Middle East.

In the United States, annual consumption is just about matched by the new discovery rate, with a ten-year reserve ahead. If this balance can be maintained, all is well. But production is rising and reserves are dropping. Furthermore, investors are becoming more and more interested in secondary recovery from already known and developed fields; this is a dangerous state of affairs, for it indicates lack of confidence in further wildcatting. A recent survey by Hill, Hammar, and Winger (1957) showed that, allowing for a plausible minimum ultimate recovery of 250 billion barrels in the United States, a peak of production will be reached about 1980, dropping away sharply about 30 to 40 years from now. Eugene Ayres (1956) presented a rather similar picture.

The long-range solution to this anticipated shortage is importation from the Middle East, Canada, and the Caribbean. However, the extra-American world consumption is rising very fast and may be expected to equal that of the United States by 1966. Owing to the relatively undeveloped state of many overseas countries, this foreign demand may reasonably rise at an ever-increasing rate as those states become more and more industrialized. Thus, unless an altogether remarkable increase in foreign reserves takes place, the foreign and thus the world total production will follow the expected United States picture to a peak and drop away rather sharply in 30 to 40 years time.

Future Development.

There are still a number of serious unknowns. One of these is the question of development of foreign reserves. It may be possible to stretch the period of optimum production by wise planning and conservation. Undoubtedly there are great fields awaiting discovery; the geological evidence points unmistakably in that direction. However, unless an immense wastage of capital is to be condoned ,some more rational techniques and organization of oil search must be envisaged. At present an astonishing amount of haphazard wildcatting is still indulged in.

The statistical approach, given only in broad outline in this paper, to logical basin classification and appraisal is now offered as a modest contribution to this great problem.

Nevertheless, it must be recognized that, regardless of new discoveries, sufficient is now known of world basins to be able to predict the ultimate decline of petroleum production. Crude oil seems destined to become so scarce and costly that it may have to be reserved for petrochemicals and other specific uses, and its wholesale use for fuel will have to cease, to be replaced by synthetics, uranium-type energy sources, and in part by a return to coal. Reserves of coal in the United States are also dropping, but in many parts of the world there are still great untapped potentials. The development of a synthetic, petroleum-like combustible (produced by a uranium-powered industry) seems to be a not unreasonable technological solution to our long-range dilemma.

CONCLUSIONS.

General.

1. Out of a total land area in the world of 150×10^6 km², sedimentary basins cover 48×10^6 km², of 32 % of the total; again, if the continental shelves of basin-character *are* included, the figure becomes 55.2×10^6 km², some 32 % of the total continent plus shelf area.
2. Large northern continents show an average of 35 % basin-covered, but smaller southern continents are about 50 % basin-covered.
3. Average thickness of sediments per basin for the world is 5,100 m., ranging from thinnest (Africa), with 2,800 m., to thickest (South America) with 5,300 m. Average thickness over the entire land area is 1,840 m.
4. Average size of basins (for world) is 180,000 km², ranging from autogeosynclines (520,000 km²) to epieugeosynclines (49,000 km²).
5. Of geosynclinal types, autogeosynclines cover the largest area (37 %) and epieugeosynclines (3 %) the least.
6. In frequency paraliageosynclines are the most numerous (33 %) and zeugogeosynclines (8 %) are the least.
7. Shape in plan is expressed by a shape Constant (ratio of width to length), autogeosynclines being about 1 : 2.5, and taphrogeosynclines about 1 : 7 (for the mean).
8. In thickness, the paraliageosyncline average is moderate (3.500 m.), the exogeosyncline is high (5,200 m.), and the autogeosyncline is low (3,100 m.).
9. Total thickness for all world basins is 1,480,000 m., which gives an average thickness/area relationship (m/km²) of 1 : 38.
10. Kay's classification of parageosynclines (1951) is essentially substantiated by the statistics. The basins are often gradational, but not always in the same order. Therefore the utilitarian value of the terms is substantiated.
11. Correlation of the basin types with the age of their respective basements shows that the older the basement the larger the superimposed basins, and vice versa. Older superimposed basins are smaller than younger ones for any given basement.
12. Continental shelves are only occupied by basins to a matter of 30 % by area; the rest are youthful platforms, suggesting the relatively recent collapse of those continental margins.
13. Deep-sea sedimentation is of the order of 1 mm. for every

5000 years up to the Cretaceous and 1 mm. for every 100 to 300 years since the Cretaceous (the appearance of pelagic foraminifera). The result would be an average sedimentary eustatic rise of 1 mm. per 5000 years. This is not sufficient to contribute greatly to the major marine transgressions of the geological past.

14. Neritic sedimentation is a great deal faster than deep sea, but in the course of geological time much of it is recycled. A calculation of the total volume of neritic (and continental, or minor fraction) sediment today, as determined from the capacity of all non-folded basins on the continents and in the continental shelves (inclusive of slopes), is 2.8×10^8 km^3.

15. Excluding mobile belts, whose subsidence often may exceed rates of accumulation, the volume of neritic sediments in the epicontinental and intermediate areas would correspond to a worldwide eustatic rise of 780 m.

16. If, for the purpose of a model, 50 % of the total neritic sediments are taken as having accumulated in the 60×10^6 years since the Cretaceous, this would indicate a mean eustatic rise of 1 mm. every 150 years.

17. Consideration of rates of sedimentation and subsidence are compared with isostatic compensation (or reaction) rates dependent upon the deglaciation of Scandinavia. The reaction time is found to be at least three times slower than the deglaciation, and in sedimentary basins the sedimentation rate seems to be greatly in excess of the isostatic subsidence rate.

18. Isostatic reaction to sedimentation cannot therefore explain the primary subsidence of sedimentary basins, the cause of which lies in forces outside of the sedimentary process. For protracted periods, the subsidence rate may have reached or exceeded 1 meter per century in the most active (but still not grossly deformed) basins.

19. Because sediment is eroded and transferred from enormous areas drained by major rivers and deposited in relatively small basins, there will be a dissimilar spread of matter by subcrustal flowage. This is asymmetric because little elevation occurs on the thalassocratonic side. The area ratio of downwarp to upwarp may range from 1 : 3 to 1 : 10 or more. The amount of uplift (in actual elevation) must normally be considerably less than the amount of downwarp.

20. It is anticipated that, by examining the stratigraphic records of individual basins, definite rate and volume figures will be determined for subcrustal flow. Earthquake seismology may provide a correlation between basin depth and crustal thickness.

Economic Significance.

1. It may be concluded from the above figures that the volume of sediments that lie below 32 % of the surface of the continents (plus shelves) represent the absolute limit of potential oil-bearing strata.
2. From this figure, however, must be subtracted the proportion of continental to marine facies in the underlying beds, which, with other refinements of second order, will materially reduce the over all potential of oil-bearing rocks.
3. A great deal has been written and said about unlimited development of the world's oil potential, and recently Wallace Pratt outlines his opinions as to an ever-expanding horizon of oil reserves, provided sufficient exploration was carried out. The absolute ceiling on total marine sediments (unmetamorphosed) proves this sanguine view to be over-optimistic.
4. In fact, a consideration of world oil reserves, estimates of increased consumption, and review of the limited number of basins still totally unexplored, leads one to the conclusion that within 30 to 40 years a fundamental shift will be taking place in the economic use of oil : from everyday fuel and heating to petrochemicals and specialized purposes. Its place may be taken by uranium-type fuels, and in part a return to coal; resources in both of these are still tremendous.
5. As an aid to oil exploration, and in particular for obtaining economics in initial drilling costs, the statistics and formulae for specific basin types, now being developed, should permit a much more accurate prediction of expectable thicknesses and facies in relatively unknown regions.

References.

Ayres (Eugene), 1956 : « The fuel situation », Scientific American, vol. 195, n° 4 (Oct.), pp. 43-49.

Boutakoff (N.), 1952 : The great-circle stress pattern of the earth, Australian Jour. Sci., vol. 14, pp. 108-111.

Brock (B. B.), 1956 : « Structural mosaics and related concepts », Trans. Geol. Soc. South Africa, vol. 59, pp. 149-197.

Cloos (H.), 1937 : Zur Grosstektonik Hochafrikas und seiner Umgebung, Geol. Rundschau, Bd. 28, Heft 3-4, pp. 333-348.

Fairbridge (R. W.), 1950 : Problems of Australian Geotectonics, Scope (Jour. Sci. Union, Univ. W. A.), vol. 1, n° 5, pp. 22-28.

FAIRBRIDGE (R. W.), 1955 : Warm marine carbonate environments and dolomitization, Tulsa Geol. Soc. Digest, vol. 23, pp. 39-48.

FISK (H. N.) and MCFARLAN (E.), 1955 : Late Quaternary deltaic deposits of the Mississippi River, Geol. Soc. Amer., Sp. Pap. 62, pp. 279-302.

GUTENBERG (B.), 1941 : Changes in sea level, postglacial uplift and mobility of the earth's interior, Bull. Geol. Soc. Amer., vol. 52, pp. 721-772.

HEAPS (H. S.), 1953 : An analysis of downpunching, Tr. Roy Soc. Can., vol. 47, Sec. 14, pp. 17-21.

HILL (K. E.), HAMMAR (H. D.), and WINGER (J. G.), 1957, « Future growth of the world petroleum industry », New-York (Chase Manhattan Bank publ.).

HILLS (E. S.), 1946 : Some aspects of the tectonics of Australia, Jour. & Proc. Roy. Soc. N. S. W., vol. 79, pp. 67-91:

KAY (Marshall), 1951 : North American geosynclines, Geol. Soc. Amer., mem. n° 48.

KAY (Marshall), 1955 : « Sediments and subsidence through time », Geol. Soc. Amer., sp. pap. 62, pp. 665-684.

KÖLBEL (H.), 1945 : « Die tektonische Entwicklung Australiens », Geotektonische Forschungen, n° 7/8, pp. 154-209.

KOSSINNA (E.), 1921 : « Die Tiefen des Weltmeeres », Veröff. Inst. f. Meereskunde, Berlin, N. F., A. Geogr. — naturw. Reihe, n° 9, 70 p.

KOSSINNA (E.), 1933 : Die Erdoberfläche, in Handbuch der Geophysik, vol. 11, pt. 6, pp. 869-952.

KRENKEL (E.), 1925 : Geologie Afrikas, Berlin (Bornträger), vol. 1, 461 p.

KUENEN (P. H.), 1946 : « Rate and mass of deep-sea sedimentation », Amer. Jour. Sci., vol. 244, pp. 563-572.

KUENEN (P. H.), 1950 : Marine Geology, New-York (Wiley), 568 p.

NISKANEN (E.), 1939 : « On the upheaval of land in Fennoscandia », Isostatic Inst., Int. Assoc. Geod., Helsinki, publ. n° 6.

NISKANEN (E.), 1943: « On the deformation of the earth's crust under the weight of a glacial load and related phenomena », Ann. Acad. Sci. Fenniae (Helsinki), A 111, n° 7, 59 p.

SOLLAS (W. J.), 1903 : The figure of the earth, Quart. Jour. Geol. Soc., London, vol. 59, pp. 180-188.

SONDER (R. A.), 1956 : « Mechanik der Erde », Stuttgart (Schweizerhart'sche Verlag.), 291 p.

STILLE (H.), 1935 : « Der derzeitige tektonische Erdzustand », Sitzb. preuss. Akad. Wiss., Berlin, Phys. Math. Kl., vol. 13, pp. 179-219:

STILLE (H.), 1936, « The present tectonic state of the Earth », trans., Bull. Amer. Assoc. Petr. Geol., vol. 20, pp. 849-880.

SUESS (E.), 1904-24, The face of the earth, Oxford (trans. by Sollas), 5 vols.

VENING MEINESZ (F. A.), 1947, Shear patterns of the earth's crust, Trans. Amer. Geophys. Union, vol. 28, pp. 1-61.

WEEKS (L. G.), 1952, « Factors of sedimentary basin development that control oil occurrence », Bull. Amer. Assoc. Petr. Geol., vol. 36, pp. 2071-2124.

YOUNG (A.), 1953, « Glacial eustasy and the rotation of the earth », Monthly Notices, Roy. Astr. Soc., Geophys. Suppl., vol. 6, pp. 453-457.

TABLE DES MATIÈRES

TOULOUSE. — IMPRIMERIE ÉDOUARD PRIVAT. — 4133-10 59
PRINTED IN FRANCE.